Volume 93, Number 3, May–June 1988
Journal of Research of the National Bureau of Standards

Contents

Volume 93, Number 3, May-June 1988
Journal of Research of the National Bureau of Standards

Accuracy in Trace Analysis

Volume 93, Number 3, May–June 1988
Journal of Research of the National Bureau of Standards

Accuracy in Trace Analysis

Volume 93, Number 3, May–June 1988
Journal of Research of the National Bureau of Standards

Accuracy in Trace Analysis

Volume 93, Number 3, May–June 1988
Journal of Research of the National Bureau of Standards

Accuracy in Trace Analysis

Volume 93, Number 3, May–June 1988
Journal of Research of the National Bureau of Standards

Accuracy in Trace Analysis

Volume 93, Number 3, May–June 1988
Journal of Research of the National Bureau of Standards

Accuracy in Trace Analysis

Volume 93, Number 3, May–June 1988
Journal of Research of the National Bureau of Standards

Accuracy in Trace Analysis

Volume 93, Number 3, May–June 1988
Journal of Research of the National Bureau of Standards

Accuracy in Trace Analysis

I. Plenary Lectures

History of Trace Analysis

H. A. Laitinen

Department of Chemistry
University of Florida
Gainesville, FL 32611

In the era of classical analysis when major and minor constituents of materials such as rocks and ores were determined by gravimetric and titrimetric methods, a measure of the quality of an analysis was the closeness to which the summation of constituents approached 100%. Trace constituents were considered to be those known to be present but in amounts so small that they made no appreciable contribution to the summation. An early authority was Hillebrand [1], who in 1919 wrote his classic book "Analysis of Silicate and Carbonate Rocks" and used the word "trace" to designate constituents present below the limit of quantitative determination, which meant below 0.01 or 0.02 percent. Sandell [2], in his 1944 book "Colorimetric Determination of Traces of Metals," considered major constituents to be those present in amounts greater than 1%, minor constituents to be those present in amounts between 0.01 and 1%, and trace constituents those below 0.01%.

The modern definition of "trace" is more flexible, as illustrated by a quotation from a 1965 book, "Trace Analysis" edited by George Morrision [3]: "The connotation of the term "trace" varies with the background or interests of the reader." In that book, the upper limit was considered to be about 100 ppm by weight, and the term "ultra-trace" was used for constituents below 1 ppm. To quote further, "any sharp division is, of course, superfluous, and will depend on the nature of the sample to be analyzed, the analytical technique employed, and the analyst."

For trace analysis to emerge as a specialty in its own right, two conditions had to be met: specific needs and applicable methods. Qualitative methods in general emerged much earlier than quantitative ones. Quite a few qualitative tests and even a few quantitative methods of great sensitivity existed before the turn of the century, but they remained largely unused as interesting curiosities until a need arose. The decade of the 1940s represented a watershed in creating a variety of new demands for analytical methods of exceptional sensitivity and difficulty. World War II had quite a stimulating effect with respect to new needs, but it also stifled free publication for several years, with the result that shortly after the end of the war in 1945, there was a release of enormous amounts of previously classified material for publication. Methods and instrumentation developed to solve specific problems now became available for wider application.

It is now convenient to consider five periods in history—(1) antiquity to the beginning of modern chemistry late in the 18th century, (2) late 18th century through the 19th century, (3) the period from 1900 to 1939, (4) the decade of the 1940s, and (5) the period from 1950 to the present.

Period 1, Antiquity to Late 18th Century

Probably the earliest example of trace analysis is fire assay or cupellation, to which several references are made in the Old Testament.

Szabadvary [4] states that "Pliny records the use of extract of gall nuts as a chemical reagent when soaked on papyrus. Adulteration of copper sulfate with iron sulfate could be detected by the papyrus becoming black when dipped in the sulfate solution." This test for iron, first described in 61 A.D., emerges again in 1576 (Gesner) and 1597 (Libavius) [5]. Apparently the first use of gall-nut powder for a quantitative analysis was by Robert Boyle to estimate the amount of iron in natural waters (1684). The limit of detection was estimated to be 1 part in 600 or 160 ppm. This reagent was also

used for copper. Boyle suggested other plant extracts as reagents but these did not prove to be reliable. He introduced a new reagent he called "volatile sulphureous spirit," later identified by Szabzadvary as hydrogen sulfide, which did not receive attention as an analytical reagent for another century. Boyle is credited with the first use of the term "chemical analysis" as we know it today in 1654, and with the introduction of litmus as an acid-base indicator.

The phlogiston era, from the late 17th to the late 18th century, was essentially barren from the viewpoint of trace analysis. An exception is the work of Marggraf (1709–82), who used the Prussian Blue test for iron, a flame test to distinguish between sodium and potassium salts, and the microscope as an analytical instrument. Another important chemist of this era was Torbern Bergman (1733–84), who wrote the first analytical textbook (1780) and originated analytical chemistry as a distinct branch of chemistry [5].

Period 2, Late 18th Century to 1899

Modern chemistry began to flourish with the abandonment of the phlogiston theory, but for a long time trace analysis remained of interest for only a few constituents of special value or special effects, such as imparting color, taste, or odor to drinking water.

Colorimetry developed relatively early in the primitive form of visual comparison of the intensity of color of an unknown in a cylindrical tube with that of a series of standards of known concentration. Some early examples are the estimation of iron or nickel in a cobalt ore (Lampadius, 1838), copper via the ammonia complex (Jacquelain, 1846), iron via the thiocyanate complex (Herapath, 1852), titanium via hydrogen peroxide (1870), hydrogen sulfide via methylene blue (1883), and silica via molybdosilicic acid (1898) [5]. The Duboscq colorimeter (1854) represented a breakthrough in permitting the relative light paths of the standard and unknown to be varied mechanically until an equal intensity is observed. This instrument remained in common use until the introduction of the photoelectric colorimeter in the late 1920s. Some of these early methods had limits of detection and determination in the microgram range and could be called trace analytical methods, but the need for such methods remained rather specialized and limited throughout the 19th century and the early 20th century.

An outstanding development of the 19th century was atomic emission spectroscopy, introduced by Bunsen and Kirchhoff in 1860 [6]. Talbot, in Scotland, had used a spectroscope to observe flame colors as early as 1826, and had suggested the use of this method for trace analysis, but it attracted little interest for several decades. It is interesting to speculate on the reason for this long gap. Talbot had observed the difference between lithium and calcium salts and had noted the great sensitivity of the method, but he did not pursue the scope of the method or contribute to the fundamental understanding of the subject. Bunsen and Kirchhoff, on the other hand, showed the reason for the Fraunhofer lines of the solar spectrum which had been observed as early as 1814, made quantitative studies of emission and absorption, and clearly associated specific emission lines with elements rather than compounds. The Bunsen burner also was a simple and practical emission source. Their method rapidly saw many applications, including the discovery of several elements [Cs, Rb (1860), Tl (1861) and In (1864)].

However, apart from Bunsen's laboratory, the method did not see general use for several decades, even for qualitative purposes. Slavin [7] has traced several reasons for this neglect: (a) Flame sources showed poor sensitivity for metals other than the alkali metals and alkaline earths; (b) While electrical discharges had long been known to produce spectra of almost all metals, there were not convenient means of providing electric current in Bunsen's day; (c) There were no wavelength tables available to interpret the complex arc and spark spectra; and (d) Photographic recording was not in general use until later. To these reasons Winefordner added the general inertia of the scientific community. As recently as 1910, H. Kayser stated "There is little prospect that in the future qualitative analysis will apply spectroscopic methods to a large extent . . . I have come to the conclusion that quantitative spectroscopic analysis has shown itself to be impractical." Slavin remarks: "Thus by 1920 all the conditions needed for a system of chemical analysis by spectroscopy existed. We had excellent instruments, good photographic emulsions, a power distribution network, and basic theory. However, chemists were very slow to take advantage of this powerful tool, even for simple qualitative identifications. They still relied on the classical instruments, the test tube, the blowpipe, and the nose." It was left for physicists, astronomers, and

others to develop the method until the 1930s.

Electroanalytical chemistry can be traced back to 1833, when Faraday discovered the laws of quantitative electrolysis. Electrogravimetry, which could in some cases be applied to trace analysis, dates back to 1864. Real advances, however, were not to come about until the emergence of solution physical chemistry around the turn of the century.

O'Haver [8] has traced the development of luminescence spectrometry (the measurement of fluorescence and phosphorescence) in analytical chemistry. Fluorescence has been recognized since 1833, when Brewster described the emission of red light by an alcoholic extract of green leaves (chlorophyll) and described the phenomenon as "dispersion" [9]. The term "fluorescence" was introduced by Stokes, who in 1852 first recognized that the emitted light was of a longer wavelength than the exciting radiation, and who proposed the use of fluorescence as an analytical tool in 1864. The first use of fluorescence in trace analysis was the determination of aluminum by means of the fluorescence of the morin complex by Goppelsroder in 1867 [10]. Until 1920, fluorescence intensities were estimated by visual comparator methods, and further development awaited the introduction of more advanced instrumentation.

A closely related method is phosphorescence, which is characterized by a time delay in the emission. This phenomenon has been recognized since 1568, when Cellini described a luminescent diamond [11]. A great many phosphors were discovered during the 17th and 18th centuries, but little progress was made until Becquerel devised the first phosphoroscope in 1858 and established the exponential decay law in 1861. Quantitative trace applications, however did not emerge until the 1950s.

Period 3, 1900–1939

The whole nature of analytical chemistry underwent a profound change when the principles of physical chemistry began to be applied systematically to the understanding of analytical procedures. A highlight was in 1894, when Wilhelm Ostwald, one of the leading physical chemists of the day, published a book entitled "Die Wissenschaftlichen Grundlagen der Analytische Chemie." Ostwald showed how ionic equilibria could be applied to acid-base and precipitation reactions, how precipitates undergo recrystallization upon standing (Ostwald ripening), etc.

Oddly enough, he did not mention the Nernst Equation, which had been published in 1889 [12] while Nernst was in Ostwald's laboratory. Nevertheless, Kolthoff [13] has characterized Ostwald together with Gibbs, van't Hoff and Arrhenius, as "the founders of physical chemistry, and, indirectly, of scientific analytical chemistry." It was Salomon [14], in Nernst's laboratory, who in 1897 performed the first "galvanometric" titration, the forerunner of the modern biamperometric titration. Nernst and Merriam [15], in 1905, established the basis of steady state voltammetry using stationary and rotating electrodes and interpreted them on the basis of the Nernst diffusion layer. These methods were not clearly understood until later, when polarography had been developed, and they did not receive application until the 1940s.

Sorensen's development of the concept of the pH in 1909 led to a direct application of the Nernst equation to trace analysis [16]. The development of the glass electrode as a pH electrode by Haber and Klemensiewicz [17], also in 1909, was later to revolutionize pH measurements as soon as reliable electronic instruments became available for measurements using the high impedance membranes. There might be some question about the inclusion of pH as trace analysis, but considering the fact that the ion selective electrodes are based on the same principle this inclusion appears appropriate.

Potentiometric titrations also originated with Nernst. A great many analytical applications were made by pioneers such as Erich Müller and I. M. Kolthoff during the 1920s, but the emphasis was on accurate and selective titrations rather than on trace analysis.

The discovery of polarography in 1922 [18] by Heyrovsky was landmark because it introduced a new approach to trace analysis. During the period 1922–39, a great many publications on classical polarography appeared, mainly in the *Collections of the Czechoslovak Chemical Communications*. Many trace analytical applications were described for inorganic, organic, and biological systems. Although Kolthoff and his students had been involved in polarographic research since 1935, no publications emerged from his school until 1939 [19]. European laboratories were making many applications, but the only commercial apparatus available was the original Nejedly instrument introduced in 1925 in Prague and no English language book was available. The method required considerable investment in effort for sufficient understanding, and did not lend itself to empirical applications without this

understanding. Applications were relatively few in the U.S.A. through the 1930s, but the picture was soon to change with the appearance of the Kolthoff-Lingane book "Polarography" in 1941 and with the introduction of U.S.-made instrumentation.

The most sensitive trace analytical method cited by Sandell, op. cit. is the isolation of a bead of gold from two liters of sea water followed by its microscopical measurement. This method, described by Fritz Haber in 1927 [20], was used to estimate that sea water contained variable amounts of gold, on the order of 10^{-10}%, depending on the locality. The accepted average value is 4×10^{-10}% or 4 μg/L.

Some of the early colorimetric methods have already been mentioned. With the development of the photoelectric colorimeter and the spectrophotometer and the increasing demand for trace methods during the 1930s and 40s, and with the increasing knowledge about solution equilibria involving coordination compounds, a great many sensitive trace methods emerged. Especially noteworthy is the dithizone method, based on selective extraction of trace metals as dithizone complexes to enhance both the selectivity and sensitivity of the methods. Sandell [2] gave a practical limit of about 0.1 ppm for quantitative colorimetric determinations in solid samples.

Fluorescence methods were stimulated by the introduction of a photoelectric fluorometer by Jette and West in 1928 [21]. Cohen, in 1935, described a simple fluorometer and depicted a typical analytical calibration curve [18]. Finally, invention of the photomultiplier in 1939 greatly improved the sensitivities of fluorescence methods. The first complete commercial fluorescence spectrometer was introduced by Aminco in 1955.

A special form of luminescence is observed when certain metal oxides containing trace quantities of activating elements are placed at the outer edge of a hydrogen diffusion flame. This phenomenon was observed as early as 1842 by Balmain and termed *candoluminescence* by Nichols in 1928. Its use in qualitative analysis dates back to Donau in 1913, but its use as a quantitative trace method is primarily due to Townshend and Belcher, beginning in 1972 [23]. It has not seen extensive application, evidently because of the inconvenient sample preparations required.

Although catalyzed reactions have been long recognized and used as the basis of sensitive qualitative tests, the first quantitative use of reaction rates in trace analysis appears to be the work of Sandell and Kolthoff [24] in 1934, who showed that the rate of the Ce(IV)-As(III) reaction was proportional to the concentration of iodide present as a catalyst, and used the rate measurement to estimate iodide concentrations down to 20 ppb.

Period 4, the 1940s

The decade of the 1940s represents a special time in the history of trace analysis because the outbreak of World War II in September 1939 suddenly cut off a great deal of international communication. Even domestic communication was impeded because of the secrecy of several wartime research programs. These research programs introduced an urgent need for trace analytical methods of a wide variety. In the years immediately following the end of the war in 1945, a great surge of publication occurred. Fortunately, the ACS had foreseen the revolutionary changes occurring in analytical chemistry, and had prepared for the flood of publications. In 1943, Walter J. Murphy became editor of *Industrial and Engineering Chemistry* and of its *Analytical Edition*. He soon brought in L. T. Hallett as an associate editor, and they began to lay plans for a separate analytical journal. Ralph H. Müller began a column on Instrumentation in 1946, a new format had been adopted by 1947, and in 1948 the new name of *Analytical Chemistry* became fully operational.

Upon the outbreak of World War II, the delivery of the Nejedly Polarograph was cut off, and the E. H. Sargent company was granted the right to market U.S.-made instruments under the same name. The first U.S.-made photographic-recording instruments of 1940 were later replaced by pen-and-ink instruments introduced by Sargent and by Leeds and Northrup. For some 25 years, polarography had dominated electroanalytical chemistry, but beginning in the 1940s other microelectrode techniques began to supplant and replace classical polarography.

The long time interval between the first discovery of the principles of steady state voltammetry and of amperometric titrations and their modern usage has already been noted. There are other interesting gaps of this sort. Coulometry could be said to date back to Faraday, but it did not emerge as a modern analytical technique until 1938, when Szebelledy and Somogyi [25] introduced coulometric titrations at constant current. The companion

technique of coulometric analysis at controlled potential was pioneered by Hickling's [26] development of the electronic potentiostat in 1942, and Lingane's [27] applications of exhaustive electrolysis in the late 1940s. These applications were hampered by the lack of an electronic coulometer. The modern form of this instrument, based on storing a portion of the electric charge in a capacitor and measuring the voltage drop across the capacitor as a function of time, could not be developed until advances in dielectric materials and electronic measurements had occurred.

Of the wartime programs, the best known is the nuclear energy program, which put severe demands upon trace analysis capabilities. Not only were materials such as graphite needed in unheard-of purity levels, but methods were needed for elements that did not even exist in nature, and for elements in matrices of exceptional complexity, such as fission products. Methods were needed for accurate isotope ratios, and for extremely small amounts of elements of unknown chemistry, the transuranium elements.

Less generally recognized are the other classified programs of the era. The antimalarial program required analytical methods for new drugs in blood plasma at concentration levels that kept decreasing as the drugs improved. Here extraction and fluorescence methods sensitive to ppb levels were devised. Another wartime effort was the synthetic rubber program which involved emulsion polymerization for the first tine in the U.S., and which brought demands for trace analysis methods not only in the emulsion system but for the raw materials and products. In the area of chemical warfare, trace methods were needed for known chemical agents as well as for new ones being developed.

These wartime demands spawned a reexamination of many existing trace methods, the adaptation of old methods to new problems, and the creation of entirely new approaches. Instrumentation often had to be improved to meet new demands, but electronics was still in the era of vacuum tubes and the digital computer had not yet been developed, so much remained to be done in the postwar period. Let us examine a few of the wartime advances.

In 1939, mass spectrometry was still in a relatively primitive state as far as trace analysis is concerned [7]. The early instruments of J. J. Thomson, A. J. Dempster, and F. W. Aston were primarily used to identify nuclides of the various elements. A. O. C. Nier, in the 1930s, greatly refined the quantitative measurement of isotope ratios, and early in the nuclear program designed instruments for isotopic analysis of uranium and hydrogen. Organic MS analysis was developed primarily for hydrocarbon analysis and applied during the wartime polymer program. In 1945, the fragmentation patterns of aliphatic hydrocarbons were published by H. W. Washburn et al. of the Consolidated Engineering Co., which introduced the first commercial MS instrument shortly thereafter.

Ion exchange had been recognized since 1850, but few analytical applications had been made by 1939. The first synthetic ion exchangers appeared in the mid-30s, but the real impetus for analytical separations came during the nuclear program when rapid rare earth separations became necessary. These developments, both at Oak Ridge under G. E. Boyd and at Iowa State under F. H. Spedding, were published in 1947 [28,29] and led to a large number of analytical applications. The polystyrene-based ion exchange resins, introduced in 1944, form the basis of modern applications.

Infrared spectrometry, in 1939, was still largely a specialized structural tool although a few analyses of major and minor constituents had been reported. A key publication by Norman Wright of Dow in 1941 showed the possibility of organic analysis by IR [7]. The wartime polymer program gave a great impetus for applications such as monitoring hydrocarbon purity and measuring side vinyl groups in elastomers. Commercial instrumentation, beginning in 1942 with the Beckman IR-1, and in 1944 with the Perkin-Elmer Model 12A, moved infrared gradually from the physics laboratory into analytical applications. Real stimulus came later, with the introduction of the Perkin-Elmer Model 137, a relatively low cost bench top instrument, which has been succeeded by a series of instruments designed for general use.

In a similar way, UV spectroscopy was stimulated to emerge as an everyday analytical method through the introduction of the Beckman DU instrument in 1941 [7]. Publication of many wartime applications was delayed until the late 1940s.

Atomic emission spectroscopy, as mentioned above, remained largely a qualitative method until the introduction of methods for comparison of line intensities on photographic plates were worked out in the 1920s and 30s. These methods included the log sector and step sector rotating disks and the microphotometer. The atomic emission method remained relatively cumbersome and inexact until the direct reading spectrometer became a reality in

the late 1940s. For this to happen, the photomultiplier tube and associated electronics had to be developed. Many later developments have involved multichannel capabilities and computerized data processing.

Electroanalytical methods likewise found many trace applications stimulated by wartime needs. For example, amperometric titration methods found application for monitoring mercaptan levels in emulsion polymerization systems, and in coulometric titrations of trace arsenic at micromolar concentration levels. Linear sweep and cyclic voltammetry were studied independently in several countries although publication did not emerge until after the war. Several electroanalytical methods were hampered by instrumental limitations which were gradually overcome in postwar years by improvements in oscilloscopes, development of solid state electronics, and the microcomputer.

Period 5, 1950 to Present

The invention of the transistor in 1947 proved to be critical in revolutionizing instrumental approaches to trace analysis. Not only were solid state electronic devices more reliable, stable, sensitive, and less expensive than their vacuum tube counterparts but they consumed far less power and were capable of miniaturization. The microcomputer became so much cheaper and smaller that it became practical to incorporate data processing elements into individual instruments. The laser and fiber optic techniques have permitted miniaturization of a variety of optical methods. The recent history of many trace methods has involved the use of long known principles of physics and rendering them practical for analytical applications through modern instrumentation.

Electroanalytical chemistry since 1950 has moved in several directions, including (a) ion selective electrodes, (b) other electrochemical sensors, and (c) combinations of electrochemical and optical techniques. These will be considered in turn.

a. Ion selective electrodes in their modern forms are relatively recent developments, beginning in the 1960s. As early as 1923, Horovitz [30] showed that glass electrodes responded to ions other than the hydrogen ion, e.g., sodium, potassium, silver, and zinc ions especially at lower acidities. Eisenman et al. [31] pioneered in the theoretical interpretation of mixed response of glass membranes to cations.

A few solid state membrane electrodes were described by Trümpler [32] in 1921, Tendeloo [33] in 1936, and to Kolthoff and Sanders [34] in 1937. No important applications were made until the work of Pungor et al. in the 1960s [35]. Pungor described composite electrodes of solid particles imbedded in silicone rubber which acted as solid membranes. A landmark discovery was the solid state fluoride sensing electrode of Frant and Ross [36] in 1966. Another landmark was the introduction of liquid membrane sensors. As early as 1933 Beutner [37] studied water-immiscible organic liquids containing mobile ionic or inorganic components and concluded that such membranes might respond to changes in external solution composition. Liquid membrane sensors for calcium ions were introduced in 1967 by Ross [38] and many others soon followed.

The idea of using a glass electrode for the sensing of gases originated in 1958 with Severinghaus [39] who coupled a CO_2 diffusion membrane to the glass electrode. This has stimulated several other sensors for gases which affect the pH of water, as well as composite electrodes consisting of a primary detector electrode coupled with some sort of specific generating system. The nature of the generating system has been varied widely. The earliest seems to be the enzyme-substrate system urease-urea, sensed by Guilbault and Montalvo [40] in 1970 with a glass electrode to detect ammonium ions for measuring urea. Rechnitz [41] has been especially active in this field, devising not only enzyme-based electrodes, but electrodes based on antigen-antibody interactions, and sensors using plant or animal tissue membranes and even living organisms.

A different principle used for membrane sensors was introduced in 1956 when L. C. Clark [42] used a diffusion membrane to obtain stable diffusion-limited electrolysis currents at stationary electrodes. The first application, for monitoring dissolved oxygen, was soon commercialized but its obscure publication delayed the further exploitation of this principle.

b. Electrolytic techniques shifted away from classical polarography to other microelectrode techniques. Several reasons for this shift of emphasis can be traced in retrospect: (a) While diffusion theory to the dropping electrode was understood relatively early (Ilkovic, 1934) [43], many phenomena related to electrode kinetics remained ill-understood until Koutecky in 1953 [44] showed the complex relationship between diffusion and kinetics at

the dropping electrode. (b) Instrumentation for current-time-potential measurements was primitive until the 1940s and later. Transient and pulse techniques lent themselves more simply to stationary electrodes than to the dropping electrode. (c) The development of the rotating disk and the ring disk electrodes by Levich in the 1940s provided an accurate means of defining mass transport and for studying transitory intermediates formed at electrodes.

Classical polarography played a key historic role in leading to the development of various microelectrode methods. A good example is chronopotentiometry, or measurement of transition times during electrolysis at constant current under diffusion control. The theory of transition times dates back to Sand (1901) [45] who verified the equation for long transition times with special precautions to avoid connective disturbances. Gierst and Juliard in 1953 [46] used a slowly dropping electrode to verify Sand's equation for short transition times, thus illustrating the stimulating effect of polarography on other microelectrode techniques. Chronopotentiometry is also an example of a rapid rise and fall of a technique. After a flurry of papers in the 1950s and early 60s, it became recognized that the theoretical difficulties of eliminating charging currents limited the accuracy of the technique, which now is largely used for diagnostic purposes such as determining whether a soluble or insoluble product is formed. Pulse polarography, which grew out of classical polarography, is another example. In its first version by Barker [47] it was shown to be far more sensitive than the classical method, but it did not gain wide use because of its electronic complexity until greatly simplified versions were described by Parry and Osteryoung [48] and developed commercially by PAR. Ultramicroelectrodes have been found to have theoretical and practical advantages which require modern measurement techniques for their full realization. New electrode materials and modified electrode surfaces are enlarging the horizons of electroanalysis. Another capability of modern instrumentation is to use a variety of different applied signals and output measurements on a given cell setup to permit signal storage and retrieval.

c. Combinations of optical and electrochemical techniques such as electrochemiluminescence, and combinations of electrochemical sensors with separation techniques such as HPLC, are finding applications, especially in bioanalytical chemistry. The concept of fiber optic sensors goes back to 1976 [49], when they were suggested for monitoring a number of physical properties. The name "optrodes" and the idea of chemical sensing originated in 1983 with Thomas Hirschfeld et al. [50]. Although electroanalytical techniques are often fully competitive in sensitivity with spectrochemical methods and cheaper in instrumentation, they often fail to be considered because they may be more limited in scope and more demanding in knowledge of solution chemistry.

Curiously enough, the atomic absorption method did not emerge until 1955. The hollow cathode tube of Walsh was largely responsible for its spectacular rise thereafter. Another factor, however, was that the need for trace analytical data increased greatly during the 1950s and 1960s. For example, environmental chemistry stimulated interest in measuring pollutants, and increasing awareness of the effects of trace constituents in materials such as alloys and solid state electronics materials provided an enormous stimulus.

The technique of atomic fluorescence spectroscopy was suggested by Alkemade in 1962 and introduced analytically by Winefordner, who remarked in 1976 "The method has not become popular despite significant advantages over atomic absorption in some cases. The reasons are not very clear. Lack of commercial instrumentation may be part of the explanation, but more likely it is the overwhelming popularity of atomic absorption methods. Atomic fluorescence has not yet made it into the club" [7]. Ten years later, he said that his statement is still true despite the introduction of a commercial instrument. An added reason is the emergence of plasma emission sources, especially the inductively coupled plasma or ICP, which have become increasingly important in recent years. Introduced simultaneously by Fassel and by Greenfield in 1964, it has been intensively investigated by Fassel more recently. Being commercially available and applicable to multi-element analyses of great sensitivity, ICP spectroscopy has become the most important of present-day emission spectrochemical methods.

Chemiluminescence has been known since the 19th century but only in recent years has it seen extensive use in trace analysis because of a lack of selectivity. By controlling the reaction conditions and by improved instrumentation it is now possible to determine many substances including trace metals, oxidizing and reducing gases, and biochemicals by direct or indirect methods involving chemiluminescence. The measurements are usually

transient in character so they require advanced instrumentation for their full exploitation. No doubt this is the reason for the slow development of this method. Another factor is the need for careful consideration of the chemical reactions involved.

The use of catalyzed reactions, and of kinetic methods in general was delayed until the development of instrumentation made possible the convenient measurement of reaction rates, even though the theoretical basis of such methods was well understood. For example, glucose oxidase has been used as a specific catalyst since 1957 [52] for the determination of glucose in blood serum via the production of hydrogen peroxide which reacts with a dye to form a colored reaction product. By designing an instrument for the automatic measurement of the initial reaction rate, Malmstadt and Hicks [53] in 1960 described a refined and specific method for glucose.

A different type of application of enzymes arose with the use of immobilized enzymes at an electrode surface. The first use of such an immobilized enzyme appears to be that of Clark and Lyons [54] in 1962, who immobilized glucose oxidase at a membrane-coated electrode and sensed the hydrogen peroxide amperometrically. The potentiometric enzyme electrodes have been mentioned above.

During the 1960s the development of the microcomputer made it possible to automate the measurement of the initial reaction rate by using the small change in voltage output of a transducer to register a small change in concentration. The transducer could be based on various principles, such as measurement of potential, current, or absorbance. Although some notable examples of trace analysis by non-catalytic methods have been described, the vast majority of kinetic trace methods are based on catalytic reactions.

Nuclear methods have existed in principle since the discovery of radioactivity at the turn of the century. Tracer techniques using naturally occurring isotopes date back at least to 1919, when Paneth used thorium B, a naturally occurring isotope of lead as a tracer to study the reactions of lead. With the discovery of artificial radioactivity in 1934, tracer techniques became more general. By the late 1930s Kolthoff was using radioactive bromine, prepared by using a radon-beryllium neutron source to study the aging of silver bromide [55]. Activation analysis dates back to 1938, when Seaborg and Livingood determined gallium in iron at the 6 ppm level using a cyclotron source. However, it was not until the nuclear reactor was available as a high flux neutron source in 1946 that neutron activation analysis became an important trace technique. Radioactive tracer isotopes as well as enriched stable isotopes soon became available for many applications of isotope dilution analysis.

The gas chromatographic method had been mentioned in a 1941 publication [56] but it lay dormant for 10 years before being revived by the same worker, A. J. P. Martin [57]. Liquid-liquid partition chromatography actually did see limited applications during the 1940s, and the Craig countercurrent extraction method was widely used in biochemical laboratories, but GC escaped attention. As it happened, Martin and Synge were engaged in unrelated wartime research soon after the 1941 publication, and it was not until 1948 when Martin and James resumed work on the idea. No doubt a contributing factor to this long neglect was the fact that the original publication in *Biochemical Journal* was not available during the war in many countries, and in any case, this journal was not one that most analytical chemists would consult. Soon after the publication of several papers in the early 1950s, commercial development followed. In the U.S., apparently the first GC was built at Monsanto by Ralph Munch in 1953 and described at a Gordon Conference in 1954. It used a thermal conductivity detector. By 1955 commercial equipment was available. Many of the early applications were for major and minor constituents in mixtures and for analysis of small samples, but later, trace methods became important, especially after the introduction of more sensitive detectors such as the flame ionization detector in 1958. About the same time, the open tubular column or capillary column GC, and GC-MS were developed, both of which greatly expanded trace applications. Commercial GC-MS did not become available until around 1970, because of the need for small dedicated computers to handle the voluminous amount of data.

The introduction of ion chromatography by Small et al. [58] in 1975 as a special form of ion exchange represented an important advance in trace analysis especially for anions but also for mixtures of cations. For extremely dilute samples, a preconcentration step can easily be added to collect ions from a large sample onto a precolumn, from which they are eluted into a separation column.

Liquid chromatography underwent a revolution starting in 1967 with the introduction of the Waters ALC 100 high pressure liquid chromatography system. The letters HPLC were first used to designate

high pressure liquid chromatography and later high performance liquid chromatography. Coupling of LC with MS began in 1973–74 with the publication of results from the laboratories of E. C. Horning, F. W. McLafferty, and R. P. W. Scott. However, early efforts were fraught with difficulties due to the need for removing the solvent, and even today improvements are being actively pursued.

Mass spectrometry has continued to develop in several forms as an important trace analytical method. Spark source MS dates back in principle to Dempster in 1934 but modern instrumentation and quantitation did not come about until the 1950s. Time of flight MS originated with A. E. Cameron in 1948 and was commercialized by Bendix in 1955. Secondary ion MS, using an ion beam to sputter material from a solid surface, emerged in the 1960s and is important both in the imaging and ion probe configurations. Tandem mass spectrometry (MS/MS) was first introduced as a structural tool in the mid-1960s but it did not become important as a trace analytical method until the triple quadrupole system of the late 1970s. The quadrupole MS dates back to Paul and Räther in 1955, and became commercially available during the 1960s. The triple QMS system, developed by Yost and Enke in 1978 and commercially available since 1981, is becoming increasingly important in trace analysis, especially for complex organic mixtures. Still another variant is ICR MS, or ion cyclotron resonance mass spectrometry, which originated in principle as the Omegatron at NBS in 1950, and which became commercially available from Varian in 1967. The Fourier transform version, introduced in 1974, has improved its applicability to analytical problems, but it is still not primarily a trace analytical instrument.

X-ray emission is another trace analytical method that was slow to develop. The principles were known at the time of Moseley (1913), who discovered the concept of atomic numbers, but analytical applications were slow to emerge. Birks, who with Friedman introduced the modern version of the x-ray fluorescence in 1948, has traced the slow development of the method over the intervening 35-year period [7]. In 1914, de Broglie had demonstrated the excitation of fluorescence x-rays outside the x-ray tube; Jonsson in 1927 had made accurate intensity measurements by means of a Geiger counter; von Hevesy published a book in 1932 laying out the principles of x-ray emission analysis; and a Russian book by Borovskii and Blokhin in 1939 formed the basis of a course on the subject at Moscow University. However, in the period between 1932 and 1948, hardly any publications appeared on the subject. Birks remarks that the modern development "was not deliberate but rather the result of a chance observation of strong background interference in x-ray powder diffraction patterns of Fe compounds when using a Cu target x-ray tube." "Changing to an Fe-target tube eliminated the background difficulties, but Friedman recognized the potential of using the fluorescent excitation as a means of elemental analysis." Birks, in following the later development of x-ray emission through the 1950s to the 70s, states that we "observe that its success depended not on new x-ray principles but almost entirely on various kinds of improvements in electronics."

The electron microprobe, also based on x-ray emission, was patented in 1947 by Hillier of RCA in 1947 but he did not pursue the method and Guinier and Castaing reported on their conversion of the electron microscope to a microprobe in 1949. An independent development by Borovskii in the U.S.S.R. occurred about the same time. The microprobe was of special significance because it permitted the direct observation of spatial distribution of constituents that on the basis of average composition would be trace constituents but would sometimes have pronounced effects because of segregation in regions of higher concentration such as grain boundaries. A closely related technique allowing for finer spatial resolution at the expense of selectivity and sensitivity is the use of energy-dispersive x-ray analysis of surfaces with the scanning electron microscope, developed during the 1960s.

Another important x-ray technique is x-ray photoelectron spectroscopy (XPS or ESCA), developed in the late 1960s by Siegbahn. Analytical applications were greatly stimulated by the publication of a monograph in 1967 and by the introduction of commercial instrumentation in 1970. More recently, the trend has been to incorporate ESCA measurements with other ultrahigh vacuum spectroscopy techniques involving a number of different excitations (photon, ion, or electron) and various types of signal (photon, ion, or electron). Although these are primarily surface techniques where the local concentration is not necessarily at the trace level, the extreme sensitivity of the techniques suggests their inclusion in any discussion of trace analysis. Ion etching of the surface permits probing of composition into the third dimension.

From these historical examples it is clear that long delays often occurred between the discovery of a trace method and its practical application. Several reasons for these delays can be found in retrospect. Sometimes, as in the case of amperometric titrations and voltammetry, the theory was ill-understood at the time of the original discovery. In other cases, e.g., gas chromatography, the seminal publication did not reach the proper readership for a long time. In still other cases, as in chronopotentiometry, the basic theory was well known but the measurements could not be put to practice because of the lack of instrumentation. Another factor was that certain types of measurements required special materials for their exploitation, as in the case of thermometric measurements which were facilitated by the development of the thermistor. Finally a need must exist before widespread use of a method will occur. Oftentimes more than one of these factors came into play, as in the case of atomic emission spectroscopy.

If we look at trace analytical methods as a group, we find a parallelism during the past 50 years regardless of the early history. In the first place there was not a great emphasis on quantitative applications of trace methods until the need arose, so many fundamental findings tended to lie stagnant until about 1940. Secondly, instrumentation was relatively primitive until the 1930s when electronics began to play a significant role. Electronic instrumentation was to undergo two major leaps ahead, first the change from vacuum tube to solid state electronics, and second with the emergence of the microcomputer, which became small enough and inexpensive enough to become an integral part of the measurement system. The availability of commercial instrumentation has also been an important factor in the use of a particular approach.

It may also be relevant to consider the reasons for the popularity of certain trace methods in relation to others. Among the factors that determine which method is to be used for a given problem (given that the sensitivity is adequate) are the following:

A. Type of sample. Solid samples may be analyzed directly by some methods but require dissolution for others. The dissolution process may be so time consuming as to rule against the use of some methods. Similarly, gaseous samples and liquid samples may be directly analyzed by some methods but require conversion in others.

B. Homogeneity of samples. Some methods inherently examine extremely small samples, and therefore are more susceptible to sampling errors if the average composition is sought. Conversely, if distribution is to be studied, a method of sufficient spatial resolution is required.

C. Cost of equipment. Some methods require enormous capital investments, which may or may not be justified by the nature of the problem.

D. Cost of personnel. Some methods are easily converted to a routine procedure that gives reliable results in the hands of a technician trained specifically for that procedure, while other methods inherently involve adjustments depending on the sample and therefore need personnel of greater training. This factor is important, for example in the relatively great usage of spectroscopic methods for trace metal determination as compared with electrochemical methods, which involve much lower investments in capital equipment.

E. Type of information needed. If just elemental composition is required, it is better to use a method insensitive to the chemical state of the elements. By the same token, such a method will not give information as to the chemical state, if that information is required. Neutron activation analysis is a good example of a method insensitive to chemical state, while electrochemical methods do respond to chemical state, and therefore provide information of this type.

F. Speed. Some problems require rapid response, and therefore require a method of appropriate speed. Continuous analysis of a flowing stream represents a problem requiring a rapid response time.

G. Dynamic range. Some methods will respond to samples ranging widely in composition, while others need a prior adjustment by dilution or concentration to bring samples into their dynamic range.

H. Selectivity. Some methods are subject to numerous interferences unless provision is made for prior separations. Nevertheless, if the interferences are known to be absent, such a method may find uses in special situations.

I. Number of samples to be analyzed. The analysis of a single sample may lead to a different choice of method than the analysis of a series of samples. Furthermore, the chosen method may be different in different laboratories depending on the available equipment and personnel.

It has been my purpose to discuss the origins of a variety of trace analytical methods and to examine the reasons for the sometimes halting nature of their development into modern form. It would also

be proper to consider recent trends, which are a useful guide to future expectations, and to make a critical comparison of the various trace analytical methods. However, there are to be two talks on the present day status of trace analysis, so these topics are better left for my colleagues.

References

[1] Hillebrand, W. F., "Analysis of Silicate and Carbonate Rocks," Bull. 700, U.S. Geological Survey, 1919.
[2] Sandell, E. B., "Colorimetric Determination of Traces of Metals," Interscience, NY, 1944.
[3] Morrison, G. H., Ed., "Trace Analysis, Physical Methods," Interscience, NY, 1965.
[4] Szabadvary, F., and Robinson, A., in "Comprehensive Analytical Chemistry," Suehla, G., Ed., Volume X, Elsevier, Amsterdam, 1980, p. 65.
[5] For references, see Szabadvary and Robinson, op. cit.
[6] Kirchhoff, G., and Bunsen, R., Pogg. Ann. **109**, 160 (1860).
[7] Laitinen, H. A., and Ewing, G. W., Eds., "A History of Analytical Chemistry," Division of Analytical Chemistry, ACS, 1977.
[8] O'Haver, T. C., J. Chem. Educ. **55**, 423 (1978).
[9] Brewster, D., Trans. Roy. Soc. Edinburgh **12**, 538 (1833).
[10] Göpelsroder, F., J. Prakt. Chem. **101**, 408 (1867).
[11] Harvey, E. N., "A History of Luminescence," Am. Philosophical Soc., Philadelphia, 1957.
[12] Nernst, W., Z. Phys. Chem. **4**, 129 (1889).
[13] Kolthoff, I. M., Anal. Chem. **45**, 24A (1973).
[14] Salomon, E., Z. Phys. Chem. **24**, 55 (1897).
[15] Nernst, W., and Merriam, E. W., Z. Phys. Chem. **53**, 235 (1905).
[16] Sörensen, S. P. L., Biochem. Z. **21**, 131, 201 (1909).
[17] Haber, F., and Klemensiewicz, Z. Phys. Chem. **67**, 385 (1909).
[18] Heyrovsky, J., Chem. Listy **16**, 256 (1922).
[19] Kolthoff, I. M., and Lingane, J. J., Chem. Rev. **24**, 1 (1939).
[20] Haber, F., Angew. Chem. **40**, 303 (1927).
[21] Jette, E., and West, W., Proc. Roy. Soc. (London) **A21**, 299 (1928).
[22] Cohen, F. H., Rec. Trav. Chim. **54**, 133 (1935).
[23] Belcher, R., Bogdanski, S., and Townshend, A., Talanta **19**, 1049 (1972).
[24] Sandell, E. B., and Kolthoff, I. M., J. Amer. Chem. Soc. **56**, 1426 (1934).
[25] Szebelledy, L., and Somogyi, Z., Z. Anal. Chem. **112**, 313 (1938).
[26] Hickling, A., Trans. Faraday Soc. **38**, 27 (1942).
[27] Lingane, J. J., J. Amer. Chem. Soc. **67**, 1916 (1945).
[28] Boyd, G. E., et al., J. Chem. Soc. **69**, 2849 (1947).
[29] Spedding, F. H., et al., J. Amer. Chem. Soc. **69**, 2777 (1947).
[30] Horovitz, K., Z. Phys. **15**, 369 (1923).
[31] Eisenman, G., Rudin, D. O., and Casby, J. U., Science **126**, 871 (1957).
[32] Trümpler, G., Z. Phys. Chem. **99**, 9 (1921).
[33] Tendeloo, H. J. C., J. Biol. Chem. **113**, 333 (1936).
[34] Kolthoff, I. M., and Sanders, H. L., J. Amer. Chem. Soc. **59**, 416 (1937).
[35] Pungor, E., and Hollos-Rokosinyi, E., Acta Chim. Hung. **27**, 63 (1961).
[36] Frant, M. S., and Ross, J. W., Jr., Science **154**, 1553 (1966).
[37] Beutner, R., "Physical Chemistry of Living Tissues and Life Processes," Williams and Wilkins, Baltimore, 1933.
[38] Ross, J. W., Science **156**, 1378 (1967).
[39] Severinghaus, J. W., and Bradley, A. F., J. Appl. Physiol. **13**, 515 (1958).
[40] Guilbault, G., and Montalvo, J., J. Amer. Chem. Soc. **92**, 2533 (1970).
[41] Rechnitz, G. A., Anal. Chem. **54**, 1194A (1982).
[42] Clark, L. C., Trans. Amer. Soc., Artificial Internal Organs **2**, 41 (1956).
[43] Ilkovic, D., Coll. Czech. Chem. Comm. **6**, 498 (1934).
[44] Koutecky, J., Chem. Listy **47**, 323 (1953).
[45] Sand, H. J. S., Phil. Mag. **1**, 45 (1901).
[46] Gierst, L., and Juliard, A., J. Phys. Chem. **57**, 701 (1953).
[47] Barker, G. C., and Gardner, A. W., Z. Anal. Chem. **175**, 79 (1960).
[48] Parry, E. P., and Osteryoung, R. W., Anal. Chem. **36**, 1366 (1964).
[49] Vali, V., and Shorthill, R. W., Appl. Opt. **15**, 1099 (1976).
[50] Hirschfeld, T., Deaton, T., Milanovich, F., and Klainer, S., Opt. Eng. **22**, 527 (1983).
[51] Wehry, E. L., Anal. Chem. **58**, 13R (1986).
[52] Hugget, A. St. G., and Nixon, D. A., Biochem. J. **66**, 12P (1957).
[53] Malmstadt, H. V., and Hicks, G. P., Anal. Chem. **32**, 394 (1960).
[54] Clark, K. C., and Lyons, C., Ann. N.Y. Acad. Sci. **102**, 29 (1962).
[55] Kolthoff, I. M., and O'Brien, A. S., J. Chem. Phys. **7**, 401 (1939).
[56] Martin, A. J. P., and Synge, R. L. M., Biochem. J. **35**, 1358 (1941).
[57] James, A. T., and Martin, A. J. P., Biochem. J. **50**, 679 (1952); Analyst **77**, 915 (1952).
[58] Small, H., and Stevens, T. S., Anal. Chem. **47**, 1801 (1975).

Volume 93, Number 3, May–June 1988
Journal of Research of the National Bureau of Standards

Accuracy in Trace Analysis

Trace Analysis by Degrees: An Academic Perspective

George H. Morrison

Baker Laboratory of Chemistry
Cornell University
Ithaca, NY 14853

The increasing awareness of the important role of very small amounts of chemical species in chemical, physical, and biological systems has greatly stimulated the refinement and extension of analyses at these levels. The analytical requirements imposed by the minute quantities and typically complex systems involved has led to the development of methodology and instrumentation so specialized as to warrant consideration as a distinct field of analytical chemistry—trace analysis. One of the aims of this symposium is to gain an accurate assessment of the current state of this field, and this paper is an attempt to present this status from an academic perspective.

In order to discuss any specialty in analytical chemistry as carried on in colleges and universities, it is necessary to first review the current status of the whole discipline. It must be stated that the main missions of universities are teaching and research, and chemistry, one of the basic sciences, is an essential discipline in most colleges and universities. How does analytical chemistry fare in academe? A review of the American Chemical Society Directory of Graduate Research lists faculties, publications and theses in chemistry and other related disciplines at universities in the United States and Canada. A review of the 1985 edition, the latest available, reveals that of the 315 chemistry departments listed, 201 include analytical chemistry with 510 analytical faculty members. It is obvious that these departments cover a wide range of sizes, so that some of the smaller institutions are less structured. Of these 201 departments, 80 have at least three or more analytical chemistry faculty members. What becomes quite apparent from a review of the data is that while analytical chemistry is not formally included in every department, there are a significant number of strong analytical departments in the United States and Canada to advance the science adequately. In this environment we can now turn our attention to trace analysis.

With regard to trace analysis research, two major approaches are evident: development of new techniques and methodology, and application to important problems. Because the field of trace analysis is so broad, I have chosen to limit my evaluation to trace element analysis, the area of my expertise. This specialty can be conveniently divided into three categories: bulk analysis, spatially resolved analysis, and speciation. In the area of applications, trace analytical research is being pursued by a good number of faculty to solve important biomedical, environmental, solid state materials, and geochemical problems.

Among the techniques currently being employed for bulk trace analysis, electroanalytical, atomic spectroscopy, x-ray fluorescence, activation analysis, and mass spectrometry are the most advanced and most used. A review of bulk trace techniques over the past 40 years indicates continuous progress in each of these categories. See figure 1. Thus, each of these techniques has continuously been used and kept viable with novel research advances. The current exciting areas in each of these categories include modified electrodes, inductively coupled plasma spectroscopy (ICP), proton induced x-ray emission spectroscopy (PIXE), charged particle and prompt gamma activation analyses, and ICP-mass spectroscopy.

While there will always be a need for more sensitive bulk trace methods of broad scope, there has been increased interest in recent years in localization of elements in solid samples. These spatially resolved methods of trace analysis can establish the distribution of many elements with spatial resolutions at the micrometer level or better. Table 1 lists

some of the more popular methods, their resolution and sensitivity. Included are electron probe microanalysis (EPMA), scanning Auger microscopy (SAM), secondary ion mass spectrometry (SIMS), laser microprobe mass analysis (LAMMA) and proton induced x-ray emission spectroscopy (PIXE). The object of these spatially resolved methods is to correlate elemental concentration with morphology to explain the properties of various heterogeneous samples in solid state, metallurgical, biological, geological, etc. problems.

Table 1. Spatially resolved methods in trace element analysis

Method	Resolution	Sensitivity[a]
EPMA	0.01 – 1 μm	ppth
SAM	0.05 – 0.5 μm	ppth
SIMS	0.1 – 0.5 μm	ppth–ppm
LAMMA	0.5 – 1 μm	ppm
PIXE	500 – 2500 μm	ppm–ppb

[a] ppth—parts per thousand; ppm—parts per million; ppb—parts per billion.

One of the more powerful spatially resolved methods, SIMS or ion microscopy, can determine the distribution of all elements at the ppm level or better. Both stigmatic and scanning ion microscopes are being used with spatial resolutions of 50–100 nm. Of particular importance is the use of the technique for subcellular elemental mapping of tissue sections and cultured cells to solve physiological, pathological, and toxicological problems in biology and medicine.

The third category in trace element analysis is the study of the speciation of an element, i.e., the determination of the various individual physicochemical forms. This is of great interest, especially in environmental analysis, because the toxicity of an element depends on its chemical form. Similarly in biology and medicine, elements such as chromium can be associated with several diseases while in the Cr(VI) state, however, Cr(III) is relatively non-toxic. Thus, elements can be present in many forms in samples, including the zerovalent metal, the free ion, an organometallic complex or a chelate. These different chemical forms of an element greatly influence its toxicity, bioavailability, bioaccumulation, and transport. Unfortunately, very little has been done to date in the area of speciation analysis. What has been done involves the use of a variety of separation and concentration techniques followed by the use of one of a number of detection methods. As can be appreciated, the use of these wet chemical methods requires great care to ensure the preservation of the chemical form of the species during the analysis. Some physical techniques can provide information on the chemical state of elemental species in solids. They include x-ray photoelectron spectroscopy (XPS), Auger electron spectroscopy (AES including SAM), and x-ray absorption fine structure spectroscopy (EXAFS). Current trends in trace element analysis include preconcentration methodology, multi-element methods, hybrid methods, and single atom detection.

Thus, the field of trace element analysis has continued to grow vigorously over the years with the advent of new and more sophisticated instrumentation and the increasingly more demanding needs for complete characterization of complex systems in science and technology. The colleges and universities have contributed significantly to this advancement through both fundamental research and in educating generations of students who have continued to work in this exciting field in university, industrial, and government laboratories.

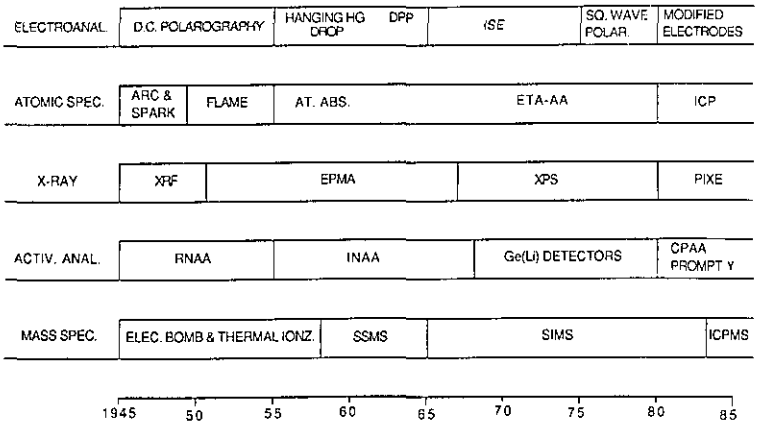

Figure 1. Progress in trace element analysis.

Volume 93, Number 3, May–June 1988
Journal of Research of the National Bureau of Standards

Accuracy in Trace Analysis

The Importance of Quantitative Trace Analysis in Industry Today

Bernard J. Bulkin

Director, Analytical Sciences Laboratory
BP America Research & Development
Cleveland, OH 44128

Trace analysis in the industrial analytical laboratory represents a substantial portion of the overall lab workload. This paper will explore some of the kinds of analyses that are done, why they are done, and what the limitations are to our current capabilities.

"Industry" represents the full diversity of analytical problems, and even within one company, such as BP America, important trace quantitation problems can arise from petroleum products, ceramics, minerals, biological materials, chemicals, catalysts, and, of course, environmental samples relating to all of these. It would be impossible to review all of the trace analytical methods used for such a diverse set of samples, to compare relative merits, or to in any way survey the field of trace analysis in industry. Rather, this paper looks at certain major themes that are driving the entire area, overlapping many techniques in each case.

For all of the diversity of quantitative industrial trace analysis, three motivational themes seem to dominate: samples where the trace quantity provides the value to a product; samples where trace species degrade the value of a product; and, samples where trace species represent a potential hazard to human, animal or plant life. In suggesting these categories, and in the subsequent discussion, I am removing from the realm of trace analysis problems in which the analyte is in high concentration but small quantity. For some techniques these may present the same problem as low concentration trace analysis, but increasingly, we find that instrumentation has evolved considerably in the ability to handle small samples.

The first category, trace quantities as key to product value, is probably most noticeable in importance today for the electronics industry. While classical chemistry recognized the importance of certain trace elements or compounds, it was the electronics industry, beginning in the earliest days of the transistor and continuing to the present, that turned this into a picoscience.

Examples in other aspects of chemistry and materials science abound. Modern heterogeneous catalysts have derived selectivity and activity from trace elements. Metallurgists, ceramists, and polymer scientists can bring about significant improvements in material properties by adding trace quantities of appropriate substances.

The analytical challenge here has been considerable. In many cases we are asked to analyze very low levels, with a high degree of quantitation, and on solid phases. It is the latter point that probably has provided the greatest challenges and the most innovative solutions. The triumphs of SIMS, an industrial innovation, despite its being a destructive technique, are to be particularly noted in this field. Many advances have also come from Fourier transform techniques, in NMR, IR, and mass spectrometry. Even in such well developed areas as atomic spectroscopy, the introduction of low temperature plasma ashing and acid digestion using sealed Teflon vessels has permitted dissolution of solids with almost no loss or contamination.

There still remains much to be done. While SIMS provides some depth profiling, we continue to be challenged by deep interfaces. These are of great importance, but analytical methodology for reaching and analyzing them is decades behind our ability to deal with surfaces.

The second area is also a well established problem in the electronics industry, but pervades much of the rest of chemistry. While some trace elements provide catalyst selectivity, others are potent catalyst poisons. Relatively low levels of metals in coke (iron, nickel, vanadium) result in substantial drops

in selling price. We see cases of all sorts where it is necessary to find analytical methods that will aid in anticipating the trace levels that will degrade quality of a product.

In many respects, the analytical problems associated with this category are not distinct from those of the first group of samples. Once again, for example, we see the value of analytical techniques such as SIMS. Other techniques, well established years ago, are experiencing varying degrees of revival to meet the analytical challenges of difficult samples. Neutron activation analysis, particularly for refractory materials, is being increasingly used. In the electronics industry, the degree of natural radioactivity in materials is an important property, and analytical chemists are being called upon increasingly to revive what may be long dormant knowledge of radiochemical methods.

Laser analytical methods are also becoming far more important. There are, for example, electrodeposition processes that will concentrate the trace element in a plating bath from the ppb level to the ppm level in the final device. It is necessary to find methods that will analyze the bath, and even monitor the depletion kinetics of the trace elements. Laser methods often are suitable here.

And we should not forget tried and true electrochemical or wet methods. As will be discussed in more detail below, such methods are particularly amenable to being carried out with laboratory robots, leading to high quality results and low cost for repetitive analysis.

The third category probably represents a large, distinct sub-discipline of analyses—environmental trace analysis, that is best dealt with separately. There is, to be sure, a set of established methodologies here. Most are considered to be adequate in terms of sensitivity, although there is certainly considerable merit to many of the active research projects in developing new methodologies for trace analysis of environmentally important species.

What is a problem, and a major one, in environmental trace analysis, is the analytical reproducibility of the established methods. Even more important than standard deviations within a single laboratory running replicate samples is the interlaboratory variance. Several publications, mostly citing older studies, have already documented the extent of this problem. The problem is also made evident by looking at the standards for interlaboratory comparison of results in the actual regulations. The extent of the problem is confirmed by recent interlaboratory tests conducted by government or independent industry groups, and by our own evaluation of contract analytical laboratories.

One approach to attacking this problem is increased use of laboratory robotics in environmental trace analysis. The original motivation for the application of laboratory robots to this area was to reduce costs and sample turnaround time. These motivations are valid, and straightforward economic analysis demonstrates that laboratory robots have a rapid payback in environmental trace analysis.

However, the impact of the laboratory robot on improved quantitation may, in the end, be as important a reason for adopting this approach. Again, there are two aspects. First, the robot carries out all operations in a far more reproducible manner than can several different human analysts, and thus directly leads to better analytical results. This will be demonstrated with the specific example of purge-and-trap analysis of volatile organics. Second, even when the robot is not to be used for an analysis on a long term basis, it is a powerful tool for method development. Using a laboratory robot, it is possible to explore the parameter space of an analytical method rather quickly and systematically, to minimize imprecision and eliminate sources of variation/bias. The optimized method, even if ultimately performed by humans, then gives improved results.

Robots are also very amenable to improved quality control in environmental analysis. Automated blanks and spiking stations have been designed and applied to these analyses. But one can go beyond this, to eliminate the biases that appear to creep into QC, by having the robot carry out blanks, spiked samples, etc., on a random basis. This should greatly improve data quality.

We recognize that in most large companies, our field of endeavor is now best described as Analytical Sciences. There is a major role for chemistry, but also roles for materials science, physics, engineering, and statistics. We need a diverse set of skills, and an ongoing research effort to keep up with the problems generated by industrial products. It seems likely that in pursuing this research effort, trace analysis will be an ongoing theme for a long time to come.

Volume 93, Number 3, May-June 1988
Journal of Research of the National Bureau of Standards

Accuracy in Trace Analysis

The Role of Robotics in the Laboratory of the 80s

James N. Little

Zymark Corporation
Zymark Center
Hopkinton, MA 01748

A new technology, robotics, already being used in other fields, is slated to have a major impact in automating operations and procedures performed in chemistry laboratories during the eighties. Introduced only 5 years ago, it has become the fastest growing new technology for the laboratory. An introduction to laboratory robotics, which combines the technologies of chemistry, analytical instrumentation, computers and robotics, will be presented first.

Laboratory automation, once limited to computerized data reduction, can now include sample handling and sample preparation, wet chemistry procedures, and instrumental analysis.

Laboratory robots, utilizing programmable computers, can be easily reprogrammed to do a variety of laboratory procedures and thus, do not require a large quantity of identical, repetitive operations to justify the investment in capital and time.

Examples will be given in automated sample preparation for a variety of trace organic and inorganic analyses.

GC and HPLC applications represent 40% of the current installed base of 1000 laboratory robotic systems. Trace chromatographic assays require many steps (i.e., filtering, extraction, evaporation, etc.) and put tremendous strain on laboratory personnel to maintain acceptable precision levels. Laboratory robotics systems typically improve precision by a factor of 2 or 3 and maintain that precision over extended periods of time. Derivatization, which is routinely used in trace chromatographic analyses, can be easily automated with robotics and eliminates the analyst's exposure to highly reactive chemicals. Robotics systems can also perform analyses in a serialized mode versus a batch mode. Serialization allows each sample to have the same time history, important in derivatization experiments where possible side reactions can occur causing increased error. Serialization also increases the throughput of samples versus a batch mode.

Automation of wet digestion procedures for trace inorganic analyses has been accomplished using laboratory robotics. Manual procedures require constant attention by an experienced chemist while being exposed to corrosive chemicals and fumes.

Laboratory robotics is finding increased use in microbiological laboratories where a sterile environment must be maintained and care must be taken so that people do not contaminate the experiments.

To improve their utility in the laboratory, robotic systems often must "interface" with standard analytical instruments. This "interface" may include a mechanical handshake to put the sample into the instrument as well as an electronic interface. The electronic interface can be as simple as turning the instrument on and off to completely controlling all parameters on the front panel. Interfaces are available for GC, HPLC, UV/VIS, NMR, titrators, viscometers, computers, ICP, physical testing instruments, etc. Bar code reading systems can also be interfaced to robotic systems allowing sample identification and method selection to be automatically entered.

Laboratory robotics is having an impact on analytical methods, laboratory layout, staffing, type of staffing and work flow. This new level of automation, achieved with laboratory robotics, brings substantial gains in laboratory performance.

Volume 93, Number 3, May–June 1988
Journal of Research of the National Bureau of Standards

Accuracy in Trace Analysis

Chemometrics and Standards

L. A. Currie

Center for Analytical Chemistry
National Bureau of Standards
Gaithersburg, MD 20899

1. Introduction

Standards are central to the achievement and maintenance of accuracy in trace analysis. This fact is well-known and well-accepted in the international analytical chemical community, where "standards" are generally considered to be *Standard Reference Materials* (SRMs) or *Certified Reference Materials* (CRMs). The term, standards, however, is multivalued, as noted recently by a former Director of the National Bureau of Standards [1]. That is, even in our more conventional view of trace analysis, we must consider in addition to standard materials: standard procedures (protocols), standard data (reference data), standard units (SI), standard nomenclature, standard (certified) instruments, and standard tolerances (regulatory standards, specifications, norms) [2]. It is interesting, in light of these several types of "standards" which have some bearing on accuracy in trace analysis, to consider the possible significance of standards in and for Chemometrics.

To pursue this objective, we first must have a common understanding of the meaning of the term, chemometrics, and what significance it may have for accurate trace analysis. A concise definition is given by the subtitle of the volume which resulted from the first NATO Advanced Study Institute on Chemometrics, i.e., "Mathematics and Statistics in Chemistry" [3]. Implications for accuracy, especially accuracy in trace analysis, are immediately evident. That is, wherever mathematical or statistical operations contribute to the experimental design, data evaluation, assumption testing, or quality control for *accurate* chemical analysis, "chemometric standards" are at least implicitly relevant.

The major part of this paper will be devoted to an explicit discussion of such chemometric standards, including case studies drawn from recent research at the National Bureau of Standards. The discussion will be placed in the framework of the Analytical System, or Chemical Measurement Process (CMP), for such a perspective makes it possible to consider logically a "theory of analytical chemistry"; and certainly chemometrics is a very important part of such a theory [4,5]. To set the stage, the next section will include a brief view of the current content of Chemometrics, together with a summary of its history and literature. This article will conclude with a glimpse at the future of chemometrics, with special emphasis on means to achieve increased accuracy in our chemical measurements and increased understanding of the external (physical, biological, geochemical) systems which provide the driving forces for analytical chemistry.

2. A Brief History

The content of Chemometrics, as viewed by the "Working Party on Chemometrics" of the Union of Pure and Applied Chemistry (IUPAC), is given in table 1 [6]. Included in the second, major portion of the table are titles for some 30 chapters which comprise an overview document being prepared for IUPAC. Two points are evident from the list of titles: (1) the scope of chemometrics is very broad indeed, encompassing significant portions of applied mathematics; (2) as implied by the name, major emphasis is given to measurement, specifically chemical measurement. In a narrower sense, chemometrics is sometimes viewed as the intersection of statistics and analytical chemistry, as seen by the emphasis on experimental design, control, and the analysis of signals and analytical data. The several chapters on signal and data analysis include such topics as filtering, deconvolution, time series analysis, exploratory data analysis, clustering, pattern recognition, factor analysis, and (multivariate)

regression. Standards and analytical accuracy have special relevance to the chapters on terminology, precision and accuracy, performance characteristics, calibration, analysis, and quality control.

Table 1. What is chemometrics?

1. NATO Advanced Study Institute (1983) "Chemometrics: Mathematics and Statistics in Chemistry"	
2. IUPAC—Working Group on Chemometrics (1987)	
Scope	
Producing Chem. Information	Notation & Terminology
Precision & Accuracy: intralab, interlab	
Calibration: univariate, multivariate	Relating Chemical & Non-Chemical Data
Information Theory	Performance Characteristics
Optimization & Exptl. Design: sequential, simultaneous	
Signal Analysis: 4 chapters	Data Analysis: 8 chapters
Expert Systems: custom made, knowledge engineering tools	
Operations Research	Graph Theory
	Robotics
Computational Techniques (future strategies)	
Chemical Image Analysis	Sampling Strategies
Quality Control	Systems Theory

A brief, chronological history of chemometrics is presented in table 2. To convey information on both the history and the literature of this discipline, we have indicated milestones in the form of selected references, to the extent possible. Impressive, recent growth is seen by the fact that the first two textbooks and the first two journals, specifically devoted to chemometrics, were published within the last 2 years. Looking to the beginning of this history (bottom of table 2), we find the name of Jack Youden, certainly one of the earliest and most notable chemometricians, whose excellent guide to chemometrics was published some 20 years prior to the invention of the term. (Youden, incidentally, was a *proper* chemometrician, in that he began his career as a chemist, and then went on to become a distinguished statistician.) The journal *Analytical Chemistry* has long served chemometrics well, through its biennial fundamental reviews of the subject, starting well before the term was known. As indicated in table 2, the term "chemometrics" was conceived by Svante Wold, in January 1971. The reader's attention is called to the interesting paragraph by Wold, in reference [7], which details the beginnings of chemometrics, including the start of the Chemometrics Society by Wold and Kowalski, in Seattle on 10 June 1974. The intervening decade, culminating in the forementioned NATO Advanced Study Institute, saw rapid growth in chemometrics education and research, much of it promulgated by the Chemometrics Society and published in journals such as *Analytical Chemistry* and *Analytical Chimica Acta*. Also, there appeared several notable texts which were largely chemometric in content, if not in title [8–13].

Table 2. A brief history

IUPAC (1987):	Report on Chemometrics (D.L. Massart, M. Otto)
Two textbooks:	"Chemometrics: a textbook" (1987, Elsevier) (Massart, Vandeginste, Deming, Michotte, Kaufman)
	"Chemometrics" (1986, Wiley) (Sharaf, Illman, Kowalski)
Two Journals:	Journal of Chemometrics (Jan. 1987) (Ed. Kowalski, Wiley)
	Chemometrics and Intelligent Laboratory Systems (Nov. 1986) (Ed. Massart; Elsevier)
Chemometrics Conference:	(NBS, May 1985)—dedicated to W. J. Youden (Spiegleman, Sacks, Watters; NBS J. Research 90 [6])
NATO Advanced Study Institute on Chemometrics:	*(Cosenza, Sept. 1983)* (Kowalski)
"Chemometrics: Theory and Application" (1977)	(Ed. Kowalski; ACS Sympos 52)
Chemometrics Society founded (Seattle, 1974) (S. Wold, B. Kowalski)	
CONCEPTION—S. Wold (1971) (J. Chemometrics, V.1, No. 1, p. 1, Jan. 1987)	
Analytical Chemistry (ACS), Reviews on statistics . . . mathematics . . . chemometrics (even years)	
W. J. Youden, "Statistical Methods for Chemists" (1951, Wiley)	

To complete this brief look at the content, history and literature of chemometrics, it is fitting to refer to the Chemometrics Conference held at NBS just 3 years ago. It was a special meeting in many respects, for it epitomized the interdisciplinary nature and increasing scope of chemometrics; and it was "probably the first (such meeting) in the United States by that title" [14]. The meeting was jointly planned by an interdisciplinary team, consisting of a chemist and two statisticians. It was jointly sponsored by two national chemical and two national mathematical societies. Finally, it contained an extremely effective and balanced blend of experts from the two disciplines: mathematicians (and statisticians) providing critiques of chemometrics presentations by chemists, and chemists providing critiques of the presentations by mathematicians. The synergism resulting from this approach is evident from examining the proceedings [14]. It is appropriate to conclude with reference to this volume, for it was dedicated to W. J. Youden, our first chemometrician in table 2.

3. Chemometric Standards and the Analytical System

3.1 Standards

The agenda for chemometrics, from the perspective of standards, is outlined in table 3. First, we must deal with the issue of nomenclature. Because of the relatively recent formal emergence of chemometrics, and because of its interdisciplinary character, this is a very important matter for our early attention. Nomenclature, in this context, refers to much more than terminology. That is, it includes basic meaning and explicit formulation of concepts falling within the scope of mathematics and chemistry. The efforts of IUPAC, both in the Commission on Analytical Nomenclature [15] and as outlined in table 1 [6], will be extremely helpful in this fundamental task for chemometrics—to assure that chemists and mathematicians "speak the same language" where that language maintains as much self consistency as possible with the slightly diverse languages of the separate disciplines. (To some extent, we shall have to accept a bilingual dictionary. For example, "efficiency," "consistency," and "sample," have somewhat different implications in statistics and analytical chemistry.)

Table 3. Chemometric standards

Nomenclature (terminology, concepts, formulation)
Standards for accuracy (entire chemical measurement process)
detection, identification, estimation, uncertainties, assumptions
evaluation of chemometric techniques, software, algorithms
validation through "standard" data; interlaboratory exercises
design to meet external needs for adequate, accurate chemical information
Advance the state of the art; stimulate multidisciplinary cooperation

Supporting standards for accuracy, for the entire Chemical Measurement Process, is perhaps our most important task. The primary components are indicated under the second heading in table 3. Most important is a rigorous approach to the specification and evaluation of the fundamental characteristics of analytical methods and analytical results, such as detection, identification, and quantification (estimates and uncertainties). A combination of chemical knowledge (or "chemical intuition") and statistical expertise in this effort is the best means to assure validity and control through the specification and testing of assumptions. A second level of control which represents a special responsibility for chemometrics is the production and evaluation of quality software and algorithms—a responsibility which is being met in both chemometrics journals. The logical extension of chemical software standards is found in chemometric validation, or Standard Test Data (STD), designed to guarantee quality for the Evaluation step of the CMP. STD thus parallel SRMs for accuracy assurance in both intra- and interlaboratory environments [16]. It is worth emphasizing that with the enormous progress in laboratory automation, and the substitution of machine intelligence for human intelligence, quality control of the mathematical or chemometric phase of the CMP becomes ever more urgent. Direct instrument responses are increasingly unavailable for the expert scrutiny of the analyst, and automatic results are produced with little indication of the assumptions involved or numerical validity (and robustness to outliers) of the computational methods.

The last "standard" indicated in table 3 relates to design. Design of the sampling, measurement, and data evaluation steps of the CMP to meet specified needs, is really the *first* responsibility of chemometrics. A careful blend of statistical expertise and chemical knowledge once again is the best means for meeting the accuracy or information requirements of the CMP. Inadequate attention to design is perhaps the most serious fault in ordinary chemical analysis. Either inconclusive or inadequate chemical results are obtained, using the samples and methods at hand, or costs are needlessly high in obtaining the relevant information. This area constitutes one of the greatest opportunities for chemometrics for attaining requisite accuracy at minimal cost; appropriate methods include information and decision theory, statistical design and optimization techniques, and exploratory multivariate approaches such as pattern recognition and cluster analysis [3].

3.2 The Analytical System

A "systems perspective" for the CMP has been promulgated by a number of eminent analytical chemists over the past 2 decades. One of the earliest and most noteworthy efforts was made by the *Arbeitskreis "Automation in der Analyse"* beginning in the early 70s [4]. The systems and information theoretic view, which was pioneered by members of this circle, such as Gottschalk, Kaiser, and Malissa, is even more relevant today, and it offers perhaps the best model for an integrated chemometric approach to accuracy. Considering a simplified representation of the CMP or analytical system presented for this purpose in reference [16] (fig. 2), for example, it is clear that not only is there material flow through the system, in terms of sampling, sample preparation, and measurement, but there is also the flow of information, and unfortunately noise. Treating the CMP as an integrated system is essential for the optimal application (cost vs accuracy) of chemometric tools for design, control, calibration, and evaluation. Interfaces between the several steps of the CMP must be astutely matched to prevent information loss, and data evaluation and reporting techniques must be recognized as part of the overall measurement process, capable of preserving or distorting information just like the chemical and instrumental steps. The CMP or analytical system model can be especially helpful in planning for accuracy through appropriate points of introduction of SRMs and STD, and for explicit treatment of feedback, where initial results are utilized for improved, on-line redesign ("learning") of the CMP.

Extended discussion of the analytical system is beyond the scope of this paper, but its introduction is essential for a meaningful consideration of the relationship of chemometrics to accuracy and standards, as indicated above. The system view is obviously important for designing or investigating overall performance characteristics, such as the blank, recovery, specificity, and systematic and random error—through propagation techniques [17]. That is, if one wishes to achieve an overall precision, or detection limit, or identification capability, then the design of an optimal system must take into consideration the corresponding parameters for each step of the CMP, from sampling through data evaluation. *Such an integrated approach to design, with the help of chemometric techniques, is as relevant to the design of self-contained automated and intelligent analytical instruments, as it is to the design of an integrated analytical approach of an entire organization (such as* CAC*) to a broader analytical question, such as the selection and certification of Standard Reference Materials* [4,12].

3.3 Hypothesis Testing and the CMP

Fundamental questions to be addressed by measurement science can often be posed as hypotheses, to be tested or evaluated via analytical measurements. The formation of meaningful hypotheses or models of the external (environmental, biological) system is the business of expert scientists within that discipline. The testing of such hypotheses, through analytical measurements, is the business of expert analytical chemists. From this perspective it is clear that hypothesis testing captures the essence of the scientific method. It *must* therefore be a key feature of any "theory of Analytical Chemistry." This is especially important for chemometrics, for hypothesis testing forms one of the cornerstones of modern statistics. By capitalizing on the elegant statistical tools that have been developed for agricultural or biological testing, for example, we can generate an objective and optimal approach to the design of the CMP. That is, by combining excellent knowledge of chemistry with that of modern statistics, we can construct CMPs which are guaranteed to have sufficient (statistical) power to meet the specified analytical needs. In this respect, we shall be responding to a famous challenge by Kaiser [18], that analytical chemists learn to match optimally

the "space of analytical methods" with the "space of analytical problems."

Some of the ways in which hypothesis testing impacts analytical accuracy, in terms of the fundamental parameters of analytical chemistry, are presented in table 4. Figures 1 and 2 convey the elements of this theory together with its application to detection and univariate identification, respectively [19]. Further details cannot be presented here, but it should be noted that accuracy in trace analysis demands quantitative chemometric approaches to detection, identification, and quantification (uncertainty evaluation), plus model and assumption validation. Inadequate attention to this matter, and imperfect understanding of the fundamental (α, β errors) limitations of hypothesis testing, i.e., chemical measurement, continue to produce very erroneous conclusions regarding the results or power of our analytical techniques [19]. It is especially interesting and important to consider this in terms of the final, data evaluation step of the CMP, in view of the expanding use of "intelligent" and automated instrumentation, which generally includes "black box" data evaluation. Monitoring the accuracy of such internal algorithms is clearly one of the critical tasks of chemometrics in the near future, one for which Standard Test Data (STD) may play an important role. The need is exhibited in figure 3, where perfectly visible gamma ray peaks remain "undetected" by a widely used instrumental gamma ray analytical system [20].

Table 4. Analytical accuracy and hypothesis testing[a]

Hypothesis formation (external system model)
Design of the measurement process—external (x, l, t)
—internal (MP, EP)
Hypotheses to be tested:
model (simplest internal: $y=B+Ax+e_y$)
detection, discrimination (estimation)
no. of components (knowledge, "fit," constraints)
identification (informing variable; pattern)
error structure (stationary, white, cdf, variance, bias)
Some diagnostics—z, t, t', K-S, χ^2, $\chi^{2'}$, F, residual patterns, ...

[a] Symbol explanation: x, l, t=sampling species, location(s), time(s), MP, EP=measurement and evaluation steps of the CMP, t', $\chi^{2'}$=noncentral t and χ^2 statistics; K-S=Kolmogorov-Smirnov statistic.

Before leaving this survey of fundamentals, we must emphasize the importance of the first syllable. Chemometrics differs from statistics and mathematics in that chemical intuition or expertise forms an essential part of the activity. As mentioned above, hypothesis formation, which is necessarily the first step in designing a scientific experiment, requires disciplinary expertise. Accuracy in data evaluation or experiment control, for example, can only be expected when the chemometric techniques employed recognize the range of possible alternative hypotheses (models or assumptions). This is the crux of setting reliable bounds for systematic error, or in establishing "definitive" analytical methods. Empirical rules or heuristic techniques adapted to this purpose should be viewed with some caution. Examples of problems demanding chemical expertise for alternative hypotheses are identification, and the assessment of blank and matrix effects [17, 19 (ch. 16)]. In figure 2, for example, knowledge of the alternative was essential to compute the identification power of the test. In the more general case, where chemical species are identified on the basis of spectral or chromatographic patterns, we must know the locations and uncertainty characteristics of *all* "nearby" patterns to assess the identification power for a given null pattern, or to design a measurement process meeting prescribed identification capabilities. In moving from the universe of all possible neighboring spectral patterns, to the universe of possible interferences [21] or calibration models, for example, chemometrics faces a considerable challenge.

4. Selected Illustrations

To illustrate the relevance of chemometrics to the assurance of accuracy in trace analysis, we shall examine three recent and continuing investigations from our laboratory. The first has been selected as an example where quantitative hypothesis testing techniques have been applied to one of the fundamental elements of any analytical system: the noise. The second relates to an exploratory research study which seeks to relate patterns of laser microprobe mass spectra to sources of combustion particles ("soot") in the atmosphere. It illustrates the importance of *chemical* information (or "intuition") to maintain accuracy in the application of multivariate data analytical techniques. The third illustration speaks to the need for STD, both for monitoring accuracy in complex chemical data evaluation, and as a stimulus for research for improved chemometric techniques and understanding of the data evaluation process.

4.1 Counting Statistics—Are They Poisson?

The two fundamental model characteristics of analytical signals are the functional relation, connecting the expected value of the signal to the analyte concentration, and the error structure, as indicated in table 4. Accurate measurements and accurate assessment of method performance characteristics demand knowledge of both. In this section we describe an experiment designed to investigate the statistical properties and the causal characteristics of the noise component in counting experiments. Such experiments, where individual atoms, ions, or photons are counted, comprise some of the most sensitive in analytical measurement. In many such cases it is assumed that the limiting counting noise is Poisson in nature. Since the variance of the Poisson distribution is equal to the mean, such an assumption leads to a simple error (standard deviation) estimate, and error propagation techniques may then be used for estimating uncertainties for net signals and analyte concentrations.

The primary objective of our investigation of noise was to test the validity of the Poisson hypothesis for very low-level counting data, with special emphasis on background counts. The validity of the Poisson assumption has long been one of the more intriguing questions in nuclear physics and chemistry, and it has therefore been the subject of some notable experiments [22]. Our experimental system was uniquely designed to permit a much more stringent test of this hypothesis, as it provided individual arrival times for more than a million events. A second objective, if the Poisson assumption proves valid, is to provide a physical random number generator—a device operating by the laws of physics, to generate random numbers for use in numerical simulations, as an alternative to numerical pseudo-random numbers.

A practical objective for investigating the low-level counting noise distribution derives from our physical knowledge of the measurement system, i.e., our knowledge of potential alternative hypotheses. Perhaps the most important such alternative is the possibility of correlated events in the radiation detector, which could have a profound influence on the magnitude and variability of our background noise. As indicated in figure 4, the effective background is reduced by about a factor of 100 through anticoincidence shielding. If, due to wall or gas impurity effects, just 1% of the electronically canceled events were to produce a secondary, time delayed event in the central detector, the effective background would be doubled! Time series and distributional analysis of the background noise thus allows us to investigate this alternative process. Knowledge of the statistical power of the null (Poisson) hypothesis test against this particular alternative is therefore vital both for the construction of valid uncertainty intervals, and for understanding the basic physics and chemistry of the background events. One illustration of the distributional analysis is given in figure 5, where χ^2 is used to test deviations from the expected exponential distribution of time intervals between events. Further discussion of this investigation, including a tabulation of six alternative hypotheses, is given in reference [23]. Further investigation of sources of background noise is currently underway, using multivariate exploration of pulse shape characteristics.

4.2 Multivariate Exploratory Analysis: Origins of Atmospheric Soot Particles

Perhaps the best known applications of chemometrics involve multivariate techniques such as principal component analysis (PCA) and cluster analysis. Such techniques have reached a high degree of sophistication, as exploratory tools for the classification of samples which may be characterized by multivariable patterns or "spectra." An excellent introduction to the principles and methods of the "soft" or empirical multivariate modeling techniques is given in reference [24]. PCA and related techniques are especially useful for data exploration, in that they permit ready visualization of sample relationships, provided there are not too many independent components in the system under investigation. Thus, a collection of mixtures of two components having quite complex, yet different, spectra or chemical patterns, can be represented by a set of points in a plane, or on a line if the mixtures are normalized. If the pure components are represented, they appear as the end points. Two dimensional PCA plots thus allow us to display relations among mixtures of three normalized components; and three dimensions increases the display capability to four components. Beyond exploratory display capability, several methods of multivariate chemical analysis may be employed for quantitative estimates for the number and identity of components, and for the analysis of mixtures [25]. These are outgrowths of the seminal work of Lawton and Sylvestre [26].

The interplay between the multivariate display techniques and chemical "intuition" (experience, knowledge) is exhibited in our investigation of laser microprobe mass spectra (LAMMS) of individual soot particles formed from the combustion of wood and fossil fuel. The scientific basis for our interest in this problem derives from the potential health effects of combustion particles, which often carry mutagens, on the one hand, and the geochemical and climatic implications, on the other. The ability to infer combustion sources for individual soot particles could add greatly to our understanding of climatic perturbations and perhaps even such phenomena as the Tertiary-Cretaceous Extinction [27]. PCA data exploration was attractive for this study because the system was relatively simple in terms of intrinsic structure (two components), but relatively complex in terms of both the graphitic soot formation and laser plume ion formation processes. The work demonstrates an extremely important point with respect to accuracy, however. That is, the importance of having thoroughly reliable chemical information for validation of the exploratory techniques. This is shown in figure 6. The upper part of the figure shows the successful classification of wood vs hydrocarbon fuel soot particles on the basis of their positive ion laser microprobe mass spectra. Application of this model, which was developed for laboratory-generated particles, to soot particles collected in the field (urban atmosphere), however, would lead to erroneous conclusions (misclassification). The failed classification shown in the lower part of the figure was discovered through the use of an independent tracer of *known accuracy*, ^{14}C, for source discrimination [28]. Subsequent research on this very important basic and practical problem has led to some understanding of the reason for the difference between laboratory and field particles, a basic issue being sensitivity of certain species (features) to deviations from the two-source, linear model. This example illustrates one of the more important cautions in the use of multivariate techniques, such as PCA and factor (FA) analysis: namely, the influential character of outliers and departures from assumptions. Further investigation of the atmospheric particles has shown the utility and relative robustness of selected negative ion carbon clusters for combustion source discrimination, as shown in figure 7. Unlike PCA and FA approaches to exploratory multivariate data analysis, the coordinates of the "bi-plot" of figure 7 are *not perturbed by outliers*. Also, they are often more readily interpretable chemically than eigenvectors, though clearly they do not possess the dimension reduction efficiency of PCA.

4.3 Standard Test Data

A special task for chemometrics is guaranteeing the accuracy of the data evaluation phase of the chemical measurement process. An important element in the task is the development of representative, reference data sets having known characteristics, for testing the validity of data evaluation. Such "standard test data" (STD) thus play the same role for data evaluation that SRMs do for procedure evaluation. STD are likely to become increasingly important as the data evaluation step becomes more complex, and as it becomes less accessible to the user, as in automated analytical systems. The nature and importance of STD for assessing interlaboratory precision and accuracy have been well demonstrated by exercises based on univariate gamma ray spectral data created by the International Atomic Emergy Agency (IAEA) [29] and multivariate atmospheric data created by NBS [30]. The parallelism with SRMs has been further established for the former STD through incorporation into the catalog of the IAEA's Analytical Quality Control Service Program [31]. A brief description of the objectives and outcome of the multivariate STD exercise follows. (A more extended review of both exercises may be found in reference [16].)

The objective of the multivariate STD exercise was to evaluate the resolving power, and precision and accuracy of all major mathematical techniques employed for aerosol source apportionment, based on linear models incorporating chemical "fingerprints" or spectra. To adequately test these techniques, which comprised various forms of multivariate factor or regression analysis, it was necessary to generate data matrices which were realistic simulations of the variations in source mixes found in an urban airshed. Also important was a realistic injection of random errors characterizing pure source profiles as well as "measured" ambient samples. This was accomplished by means of the linear equation given below, where the S_{jt} were generated by applying a dispersion model incorporating real meteorological data to two urban (geographic) models. The STD generation scheme is illustrated for one of these urban models in figure 8.

Generating Equation

$$\tilde{C}_{it} = \sum^{P} [\tilde{A} - e_m - e_H]_{ij} S_{jt} + e_{it},$$

where: t = sampling period $[1 \leqslant t \leqslant 40]$
$\tilde{C}_{it}$ = "observed" concentration of species—i, period—t $[1 \leqslant i \leqslant N, N \leqslant 20]$
S_{jt} = true intensity (at receptor) of source—j $[1 \leqslant j \leqslant P, P \leqslant 13]$
$\tilde{A}_{ij}$ = "observed" source profile matrix (element—i,j)
e_i = random measurement errors, independent and normally distributed
e_m = systematic source profile errors, independent and normally distributed (systematic, because fixed over the 40 sampling periods)
e_H = random source profile variation errors, independent and log-normally distributed

The outcome of the exercise was instructive. Though results for the several techniques were generally correlated, and agreement with the "truth" was generally within a factor of two, some important differences and discrepancies were observed. For example, FA methods in contrast to weighted least squares estimation ("chemical mass balance") could not provide estimates for all components. They were limited to a collection of four or five component classes. Also, presumably identical methods, operating on strictly identical data resulted in differing component estimates as well as different standard error (SE) estimates. Comparing the actual distributions of residuals to the quoted SEs, we found the latter to vary from gross underestimates to gross overestimates. It was clear from this exercise that results depended heavily on "operator judgment," i.e., unique solutions could not be obtained without the use of certain, often implicit assumptions or decisions. It can be shown that problems of this sort, and in fact a large fraction of the multivariate problems in chemistry, are underdetermined or heavily dependent on assumptions. This is a challenge to chemometrics. Chemical knowledge combined with astute design should eliminate some of the inaccuracy connected with model selection, error treatment, and incautious use of criteria such as non-negativity.

Just as with SRMs, the above intercomparison was not the last word with this data set. Rather it has served as a test bed for additional and newly-developed methods of multivariate chemical data analysis [16], the most recent of which involves a new, more accurate representation of multivariate data by "parallel coordinate" systems [33]. In the future, we would expect STD to continue to serve the mutiple purposes of chemometric quality control for both conventional and automated analytical systems, assessment of interlaboratory or interalgorithmic accuracy, and as stimuli for chemometric research on complex, multicomponent systems.

5. Summary and Forecast

In conclusion, let us consider for a moment the matter of forecast, as viewed from two perspectives: (1) What may be forecast for the future of chemometrics in relation to standards and accuracy? (2) What directions are envisioned if we are to use chemometrics to improve our ability to understand and forecast the behavior of external systems, such as the environment? Key issues which comprise the answer to the *first question* are:

- Nomenclature, including rigorous terminology and formulation of the performance characteristics of the CMP, plus standard nomenclature for methods of CMP design, control and evaluation derived from applied mathematics.
- Optimal design of the overall analytical system to meet prescribed analytical needs and accuracy limits, utilizing detailed chemical knowledge of the characteristics of the individual CMP steps.
- Attention to the validity of the analytical model, both the functional relationship and the noise models; specification of hypotheses and tests having adequate power with respect chemically significant alternative hypotheses.
- Assessment of the accuracy of mathematical techniques as applied to chemical data, via algorithm or software evaluation, or overall data reduction evaluation using STD.
- Development of new methods of increased accuracy by iteratively linking CMP design, chemical separation, instrumental measurement and data evaluation, to reduce dependence on unverified assumptions, and to improve precision through interference reduction and application of expert knowledge.

The *second question* relates to the fact that data-based, empirical models cannot be relied upon to provide information beyond their immediate domain. That is, if we wish to be in a position to make

accurate forecasts, or even accurate interpolations, for a given system, *there is no substitute for a detailed mechanistic understanding* of the properties (model) of that system. It is in this area that chemometrics, and analytical chemistry, have their greatest promise for the future. This prospect is best viewed in terms of a pair of interacting systems. The first system represents the *raison d'être* or driving force for analytical chemistry; it is the external system which depends on chemical analyses for its elucidation or control. The second system is the analytical system or CMP. Chemometrics has long recognized the linkage between these two systems, but much of the work has been based on sampling and measurements designed to establish empirical patterns, or "soft modeling" [34].

Soft modeling, which might be viewed as an outgrowth of empirical, statistical modeling, is extremely important for exploratory studies, and for providing statistical descriptions of empirical relationships in complex chemical or biological systems. In contrast, "hard global models . . . have great advantages both in their far-reaching predictions and their interpretation in terms of fundamental quantities." And, unlike soft models, "the deviation between the hard model and the measured data must not be larger than the errors of measurement" (Wöld and Sjöstrom, pp. 243ff. [34]). Increased movement in chemometrics toward hard modeling is clearly attractive because of the potential for increased basic understanding and increased accuracy; it is realistic in view of the enormous advances during the last decade in sampling and measurement capabilities, and especially in computational capacity.

The transition toward more accurate representation of the external physical, chemical or biological systems which analytical chemistry must serve is outlined in table 5. To complement Wold's basic categories, we present the "musical" classification of Douglas Hofstadter [35], and the mechanistic model categories often used to describe biological or environmental systems [36]. Hofstadter's descriptors are apt. They convey succinctly the increasing sophistication of models ("analogies") in an area of enormous intrinsic complexity—artificial intelligence. The flow of models for the environmental system brings us immediately back to analytical chemistry and chemometrics. That is, the linear model, such as that described in section 4.3 is our simplest representation for an environmental system. Consistency and accuracy, governed by measurement error alone, cannot be generally expected with so simple a model. Improvements may be gained through: (1) combined chemometric techniques, such factor analysis followed by time series analysis, to explore the dynamics of the system [37]; and (2) "hybrid" modeling to take into account certain non-linearities such as homogeneous and heterogeneous reactions [38]. Major progress in understanding and monitoring an environmental system comes when natural "compartments" may be defined, with differential equations describing transfers between compartments [39]. When the compartmental description is inadequate, one must consider an even more detailed description of the system, generally by taking into consideration its full dynamic space-time character through the use of coupled equations representing transport and reaction [40]. These last two categories of modeling and measurement are important for assessing the potential impact of human activities on climate, in connection with the "CO_2" problem, and the coupled reactive system CO-OH-CH_4, respectively [41].

Table 5. The transition from empirical to mechanistic modeling

Model classes [empirical → mechanistic]		
S. Wold[a]	D. Hofstadter[b]	Environ. system
	"Muzak"	Linear[c]
"Soft"		↓ hybrid[d]
	"Jazz"	Compartment[e]
"Hard"		
	"Classical Music"	Full dynamic[f]

[a] See reference [34].
[b] See reference [35].
[c] Multivariate source apportionment (conservative tracers) [32].
[d] Particle—sulfate system apportionment [37,38].
[e] CO_2 system: troposphere-biosphere-ocean; biological systems [36,39].
[f] CO-OH-CH_4 system (production, transport, reaction) [40,41].

We face very important opportunities to gain increased fundamental knowledge of the nature (mechanistic models) and state of external (environmental, biological) systems through the use of hard, or at least harder, models to guide the sampling and measurement designs for these systems. By working closely with expert theoretical geochemists or biochemists, for example, chemometricians have the opportunity to design the analytical

measurement process to optimally test alternative external models, to better estimate their parameters, and to more accurately evaluate their present state and future course [42].

Acknowledgment

It is a pleasure to acknowledge coworkers G. Klouda, J. Tompkins, C. Spiegelman, and D. Walczak who participated in research described in section 4.1; R. Fletcher and G. Klouda, who participated in section 4.2 research; and R. Gerlach and C. Lewis, plus numerous receptor modelers, who participated in section 4.3 research. In addition, special thanks go to J. Winchester for his stimulating thoughts and questions regarding atmospheric chemistry and CMP design, during his recent sabbatical at NBS.

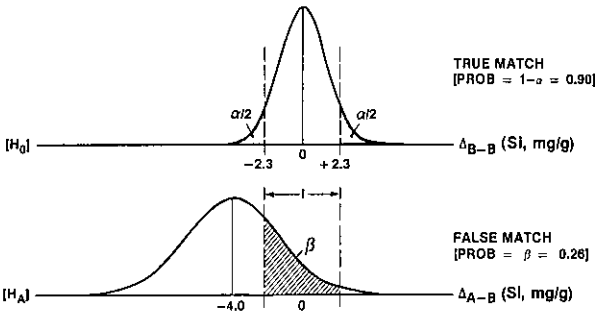

Figure 2. Hypothesis testing formulation for identification in analytical chemistry. Probability density functions are given for the difference in composition (*Si*) for particles emanating from the same source vs two different sources [19].

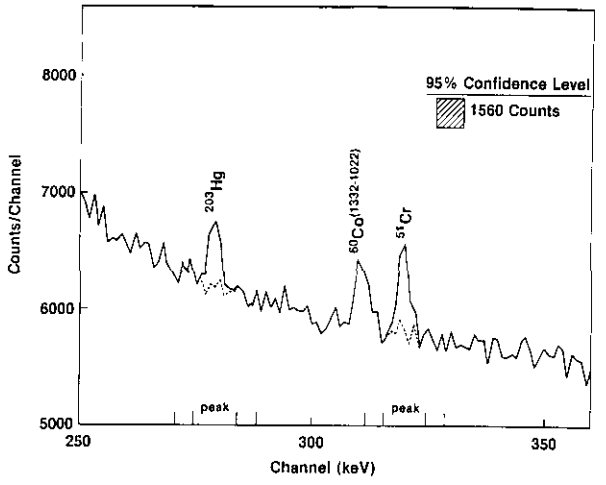

Figure 3. Clearly visible gamma ray peaks (^{203}Hg, ^{51}Cr), which were not detected above a ^{60}Co background in the IAEA practical examination of commercial software [20].

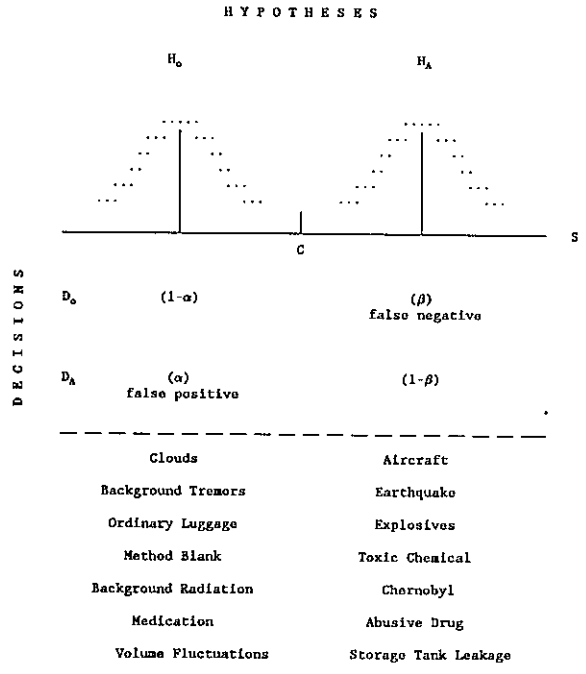

Figure 1. Hypothesis testing and societally important detection decisions. Sets of null (H_0) and alternate (H_A) hypotheses are listed below a Truth Table and stylized probability density functions [19].

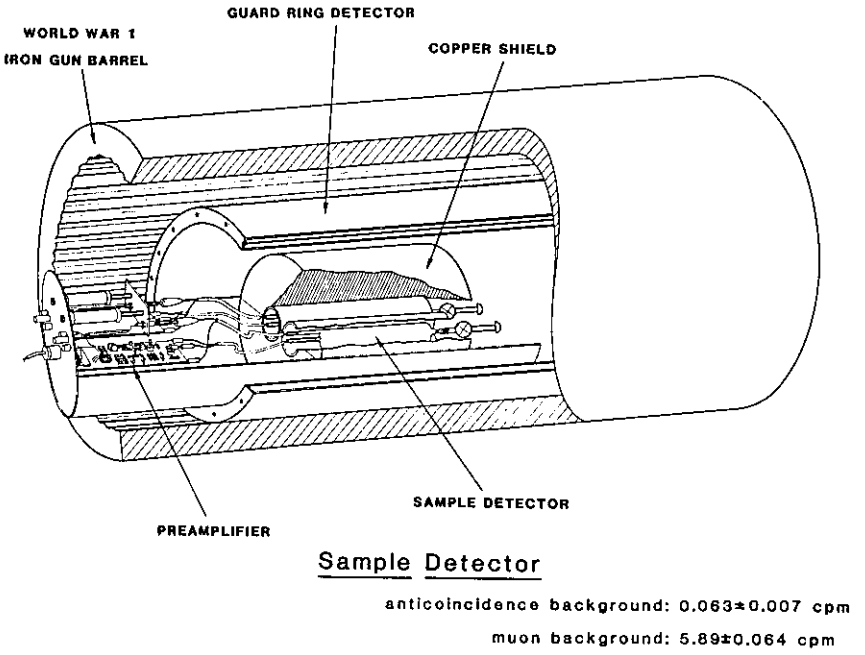

Figure 4. Low-level counting system. Penetrating cosmic rays (mu mesons) are removed as a background component of the sample detector by coincidence with the guard ring detector, reducing background by two orders of magnitude. (Uncertainties shown correspond to the Poisson standard deviations for a 24 hour counting period.)

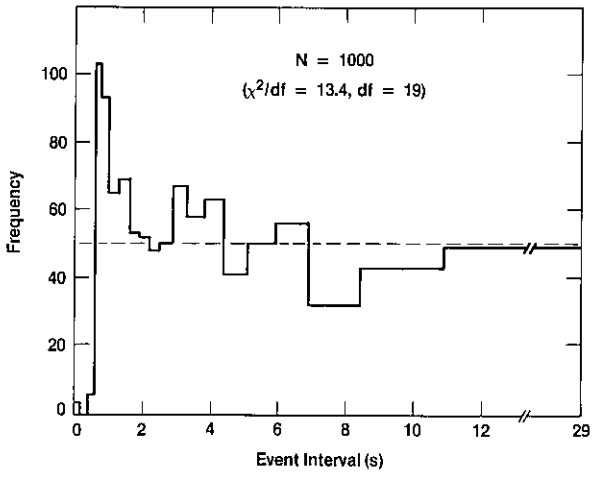

Figure 5. Chi-square test of the empirical equal probability histogram for low-level counting data [23].

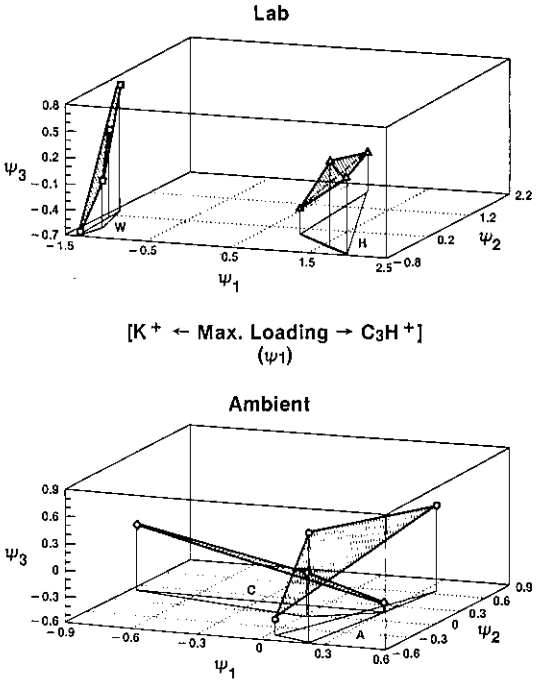

Figure 6. Isometric PCA projections of Lab and Ambient particle LAMMS positive ion spectra on the first three eigenvectors. Soot particles from wood are denoted "W" and "C"; those from hydrocarbon fuel are denoted "H" and "A." Feature (mass) selection on the basis of "characteristicity" preceded the principal component analysis [28].

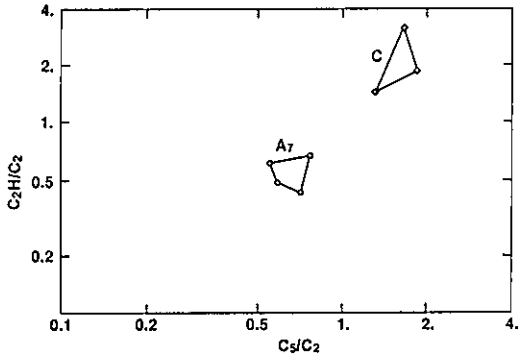

Figure 7. Bi-plot showing negative ion carbon cluster discrimination of LAMMS spectra from ambient atmospheric soot formed from the combustion of hydrocarbon fuel ["A"] and wood ["C"].

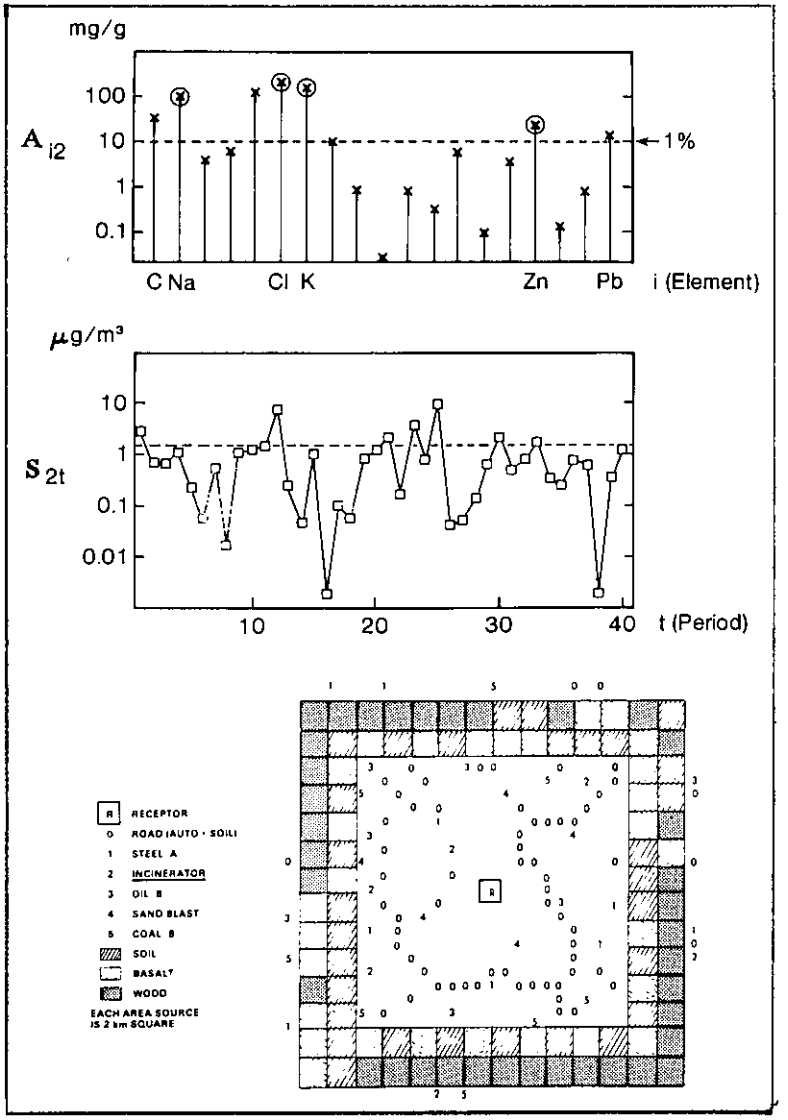

Figure 8. Source apportionment STD. A_{i2} represents the source profile vector for source-2 (incinerator); S_{2t} represents the source intensity time series for the same source. The lower portion of the figure shows the aerosol source emission map [16].

References

[1] Branscomb, L., Science and Technology in the Public Interest: the National Bureau of Standards in the Post-War Era, 1945-85, to be publ., the Johns Hopkins Press, S. W. Leslie and R. H. Kargon, Eds. (1988).
[2] Brady, E. L., and Edgerly, D., "International Technical Cooperation: A Case Study—the Treaty of the Meter and the International Organization for Legal Metrology," J. Wash. Acad. Sci. 77, 93 (1987). See also the International Vocabulary of Basic and General Terms in Metrology, International Organization for Standardization, Geneva (Metrologia, 1984).
[3] Kowalski, B. R., Ed. Chemometrics: Mathematics and Statistics in Chemistry, (Reidel Publishing Co.) 1984.
[4] Gottschalk G., and Marr, I. L., Talanta **20**, 811 (1973), Kaiser, H., Spectrochim. Acta **33B**, 551 (1978).
[5] Ramos, L. S., Beebe, K. R., Carey, W. P., Sanchez, M. E., Erickson, B. C., Wilson, B., Wangen, L. E., Kowalski, B. R., Anal. Chem. **58**, 294R (1986). [Review and bibliography].
[6] Otto, M., and Massart, D., Ed. Report on Chemometrics, IUPAC Working Party on Chemometrics (1988). See also: IUPAC news item in Chemom. and Intellig. Lab. Systems **1**, 6 (1986).
[7] Editorial, J. Chemom. **1**, 1 (1987).
[8] Massart, D. L., Dijkstra, A., and Kaufman, L., Evaluation and Optimization of Laboratory Methods and Analytical Procedures, New York, Elsevier, 1978.
[9] Eckschlager, K., and Štěpánek, V., Information Theory as Applied to Chemical Analysis, J. Wiley-Interscience, New York, 1979.
[10] Liteanu, C., and Rîcă, I., Statistical Theory and Methodologyof Trace Analysis. New York: John Wiley & Sons, 1980.
[11] Malinowski, E. R., and Howery, D. G., Factor Analysis in Chemistry, John Wiley & Sons, New York (1980).
[12] Kateman, G., and Pijpers, F. W., Quality Control in Analytical Chemistry, New York: John Wiley & Sons, 1981.
[13] Massart, D. L., and Kaufman, L., The Interpretation of Analytical Chemical Data by the Use of Cluster Analysis, John Wiley & Sons, Inc., New York, 1983.
[14] Spiegelman, C., Watters, R. L., Jr., and Sacks, J., Ed., Chemometrics Conference, J. Res. Natl. Bur. Stand. (U.S.) **90**, 391 (1985).
[15] IUPAC, Commission V.3, Compendium of Analytical Nomenclature (1978, 1986), Recommendations for Nomenclature in Evaluation of Analytical Methods, (1987, in review), Nomenclature of Sampling in Analytical Chemistry (1987, submitted for publication).
[16] Currie, L. A., J. Res. Natl. Bur. Stand. (U.S.) **90**, 409 (1985).
[17] Kelly, W. R., and Hotes, S. A., J. Res. Natl. Bur. Stand. (U.S.) **93**, 1 (1988). Parr R. M., IAEA Users' Guide on Limit of Detection, in preparation. (See also reference [15], and reference [19], chapter 9.)
[18] Kaiser, H., Anal. Chem. **42**, No. 2, 24A, **42**, No. 4, 26A (1970).
[19] Currie, L. A., Ed. Detection in Analytical Chemistry, Amer. Chem. Soc. Sympos. Ser. 361, (1988). Background for figures 1 and 2 is further discussed in chapter 1.
[20] Reichel, F. and Schelenz, R., Practical Estimation of the Limit of Detection in Gamma Spectrometry Using a Commercially Available Program, Chemistry Unit, IAEA Laboratories, 1985.
[21] Rogers, L. B., "Interlaboratory Aspects of Detection Limits Used for Regulatory/Control Purposes," chapter 5 in reference [19].
[22] Berkson, J., Intern. J. Appl. Rad. Isot. **26**, 543 (1975), Cannizzaro, F., Greco, G., Rizzo, S., and Sinagra, E., Intern. J. Appl. Rad. Isot. **29**, 649 (1978).
[23] Currie, L. A., "Chemometrics and Analytical Chemistry," in reference [3], p.115.
[24] Wold, S., Albano, C., Dunn, III, W. J., Edlund, U., Esbensen, K., Geladi, P., Hellberg, S., Johansson, E., Lindberg, W., and Sjöström, M., "Multivariate Data Analysis in Chemistry," in reference [3], pp. 17-96.
[25] Sharaf, M. A., and Kowalski, B. R., Anal. Chem. **54**, 1291 (1982), Windig, W., McClennen, W. H., and Meuzelaar, H. L. C., Chemom. Intell. Lab. Systems **1**, 151 (1987).
[26] Lawton, W. H., and Sylvestre, E. A., Technometrics **13**, 617 (1971).
[27] Wolbach, W., Lewis, R. S., and Anders, E., Science **230**, 167 (1985).
[28] Currie, L. A., Fletcher, R. A., and Klouda, G. A., Nucl. Instrum. Meth. **B29**, 346 (1987).
[29] Parr, R. M., Houtermans, H., and Schaerf, K., The IAEA Intercomparison of Methods for Processing Ge(Li) Gamma-Ray Spectra, "Computers in Activation Analysis and Gamma-Ray Spectroscopy," U.S. Dept. of Energy, Sympos. Ser. 49, 544 (1979).
[30] Currie, L. A., Gerlach, R. W., Lewis, C. W., Balfour, W. D., Cooper, J. A., Dattner, S. L., DeCesar, R. T., Gordon, G. E., Heisler, S. L., Hopke, R. K., Shah, J. J., Thurston, G. D., and Williamson, H. J., Atmospheric Environment **18**, 1517 (1984).
[31] International Atomic Energy Agency: "Analytical Quality Control Service Programme, Intercomparison Runs, Certified Reference Materials, Reference Materials" 1986-87.
[32] Stevens, R. K., and Pace, T. G., Atmos. Environ. **18**, 1499 (1984).
[33] Wegman, E. J., "A Parallel Coordinate Approach to Statistical Graphics," Computer Graphics Conference Proceedings, 3, 574-580 (National Computer Graphics Assoc., 1987).
[34] Wold, S., and Sjöström, M., "SIMCA: A Method for Analyzing Chemical Data in Terms of Similarity and Analogy," in Kowalski, B. R., Ed., Chemometrics: Theory and Application, Amer. Chem. Soc. Sympos. Ser. 52, 243 (1977). See also: Vogt, Nils, Chemom. Intell. Lab. Systems **1**, 213 (1987).
[35] Hofstadter, D. R., "Flexible Concepts and Creative Analogies: a Computer Model," lecture given at NASA-Goddard, Greenbelt, MD (May 1986). See also Hofstadter, D., Sci. Amer. **247**, 16 (July 1982), **249**, 14 (July 1983).
[36] World Meteorological Organization, The Physical Basis for Climate Modeling, GARP 16, WMO, Geneva (1975), International Commission on Radiological Protection, Report of the Task Group on Reference Man, ICRP Publ. No. 23 (Pergamon Press, London, 1975).
[37] Wang, M. X., Winchester, J. W., and Li, S. M., Nucl. Instrum. Meth. **B22**, 275 (1987).
[38] Lewis, C., and Stevens, R. K., Atmos. Environ. **19**, 917 (1985).
[39] Lai, T. L., J. Res. Natl. Bur. Stand. (U.S.) **90**, 525 (1985). Oeschger, H., Siegenthaler, U., Schotterer, U., and Gugelmann, A., Tellus **27**, 168 (1975).
[40] National Research Council, Global Tropospheric Chemistry, National Academy Press, Washington, 1985.
[41] Thompson, A. M., and Cicerone, R. J., J. Geophys. Res. **91**, 10853 (1986).
[42] A prototypical example of such a "chemometric" model evaluation plan is the NBS report to Congress: "An NBS Pilot Program in Model Evaluation Related to Climate Modeling and Atmospheric Heating by Carbon Dioxide" which was prepared by an interdisciplinary team of chemists, mathematicians, and physicists (1979).

Volume 93, Number 3, May–June 1988
Journal of Research of the National Bureau of Standards

Accuracy in Trace Analysis

Process Analytical Chemistry

Bruce R. Kowalski

Center for Process Analytical Chemistry
Department of Chemistry BG-10
University of Washington
Seattle, WA 98195

Chemical analysis can be thought of as a means to obtain chemical information on a chemical system or process. Traditionally, the system or process is sampled and the samples are transported to the analytical laboratory where analytical procedures and instruments are used to generate data which are then converted to chemical information by calibrated mathematical models. Unfortunately, this valuable information is not used or needed in the laboratory. Further, it is currently being recognized that sampling errors and time delays associated with sample transport and analysis make it nearly impossible to control complex chemical processes with the required degree of success. Traditionally, chemical engineers have relied predominantly on pressure, temperature, and flow sensors to monitor and control their processes. More recently, there have been increasing attempts to make laboratory instruments "process hardened" and move from "off-line" to "at-line" analysis. In addition, there has been a growing demand for the development of novel sensors to allow for true "on-line" analysis and control (and also the development of noninvasive sensors for some problematical process applications). Process Analytical Chemistry [1] seeks to create new sensors and analytical instruments that can be used as integral parts of a wide range of chemical processes for process monitoring and control.

The Center for Process Analytical Chemistry (CPAC) at the University of Washington was founded as a University/Industry Cooperative Research Center established by a grant from the National Science Foundation. CPAC serves as a focus for basic research in process analytical chemistry as well as a clearinghouse for information on analytical methods and a training ground for scientists and engineers skilled in on-line chemical processing, monitoring and control.

Trace analysis in process analytical chemistry has not received the same emphasis as it has, say, in environmental or health sciences. More often than not, process engineers would prefer to follow the concentrations of major reaction products for on-line control. This may be because new process analytical sensors and instrumentation capable of trace analysis have not met the severe tests required for use with process streams. CPAC researchers are working on new methods and applications designed to contribute to improved accuracy in trace, minor and major component analysis. Among these contributions are included chemometric methods for designing optimal arrays of sensors [2] and characterizing performance as they are developed [3]. The characterization of sensor arrays, based on the concept of net analyte signal [4], allows analytical chemists to estimate the sensitivity, signal to noise ratio, selectivity, and limits of determination for individual analytes. Using these statistics embedded in an expert system being assembled at CPAC, the analyst will be able to construct sensor arrays or select wavelengths that will meet the accuracy requirements for given analytes in a variety of sample matrices.

The use of nonselective arrays of sensors or multiple wavelengths is important for process analytical chemistry where the development of fully selective sensors is often too costly. For this reason, CPAC has supported work on new multivariate calibration [5] methods and has even provided a theoretical foundation for partial least squares [6], a method enjoying popularity in industrial applications. Previously, the use of these multivariate methods had the disadvantage that predicted analyte concentrations on real samples were not accompanied by confidence level estimates. This is because the three sources of error (calibration sensor responses, "known" concentrations, and sensor

responses from the unknown samples) combined in a very complex manner. In view of the importance of accuracy in process modelling and control, CPAC researchers have developed a method to estimate accurately the variance of concentrations predicted from multivariate calibration models that include all sources of error [7]. The method separates bias from precision and can therefore be used as an estimate of accuracy.

References

[1] Callis, J. B., Illman, D. L., and Kowalski, B. R., Process Analytical Chemistry, Anal. Chem. **59**, 624A (1987).
[2] Carey, W. P., Beebe, K. R., Kowalski, B. R., Illman, D. L., and Hirschfeld, T., Selection of Adsorbates for Chemical Sensor Arrays by Pattern Recognition. Anal. Chem. **58**, 149 (1986).
[3] Carey, W. P., and Kowalski, B. R., Chemical Piezoelectric Sensor and Sensor Array Characterization. Anal. Chem. **58**, 3077 (1986).
[4] Lorber, A., Error Propagation and Figures of Merit for Quantitation by Solving Matrix Equations. Anal. Chem. **58**, 1167 (1986).
[5] Beebe, K. R., and Kowalski, B. R., An Introduction to Multivariate Calibration and Analysis. Anal. Chem. **59**, 1007A (1987).
[6] Lorber, A., Wangen, L. E., and Kowalski, B. R., A Theoretical Foundation for the PLS Algorithm, J. Chemometrics **1**, 19–31 (1987).
[7] Lorber, A., and Kowalski, B. R., Estimation of Prediction Error for Multivariate Calibration, in press. J. Chemometrics (1987).

Volume 93, Number 3, May–June 1988
Journal of Research of the National Bureau of Standards

Accuracy in Trace Analysis

Expert Systems and Robotics

T. L. Isenhour

Department of Chemistry
Kansas State University
Manhattan, KS 66506

and

J. C. Marshall

Department of Chemistry
Saint Olaf College
Northfield, MN 55057

In this paper, we will discuss the interface between expert systems and laboratory robotics. We will use examples from our recent research to illustrate how we are building an effective interface and indicate where we think this research will lead.

What are expert systems? As an operational definition we will adopt the following:

> Expert Systems are a sub-specialty in artificial intelligence (AI). The term is generally understood to mean a "knowledge-based" or "knowledge-driven" system designed to represent and apply factual knowledge in specific, very limited areas of expertise.

In the early sixties, AI researchers attempted to simulate the complicated process of thinking by finding general methods for solving broad classes of problems. This proved too difficult and such attempts failed. In the early seventies the problem was reformulated to include careful attention to data structures but the emphasis was still on general knowledge. Progress was still limited. In the late seventies the problem was further refined to focus almost completely on the knowledge representation. The goal was to make intelligent programs by providing them with high quality, domain-specific knowledge about some limited problem area. This strategy is much like that used by a human expert and gives rise to the term "expert system."

What domains are appropriate for expert system work? First and foremost, for the present state of expert systems technology the problem domain must be of limited scope. A majority of the people within the application field must agree that real experts do exist. The problem must be knowledge, not data, intensive. A problem is knowledge intensive if there is substantial variability in people's ability to solve it. The problem must not require information from visual input. Multiple answers from the same input data can be handled but with limited success. Perhaps the best test of all for a potential candidate for expert system work is the so-called "telephone test." If you have a problem and you are confident that if you called some known expert in the field, he or she could solve the problem for you in 30 minutes or less over the phone, then the problem is likely to be amenable to an expert system solution.

How do expert systems compare with human experts? The popular press has tended to be wildly optimistic about the present state of expert systems development. While many useful expert systems are available, they apply to very limited problem domains. In such domains expert systems can quickly provide answers that are consistent and objective. Expert systems can capture human expertise and make it permanent, widely available and easily portable. However, current expert systems lack the creativity and adaptability expected of a human expert.

How do expert systems work? Regardless of the details of the implementation, an expert system is a program driven by an inference engine towards a specific goal. It is, in the limit, a remarkably simple

process involving a cleverly ordered series of "if tests." A potential difficulty is, when the problem gets large and consequently the number of rule structures in the data base increases, an expert system can become difficult to modify, hard to debug and slow to execute.

Expert Systems for Data Management

Chemists, particularly analytical chemists, have historically been very concerned with the storage and retrieval of information. Spectral libraries are a common example. There is presently much interest in the potential of so-called "smart data bases" [1]. The fundamental idea is that a data base is represented as a collection of executable statements rather than facts.

The smart data base concept is a subtle strategy that can be illustrated with a trivial example involving the periodic table. The entries of the data base all conform to the PROLOG predicate ATOMIC and become executable statements; as such they are no longer passive facts. The PROLOG definitions and data base entries for a small part of this periodic table are shown in figure 1. In this example, apart from the definitions, there are no program statements other than the data base. A compelling advantage is that all of the features of the AI language used (in this case PROLOG) are available to form queries and the inference engine interrogates the file automatically. This is illustrated in figure 2.

Methods Development Using Expert Systems and Robotics

A central theme in our research for the past several years has been the idea of the *Analytical Director*. Laboratory robots can carry out simple repetitive tasks, following an invariant set of rules. However, when a robot becomes a mechanical extension of a control program that has logic capability the whole becomes greater than the sum of the parts. The *Analytical Director* project is an expert system driven robot that combines knowledge about analytical chemistry with laboratory robotics. The system is presently capable, in a limited way, of designing procedures for analysis, testing and modifying such procedures, and finally archiving the modified procedure for future reference. The flexible library facilities of the *Analytical Director* are possible because of the "smart data" capabilities inherent in the logic based programming languages.

The current implementation of the *Analytical Director* is a Zymark robot running under control of the ARTS [2] software system, an expert system driven robotics language. The control computer is a simple PC.

To demonstrate an application of the *Analytical Director*, the development of a complexometric titration procedure [3] is shown as a flow chart in figure 3.

A successful complexometric titration requires that the conditions be adjusted so as to insure a conditional stability constant of about 1×10^5. Choices to be made include the pH, the titrant, the masking agent or agents used and the method of endpoint detection. A vast literature exists on complexometric titrations. Some of this information is part of the knowledge base used by the ARTS system. The system not only starts with a knowledge base, but can continually update that knowledge base using results of experiments. The user is given the opportunity to specify some or all of the parameters that he/she wishes. The system will not override user input even though it may be wrong. The system will fill in missing user input from its knowledge base. The success or failure of a determination is stored by the system for future use.

Experimental results for the triplicate determination of Ni^{+2} by complexometric titration are shown in table 1 and compared with results obtained with manual titrations.

Table 1. Comparison of expert system and human counterpart. Results for the titration of a Ni^{2+} solution using 0.1004M EDTA without an indicator. Absorbance data were collected at 480 nm

	Expert system	*Human*
Trial 1	0.1006	0.0981
Trial 2	0.1004	0.0981
Trial 3	0.1007	0.0983
Average	0.1005_7	0.0981_7
Standard deviation	0.0001_5	0.0001_2
%Standard deviation	0.15	0.12

Building Expert Systems from Chemical Data

One of the most difficult problems with expert system work is creating an efficient knowledge base. When the knowledge base gets large, it becomes imperative to create the most efficient possible production rules. The knowledge base used by an expert system can be most efficiently structured as a set of rules that describe the minimal decision tree spanning the data. The root node of this tree is the attribute of the data that minimizes the number of branches from the root. Each branch from the root node contains a different value of the root attribute and creates second level nodes. These second level nodes may be branched further using attributes different from the previous attributes used to split the data. The class attributes and values will occupy terminal nodes in the decision tree. If more than one attribute is used to describe the data, the decision tree will not be unique. As the number of attributes required to describe the data increases, the number of possible decision trees increases combinatorially.

For this task we have implemented the ID3 (iterative dichotomizer 3) algorithm [4–6], originally developed for organizing and optimizing chess end-game strategies.

The ID3 algorithm is based on information theory and uses the entropy of classification. The entropy of classification is a measure of the entropy resulting from classifying an object in a particular class. The algorithm will first determine the attribute to use for the root node of the tree so that the number of branches from the root node are minimum. Each branch from the root node represents a unique value of the root attribute. The algorithm is then applied recursively to all the second level nodes, and all subsequent nodes spawned by each of the second level nodes.

We have implemented the ID3 algorithm (7) in PROLOG so that it accepts classification data and determines an efficient set of rules spanning the data. The program will then produce a file of rules that can be used directly by an expert system as an efficiently ordered knowledge base.

A simple example of how this works uses the infrared data in table 2. These data are applied to identifying substituted benzenes from their infrared absorption spectra.

There is enough information in the first two bands to answer the question. There is no information in the last two bands relevant to this question.

Table 2. Infrared data for some substituted benzenes

Compound name	Degree of substitution	IR ranges in cm^{-1}				
		650–699	700–749	750–799	800–849	850–899
toluene	MONO	S[a]	S	W	W	W
m-xylene	META	S	W	S	W	W
o-xylene	ORTHO	W	S	S	W	W
p-xylene	PARA	W	W	S	W	W

[a] S=strong; W=weak.

From these data, the algorithm outputs the information tree shown in figure 4. Not shown is the set of syntactically correct PROLOG production rules generated by the program that span the tree in figure 4.

Conclusion

The purpose of this research is the combination of logic programming with laboratory robotics. The goal of this research is the creation of the *Analytical Director*, an intelligent laboratory robotics system that will be able to develop, test and modify laboratory procedures without human supervision.

Acknowledgment

This research was supported by the National Science Foundation under grant number CHE-8415295.

```
        /*PROLOG data base example*/
domains
        name,symbl = symbol
        number = integer
        weight = real
predicates
       atomic(name,symbl,number,weight)
clauses
        atomic("Hydrogen","H",1,1.008).
        atomic("Helium","He",2,4.003).
        atomic("Lithium","Li",3,6.941).
        atomic("Beryllium","Be",4,9.012).
        atomic("Boron","B",5,10.81).
```

Figure 1. PROLOG data base example.

```
Goal: atomic(Name,Symbol,Number,Weight),Number>1,Weight<10
Name=Helium, Symbol=He, Number=2, Weight=4.003
Name=Lithium, Symbol=Li, Number=3, Weight=6.941
Name=Beryllium, Symbol=Be, Number=4, Weight=9.012
3 Solutions
Goal: atomic(Name,"B",Number,Weight)
Name=Boron, Number=5, Weight=10.81
1 Solution
Goal: atomic(Name,Symbol,5,Weight)
Name=Boron, Symbol=B, Weight=10.81
1 Solution
```

Figure 2. PROLOG data base interrogation examples.

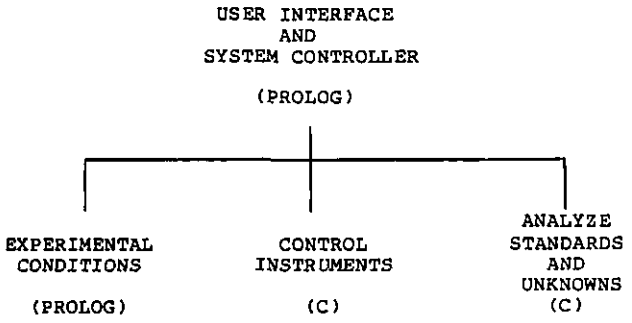

Figure 3. Complexometric titrations under expert system control.

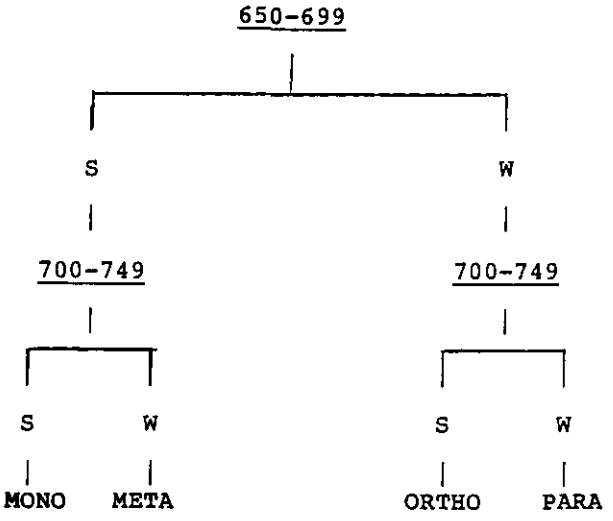

Figure 4. Decision tree generated from data in table 2.

References

[1] Schur, S., AI Expert 3, 26 (1988).
[2] Schlieper, W. A., Isenhour, T. L., and Marshall, J. C., Anal. Chem., in press.
[3] Schlieper, W. A., Isenhour, T. L., and Marshall, J. C., Complexometric Analysis Using an Artificial Intelligence Driven Robotic System, J. Chem. Inf. Comput. Sci., in press.
[4] Quinlan, J. R., Learning Efficient Classification Procedures and Their Applications to Chess End Games, in Machine Learning—An Artificial Intelligence Approach, Michalski, R. S., Carbonell, J. G., Mitchell, T. M., (Eds.), Tioga Publishing Company, Palo Alto, CA (1983).
[5] Thompson, B., Thompson, W., Byte **11**, 149 (1986).
[6] Derde, M., Buydens, L., Guns, C., and Massart, D., Anal. Chem. **59**, 1868 (1987).
[7] Schlieper, W. A., Isenhour, T. L., and Marshall, J. C., Using Analytical Data to Build Expert Systems, submitted, J. Chem. Inf. Comput. Sci.

Volume 93, Number 3, May–June 1988
Journal of Research of the National Bureau of Standards

Accuracy in Analysis: The Role of Standard Reference Materials

Stanley D. Rasberry

Office of Standard Reference Materials
National Bureau of Standards
Gaithersburg, MD 20899

1. Introduction

What one question haunts the best of analytical chemists when their day's work is done? Four of the main questions that arise regarding any analytical method are:

—Is it sensitive enough for the level of detection required?
—Is it free of interferences for the desired analyte?
—Is it precise, so that the results are reproducible?
—Is it accurate, so that the results approach true values?

Probably it is the last of these questions that brings the greatest difficulty and the most soul searching to the analyst. If this were not the case, why are there so many cars in chemistry building parking lots on weekends and holidays? Why are analysts often reluctant to report results without "just one more retest"?

This paper will attempt to pick apart some of these questions. While it may answer none of them conclusively, it is aimed at demonstrating the role of Standard Reference Materials (SRMs) in the analyst's pursuit of accuracy. In the case of trace analysis near the detection limit of state-of-the-art methods, certifiers of reference materials face a very special problem: certified error limits often seem unacceptably high when considered on a relative basis. This paper will include a brief discussion of this problem.

2. Role of Standard Reference Materials (SRMs)

Simply stated, the National Bureau of Standards (NBS) produces SRMs to help people bring quality assurance to their measurements. In some cases instruments require SRMs for calibration. In most cases measurement accuracy should be validated by use of a certified reference material.

In the mining and manufacturing industries, at least four major stages of activity require measurements and thus some form of measurement quality assurance:

—Raw Materials.
—Finished Materials.
—Subcomponents.
—Products.

At the first two stages, the measurements are most likely to be chemical analyses. At later production stages, measurements are more apt to be physical or engineering tests. Increasingly, SRMs are also being produced for use in these later stages of production.

Today, the U.S. economy has shifted from manufacturing to an emphasis on the service sector. Chemical analysis plays an important role in this sector, too. Here we often find measurement quality assurance needs for analyses in such service areas as: environmental, clinical, geological, and energy. SRMs are underutilized by the service sector and could be very helpful to future improvements in quality assurance of measurements.

A third community that has a heavy focus on measurements is the academic and R&D community. Here is where we get most of our new concepts for instrumentation and measurement methods. When new developments are tried out in the lab and reported in the literature, SRMs have a critical role in helping the researchers assess the accuracy of what they have wrought.

3. Concern About Accuracy

In certifying SRMs, the goal at the NBS is to give a true value at a stated level of accuracy for each property certified [1]. Notice the word accuracy rather than precision. The concept of accuracy is focused on arriving at the "true" or "actual" value of a property. Real world materials are usually not completely uniform, so the true value may differ for different samples taken from the material. Provided the differences are small, they may be covered in an accuracy statement representative of the entire lot. Large differences require rejection of the lot or individual certification of each sample.

Conversely, precision gives no indication of how closely a set of measurements approaches the true value. The concept of precision is focused on how tightly clustered a set of measurements is. Said another way, one can have a set of measurements which is extremely precise, but also extremely wrong. Precision may be viewed as a necessary but not sufficient precursor of accuracy.

I have tried to establish an estimate of accuracy that a wide range of chemists and methods realize at trace levels. To do this, I have used a literature survey [2] which has reviewed more than 100 papers citing results of analysis of SRM 1571, Orchard Leaves. In table 1 are summarized the results found for two elements (iron and aluminum) which are present at about 300 μg/g. Note that iron is certified by NBS, while aluminum is not. Similarly, one certified element (strontium) and one element not certified (titanium) in SRM 1571 are shown and are at about one order of magnitude lower concentration. A more detailed view of the analytical accuracy is given in the next two tables.

Table 1. 1571 Orchard Leaves (μg/g)

Element	NBS	Literature [2] $X+S(n)$	Range
Fe	300±20	284± 28(109)	121 -884
Al		320±110 (41)	99 -824
Sr	37± 1	37± 4 (39)	14.5-118
Ti		24± 9 (7)	2.4-191

Table 2 shows that the range of values for the 109 determinations of iron (certified) is no greater than the range of 41 determinations of aluminum (not certified). For each element the three highest and three lowest values reported are shown together with the certified or mean value. What is critical to note is that uncertainty statements provided in the literature may be unfoundedly optimistic but are substantially improved when a certified value is available.

Table 2. 1571 Orchard Leaves (μg/g) literature [2]

Element:	Iron	Aluminum
	884	824± 50
High:	450±70	520±180
	370±45	460± 7
	300±20[a]	320±110[b]
	205±37	146± 20
Low:	145± 4	140± 8
	121	103± 22

[a] Certified concentration.
[b] Literature mean for aluminum.

The situation is similar for lower concentrations, as shown in table 3. Here uncertainty estimates for titanium are in error by as much as 5000%. Note from tables 1 and 3 that at least six of the seven analysts reporting titanium do not include, within their uncertainties, the mean of the seven determinations.

Table 3. 1571 Orchard Leaves (μg/g) literature [2]

Element:	Strontium	Titanium
	118	191 ±33
High:	53 ±4	96 ±12
	45 ±2	60
	37 ±1[a]	24 ± 9[b]
	31 ±3.3	17.2± 0.3
Low:	28.0±0.6	6.6± 0.5
	14.5±2.5	2.4± 0.4

[a] Certified concentration.
[b] Literature mean for titanium.

4. Concern that SRMs Are Underutilized

It is very difficult to estimate the degree to which SRMs are utilized when their use is warranted. Review of sales records gives the rather imprecise "feeling" that usage in mining and manufacturing may exceed 10% of the applicable occasions. However, in the service sector, a 1% usage rate may be a better estimate. An open question is,

"Are chemists receiving an adequate education in the use of Standard Reference Materials?"

In the academic and R&D sector a very rough idea of the rate of usage can be established by examining papers where the use of SRMs would have been helpful to validate new work. In tables 4 and 5, we have a survey of SRM use taken from periodicals spaced 10 years apart.

Table 4. Survey of three August 1977 periodicals to compare potential and actual use of SRMs

	Articles employing SRMs	
Periodical	Should have	Did
American Laboratory	Not available	
Applied Spectroscopy	4	0
Analytical Chemistry	10	4
Total	14	4
% Using	29%	

Table 5. Survey of three August 1987 periodicals to compare potential and actual use of SRMs

	Articles employing SRMs	
Periodical	Should have	Did
American Laboratory	7	4
Applied Spectroscopy	6	2
Analytical Chemistry	7	1
Total	20	7
% Using	35%	

The precision of the data probably does not warrant concluding that usage rates have changed between 1977 and 1987. However, the data do provide gratifying evidence that researchers realize some value in reporting validation of new work by SRMs. I feel that a usage factor of at least 50% should be obtainable in this sector. Could it be obtained if reviewers of papers were a bit more insistent that reported results include SRMs when available?

5. Certification of SRMs

At NBS, we cannot rely only on assessments of measurement precision to set uncertainty limits [1]. Instead, an individually tailored program is set up for the project design, measurement, and certification of each SRM. Typically, this program will include measurement by more than one method and in more than one laboratory. Unless SRM units are individually certified, the program also must assess the homogeneity of the lot of material.

At each step of the program careful attention is given to precision of results from each method and each laboratory. Statistical assessments are made of homogeneity, which can be considered the material component to imprecision, in contrast to the precision of various measurements made on the material.

By the end of the measurement process, the measurement experts and the project manager have in hand far too much data to put onto a certificate. Their job is to distill those data into one meaningful uncertainty statement for each value certified. Obviously, they must take into account the precision of all the measurements and the homogeneity of the material, but, more importantly, they must zero in on the true value. They must cross-compare data from different, independent methods. They often need to evaluate data from different laboratories. They must probe for systematic errors or bias in methods and instruments, including examination of such questions as recoveries and results on control samples.

Finally, they decide on the best possible description of the stated level of accuracy for the certification. Sometimes this parameter is stated as a tolerance interval; more often, it is simply given as an estimated uncertainty. The important factor to reiterate is that the uncertainty statement is more than a precision statement. Typically, the uncertainty will include the combined effects of method imprecision, possible systematic errors among methods, and material variability.

In cases where certification is for an element near the detection limit of state-of-the-art methods, it is usual for relative uncertainties to be large. For example, an element that can be certified at 1 ± 0.8 ng/g may seem to have an unacceptably high relative uncertainty of $\pm 80\%$. However, the absolute error is quite small and defines the presence of one more element in the SRM to within ± 0.8 ng/g. Until the methods for that particular element are improved, a certification with large relative uncertainty is all that is possible.

6. Consideration for SRM Users

As instrumental methods become very precise, users of a single, precise method begin to question why that method is so much more precise than the uncertainties on NBS certificates [1]. They wonder why NBS is "working at such low precision." NBS uncertainty limits will always be wider than the precision obtained in any of the individual measurement methods used in certification.

It is good for users to have highly precise methods because they serve as a precursor to their attaining accurate measurement. In a sense it means they are ready to make full and effective use of SRMs to calibrate or validate their measurements. But users must be cautioned never to assume that good precision implies accuracy, without the confirmation by SRMs.

References

[1] Rasberry, S. D., Reference Materials, Amer. Lab. **19**, 130–131 (1987).

[2] Gladney, E. S., Burns, C. E., Perrin, D. R., Roelandts, I., and Gills, T. E., 1982 Compilation of Elemental Concentration Data for NBS Biological, Geological, and Environmental Standard Reference Materials, NBS Spec. Publ. 260-88 (March 1984).

Volume 93, Number 3, May–June 1988
Journal of Research of the National Bureau of Standards

II. Considerations of the Measurement Process

Quality Assurance and Reference Materials for Trace Analysis

Accuracy in Trace Analysis

G. Kateman

Laboratory for Analytical Chemistry
Faculty of Sciences, Catholic University
of Nijmegen, Toernooiveld,
6525 ED Nijmegen, The Netherlands

Most analytical measurements are not absolute but depend on the correlation between physical phenomena and some intrinsic property, e.g., concentration. Therefore, calibration is an indispensable part of analytical chemistry. Unfortunately, calibrations are not free from interference by the environment. This disturbing environment can be the micro-environment, components in the sample that influence the calibration line. As a rule this interference is usually constant, though not always (e.g., separation processes).

The macro-environment, however, changes continuously. Temperature, pressure, chemicals, and man are stationary only during a short time. These influences will be seen as random fluctuations or, when autocorrelated, as drift. One approach is to monitor the properties of the calibration system internally by incorporating a calibration system and a measuring system. By monitoring the calibration system, the results of the unknown can be corrected. Kalivas and Kowalski [1] described the solution for the multicomponent situation, using the generalized standard addition method (GSAM). By treating drift as a time dependent component they obtain the equation

$$\Delta q_{m,l} = \sum_{s=1}^{r} \Delta n_{m,w} K_{s,l} + (V_m t_m - V_0 t_0) K_{t,l}$$

where $q_{m,l}$ = the volume corrected response
$n_{m,s}$ = the total number of moles of component s
$K_{s,l}$ = linear response constant for the l-th sensor to the s-th component
m = number of additions of analyte
t_m = time elapsed from initial measurement up to the m-th addition
V_m = volume after m-th addition

Smit, Mars, and Kraak [2] developed a method to calibrate during a chromatographic run by applying correlation chromatography. In this technique a sample is introduced into a chromatographic column not as a single pulse, but according to a "Pseudo Random Binary Sequence" (PRBS). Smit et al. proved that it is possible to introduce more samples simultaneously, though at the expense of lengthening the PRBS sequence. Any disturbance of the system during the determination acts immediately on the calibration sample, giving a calibration factor that is obtained under ideal circumstances. Other techniques depend on prediction of the behavior of the calibration system. In this case a model is required. Assuming that drift in a calibration can be modelled as an autocorrelated random variation with known correlation constant, Tx, the future values can be predicted according to

$$\hat{x}(K+\tau) = \alpha^{\tau} \cdot x(K)$$

where $x(K)$ is the normalized value of the calibration factor.

Predicting $\hat{x}(K+\tau)$ over a time span τ is feasible only when the predicted values do not deviate more than a preset value, T_r. Müskens [3] derived that

$$\tau = -Tx \ln\{Tr\, x(K) + N[x(K)^2 - q(Tr^2 - N^2)]^{\frac{1}{2}}[x(K)^2 + qN^2]^{-1}\}$$

where $q = (\sigma_x^2 + \sigma_a^2)\sigma_x^{-2}$, and σ_a = the standard deviation of a measurement.

A powerful method which uses all available information is "state estimation" or Kalman filtering. Information from the past, or when starting the measurement from an educated guess, is used to predict the situation in the present.

$$\hat{x}(K) = F\bar{x}(K-1) - w(K-1),$$

where $\hat{x}(K)$=predicted state (e.g., concentration) at time K, $\bar{x}(K-1)$=the estimation of x at $K-1$, F=the transition function, and $w(K)$=the variance of noise.

The next step is to do a new measurement $z(K)$.

$$\bar{x}(K)=\hat{x}(K)+G(K)[\hat{x}(K)-H(K)z(K)],$$

where $H(K)$=calibration factor.

The estimate $x(K)$ is the best estimate that is possible. The weighting factor

$$G(K)=P(K)[P(K)+R(K)]^{-1}$$

depends on the fluctuations in the system, expressed as covariance $P(K)$ and the measuring error R(K).

A Kalman filter enables the on-line estimation of calibration parameters, intercept, sensitivity and drift (of both intercept and sensitivity). The filter requires a model of the system, including system noise and measurement noise. When a good model is available, the filter can predict future values or estimate best values of the changing parameters. These figures may be used to determine when a recalibration is required.

Making a number of assumptions, the usual Kalman filter algorithms can be used resulting in [4,5,6]

$$\hat{x}(K)=F(K)\bar{x}(K-1)$$
$$\hat{P}(K)=F(K)\bar{P}(K-1)F'(K)+Q(K-1)$$
$$\bar{x}(K)=\hat{x}(K)+G(K)\{z(K)-h'(K)\hat{x}(K)\}$$
$$\bar{P}(K)=\hat{P}(K)-G(K)h'(K)\hat{P}(K)$$
$$G(K)=\hat{P}(K)h(K)\{h'(K)\hat{P}(K)h(K)+R(K)\}^{-1}.$$

The quality performance of the system is controlled on-line by comparison with a predefined criterion. The decision to re-calibrate is followed by optimization of the concentration standards available. The example given treats drift as a deterministic phenomenon. Poulisse [7,8] indicated another approach, considering drift as a stochastic phenomenon. A novel approach aiming at the elimination of the human factor in calibration is the use of expert systems. An expert system allows the objective use of a large knowledge base. This knowledge base consists of facts and rules, the results of long experience. A so-called inference machine searches for the right solution given a set of starting parameters or states the starting parameters when the goal has been stated. Since the computer will not be annoyed when repeatedly asked for the conditions for a good calibration and can deliver calibration correction factors for each situation, it can be expected that this approach will give better calibration results. However, no conclusive results have been reported so far.

References

[1] Kalivas, J. H., and Kowalski, B. R., Anal. Chem. **54**, 560 (1982).
[2] Smit, H. C., Mars, C., and Kraak, J. C., Anal. Chim. Acta **181**, 37 (1986).
[3] Müskens, P. J. W. M., Anal. Chim. Acta **103**, 445 (1978).
[4] Thijssen, P. C., Wolfrum, S. M., Smit, H. C., and Kateman, G., Anal. Chim. Acta **156**, 87 (1984).
[5] Thijssen, P. C., Smit, H. C., and Kateman, G., Anal. Chim. Acta **162**, 253 (1984).
[6] Poulisse, H. N. J., and Engelen, P., Anal. Letters **13** (A14), 1211 (1980).
[7] Poulisse, H. N. J., "State- and parameter estimation as chemometrical concepts," thesis, Nijmegen 1983, chapter 6.
[8] Poulisse, H. N. J., "State- and parameter estimation as chemometrical concepts," thesis, Nijmegen 1983, chapter 8.

Design of Cost-Effective QC Procedures for Clinical Chemistry Assays

James O. Westgard

Department of Pathology and
Laboratory Medicine
Medical School, Medical Technology Program
School of Allied Health Professions
University of Wisconsin
Madison, WI

Introduction

In clinical laboratories, the major production processes are analytical processes. Quality management strategies must include approaches for optimizing the cost-effectiveness of analytical processes. "Cost-effective QC," in this context, is concerned with selecting or designing a quality control procedure that maximizes both the quality and productivity of an analytical process [1]. There are many factors that need to be considered, including the medically required quality for the analyte being measured, the characteristics of the measurement procedure (type of process or system, precision,

accuracy, drift stability, and frequency of occurrence of errors), the type and structure of the errors occurring (random or systematic, intermittent or persistent), and the error detection and false rejection characteristics of the control procedure itself (probabilities for rejection, average run lengths).

To assess the possible interactions of these many factors, it is necessary to have a "design tool" such as a quality-productivity model, which is based on the industrial concept of quality-costs. With the aid of such models, the effects of these many factors can be predicted, facilitating the planning of analytical processes that will provide cost-effective operation.

Quality-Productivity Models

The industrial concept of "quality costs" was described by Feigenbaum in 1956 [2]. Quality costs include components of prevention costs, appraisal costs, and failure costs, including both internal and external failure costs. When costs are restricted to process costs in terms of samples analyzed or repeated, prevention costs are losses of samples for calibration, and appraisal costs are losses for analyzing control samples, both of which can be estimated from knowledge of the physical variables of the analytical system and process. Failure costs are losses for repeat runs and repeat requests, which can be predicted from performance characteristics of the measurement and control procedures. These losses, described in terms of the process variables and characteristics, provide an estimate of process waste. Test yield, or productivity, is estimated by the difference between the maximum output and the process waste (1−[average quality costs or losses]).

Table 1 provides an example quality-productivity model for a batch analytical process subject to intermittent errors.

Table 1. A quality-productivity model for describing the quality and productivity of a batch analytical process subject to intermittent analytical errors

Measure of quality is "defect rate"

Defect Rate$=f(1-P_{ed})$

Measure of productivity is "test yield"

$$\text{Test Yield}=1-\frac{C+N}{T}-\frac{Sp}{T}\,[R_{tr}fP_{ed}+R_{fr}(1-f)P_{fr}+R_{fa}f(1-P_{ed})+R_{ta}f(1-P_{ed})(1-f)(1-P_{fr})]$$

where the terms are characteristics of the measurement and control procedures, and laboratory policies for repeat runs

- f is the frequency of occurrence of errors
- P_{ed} is the probability for error detection
- P_{fr} is the probability for false rejection
- C is the number of calibrators
- N is the number of control measurements per run
- Sp is the number of patient specimens
- T is the total samples in a run $(C+N+Sp)$
- R terms are rerun factors for true reject, false reject, false accept, and true accept runs

Example Application

Let us assume a batch process having 30 samples per batch that is calibrated once a week, requiring six calibrators (C) be analyzed in duplicate. Assume a workload requiring one run per day for 6 days in a week, thus (C) averages one per run for this example. We then postulate a design for a control procedure, enter the number of control measurements per run (N), and the probabilities for false rejection and error detection (for medically important errors), as determined from power function graphs obtained by a computer simulation program [3]. Complete details of this example are found elsewhere [1].

Figure 1 shows the performance of a multi-rule procedure [4] for $N=2$ and $N=4$. For an unstable measurement procedure having a frequency of errors of 0.10 (or 10%), doing more quality control actually provides higher quality and higher productivity. Doubling the number of controls per run actually reduces the cost. For a stable measurement procedure, with a frequency of errors of 0.01 (or 1%), higher productivity is achieved with $N=2$.

Figure 2 compares the performance of three different control procedures having $N=2$. For a stable measurement procedure, the use of 3s control limits (1_{3s} control rule) or a multi-rule control pro-

cedure [3] provides high quality (low defect rate) and high productivity (high test yield). For an unstable measurement procedure, say a frequency of errors of 0.20 (or 20%), the use of 2s control limits (1_{2s} control rule) provides better quality and higher productivity.

Figure 3 shows a comparison of three different control procedures, with different rules and with different N's, all giving nearly the same quality or defect rates. Multi-rule with $N=4$ or 1_{2s} with $N=2$ provide more cost-effective operation than 1_{3s} with $N=8$.

Implications for Selecting and Designing QC Procedures

Given the practical limitations of two to four control measurements per run due to short runs for fast turnaround of results, it is impossible to have an ideal control procedure with *both* high error detection and low false rejection. However, a laboratory can have *either* high error detection or low false rejection if it knows which is more important for the particular application.

Because the performance of an analytical process depends on its stability, i.e., its frequency of errors (f), the control procedure can be tailored to fit that frequency of errors. For measurement procedures having a low frequency of errors, the QC procedure should be selected or designed primarily for a low probability of false rejection, with secondary concern for error detection ("low-f design"). When there is a high frequency of errors, the QC procedure should be selected or designed for high error detection, with little regard for its probability for false rejection ("high-f design").

One useful strategy is to change control procedures depending on the recent history of the measurement procedure, switching from "low-f" to "high-f" designs, as necessary. Whenever the analyst is suspicious that performance is deteriorating, the "high-f" design can be used. When the process is running smoothly, the "low-f" design can be used.

Another strategy is to systematically switch from one design to another as the analytical process goes through its normal operational cycle. For example, at the beginning of the day, test the process carefully using a "start-up" design having high error detection; following successful completion of that testing, switch to a "monitoring" design having very low false rejection; and, over the course of the day, use a "prospective" design to analyze the accumulated control measurements and trigger preventive maintenance procedures prior to tomorrow's run. Such "multi-stage" designs provide a systematic tailoring of the control procedure to fit the changing operation conditions of the measurement procedure.

Doing "cost-effective QC" in clinical laboratories means using individualized designs of QC procedures that fit the measurement procedures to be monitored. A comprehensive design tool would be useful to help users study and plan their analytical processes. It should provide a wide variety of control rules, incorporate computer simulation to provide the performance characteristics of the selected QC procedure, utilize more realistic error distributions to represent stable and unstable performance, offer choices of intermittent and/or persistent error conditions, and permit input of information on the factors and variables needed to customize the quality-productivity model to fit individual analytical systems.

Routine implementation of such individualized QC designs also would be aided by more advanced QC programs in laboratory information systems. The programs should permit analysts to choose the control rules and the number of control measurements, to select how the rules are applied across materials and/or runs, to specify whether the control signal is a rejection or warning for preventive maintenance, and to define two or more QC procedures that could be employed on a single measurement procedure.

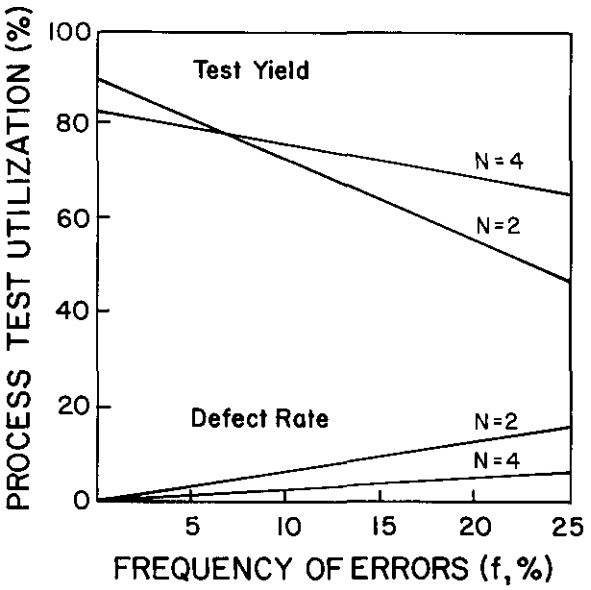

Figure 1. Comparison of quality (defect rate) and productivity (test yield) for a batch analytical process using a multi-rule control procedure with $N=2$ and $N=4$. From reference [1].

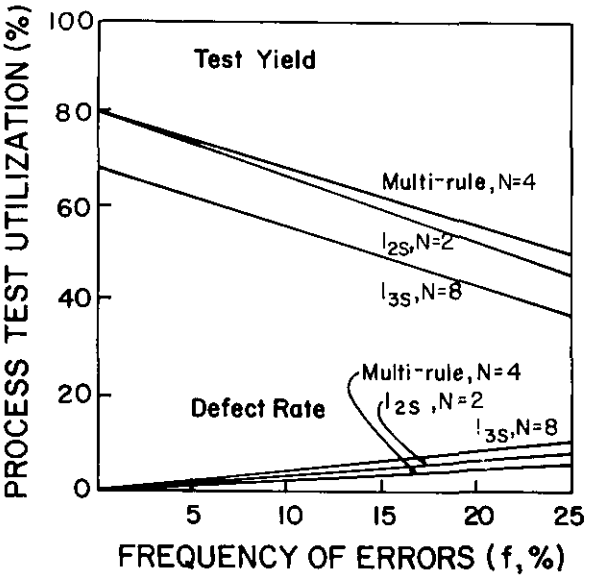

Figure 3. Comparison of quality (defect rate) and productivity (test yield) for a batch analytical process with different control rules and different N's. From reference [1].

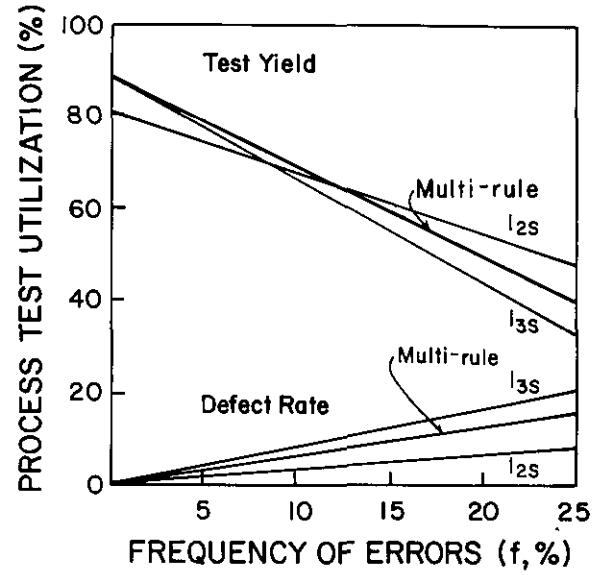

Figure 2. Comparison of quality (defect rate) and productivity (test yield) for a batch analytical process with different control rules all using $N=2$ (2 control measurements per run). From reference [1].

References

[1] Westgard, J. O., and Barry, P. L., Cost-Effective Quality Control, AACC Press, Washington, DC (1986).
[2] Feigenbaum, A. V., Harvard Bus. Rev. **34**, 93 (1956).
[3] Westgard, J. O., and Groth, T., Clin. Chem. **25**, 863 (1979).
[4] Westgard, J. O., Barry, P. L., Hunt, M. R., and Groth, T., Clin. Chem. **27**, 493 (1981).

Statistical Models in Quality Control for Trace Analysis

Robert S. Elder

FSIS Science, Room 612 Annex
U.S. Department of Agriculture
Washington, DC 20250

1. Introduction

It is well known that there are important factors affecting accuracy in trace analysis, such as handling loss, contamination and purity of reagents.

The contention of this paper is that the statistical model for analytical error is another important factor, that currently is receiving much attention. A normal distribution is the model upon which the statistical procedures used in laboratory quality control (QC) customarily are based. However, examinations of certain analytical procedures and results of trace analyses reveal features that are inconsistent with normality.

2. Alternate Models

The three models to be discussed are the normal distribution, the lognormal distribution, and no distribution. There are good reasons for expecting one of these models to be appropriate in many circumstances.

The normal distribution is symmetric, bell-shaped, and of unbounded range. It is characterized by two independent parameters, its mean (μ) and standard deviation (σ), which can be directly associated with analytical bias and precision. One reason for the widespread applicability of this model is the Central Limit Theorem, the practical result of which is that sums of random variables tend to be normally distributed under mild conditions. Based on the Central Limit Theorem, it has been said that "in the case of a well devised analytical system of measurement and a properly performed analysis . . . analytical results will be normally distributed or, at least, almost so" [1]. This statement assumes that analytical errors are additive.

The lognormal distribution [2] is asymmetric, bounded below by zero, and is defined by the function

$$f(x)=\exp[-(\log(x)-\alpha)^2/2\,\delta^2]/(2\pi\delta^2 x)^{1/2}$$

The distribution takes its name from the fact that if x is lognormally distributed, $\log(x)$ is normally distributed. The mean and standard deviation of the distribution are $\mu=\exp(\alpha+1/2\delta^2)$ and $\sigma=\mu\cdot(\exp(\delta^2)-1)^{1/2}$; thus the coefficient of variation (CV) is constant with respect to the mean. For QC use one can reparameterize the model to make the mean and coefficient of variation the basic parameters (by defining $\delta^2=\log[1+(CV/100)^2]$ and $\alpha=\log(\mu)-\delta^2/2$). In addition, the model can be generalized to shift its origin from zero to γ by taking $\log(x+\gamma)$ to be normally distributed.

Figure 1 illustrates how the skewness of the distribution increases as the CV increases. For CVs of less than 10%, the model differs very little in shape from the normal distribution. (This is another reason for the usefulness of the normal model.)

Based on the Central Limit Theorem and the fact that the logarithm of a product of random variables equals the sum of the logarithms of the random variables, the lognormal model tends to be appropriate for multiplicative processes. Figure 2 shows how rapidly the distribution of a product of random variables can approach the lognormal distribution as the number of factors (n) increases.

The third alternative, no distribution, is the most likely model in the absence of effective quality control. The first job before applying statistical models and procedures is to get a distribution. "Stability, or the existence of a system, is seldom a natural state. It is an achievement . . ." [3]. Producing a consistent distribution requires serious effort from design (method development) through production (routine analysis).

3. Choosing the Right Model

One way to decide what statistical model to use is to turn to the technical literature for guidance. However, many sources do not address the subject explicitly (e.g., see the ACS Principles of Environmental Analysis [4]), and others give conflicting advice. For example, the Statistical Manual of the AOAC [5] says: "It is understood that random errors are equally likely to be positive or negative and to vary in size in a manner that is adequately described by the normal law of errors." Eckschlager and Stepanek [6] say that a shifted lognormal distribution is appropriate for concentrations above the determination limit. Thompson and Howarth [7] claim to make the "case against" the lognormal distribution.

A second approach to choosing a model is to look at data. Unfortunately, there is seldom enough data to reach a conclusion [7], or the data is messy (contains blunders and outliers and is censored below the limit of quantitation). Nevertheless, one can find clues in QC data; for example, appropriateness of CV and percent recovery as summary statistics hint at a multiplicative process and lognormality. The work of Horwitz and colleagues in relating analytical precision to concentration across many analytical methods is interesting in this regard: it shows the widespread usefulness of

the *CV* as a measure of imprecision, and shows how the total *CV* increases as the level of applicability of methods decreases [8]. At the ppb level, the Horwitz model gives a *CV* of about 45%.

The third and best method of choosing a model is to combine whatever knowledge can be obtained from data with what can be deduced from the nature of the measurement process. Is the process additive or multiplicative? There are certain common steps in sample preparation, such as concentration, dilution and extraction, that are multiplicative in nature [9,10]. An example of an analytical method with a multiplicative quantitation process is the GC/MS method for wastewater analysis [11]: the test result is a product or quotient of response factor, concentration of internal standard, peak areas, and volume of original sample. Coupled with the fact that *CV*s for this method are as high as 50%, there is good reason to expect the lognormal model to be appropriate.

4. Impact of the Lognormal Model

A legitimate concern with the lognormal model is how it will affect traditional concepts and procedures of analytical QC. The answer is that the impact ranges from negligible to serious depending on the procedure involved. Consider these examples:

(1) Repeatability interval. The distribution of the difference of two identically distributed lognormal random variables is well approximated by the normal distribution. Therefore, the impact of lognormality on this concept is negligible.

(2) Control charts. It is not necessary to work with log-transformed data to control either bias or precision. For example, bias can be monitored with a percent recovery control chart [12], and within-laboratory precision by a chart for the ratio of duplicate measurements. It becomes more important to base control limits on the lognormal rather than the normal model the farther the *CV* gets above 10%.

(3) Youden two-sample chart. Figure 3 shows the type of patterns to expect from lognormal data for two different degrees of between-laboratory variation. One should expect fan-shaped patterns with points concentrated in the first quadrant, rather than the more balanced elliptical patterns characteristic of the normal distribution [5].

(4) Outlier tests. The commonly used outlier tests are based on the normal distribution, which is symmetric, so applying such tests to lognormal data tends to give erroneous results. For example, when Grubbs test is applied to untransformed lognormal data, there is a tendency to miss real lower-tail outliers and to find too many upper-tail "outliers." The problem grows as the *CV* increases, but it is easily cured by applying the test to log-transformed data.

In conclusion, the lognormal distribution appears to be the appropriate model for some methods of trace analysis. As the *CV* increases, it becomes more important to use this model when it is appropriate; its use does not require unmanageable changes in analytical QC practices.

Acknowledgments

This paper is an expansion of part of an earlier paper coauthored with L. P. Provost [12]. A detailed critique of [12] by W. Horwitz and R. Albert [13] helped to stimulate development of additional ideas.

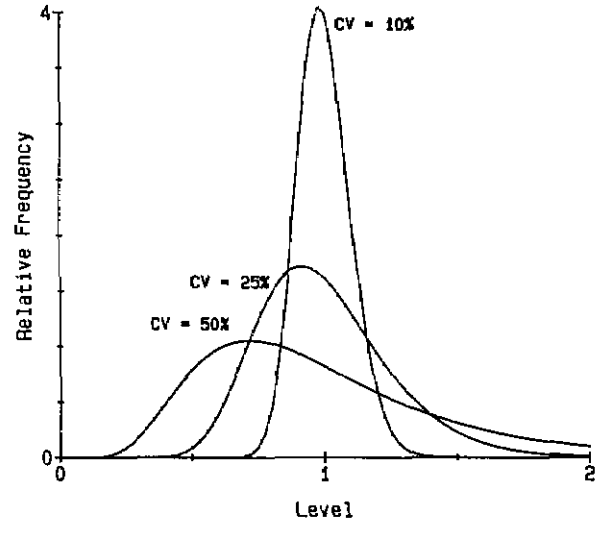

Figure 1. Lognormal distributions.

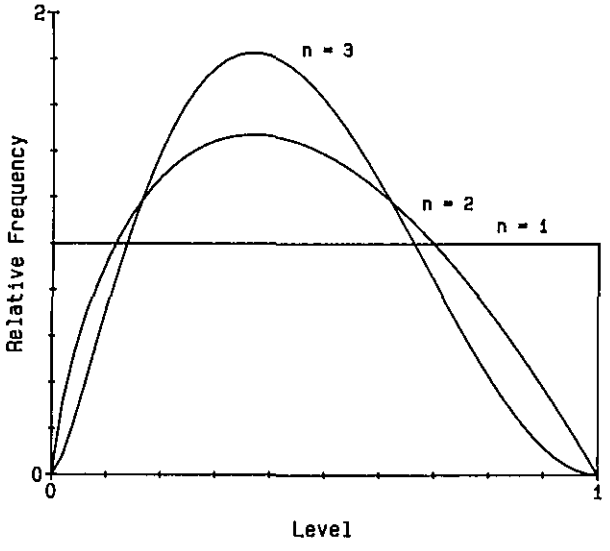

Figure 2. Distributions of geometric means of samples from a rectangular distribution.

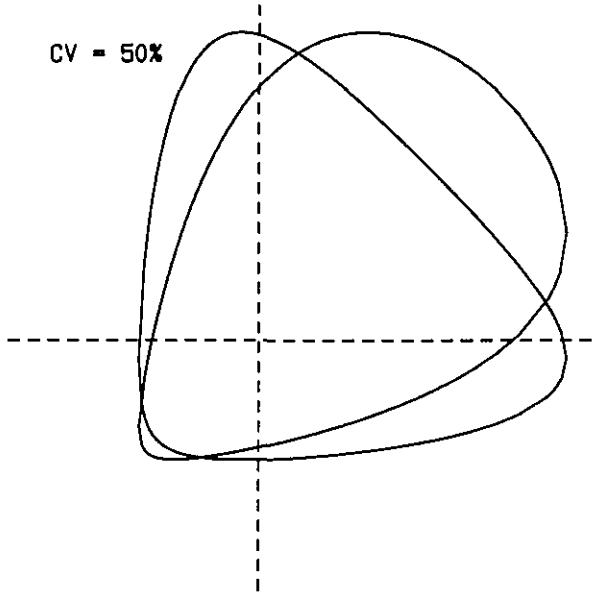

Figure 3. Expected configurations of Youden two-sample charts for lognormal data.

References

[1] Liteanu, C., and Rica, I., Statistical Theory and Methodology of Trace Analysis, Halsted Press, New York, p. 31 (1980).
[2] Aitchison, J., and Brown, J. A. C., The Lognormal Distribution, Cambridge University Press, London (1957).
[3] Deming, W. E., Quality, Productivity and Competitive Position, Massachusetts Institute of Technology, Cambridge, p. 119 (1982).
[4] ACS Committee on Environmental Improvement, Anal. Chem. **55**, 2210 (1983).
[5] Youden, W. J., and Steiner, E. H., Statistical Manual of the AOAC, Association of Official Analytical Chemists, Arlington, p. 8 (1975).
[6] Eckschlager, K., and Stepanek, V., Analytical Measurement and Information, John Wiley and Sons, New York, p. 73 (1985).
[7] Thompson, M., and Howarth, R. J., Analyst **105**, 1188 (1980).
[8] Horwitz, W., J. Assoc. Official Anal. Chem. **66**, 1295 (1983).
[9] Eckschlager, K., Errors, Measurement and Results in Chemical Analysis, Van Nostrand Reinhold, London, p. 72 (1969).
[10] Janardan, K. G., and Schaeffer, D. J., Anal. Chem. **51**, 1024 (1979).
[11] Environmental Protection Agency, Guidelines Establishing Test Procedures for the Analysis of Pollutants, Federal Register, 44, 69464–69575 (3 Dec. 1979).
[12] Provost, L. P., and Elder, R. S., Statistical Issues in QC for Trace Analysis, presented at 28th Annual Fall Technical Conference, London, Ontario (1984).
[13] Horwitz, W., and Albert, R., private communication (1985).

Quality Control in Routine Instrumental Epithermal Neutron Activation Analysis of Geological Samples

Maija Lipponen and Rolf Rosenberg[1]

Technical Research Centre of Finland
Reactor Laboratory
SF-02150 Espoo, Finland

Introduction

The Reactor Laboratory carries out analytical service by using neutron activation analysis. Altogether 50 elements are analyzed within a wide

[1] Present address: International Atomic Energy Agency, P.O. Box 100, A-1400 Vienna, Austria.

variety of geological, environmental, biological, archaeological, and industrial samples using instrumental and radiochemical thermal and epithermal neutron activation analysis. However, a major part of the analytical service is instrumental epithermal neutron activation analysis (IENAA) of geological samples and therefore only the quality control of this procedure will be discussed.

The main purpose for developing the technique was the need for a low cost and low detection limit determination of gold for geochemical exploration. The procedure used determines the concentration of 23 elements: Na, Sc, Cr, Fe, Co, Ni, Zn, As, Rb, Mo, Ag, Sn, So, Cs, Ba, La, Sm, Lu, Ta, W, Au, Th, U. A detection limit of 3 ppb for gold could only be obtained through IENAA. The required low cost and high capacity necessitated some compromises, and therefore an accuracy of ±10–20% was considered sufficient. The principal application field of the results (i.e., geochemical exploration) permits this.

Procedures for the simultaneous epithermal neutron irradiation of 600 samples and automatic measurement and data processing have been developed. A strong emphasis has been laid on the reliability of the results. This quality control has been twofold. The first stage was to show the procedure to be capable of producing results within the stated accuracy. The second stage is continuous control which ensures that the results of the routine analysis continue to fall within the stated error limits.

The Analytical Procedures

Standards

Four different standards are used to cover the 23 elements analyzed. Two of them are National rock standards produced by the Geological Survey of Finland. An aqueous solution of KBr is used as a standard for Br. The fourth is a solid SiO_2-based standard made at the Reactor Laboratory [1].

Equipment

A Triga Mk II research reactor is used for the irradiations. The reactor is run about 7 h daily from Monday to Friday. The thermal flux is $1.2 \cdot 10^{12}$ $cm^{-2}s^{-1}$ and the Cd-ratio for gold is 2. Twenty of the irradiation positions are used for thermal irradiations and 20 for epithermal irradiations. The epithermal flux is attained by using containers of aluminium 3 cm $\phi \times 25$ cm in size, lined with 1 mm of cadmium and again with 0.2 mm of aluminium. These containers are permanently located in the reactor and are only taken up to change samples.

Measurements are performed with automatic γ-spectrometers comprising a Ge(Li) or a Ge detector with auxiliary electronics, a sample changer, a multichannel analyzer, a microcomputer, and input/output devices [2]. This system automatically measures a series of samples and simultaneously calculates the elemental concentrations that are printed on paper and cassette.

Procedure for ENAA

The standards and powdered samples are weighed into polyethylene capsules with an inner volume of 0.5 mL. One irradiation series comprises four standards, 12 control samples, and 144 samples. These are inserted into cadmium containers and irradiated for 1 week.

The sample codes and weights are printed on floppy disks from which they are copied on a cassette for input into the computer memory at the start of a measurement series. After a decay time of 4–6 days, the samples are measured for 20 min/sample. Four series are measured in a week.

While this paper was being written, the computing and data input were centralized by connecting all the analyzers to one IBM/AT computer.

Quality Control

Development of Procedure

In developing the analytical procedure, the following aspects were considered: detection limits, cost, and accuracy. To decrease the cost, only a moderate accuracy, ±10–20%, was sought. The main consequences of this are: 1) there is no need to correct for the moderate flux variations between samples irradiated in one plane, and 2) a low activity and relatively short measurement time causing non-ideal counting statistics, is acceptable. In almost all other respects the maximum accuracy could be sought.

The possible errors include: sample representativity; contamination; weights; standards; flux variation; interfering nuclear reactions; neutron absorption; counting geometry; gamma-ray absorption; pulse pile-up, analyzer dead time; and interpretation of gamma-ray spectra.

The small sample size calls for a very homogeneous sample. This can be taken care of for all elements except gold. Additionally, contamination is a special problem to be addressed in the case of gold.

The standards are analyzed in our own laboratory using specially prepared liquid standards and earlier established standards. They are checked against international reference samples.

Figure 1 shows the flux variation in the irradiation positions used. The average variation within the plane is ±3%. The horizontal variation within one container is about ±3%. The average flux difference between the layers of the samples is corrected for by using predetermined flux correction factors. Thus the average flux variation of individual samples relative to the standards is less than ±10%.

With the exception of nickel, the analysis is based on (n;γ) reactions. The same radionuclides can be produced by the fission of ^{235}U, ^{238}U and ^{232}Th and by fast neutron reactions. Of the latter, only $^{54}Fe(n;\alpha)^{51}Cr$ can constitute a serious source of error. The effect of Ti, $^{46}Ti(n;p)^{46}Sc$, cannot be corrected without analyzing Ti separately, but it is negligible in most cases. The effect of the fission products is usually negligible, but has to be kept in mind.

With the small samples used, neutron absorption is negligible except in the case of gold. In average gold concentrations of less than 1 ppm, it has not been of significance, but in some cases intercomparisons with other analytical techniques have shown a 10% negative error in concentrations of 10 ppm or higher.

Errors in the counting geometry can be avoided by always filling the capsules. The sample positioning, effected by means of the sample changer, is accurate.

Gamma-ray absorption is negligible with the small samples and relatively high gamma-energies used. With a few exceptions the sample activity is so low that the analyzer dead time is ~3%. Therefore the dead time correction is accurate and pulse pile-up negligible.

The statistical error is quite a good estimate of the total error in the peak intensity, as calculated by the computer program in use [3].

A set of USGS geochemical standards was analyzed to check the overall behaviour of the procedure [4]. The agreement was satisfactory.

Quality Control of Routine Analysis

The purpose of this exercise is to assure that the analysis is continuously performed according to the criteria determined when the procedure was developed. Possible errors include: wrong standards; sample in wrong place during irradiation or measurement; Cd-lock of irradiation capsule ajar; wrong input data; malfunction during measurement; and too active a sample.

A number of control functions and samples are used to avoid the errors mentioned above or to find them after their occurrence.

Figure 2 shows the irradiation configuration and figure 3 the measurement configuration of one series of samples. The control samples are used to check that the samples are in the intended positions during irradiation so that the flux corrections will be right. It has happened that one sample tube is upside down during irradiation. Possible changes in the flux distribution due to other reasons can also be detected in this manner.

The results of the control samples are automatically compared with the "true values," and if a difference greater than ±10% is found, a warning is given. The results are then controlled manually to find out the reason for the error. A warning is also given if a sample is too active.

Table 1 gives typical long-term results of a control sample. The results of 33 samples were collected over a period of 6 months.

Conclusions

IENAA has now been used for 7 years in the Reactor Laboratory. Annually 6000–1300 samples have been analyzed. The reliability of the results has been improved by increasing the number of control samples. The automated data control by the program has also been developed to prevent errors in advance and to aid in studying the results. Because most of the samples are analyzed for geochemical exploration, the acquired accuracy of ±10–20% is sufficient.

Volume 93, Number 3, May–June 1988
Journal of Research of the National Bureau of Standards

Table 1. The mean value ($\bar{x}\pm$S.D.) of 33 control samples and the calculated error from the recommended value. The sample is a rock standard produced by the Geological Survey of Finland

Element	Mean value (ppm)	Recommended value (ppm)	Relative Difference (%)
La	82±5	88	6.8
Sm	7.1±0.6	7.8	9.9
Fe	14400±1800	15600	7.7
Co	24.2±1.8	25	3.2
Na	21800±2000	22000	0.9
Sc	3.4±0.4	3.5	2.9
Ba	1090±100	1100	0.9
Cs	6.3±0.5	6.5	3.1
Rb	220±20	225	2.2
Ta	2.2±0.3	2.3	4.3
U	12.7±1.0	13	2.3
Th	52±3	53	1.9

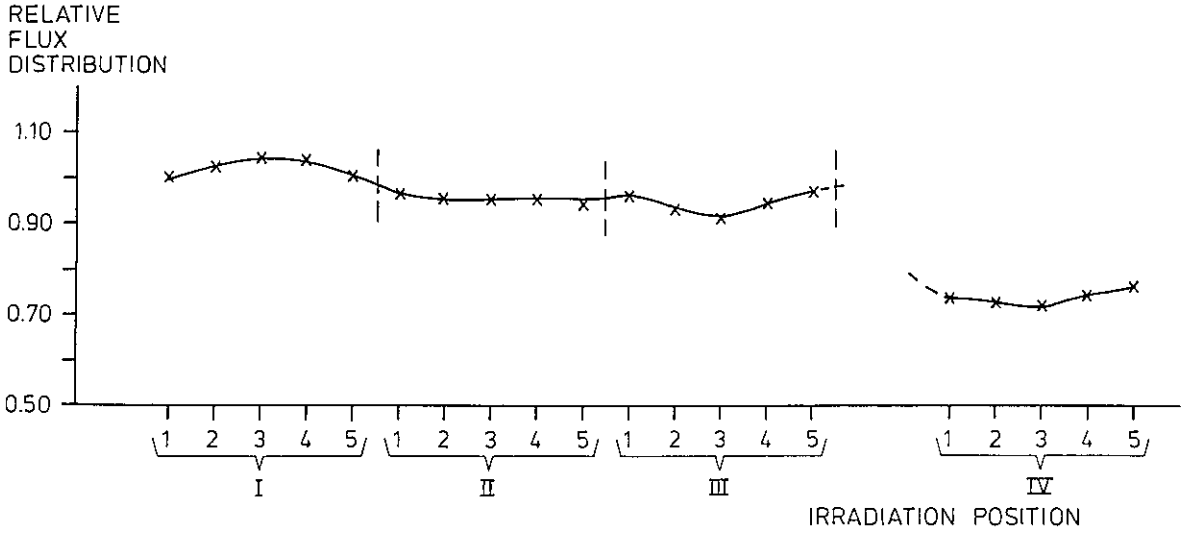

Figure 1. Flux variation in irradiation position.

Volume 93, Number 3, May–June 1988
Journal of Research of the National Bureau of Standards

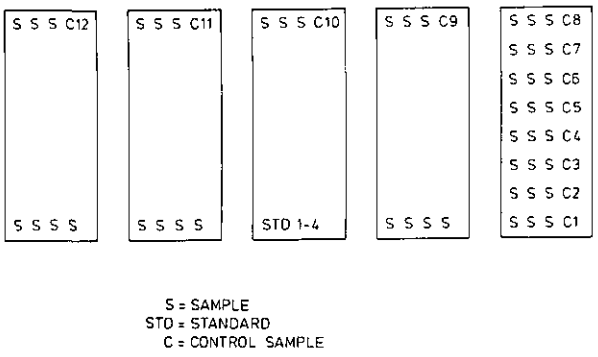

Figure 2. Irradiation configuration.

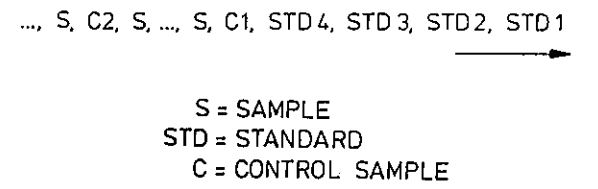

Figure 3. Measurement configuration.

References

[1] Date, A. R., Preparation of Trace Element Reference Materials by a Co-precipitated Gel Technique, Report No. 101, Institute of Geological Sciences, London, March 1977.
[2] Vänskä, L., Rosenberg, R. J., and Pitkänen, V., Nucl. Instrum. Methods **213**, 343 (1983).
[3] Rosenberg, R. J., and Vänskä, L., STOAV84, a Computer Program for an Automatic Gamma Spectrometer for Activation Analysis, Technical Research Centre of Finland, Research Notes 415, Espoo, 1985.
[4] Rosenberg, R. J., Kaistila, M., and Zilliacus, R., J. Radioanal. Chem. **71**, 419 (1982).

Importance of Chemical Blanks and Chemical Yields in Accurate Trace Chemical Analysis

W. R. Kelly and S. A. Hotes

Inorganic Analytical Research Division
Center for Analytical Chemistry
National Bureau of Standards
Gaithersburg, MD 20899

1. Introduction

"The fundamental limitation to accuracy in chemical analysis is systematic error" [1]. Systematic error arises whenever the actual nature of the measurement process differs from that assumed. For a measurement to be both accurate and precise the measured value must be corrected for all sources of systematic error or bias and the true value must lie within the stated uncertainty with some stated level of confidence. Accurate chemical determinations require accurate knowledge of the chemical blanks and chemical yields at each stage of the separation process. A true blank correction can only be made if the exact functional form of the blank correction is known. If the blank correction is not exact, a bias may be introduced in the final value.

Murphy has noted that the analytical blank may be considered the "Achilles Heel" in chemical analysis [2]. Frequently, precise and otherwise accurate methods produce highly biased results from a lack of knowledge of, or improper consideration of, the chemical blank. For many types of measurements it is frequently necessary or highly desirable to isolate the element of interest in essentially pure form from the matrix in which it is found. This procedure typically involves decomposition of a sample with mineral acids and isolation of one or more elements by several solvent extraction or ion exchange steps. In each purification step, sample and blank atoms may be lost resulting in blank amplification in succeeding steps. The relationship between chemical yields and blank amplification is seldom discussed in the literature. Although blanks are frequently discussed in the chemical literature and guidelines for evaluating the blank correction have been published (see e.g., [3]), we are aware of only a few papers where the relationship between blanks and chemical yields is discussed [4–7].

Volume 93, Number 3, May–June 1988
Journal of Research of the National Bureau of Standards

In this note, we limit our focus to the effect of chemical blanks and chemical yields on the accuracy of chemical measurements. Their effect on both accuracy and precision will be discussed in more detail in a later paper.

2. Definition of Chemical Yield and Chemical Blank

For this discussion the term chemical yield is synonymous with the term recovery which refers to the fractional amount of a substance reclaimed from a purification process. We will take the following as an operational definition of the chemical blank: the chemical blank is the sum of all sources of the element or compound being determined that is not indigenous to the sample but is measured by the detector. Chemical species other than the analyte of interest that give the same response in the detector are not considered chemical blank.

3. Accuracy

An accurate measurement is one which obeys the following condition:

$$|M_c - T| = 0 \tag{1}$$

where T is the true value and M_c is the corrected experimentally measured value given by one of the following two relations:

$$M_c = f(M, B_i, Y_j) \tag{2a}$$

$$M_c = M - f(B_i, Y_j) \tag{2b}$$

In actual practice we say that a measurement is accurate if it differs from the true value by less than some specified amount, say ϵ:

$$|M_c - T| < \epsilon \tag{3}$$

where B_i and Y_j are the chemical blanks and chemical yields which are subject to the boundary conditions:

$$b_k - < B_i < b_l \tag{4a}$$

$$y_k < Y_j < y_l \tag{4b}$$

where the absolute magnitude of the upper and lower bounds may or may not be equal. We are interested in examining the functional form [eqs (2a) and (2b)] that relates the measured value, the chemical blanks, and the chemical yields. In particular we wish to know under what conditions, if any, measurements can be made to obey eq (1).

4. Difference Between External and Internal Techniques

Chemical techniques can be grouped into two broad categories. For convenience, we will refer to techniques that have an internal standard as internal techniques whereas those that require external standards as external techniques. An example of an internal technique is isotope dilution in which an enriched or radioactive isotope of the element of interest is added to the sample. After dissolution of the sample and separation of the element of interest from the matrix the isotopic ratio of the mixture is then measured. Examples of the external techniques are the many spectroscopic techniques that compare the response of the sample to that of a standard. We wish to consider the functional form of several blank corrections and compare these to the exact blank corrections to ascertain the magnitude of the bias that is introduced. We will assume that measuring devices in both the internal and external cases are perfect and introduce no error. We will assume that both techniques must dissolve the sample and chemically separate the element of interest by an n-step separation process. During the dissolution step the sample picks up a reagent blank, B_R, and at each successive separation step the sample is subject to a blank B_i. After the chemical separation process the sample encounters an instrumental blank or loading blank inherent to the measurement system designated as B_L. We will consider the case which is encountered in most instances in chemical analysis in which both sample and blank are lost together for a two-step ($n=2$) separation process.

4.1 External Case

For the external case the measured value is given in general by the following relation:

$$M = (T + B_R)\prod_{j=0}^{n} Y_j + \sum_{i=1}^{n} B_i \prod_{j=i}^{n} Y_j + B_L \tag{5}$$

which gives for $n=2$ the following:

$$M=Y_0Y_1Y_2T+Y_0Y_1Y_2B_R+Y_1Y_2B_1 + Y_2B_2+B_L \quad (6)$$

which on rearrangement gives for the true value the following:

$$T=\frac{M}{Y_0Y_1Y_2}-\left[B_R+\frac{B_1}{Y_0}+\frac{B_2}{Y_0Y_1}+\frac{B_L}{Y_0Y_1Y_2}\right] \quad (7)$$

Therefore, for the external technique eq (1) only holds true when the right hand side of eqs (2) and (7) are identical. It is evident from eq (7) that to measure the analyte accurately requires knowledge of eight unknowns. Note that the measured value must be divided by the total chemical yield before applying the blank corrections. Therefore, even if the chemical blanks are negligible the measured value will be less than the true value for yields less than unity.

4.2 Internal Case

For the internal case the measured value, M, is given in general by the following:

$$M=T+B_R+\sum_{i=1}^{n}B_i\prod_{j=0}^{i-1}Y_j^{-1}+B_L\prod_{j=0}^{n}Y_j^{-1} \quad (8)$$

which gives on rearrangement for $n=2$ the following for the true value, T:

$$T=M-\left[B_R+\frac{B_1}{Y_0}+\frac{B_2}{Y_0Y_1}+\frac{B_L}{Y_0Y_1Y_2}\right] \quad (9)$$

which is similar to eq (7) for the external case but with the very important difference that the measured value is not divided by the total chemical yield. Therefore, if the chemical blanks are negligible the measured value will be equal or very close to the true value. This is a unique advantage of isotope dilution compared to other techniques. It is commonly stated that the accuracy of isotope dilution is independent of chemical yields. However, it is important to emphasize that the chemical yield does in fact enter into the final value of an isotope dilution measurement in the blank correction terms as shown in eq (9). This fact is frequently overlooked or not considered when measurements are reported.

5. Comparison of External and Internal Methods

A simple way of illustrating the differences between the two methods is to consider the case which is often encountered in trace determinations where the blank approaches the size of the analyte of interest. For illustration let us assume that $T=10$, $B_R=1$, $B_1=2$, $B_2=2$, $B_L=0.1$, and $Y_0=1$.

5.1 Case A—No Blank or Yield Correction

In figure 1, the measured values for the external [eq (6)] and internal [eq (8)] techniques are plotted assuming no corrections for chemical blanks or chemical yields. Note that the internal method is close to the true value but is biased in the positive direction for all values of Y_1. Because Y_2 only appears as a coefficient of B_L, the measured value is not strongly influenced by the value of Y_2 [see eq (8)]. The measured values from the external technique define a line of negative slope whose intercept is strongly influenced by the value of Y_2. As Y_2 becomes smaller the line moves to lower values.

5.2 Case B—Total Blank Correction, No Yield Correction

This is the type of correction that is frequently used by chemists and is referred to as a straight blank correction. In this case the total chemical blank, $B_T=B_R+\Sigma B_i+B_L$, is subtracted from the measured value, M. This gives for the external and internal techniques the following two equations which are plotted in figure 2 for $Y_2=1$:

External Technique

$$M_c=T(Y_0Y_1Y_2)+B_R(Y_0Y_1Y_2-1) + B_1(Y_1Y_2-1)+B_2(Y_2-1) \quad (10)$$

Internal Technique

$$M_c=T+B_1\left(\frac{1}{Y_0}-1\right)+B_2\left(\frac{1}{Y_0Y_1}-1\right) + B_L\left(\frac{1}{Y_0Y_1Y_2}-1\right) \quad (11)$$

From inspection of eqs (10) and (11) one can see that for the external case $M_c \leqslant T$ for all values of B_i, whereas the converse ($M_c \geqslant T$) is true for the internal case. As Y_2 becomes smaller the external

line drops to lower and lower values whereas the internal line is essentially unchanged due to the small dependence of eq (11) on Y_2. It is clear from figure 2 that the internal method gives a more accurate result for all values of B_i and Y_j.

5.3 Exact Correction—Internal Case

It should be noted that with isotope dilution it is possible to measure the chemical yield at any point in the chemical separation for each sample by adding another isotope to the sample. For the case of $n=2$, if one knows the B_i's, and determines the chemical yield after step 1, this allows the following approximate blank correction to be used:

$$f(B_i, Y_j)=B_R+B_1+\frac{B_2}{Y_0Y_1}+\frac{B_L}{Y_0Y_1} \quad (12)$$

Subtracting the r.h.s. of eq (12) from the r.h.s. of eq (8) gives the following for the corrected value:

$$M_c=T+B_1\left(\frac{1}{Y_0}-1\right)+B_L\left(\frac{1}{Y_0Y_1Y_2}-\frac{1}{Y_0Y_1}\right) \quad (13)$$

which for $Y_0=1$ is a function of only B_L and the chemical yields. Since the coefficients of B_1 and B_L are positive $M_c \geqslant T$. Equation (13) yields values which differ from the true value by a very small amount. For example, for $Y_1=Y_2=0.5$ eq (13) equals $T+2B_L$.

6. Conclusions

The important point is that all approximations to the blank and yield correction introduce a systematic error into the final result whose magnitude will depend on the Sample/Blank ratio, the chemical yields, and blanks for individual steps in the separation process for $n \geqslant 1$. If chemical yields cannot be determined, they should be bounded. The number of separation steps should be kept as small as possible because the number of unknowns is equal to $2n+4$. For $n=2$, a nearly exact solution can be used in isotope dilution determinations which is not true for the external method case because the yields must be determined in parallel experiments and cannot easily be determined on an individual sample.

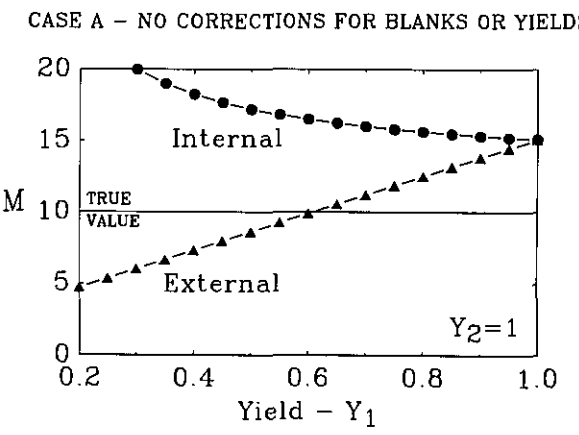

Figure 1. Plot of the measured values for the External [eq (6)] and the Internal [eq (8)] methods.

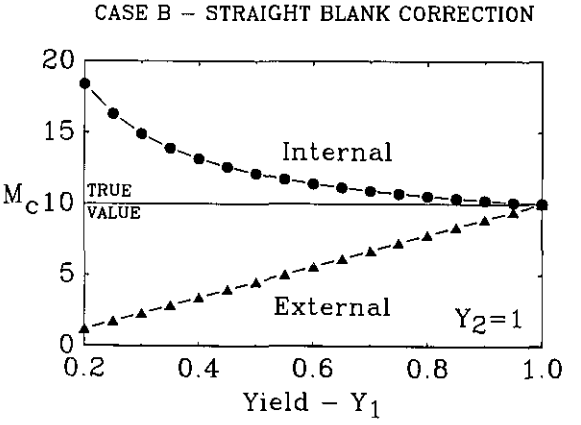

Figure 2. Plot of the corrected measured values [eqs (10) and (11)] using as the blank correction total subtraction of the chemical blank.

References

[1] Currie, L. A., and DeVoe, J. R., Systematic Error in Chemical Analysis, in Validation of the Measurement Process, ACS Symposium Series, No. 63, DeVoe, J. R., Ed., American Chemical Society: Washington, DC (1977) 114–139.

[2] Murphy, T. J., The Role of Analytical Blank in Accurate Trace Analysis, in Accuracy in Trace Analysis: Sampling, Sample Handling, Analysis, LaFleur, P. D., Ed., U.S. Government Printing Office: Washington, DC (1976) 509–539.

[3] Taylor, J. K., J. Test. Eval., 54 (1984).

[4] Stukas, V. K., and Wong, C. S., Accurate and Precise Analysis of Trace Levels of Cu, Cd, Pb, Zn, Fe, and Ni in Seawater by Isotope Dilution Mass Spectrometry, in Trace Metals in Sea Water, Wong, C. S., Boyle, E., Bruland, K. W., Burton, J. D., and Goldberg, E. D., Eds., Plenum Press (1983) 513–536.

[5] Patterson, C. C., and Settle, D. M., The Reduction of Orders of Magnitude Errors in Lead Analyses of Biological

Materials and Natural Waters by Evaluating and Controlling the Extent and Sources of Industrial Lead Contamination Introduced During Sample Collecting, Handling, and Analysis, in Accuracy in Trace Analysis: Sampling, Sample Handling, Analysis, LaFleur, P. D., Ed., U.S. Government Printing Office: Washington, DC (1976) 321-351.

[6] Kelly, W. R., and Fassett, J. D., Anal. Chem. 55, 1040 (1983).

[7] Kelly, W. R., Fassett, J. D., and Hotes, S. A., Health Phys. 52, 331 (1987).

The Importance of Quality Assurance in Trace Analysis

John K. Taylor

National Bureau of Standards
Gaithersburg, MD 20899

1. Introduction

The quality of data must be known if it is to be used in any logical sense in any decision process. Data must be both technically sound and defensible. This simple statement seems axiomatic, yet its impact only recently has been widely recognized. And even today, much of the data generated for environmental, health, and other vital purposes is of questionable quality.

Data quality has impact on the attainable accuracy of every measurement. In trace analysis, which is often pushing the lower limits of measurement, it influences the decision of whether the measured value has any significance, whatsoever.

The effect of data quality on any analytical decision is illustrated in figure 1. The total uncertainty is indicated by the bounds for bias (dotted areas) and the random component (curve enclosed areas). A value just at the decision level, D, has some probability of being either larger or smaller than that *measured*. Even a value of A, well above D, has a probability of being smaller, changing the decision from YES to NO, and conversely for a value B. The indecision zone is clearly a function of imprecision and bias, both of which must be known and estimated.

A similar situation exists for the decision of detection, shown in figure 2. Detection consists in whether a measured value is larger than its uncertainty, and data are only quantitatively useful if their relative uncertainty is reasonably smaller than the measured values. The limit of detection (LOD) and the limit of quantitation (LOQ) depend on the magnitude of the standard deviation and the bounds for bias. The limits in figure 2 correspond to those recommended by the American Chemical Society, Committee on Environmental Measurement [1].

It should be clear that data uncertainty must be known and the measurement system must be stable if data are to be used with confidence. Their quality must be assured by the producer and to the user(s). Until a measurement system has achieved statistical control, it cannot be considered in any logical sense as measuring anything at all [2].

2. What is Quality Assurance?

Quality assurance consists of all activities undertaken to produce data of evaluated quality [3]. It consists of two separate but related activities: Quality Control—What is done to obtain data of acceptable quality, and Quality Assessment—What is done to evaluate the quality of the data produced.

3. Quality Control

All sources of variability of the measurement process must be stabilized and optimized, consistent with the end use of the data. Bias control must be implemented as well. All of these become extremely critical in trace analysis. The major sources of imprecision and bias are shown in table 1. The impacts indicated are for the average case and will differ in importance according to the situation and the degree of control that is achieved.

Table 1. Sources of uncertainty in trace measurements

Source	Impact	Precision	Bias
Sample	high-to-extensive	m	M
Sub-sampling	high	M	M
Chemical operations	high	M	M
Losses	high	m	M
Contamination	medium-to-high	M	M
Blank	medium-to-high	m	M
Calibration	medium-to-high	m	M
Instrumentation	low-to-medium	m	m

m=minor contributor
M=major contributor

Quality control is achieved by careful attention to all factors that affect uncertainty. These may be classified in the general categories shown in table 2 [4]. The emphasis is on doing what is necessary, doing it right, and doing it consistently. The latter is achieved by following optimized protocols. While most of the elements in table 2 are self evident, the acronyms may be less familiar.

Table 2. Elements of quality control[a]

Competent personnel
Suitable facilities
Appropriate methodology
Adequate calibration
GLPs
GMPs
SOPs
PSPs
Inspection
Documentation

[a] See reference [4] for a detailed discussion of the elements.

GLPs— Good Laboratory Practices: protocols that define how general operations are to be carried out.

GMPs—Good Measurement Practices: protocols that define how technique-specific operations are to be carried out.

SOPs— Standard Operations Procedures: protocols that define how measurement and sampling operations are to be carried out.

PSPs— Protocols for Specific Purposes: protocols that define how an entire measurement program is to be carried out.

4. Quality Assessment

The elements of quality assessment are shown in table 3. They are rated according to their importance in evaluating imprecision (P) and bias (B), and also whether they can be provided by a laboratory's internal (I) resources or whether they are provided externally (E). It is evident that precision evaluation, a prerequisite to bias evaluation, should be relatively easy for a laboratory to accomplish without external assistance. Bias evaluation can be done internally, but is is time consuming and requires external inputs if it is to be objective. Both kinds of evaluation must be consistently monitored, preferably using control charts. The consistent measurement of reference materials is the procedure of choice whenever possible. The importance of audits, both internal and external, to monitor both performance and conformance to quality assurance standards is obvious. And, of course, every concerned analyst and analytical laboratory must critically review its outputs (introspection).

Table 3. Elements of quality assessment

Element	Impact	Source	
Replicate measurements	P	I	
Reference materials	B		E
Definitive measurements	B	I	E
Independent methods	B	I	
Spikes	B	I	
Surrogates	B	I	
Collaborative testing	B		E
Audits	P/B	I	E
Control charts	P/B	I	
Introspection	P/B	I	

5. Conclusion

Quality assurance must be extended to every operation that affects the final measured result if valid conclusions are to be made. That is to say the sample, the sampling operation, blanks, calibration, and measurement.

One must always distinguish between attainable accuracy and the accuracy actually attained. The state-of-the-process is often significantly less than the state-of-the-art, resulting from ill-defined tolerances, inadequate control, poorly designed measurement system, and inappropriate use of methodology. All can become major limitations in trace analysis.

Quality is only achieved by consistent and diligent effort and it is best achieved by developing and following an appropriate QA program. But QA is more than a system. It is a philosophy, and indeed a way of life. As a system, it is doomed to disappointment, if not failure. As a philosophy, there is some hope for success. As a system and a philosophy, that is to say a way of life, the prospects for quality data are excellent [5].

Volume 93, Number 3, May-June 1988
Journal of Research of the National Bureau of Standards

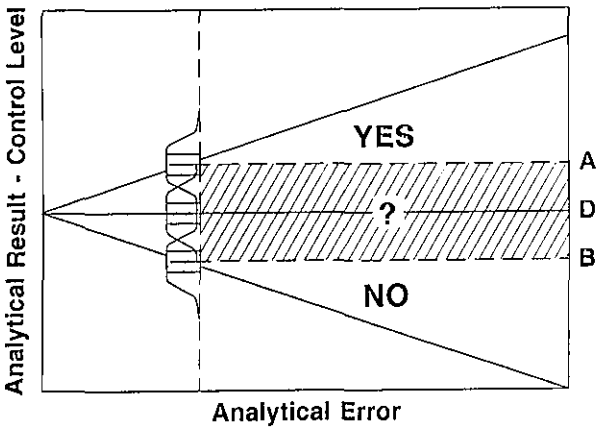

Figure 1. Effect of data quality on analytical decision.

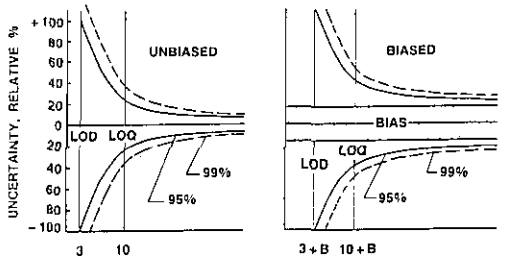

Figure 2. Effect of data quality on decision of selection.

References

[1] Am. Chem. Soc. Report, Principles of Environmental Measurement, Anal. Chem. **55**, 2210 (1983).
[2] Eisenhart, C., J. Res. Natl. Bur. Stand. **67C**, 161 (1963).
[3] Taylor, J. K., Anal. Chem. **53**, 1588A (1981).
[4] Taylor, J. K., NBSIR 85-3104, Natl. Bur. Stand., Gaithersburg, MD 20899.
[5] Taylor, J. K., The Quest for Quality Assurance, Am. Lab. pp. 67-75 (October 1985).

A New River Sediment Standard Reference Material

Michael S. Epstein, Barry I. Diamondstone, and Thomas E. Gills

National Bureau of Standards
Gaithersburg, MD 20899

and

John R. Adams

U.S. Army Corps of Engineers
Buffalo, NY 14207

Several sediment reference materials are available for use in assuring the quality of environmental measurements. These materials have been prepared by various organizations throughout the world, and include bottom sediments from numerous aqueous environments (rivers, ponds, bays, streams, gulfs, etc.) for which either certified or consensus concentration values of inorganic or organic constituents are or soon will be available [1]. As a result of the decreasing supply of Standard Reference Material (SRM) 1645, River Sediment, the NBS Office of Standard Reference Materials authorized the evaluation of candidate materials for a new river sediment SRM. Considerable emphasis was placed on assuring the homogeneity of the sample, the quality of the analyses, and the selection of certified constituents throughout the development of this material, SRM 2704.

Sample homogeneity and analysis quality are reflected in the uncertainty limits that are placed on the certified values. These limits can be used as a realistic estimate of the sum of error sources associated with the collection, processing, and certification of each element in the sample matrix. In round-robin type protocols involving inter- and intra-laboratory comparisons, it has been observed that within-method uncertainties are often significantly less than between-method uncertainties. Assuming that appropriate sampling protocols were followed and that the confidence limits reported for individual methods are not underestimated, it is reasonable to conclude that the imprecision and bias of individual techniques used by different laboratories produces a significant uncertainty in the approved value. As the constituent concentrations

in these materials decrease, the uncertainty associated with reported values increases, since matrix interferences and contamination make larger contributions to the overall uncertainty of the individual analytical techniques. At the lowest concentrations, where the analyst begins to approach the detection limit of the technique, fundamental noise sources [2] become a major source of imprecision, and the number of useful techniques becomes limited.

Ideally, homogeneity information should provide an estimate of the amount of material required so as not to exceed a series of defined sampling uncertainties for each certified element. As discussed by Kratochvil and Taylor [3], homogeneity is estimated using the relationship $WR^2=K_s$, where W is the weight of sample, R is the %RSD of sample composition, and K_s is Ingamell's sampling constant, which is the weight of sample required to limit the sampling uncertainty to 1% with 68% confidence. The sampling constant can be determined by estimating the between-sample standard deviation from a series of measurement sets of different sample weights.

The planning that goes into the preparation of an SRM includes the selection of analytical techniques which have been shown to have adequate sensitivity and precision for specific analyses. In a laboratory such as NBS, which is dedicated to certification work, it usually is easier to select appropriate analytical methods that have been refined over the years, and to run these procedures by trained measurement experts, with readily implemented controls. The controls available in a dedicated certification laboratory usually result in much lower uncertainties than would be possible using a large number of cooperating laboratories in a round-robin consensus approach to certification. The goal of this project was to reduce the uncertainty associated with certified values for the new river sediment below those previously attained for SRM 1645.

Although the ideal sediment reference material should be certified for both inorganic and organic constituents, this is not always possible because the criteria for collection, processing and storage often are different for these two types of constituents. Often, the most desirable equipment for the collection of materials to be certified for organics are the most probable sources of contamination to an analyst interested in inorganics, and *vice versa*. The collection and processing procedures developed for SRM 2704 were designed to minimize inorganic contamination, but where possible, steps also were taken to keep organic contamination to a minimum.

Four grab samples of sediment were collected from the Buffalo, NY area in April of 1985. A series of tests were conducted to develop a scheme for producing a fairly homogeneous sample from a bulk sample, to evaluate various techniques for putting the sample in solution, and to determine the concentrations of the elements of interest. Based on the results of these tests, it was decided to sample from the bottom of the Buffalo River, in the vicinity of the Ohio Street bridge. The Buffalo River sediment was collected in cooperation with the U.S. Army Corps of Engineers in late November 1986, using an unpainted, cleaned, and rinsed clamshell bucket suspended from the crane of a derrick boat. It was known that the sampling site had not been dredged in over 2 years. A sample of proximately 12 to 24 inches of sediment was removed from each full bucket. The dredged sediment was transferred into 55 gallon steel drums lined with teflon bags nested inside of polyethylene bags. Teflon-coated shovels were used to transfer the material to the drums, and care was taken to ensure that the material transferred was not in direct contact with the inside of the bucket (fig. 1). Once the drums were filled, the bags and drums were sealed and transferred to a refrigerated truck. The entire collection was then transported to a facility where it was freeze-dried, screened to pass a 100-mesh sieve, and mixed in a stainless steel blender. The blended material was evaluated for gross homogeneity, and the bulk lot was radiation sterilized at a minimum dose of 2.5 megarads.

The relative homogeneity of the material was assessed using analysis of variance (ANOVA) to separate bottle-to-bottle, sample-to-sample, and instrument variance. Instrument measurement precision was degraded to approximately 1–2% relative by the high dissolved solids content of the samples. No inhomogeneity for Na or Si could be detected when compared to the instrumental measurement variance. Inhomogeneity was definitely observed for the Cr, and marginally for the Fe. Based on this information, the material was reblended. The material was then bottled in 50 g units, producing a total of 3305 units. Fifty bottles, randomly selected from the entire population, were used for the analytical measurements.

The corroborating laboratories and the techniques selected for certification analysis are listed in table 1. Each laboratory was given a set of in-

structions which detailed the number of samples to be analyzed, the dissolution procedures, the control samples to be analyzed, and the information relative to method bias and precision which should be included with the individual reports of analysis. It is expected that all results will be received by the end of 1987, and the new SRM should be available by the spring of 1988.

References

[1] Russel, D. S., Available Standards for Use in the Analysis of Marine Materials, Report NRCC 23025, Marine Analytical Chemistry Standards Program, National Research Council of Canada, Ottowa (1984).
[2] Epstein, M. S., and Winefordner, J. D., Prog. Anal. Atom. Spectrosc. **7**, 67 (1984).
[3] Taylor, J. K., Anal. Chem. **55**, 6, 600a (1983).

Table 1. Corroborating laboratories and techniques selected for certification analysis

Corroborating Laboratories
National Research Council of Canada, Analytical Chemistry Divison
Los Alamos National Laboratory
Oak Ridge National Laboratory
Penn State University, Mineral Constitution Laboratory
Shanghai Institute of Testing Technology, Peoples Republic of China
Virginia Institute for Marine Science
Analytical Techniques
Inductively Coupled Plasma Spectroscopy (ICP)
Instrumental Neutron Activation Analysis (INAA)
Inert Gas Fusion (IGF)
Cold Vapor Atomic Absorption Spectroscopy (CVAAS)
Polarography
Isotope Dilution Mass Spectrometry (IDMS)
Gravimetry
Inductively Coupled Plasma—Mass Spectrometry (ICP-MS)
Laser Enhanced Ionization Spectroscopy (LEI)
Potentiometry
Direct Current Plasma Spectroscopy (DCP)
Ion Chromatography (IC)
Coulometry
Photometry
Hydride Generation Atomic Absorption Spectroscopy (HGAAS)

Figure 1. River sediment being transferred from collection bucket to teflon-lined barrels using teflon-coated shovels.

Volume 93, Number 3, May–June 1988
Journal of Research of the National Bureau of Standards

Accuracy in Trace Analysis

U.S. EPA Reference Standards and Quality Assurance Materials for the Analysis of Environmental Pollutants

R. E. Thompson, J. R. Tuschall, and T. M. Anderson

Northrop Services, Inc.—Environmental Sciences
Research Triangle Park, NC 27709

"The quality of all analytical measurements rests ultimately upon the quality of reference materials employed." This statement is especially appropriate in the determination of trace contaminant residues in environmental matrices. To support the need for a certified, quality-controlled, common database in the analysis of pollutant chemical agents in environmental substrates, the U.S. EPA's Environmental Monitoring Systems Laboratory (Las Vegas) and Environmental Monitoring and Support Laboratory (Cincinnati) jointly maintain several repositories of analytical grade reference materials under the Agency's Quality Assurance Reference Materials (QARM) Project. Operated under contract by Northrop Services in Research Triangle Park, NC, the Project currently offers standards of some 2700 compounds of environmental concern, including pesticides and their metabolites and degradation products; PCBs, chloro- and bromodibenzodioxins and furans, and other halogenated organics; plasticizers; nitrosamines; polynuclear aromatics; and heavy metals and metalloids. Included among these are the Agency-identified compounds commonly known as the "priority pollutants," those materials regulated under Appendix VIII (RCRA) and CERCLA (Superfund) legislation, and groundwater monitoring compounds.

The program is currently being supplied by nearly 200 chemical manufacturing companies and 33 chemical supply houses. Additional commercially-unavailable compounds, especially select environmental reaction and degradation products, are synthesized and purified in-house. Standards are offered, without charge, to any and all laboratories worldwide engaged in environmental monitoring, research, and/or regulatory and enforcement activities. During 1986, more than 150,000 standards were distributed in response to 7,000 requests.

The analyst using Project standards expects the highest quality materials at accurate purity values and concentrations (for solutions), often without knowledge of how the integrity of each is established and maintained. Prior to distribution, each compound is subjected to a rigorous quality assurance program, including (1) component identification, (2) purity assay of neat materials, (3) concentration verification of solutions, and (4) stability studies, using a variety of instrumental methods.

Although acquired materials typically include a percent purity value, each is individually reanalyzed in a series of steps. Chemical identity is verified by mass spectrometry, introduced via gas chromatograph or alternately, by direct insertion probe. For select compounds, other spectroscopic methods—IR, NMR, and ultraviolet spectroscopy—are supplementally employed.

Subsequently, chemical purity is assayed by (at least) two methods, normally one chromatographic (GC, HPLC, TLC) and one non-chromatographic (DSC, NMR, IR, etc.). Establishing purity of a neat material is often complicated by the lack of a uniform response for all components to a single mode of detection. Electron capture, flame ionization, nitrogen-phosphorus, Hall, or mass spectrometric detection are the chromatographic methods of choice for most compounds, whereas HPLC or TLC are used for highly polar or thermo-labile materials. Purity is established by the ratio of peak area of the compound of interest to the combined peak areas for all eluting components. Implicit in this procedure is the assumption that all components elute and produce equal response at the detector. For FID or MS (positive electron impact), the assumption of equal responses is reasonably accurate, although some differences in relative response are inevitable.

Non-chromatographic methods of purity analysis include ultraviolet spectroscopy, NMR, melting point, and differential scanning calorimetry (DSC). The latter method is frequently used for high-purity compounds because the method is typically reliable at purities $>97\%$ and useful for a wide variety of compounds. In DSC analysis, purity is estimated using a van't Hoff plot of melting point data. Typically, agreement of results among methods is within 1–2% and an average value is reported. However, in some cases, a substantial discrepancy in results is observed, necessitating further analyses.

Additionally, isotopic purity of compounds enriched with stable isotopes (^{13}C, ^{37}Cl, D) is established by mass spectrometry. Typical purity of materials distributed exceeds 99%.

The two other components of the quality assurance program that apply to materials available in solution form are concentration verification and stability studies. Subsequent to loading 1.5 mL of a prepared standard solution into several thousand ampuls, a random sample is analyzed from each of three groups (early, middle, and late) of ampuls filled. Analysis (in-house as well as by external referee laboratories) by GC, HPLC, or ultraviolet spectroscopy is performed to establish that concentrations of solutions are within 10% of the target value. Similarly, stability studies (again, on randomly selected ampuls) are performed at predetermined intervals for the duration of storage to verify concentration for prepared solutions in each solvent used. Any compound determined to be unstable is freshly prepared and again subjected to the entire QA program prior to distribution.

In addition to analytical standards, the program supports laboratory quality assurance efforts with other services. Florisil, a differential adsorbent useful in sample clean-up and multiresidue extractions, is available, as are several pre-coated GLC column packings particularly suitable for environmental analysis. Each batch is screened and certified for acceptable separation and recovery, and each sample is provided with an accompanying performance specification sheet and elution profile.

Four times per year, under the Intercomparison Studies project, "spiked" matrix reference materials are provided to laboratories electing to participate in EPA's interlaboratory quality assurance program. Porcine fat, human blood plasma, human urine, and water-miscible solvents are custom-spiked with multi-compound residue levels of various compounds. Field laboratories analyze these materials and return results to be graded in an effort to assess instrumentation accuracy and precision as well as analytical techniques. These samples typically serve a dual purpose as (1) check samples of unknown composition for laboratory intercomparison and (2) after composition is disclosed, internal laboratory control samples for the next 3–6 months.

Technical manuals on analytical methods, analytical quality control, standards preparation, and related topics are also available. An extensive technical library is maintained for requestors' needs, complete with direct terminal access to several major computerized chemical databases. Technical information specialists provide assistance to laboratories with chemical/physical/toxicological data; sample preparation and analytical methodology; instrument troubleshooting; synthesis and purification methods; quality assurance procedures; transportation and waste disposal protocols; and a wide variety of related information. More than 4,000 environmental monitoring and research laboratories in 93 countries are currently utilizing program services.

Volume 93, Number 3, May–June 1988
Journal of Research of the National Bureau of Standards

Industrial Trace Analysis

Characterization of High Purity Silicides

Purneshwar Seegopaul and Maria C. L. Williams

Materials Research Corporation
Orangeburg, NY 10962

The semiconductor industry has produced some exciting and dramatic advances in technology whose impact has been felt universally. Integration of an increasing number of devices on single microchips has necessitated the use of specialized and highly pure materials. The interconnect materials pose unique difficulties as resistivity limitations are reached with the traditional aluminum and polysilicon. Silicides are now being utilized to overcome some of these limitations in interconnect technology. These silicides are basically compounds of silicon with the refractory element of choice in varying stoichiometries that fit the need of the process and metallization sequence. Some common silicides are compounds of silicon and tantalum, tungsten and molybdenum. Silicides are produced by melting silicon with the refractory element of interest.

Characterization of high purity silicides involves both physical and chemical properties. Table 1 lists some of the parameters involved in characterization of these materials. This discussion will focus on the chemical properties of purity and stoichiometry. The silicon to metal ratio is critical to the needs of the application and impurities are incompatible with yield, quality, and reliability of the devices.

Table 2 describes a general strategy in generating the purity and stoichiometry of the silicides. Both "wet" solution-based and "solid"-based methods are exploited for optimum analytical yield and reliability. The techniques include spectroscopic methods for compositional and impurity determination and "LECO" combustion methods for gases. The spectroscopic techniques include atomic absorption, atomic emission, x-ray and mass spectroscopy.

Table 1. Characterization of high purity silicides

Physical properties
Resistivity
Density
Homogeneity
Grain size
Microstructure
Mechanical strength
Temperature profiles
Chemical properties
Etchability
Purity
Stoichiometry
Thin film properties
Physical
Chemical

Table 2. Analytical chemistry of silicides

Analytical parameters	
Stoichiometry	—Composition
Purity	—Impurity content
Techniques	
"Wet" solution-based methods	
a. Atomic absorption spectroscopy	
Flame/graphite furnace	
b. Plasma emission spectroscopy	
Direct current plasma (DCP)	
Inductively coupled plasma (ICP)	
"Solid"-based methods	
a. Energy dispersive x-ray spectroscopy	
b. Mass spectroscopy	
Glow discharge	
Spark source	
c. Combustion "LECO" methods	

Sampling and dissolution of the material for the solution methods are critical. Powdered samples are mixed and blended to ensure homogeneity, while large samples are reduced to small pieces followed by random sampling for dissolution. Dissolution of the silicides introduces the need for special precaution to prevent loss of silicon through

volatilization. This is obviously critical in the compositional analysis. Methods for dissolution are generally based on acid or fusion procedures. The fusion methods use sodium peroxide/sodium carbonate mixtures while the acidic methods utilize a mixture of hydrofluoric acid, nitric acid and water. This work is based on a rapid acidic dissolution method at room temperature. Previous acid methods were very lengthy and involved used of a liquid nitrogen blanket for cooling. The accuracy and precision of this technique were studied and table 3 shows correlation data for % silicon determination by several techniques. The excellent agreement demonstrates the validity of the rapid acidic dissolution without loss of silicon. The % silicon is routinely measured by atomic absorption techniques with a wavelength of 251.6 nm in a nitrous oxide/acetylene flame. The data in table 3 clearly show that any of these methods may be used for this analysis.

Table 3. Correlation data of % Si in silicides

Sample	Atomic absorption		Atomic emission			
			DCP		ICP	
	Duplicate	%Rec	Duplicate	%Rec	Duplicate	%Rec
$MoSi_{2.0}$	36.88	99.5	37.69	99.2	36.84	99.9
	37.00		36.76		36.59	
$MoSi_{1.7}$	32.60	99.2	32.80	99.1	32.60	98.5
	33.60		32.60		32.40	
$TaSi_{2.5}$	27.98	99.0	28.60	98.4	29.00	99.2
	27.70		27.90		28.50	
W_5Si_3	8.20	99.0	8.40	98.9	8.43	98.8
	8.30		8.32		8.42	

As discussed earlier, a combination of analytical techniques are used for determining the impurities in the silicides. These impurities are generally metallics, gases and interstitial elements. The determination of metallics is accomplished by the spectroscopic methods while the gases are measured by combustion type techniques.

The determination of metallics involve sampling, etching to remove surface contamination and dissolution to a 2.5 % w/w solution for analysis. Matrix matching is critical for accurate and precise analysis. All standards are, therefore, properly matrix matched to reflect the stoichiometry of the silicide being analyzed. Incorrect matrix matching results in the suppression or enhancement of the signals used to generate final analytical values. Reference and duplicate samples are routinely analyzed to ensure accuracy and precision. The routine methods consist of ICP and DCP plasma emission spectroscopy and atomic absorption spectroscopy. The ICP spectrometer is equipped with a holographic grating while the DCP spectrometer has an Echelle grating.

Table 4 shows some correlation data of impurities determined in a moly silicide by different techniques. Most of the elements showed excellent agreement between the methods used to generate the data. Copper and chromium gave poor recovery type data in the plasma emission techniques and are analyzed by atomic absorption methods. Interlaboratory studies of silicide analysis were also conducted and the results again revealed excellent correlation.

Table 4. Correlation results of impurities

Analyte	AAS	DCP	ICP	MS
	(ppm)			
Al	<1	<1	0.8	1
Ca	<1	0.9	1.1	0.7
Cu	6	20	14	5
Cr	4	14	25	3
Ni	9	6	6	3
Co	3	<1	<1	0.04
Mg	<1	3	<1	1
Fe	18	17	20	15
Mn	<1	<1	<1	0.1

This discussion highlighted the importance of silicides in the semiconductor industry and the need for accurate and precise analysis. Purity and composition can be readily determined by both atomic absorption and plasma emission techniques.

Volume 93, Number 3, May-June 1988
Journal of Research of the National Bureau of Standards

Accuracy in the Determination of Chlorinated Dibenzo-p-Dioxins and Dibenzofurans in Environmental Samples

L. L. Lamparski and T. J. Nestrick

The Dow Chemical Company
Michigan Applied Science and Technology
Laboratories, 574 Building
Midland, MI 48667

The analytical chemist involved in industrial trace analysis is frequently confronted with many varied problems. Programs to produce acceptable data can be divided into two classes depending upon the level of quality assurance that is required. Frequently, unvalidated analytical procedures can be used to generate data for screening programs or process control. On the other hand, validated methods with rigorous quality assurance guidelines are absolutely necessary for work involving product specifications, industrial hygiene, or regulatory matters.

When the analyst is asked to develop a trace analytical method, he must determine the end-use of the data. There are many parameters which must be factored into the analytical method. The analyst would like to build into the method the highest achievable sensitivity, accuracy, and reliability; and the customer wants the lowest cost and fastest analysis time possible. We can see then, from a practical viewpoint, the method development begins with a series of compromises. When implemented properly, these compromises can improve the overall quality of the method.

The American Chemical Society has published "Principles of Environmental Analysis" [Anal. Chem. 55, 2210 (1983)] to aid in designing analytical measurements on environmental samples. The relationship between the number of samples necessary to obtain data within a defined acceptable error, and the standard deviation of the method, is shown by the equation:

$$N = \frac{(Z\sigma)^2}{E} ,$$

where N equals the number of measurements necessary, Z equals the standard normal variate based upon the level of confidence, σ equals the standard deviation of the method, and E equals the tolerable error in the estimate of the mean. Obviously, for constant values of Z and E, N is proportional to σ^2. Any changes in an analysis method that increase σ will result in an exponentially larger increase in N. When a high degree of accuracy is required, an analytical method with a small σ will have a smaller value of N and require fewer measurements. In fact, by building the highest possible degree of reliability into a method, it may be possible to actually decrease the amount of time necessary to run N analyses. The method reliability can be improved by eliminating or at least recognizing factors which can lead to either high or low results.

High results can be caused by contaminated internal standards or reagents, interferences in the sample, or matrix effects caused by co-extractives in the sample extract. We have taken precautions to minimize the potential for these problems in our method for the determination of chlorinated dibenzo-p-dioxins (CDDs) and dibenzofurans (CDFs) by addressing each area.

1) Isotopically-labeled internal standards can be contaminated with native analyte or with other labeled impurities which could potentially lead to high results. Prior to the use of any internal standard in a sample analysis, we perform an extensive series of GC-MS analyses to verify chemical identity, isotopic purity, chemical purity, and absence of analyte contamination. To date, ~40% of purchased internal standards have failed to meet the criteria for use in our method.

2) Positive reagent blanks can originate from poor equipment cleaning, environmental contamination of sample extracts, or from contamination of chemicals or adsorbents used in the sample preparation. We have imposed a rigorous quality assurance program which involves analysis of a reagent blank with every set of three samples. A positive reagent blank can result in rejection of data and reanalysis of samples after the source of contamination is identified and eliminated.

3) Interferences in sample extracts are minimized by application of identification criteria which include multiple liquid chromatographic separations and gas chromatography-mass spectrometry separation and measurement.

4) Matrix effects can cause high results by changing the mass spectrometer response. The use

of an analyte specific clean-up is useful in minimizing this problem. Identification of the species producing the effect and application of specific clean-up steps can eliminate problems.

Low results can result from incomplete analyte extraction, loss or degradation of the analyte during sample clean-up, or matrix effects. These problems can be eliminated by a careful evaluation of each of the steps employed in the sample preparation.

1) Extraction efficiencies can be improved by dissolving the sample matrix whenever possible and determining the optimum solvent for analyte extraction. When dissolution of the matrix is not practical, an exhaustive extraction procedure with an optimum solvent should be used.

2) Loss or degradation of the analyte can be controlled by determining the recoveries of all analytes through each clean-up step. An understanding of the chemical and physical properties of the analyte will not only improve recoveries, but also can allow optimization of each clean-up step.

3) Matrix effects leading to low results generally are caused by exceeding the capacity of the clean-up procedure for either analytes, related compounds, or coextractive species. This "overloading" can change the chromatographic retention of the analyte. In general, these effects can be minimized by decreasing the sample size or using a high-capacity pretreatment step to remove the coextractives.

Application of these precautions can result in a method which does not generate false positive or false negative results. A recent collaborative study to determine fortified levels of CDDs and CDFs in human adipose tissue at 5–50 pg/g has been completed by eight laboratories highly experienced in the determination of CDDs and CDFs [Albro et al., Anal. Chem. **57**, 2717 (1985)]. By implementing the practices described above, laboratory 2 avoided generating either unaccountably high or low results (table 1).

The apparent drawback of the laboratory 2 method is the relatively long analysis time per sample. However, when the standard deviation of the recoveries for each laboratory is calculated and used in the equation to determine the relative time to analyze N samples (measurements necessary to yield data of defined statistical reliability), method 2 can actually generate data with a specified precision in the shortest time.

Table 1. Interpretation of recovery data from CDD/CDF collaborative study

	Lab 1	Lab 2	Lab 3	Lab 4	Lab 5	Lab 6	Lab 7	Lab 8
Avg. analysis time days/sample	0.9	2.6	0.6	1.0	1.0	1.5	–	2.5
Number of values unaccountably high	4	0	2	6	2	3	16	3
Number of values unaccountably low	0	0	0	1	10	8	7	0
Avg. recovery	115%	97.7%	114%	147%	97.0%	50.3%	135%	151%
σ (S.D. rec.)	51%	19%	48%	94%	143%	39%	123%	64%
n	26	23	23	26	23	26	23	25
Rel. time to N	2.5	1	1.5	9.2	22	2.4	–	11

$N \propto \sigma^2$.

Relative time to $N = \dfrac{(\sigma_{Lab})^2 \times \text{days/sample}}{(\sigma_{Lab2})^2 \times 2.6 \text{ days/sample}}$.

Pharmaceutical Trace Analysis

D. Scott Aldrich, Steven J. Borchert, Amy Abe[1], and James E. Freeman

The Upjohn Company
Kalamazoo, MI 49001

Trace analysis can have various meanings, depending on the context of the problem at hand. This paper focuses on one aspect of trace analysis relevant to quality control in the pharmaceutical industry. Trace levels of contaminants in pharmaceutical materials and products can present significant analytical challenges in many ways. For example, organic impurities in drugs and drug products are typically controlled to levels from 0.01–1.0%. Detecting and quantitating species at these levels represents a complex problem in

[1] The Sherwin-Williams Company, Chicago, IL.

mixture analysis. The development of such methods frequently requires the analysis of overlapped chromatographic peaks and chemically labile species. For compounds of acute toxicological concern, part-per-billion (ppb) levels must sometimes be monitored. Apart from toxicology issues, some chemical contaminants present at a few ppm can produce undersirable color or odor in a product.

Although the above examples represent everyday problems in pharmaceutical trace analysis, the focus of this paper is in another area: the detection, identification, and control of trace levels of insoluble material in drug solutions. Insoluble materials can occur as individual particles visible to the eye, visually perceptible haze, or subvisible particles. Some medical evidence of the consequences of particulate matter entering the bloodstream does exist [1–3]. Furthermore, various compendial regulations limit the numbers and sizes of particles allowed in parenteral drug products [4–6]. For example, no particles visible to the eye may be present. Recent trends within the pharmaceutical regulatory community indicate increasingly restrictive requirements pertaining to particulate matter.

The particle size range of interest for pharmaceuticals is 5–100 μm. The lower limit is determined by the size of capillary blood vessels, and the upper limit is the threshold of visible detection. That this type of contamination is a trace analytical problem can be appreciated from the data in table 1. The concentrations of particles fall in the ppm range, and typically as little as a few nanograms of material must be detected and analyzed.

Table 1. Mass and concentration of 1 g/cm^3 spherical particles at various regulatory limits

Limit	Particle mass per container (μm)	Particle concentration (ppb)
One 100-μm particle per 10-mL container	0.52	52.
1000 2-μm particles per mL	0.0042	4.2
100 5-μm particles per mL	0.0065	6.5
50 10-μm particles per mL	0.026	26.
5 25-μm particles per mL	0.041	41.

Because particulate matter must be controlled on a routine basis, the best approach to dealing with such problems is in the formulation and manufacturing design stages. We have followed this strategy: (1) detection and problem definition, (2) isolation and sample preparation, (3) identification, and (4) elimination of the mechanism of particle formation [7]. The following discussion includes brief descriptions of each of these points and examples of actual problems we have encountered.

The characteristics of human and instrumental particle-detection technology have been thoroughly described in the literature ([7], and references therein). Two alternatives exist for detecting "visible particles," i.e., particles >100 μm. Human visual inspection, while sensitive and selective as to its ability to classify particle types, suffers from inspector fatigue and poor reproducibility. This process has been shown to be probabilistic, not deterministic: it cannot detect visible particles with 100% certainty. Machine visual inspection is more reproducible and possesses a lower particle-size detection limit. Subvisible particles must not only be detected, but also sized and counted. A number of instrumental approaches to this problem have been developed, but the method based on detecting and sizing particles by their ability to block a light beam has been almost universally adopted by the pharmaceutical industry.

Proper definition of the problem as, for instance, individual large particles, haze, etc. is important for the next steps, which involve isolation of the particles and preparing them for analysis. Commonly, only a small number of product containers with only a few particles are available for analysis. The most common isolation techniques are filtration and single-particle isolation by micropipette. The surface on which particles are isolated can determine what subsequent analytical techniques can be applied. We have found the use of gold-coated membrane filters to be particularly useful when surface-sensitive spectroscopic techniques are to be used.

Microscopy is invariably the first technique applied to particle analysis: microscopy is sensitive, with a detection limit of one picogram, and it is ideally suited to assessing the heterogeneity of the isolated particles. Light microscopy techniques can determine refractive index, crystal form, solubility, thermal properties, and some chemical properties. Elemental analysis (scanning electron microscopy/x-ray fluorescence, ESCA), molecular spectroscopy (infrared, Raman, mass spectrometry), and other techniques (light scattering, x-ray diffraction, chromatography) must frequently be used to completely identify particulate matter. Importantly, SEM/XRF, Raman, and infrared spectroscopy can each be used to analyze nondestructively single particles.

Identification includes not only chemical identity, but also the source of the particles. Particles can arise from the manufacturing environment, packaging materials, or the drug solution itself. The examples described below illustrate two such sources. Once the mechanism of particle formation is understood, steps to eliminate it from the product design can be taken.

In the first example, large visible particles were detected in a diluent solution used for reconstituting lyophilized drug powders. The solution contained water, methyl and propyl paraben, and sodium pantothenate. Microscopy revealed a heterogeneous matrix, one component of which was identified by infrared spectroscopy as silicone oil. SEM/XRF analysis revealed the presence of Cu and S; the remainder of the particles was organic in nature. Using x-ray fluorescence and atomic absorption spectroscopy, Cu was quantitated in solution at about 1 ppm and traced to the lot of sodium pantothenate used for these preparations. Product manufactured from other lots of sodium pantothenate containing lower levels of Cu did not produce a significant amount of precipitate.

Copper alone could not account for the formation of the precipitate, and the presence of silicone oil implicated the lubricated rubber stoppers. A series of experiments demonstrated that both the presence of Cu and contact with the rubber stoppers used in the product were necessary to form particles. Subsequent mass spectral analysis of the particles confirmed the presence of a common vulcanizing agent, 2-mercaptobenzothiazole (MBT). MBT is known to be extracted from rubber by contact with aqueous solutions, and its reaction with Cu yields a highly insoluble complex [8–10]:

$$\mathrm{Cu}+2\,\mathrm{MBT}=\mathrm{Cu(MBT)_2}, \qquad K_{sp}=10^{-21}\ .$$

Experiments confirming the Cu concentration dependence of particle formation, as well as identification of the individual components, were important to discovering this mechanism. An obvious solution to this problem is the use of stoppers which do not contain MBT.

In the second example, particles were observed as a fine "smoke" in a new product under development. Interestingly, the smoky character of the particles prevented their detection by machine inspection; only careful human inspection revealed their presence. Microscopically, these particles were amorphous flakes 10–30 μm in size. SEM/XRF analysis did not detect elements of atomic number >9. ESCA detected significant amounts of only C and O, and high-resolution measurements suggested the presence of an ester functional group. Infrared analysis detected carbonyl and C–O–C stretching frequencies characteristic of aromatic esters, and Raman spectroscopy confirmed the presence of aromatic functionality with a band at 1000 cm^{-1}. Mass spectrometry revealed several series of repeating mass fragments and, hence, the polymeric nature of the particles. A detailed analysis of the infrared and mass spectra (figs. 1 and 2), followed by analysis of specially synthesized authentic material, confirmed the identity of the particles as poly(diethyleneglycol)isophthalate. This material was subsequently traced to filtration equipment used during synthesis of the drug.

These examples illustrate the wide range of techniques which can be used to identify particulate matter. Detection and resolution of such problems contributes significantly to the design and manufacture of high-quality pharmaceutical products.

Acknowledgments

The authors would like to acknowledge the contributions of Robert S. Chao, Frank W. Crow, Wayne K. Duholke, Lloyd E. Fox, Ronald W. Maxwell, and Robert D. White.

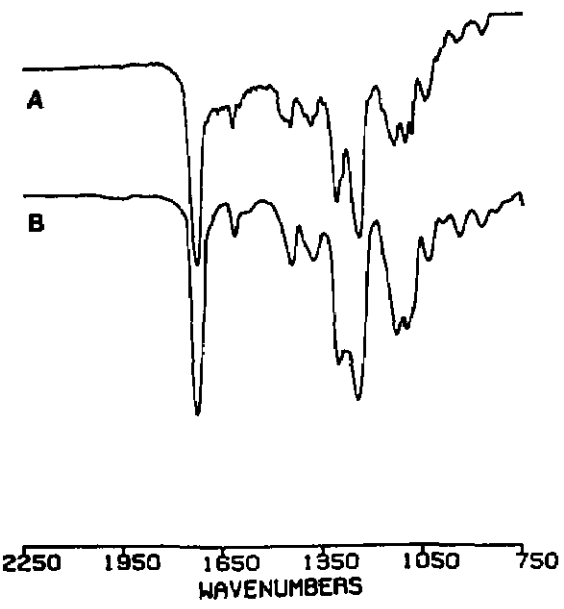

Figure 1. Infrared spectra of (A) particles and (B) synthetic poly(diethyleneglycol)isophthalate.

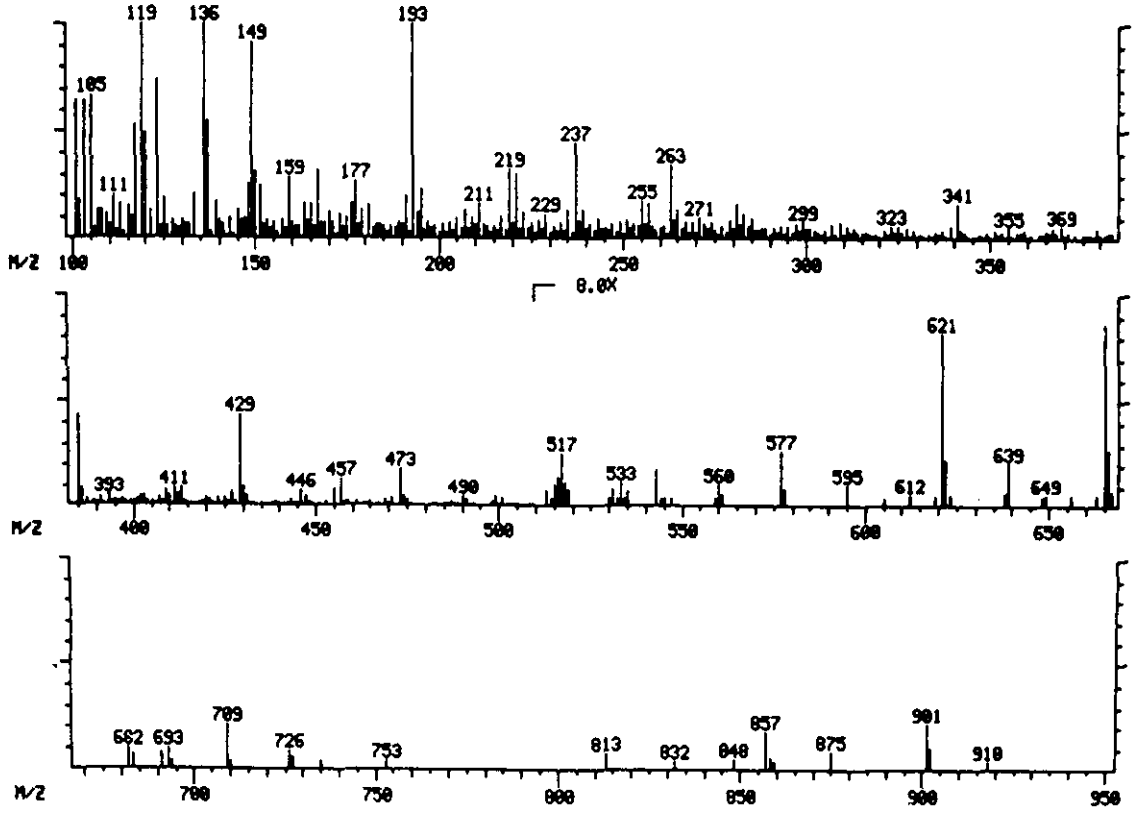

Figure 2. Desorption chemical ionization mass spectrum of particles.

References

[1] Turco, S., and Davis, N. M., Hosp. Pharm. **8**, 137 (1973).
[2] Thomas, W. H., and Lee, Y. K., N. Z. Med. J. **80**, 170 (1974).
[3] Akers, M. J., Parenteral Quality Control: Sterility, Pyrogen, Particulate, and Package Integrity Testing, Marcel Dekker, Inc., New York (1985) p. 143.
[4] The United Stated Pharmacopoeia, Twenty-First Revision, Mack Publishing Company, Easton, PA (1984).
[5] British Pharmacopoeia 1980, Volume II, University Press, Cambridge (1980).
[6] The Pharmacopoeia of Japan, Part I, Tenth Edition, Yakuji Nippo, Ltd., Tokyo (1982).
[7] Borchert, S. J., Abe, A., Aldrich, D. S., Fox, L. E., Freeman, J. E., and White, R. D., J. Parenteral Sci. Technol. **40**, 212 (1986).
[8] Boyett, J. B., and Avis, K. E., Bull. Parenteral Drug Assoc. **29**, 1 (1975).
[9] Prajapati, S. N., et al., J. Inst. Chem. Calcutta **47**, 99 (1975).
[10] Rusina, O. N., Mater. Nauch-Tekh. Kanf Sev-Kavkaz Gornomet. Inst. 69 (1970).

Organic Microanalysis of Submicrogram Samples

Douglas B. Hooker and Jack DeZwaan

The Upjohn Company
Kalamazoo, MI 49001

1. Introduction

Information on the elemental composition of materials can be of great value in a variety of research problems. Obtaining this information is a problem in cases where only a very small amount (micrograms) of material is available since conventional microanalytical techniques require much larger (milligram) samples for each elemental determination. In these situations, a method which would determine all the elements present using a single, submicrogram sample would be useful.

Atomic emission generated from samples which have been introduced into a microwave plasma (MIP) has been investigated extensively as a means of element specific detection and as a means of elemental ratio determination [1,2]. Microwave plasmas generated in a helium carrier are especially useful because high levels of excited atomic states of several interesting nonmetals such as carbon, nitrogen, phosphorous, sulfur and the halogens can be generated [3,4]. Simultaneous measurement of emission from the desired elements provides the potential for multielemental determination using a single submicrogram sample.

Although gas phase procedures for introducing samples into microwave plasmas have been the most reliable, they cannot be used with most solid samples. Electro-thermal procedures have also been reported for some sample types [5,6]. The more general method of sample introduction for nonvolatile samples reported here uses a fine quartz filament to deliver a sample to a low pressure microwave plasma. This procedure delivers the sample to the plasma intact, producing sharp responses of around a second in duration at all emission wavelengths. A series of samples containing C, S, F, and Cl are used to evaluate the performance of this technique in determining elemental ratios in solid, nonvolatile samples and in predicting empirical formulas with complementary mass spectral data.

2. Experimental

The data were generated on a commercial instrument, the MPD 850 (Applied Chromatography Systems, Lutton, Bedfordshire, U.K.). This instrument was designed as a gas chromatographic detector and was modified for solid sample introduction. The MIP was produced in a 1/4-wave Evanson type cavity using chromatographic grade helium at ~10 torr, containing about 0.2% oxygen to prevent carbon buildup on walls of the quartz tube confining the plasma. Forward microwave power of 100 watts at 2.45 GHz was used with minimal reflected power. The grating produced a reciprocal dispersion of 1.39 nm/mm (first order).

Elemental emission was detected simultaneously at the wavelengths shown in table 1. The photocurrents were amplified and digitized (120 Hz) and stored on a Harris H1000 computer.

The sample delivery device, illustrated in figure 1, consists of a quartz filament (0.0776–0.102 mm diameter) inside a hollow-fused silica guide (OD=0.42 mm and ID=0.32 mm). This assembly was contained within the enclosed vacuum manifold. Individual magnets were attached to both the filament and the guide tube which allowed them to be moved in tandem or individually with magnets on the outside of the manifold.

Table 1. Wavelengths monitored and the slit widths used to monitor atomic emission

Element	Wavelength (nm)	Slit width (μm)
Carbon	247.86	75
Chlorine	479.45	50
Sulfur	545.39	50
Fluorine	685.60	75

Samples were loaded from chloroform solution directly onto the quartz fiber using a 10 μL Hamilton syringe at Port A. The solvent was allowed to evaporate before analysis. Complete solvent removal was established by the absence of carbon or chlorine atomic emission after the plasma was triggered. After being loaded, the fiber was drawn up into the guide tube and the assembly was lowered in tandem to a point just above the plasma. The fiber was then lowered directly into the upper portion of the plasma. After sample vaporization the fiber could be raised back into the guide tube and the assembly raised in the manifold for reloading.

3. Results and Discussion

The structures of the samples used are given in figure 2. The responses shown in figure 3 are typical of those obtained using sample sizes of about 500 nanograms. For illustration they have been offset and normalized so that the largest signal is full scale. The responses are all sharp with a half-width of under a second and a high signal to noise ratio for all elements. Within seconds of the initial analysis, the quartz fiber was reinserted into the plasma. No observable responses were observed for any of the samples following this procedure indicating that the sample was completely transferred to the plasma on the initial insertion.

The elemental responses were quantitated by peak integrations and these responses were used in eq (1) to give the data shown in table 2.

Table 2. The number of heteroatoms per molecule calculated from the experimentally determined elemental response ratios. Each result is the average of four separate determinations. The standard deviations are given in parentheses

Empirical Formula	F atoms	S atoms	Cl atoms
$C_{23}H_{29}NO_2F_2Cl$	2.4 (0.11)	0.017	0.97 (0.25)
$C_{27}H_{22}O_3F_4S$[a]	4.0 (0.1)	0.91 (0.07)	0.1
$C_{10}H_{13}N_2O_3SCl$[b]	0.004	1.00 (0.03)	1.00 (0.11)
$C_9H_5NOCl_2$	0.006	0.004	2.5 (0.4)
$C_9H_9NOS_2$	0.001	2.3 (0.2)	0.03
$C_{10}H_7NO_3FCl$	0.96 (0.01)	0.004	1.1 (0.3)
$C_{15}H_{13}O_2F$	0.83 (0.01)	0.007	0.02

[a] Used as calibration standard for F.
[b] Used as calibration standard for S and Cl.

$$X_{sam} = \frac{c_{std}}{x_{std}} \cdot \frac{X_{std}}{C_{std}} \cdot \frac{x_{sam}}{c_{sam}} C_{sam}, \quad (1)$$

where c and x are the integrals obtained for carbon (c) and the heteroatom (x) and C and X are the number of carbons (C) and heteroatoms (X) appearing in the empirical formula.

Each of the responses in table 2 is the average of four independent sample runs, with at least two different quartz fibers and plasma tubes used for each compound. When the experimental values are rounded to the nearest whole number they agree with the value expected from the empirical formula.

While it is true that the value of C_{sam} in the above expression will not be known for actual samples, the measured mass of the material is often available from mass spectrometry. Knowing the exact mass allows information on possible empirical formulae to be generated especially if information on the heteroatoms present is available. This is illustrated in table 3 for the mass of 502.1226 derived from the empirical formula $C_{27}H_{22}F_4O_3S$. Using all possible values of carbon from tables 3 as C_{sam} in eq (1) along with the ratio of area responses obtained for compound 1 in figure 2, it is possible to determine the empirical formula of this sample.

While the unique selection of an empirical formula is not always possible, the number of choices is always greatly reduced using information on elemental ratios especially if the number of elements measured is increased.

Table 3. Empirical formulae within 5 millimass units of 502.1226 when heteroatoms are constrained to the ranges $0 \leqslant F \leqslant 5$, $0 \leqslant O \leqslant 5$ and $0 \leqslant S \leqslant 2$

C	H	F	O	S
33	17	3	2	0
30	18	4	3	0
35	18	0	4	0
27	19	5	4	0
32	19	1	5	0
36	19	1	0	1
33	20	2	1	1
30	21	3	2	1
27	22	4	3	1
32	22	0	4	1
24	23	1	5	1
29	23	1	0	2
33	23	1	0	2
30	24	2	1	2
27	25	3	2	2
24	26	4	3	2
29	26	0	4	2
21	27	5	4	2

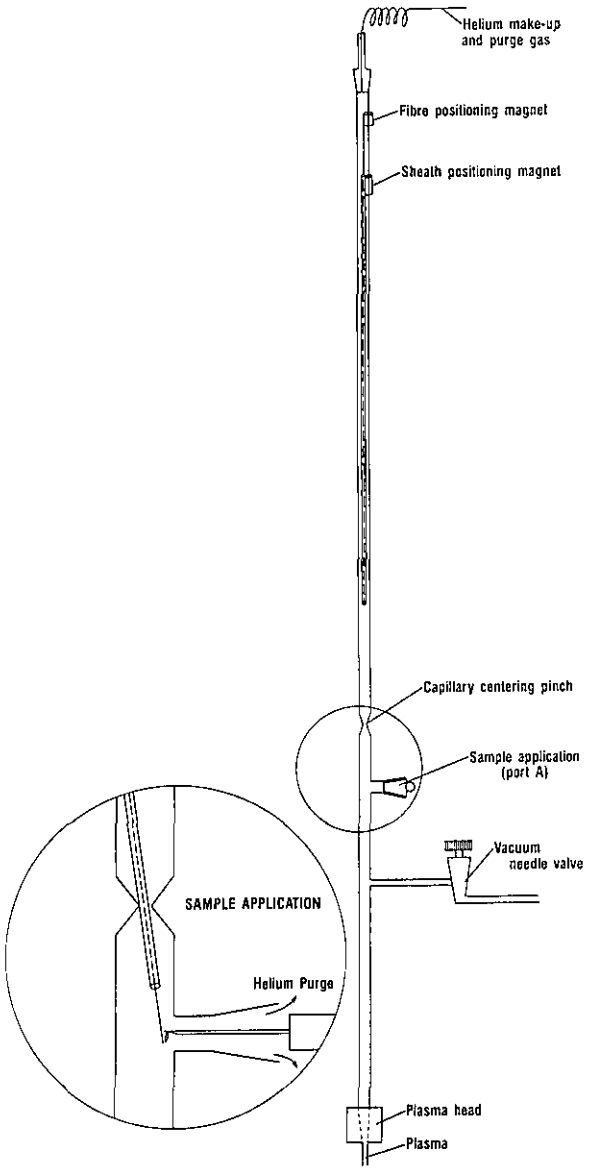

Figure 1. Device used to deliver solid samples to the plasma. Sample is loaded onto the quartz filament at port A using a Hamilton syringe as shown in the insert.

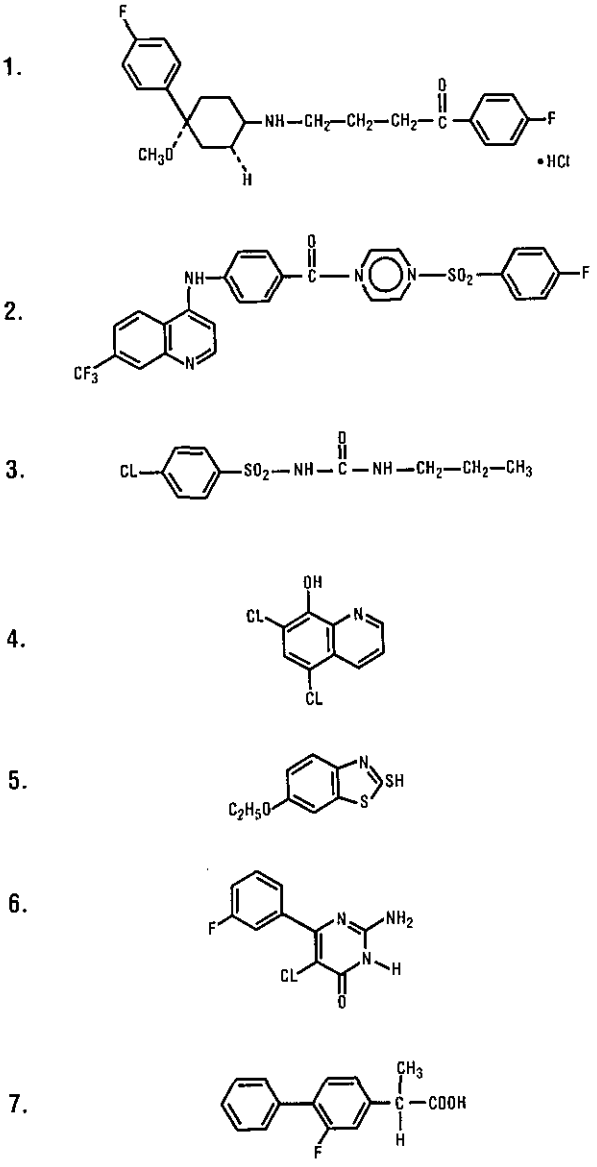

Figure 2. Structures of the nonvolatile samples studied.

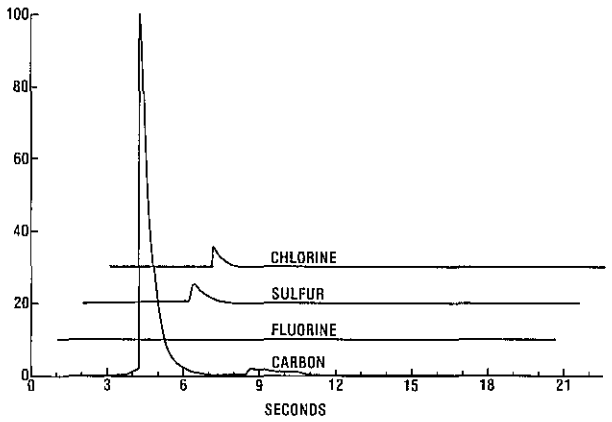

Figure 3. Typical responses obtained for a 500 ng sample.

4. References

[1] Uden, P. C., Slatkavitz, K. J., and Barnes, R. M., Anal. Chim. Acta **180**, 401 (1986).
[2] Freeman, J. E., and Hieftje, G. M., Spectrochim. Acta **40B**, 653 (1985).
[3] Bauer, C. F., and Skogerboe, R. K., Spectrochim. Acta **38B**, 1125 (1983).
[4] VanDalen, J. P. J., DeLezenne Coulander, P. A., and DeGalen, P. A., Anal. Chim. Acta **94**, 1 (1977).
[5] Mitchell, G. D., Aldous, K. M., and Canelli, E., Anal. Chem. **49**, 1235 (1977).
[6] Carnahan, J. W., and Caruso, J. A., Anal. Chim. Acta **136**, 261 (1982).

Ethyl Carbamate Analysis in Fermented Products: A Comparison of Measurements of Mass Spectrometry, Thermal Energy Analyser, and Hall Electrolytic Conductivity Detector

M. J. Dennis, N. Howarth, R. C. Massey, D. J. McWeeny, I. Parker, M. Scotter, and J. R. Startin

Food Science Laboratory
Ministry of Agriculture
Fisheries and Food
Norwich and London, U.K.

1. Introduction

Ethyl carbamate occurs in some alcoholic beverages in concentrations ranging from <10 μg/L to >1000 μg/L. Typically, the concentration is low in wine and high in some spirits; the concentration is particularly high in some plum brandies but is low in gin and vodka. Literature methods [1,2,3] rely on sample clean-up followed by packed-column GC and detection by FID, alkali flame ionisation, electron capture, or Coulson electrolytic conductivity detector and allow measurements down to 10 μg/L. The clean-up procedure required for levels below 100 μg/L is extensive and MS confirmation is still required.

In the course of a study of ethyl carbamate levels in alcoholic beverages on sale in U.K., different methods of separation and measurement were assessed. Using extracts prepared by the clean-up procedure described below the three measurements were carried out within MAFF Food Science Laboratory over a period of some weeks by separate groups using respectively GC-Hall Electrolytic Detector, GC-Thermal Energy Analyser and GC-Mass Spectrometry. Results are shown in table 1.

Table 1. Comparison of results for ethyl carbamate (μg/L) obtained from different detectors

Sample	Mass spectrometer (*m/z* 62)	TEA detector	Hall detector
Bourbon Whiskey a[a]	216[a]	204	176
b	212[b]	208	184
Scotch Whiskey a[a]	75	80	72
b	77	99	84
Red Wine a	22	16	13
b	Not analysed	13	10

[a] Each sample was extracted and concentrated in duplicate (a and b). Each concentrate was then analysed by the different detectors.
[b] Confirmed from *m/z* 61, 74.

2. Extraction and Clean-Up Procedure

Samples were diluted to $<5\%$ alcohol and 50 mL passed down a Chemtube (CT 2050, Analytichem) or Extrelut (Merck, 42g). Ethyl carbamate was eluted with 3×50 mL dichloromethane, the extract was dried on a sodium sulphate column and concentrated to 4 mL prior to passage down a Florisil Sep-Pak (Waters) pre-rinsed with dichloromethane. The Sep-Pak was rinsed with dichloromethane and ethyl carbamate was eluted with 7% (V/V) methanol in dichloromethane (5 mL) and concentrated to about 0.7 mL in a micro Kuderna-Danish evaporator. Final volume was measured by syringe. Average recoveries were 84% (minimum 75%).

3. GC Conditions

Slightly different gas chromatographic conditions were employed for each detector to gain optimum performance from each instrument. The following, used for the thermal energy analyser (TEA) detector, was typical. CP Wax 52 CB column (Chrompack), 25 m × 0.31 mm I.D., 0.21 μm film thickness, temperature programme 65 °C (for 1 min) then 10 °C/min to 100 °C and 20 °C/min to 200 °C (for 10 min).

On-column injection (2 μL) with secondary cooling was employed with helium carrier gas (0.6 bar).

4. Detector Operating Conditions

Hall 700A Electrolytic Conductivity Detector (Tracor) was used in nitrogen-mode without scrubbing; furnace 840 °C; isopropanol:water (1:1) electrolyte at 0.4 mL/min with manual venting; hydrogen flow 40 mL/min.

Thermal Energy Analyser Model 610 (Thermedics) was used in the nitrogen mode; interface temperature 200 °C; furnace 800 °C; reaction chamber pressure 2 mm Hg; no make-up gas.

VG 7070H mass spectrometer was used in E.I. mode (70 eV, 200 μA trap current, 200 °C) with interface heater at 200 °C. Selected ions were monitored (*m/z* 61, 62, 74).

5. Discussion

The Chem-Tube/Extrelut clean-up saved much time in clearing dichloromethane:water emulsions. The Florisil Sep-Pak allowed further clean-up in about 1 minute and although not strictly required for TEA purposes was necessary if a full mass spectrum is required for confirmatory purposes and greatly extends capillary column life.

Hall Electrolytic Conductivity gave a high background signal due to HCl from dichloromethane; this could be avoided by changing the solvent to ethyl acetate or (more conveniently) by manual venting of the detector until just before ethyl carbamate elutes. The scrubber system was not used as it adversely affected peak width without significantly reducing background noise. Instrument behaviour was variable and optimum performance demanded considerable operator skill. Figure 1 shows a typical chromatogram.

The mass spectrum of ethyl carbamate is shown in figure 2(a). Monitoring *m/z* 62 provided high selectivity and a 1 μg/L detection limit. The relative heights of *m/z* 62, 61, and 74 were used to confirm identity/purity. A typical chromatogram, monitoring *m/z* 62 is shown in figure 2(b).

The Thermal Energy Analyser, like the Hall, showed relatively few peaks but gave very stable performance (fig. 3). Blanks were consistently below the detection level (1 μg/L); duplicates were within 5% of the mean. Duplicate analyses on three separate days showed a coefficient of variation of 6.34% for the six analyses of a bourbon whiskey containing 300 μg/L ethyl carbamate.

6. Conclusions

A rapid clean-up procedure followed by GC-TEA separation and measurement suitable for routine analysis of ethyl carbamate down to 1 μg/L in alcoholic beverages has been developed. Results correlate well with data from alternative detector systems. Fuller details are reported elsewhere [4].

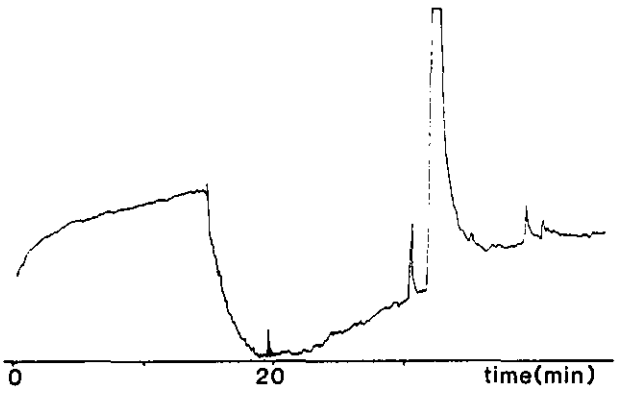

Figure 1. Capillary GC analyses of ethyl carbamate in whiskey using Hall 700A electrolytic conductivity detector. Shadowed area, 32 μg/L.

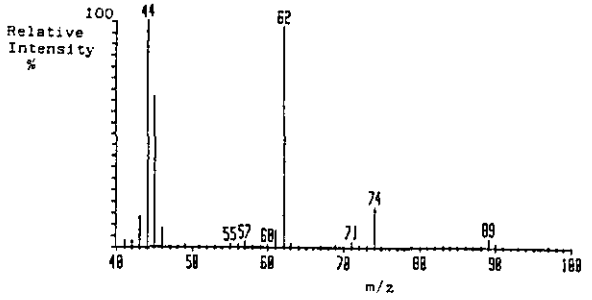

Figure 2(a). Electron impact spectrum of ethyl carbamate.

Figure 2(b). Capillary GC-MS analysis (m/z 62) of ethyl carbamate.

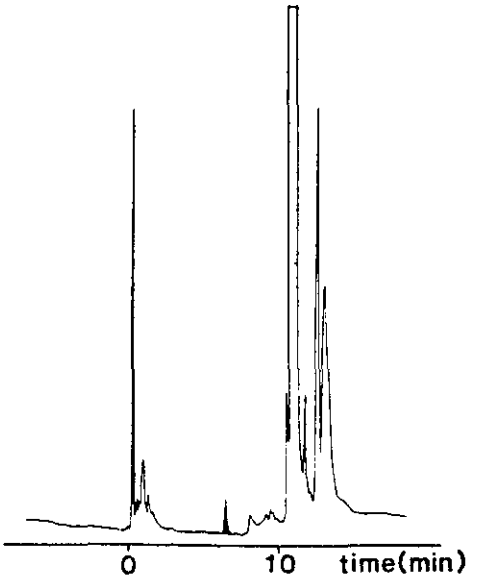

Figure 3. Capillary GC analysis of ethyl carbamate in whiskey using thermal energy analyser (nitrogen mode). Shadowed area 43 μg/L.

7. References

[1] Walker, G., Winterlin, W., Fonda, H., and Seiber, J., J. Agric. Food Chem. **22**, 944 (1974).
[2] Ough, C. S., J. Agric. Food Chem. **24**, 323 (1976).
[3] Joe, F. L., Kline, D. A., Miletta, E. M., Roach, J. A. G., Roseboro, E. L., and Fazio, T., J. Assoc. Off. Anal. Chem. **60**, 509 (1977).
[4] Dennis, M. J., Howarth, N., Massey, R. C., Parker, I., Scotter, M., and Startin, J., J. Chromatog. **369**, 193 (1986).

Volume 93, Number 3, May-June 1988
Journal of Research of the National Bureau of Standards

Chemometrics

Multicomponent Analysis in Static and Flow Systems Using Digital Filters

Steven D. Brown, Todd Q. Barker, Harlan R. Wilk, and Stephen L. Monfre

Department of Chemistry and Biochemistry
University of Delaware
Newark, DE 19716

1. Multicomponent Analysis as a Routine Analytical Tool

Many samples require rapid quantitative analysis of several components without taking the time required for separation of the components either from each other, or from the sample matrix. This need is especially critical for samples whose existence in some detection zone is transient, either because of some chemical reaction or because of sample transport rates through the analysis manifold. Mathematical analysis of data collected on such systems offers a practical route to the enhancement of detector selectivity without significant degradation of detection limits.

2. A Brief Review of Digital Filters

A set of techniques which is particularly suited to use in the analysis of transient responses involves the use of digital filters based on the Kalman algorithm [1]. The Kalman filter is a recursive, digital filter which uses models for the measurement and optimal estimates of the system states as well as errors associated with those estimates. In essence, these filters make use of empirical models of analyte responses, as well as any available theory, to enable the resolution of overlapped responses from the chemical components of a mixture. The recursive nature of these filters makes them attractive for "on-line" analysis, because they can process data point-by-point, using only points with high information content, and because concentration estimates can be developed in "real time." There have already been a number of applications in analytical chemistry [2].

Because these filters are not demanding of memory, and because the simpler forms do not require extensive matrix manipulations, they are easy to implement on a small, low-cost computer. More complex filters can be developed to detect, and even to correct, errors in the chemical models used for the multicomponent analysis. These filters, as well as other "quality assurance" software, can be run as hierarchical filters, with the simple filters acting as intelligent data collectors, and the more complex large filters monitoring the performance of the multicomponent analysis accomplished by the simpler filters. These methods are also easily merged with other chemometric methods, such as factor analysis, to permit more complex, off-line calculations as necessary to provide for improved calibration models, or to model new chemical systems planned for routine study.

3. Three Applications of Digital Filters in Multicomponent Analysis

This paper reports some applications of three new Kalman filters. The first application demonstrates the feasibility of filter-based multicomponent analysis in the Fourier domain, or in fact any other domain reached by a linear transformation from the time domain. Multicomponent analysis in these domains has a number of advantages for real-time analysis: the nature of model errors is changed, and "on-line" FTIR-based multicomponent analysis is made feasible. Figure 1 illustrates filtering of FTIR data in the Fourier domain.

The second application involves the development of new adaptive filters for detection and correction of model error, based on the entropy of the filter innovations. A simplex algorithm is used to drive a sub-optimal adaptive filter to the "best" (minimum entropy) fit, faster and with less error than with other adaptive filters [3]. We have been investigating the convergence properties of this filter. As figure 2 demonstrates, a fairly wide range of

initial guesses results in accurate concentration estimates, even when model error occurs *prior* to regions which are correctly modeled in a spectrum.

The final application involves the "in-line" application of Kalman filtering for filtering and quantitation of species observed across the interface created, for example, by injection of a basic solution into a flowing, acidic carrier. These interfaces are typical of those observed in flow injection experiments carried out with low dispersion. Spectroscopic data are collected using diode array spectrometry, and the resulting three-dimensional data are filtered to obtain concentration estimates for all absorbing species across the interface of carrier and bolus, and across the bolus as well. Figure 3 shows the distribution of species for nicotinic acid and nicotinate ion across an HCl-NaOH interface. The estimated concentrations of the species have less than 2% error without separation or internal standards.

Acknowledgments

This work was supported by the U.S. Department of Energy under grant DE-FG02-86ER13542.

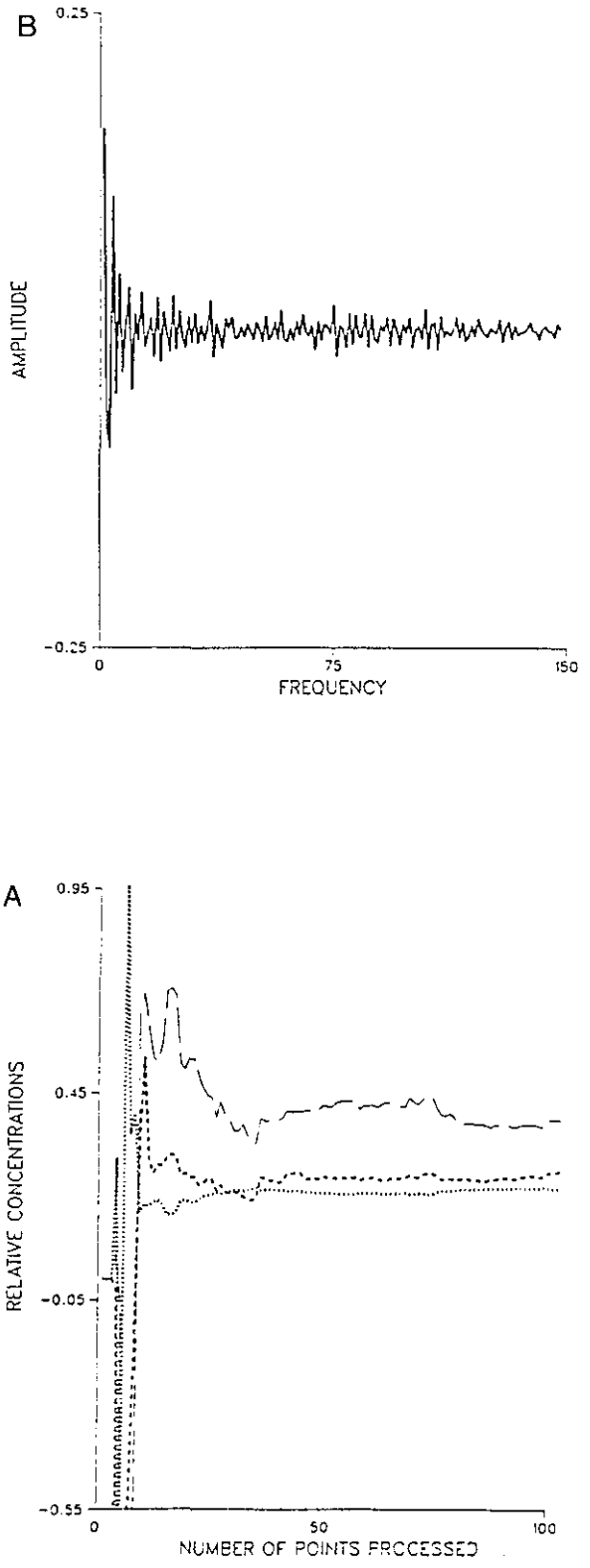

Figure 1. Fourier-domain filtering of spectroscopic data. **A.** Evolution of states for Kalman filtering of multicomponent infrared data. **B.** Portion of interferogram used in filtering multicomponent data.

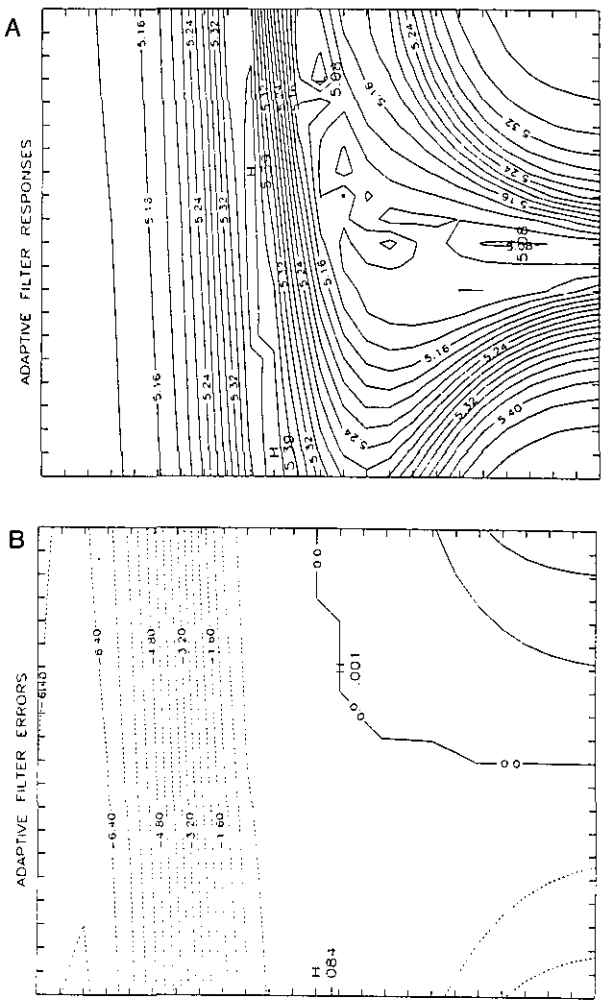

Figure 2. A. Entropy surface for innovations from a covariance-matched adaptive filter. The ordinate is the initial guess for the concentration of the modelled component. The abscissa is the initial guess of the covariance matrix element associated with that concentration. **B.** Error surface for estimates produced from a covariance-matched adaptive filter as a function of the initial guesses of the concentration and its covariance. Abscissa and ordinate are as in **A.**

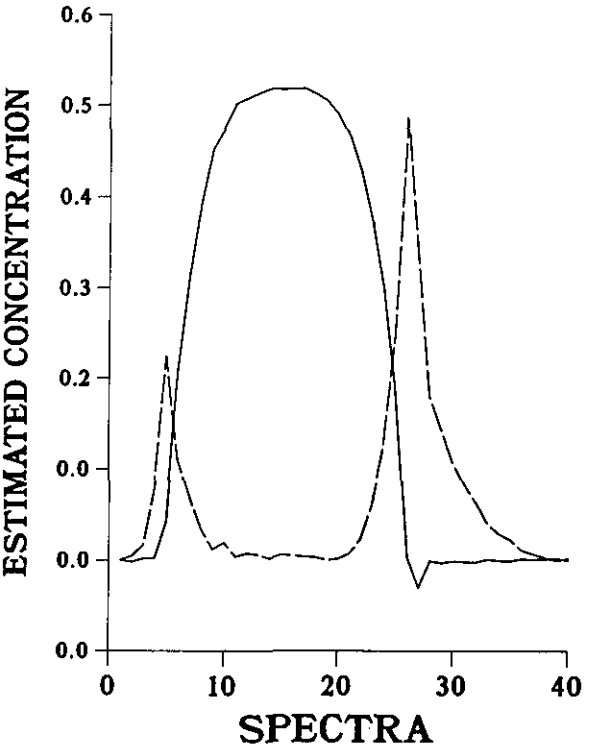

Figure 3. The Kalman filter estimated distribution of nicotinic acid species across an acidic bolus injected into a basic carrier undergoing laminar flow. The dashed line refers to the nicotinate ion, while the solid line refers to nicotinic acid.

References

[1] Gelb, A., ed., Applied Optimal Estimation, MIT Press, Cambridge, MA (1974), pp. 102–142.
[2] Brown, S. D., Anal. Chim. Acta **181**, 1 (1986).
[3] Brown, S. D., and Rutan, S. C., J. Res. Natl. Bur. Stand. (U.S.) **90**, 403 (1985).

Volume 93, Number 3, May-June 1988
Journal of Research of the National Bureau of Standards

Evolutionary Factor Analysis

K. Schostack, P. Parekh, S. Patel, and E. R. Malinowski

Department of Chemistry and Chemical Engineering
Stevens Institute of Technology
Castle Point, Hoboken, NJ 07030

Because of chemical interconversion, many chemical systems cannot be physically separated, making chemical identification and quantification difficult. The spectra (IR, UV, Visible, Raman, CD, etc.) of such systems exhibit overlapping contributions of uncataloged components, confounding the identification as well as the quantification. Strategies based on factor analysis [1], a chemometric technique for handling complex multi-dimensional problems, are ideally suited to such problems. Abstract factor analysis (AFA) reveals the number of spectroscopically visible components. Evolutionary factor analysis (EFA) [2–4] takes advantage of experimental variables that control the evolution of components, revealing not only the concentration profiles of the components but also their spectra even when there are no unique concentrations or spectral regions.

Evolutionary factor analysis makes use of the fact that each species has a single, unique maximum in its evolutionary concentration distribution curve. We have recently applied this self-modeling method to the infrared spectra of stearyl alcohol in carbon tetrachloride solution. The evolutionary process of this system was achieved by increasing the concentration of stearyl alcohol from 0.0090 to 0.0800 g/L in 15 stages, each time recording the IR spectra from 3206 to 3826 cm^{-1}. The spectra were corrected for baseline shift, solvent absorption and reflectance losses. The 15 spectra were then digitized every 3 cm^{-1} and assembled into a 35×15 absorbance matrix $[A]$ appropriate for factor analysis.

The factor indicator function [1], the reduced eigenvalue [5] and cross validation [6] indicated that three species contribute to the observed spectra. Thus AFA expresses the data matrix as a product of a 35×3 absorptivity matrix $[E]_{abst}$ and 3×15 abstract concentration matrix $[C]_{abst}$.

$$[A]=[E]_{abst}\,[C]_{abst}$$

Because the abstract matrices are mathematical solutions devoid of chemical meaning, they must be transformed into physically meaningful absorptivities and concentrations. This is accomplished by target transformation factor analysis (TFA) [1], a powerful technique which allows one to test factors *individually* without requiring any *a priori* information concerning the other factors. A test vector C_{test} emulating an evolutionary profile can be converted into a predicted vector C_{pred} that lies completely inside the factor space by finding a transformation vector T that minimizes the sum of squares of the difference between C_{test} and C_{pred}. Accordingly, C_{pred} is given by:

$$C_{pred}=T[C]_{abst}$$

in which $T=C_{test}\,[C]'_{abst}\,\{[C]_{abst}\,[C]'_{abst}\}^{-1}$

The prime indicates matrix transposition.

These equations were used to target test 15 ideal (Dirac delta function) concentration profiles, represented by uniqueness tests for each column of the absorbance matrix. A uniqueness vector consists of zeros for all elements except the one in question, which contains unity:

$$\begin{aligned}C_1&=(1,0,0,\ldots,0,0,0)\\C_2&=(0,1,0,\ldots,0,0,0)\\&\cdots\\C_{15}&=(0,0,0,\ldots,0,0,1)\end{aligned}$$

The three predicted vectors with maxima corresponding to the unique point of the respective test vector were retained as likely candidates. These crude profiles were refined, individually, by applying simplex optimization to the respective transformation vector, using a response function designed to minimize negative concentration points and double maxima in the profile.

Further refinement was achieved by the following iteration. Because negative regions are meaningless, all data beyond the boundaries marked by the first negative regions encountered on the left and on the right of the peak maximum were truncated. These profiles were normalized so the sum of squares equals unity and then assembled into a concentration matrix $[C]$. The pseudoinverse equation

$$[E]=[A]\,[C]'\,\{[C]\,[C]'\}^{-1}$$

was used to calculate the spectral matrix, followed by another pseudoinverse

$$[C]=\{[E]'\,[E]\}^{-1}\,[E]\,[A]$$

to recalculate the concentration profiles. This process (truncation, normalization and pseudoinverse followed by pseudoinverse) was repeated until no further refinement occurred.

The concentration profiles and spectra of the three unknown components of stearyl alcohol in carbon tetrachloride obtained in this manner were found to make chemical sense.

This EFA procedure, unlike others, was successful in extracting concentration profiles from situations where one component profile was completely encompassed underneath another component profile.

References

[1] Malinowski, E. R., and Howery, D. G., Factor Analysis in Chemistry, Wiley Interscience, New York (1980).
[2] Gemperline, P. G., J. Chem. Inf. Comput. Sci. **24**, 206 (1984).
[3] Vandeginste, B. G. M., Derks, W., and Kateman, G., Anal. Chim. Acta **173**, 253 (1985).
[4] Gampp, H., Maeder, M., Meyer, C. J., and Zuberbuhler, A. D., Talanta **32**, 1133 (1985).
[5] Malinowski, E. R., J. Chemometrics **1**, 33 (1987).
[6] Wold, S., Technometrics **20**, 397 (1978).

Chemometrics in Europe: Selected Results

Wolfhard Wegscheider

Institute for Analytical Chemistry
Mikro- and Radiochemistry
Technical University Graz, A-8010 Graz, Austria

Chemometrics is a very international branch of science, perhaps more so than chemistry at large, and it is therefore appropriate to question the suitability of the topic to be presented. It is, however, the author's opinion that the profile of European chemometric research has a couple of distinct features that may originate more in the structure of the educational system than in the actual research topics. The profile as it will be presented is the one perceived by the author, and therefore comprises a very subjective selection of individual contributions to the field. Obviously, this is not the place to offer a review on chemometrics, let alone one that is restricted to a continent.

The definition of chemometrics [1] comprises three distinct areas characterized by the key words "optimal measurements," "maximum chemical information" and, for analytical chemistry something that sounds like the synopsis of the other two: "optimal way [to obtain] relevant information."

Information Theory

Eckschlager and Stepanek [2–5] pioneered the adaption and application of information theory in analytical chemistry. One of their important results gives the information gain of a quantitative determination [5]

$$\hat{I}\,(q\|p)=\ln\frac{(x_2-x_1)\sqrt{n_A}}{s\sqrt{2\pi e}} \qquad (1)$$

where q and p are the prior and posterior distribution of the analyte concentration for the specific cases of a rectangular prior distribution in (x_1,x_2) and a Gaussian posterior with a standard deviation s determined from n_A independent results. The penalty for an inaccurate analysis is considerable and can be expressed as

$$\hat{I}\,(r;q,p)=\hat{I}\,(q\|p)-\frac{n_A}{2}\left(\frac{d}{s}\right)^2 \qquad (2)$$

with d the difference between obtained value and the true value of x. The concept has also been extended to multicomponent analysis and multimethod characterization. In the latter case, correlations between the information provided by the different methods need to be accounted for. Given the cost of and time needed for an analysis, *information efficiency* can be deduced in a straightforward manner [2]. Recently, work was published [5] suggesting the incorporation of various relevance coefficients; this, indeed, is a very important step since it provides a way to single out the information that is judged to be relevant for a given problem. It also opens up the possibility to draw on information theory for defining objective functions in computer-aided optimization of laboratory procedures and instruments.

Optimization of Chromatographic Separations

In the area of optimization, significant activity is spotted in chromatography since systematic strategies for tuning the selectivity are badly needed. Due to the randomness of elution, a hypothesis supported recently by Martin et al. [6], peak overlap is the rule rather than the exception even for systems with high peak capacity. Assuming equiprobable elution volumes for all analytes, the authors [6] have derived from standard probability theory an expression for the probability that all analytes are separated. An evaluation of eq (9) in reference [6]

$$P_{m,n}(m)=\left(1-\frac{m-1}{n-1}\right)^{m-2} \qquad (3)$$

(m the number of components, n the peak capacity of the system and $P_{m,n}(m)$ the probability that all components are separated) is provided in table 1 and shows that the absence of overlap is really very improbable except in cases of an extremely high ratio of peak capacity/number of components. The necessity of a separate optimization for each mixture of compounds is thus the rule and not an exception.

Chromatographic optimization cannot be reliably accomplished, however, by direct search techniques like the SIMPLEX, since each change of elution order corresponds to a minimum in the objective function. For multimodal surfaces, techniques that model the retention behaviour of each analyte separately and subsequently assemble a response function for a grid-like pattern in the space of experimental variables seem to be most promising [7]. Lankmayr and Wegscheider [8] have suggested to use a "moving least-squares" algorithm known from the interpolation part of the X-ray fluorescence program NRLXRF [9] for modelling elution. This results in an efficient optimization that is not stranded on secondary maxima of the response surface. A flow chart of this procedure is provided in figure 1. The efficiency stems mainly from three things: (i) a first estimate of the optimum can be made from only two chromatographic runs under different conditions; (ii) additional data can be incorporated to update the model of the response surface as they become available; and (iii) if required, additional experimental variables can be entered in the optimization at any stage. A drawback of this and all similar approaches is that an assignment of the peaks to the analytes is required at each stage. Currently, experimental work is under way to evaluate fuzzy peak tracking based on peak area and mean elution order [10].

Selectivity and Multicomponent Analysis

In spite of the great advances in the development of methods at trace levels, neither current separation techniques nor the detection principles are sufficiently selective. An attempt was recently made to redefine selectivity in chemometric terms, since Kaiser's well received proposal on this subject fails in two ways [11]. First, it does not give a clear account of the interrelationship between selectivity, accuracy and precision, and second it gives a value of infinity for full selectivity, a somewhat fuzzy result. By Taylor expansion, any multicomponent calibration system can be assessed for its selectivity by the condition number of the sensitivity matrix, cond(K); the condition number assumes the value of one for full selectivity and grows as the mutual dependence of the columns of K increases. Since the condition number can also be shown to relate to the analytical error, it was termed "error amplification" factor [12]. It can thus be regarded a prime concern in multicomponent analysis to find suitable means to minimize the condition number.

Recently, a chemometric approach was suggested by Lohninger and Varmuza [13], who derived a linear discriminator to serve as a selective detector for PAH in GC-MS. This was accomplished by selecting the best of 40 proposed features both in terms of discriminatory power against NOT-PAHs and by a rigorous sensitivity analysis to discard those that are unreliable in the presence of experimental error. The authors claim a recognition rate of 99%. Surely the concept is in its infancy, but the chemometric detector may well have potential in other areas, as well.

Partial Least Squares and Multivariate Design

Relating sets of measurements to each other is frequently done by least squares techniques. Among those, the partial least squares (PLS) algorithm as developed by Wold et al. [14] is most popular among chemometricians. As opposed to

principal component regression, another remedy in case of collinearity, PLS enhances relatively small variance structures if they are relevant for predictions of Y from X. This is done by using eigenvectors of $X'YY'X$ instead of $X'X$ as done in principal components analysis [15]. The most recent application of PLS are in quantitative structure activity relation (QSAR) studies of various classes of compounds.

Examples are contained in reference [16] and briefly outlined in reference [17]. For a series of bradykinin—potentiating pentapeptides, a model was derived to predict the biological activity of another set of peptides by describing the amino acid sequence from principal properties of single amino acids. These principal properties were deduced from 29 parameters by principal components analysis. These same principal properties can be used to design an approximate fractional factorial function with 16 different structures that effectively spans the space in terms of the 29 parameters initially judged useful for the description of the relation between structure and biological activity. This gives a guideline for the synthesis of good candidate peptides. As pointed out by Wold and coworkers [17], current advice in peptide design is to change the amino acid in only one position at a time, in clear contrast to what has been shown to be efficient screening of design variables.

Table 1. Probability that all components in a mixture are separated

Peak capacity	number of components	probability
50	5	0.77
	10	0.20
	20	1E -4
100	5	0.88
	20	0.02
	50	5E -15
1000	5	0.99
	50	0.09
	100	4E -5

Fuzzy Theory in Analytical Chemistry

An important strength of chemometrics as applied in analytical chemistry must be to utilize the wealth of statistical, numerical, computational methods available and choose the appropriate one in each instance. Recently, fuzzy theory was introduced in analytical chemistry [18]. Its basic notion is that crisp sets and numbers are replaced by their fuzzy analogues, to allow for variability on a non-probabilistic basis. The type of variability is defined in a so-called membership function that can be constructed from supplemental knowledge or subjective judgement by an expert in the field. By doing this, each number manipulated also carries information on its spread. Important applications of fuzzy theory so far have been library searching [19], pattern classification [20], and calibration with linear and non-linear signal/analyte dependencies in the presence of errors in x and y [21]. In the future, the incorporation of fuzzy information in expert systems will undoubtedly play a major role.

Conclusions

As pointed out at the beginning, this is only a subset in terms of volume of work done in chemometrics in Europe today. It is hoped that the reader finds this useful since it is regarded as typical. Other papers in this volume will cover calibration [22], evolving factor analysis [23], and expert systems in analytical chemistry [24], all being subjects of intense study in European laboratories. More traditional fields, for example, cluster analysis and pattern recognition, although very actively pursued, have not been included in this abstract [25].

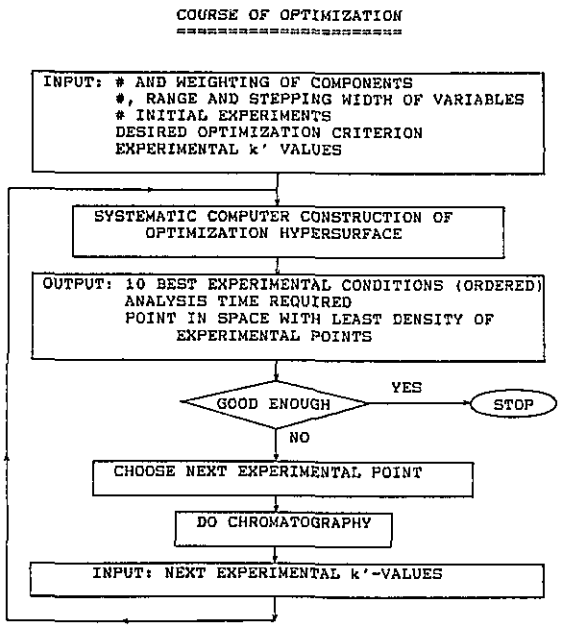

Figure 1. *Flow chart for using the "moving least-squares" algorithm [8].*

References

[1] Frank, I. E., and Kowalski, B. R., Chemometrics, Anal. Chem. **54**, 232R (1982).
[2] Eckschlager, K., and Stepanek, V., Information Theory as Applied to Chemical Analysis, Wiley, New York (1979).
[3] Eckschlager, K., and Stepanek, V., Anal. Chem. **54**, 1115A (1982).
[4] Eckschlager, K., and Stepanek, V., Analytical measurements and Information, Research Studies Press, Letchworth (1985).
[5] Eckschlager, K., and Stepanek, V., Chemom. Intell. Lab. Syst. **1**, 273 (1987).
[6] Martin, M., Herman, D. P., and Guiochon, G., Anal. Chem. **58**, 2200 (1986).
[7] Schoenmakers, P. J., Chromat. Lib. **35**, Elsevier Science Publishers, Amsterdam (1986).
[8] Lankmayr, E. P., and Wegscheider, W., Automated Optimization of HPLC Separation Methods, Pittsburgh Conference and Exposition, New Orleans, 1985.
[9] Criss, J. W., NRLXRF, A Fortran Program for X-ray Fluorescence Analysis, distrib. through COSMIC, Suite 112 Barrow Hall, Athens, GA (1977).
[10] Otto, M., Wegscheider, W., and Lankmayr, E. P., A Fuzzy Approach to Peak Tracking in Chromatographic Separations, submitted (1987).
[11] Otto, M., and Wegscheider, W., Anal. Chim. Acta **180**, 445 (1986).
[12] Jochum, C., Jochum, P., and Kowalski, B. R., Anal. Chem. **53**, 85 (1981).
[13] Lohninger, H., and Varmuza, K., Anal. Chem. **59**, 236 (1987).
[14] Wold, S., Wold, H., Dunn, W. J., III, and Ruhe, A., Umea *University, Report UMINF-83.80,* 1982.
[15] Martens, H., Multivariate Calibration: Combining Harmonies from an Orchestra of Instruments into Reliable Predictions of Chemical Composition, 46th Session of the Intern. Statistical Institute, Tokyo (1987).
[16] Hellberg, S., A Multivariate Approach to QSAR, Research Group for Chemometrics, Umea University (1986).
[17] Wold, S., Sjoestroem, M., Carlson, R., Lundstedt, T., Hellberg, S., Skagerberg, B., Wikstroem, C., and Oehman, J., Anal. Chim. Acta **191**, 17 (1986).
[18] Bandemer, H., and Otto, M., Mikrochim. Acta 1986 II, 93.
[19] Blaffert, T., Anal. Chim. Acta **161**, 135 (1984).
[20] Otto, M., and Bandemer, H., Anal. Chim. Acta **184**, 21 (1986).
[21] Otto, M., and Bandemer, H., Chemom. Intell. Lab. Syst. **1**, 71 (1986).
[22] Kateman, G., J. Res. Natl. Bur. Stand. (U.S.) **93**, 217 (1988).
[23] Schostack, K., Parekh, P., Patel, S., and Malinowski, E. R., J. Res. Natl. Bur. Stand. (U.S.) **93**, 256 (1988).
[24] Janssens, K., Van Borm, W., and Van Espen, P., J. Res. *Natl. Bur. Stand. (U.S.) 93, 260 (1988).*
[25] Derde, M. P., and Massart, D. L., Anal. Chim Acta **191**, 1 (1986).

Increased Accuracy in the Automated Interpretation of Large EPMA Data Sets by the Use of an Expert System

K. Janssens, W. Van Borm, and P. Van Espen

Department of Chemistry
University of Antwerp (UIA)
Universiteitsplein 1
B-2610 Wilrijk/Antwerp, Belgium

1. Introduction

Characterization of particulate material is one of the major applications of Electron Probe Micro Analysis (EPMA). This involves the collection of an energy dispersive x-ray spectrum for each particle to determine its chemical composition. Since for each aerosol sample typically 1000 particles are measured, very large data sets are obtained. Because of limitations in computer time and mass storage capacity, these spectra are not stored but are processed on-line, i.e., they are converted into tables of peak energies and intensities, permitting

the characterization of 1000 particles in 4 hours of instrument time without operator intervention. The off-line data processing consists of the interpretation of the peak table associated with each particle in terms of their chemical constituents. By using the Kα or Lα lines of each element, a particle vs elemental x-ray intensity matrix is built which is issued as input for multivariate classification techniques.

Since almost all detailed spectral information is lost in the initial data reduction process, qualitative interpretation by a conventional computer program produces erroneous results when peak overlap occurs. However, as human interpreters can obtain better results based on the same limited information, it was decided to capture the additional interpretation knowledge used by the chemist into an expert system, implemented in the OPS5-language [1]. Before the expert system starts an interpretation session, the peak tables generated during the on-line data reduction phase (see table 1a) are converted into a representation which is more suitable for the expert system. For each peak, a library of principal x-ray lines is searched. Since each peak can be associated with several types of x-ray lines of different elements (e.g., a peak at 1.479 keV corresponds to Al-K or Br-Lα), a (sparse) matrix of possible identifications is obtained (see table 1b). These matrices are read directly by the expert system.

2. The Expert System

Inside the expert system's data base, the data present in each row of an identification matrix are stored into an OPS5 working memory element (WME) of type "PEAK." WME's are complex data structures having several distinct fields. The structure of a peak-WME is represented in figure 1a. As in the identification matrices, each peak can be associated with seven elements. A probability value (e.g., $p_{K\alpha}$, $p_{K\beta}$, ...) corresponds with every association. X-ray data pertaining specifically to a chemical element is stored into WME's of type "ELEMENT" (see fig. 1b).

Schematically, the functioning of the expert system is represented in figure 2. The systems production rules are organized in several modules (e.g., CLEAN, ANALYZE, OVERLAP, ...) each dealing with a particular phase of the interpretation. Interaction between the modules is handled by meta-rules. Table 2a lists a meta-rule and its OPS5-equivalent. At present, the knowledge base contains about 80 chemical knowledge rules. Table 2b lists a rule from the CLEAN module. By using these rules, the system decreases/increases the probability values of a peak as more evidence is found that the associated chemical element is absent/present. The functioning of the expert system is described in more detail elsewhere [2].

Table 1a. Peak table

Peak Number	Intensity (counts)	x-ray energy (keV)
1	167	1.244
2	212	1.479
3	1147	1.742
4	379	3.682
5	1724	4.511
6	301	4.928
7	289	5.894
8	12873	6.392
9	1666	7.043

Table 1b. Identification matrix obtained after data reduction of a spectrum collected from a Mg, Al, Si, Al, Ti, Mn and Fe containing particle

	Possible Identifications					
Kα	Kβ	Lα	Lβ1	Lβ2	Lγ	Mα
Mg	**	As	**	**	**	**
Al	**	Br	**	**	**	**
Si	**	**	**	**	**	**
Ca	**	**	Sn	**	**	**
Ti	**	Ba	**	**	**	**
V	Ti	**	**	**	**	**
Mn	Cr	**	**	**	**	**
Fe	**	**	**	**	**	**
**	Fe	**	**	**	**	**

3. Results and Discussion

The performance of the expert system (method A) was evaluated by comparing the expert system results with those obtained by manual interpretation (method B) and by a conventional FORTRAN interpretation program (method C), using aerosol samples collected in a suburban area [3]. The conventional program operates by summing all peak tables of a data set, yielding a summary spectrum. A set of windows is constructed in which the peak intensities are accumulated while the window positions and widths are continuously adjusted during the summing process. After the summation, each

window is associated with a chemical element by comparing its mean energy with energies of principal x-ray line energies after which the elements associated with each individual particle are determined. Thus, a particle vs elemental x-ray intensity matrix is obtained.

Table 2a. Example of one of the expert systems meta-rules

Rule	**Go back to "CLEAN" phase after "INTENS"**
If	the current interpretation phase is "INTENS" one or more "INTENS"-rules has been used
Then	modify the interpretation phase to "CLEAN" *set the number of used "CLEAN"-rules to zero.*

OPS5-form:

```
(p intens::control:back-to-clean
      {<PHASE> (phase ^name intens ^intenscount > 0)}
→     (modify <PHASE> ^name clean ^cleancount 0))
```

Table 2b. Example of one of the rules from the CLEAN module, which removes Kβ-entries for a given element if no Kα-entry is found in the data base

Rule	**Remove isolated Kβ-entries from the database**
If	the current interpretation session is "CLEAN" a peak is found corresponding to the Kβ-line of an element *no peak is found which corresponds to the Kα-line* of this element
Then	remove the Kβ-entry from the data base.

OPS5-form:

```
(p clean::k:kb-no-ka
      {<PHASE> (phase ^name clean ^cleancount <n>)}
      {<KB-PEAK> (peak ^kb {<el> <> **})}
      --(peak ^ka <el>)
→     (modify <KB-PEAK> ^kb **)
      (modify <PHASE> ^cleancount (compute <n> + 1)))
```

As an illustration, the fine fraction of a data set of 1000 particles is considered below. After performing the qualitative interpretation of the data set in three different ways, the composition of each particle was calculated using a standardless ZAF correction procedure [4]. The resulting three data matrices were subsequently used as input to hierarchical cluster analysis (using Ward's errors sum strategy) to extract information on the different types of particles present in the sample. The resulting dendrograms are shown in figure 3. Although at first glance dendrogram C differs greatly from dendrograms A and B, roughly the same groups of particles can be distinguished. When the soil dust (Si,Al) or gypsum (Ca,S) groups are compared among the three dendrograms, approximately the same mean composition is obtained. However, when the particles containing heavy metals are considered, significant differences appear:

- In all dendrograms the Pb group consists of two subgroups. In A and B, the first subgroup mainly contains Pb (70%) and Br (24%), the second almost pure Pb (93%). In dendrogram C, however, both groups also contain S, with mean compositions of 60%Pb, 20%Br, 8%S and 82%Pb, 11%S respectively. Clearly, method C could not distinguish between S-Kα and Pb-Mα while method A could.
- Similarly, in the Zn containing particles, Na is found in all cases by method C since Na-K overlaps with Zn-Lα while no Na is found by either the manual or expert system interpretation methods.
- In the V,Ni group, two subgroups also appear, one contains soil dust elements and the other does not (methods A and B). In dendrogram C however, because the interpretation program found Cr in some of these particles, two other groups (containing Cr and not containing Cr) were formed. In this case, the interpretation errors not only yield incorrect particle compositions but have the more important effect of influencing the way particles are clustered together by introducing non-existent correlations.
- In dendrograms A and B, a number of particles of miscellaneous composition is present which do not belong to any of the larger groups. Among them is a group of five Ti particles and one Ba particle. Also pure As and Se particles are present and were identified by both the expert system and the human interpreter. In dendrogram C, however, the As particle belongs to the Pb group while a cluster of six Ba particles is present. Although the significance of these few particles in the entire data set is very small, this shows that the expert system is also capable of handling exotic particles correctly while the conventional program is clearly not.

A significant drawback in the use of the expert system is the considerable amount of computer memory and time it requires. While the conventional program takes about 5 min CPU-time to interpret a data set of 1000 particles. the expert system takes approximately 30 min, depending on the number of peaks in each spectrum.

Conclusion

In this work, an expert system, implemented in the language OPS5, for the automated interpretation of large EPMA data sets is discussed. The

interpretation results were evaluated by comparing them with those obtained from a manual interpretation method and from a conventional interpretation program using a windowing technique. This comparison shows that the results produced by the expert system are in good accordance with the results obtained by manual interpretation since the expert system is able to deal with the frequently occurring case of spectral overlap and retains only physically realistic identification possibilities.

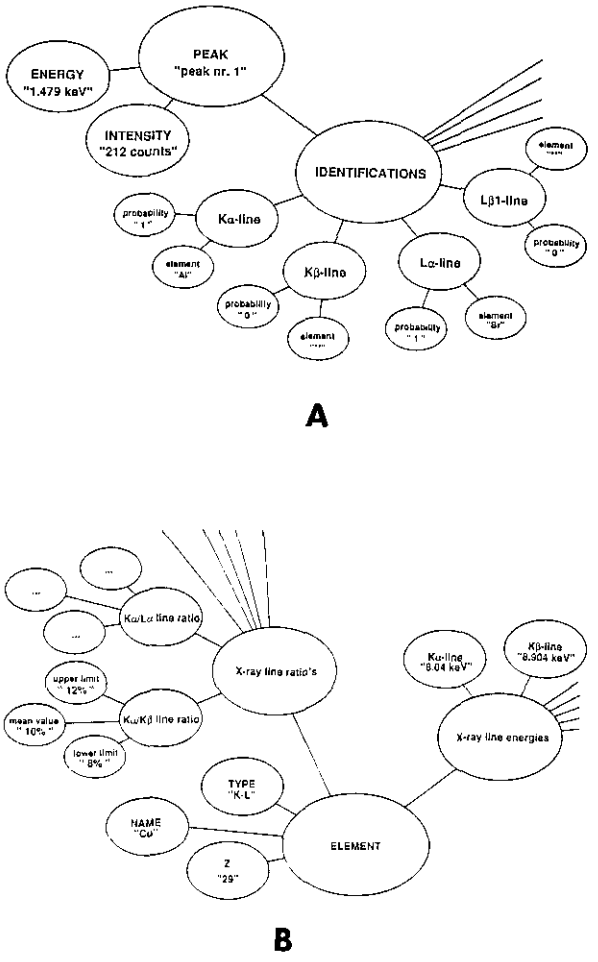

Figure 1. Structure of the PEAK and ELEMENT-type of data objects used by the expert system to store peak- and element-specific information.

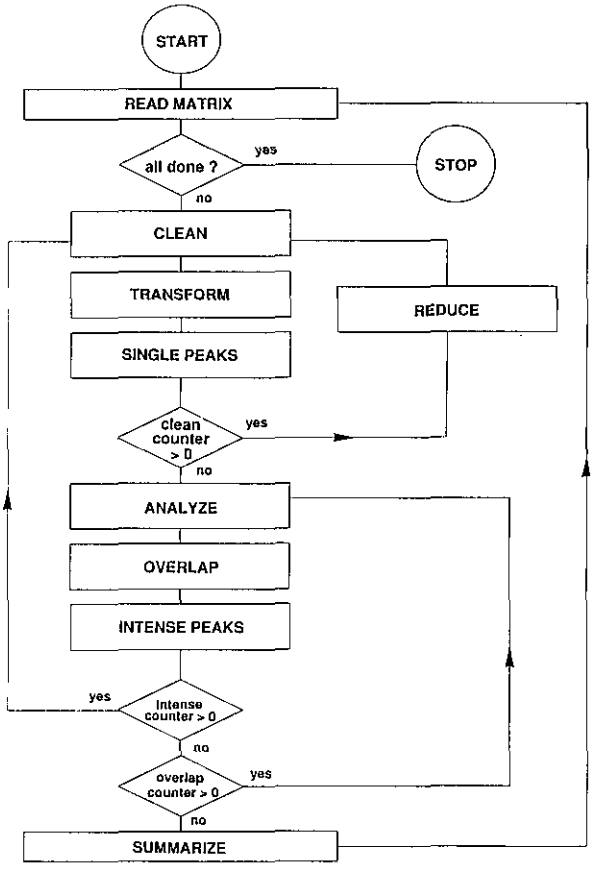

Figure 2. Schematic overview of the interaction between the rule modules present in the expert system's knowledge base.

Volume 93, Number 3, May-June 1988
Journal of Research of the National Bureau of Standards

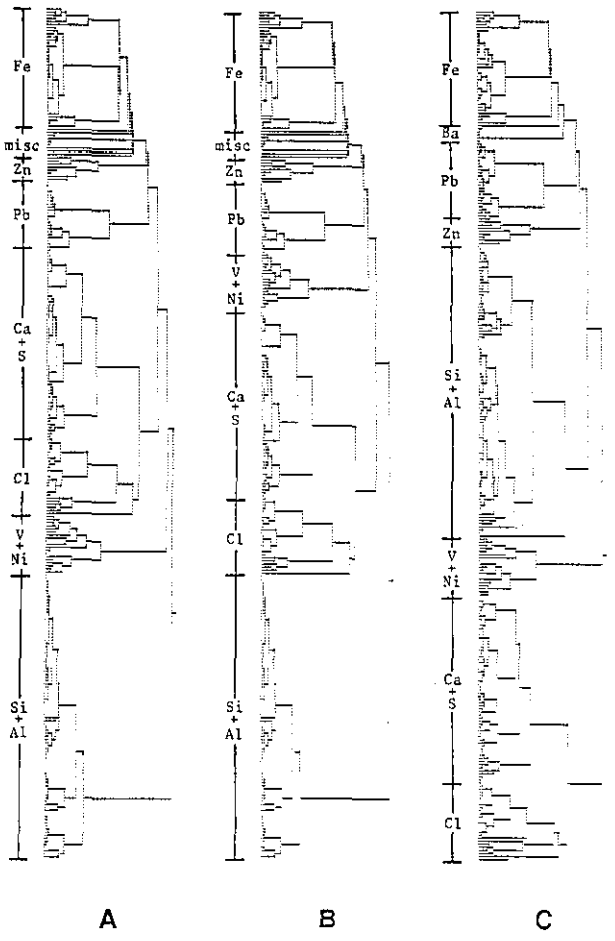

Figure 3. Dendrograms obtained by applying hierarchical cluster analysis to the same data set using different interpretation methods: (a) expert system, (b) manual interpretation, (c) conventional program.

References

[1] Forgy, C. L., OPS5 User's Manual, Technical Report CMU-CS-81-135, Dept. of Computer Science, Carnegie Mellon University (July 1981).

[2] Janssens, K., Dorinné, W., Van Espen, P., Chemo. Lab, The development process of an expert system for the automated interpretation of large EPMA data sets, submitted.

[3] Van Borm, W., Adams, F., Maenhaut, W., Environ. Sci. Technol., Source apportionment of air particulate matter in Antwerp, Belgium, submitted.

[4] Raeymaekers, B., Van Espen, P., Adams, F., Anal. Chem., A fast standardless ZAF correction for Electron Probe Micro Analysis, submitted.

Heteroscedastic Calibration Using Analyzed Reference Materials as Calibration Standards

Robert L. Watters, Jr.

National Bureau of Standards
Gaithersburg, MD 20899

and

Raymond J. Carroll and Clifford H. Spiegelman

Department of Statistics
Texas A&M University
College Station, TX 77843

Many instrumental analytical techniques exhibit a definable relationship between instrument response and analyte concentration over wide concentration ranges. This response is usually fit to an accepted model during the calibration phase of the measurement process. Often the calibrated concentration range (x values) is such that the measured response (y values) exhibits non-constant variance. The use of weighted regression techniques to properly estimate model parameters for this case has been described for a number of analytical applications. *An inherent, if not stated, assumption in* these treatments is that negligible error resides in the concentrations of the calibration standards.

A separate issue regarding calibration is the desire to minimize bias in the analysis by using calibration standards that are matched to the sample to be analyzed. It has been suggested that analyzed reference materials (ARMs) of a chemical matrix similar to that of the sample be used as calibration standards. Since the concentrations of analytes in these materials are estimates from measurements with error, using ARMs as *calibration standards* leads to errors in both x and y values for fitting the model. Therefore, the standard regression assumptions are not valid. A number of schemes have been developed for treating the calibration problem where both x and y have errors. However, when this problem is combined with heteroscedastic calibration, appropriate procedures are more complex.

We have recently reported an approach to heteroscedastic calibration that yields multiple-use calibration estimates and confidence intervals [1]. *The first step is to obtain calibration* data from

standards, which provide both estimates of the instrument response and its variability over the concentration range of interest. These estimates of uncertainty are fitted to a model for errors in y,(σ_y) in an iterative fashion. Each iteration is a weighted fit of the error model. The weights, $1/\sigma_y^2$, are calculated from the estimates of σ_y from the previous fit. Once the coefficients of the error model are obtained, a final set of σ_y's is calculated and used for the weighted fit of the calibration curve. Uncertainty bands over the calibrated range are then constructed by combining the uncertainty interval for successive measurements of unknown samples and the calibration band uncertainty. Concentration estimates and confidence intervals for the unknowns can then be obtained (cf. ref. [1], fig. 3). To combine this approach with the problem of errors in x, we apply adjustments to both the error model fit and the calibration curve fit. The matrices used in the calculations contain standards concentration data, error estimates for both y and x, the estimated calibration curve slope, and the coefficients for y-error model.

Care must be exercised in using this approach, because the general problem of calibrating with analyzed reference materials can violate some key assumptions regarding the calibration model. Analyzed reference materials are often complex solids that may be impossible to completely dissolve. Reference value estimates and uncertainties cannot be used for analytes lost in the dissolution process. Furthermore, preparation of calibration standards with analyte concentrations at various levels over the range of calibration will also result in matrix concentrations that also vary. If chemical matrix-matched calibration is required to reduce systematic errors in the analysis, various dilutions of analyzed reference materials are likely to change the slope of the calibration curve at each calibrated point. When analyzed reference materials are diluted into a constant chemical matrix, this type of calibration may be appropriate. Examples of this would include the mixture of geological materials in an excess of fusion flux for dissolution or the dilution of wear metals in oil standards in a constant excess of organic solvent.

Reference

[1] Watters, Robert L., Jr., Carroll, Raymond J., and Spiegelman, Clifford H., Anal. Chem. **59**, 1639 (1987).

Volume 93, Number 3, May–June 1988
Journal of Research of the National Bureau of Standards

Accuracy in Trace Analysis

Sample Preparation and Chemical Separations/Manipulations

The Role of the Robot in the Chemical Laboratory

C. H. Lochmüller

The Department of Chemistry
Duke University
Durham, NC 27706

The robot, a natural extension of the development of automation in the chemical laboratory, has recently enjoyed a flowering of interest. Robotics provides the missing link for the complete automation of standardized and new procedures by allowing the instrumentalist the option of mass-moving within the envelope of a laboratory experiment. It must be made clear that robotics is not a separate area but simply a sub-discipline within the general area of chemical instrumentation. Nothing that is done by a robot could not be done by a piece of "hard" instrumentation. The advantage of the robot is that it is "soft" instrumentation [1]. Soft instrumentation permits the laboratory worker to reprogram the manipulations carried out by automated equipment when a change is necessary in an established protocol.

Robotics has enjoyed a burst of interest because there are many established analytical procedures which involve substantial human interaction and which depend for their precision on the adaptation of humans to a protocol for a given task. It is the common experience of many laboratory managers that a technician requires a significant period of time to develop the technique required for good precision. This period of attainment of good precision is followed by a period of acceptable performance. If the task is a monotonous one, then the period of good performance is often followed by a decline in precision resulting from a growing human disinterest in the task itself. Robots provide a disinterested approach to the performance of such routine tasks and their training period differs little from the training period of a human operator.

Many administrators and laboratory managers are disappointed that robots require a significant period of time to be integrated into the laboratory environment. Robots, operating as they do as one-, or, at best, two-armed mechanical laboratory assistants incapable of vision and with limited sense of touch, require the conversion of human-assisted laboratory procedures to robot-assisted laboratory procedures and this requires training. This training often involves personnel of equivalent or higher level than would normally be assigned to the task that will be ultimately robotized. In fact, it is not unusual that the first robot installation of a kind will require 3 to 4 months of continuous effort by a team of two or three laboratory personnel, usually including one Ph.D., to be successfully implemented.

The whole problem is not the easy implementation of the number of steps required in the human-assisted example but rather the validation at every step carried out by this essentially blind, one armed, limited sensual capability laboratory assistant, the robot. In fact, most laboratory procedures, even those involving 10 or more steps, can be implemented in a laboratory using a robot within 10 days. The additional time of 4 months involves establishing those validation steps so critical to insuring that what this mindless assistant does can be traced and that anomalous results can be explained. It is this additional work that generates a sense of frustration in some laboratory personnel attempting to introduce robotics.

The more human a current robotic system is the less flexible it is. Human laboratory systems are currently defined in marketing terms as those which are essentially "turn key" systems which require little if any training by the laboratory personnel in order to perform routine tasks. Examples of this include the "PYE" approach of Zymark and the more recent contributions of Waters. Many routine sample separation operations can indeed be programmed with relative ease in either of these environments. However, robotics can contribute much more to laboratory exercise than the routine unit operations of filtration, extraction, etc. [2]. It is possible to train the robot to operate human-engineered machinery including a keyboard so that during the off hours when the robot is working alone in the laboratory it can, by access to expert

systems, modify analytical procedures within established limits in order to restore analytical capability and, therefore, maintain productivity [2].

This paper, while reviewing progress in the introduction of robotics in the laboratory, will also illustrate the inclusion of various elements that are beyond the routine sample preparation operation in nature and which includes optimization of analytical conditions and referral to residing experts systems for decisions related to the next best test to perform [3]. It is true that 99% of current robot installations perform routine tasks which could be easily described by decision trees or flow programming. It is also true that robotic installations of the future, or broadly defined as simply the mass-moving component of current robotic systems, will make decisions based on intelligence bases which will involve an almost cybernetic or "clever" decision basis. Attempts to extrapolate current capability into future capability will be made.

References

[1] Lochmüller, C. H., and Lung, K. R., Anal. Chim. Acta. **183**, 257 (1986).
[2] Lochmüller, C. H., and Lung, K. R., J. Liq. Chrom. **9**, 2995 (1986).
[3] Lochmüller, C. H., Lloyd, T. L., Lung, K. R., and Kahlurand, M., Anal. Lett. **20**, 1237 (1987).

Laboratory Robotics in Radiation Environments

Tony J. Beugelsdijk and Dan W. Knobeloch

Mechanical and Electronic Engineering Division
Los Alamos National Laboratory
Los Alamos, NM 87544

Radiation environments pose special problems for the implementation of robotic systems. A large part of the robotic effort at Los Alamos National Laboratory is spent addressing these issues and modifying commercial robotic equipment for these environments. This paper will briefly summarize some of the problems encountered and the solutions we have implemented on three laboratory robotic systems. The degree of modification increases with each system described. This succession of experiences has led us to begin the design of our own laboratory robotic arm compatible with this environment. This effort will also be described.

Problems associated with radiation have their origins in the types of radiation encountered [1]. By far the most common are alpha and beta emitting sources. For through-space radiation, these are fairly easily dealt with by simple shielding of sensitive robotic components. Contact radiation must be avoided, however, by careful control of the particulate levels within the workcell, by physical enclosure of semiconductor components, and by gas purging. Coatings must also be removed and polymeric materials must be replaced with metal wherever possible.

Gamma and neutron sources are much more difficult to deal with due to their penetrating nature. Here, successful approaches involve the considerations for alpha and beta sources as well as remoting electronics to outside the containment area. Maintainability issues also surface for these types of radiation. Where components are likely to fail, ease of replacement becomes key, especially while wearing thick, lead-lined gloves.

An initial laboratory robotic project involved the preparation of samples containing plutonium and americium prior to radiochemical counting for these elements [2]. This system was built around commercially available components acquired from the Zymark Corporation. The robot performed multiple dilutions and extractions in addition to weighing, centrifugation, and incubations for each sample. Final preparations consisted of a dried droplet (90 microliters) on a glass cover slip which is submitted for gross alpha measurement and a test tube containing two milliliters of solution for gamma counting. The results of both measurements are taken together in the final calculations for the plutonium and americium content of the original sample.

Modifications to this system were minor due to the predominance of alpha radiation and extremely low levels of americium (<100 ppm), a gamma source. Shielding from the lab environment was accomplished with a plexiglass hood enclosure built specifically to fit over the robot and its modules. A slight negative pressure is maintained within this enclosure.

A second application involved dispensing aliquots of radioactive solutions [3]. These solutions came from dissolved core samples taken from the Nevada Test Site after a test firing. A corrosion

resistant version of the standard Zymark arm was chosen for this project. A special problem was posed, however, in the handling of these solutions in the volumes required (10–300 mL) without contaminating the delivery devices. A solution was found through the use of peristaltic pumps and three-way pinch valves. These components were assembled into a pump station controlled by digital signals from Zymark's Power and Event Controller [4]. Between test firings, the tygon tubing is replaced to avoid cross-contamination. In addition, the master solutions are shielded in a lead brick lined enclosure—the robot workcell is itself not enclosed.

The system that required the most extensive modification is currently enclosed in a stainless steel glovebox [5]. This application called for the transfer of samples of Pu-238 oxides into and out of calorimeters for measurement of their heat output. Pu-238 is an intense alpha emitter and, as an oxide, the particulate acquires a charge. These charged particles are very mobile, quickly contaminate any space, and even migrate into conductors shorting them eventually. All drive electronics were removed from the Zymark robot base and wrist, coatings were removed, and all plastic components were replaced with metal. The only components remaining with the robot arm are the servo motors and feedback potentiometers. Remoted electronics were placed in a separate housing and cabled to through the wall of the glovebox using special hermetically sealed feedthrough connectors.

Our experience with radiation environments, gloveboxes, and existing laboratories have led us to begin design of our own robotic arm. The system will be of a gantry geometry and be modular in the x and y dimensions in increments of 6 inches. This will allow us to size the robot to the existing work space and the intended application. The z-axis will be telescoping in on itself to limit the overall height of the robot. The gantry design permits maximum use of the bench space or glovebox floor for modules, while the robot itself uses previously unused space overhead. Laboratory remodelling costs will thus be circumvented. Additional specifications have been reviewed by many researchers and address such areas as material compatibility, precision, controller architecture, tool changing, etc. The arm will be compatible with other commercially available laboratory robotic modules (i.e., syringe stations, balances, centrifuges, etc.). We anticipate having prototypes available within 2 years.

References

[1] Beugelsdijk, T. J., and Knobeloch, D. W., J. Liq. Chrom. **9**, 3093 (1986).
[2] Beugelsdijk, T. J., Knobeloch, D. W., Thurston, A. A., Stalnaker, N. D., and Austin, L. R., Robot-Assisted Sample Preparation for Plutonium and Americium Radiochemical Analysis, in Advances in Laboratory Automation-Robotics 1985, Strimaitis, J. R., and Hawk, G. L., eds., 283.
[3] Bowen, S. M., Beugelsdijk, T. J., and Knobeloch, G. W., Nevada Test Site Solution Dispensing Robotics System, in Advances in Laboratory Automation-Robotics 1986, Strimaitis, J. R., and Hawk, G. L., eds., 347.
[4] Beugelsdijk, T. J., Bowen, S. M., Waters, D. S., and Schneider, D. N., A Non-Contact Pump Station for the Delivery of Radioactive Solutions, Zymark Newsletter **2**, 8 (1985).
[5] Knobeloch, D. W., Austin, L. R., Latimer, T. W., and Schneider, D. N., Automation of the Calorimetry Step for Production of Plutonium-238 Oxide Fueled Milliwatt Generators, in Advances in Laboratory Automation-Robotics 1985, Strimaitis, J. R., and Hawk, G. L., eds., 313.

Microwave Acid Sample Decomposition for Elemental Analysis

H. M. Kingston and L. B. Jassie

Center for Analytical Chemistry
Inorganic Analytical Research Division
National Bureau of Standards
Gaithersburg, MD 20899

Appropriate sample preparation is essential to achieve both accuracy and precision in the analysis of materials. This preliminary step is one of the most time-consuming parts of many analyses and has become the rate limiting step for such multi-element techniques as ICP, XRF, and ICP-MS. Acid dissolution of biological and botanical samples can take from 4 to 48 hours using classical digestion techniques. Many of these same samples require only 10 to 15 minutes with microwave digestions, dramatically reducing preparation times. Volatile elements such as selenium, phosphorus, tellurium, and vanadium can be retained quantitatively in a sealed vessel using microwave decomposition prior to instrumental analysis [1]. The technique has been tested on all the major sample types including biological, botanical, geological, alloy, and glassy samples and has demonstrated advantages for each of these sample groups.

The development of real-time monitors for temperature and pressure in the microwave environment permits the investigation of closed vessel digestion using microwave energy as the heat source. It is necessary, however, to have an understanding of the fundamental concepts controlling interactions between microwave energy and the acid solution containing the sample.

Research has been conducted to identify these fundamental relationships and to develop methods that allow the analyst to predict, before programming and running the equipment, the conditions that will be generated during microwave digestion. This has been accomplished by measuring many of the parameters required to calculate the microwave power absorption by the mineral acids. Once the amount of energy that will be absorbed by a quantity of acid is determined, the equation is solved for the final temperature that will be reached by the sample at specific power settings. This method of predicting the temperature, or the time it takes to reach a particular temperature is useful in estimating the decomposition conditions [2].

This work has led to many new applications. Because microwave digestions occur in a well-defined, precisely controlled system, it is suitable for integration into automated applications. Acid digestion conditions have previously been too arbitrary for automation. With direct control of the power, the acid temperature, and the time for digestion, the microwave technique has become sufficiently structured so that it is possible to automate sample decomposition prior to instrumental analysis. New microwave-transparent vessels made of PFA Teflon and specifically engineered for this purpose permit the use of high temperatures (180–250 °C) and pressures (1000 kPa or 10 atm).

Because microwave energy is transferred directly to the acid, the reproducibility of decomposition conditions is better than can be achieved by traditional hotplate heating. Figure 1 shows the excellent reproducibility of sample conditions; it compares the temperature profile of two sets of six rice flour samples digested separately. The maximum difference between the sample temperatures at any point on the curve is 1.7%. Not only do the samples reach the same end point, but they achieve the same conditions at every point within this uncertainty.

Specific temperatures were identified for the rapid decomposition of the three basic components of biological and botanical matrices in nitric acid. Carbohydrate matrices decompose rapidly at a temperature of 140 °C, protein molecules rapidly decompose at 150 °C, and lipid molecules decompose at approximately 160 °C. These temperatures were determined by observing the nitric acid decomposition of each of these biological components separately. Three carbohydrates were used (soluble starch, amylopectin-amylose and glucose). The proteins were modeled by using Albumin (SRM 926, a pure protein), and tristearin (C-18, fatty acid ester) was used for the lipids. The oxidation by nitric acid was determined by measuring a rapid rise in pressure inside the closed container during a small change in solution temperature.

Biological materials decompose rapidly at temperatures that are closely related to their major components. Because the biological matrix is converted to CO_2 and nitric acid is converted to NO_2, these gaseous decomposition products produce a sharp rise in pressure with barely perceptible temperature changes. This rise is a good indication of the occurrence of decomposition. Figures 2 and 3 show the increase in pressure with the increase in temperature for bovine liver compared to albumin and to tristearin. The decomposition of bovine liver resembles tristearin rather than albumin. Tristearin requires a higher temperature to oxidize in nitric acid than does albumin. It appears that the more acid-resistant component of the matrix may be left intact if the conditions are not vigorous enough. Even at conditions that decompose the carbohydrate, protein and fatty acid molecules, certain organic moieties, such as the nitrobenzoic acids, remain after treatment with nitric acid. The nitrobenzoic acids are formed by the nitration of the aromatic rings of certain amino acids and they do not degrade further [3].

An additional test to observe the completeness of the digestion with time was carried out by decomposing albumin. It was first digested for 10 minutes under normal conditions, then cooled to room temperature, and digested a second time. Figure 4 shows that the pressure versus temperature curves for the two tests are very different. The second decomposition curve resembles the partial pressure of pure nitric acid heated under these same conditions; this comparison is shown in figure 5. The fact that no additional pressure was developed during the second heating indicates that all the oxidation occurred in the first 10 minute exposure to nitric acid under these specific conditions of temperature and pressure. These results indicate that rapid oxidation of biological samples can be achieved in

approximately 10 minutes. The high temperature required for rapid oxidation of samples can be achieved reproducibly in a short period of time. These conditions require inert, closed vessels that can withstand substantial pressures and temperatures.

Because of the precise reproducibility of the conditions and decomposition, microwave dissolution has great potential as a tool in analytical laboratories. This new technique effectively addresses the problems of precision, accuracy and efficiency.

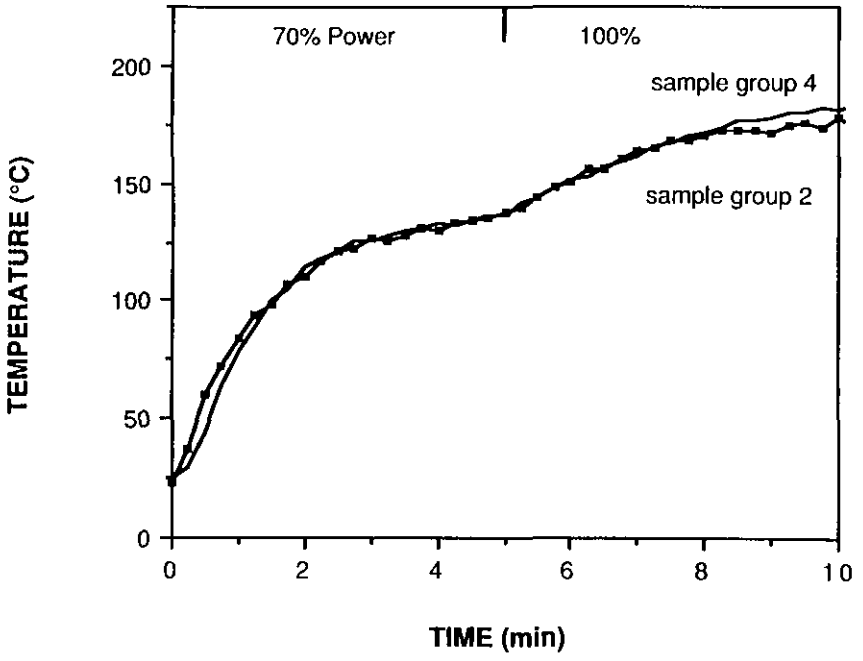

Figure 1. Temperature reproducibility of two sets of six samples each of 1 g of rice flour in 14 g of nitric acid.

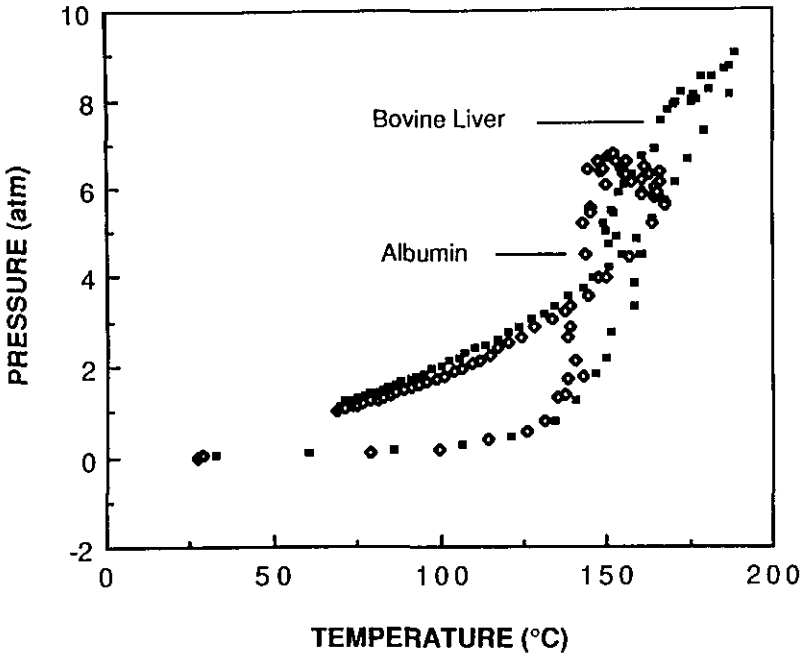

Figure 2. A comparison of the temperature versus pressure profile of acid decomposition of a biological tissue with that of a pure protein in the same acid.

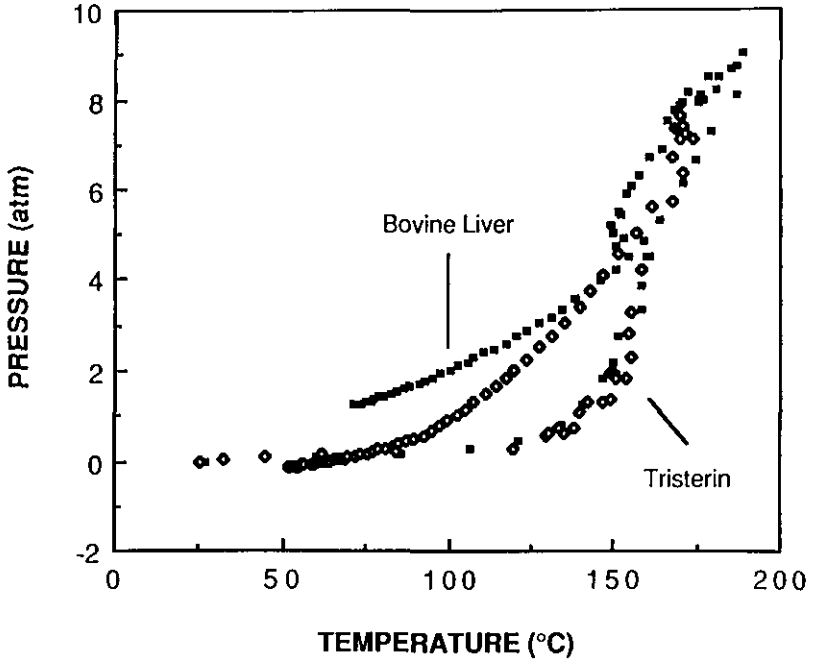

Figure 3. A comparison of the temperature versus pressure profile of acid decomposition of a biological tissue with that of a pure lipid.

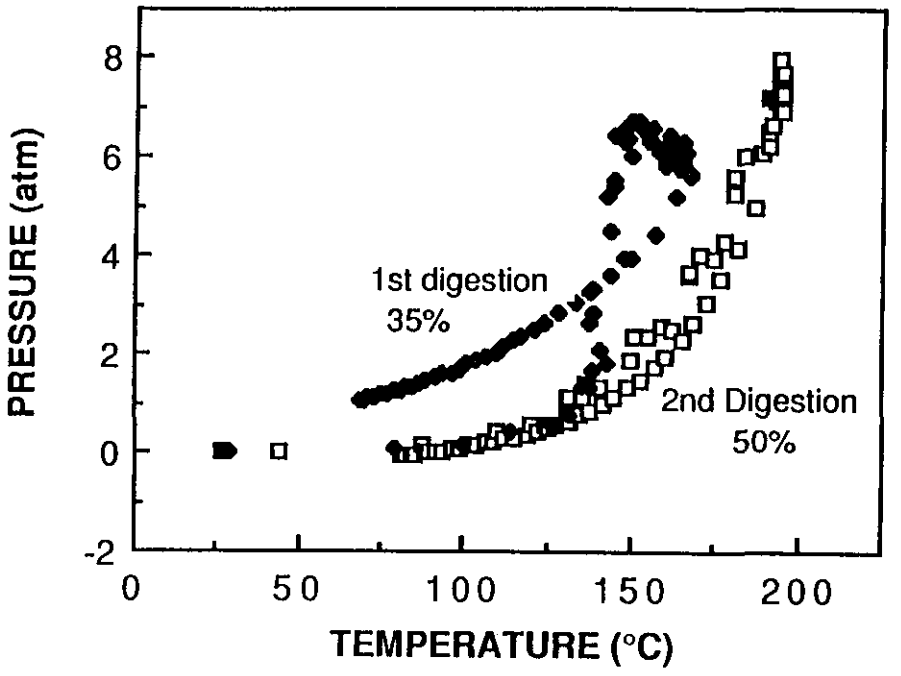

Figure 4. Temperature versus pressure profiles of the first and second digestions of a pure protein in nitric acid.

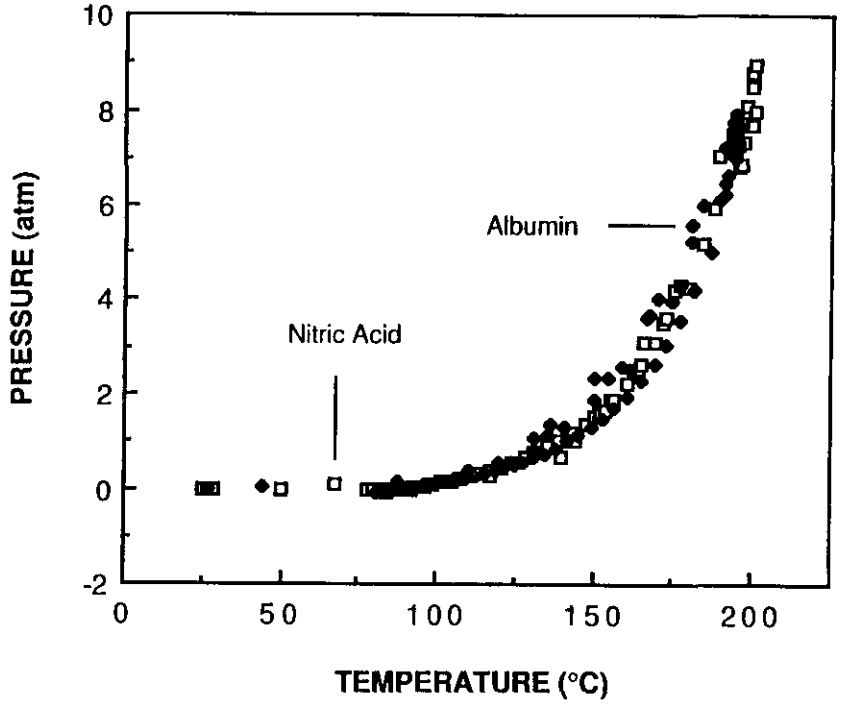

Figure 5. A comparison of the temperature versus pressure profile of the second digestion of a pure protein in nitric acid with that of nitric acid itself.

References

[1] Paterson, K. Y., Veillon, C., and H. M. Kingston, "Microwave Digestion of Biological Samples for Selenium Analysis by Electrothermal Atomic Absorption Spectrometry" in Introduction to Microwave Sample Preparation: *Theory and Practice, H. M. Kingston and L. B. Jassie, eds.*, ACS Reference Book Series, in press.
[2] Kingston, H. M., and Jassie, L. B., Anal. Chem. **58**, 2534 (1986).
[3] Pratt, K. W., Kingston, H. M., MacCrehen, W. A., and Koch, W. F., "Voltammetric and Liquid Chromatographic Identification of Organic Products of Microwave-Assisted Wet Ashing of Biological Samples" in press.

Solid Phase Extraction on a Small Scale

Gregor A. Junk and John J. Richard

Ames Laboratory (USDOE)
Iowa State University
Ames, IA 50011

1. Introduction

A wide range of sample size, flow rate, cartridge size, and volume of eluting solvent has been reported for the solid phase extraction (SPE) from water of a wide variety of organic compounds. Water sample volumes from 20–2000 mL, flow rates from 2–200 mL/min, cartridge sizes from 100–1200 mg, and volumes of eluting solvents from 0.1–5 mL have been used. At our laboratory, we have been able to achieve a concentration factor of 1000 and recoveries greater than 80% for pesticides [1] and tributyltin chloride [2] present at 0.1 ng/mL in water volumes of 100 mL. These results were obtained using 0.1 mL or less of ethylacetate to elute small cartridges containing 100 mg of C-18 bonded porous silica.

In this paper, we report the verification of this technique by extension to additional pesticides and polycyclic organic materials (POMs) and by field studies of surface and ground water samples where the SPE results are compared to those from conventional, accepted extraction procedures such as Amberlite XAD-2 [3] and solvent extraction.

2. Experimental

2.1 Extraction Procedures

2.1.1 Pesticides Cartridges containing 100 mg C-18 bonded porous silica, purchased from J. T. Baker (Phillipsburg, PA), were washed with about 3 mL of ethylacetate, followed by one column volume of methanol which was subsequently displaced with organic-free water. One hundred μL of the standard pesticide spiking solution were added to 100 mL of water which was then forced through the cartridge, using a 50 mL glass syringe, at a flow rate of about 25 mL/min. The C-18 bonded porous silica was then dried by drawing room air through the cartridge using the vacuum from a water aspirator. The adsorbed pesticides were eluted by gravity flow of ethylacetate.

For on-site adsorption of the pesticides from collected surface water samples, the cartridges were preconditioned in the laboratory by washing with ethylacetate and methanol. The methanol was displaced with water and the cartridges were capped and transported to the sampling site where two 50 mL volumes of surface water were passed through each cartridge using a glass syringe. The cartridges were then returned to the laboratory for drying and elution. Duplicate water samples were collected in 4 L amber bottles and returned to the laboratory for processing using the XAD-2 procedure [3].

2.1.2 Polycyclic Aromatic Hydrocarbons (PAHs) The PAHs were tested at 10 ng/mL using the same procedure used in the pesticide study. Recoveries were checked for partially dried cartridges using 100 μL of benzene eluent. For field samples, solvent extraction with methylene chloride was used for comparison of recoveries with those obtained using C-18 bonded porous silica.

Standard capillary GC analyses were employed for the analyses of all eluates and extracts.

3. Results and Discussions

3.1 Pesticides

The recovery results from a previous study [1] and new results for some additional herbicides and insecticides are given in table 1.

Table 1. Recovery of pesticides spiked into 100 mL of water

Compounds	%Rec [a]	Compounds	%Rec [a]
Herbicides		Organochlorines	
Alachlor	91	Chlordane	82
Atrazine	80	p p -DDE	81
Cyanazine	92	Endrin	106
Metolachlor	88	Hept. Epoxide	88
Metribuzin	88	Lindane	98
Propachlor	90		
Trifluralin	90	Organophosphorus	
		Chloropyrifos	82
Carbamates [b]		Fonofos	96
Carbaryl	83	Ethyl Parathion	95
Carbofuran	92		

[a] Avg. Std. Dev. for 4–6 runs was 80%.
[b] Tested at 1.0 ng/mL; all others at 0.1 ng/mL.

The combination of the small particle size and high surface area of C-18 bonded porous silica insured contact of the dissolved pesticides with the adsorbent even when very rapid flow rates of up to 250 bed volumes per minute are employed. Our results and those from other investigators [4–8] indicate that flow rate does not have to be closely controlled.

Methanol and acetonitrile have been the recommended solvents for the elution of compounds sorbed to alkyl-bonded porous silicas. Many hydrophobic compounds have limited solubility in these two solvents; consequently 1–5 mL of eluting solvent are usually recommended in the SPE procedures. For pesticides, we found ethylacetate to be a superior eluent capable of recovery >90% of almost all compounds in the first 60 μL of eluate from small cartridges containing 100 mg of 40 μm bonded porous silica.

Comparative field studies are valuable for evaluating the effectiveness of different extraction procedures. In table 2, we report representative SPE results for atrazine, alachlor, metolachlor, cyanazine and metribuzin extracted from 100 mL field water samples taken from four different sites. For comparison, the results are also given for one liter volumes of these same water samples returned to the laboratory for extraction using the XAD-2 procedure [3]. These favorable comparisons for the four sample sites given in the table were also obtained for these same five pesticides in water samples taken from eight other sites located in Iowa and Nebraska.

Table 2. Results using the C-18 and the XAD-2 method for pesticides in water

Site	Extr Method	mL H_2O Extr	Concentration in μg/L Atraz	Alach	Metol	Cyana	Metri
1	XAD	3000	23.0	3.0	2.9	3.2	1.3
	C-18	25	22.5	2.9	3.0	3.1	1.1
2	XAD	3000	6.8	1.2	1.6	1.1	0.19
	C-18	25	6.7	1.3	1.2	1.2	0.15
3	XAD	3500	0.31	0.14	ND [a]	0.33	ND
	C-18	100	0.46	0.18	ND	0.42	ND
4	XAD	3500	2.2	0.60	0.37	ND	ND
	C-18	50	1.9	0.81	0.60	ND	ND

[a] ND=Not Detected.

3.2 PAHs

Favorable results, comparable to those discussed above for the pesticides, were obtained in our study of the recovery of PAHs. Good recoveries, as listed in table 3, were obtained when partially air-dried columns were eluted with 100 μL of benzene.

Table 3. Recovery of PAHs spiked into 100 mL of water

Compounds [a]	% Rec [b]
Indene	80
3-Methylindene	82
Naphthalene	83
1-Methylnaphthalene	86
Acenaphthylene	88
Acenaphthene	89
Phenanthrene	97
Fluoranthene	90

[a] Tested at 2 to 10 ng/mL.
[b] Avg. Std. Dev. for 4 runs was ±8%.

Preliminary recovery results for other POMs, such as dioxin, trichlorobenzene, fluorenone, anthraquinone, nitrofluorene and nitronaphthalene, showed greater than 90% recovery at 0.1 to 2 ng/mL in water volumes of from 1 to 100 mL.

To further verify the SPE procedure for PAHs, field samples of contaminated water were checked. Comparative values obtained using conventional solvent extraction and SPE are given in table 4. Benzene was used to elute the partially dried cartridges for the SPE procedure and methylene chloride was used for the solvent extraction of the water samples. The excellent agreement of these

results is supportive of the more convenient SPE procedure.

Table 4. Results using C-18 for SPE and methylene chloride for solvent extraction of PAHs

Compounds	Conc in μg/L	
	Solv Extn	C-18 SPE
3-Methylindene	13	13
Naphthalene	23	22
1-Methylnaphthalene	436	433
Acenaphthylene	60	69
Acenaphthene	391	376

4. Conclusions

The small size of the C-18 cartridge plus its adaptability to hand-held syringes made it ideal for field sampling. Flow rates did not have to be controlled closely to achieve efficient adsorption even at rapid flows corresponding to 250 bed volumes per minute. Nearly quantitative recoveries were obtained by eluting with as little as 100 μL of organic solvent. In addition to these significant improvements, the SPE procedure as described here, when compared to solvent extraction, retains the following advantages: economical and convenient; uses less organic solvent; requires fewer operational steps; safer because it reduces the use and disposal of toxic and flammable solvents by greater than 90%; amenable to batch processing of samples thus increasing output; and emulsions are not a problem.

5. Acknowledgment

This work was performed in the laboratories of the USDOE and supported under Contract No. W-7405-Eng-82. The work was supported by the Office of Health and Environmental Research, Office of Energy Research.

6. References

[1] Richard, J. J., and Junk, G. A., Mikrochim. Acta (Wien) **387** (1986).
[2] Junk, G. A., and Richard, J. J., Chemosphere **16**, 61 (1987).
[3] Junk, G. A., Richard, J. J., Grieser, M. D., Witiak, D., Witiak, J. L., Arguello, M. D., Vick, R., Svec, H. J., Fritz, J. S., and Calder, G. V., J. Chromatog. **99**, 745 (1974).
[4] Andrews, J. S., and Good, T. J., Am. Lab. **14**, 70 (1982).
[5] Tatar, V., and Popl, M., Fresenius Z. Anal. Chem. **322**, 419 (1985).
[6] Saner, W. A., Jadamec, J. R., Sager, R. W., and Killen, T. J., Anal. Chem. **51**, 2180 (1979).
[7] Steinheimer, T. R., and Ondrus, M. G., Anal. Chem. **58**, 1839 (1986).
[8] Renberg, L., and Lindstrom, K., J. Chromatogr. **214**, 327 (1981).

Volume 93, Number 3, May–June 1988
Journal of Research of the National Bureau of Standards

III. Quantitation in Material, Environmental, Clinical, and Nutrient Analysis

Environmental Analysis

Determination of Tributyltin in the Marine Environment

R. G. Huggett, M. A. Unger, F. A. Espourteille, and C. D. Rice

Virginia Institute of Marine Science
School of Marine Science
College of William and Mary
Gloucester Pt., VA 23062

Introduction

Tributyltin (TBT) is a biocide used in antifouling paints to protect hulls from nuisance organisms such as barnacles, worms and algae. The use of TBT paints has increased over the past decade due to its effectiveness as an antifoulant which is related to its toxicity. Water concentrations of less than 100 ng L^{-1} have been shown to harm some aquatic species in laboratory tests and observations in the natural environment indicate that levels below 10 ng L^{-1} may be harmful. Tributyltin is bioconcentrated by many species to levels of one thousand, or more, times ambient water concentrations. Sediment-water partitioning coefficients for TBT of 100–10,000 have been reported [1]. The extreme toxicity of TBT challenges the analytical chemist to accurately and precisely determine ambient TBT concentrations in water at or below 1 ng L^{-1} and in sediments and tissue at concentrations ranging from $\mu g\ kg^{-1}$ to mg kg^{-1}.

Methods and Procedures

Tributyltin is often derivatized to convert the substance to a more volatile compound to facilitate analyses [2,3]. Our methodology for water involves liquid-liquid extraction of an acidified sample with tropolone and n-hexane. This is followed by the generation of n-hexyltributyltin, using the Grignard reagent, n-hexyl magnesium bromide. The derivatized extract is then cleaned by fluorisil column chromatography and analyzed by capillary gas chromatography with flame photometric detection or gas chromatography-mass spectrometry. Tripentyltin chloride is added as an internal standard before extraction of the sample [4].

The methodology for quantification of TBT in sediments and tissue differs from the water procedure only in the extraction steps. Anhydrous sodium sulfate and precipitated silica are added to wet tissue or sediment to dessicate the sample. It is then frozen to lyse cells and ground to a fine powder consistency. The TBT is removed from the sample by soxhlet extraction with n-hexane. The extract is then processed by the same procedure used for water extracts [5].

Discussion

The methodologies described above are straightforward, but a unique set of problems emerge when attempting to quantitate TBT at low ng L^{-1} concentrations. For instance, most commercial supplies of the Grignard reagent contain organotins as contaminants. This occurs because the same inert atmosphere apparatus is often used to synthesize organotins and Grignard reagents. Some commercial Grignard reagents were found to contain TBT at levels as high as several mg kg^{-1}. A contamination-free commercial source of n-hexyl magnesium bromide has since been found which now allows us to quantify TBT in water at less than 1 ng L^{-1}.

Sediment and tissue analyses are more complex than those for water. The material is difficult to extract from these matrices and the analyst must be cautious not to degrade or alter the substance in the process. Additionally, compounds that may interfere with TBT analyses are more abundant in tissue and sediment than in water. This is particularly true for samples collected from marinas and harbors which experience hydrocarbon pollution from oil spills and bilge waters.

Sampling frequency is an important aspect of any analytical investigation involving chemical contamination of the natural environment. Our work with TBT confirms this statement. The natural variability of TBT concentrations in water, sediment or tissue is large. Table 1 shows the concentrations of TBT in 19 individual oysters, *Crassostrea virginica*, collected from a single location in the James River, VA [6]. The lowest concentration differs from the highest by more than a factor of two. Water samples collected at the same location and at the same phase of the tide can vary by an order of magnitude within a one week period. Samples collected at the same time but a few hundred meters apart can be vastly different in concentration [7]. There are a number of factors responsible for this natural variability. These include wind conditions which influence both the amplitude of the tides and the mixing of the water mass, the ever-changing number of vessels in the vicinity of the sampling sites and the age of the paint films, since the release of TBT from the paints is somewhat time dependent. Figure 1 shows the concentration of TBT in surface water (30 cm below surface) collected from the same location on high slack tides over an 18-month period. Such data indicate that TBT water monitoring programs, and perhaps monitoring programs for other dissolved constituents, must be carefully designed with particular attention given to natural variability if short-term trend analyses (e.g., over 1 or 2 years) are desired.

Table 1. Concentrations of tributyltin in oysters, *Crassostrea virginica*, from a single location in the James River, VA

Oyster	Tributyltin concentration [a] $\mu g\ kg^{-1}$
1	301
2	285
3	211
4	515
5	280
6	345
7	386
8	254
9	374
10	258
11	411
12	446
13	480
14	311
15	264
16	379
17	373
18	325
19	325
	$\bar{x} \pm sd = 343 \pm 81$

[a] Concentrations given as TBT, dry weight.

The proper interpretation of environmental chemical monitoring data depends not only on the accuracy and precision of the analyses but also on how well the samples represent the system being investigated. The authors suggest that more attention should be given to sampling in the total analytical scheme.

Acknowledgments

The authors wish to acknowledge the laboratory support of D. J. Westbrook and E. J. Travelstead. *Financial assistance was provided by the Virginia* State Water Control Board, the U.S. Navy and the Virginia Institute of Marine Science.

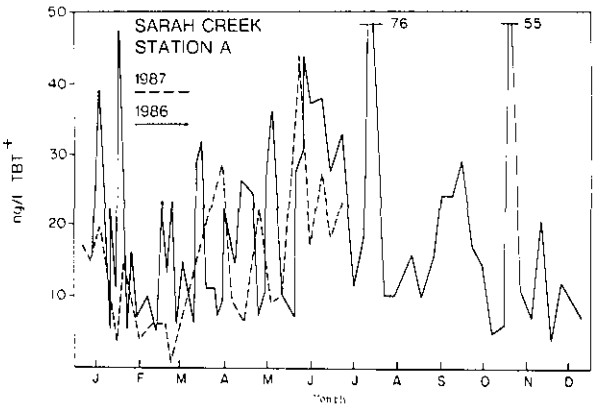

Figure 1. Tributyltin in near surface waters from Sarah Creek, VA over an 18-month period.

References

[1] Unger, M. A., MacIntyre, W. G., and Huggett, R. J., Equilibrium Sorption of Tributyltin Chloride by Chesapeake Bay Sediments, In: Proceedings of the Oceans '87, International Organotin Symposium, Halifax, Canada (1987).

[2] Maguire, R. J., Chau, Y., Bengert, G. A., Hale, E. J., Wong, P. T. S., and Kramer, O., Environ. Sci. Tech. **16**, 698 (1982).

[3] Matthias, C. L., Olson, G. J., Brinckman, F. E., and Bellama, J. M., A Comprehensive Method for the Determination of Aquatic Butyltin and Butylmethyltin Species at Ultra-Trace Levels Using Simultaneous Hybridization/Extraction with G. C./F.P.D., presented in part at American Chemical Society, Miami Beach, FL (1985).

[4] Unger, M. A., MacIntyre, W. G., Greaves, J., and Huggett, R. J., Chemosphere **15**, 461 (1986).

Volume 93, Number 3, May–June 1988
Journal of Research of the National Bureau of Standards

[5] Rice, C. D., Espourteille, F. A., and Huggett, R. J., Appl. Organometallic Chem. **6**, in press.
[6] Espourteille, F. A., Tributyltin in Oysters, *Crassostrea virginica*, and Sediments from the Chesapeake Bay, Masters Thesis, School of Marine Science, College of William and Mary, Gloucester Pt., VA (in preparation).
[7] Huggett, R. J., Unger, M. A., and Westbrook, D. J., Organotin Concentrations in the Southern Chesapeake Bay, In: Proceedings of Ocean '86 Organotin Symposium, Marine Technology Society, Washington, DC, 1262–1265 (1986).

Analysis of Gaseous and Particle-Associated PAH and Nitroarenes in Ambient Air

Janet Arey, Barbara Zielinska, Roger Atkinson, and Arthur M. Winer

Statewide Air Pollution Research Center
University of California
Riverside, CA 92521

The organic species present in ambient air vary considerably in volatility and concentration and are distributed between the gaseous and particulate phases. This distribution depends on, among other factors, ambient temperature and the composition of the particulate phase. The major sources of anthropogenic chemicals emitted into the atmosphere are combustion and volatilization, and the more volatile species are often present in high concentrations. This is demonstrated in figure 1 for a series of aromatic hydrocarbons. Literature values for ambient benzene and toluene concentrations [1] and the ambient concentration data we obtained for polycyclic aromatic hydrocarbons (PAH) at Glendora, CA, in August 1986 are shown plotted against their room temperature vapor pressures [2,3]. Thus, to measure ambient concentrations of the complete range of PAH and nitroarenes (which are generally at least an order of magnitude less abundant than the parent PAH), complementary sampling and analysis techniques are required.

Indicated in table 1 are the sampling technique(s) which provided quantitative concentration values for the listed PAH during 12-h sampling periods. The sampling techniques employed were: sampling at 1 L min^{-1} onto cartridges containing 0.1 g of Tenax GC solid adsorbent (low-flow Tenax), sampling at 10 L min^{-1} onto 0.6 g of Tenax (high-flow Tenax), sampling at 30 SCFM onto four polyurethane foam (PUF) plugs located in series downstream from Teflon-impregnated glass fiber (TIGF) filters in modified high-volume samplers, and standard high-volume sampling at 40 SCFM onto TIGF filters. Crucial to the quantification

Table 1. PAH quantitatively measured and the sampling techniques employed at Glendora, CA, in August 1986

m.w.	PAH	Low-flow Tenax	High-flow Tenax	PUF plugs	Filter	Comment
128	Naphthalene	X				Ave. 2% on back-up Tenax
142	1-Methylnaphthalene	X	X			Low- and high-flow Tenax agree
142	2-Methylnaphthalene	X	X			Low- and high-flow Tenax agree
154	Biphenyl		X			Too low to quantify on low-flow Tenax
154	Acenaphthene		X			Too low to quantify on low-flow Tenax
166	Fluorene		X			ΣPUFs ~25% high-flow value
178	Phenanthrene		X	X		<10% on 4th PUF
178	Anthracene			X		Too low to quantify on high-flow Tenax
184	Dibenzothiophene			X		
202	Fluoranthene			X		Partially gas-phase Partially "blown-off" filter <10% on filter
202	Pyrene			X		Partially gas-phase Partially "blown-off" filter <10% on filter
228	Chrysene/Triphenylene			ΣX		20–50% present on PUFs
Higher Molecular Weight PAH					X	

procedures was the utilization of a complete range of deuterated internal standards, from naphthalene-d_8 to dibenz(a,h)anthracene-d_{14}, added to the appropriate samples prior to the extraction step.

Generally the abundant volatile ambient nitroarenes, which include 1- and 2-nitronaphthalene and 3-nitrobiphenyl, are efficiently sampled utilizing PUF plugs [4]. To understand the sources of the nitroarenes observed in ambient air, isomer-specific compound identification is required [5,6]. The identification in an ambient particulate extract of the most abundant particle-associated nitroarene species as 2-nitrofluoranthene is illustrated in figure 2. Shown in this figure are the gas chromatographic/mass spectrometric (GC/MS) multiple ion detection (MID) traces for the molecular ion (*m/z* 247) of the isomeric nitrofluoranthenes (NF), nitropyrenes (NP) and nitroacephenanthrylenes (NAce) and for the molecular ion (*m/z* 256) of the corresponding perdeuterated species added as internal standards. The GC/MS identification of 2-NF and additional NF, NP and NAce isomers in ambient samples has been achieved through the use of deuterated internal standards in conjunction with the consistent chromatographic resolution and high sensitivity achievable through sample clean-up by high performance liquid chromatographic separations [7,8].

Acknowledgments

The financial support of the U.S. Environmental Protection Agency, Grant No. R-812973-01 and the California Air Resources Board, Contract No. A5-185-32 is gratefully acknowledged.

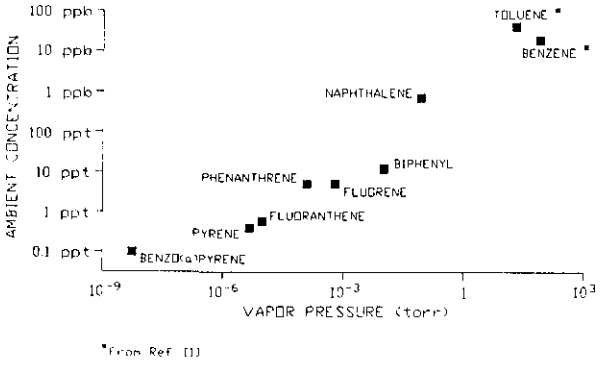

Figure 1. Plot of typical ambient concentrations of a series of aromatic hydrocarbons as a function of their room temperature vapor pressures.

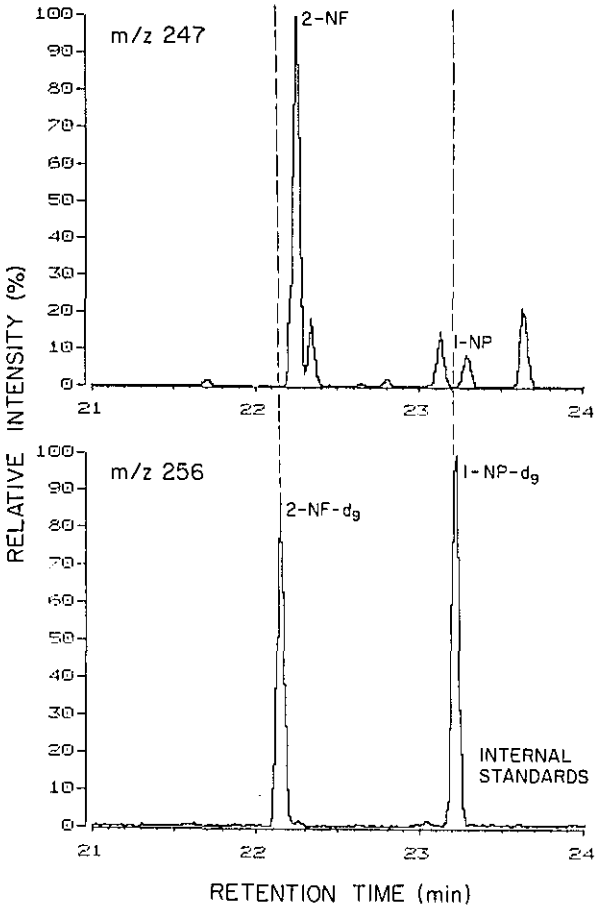

Figure 2. GC/MS MID traces of an ambient particulate sample extract showing that the most abundant NF, NP or NAce isomer is 2-nitrofluoranthene.

References

[1] Grosjean, D., and Fung, K., J. Air Pollut. Control Assoc. **34**, 537 (1984).
[2] Sonnefeld, W. J., Zoller, W. H., May, W. E., Anal. Chem. **55**, 275 (1983).
[3] Yamasaki, H., Kuwata, K., and Kuge, Y., Nippon Kagaku Kaishi **8**, 1324 (1984)
[4] Arey, J., Zielinska, B., Atkinson, R., and Winer, A. M., Atmos. Environ. **21**, 1437 (1987)
[5] Arey, J., Zielinska, B., Atkinson, R., Winer, A. M., Ramdahl, T., and Pitts, J. N., Jr., Atmos. Environ. **20**, 2339 (1986).
[6] Atkinson, R., Arey, J., Zielinska, B., Winer, A. M., and Pitts, J. N., Jr., The Formation of Nitropolycyclic Hydrocarbons and their Contribution to the Mutagenicity of Ambient Air, In: Short-Term Bioassays in the Analysis of Complex Environmental Mixtures V, Sandhu, S. S., DeMarini, D. M., Mass, M. J., Moore, M. M., and Mumford, J. S., Eds., Plenum Press, in press (1987).
[7] Zielinska, B., Arey, J., Atkinson, R., and McElroy, P. A., Nitration of Acephenanthrylene Under Simulated Atmospheric Conditions in Solution, and the Presence of Nitroacephenanthrylene(s) in Ambient Particles, Environ. Sci. Technol., submitted for publication (1987).
[8] Zielinska, B., Arey, J., Atkinson, R., and Winer, A. M., The Nitroarenes of Molecular Weight 247 in Ambient Particulate Samples, J. Chromatogr., to be submitted (1987).

Pattern Recognition Classification and Identification of Trace Organic Pollutants in Ambient Air from Mass Spectra

Donald R. Scott

U.S. Environmental Protection Agency
Research Triangle Park, NC 27711

and

William J. Dunn III and S. L. Emery

College of Pharmacy
University of Illinois at Chicago
Chicago, IL 60612

Introduction

The most frequently used method of analysis of trace organic pollutants in ambient air is gas chromatography-mass spectrometry (GC-MS). Presently, target compounds in air monitoring samples are identified from gas chromatographic retention times and a combined forward-reverse search of mass spectral reference spectra. The primary objective of this study is to develop computational pattern recognition procedures for the identification of chemical classes and, if possible, individual compounds from routine GC-MS data files. The additional information on nontarget compounds would supplement compound identifications obtained from the target list. The target set of compounds investigated consisted of 78 substituted benzenes, haloalkanes and haloalkenes.

Methods

SIMCA Pattern Recognition

SIMCA pattern recognition was developed by Wold and coworkers [1] for application to classification problems in chemistry. The technique is based on the modeling of chemical classes by disjoint principal component models. Once the class models have been determined, objects are classified by fitting their data to the class models. A standard deviation for each model is calculated from the residuals which represents a class tolerance level around the model in measurement space.

Data Analysis

In this study an IBM PC-XT microcomputer with 640K memory was used. A modified version of the SIMCA program was used for the majority of the pattern recognition calculations. The low resolution mass spectra of 78 compounds were obtained from the EPA-NIH Mass Spectral Library on an INCOS data system (see table 1). The GC-MS data files were from routine calibration and analysis performed by the Environmental Monitoring Systems Laboratory, U.S. Environmental Protection Agency, Research Triangle Park, NC.

The data were preprocessed by taking the autocorrelation transform of the mass spectra for mass lags less than 100. In the initial stages of class modeling, the autocorrelation transformed spectra for the 78 training compounds were examined for class separation with two and three dimensional principal components projections of the training data. Three different groups were found: nonhalogenated benzenes; chloroaromatics, chloroalkanes, chloroalkenes; and bromocarbons.

Principal components models were then derived for each class [2]. None of the class models

Table 1. Compounds included in this pattern recognition study

Compound	Class[a]	Compound	Class[a]
		Dibromomethane	3
		Bromoform	3
p-Xylene	1	1,2-Dichloroethane	2
1,3,5-Trimethylbenzene	1	1,1,1-Trichloroethane	2
Isopropylbenzene	1	1,1,2-Trichloroethane	2
n-butylbenzene	1	1,1,2,2-Tetrachloroethane	2
1-Methyl-4-isopropylbenzene	1	Pentachloroethane	2
o-Dichlorobenzene	2	1,1-Dichloroethane	2
p-Dichlorobenzene	2	Trichloroethene	2
1-Chloro-2-methylbenzene	2	Tetrachloroethene	2
1-Chloro-4-methylbenzene	2	Bromoethane	3
p-Chlorostyrene	2	1,2-Dibromoethane	3
1,1-Dichloroethane	2	1-Chloropropane	2
1,1,1,2-Tetrachloroethane	2	2-Chloropropane	2
1,2,3-Trichloropropane	2	1,2-Dichloropropane	2
3-Chloro-1-propene	2	1,3-Dichloropropane	2
2-Chlorobutane	2	1-Bromo-3-chloropropane	3
1,3-Dichlorobutane	2	1,2-Dibromopropane	3
1,4-Dichlorobutane	2	2,3-Dichlorobutane	2
1,4-Dichloro-2-butene (*cis*)	2	Tetrahydrofuran	0
3,4-Dichlorobut-1-ene	2	Benzaldehyde	1
1,4-Dioxane	0	1-Bromo-1-chloroethane	3
1-Chloro-2,3-epoxypropane	2	2,2-Dibromopropane	3
2-Chloroethoxyethene	2	2-Bromopropene	3
Acetophenone	1	2-Bromopropane	3
Benzonitrile	1	3-Bromopropene	3
Benzene	1	1-Bromopropane	3
Toluene	1	1-Chlorobutane	2
o-Xylene	1	1-Bromo-2-chloroethane	3
m-Xylene	1	Bromodichloromethane	3
Ethylbenzene	1	1-Bromobutane	3
Styrene	1	2,2-Dichlorobutane	2
Chlorobenzene	2	Dibromochloromethane	3
Bromobenzene	3	1,1,2-Trichloropropane	2
m-Dichlorobenzene	2	1,3-Dibromopropane	3
1-Chloro-3-methylbenzene	2	1,1,1,2-Tetrachloropropane	2
Chloroform	2	1,2,2,3-Tetrachloropropane	2
Carbon tetrachloride	2	1,3-Dibromobutane	3
Bromochloromethane	3	1,1,2,3-Tetrachloropropane	2
Bromotrichloromethane	3	1,4-Dibromobutane	3

[a] Class 1=nonhaloaromatics; class 2=chlorocarbons including aromatics and aliphatics; class 3=bromo- and bromochlorocarbons; class 0=internal standards and dioxane and tetrahydrofuran.

required more than three principal components. The largest number of autocorrelation coefficients relevant to a specific class was 40 in class 3. Eighty-six percent of the training set compounds were assigned to their correct class as a first choice and were within two standard deviations of the models.

Hierarchical Classification Scheme [2]

Once a class assignment is made, further identification of each spectrum can be made. This is done by calculating the distance, using the entire spectrum in autocorrelation space, of each compound to its three nearest neighbors in its assigned class. To obtain a specific structural assignment, the normalized correlation coefficient of the unknown mass spectrum with that of each of its three nearest neighbors is obtained. If the unknown is not identified as one of the three nearest neighbors in the first class assignment, the correlation coefficients of the three nearest neighbors in the second SIMCA class assignment are compared.

Volume 93, Number 3, May–June 1988
Journal of Research of the National Bureau of Standards

Results

GC-MS Calibration Samples

Three direct injection calibration samples, which contained all but one of the training set compounds, were analyzed [2]. Of the 77 compounds observed in the calibration runs, 84% were correctly identified. Of the 13 compounds not identified, three were correctly assigned by chemical class.

GC-MS Field Samples

The GC-MS data files for three field samples were also analyzed [3]. The identities of the target compounds were determined by using both GC retention times and a combination of forward and reverse spectral matching techniques with stringent matching parameters. The identification of other compounds not on the target list was based on a Finnigan search technique. The application of the pattern recognition scheme to the transformed data for the target compounds resulted in 88% correct classification. The compound identification results were 85% accurate.

There were 75 different nontarget compounds identified in 120 occurrences in the three samples. The classification results agreed very well for the two class 1 and class 2 spectra. However, a very large number of alkanes and alkenes were incorrectly classified as chlorocompounds. Further details of this study are given in references [2], [3], and [4].

Although the research described in this article has been funded by the U.S. Environmental Protection Agency under Cooperative Agreement CR-811617 with the University of Illinois at Chicago, it has not been subjected to Agency review. The mention of commercial products does not constitute endorsement or recommendation for use.

References

[1] Wold, S., Albano, C., Dunn, W. J. III, Edlund, U., Esbensen, K., Geladi, P., Hellberg, S., Johansson, E., Lindberg, W., and Sjostrom, M., in B. R. Kowalski (Editor), Chemometrics: Mathematics and Statistics in Chemistry, Reidel, Boston (1984), pp. 17–96.

[2] Dunn, W. J. III, Koehler, M. G., Emery, S. L., and Scott, D. R., Application of Pattern Recognition to Mass Spectral Data of Toxic Organic Compounds in Ambient Air, Chemometrics Intell. Lab. Sys., in press, Sept. (1987).

[3] Scott, D. R., Dunn, W. J. III, and Emery, S. L., Classification and Identification of Hazardous Organic Compounds in Ambient Air by Pattern Recognition of Mass Spectral Data, Environ. Sci. Tech., in press, Sept. (1987).

[4] Scott, D. R., Anal. Chem. 58, 881 (1986).

Annular Denuders and Filter Packs Designed to Measure Ambient Levels of Acidic and Basic Air Pollutants

Robert K. Stevens

U.S. Environmental Protection Agency
Research Triangle Park, NC 27711

Measurements of acidic (e.g., SO_2, HNO_3) and basic gases (e.g., NH_3) that coexist with fine particles (<2.5 μm) are used in models to assist in determining the origin and age of aerosols. Bias associated with each measurement method used to obtain this air quality data can degrade the real correlation between species. In addition, the sensitivity of most instrumental methods to measure SO_2, NH_3, HNO_3 or HNO_2 is limited to measurements at concentration levels above 2–5 ppb. Measurement of HNO_3 has also proven to be more difficult due to losses of HNO_3 in the sampling inlets used in some of the measurement procedures. Difficulties in differentiating atmospheric HNO_3 from HNO_3 produced by the dissociation of NH_4NO_3 during sampling, further complicates monitoring procedures.

Possanzini et al. [1] described the development of an annular denuder system which removes reactive gases (e.g., HNO_3, SO_2) from air samples an order of magnitude more efficiently per unit length and at lower Reynolds number than open tubular denuder designs. Recently we developed an improved version of the annular denuder that incorporates several important features to minimize losses of key species during sampling and reduce the possibility of leaks in the components that join the various parts of the system.

To demonstrate the applicability of this improved design of the annular denuder, a series of field studies were conducted in Research Triangle Park, NC during the fall of 1986 and winter of 1987. An annular denuder system (fig. 1) is composed of four components: an inlet (to remove large particles), coated denuders (to collect the acidic and basic gases), filter pack (to collect fine particles and HNO_3 that may evaporate from the filter), and a flow controller-pump assembly. In this study a new glass Teflon-coated impactor inlet was designed with a short tube extending below the impactor to prevent large particles and rain droplets from entering the impactor. With the exception of the impactor surface, the entire inlet is

coated with Teflon. The impactor surface is a sintered glass disc coated with silicone grease to prevent particle bounce. At 16.7 L/min, a 50% D_{AE}=2.64 μm cutpoint was obtained with an impactor nozzle jet diameter of 4.0 mm (Baxter and Lane [2]).

The first two denuder tubes were coated with a 1% solution of glycerine and Na_2CO_3. Anions collected on the second denuder are used to correct for any particle deposition that may have occurred in the denuders during sampling. Both denuders were extracted with ion chromatography eluent and analyzed for $NO_2^-(HNO_2)$, $NO_3^-(HNO_3)$, and (SO_2). The two filters in the filter pack were extracted with 20 mL deionized water and analyzed for $SO_4^=$ and NO_3^- content. For some portions of the study, a third annular denuder coated with citric acid was used to collect NH_3. As a result of these experiments, we have demonstrated that a relatively inexpensive ($150.00) Teflon-coated impactor will quantitatively transmit acidic gases to an annular denuder.

In addition, modifications to the annular denuder itself resulted in a reliable system for field investigations. Paired samples were run to compare the new denuder assemblies and the average percent differences between sampler results with different inlet configurations for SO_2, HNO_3, HNO_2. The differences were 3.4, 6.4, and 8.3%, respectively. During the second phase of the testing, an NH_3 denuder was incorporated into the assembly. The average % difference between two identical annular denuder systems for SO_2, HNO_2, HNO_3, NH_3, $SO_4^=$ and NO_3^- were 1.8, 5.5, 15, 16, 4.6 and 3.6%, respectively. Experiments by Appel et al. [3] indicated that HNO_3 was not retained in the Teflon-coated glass inlets.

In our study, intercomparison of denuder assemblies showed that ratios of HNO_3 to particle nitrate tended to decrease with decreasing ambient temperature and increasing humidity. This is qualitatively consistent with previous theoretical phase equilibrium calculations of NH_4NO_3.

Disclaimer. Although the research described in this article has been funded wholly by the U.S. Environmental Protection Agency, it has not been subjected to review and therefore does not necessarily reflect the views of the agency and no official endorsement should be inferred.

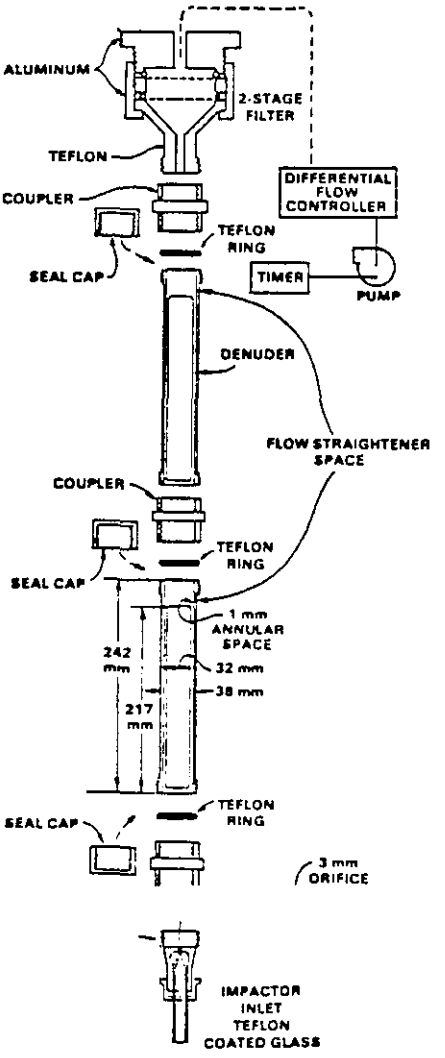

Figure 1. Annular denuder.

References

[1] Possanzini, M., Febo, A., and Liberti, A., Atmosph. Environ. 7, 2605 (1983).

[2] Baxter, T. E., and Lane, D. D., Initial performance testing of a glass jet impactor designed for use in dry acid deposition sampling, Presented at the 1987 American Assoc. for Aerosol Research, Seattle, WA. 14–17, Sept. (1987).

[3] Appel, B. R., Povard, V., and Kathney, E. L., Loss of nitric acid within inlet devices for atmospheric sampling, Paper presented at 1987 EPA APCA Symposium: Measurement of Toxic and Related Air Pollutants, Research Triangle Park, NC. 3–6 May (1987).

Volume 93, Number 3, May–June 1988
Journal of Research of the National Bureau of Standards

Accuracy in Trace Analysis

Measurement of Sunlight-Induced Transient Species in Surface Waters

Werner R. Haag

SRI International
Menlo Park, CA 94025

Sunlight irradiation of natural waters results in absorption of light by dissolved organic and inorganic compounds which then generate a variety of transient species including excited state dissolved organic materials (^{3}DOM), singlet oxygen ($^1O_2$), peroxy radicals (ROO·), hydroxyl radicals (HO·), solvated electrons (e^-_{aq}), and superoxide ion (O_2^-) [1–12]. The transient nature of these species causes both the practical aspects of and philosophy behind their determination to be different from those of conventional, more stable aquatic pollutants. Firstly, transients cannot be concentrated, separated from the water matrix, or the water removed from the light source, and therefore their analysis must be performed by *indirect* kinetic or integrative techniques. Secondly, they do not pose a human health concern because no significant exposure route exists. Ecological effects on lower organisms are possible [13] but none has been documented to date. The primary reason for their interest is that they can affect transformation of natural and man-made compounds. Such transformation can be beneficial, such as in the detoxification of pesticides [14], harmful, such as in the production of toxic peroxidic compounds in the photo-oxidation of crude oils [15], or simply of interest for the understanding of biogeochemical cycles, such as in the cycling of sulfur, nitrogen, and humic materials on geological time scales. Their quantitation allows prediction of environmental fate dynamics, and is of interest in water treatment processes where external sources of transients are added [16,17].

In order to understand how to measure transients, it is necessary to have some understanding of the factors which control their formation and consumption. Figure 1 and table 1 give an overview of some of the main processes involved. The bulk (~99%) of sunlight absorbed by DOM is converted directly to heat. About 1% of the initially formed excited state ^{1}DOM undergoes intersystem crossing to the longer-lived ^{3}DOM, which transfers the energy to oxygen to form $^1O_2$, the majority of which, in turn, decays by heating the water. A small fraction of ^{3}DOM transfers an electron to oxygen to produce O_2^-, which decays by disproportionation and some unknown reactions [12]. A minute fraction of excited state DOM ejects an electron, which is consumed rapidly by dissolved oxygen or possibly by nitrate. The radical cation formed by electron ejection may react with oxygen to form peroxy radicals, or these may be formed by addition of ground state oxygen to excited carbonyls yielding a biradical

$$^3R_2C{=}O + O_2 \rightarrow R_2C(O\cdot)OO \rightarrow R_2C{=}O + O_2 + \text{heat}$$

The factors controlling peroxy radical consumption are undefined at present, but may include disproportionation, reaction with DOM, or reversal of O_2 addition. Hyroxyl radicals are formed mostly by nitrate photolysis and consumed by reaction with DOM in fresh water or bromide ion in seawater.

The data in table 1 include only values measured or estimated thus far and therefore they do not necessarily represent all types of waters. Also, the data are of widely varying accuracy. For example, the formation and loss rates of $^1O_2$ are accurately known, but the corresponding rates for ROO· and O_2^- are crude estimates. The values for e^-_{aq}, HO·, and ^{3}DOM appear to be reliable, but there is less data available than for $^1O_2$ from which to judge accuracy and/or the range of values occurring under a broad variety of conditions. It may be assumed [1], however, that in well-oxygenated waters

$$[^3\text{DOM}] = 0.5[^1O_2]$$

and therefore many more [^{3}DOM] measurements were inherently estimated from [$^1O_2$] measurements.

Two approaches have been used to measure transient concentrations: derivative and integrative. The first involves following the light-induced rate of loss of a selective trapping agent A, added in low enough concentration that it traps only a small fraction of the transient of interest. This provision is necessary so that A does not perturb the system, i.e., it does not repress the steady state transient concentration, $[T]_{ss}$.

Table 1. Kinetic and concentration data for transients in surface water

Transient	Source	Sink[a]	k_{Sink}[b]	Formation Rate, M s^{-1}	Loss Rate, s^{-1}	Surface Concentration, M
^{3}DOM	DOM	$k_q[O_2]$	2×10^9 $M^{-1}s^{-1}$ [1]	$(3\text{-}300) \times 10^{-9}$	5×10^5	$(1\text{-}5) \times 10^{-13}$[c]
$^1O_2$	DOM	k_q (H_2O)	2.5×10^5 s^{-1} [18]	$(3\text{-}300) \times 10^{-9}$	2.5×10^5	10^{-14}-10^{-13}[d] 10^{-14}-10^{-12}[e]
ROO•	DOM	$k_t[ROO\bullet]^2$? $k_r[DOM]$	? ?	10^{-11}-10^{-10}	0.1-1 ?	10^{-11}-10^{-10}
HO•	NO_3^-	$k_r[Br^-]$[d] $k_r[DOM]$[e]	1.2×10^9 $M^{-1}s^{-1}$ [19] 2.5×10^4 L $mg^{-1}s^{-1}$ [7]	10^{-11}-10^{-10}	10^7[d] $(0.2\text{-}2) \times 10^5$[e]	2×10^{-19}[d] $(2\text{-}6) \times 10^{-16}$[e]
e^-_{aq}	DOM	$k_r[O_2]$ $k_r[NO_3^-]$	2×10^{10} $M^{-1}s^{-1}$ [20] 1×10^{10} $M^{-1}s^{-1}$ [20]	$(5\text{-}10) \times 10^{-11}$	$(0.5\text{-}1.5) \times 10^7$	$(1\text{-}2) \times 10^{-17}$
O_2^-	DOM	$k_t[O_2^-]^2$ $k_r[DOM]$	$6 \times 10^{12}[H^+]$ $M^{-1}s^{-1}$ [21] ?	10^{-11}-10^{-7} ?	10^{-3}-1 ?	10^{-9}-10^{-8} ?

[a]The species in brackets or parentheses indicates the interactant and the rate constant subscript indicates the type of interaction: q = energy transfer (quenching), t = termination of two radicals, r = other reactions.

[b]value of rate constants in previous column

[c]≥90 kJ/mol [1]

[d]Seawater

[e]Freshwater

Under these conditions

$$-d[A]/dt = k_r[T]_{ss}[A] = k_{exp}[A]$$

$$[T]_{ss} = k_{exp}/k_r$$

where k_r is the known second-order rate constant for reaction of A with T, and k_{exp} is the experimental, first-order rate constant. Such measurements are simple and give $[T]_{ss}$ directly, but it is crucial to know, at least very crudely, the first-order transient loss rate constant in the absence of A, k_d, in order to calculate the maximum concentration of A which may be used:

$$k_r[A] \leqslant 0.1\, k_d$$

An example of the repressive effect of too much trapping agent is shown in figure 2, which shows that $\leqslant 10\ \mu M$ benzene should be used when determining $[HO\cdot]_{ss}$ in this particular water sample [8].

The integrative approach involves addition of A in high enough concentration to trap all of the transient as it is formed, and measurement of the formation of a product or loss of a reactant such as oxygen:

$$-d[A]/dt = +d[Product]/dt = k'_{exp}$$

$$[T]_{ss} = k'_{exp}/k_d$$

This method has the drawbacks that it requires precise knowledge of k_d and that there is always the potential that the high concentrations of A required may affect the lifetime (concentration) of a precursor to the transient of interest. However, the method is more sensitive than the derivative technique and can give quantum yield data which can be used more generally than $[T]_{ss}$ values in making environmental fate predictions. This approach has been used successfully in the determination of $[e^-_{aq}]_{ss}$ [22], and quantum yields of $^1O_2$ production [3] and total radical production [23].

Clearly important for both methods is that the trapping agent be highly selective for the transient of interest. Testing of selectivity can sometimes be done by quantitation of products, but in some cases products from two transients are so similar that this is not possible. Kinetic tests involve addition of a second solute which modifies the transient lifetime (concentration) in a quantitatively predictable way (table 2). Usually this means adding a competitive quencher or reactant having a known rate constant and seeing if the reduction in rate of loss of the first trapping agent agrees with the predicted factor of $k_d/(k_d+k_{Modifier}[Modifier])$. The addition of D_2O as a diagnostic test for $^1O_2$ is particularly useful because it selectively causes an increase, rather than decrease, in $^1O_2$ lifetime and concentrations.

Table 2. Trapping agents, lifetime modifiers, and typical reactants for transients in surface water

Transient	Trapping Agents	k_r $M^{-1}s^{-1}$	Lifetime Modifier	$k_{Modifier}$ $M^{-1}s^{-1}$	Compounds Affected
^3DOM	1,3-pentadiene	5×10^8 [1]	O_2	2×10^9 [1]	nitro-aromatics, dienes
$^1O_2$	furfuryl alcohol	1.2×10^8 [2]	D_2O	a	furans, imidazoles
	dimethylfuran	8.2×10^8 [24]	N_3^-	5×10^8 [25]	sulfides, azo-dyes
					e^--rich aromatics
ROO•	2,4,6-trimethylphenol	$\sim 10^5$ [5]	p-methoxy-phenol	$\sim 10^5$	phenols, anilines
	p-methoxyphenol	$\sim 10^5$			azo-dyes
	p-isopropylphenol	$\sim 2 \times 10^4$			
HO•	butylchloride	3×10^9 [19]	octanol	4×10^9 [19]	most organics,
	benzene	6×10^9 [19]	(organics)	$(1\text{-}10) \times 10^9$ [19]	nitrite
e^-_{aq}	carbon tetrachloride	3×10^{10} [20]	O_2,	2×10^{10} [20]	polyhalo compounds
	2-chloroethanol	4.1×10^8 [20]	polyhalo compounds	$(1\text{-}3) \times 10^{10}$ [20]	nitroalkanes ?
O_2^-	none identified		superoxide	2×10^9 [21]	none identified
	catechol ?	2.3×10^5 [21]	dismutase		benzidines ?
	benzidine ?	$>2.5 \times 10^7$ [21]			catechols ?

[a]Increases lifetime of $^1O_2$; k_d in H_2O/D_2O mixtures is equal to $k_d^{2\,H_2O} X^{2\,H_2O} + k_d^{2\,D_2O} X^{2\,D_2O}$ where X indicates mole fraction and $k_d^{2\,H_2O} = 2.5 \times 10^5\ s^{-1}$ and $k_d^{2\,D_2O} = 1.8 \times 10^4\ s^{-1}$ [18].

Acknowledgment

The author wishes to thank J. Hoigné, T. Mill, and R. Zepp, who helped generate many of the concepts used in this paper.

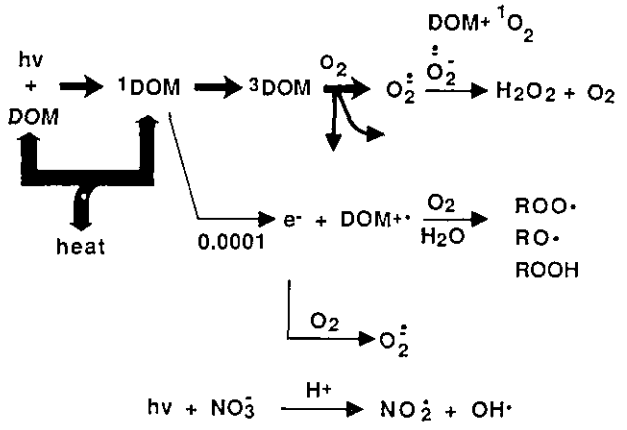

Figure 1. Photochemical pathways for transient formation in surface waters.

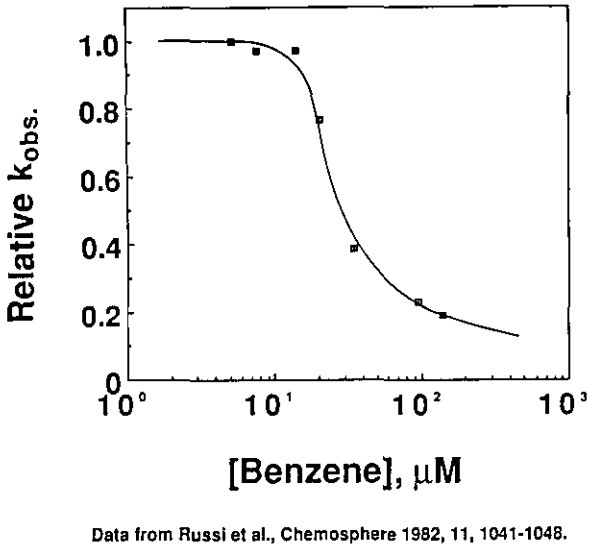

Figure 2. Sensitized benzene hydroxylation in a natural water.

References

[1] Zepp, R. G., Schlotzhauer, P. F., and Sink, R. M., Environ. Sci. Technol. **19**, 74 (1985).
[2] Haag, W. R., Hoigné, J., Gassmann, E., and Braun, A. M., Chemosphere **13**, 631 (1984).
[3] Haag, W. R., Hoigné, J., Gassmann, E., and Braun, A. M., Chemsophere **13**, 641 (1984).
[4] Haag, W. R., and Hoigné, J., Environ. Sci. Technol. **20**, 341 (1986).
[5] Faust, B. C., and Hoigné, J., Sensitized Photo-oxidation of Phenols by Fulvic Acid and in Natural Waters, Environ. Sci. Technol. (1987) accepted.
[6] Mill, T., Hendry, D. G., and Richardson, H., Science **207**, 886 (1980).
[7] Haag, W. R., and Hoigné, J., Chemosphere **14**, 1659 (1985).
[8] Russi, H., Kotzias, D., and Korte, F., Chemosphere **11**, 1041 (1982).
[9] Zepp, R. G., Hoigné, J., and Bader, H., Environ. Sci. Technol. **21**, 443 (1987).
[10] Fischer, A. M., Kliger, D. S., Winterle, J. S., and Mill, T., Chemosphere **14**, 1299 (1985).
[11] Zepp, R. G., Braun, A. M., Hoigné, J., and Leenheer, J. A., Environ. Sci. Technol. **21**, 485 (1987).
[12] Petasne, R. G., and Zika, R. G., Nature **325**, 516 (1987).
[13] Baxter, R. M., and Carey, J. H., Freshwater Biol. **12**, 211 (1982).
[14] Ross, R. D., and Crosby, D. G., Environ. Toxicol. Chem. **4**, 773 (1985).
[15] Larson, R. A., Hunt, L. L., Blankenship, D. W., Environ. Sci. Technol. **11**, 492 (1977).
[16] Hoigné, J., and Bader, H., Ozone Sci. Eng. **1**, 357 (1979).
[17] Acher, A. J., Water Sci. Technol. **17**, 623 (1985).
[18] Rodgers, M. A. J., and Snowden, J. Am. Chem. Soc. **104**, 5541 (1982).
[19] Farhataziz, and Ross, A. B., Selected Specific Rates of Reactions of Transients from Water in Aqueous Solution. III Hydroxyl Radical and Perhydroxyl Radical and their Radical Ions, NSRDS-NBS 59, Washington, DC (January 1977).
[20] Anbar, M., Bambenek, M., Ross, A. B., Selected Specific Rates of Reactions of Transients from Water in Aqueous Solution. I Hydrated Electron, NSRDS-NBS 43, Washington, DC (1973).
[21] Bielski, B. H. J., Cabelli, D. E., Arudi, R. L., and Ross, A. B., J. Phys. Chem. Ref. Data **14**, 1041 (1985).
[22] Hoigné, J., Faust, B. C., Haag, W. R., and Zepp, R. G., Aquatic Humic Substances as Sources and Sinks of Photochemically Produced Transient Reactants, ACS Symposium Series, Washington, DC, in press.
[23] Zafiriou, O. C., Measuring Photochemical Radical Fluxes in Natural Waters, Presented at the Ocean Sciences Meeting, New Orleans, LA, January, 1978. Abstract in EOS 66, 1265 (Dec. 17, 1985).
[24] Scully, F. E., and Hoigné, J., Chemosphere **16**, 681 (1987).
[25] Haag, W. R., and Mill, T., Photochem. Photobiol. **45**, 317 (1987).

Volume 93, Number 3, May–June 1988
Journal of Research of the National Bureau of Standards

Accuracy in Trace Analysis

Trace Radiocarbon Analysis of Environmental Samples

Ann E. Sheffield, Lloyd A. Currie, and George A. Klouda

National Bureau of Standards
Center for Analytical Chemistry
Gas and Particulate Science Division
Gaithersburg, MD 20899

1. Radiocarbon in the Environment

In the atmosphere, radioactive ^{14}C is produced at a roughly constant rate and decays with a half-life of 5730 y. Human activity perturbs the natural, steady-state level of ^{14}C. Combustion of fossil fuels and emission of pollutants derived from fossil feedstocks dilute ^{14}C with "dead" ^{12}C (the "Suess effect"), and nuclear weapons tests produce excess ^{14}C (the "bomb effect"). Therefore, sources are often revealed by measurement of ^{14}C in species of environmental concern, such as "greenhouse" gases (CO_2, CO, CH_4), atmospheric particles, and toxic or carcinogenic organic compounds.

Atmospheric weapons testing peaked in the early 1960s, and, in 1963, the atmospheric radiocarbon level was about twice the natural level [1]. Since then, the ^{14}C concentration has been declining, largely because of equilibration of atmospheric CO_2 with carbonate in the world's oceans. The changing distribution of "bomb" carbon in the ocean has been measured to investigate ocean circulation patterns [2,3,4]. As nuclear power plants become more widely used, they, too, may become important sources of atmospheric ^{14}C. Radiocarbon has already been exploited as an inherent tracer to investigate the dispersion of plumes from nuclear power plants [5,6,7].

2. Accelerator Mass Spectrometry

For many species of interest, the small amount of sample available requires the use of accelerator mass spectrometry (AMS) for radiocarbon analysis. A gram of modern carbon undergoes 13.56 radioactive disintegrations ($^{14}C \rightarrow {}^{12}C$) per minute; this corresponds to a ^{14}C concentration of 5.9×10^{10} atoms of ^{14}C/gC. Because AMS detects atoms rather than radioactive decays, it is far more sensitive than conventional counting methods.

In AMS, a Cs^- ion sputter source is used to produce negative ions from a sample target. The major interference with ^{14}C is ^{14}N, which does not form stable negative ions and hence is largely eliminated. In many AMS systems, the mass-14 beam is selected by a magnetic deflector and directed into a tandem accelerator. The ions are accelerated at ~3 MeV and gas-stripped. At this energy, the most probable charge state for C is +3. Interfering molecular ions, e.g., ^{13}CH and $^{12}CH_2$, are unstable in the +3 state and disintegrate completely. The ion beam is then accelerated back to ground potential, the mass-14, +3 beam is selected, and final measurement of ^{14}C occurs in E-dE/dx detectors of the type used in nuclear physics. Magnetic switching between ^{14}C and ^{13}C or ^{12}C permits the measurement of ^{14}C relative to a stable isotope.

At present, the accuracy of AMS is limited by contamination during sample preparation, sensitivity (response/^{14}C) by ionization efficiency and half-life, and precision by counting statistics and "machine reproducibility" (currently ~0.5% for mg-size samples). A sample-preparation technique developed at NBS [8] involves a closed-tube combustion of samples to CO_2 followed by a closed-system reduction to CO over hot Zn and reduction of CO to C on Fe wool. The procedure, giving an overall blank (chemistry and accelerator) of 1.9 ± 0.4 μg contemporary carbon, has been used to measure samples containing <100 μg of carbon (RSE = 10%) [9].

Development of gaseous ion sources that can accept CO_2 directly [10,11] will reduce sample handling and hence contamination. When such sources become available, combined techniques such as GC-AMS will be possible, since samples eluting from a column could be combusted to CO_2 and introduced directly into the AMS ion source [12].

3. Radiocarbon in Atmospheric Particles

Carbonaceous particles in the atmosphere are of interest not only because of their effects on visibility, climate, and health but also because they may carry toxic or carcinogenic organic pollutants. Radiocarbon analysis allows modern particles arising from biological processes or from human activities

such as wood-burning to be distinguished from those arising from fossil sources such as motor traffic and combustion of coal and oil.

Because of the large sample requirements of conventional decay counting, early work [13,14] involved collection of whole-particle samples over long periods (days). Such whole-particle samples are often biased by the presence of relatively large debris such as pollen, insect parts, and road dust, but the fine (<2.5 μm diameter) particles are of more environmental concern. Fine carbonaceous particles have a disproportionate effect on visibility and climate [15] and are in the "respirable" size range, i.e., they are retained in the lungs. Measurement of size-fractionated aerosol in Los Angeles [16,17,18] showed that the fine particles had a higher percentage of fossil, anthropogenic carbon than did larger particles.

Our involvement with EPA's Integrated Air Cancer Project (IACP) [19] allowed us to investigate the sources of different chemical fractions in fine particles. Samples were collected during winter, 1984–1985, in two cities (Raleigh, NC, and Albuquerque, NM) where the dominant carbon sources were expected to be residential wood combustion (contemporary) and motor vehicle emissions (fossil). We used oxidation with nitric acid [20] to isolate the elemental carbon fraction from selected fine-particle samples and analyzed both elemental and total carbon for ^{14}C. The results summarized in table 1 show that: (1) as expected, the fossil (motor vehicle) contribution was highest for the high-traffic intersection in the daytime and was quite low for the residential sites at night; and (2) the elemental carbon fraction had a higher fossil contribution than the corresponding total carbon in all cases. This result suggests that elemental carbon may be more useful than total or organic carbon for tracing mobile sources [21].

Finally, in a second Albuquerque study conducted in December 1985, we isolated the polycyclic aromatic hydrocarbon (PAH) fraction from fine-particle samples. The behavior of two PAH, dehydroabietic acid (DHA) and benzo(ghi)perylene (BGP), is shown in figure 1. DHA has been detected in wood smoke [22], and BGP has been suggested as a tracer for motor vehicle emissions [23]. The utility of these and other PAH as source tracers will be tested by comparing PAH-based source-strength estimates with ^{14}C results for the PAH fraction.

Acknowledgments

We thank D. J. Donahue, A. J. T. Jull, T. W. Linick, and L. J. Toolin for their participation in the AMS radiocarbon measurements, S. N. Chesler for assistance with GC measurements, and R. K. Stevens for his contributions. This work was supported in part by the U.S. Environmental Protection Agency.

Table 1. Radiocarbon results for IACP samples

Site	% Contemporary	
	Total C	Elemental C
Raleigh, residential site		
night	95±14[a] (3)[b]	60±11 (2)
Albuquerque, residential site		
night	78±6 (8)	61±10 (8)
day	66±2 (2)	40±18 (3)
Albuquerque, traffic intersection		
day	35±15 (3)	19±1 (2)

Contemporary carbon values have been adjusted for the ^{14}C content of the atmosphere.
[a] Errors shown are standard deviations.
[b] The number of samples (N) for each entry is given in parentheses.

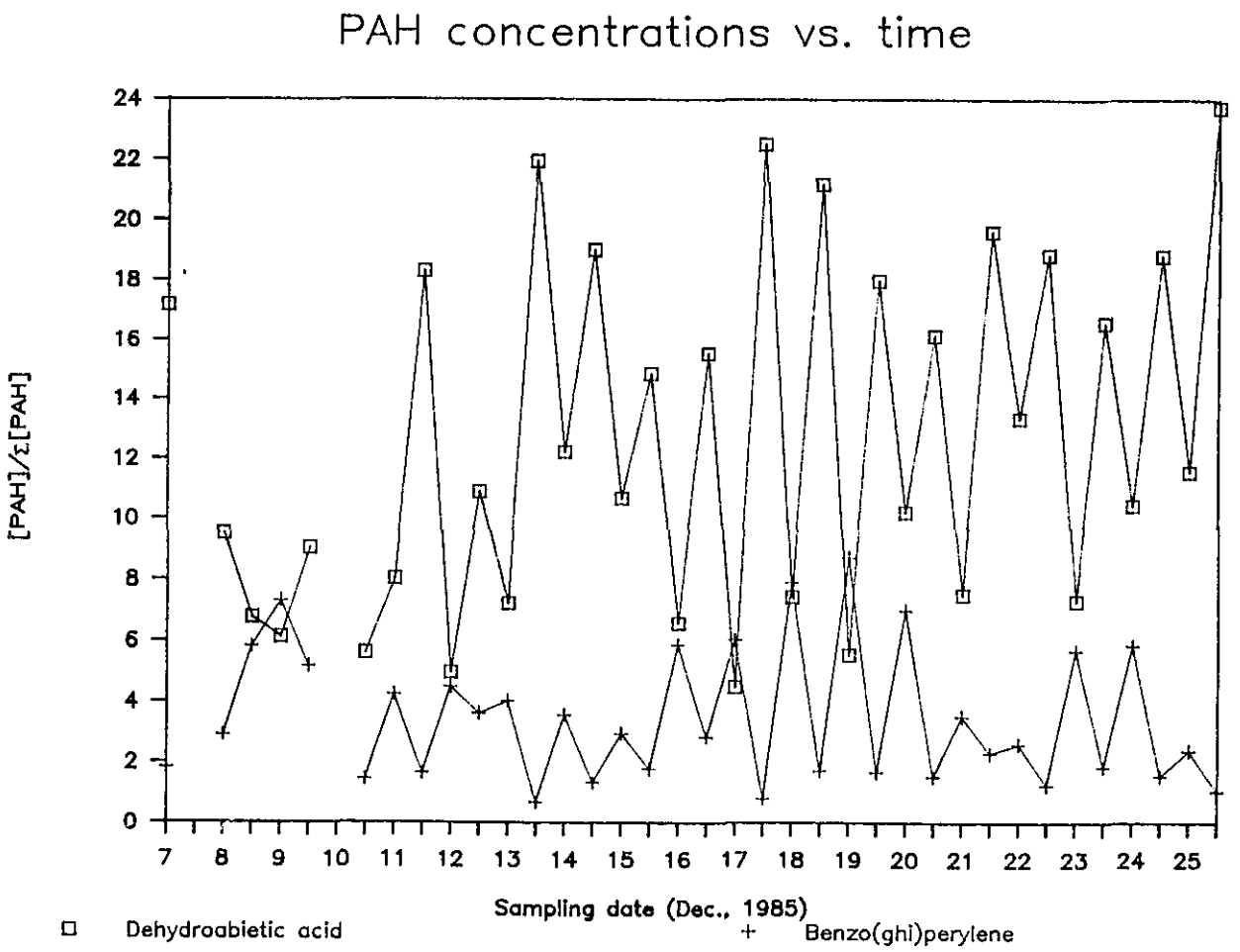

Figure 1. Variation of DHA and BGP with collection date and time in samples from a residential site in Albuquerque, NM. For each sample, PAH concentrations are expressed relative to the total mass of all PAH measured in that sample. Integral "date" values represent daytime samples; half-integral values indicate nighttime samples.

References

[1] Levin, I., Münnich, K. O., and Weiss, W., Radiocarbon (U.S.) **22**, 379 (1980).
[2] Broecker, W. S., Peng, T.-H., Ostlund, G., and Stuiver, M., Geophys. Res. (U.S.) **90**, 6953 (1985).
[3] Peng, T.-H., Radiocarbon (U.S.) **28**, 363 (1986).
[4] Schlitzer, R., Radiocarbon (U.S.) **28**, 391 (1986).
[5] Walker, A. J., Otlet, R. L., and Longley, H., Radiocarbon (U.S.) **28**, 681 (1986).
[6] McCartney, M., Baxter, M. S., McKay, K., and Scott, E. M., Radiocarbon (U.S.) **28**, 634 (1986).
[7] Otlet, R. L., Walker, A. J., and Longley, H., Radiocarbon (U.S.) **25**, 593 (1983).
[8] Verkouteren, R. M., Klouda, G. A., Currie, L. A., Donahue, D. J., Jull, A. J. T., and Linick, T. W., Phys. Res. B (Netherlands), in press (1987).
[9] Klouda, G. A., and Currie, L. A., Verkouteren, R. M., Einfeld, W., and Zak, B. D., J. Amer. Nuclear Soc. (U.S.), in press (1987).
[10] Middleton, R, Phys. Res. B (Netherlands) **5**, 193 (1984).
[11] Bronk, C. R., and Hedges, R. E. M., Phys. Res. B (Netherlands), in press (1987).
[12] Gillespie, R., Radiocarbon (U.S.) **28**, 1065 (1986).
[13] Clayton, G. D., Arnold, J. R., and Patty, F. A., Science (U.S.) **122**, 751 (1955).
[14] Lodge, J. P., Jr., Bien, G. S., and Suess, H. E., Internatl. J. Air Pollution **2**, 309 (1960).
[15] Wolff, G. T., Countess, R. J., Groblicki, P. J., Ferman, M. A., Cadle, S. H., and Muhlbaier, J. L., Atmos. Environ. (U. K.) **15**, 2485 (1981).
[16] Currie, L. A., Klouda, G. A., Continetti, R. E., Kaplan, I. R., Wong, W. W., Dzubay, T. G., and Stevens, R. K., Radiocarbon (U.S.) **25**, 603 (1983).
[17] Klouda, G. A., Currie, L. A., Donahue, D. J., Jull, A. J. T., and Zabel, T. H., Phys. Res. B (Netherlands) **5**, 265 (1984).
[18] Berger, R., McJunkin, D., and Johnson, R., Radiocarbon (U.S.) **28**, 661 (1986).
[19] Lewtas, J., and Cupitt, L., Overview of the Integrated Air Cancer Project, Proc. 1987 EPA/APCA Symposium on Measurement of Toxic and Related Air Pollutants, APCA, Pittsburgh (1987), p. 555.

[20] Sheffield, A. E., Klouda, G. A., and Currie, L. A. in preparation (1987).
[21] Klouda, G. A., Currie, L. A., Sheffield, A. E., Wise, S. A., Benner, B. A., Stevens, R. K., and Merrill, R. G., The Source Apportionment of Carbonaceous Combustion Products by Micro-Radiocarbon Measurements for the Integrated Air Cancer Project (IACP), Proc. 1987 EPA/APCA Symposium on Measurement of Toxic and Related Air Pollutants, APCA, Pittsburgh (1987), p. 573.
[22] Standley, L. J., and Simonheit, B. R. T., Environ. Sci. Technol. (U.S.) **21**, 163 (1987).
[23] Sawicki, E., Analysis for Airborne Particulate Hydrocarbons: Their Relative Proportions as Affected by Different Types of Pollution, National Cancer Institute Monograph No. 9 (1962).

The Use of Cryogenic Size Reduction to Improve Purgeable Priority Pollutant Analyses in Soil Samples

J. H. Phillips, C. A. Potera, P. M. Michalko, and J. H. Frost

Air Products and Chemicals, Inc., Allentown, PA 18195

Air Products and Chemicals has been investigating the use of cryogenics to improve the recoveries of priority pollutants from solid matrices. A significant number of benefits have been realized from cryogenic size reduction of materials prior to analysis. The precision and accuracy of trace organic analyses in solid matrices are improved by cryogenic techniques. Even the most difficult samples, from rocks to rubber, can be easily ground cryogenically. Cryogenic size reduction increases sample homogeneity, reduces analyte loss due to the heat of grinding, and improves extraction efficiency by increasing the surface area of the sample.

The Environmental Protection Agency (EPA) has proposed the Toxicity Characteristic Leaching Procedure (TCLP) to identify wastes which pose a hazard due to their potential to leach toxic species. Because the determination of volatile species was important, a Zero Headspace Extractor (ZHE) was designed to prevent volatile loss during leaching. A shortcoming of the proposed volatiles analysis is that a trade-off had been made between size reduction and volatile loss. The EPA recommends that only solids that are >9.5 mm or have a surface area of <3.1 cm^2/g be reduced.

Clays were used as the synthetic soil matrix from which volatiles would be recovered. Clays have a number of unique properties which make them ideal candidates for adsorbing and retaining volatile organics. A hardened clay matrix was produced by combining one part kaolin clay, one part sepolite clay, one part cement, and two parts water. Twenty-one volatile organic priority pollutants were spiked into the clay matrix via the aqueous portion of the formulation. The spiking was performed at two concentrations, 20 mg/kg and 2.0 mg/kg in the solid matrix.

The spiked clay samples were reduced to 9.5 mm under ambient conditions, reduced to <200 mesh at ambient temperature, or reduced to <200 mesh at cryogenic temperature (−196 °C). After size reduction, the sample was extracted for 18 h in the ZHE according to TCLP protocol. The leachate was then analyzed by purge and trap GC/MS according to the EPA method #624.

At the 20 mg/kg spike concentration, recoveries ranged from 1.2% to 20%. Recoveries never approached 100% because a significant portion of volatiles was lost to the atmosphere during mixing and hardening of the clay-cement matrix. On a relative basis, cryogenic size reduction improved recoveries three fold over ambient and minimum size reduction techniques.

At the 2 mg/kg spike concentration, the effects of cryogenic size reduction were also quantified. Recoveries were improved an average of five times over ambient and minimum size reduction. Analysis precision, as measured by the percent relative standard deviation between three extractions, was also improved. The precisions of analyses were 5.9% for cryogenic size reduction (200 mesh @ −195 °C), 13% for minimum size reduction (9.5 mm @ 20 °C) and 25% for ambient size reduction (200 mesh @ 20 °C). These results indicated that when cryogenic size reduction was not possible, minimum size reduction was preferred.

Cryogenic grinding was clearly the best size reduction technique for the preparation of samples for volatile analysis. Advantages were increased analyte recovery, better sample homogeneity, and improved extraction efficiency.

Volume 93, Number 3, May–June 1988
Journal of Research of the National Bureau of Standards

Accuracy in Trace Analysis

Determination of 3-Quinuclidinyl Benzilate in Urine

G. D. Byrd, L. T. Sniegoski, and E. White V

Center for Analytical Chemistry
National Bureau of Standards
Gaithersburg, MD 20899

The compound 3-quinuclidinyl benzilate (BZ) is a potent muscarinic cholinergic antagonist that can produce incapacitation at very small doses [1,2]. As such it can be used as a powerful psychochemical warfare agent. In response to the scheduled destruction of U.S. military stockpiles of BZ and the increased potential for worker exposure, our laboratory has developed a specific confirmatory test for human exposure to BZ. The test determines the amount of the parent compound in the urine as well as the two major metabolites, quinuclidinol (Q) and benzilic acid (BA) which are formed by hydrolysis as shown in figure 1. Previous work in our laboratory demonstrated that BA and Q could be determined in urine at their target concentration of 5 ng/mL as based on a proposed acceptable exposure level. The work described here demonstrates the recovery of the parent compound from urine at its target level and the incorporation of this method into an overall test for exposure to BZ.

Only a small percentage of unmetabolized BZ is expected to be found in the urine of exposed persons. Estimates based on the proposed acceptable exposure level require detection limits for BZ in urine of 0.5 ng/mL. Because of the complexity of the urine matrix and the variation of urine from one individual to the next, the measurement of BZ in urine at this level presents a challenging analytical problem. A method using solid phase extraction and isotope dilution GC/MS was developed to measure BZ in urine. In the procedure, a 20 mL urine sample is made basic and the BZ is removed by solid phase extraction onto a C_{18} sample preparation column. The column is washed with water and a 40% acetonitrile solution and the BZ is eluted with methanol. The eluent is blown to dryness and reconstituted in a derivatizing agent to form the trimethylsilyl derivative for analysis by GC/MS. Measurements are performed using single ion monitoring for the fragment ion $(C_6H_5)_2CO\text{-}TMS^+$ at m/z 255 and the analogous ion from the isotopically labeled internal standard (3-quinuclidinyl-^{18}O-benzilate-d_5) at m/z 260. We have been able to determine BZ in urine at concentrations less than 0.5 ng/mL. Figure 2 depicts an ion chromatogram showing detection of BZ as its TMS derivative at 0.5 ng/mL.

This method was incorporated into the overall test for exposure to BZ which determines the concentration of BZ, BA, and Q in urine. The test was validated by looking at eight different urine samples which were divided into subsamples, some spiked with known concentrations of the analytes and others left blank. Of the 18 subsamples that were analyzed for BZ, BA, and Q, nine were spiked at or just below the target concentration level, five at approximately 10 times the target level, and four were blank. The subsamples spiked at 10 times the target level were to provide information for urine samples with concentration levels that would be expected in the event of an actual exposure. The blank urine samples provided information regarding background interferences with the test over several different urines. The results of the validation test on these samples are summarized graphically in figure 3.

For all three analytes we considered the measured values close to the spiked levels. Based on the established target levels no false positives occurred for any of the three analytes in any of the four blank urines. For samples spiked near the target levels no measured value was less than 80% of the spiked value. On this basis, no false negatives were apparent. The imprecisions in the method with regard to GC/MS measurement, sample preparation, and urine-to-urine variability were more or less evenly distributed and the imprecision of a single measurement was about 15%.

Acknowledgment

This work was supported by the U.S. Army Medical Bioengineering Research and Development Laboratory.

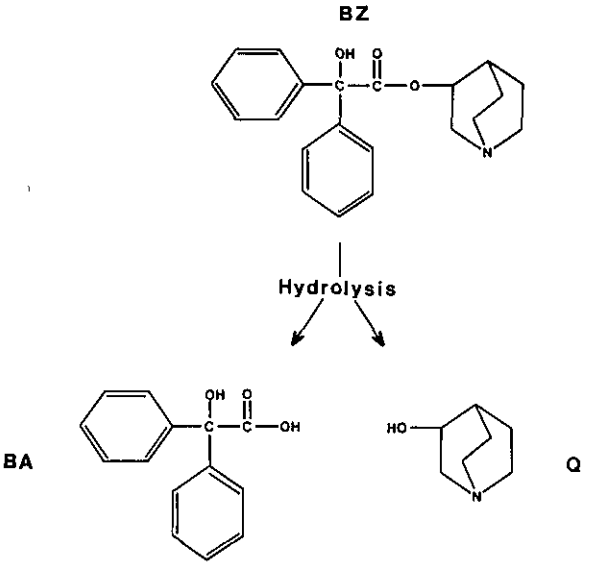

Figure 1. Hydrolysis of BZ.

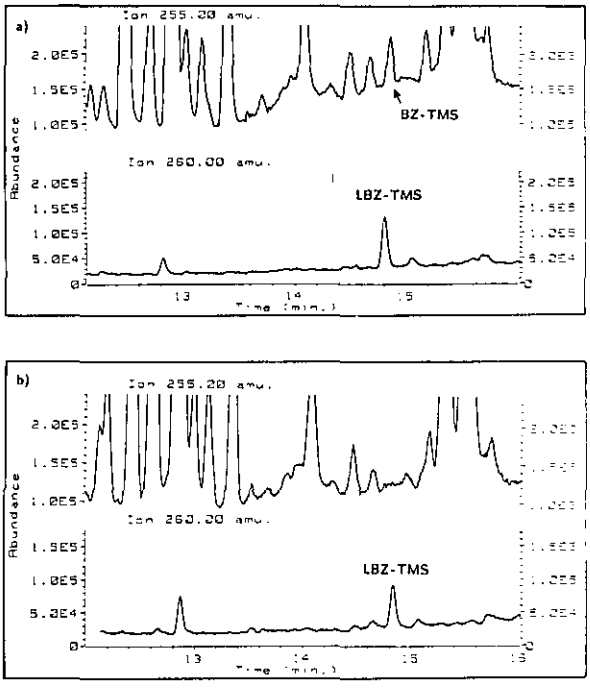

Figure 2. SIM chromatogram of *m/z* 255 and *m/z* 260 from extracts of urine a) spiked with 0.5 ng/mL BZ and b) a urine blank. BZ-TMS is the derivatized BZ and LBZ-TMS is the derivatized labeled internal standard.

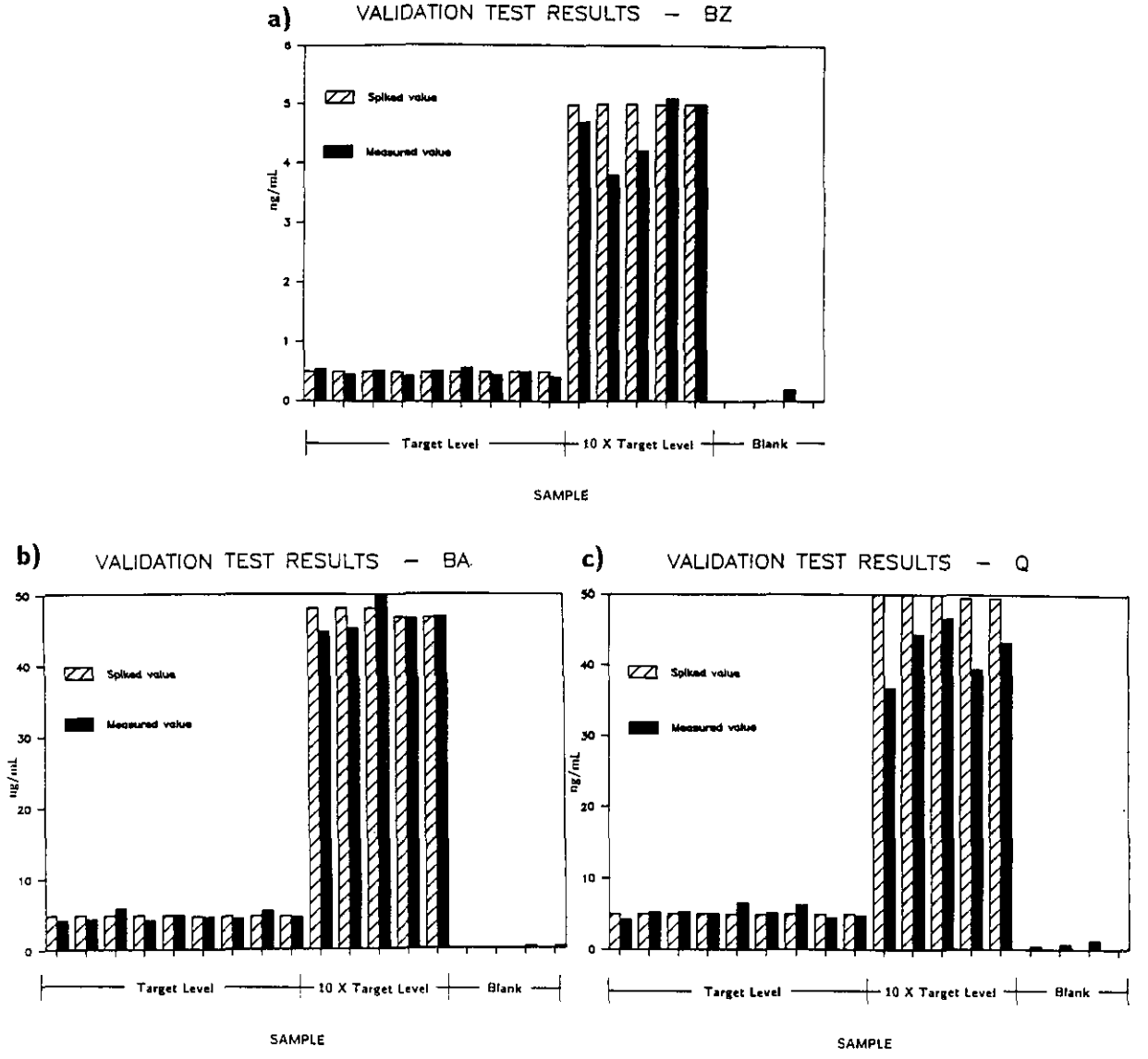

Figure 3. Graphical representation of results from validation test of analytical method for a) BZ, b) BA, and c) Q in urine.

References

[1] Albanus, L., Acta Pharmacol. Toxicol. **28**, 305 (1970).
[2] Rosenblatt, D. H., Dacre, J. C., Shiotsuka, R. N., and Rowlett, C. D., Problem Definition Studies on Potential Environment Pollutants. VIII. Chemistry and Toxicology of BZ (3-Quinuclidinyl Benzilate). Technical Report 7710, U.S. Army Medical Bioengineering Research and Development Laboratory, Fort Detrick, Frederick, MD (1977).

Volume 93, Number 3, May–June 1988
Journal of Research of the National Bureau of Standards

Range-Programming Stripping Voltammetry for Determination of Some Metals in Seawater

Myung-Zoon Czae and Jong-Hyup Lee

Department of Chemistry
Hanyang University
Seoul 133, Korea

Multielement capability of stripping analysis is one of its distinctive advantages described elsewhere [1]. Anodic stripping voltammetry with the use of differential pulse mode (DPASV) is uniquely suited [2], and therefore, applied extensively to the direct simultaneous determination of some trace metals (Zn, Cd, Pb, and Cu) in sea waters [3,4]. Even with the well-established procedure for a given sample, there still arises the problem introduced by simultaneously measuring relative concentrations of metal ions. A case in point is zinc and cadmium concentrations whose ratio sometimes is as high as 400 (12 ppb Zn/0.03 ppb Cd), and typically as high as 200 in raw surface sea waters [3]. In such a case, either one must run the entire steps separately by selecting suitable variables for each metal or pair of metals whose concentration ratio is adequate for simultaneous measurement, or the recorder scale must be changed during a single run to obtain the best results. The latter approach, difficult to achieve manually in practice, would rely on the application of an autoranging amplifier [5]. The use of an autoranging amplifier, however, has given rise to complications in evaluating the resulting voltammograms in most practical applications for analyzing seawaters [6]. The present work was initiated in order to overcome deterioration in readability and data quality, by developing a new programmed-ranging technique.

Principle of Operation

With the pulsed (commonly DP) stripping mode in the simultaneous measurements, each voltammogram peak starts from the baseline of nearly zero or very small current when moderate resolution is provided. This fact enables us to change current gain to a pre-specified value (programmed vs potential, according to the concentration ratios for a lot of samples), when the potential is scanned to a position just before the start of a subsequent peak (where pre-peak current also drops nearly to the baseline). Figure 1 illustrates the basic principle behind the programmed-ranging technique. If we incorporate an additional amplifier (fig. 1, lower large box) with a gain (programmable) of $G_j(x)$ to a prototyping polarographic analyzer's output (which otherwise would give the peak current i_j, for the jth component or peak), the overall analytical signal (I_j) will be

$$I_j = G_j(x)\, i_j \tag{1}$$

where gain $G_j(x)$ depends on some variable x. In a scheme employing an autoranging amplifier, x is I_j provided by feedback means. Thus, gain $G_j(I_j)$ varies indefinitely in a stepwise manner by a predetermined factor of $(10)^{1/2}$, 10, or several decades. This approach requires the operator's attention for marking the gain increments. We adopted a potential window, $E_{(j)}$, as x, located around the j's peak potential. The implementation of eq (1) with $G_j(E_{(j)})$, range programming (vs potential), can be provided by feedforward automatically, instead of by feedback.

The gain or range programming amplifier unit (fig. 1) comprises a comparator with variable threshold (Reference Voltage) and associated circuitry (Processing Ckt) for automatically changing the gain $G_j(E_{(j)})$ when the scanned electrode potential reaches a threshold of the jth potential window $E_{(j)}$. The value of gain G_j remains at the programmed value over the entire potential window $E_{(j)}$. The processing circuit comprises a programmable gain amplifier, counter, and multiplexer/demultiplexer (MPX) and related circuitry for performing the proper functions. By comparing the sweep potential with the set voltage, the comparator causes the counter to produce a bit control signal to the demultiplexer, which selects a gain-determining feedback resistor, and, in turn, switches the next prespecified reference voltage to the comparator.

Results and Discussion

Figure 2 shows differential pulse stripping voltammograms with a range or gain program shown in (C) for a 10 mL aliquot of the filtered seawater sample solution (0.45 μm Millipore

membrane) whose pH was adjusted to 3.0. The adverse concentration ratio (Zn/Cd) was 150. The readability, however, improved to the same order of magnitude in the range programming mode ((b) in fig. 2), without making any sacrifice in data quality. The potentiostat was a PAR Model 174A equipped with a Model 303 static mercury drop electrode.

To establish linearity between peak current and concentration, standard curves for four metals in seawater were simultaneously run at pH 3.0. Standard additions were made by adding to the 10-mL sample, 10-μL volumes of a solution containing 0.100 ppm in Cd and 1.0 ppm in Zn, Pb, and Cu. The resulting standard addition curves (shown in fig. 3) demonstrate response linearity with good precision. With the deposition potential of −1.2 V (vs Ag/AgCl) and a deposition time of 3 min, we applied the technique to analyze simultaneously more than 300 seawater and marine samples employing the standard addition calibration curve and triple spiking procedure [7], respectively.

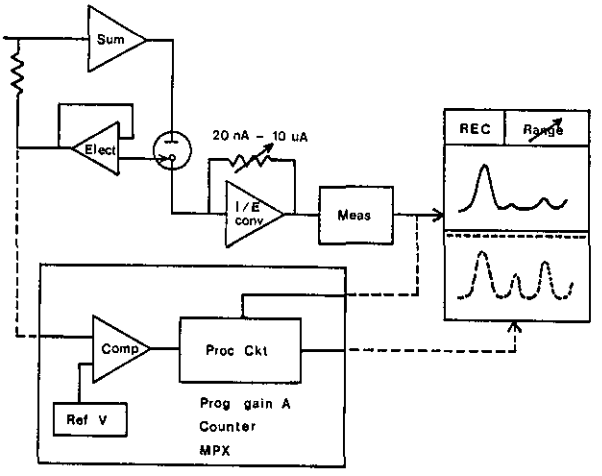

Figure 1. Schematic diagram of proposed technique.

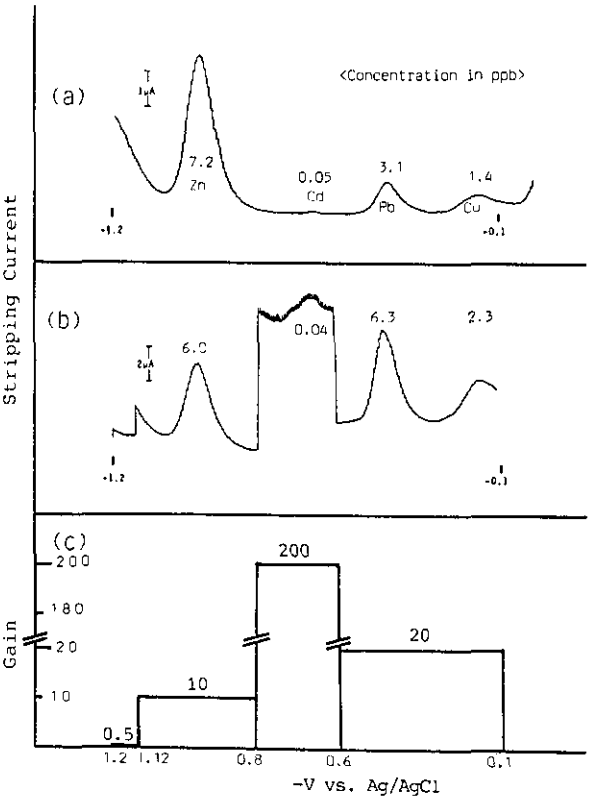

Figure 2. Typical voltammograms, (a) conventional, with deposition time of 30 min; (b) range programmed, with 3 min deposition with gain program shown in (c).

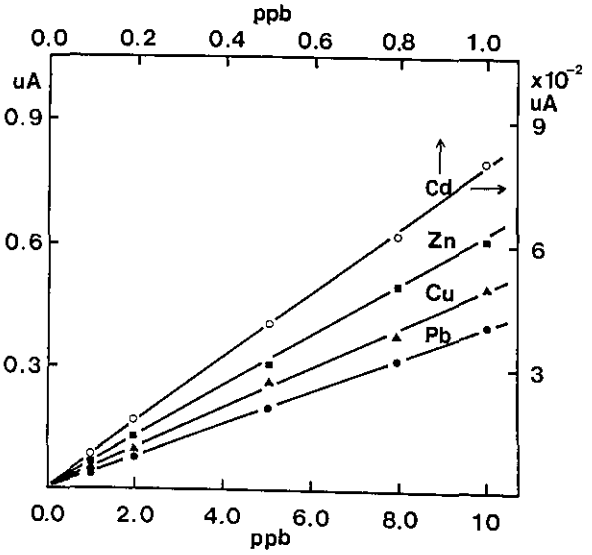

Figure 3. Standard addition calibrating curves in seawater. The peak currents are net values.

References

[1] Wang, J., Envir. Sci. Technol. 16, 104A (1982); Stripping Analysis, VCH Publishers, Inc., Deerfield Beach, FL (1985) Chap. 1.
[2] Zirino, A., Voltammetry of Natural Sea Water, in Marine Electrochemistry, M. Whitfield and D. Jagner, eds., John Wiley and Sons, New York (1981) Chap. 10.
[3] Czae, M.-Z., and Lee, J.-H., Bull. Envir. Sci. (Hanyang Univ., Seoul, Korea) 6, 153 (1985).
[4] Kim, E., Czae, M.-Z., et al., Studies on the Effect of Cooling Water to the Cultivated Marine Organism around Poryung and Samchunpo Power Plants, Part I and II, KRC-84C-J01, Korea Electric Corp., Seoul, March 1985.
[5] Ben-Yaakov, S., and Lazar, B., Talanta 27, 1061 (1980).
[6] Lee, J.-H., Autoranging Amplifier for the Simultaneous Determination of Some Trace Metals in Seawater by DPASV. Thesis (MS), Hanyang University, Seoul, Korea.
[7] Czae, M.-Z., Lee, J.-H., and Hong, T., Validation of Anodic Stripping Voltammetry for Determination of Some Metals in Sea Samples, Proc. First Korea-Japan Joint Symp. on Anal. Chem. (Korean Chem. Soc.), Seoul, Korea (April 1985) 27–36.

Computer Assisted Pesticide and PCB Identification System (CAPPIS)

Joseph E. Dierkes

New Jersey State Department of Health
John Fitch Plaza CN 361
Trenton, NJ 08625

Environmental samples (water, air, soil, etc.) are routinely analyzed in the state laboratory for pesticide and PCB residues using gas chromatographs (GCs) equipped with electron capture detectors (ECDs), and packed glass (4 mm × 2 m) columns of differing polarity. In a typical analysis, one primary column (1.5% OV-17/1.95% OV-210) is used to quantitate results obtained after confirmation by a secondary column (4% SE-30/6% OV-210) and occasionally a third column (5% OV-210, 3% OV-1, etc.).

Two standard mixtures of pesticides are injected before any samples are analyzed. After verifying retention times (RTs) for key pesticides (i.e., pp'-DDT) in these standards, actual sample analysis may begin. Should any peaks be encountered, then their RTs are compared with those of the standards. If the sample peak RT on each column used matches the RT of the pesticide standard on each column within certain limits, identification is tentatively confirmed. If a multicomponent residue such as chlordane, toxaphene, or a PCB is found, then the appropriate or suspected standard is also injected and chromatographed. Each sample chromatogram is checked for the presence and proper RT of any surrogate compounds (Mirex or dibutylchlorendate) used.

The peak height ratios between the columns are next examined for a similar ratio obtained for that of the pesticide and the standard, thus ruling out false identifications due to interferences. Following U.S.E.P.A. practice, positive matches are quantitated by a comparison (peak height or area) with known concentrations of standards, as long as the peak heights between sample and standards are within 25% of each other. If the positive result is the surrogate compound, then its percent recovery is also calculated.

It was desired to develop a computer algorithm to perform all these checks and measurements with greater accuracy and speed, provide a considerable amount of quality control documentation for large numbers of samples, and at the same time meet or surpass stringent U.S.E.P.A. and IFB analytical requirements.

To this end, a battery of GCs was interfaced with a mainframe computer system. Sample chromatograms are produced by standard 1 mV recorders and the GC signals are simultaneously digitized by analog-to-digital converters. The digitized data from each analysis are arranged into a definite set of records in a file by a modified post run program which assigns the file a unique number and stores it on the disk. Any chromatogram can be called up at a later time for access by the software package, designated CAPPIS, by referring to its file number.

This package consists of a set of simple BASIC/FORTRAN programs which could be modified to work with various analytical systems. All that would be needed would be to set up unique digitized data files and define the ways the software could access them.

After a GC is set up, its operating parameters (column types, carrier gas type and flow rate, temperature, etc.) are stored on the disk in a file generated by one of these programs. Next, retention time windows are generated by another program and also stored on disk. This completes the initial setup, and is essentially done once. Any later changes in the operating parameters, columns, or windows are

very easily accomplished by rerunning one or both of these programs.

When a series of samples is injected and analyzed, all chromatograms thus generated are labeled with sample identifications, sizes, weights, volume injected, and attenuation used with yet another program. Then, the user is ready to invoke CAPPIS to analyze the data.

This analytical package consists of a menu from which the user chooses one of [currently] three options:

1) identify and quantitate pesticide residues with two or with three columns;
2) quantitate a multicomponent sample such as a PCB, chlordane, or toxaphene, when the identity of the sample has been established;
3) compare different multicomponent standards with a multicomponent sample to deduce its identity.

Essentially, the software sorts the peak data into various sets of arrays which are then manipulated according to which option is chosen. For the first option, it compares sample chromatograms with those of different pesticide standards analyzed the same day. Positive identifications are based upon retention time matches between all the columns used as long as the RT for each peak in question is within its specified window. After passing a peak height ratio test, a result is calculated; if it is above experimentally determined detection limits, it is printed on the report.

Since it is not practical to maintain any sort of "library" of PCB patterns (due to varying detector response, operating parameters and column characteristics between different instruments), option #3 functions as a useful tool in assigning an identification between similar PCBs (e.g., Ar1248 vs Ar1254). Once the identity of a particular PCD has been established, it is a simple matter to quantitate the results with option #2.

In contrast to the manual quantitation method, the sum of the peak heights from ALL the columns used is employed for computing results, not simply the peak height from the primary column. When quantitating a set of multicomponent samples versus a standard, CAPPIS adjusts itself to varying numbers of peaks, so that the maximum possible number of peak matches can be used in each case. This provides greater accuracy and reproducibility due to an error leveling effect.

The software is open-ended. By adding additional testing loops either internally or in the form of subroutines, further refinements, currently under study in our laboratory, can be made to option #3. Peak data arrays can be extended in various directions to encompass the use of three or more different standards and/or columns. Arrays could also be added to option #1 for additional testing loops such as relative retention time ratios for deducing possible identifications of pesticides not contained in the standards.

During the past several months that CAPPIS has been in routine use, a time savings of one man-hour per instrument per day has been realized. The software has been used to successfully pass proficiency tests at the federal and state levels. Additionally, it has provided a reliable method of tracking both instrument performance and quality control trends.

Sequential Automated Analysis System for Lower Oxygenated Organic Compounds in Ambient Air

Ikuo Watanabe

The Institute of Public Health
4–6–1 Shirokanedai
Minato-ku, Tokyo 108, Japan

A completely automated system controlled by a microcomputer was developed for hourly analyses of lower oxygenated organic compounds (LO_x) in ambient air at the sub-ppb level. This system has some advantages, compared with manual procedures, including 1) good repeatability, 2) easy data processing, 3) easy accumulation of extensive data throughout the day and night, and 4) reduction of labor. Consecutive measurements using this system for 6–15 days have been carried out several times since November 1985 in Tokyo.

1. Introduction

LO_x are formed by the degradation of atmospheric hydrocarbons by free radicals, and are also emitted from various sources [1]. These compounds have been identified and measured in air [1–4], however, little is known about their concentration in the environment.

The accumulation of a large amount of data is essential for elucidation of the phenomena induced by the existence of LO_x. For this purpose, a practical and durable automated system was developed.

2. Experimental

2.1 Sampling Trap

Four kinds of adsorbents (Porapak–N, –Q, –T and Chromosorb 104) were examined for collection ability, and for desorption efficiency of LO_x and their parent compounds by heating. The results showed Chromosorb 104 (C104) to be superior to the other 3 adsorbents when a stainless steel tube (3 mm i.d. × 16 cm) packed with 0.4 g of C104 was used for the sampling tube. The collection volume of this trap for LO_x was estimated to be 2.4 L or more at 0 °C.

2.2 Sampling Air

An air sample was drawn at a height of 20 m from the ground and 3 m from the walls through a 20 m Teflon tube (6 mm o.d.) covered with a black tube. To reduce the loss of the compounds through the tube, the air sample was continuously drawn with a pump at a flow rate of 1 L/min. A portion of the air was sucked from the end of the main air stream for 30 min with a flow-controlled pump, through the sampling trap (kept at ca. 0 °C) using a flow rate of 45–50 mL/min to collect the LO_x in the air sample.

2.3 Chromatographic System

The system with an automated sampler is shown in figure 1. Two precolumns (BCEF and s.PQ in table 1) are used for the pre-fractionation of aliphatic hydrocarbons (AlHC) and aromatic hydrocarbons (ArHC), because some of AlHC overlap LO_x in chromatograms and ArHC prolong the analytical time.

The peaks in chromatograms of air samples were periodically identified by GC/MS. If the method requires sample sizes of more than 10 L, another sampling method was used [i.e., a trap (3 mm i.d. × 18 cm Teflon tube) packed with quartz wool impregnated with water was installed between 1.PQ and FID, with the LO_x peaks confirmed by their disappearance from the chromatograms].

The switching of the valves, fan, heater, cooler, GC, and data processor are controlled with a microcomputer and an interface. An air sample was ataken every hour for 30 min, and the chromatograms and the processed results were printed on chart paper and stored on floppy disks.

3. Results and Discussion

The reproducibility tests using a specially prepared gas containing LO_x at ppb levels showed that the overall system precision for LO_x was 1–5% (RSD) during one day, and the changes of the retention times were less than 0.5% (RSD). Detection limits with signal-to-noise of 4 were 0.5 ng for methanol, 0.1 ng for acetaldehyde and 0.1–0.5 ng for others. This corresponds to ca. 0.3 ppb of methanol and ca. 0.04 ppb of acetaldehyde respectively, in a 1.5 L air sample.

A typical chromatogram obtained with this system is illustrated in figure 2, showing the concentrations of some LO_x and ArHC species. Since the acetone and isopropanol peaks might contain other compounds, their values shown in figure 2 are considered to be tentative.

Table 1. Operating conditions for gas chromatograph

	Packings	Tube (SUS)	GC conditions
P1	N,N-bis(2-cyanoethyl) formamide [BCEF] on Chromosorb W (60/80)	3 mm (i.d.) 1.5 m (long)	Room temperature (18–30 °C) N_2 (38 mL/min)
P2	Porapak Q (50/80) [s.PQ]	2 mm (i.d.) 25 cm (long)	124 °C(12.5 min) – 4 °C/min(15 min) – 184 °C(25 min) N_2 (41 mL/min)
AC	Porapak Q (80/100) [1.PQ]	1.5 mm (i.d.) 4 m (long)	38.25 °C – 1.5 °C/min(14.5 min) – 20 °C/min(2.5 min) – 10 °C/min(3 min) – 2 °C/min(20 min) – 180 °C(13 min) N_2 (33 mL/min)

Volume 93, Number 3, May–June 1988
Journal of Research of the National Bureau of Standards

The monitoring of LO_x for 6–15 days has been carried out several times in the metropolitan area of Tokyo since November 1985, and data on more than 1800 samples have been obtained. Acetaldehyde, C_1-C_3 alcohols, and acetone were constantly observed in chromatograms. Acrolein, C_2-C_3 esters, propionaldehyde, C_4-C_5 ethers, and methylethylketone were occasionally detected. This system has worked satisfactorily for more than 2500 hours without any exchange of parts in the devices, and has proved to be practical and durable.

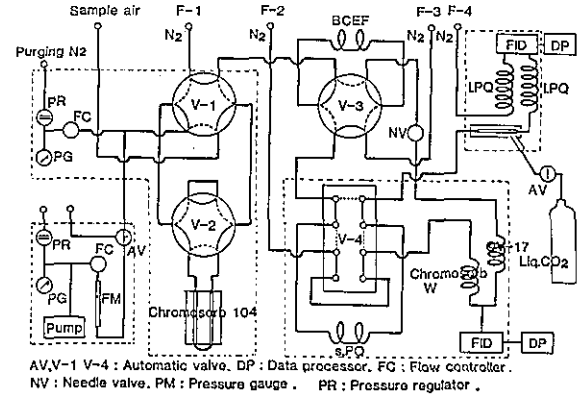

Figure 1. Schematic for automated sampling and analysis.

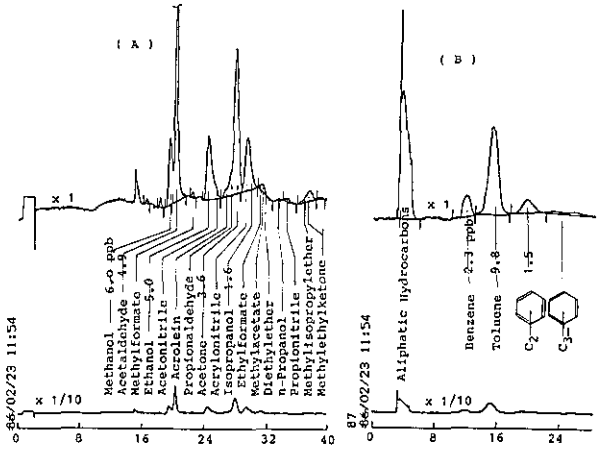

Figure 2. Gas chromatograms of ambient air (1.38 L).

References

[1] Graedel, T. E., Hawkins, D. T., and Claxton, L. D., Atmospheric Chemical Compounds, Academic Press, Inc., Orlando (1986).

[2] Bellar, T. A., and Sigsby, J. E., Jr., Environ. Sci. Technol. **4**, 150 (1970).

[3] Watanabe, I., and Yamada, S., Taikiosenkenkyu (J. Japn. Soc. Air Pol.) **13**, 259 (1978).

[4] Snider, J. R., and Dawson, G. A., J. Geophysical Res. **90(D2)**, 3797 (1985).

Trace Level Quantitation of Phenyltin Compounds Using HPTLC

K. K. Brown

Department of Chemistry
Oakland University
Rochester, MI 48063
and
Pesticide and Industrial Chemical Research Center
U.S. Food and Drug Administration
Detroit, MI 48207

P. Tomboulian

Department of Chemistry
Oakland University
Rochester, MI 48063

and

S. M. Walters

Pesticide and Industrial Chemical Research Center
U.S. Food and Drug Administration
Detroit, MI 48207

We sought to develop a rapid analytical technique for the determination of triphenyltin pesticide residues in food. HPTLC offers such an approach since it is rapid, selective, sensitive and has a high throughput [1]. The quantitative aspects of HPTLC have been documented and reviewed [2]. Conventional TLC has been used to separate butyltin compounds, subsequently detected using chemical oxidation and colorimetry of the pyrocatechol-complex [3]. TLC has also been used to speciate organotin compounds that were detected by anodic stripping voltammetry [4]. A study of the mammalian metabolism of organotins used normal and two-dimensional TLC, followed by photolysis and treatment with visualizing reagents (8-hydroxy-5-sulfonic acid, pyrocatechol violet, or dithizone) to identify the chromatographic components

[5]. Another TLC method for organotins reported retention factor values for a series of tri-, di- and monosubstituted organotins; hematooxylin was used for visualization and the good resolving capacity of TLC was demonstrated [6]. HPTLC quantitation of butyltins in a wood extract matrix has been reported using post-development photolysis and colorimetric detection by complexation with pyrocatechol violet [7]. When complexed with inorganic tin and some organotins, morin produced a fluorescent complex; this principle forms the basis of this sensitive (DTL: 10^{-7} to 10^{-9} M) and selective analytical method [8].

The present study examines the use of HPTLC with in situ post-development derivatization using morin; fluorescence detection in HPTLC typically offers greater sensitivity and selectivity than other light absorption methods [9]. Fluorescence enhancement plate coatings are an important aspect of HPTLC quantitative analysis because they produce enhanced and stabilized fluorescence on HPTLC plates [16,17].

Mixtures of tetraphenyltin (TTPT), triphenyltin chloride (TPTCl), diphenyltin dichloride ($DPTCl_2$), and monophenyltin trichloride ($MPTCl_3$) were resolved using high performance thin layer chromotography on silica gel with retention factor values of 0.80, 0.35, 0.20, 0.01, respectively. Inorganic tin impurities were strongly adsorbed and did not migrate from the origin. Diphenyltin dichloride, monophenyltin trichloride, and inorganic tin components reacted with morin to produce fluorescent complexes. Post-development exposure of the plate to ultraviolet light photodegraded the organic components which, after morin treatment, exhibited greater fluorescence than the organotins. This photolysis technique permitted the visualization of the otherwise nonfluorescent tetraphenyltin and weakly fluorescent triphenyltin spots.

The components were quantitated using scanning densitometry. The working range varied from a maximum of 222 nanograms to a minimum of 1 nanogram, depending on the particular component and the excitation wavelength chosen. Thirty standards, each containing five components, were spotted, developed, derivatized, and scanned at least three times to produce 480 pieces of data within 4 hours. Calibration curves showed an instrumental error of 1.5% relative standard deviation, and a spotter and intraplate variation of 9.0% relative standard deviation. The inherent multiplicity of high performance thin layer chromatography allows for multiple sampling and analysis, thereby yielding significantly increased precision and high sample throughput. The chromatography and detection of butyltins and cyclohexyltins were also examined.

The four chromatograms in figure 1 demonstrate the HPTLC of the compounds TTPT, TPTCl, $DPTCl_2$, $MPTCl_3$, and organic tin on silica gel using two different mobile phases, with and without the use of photolysis prior to morin derivatization and fluorescence detection. Chromatograms 1a and 1b used mobile phase A (5% acetic acid, 20% methylene chloride, 75% isooctane v/v) which completely resolves the organotins. However, $MPTCl_3$ is not moved from the origin and if inorganic tin compounds are also present $MPTCl_3$ is not resolved from them, therefore a stronger mobile phase in a separate development is required to resolve $MPTCl_3$ from inorganic tin. The efficiency is excellent with no tailing or peak asymmetry. Photolysis increases the fluorescence of each compound, and is critical for the detection of TTPT, and TPTCl. Chromatograms 1c and 1d use a stronger mobile phase B (30% acetic acid, 70% chloroform v/v). The Rf values of TTPT, TPTCl, $DPTCl_2$, and $MPTCl_3$ were: 0.85, 0.55, 0.25, and 0.00 using mobile phase A; and 0.65, 0.56, 0.14, and 0.05 using mobile phase B. TPTCl, triphenyltin hydroxide (TPTOH), and triphenyltin acetate (TPTAc) all elute as TPTAc, as established using preparative TLC and FT-IR comparisons.

The calibration curves shown in figure 2 are for $MTPCl_3$, $DPTCl_2$, TPTCl, and TTPT with the analyte-morin complex excited at 313 nm. The error bars at each measured concentration level indicate the mean value, plus and minus one standard deviation ($N=6$). The relative slope of each line correlates qualitatively to the percent of tin in each molecule; thus the detection limit is lowest for $MPTCl_3$.

Figure 3 shows 15 chromatograms from authentic organotin reference compounds that were applied to a single 10-cm × 10-cm HPTLC plate, and analyzed by the described method. The organotin samples and the corresponding peaks were: fenbutatin oxide (samples 1–3; peak A); triphenyltin oxide, TPTO (samples 4–6; peak B); monocyclohexyltin tribromide, $MCyTBr_3$ (samples 7–9; peak C); dicyclohexyltin dibromide, $DCyTBr_2$ (samples 7–9; peak D); tricyclohexyltin bromide, TCyTBr (samples 7–9; peak E); monobutyltin trichloride, $MBTCl_3$ (samples 10–12; peak F); dibutyltin dichloride (samples 10–12; peak G);

tributyltin chloride, TBTCl (samples 10–12; peak H); monophenyltin trichloride, $MPTCl_3$ (samples 13–15; peak I); diphenyltin dichloride, $DPTCl_2$ (samples 13–15; peak J); triphenyltin chloride (samples 13–15; peak K); tetraphenyltin, TTPT (samples 13–15; peak L). Each standard had an approximate mass of 10 ng except the $MBTCl_3$, and $MPTCl_3$ which were of uncertain quantity. The standards were eluted with mobile phase A to a 5-cm solvent front. The processed plate was scanned longitudinally with 15 4-cm passes to measure the fluorescence emitted at 515 nm (broad band pass filter) using 436 nm excitation. The results in figure 3 demonstrate that resolution of organotins between classes of compounds is excellent (i.e., R_4Sn, R_3SnX, R_2SnX_2, and $RSnX_3$ where R = alkyl or aryl groups).

Currently work is being done to incorporate this determinative step to quantitate TPT residues in potatoes. Quantitation of TPT at 0.1 ppm has been accomplished. Potato extracts have been screened for TPT down to 0.01 ppm. This determinative method has also been used to measure tri-, di-, and monobutyltin chloride in water down to 0.01 ppm.

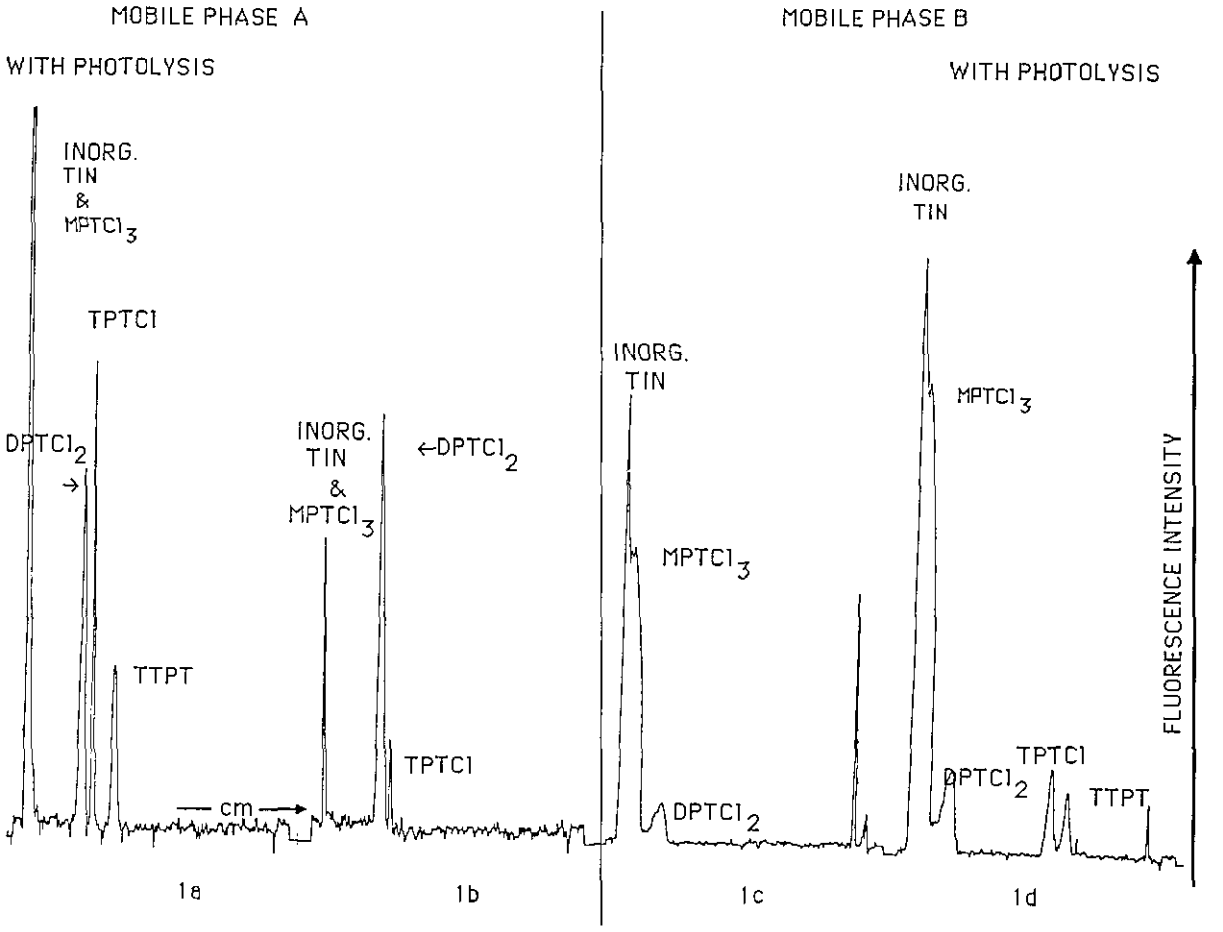

Figure 1. Four chromatograms separating inorganic tin, $MPTCl_3$, $DPTCl_2$, TPTCl, and TTPT. Chromatograms 1a and 1b used mobile phase A, and 1c and 1d used mobile phase B.

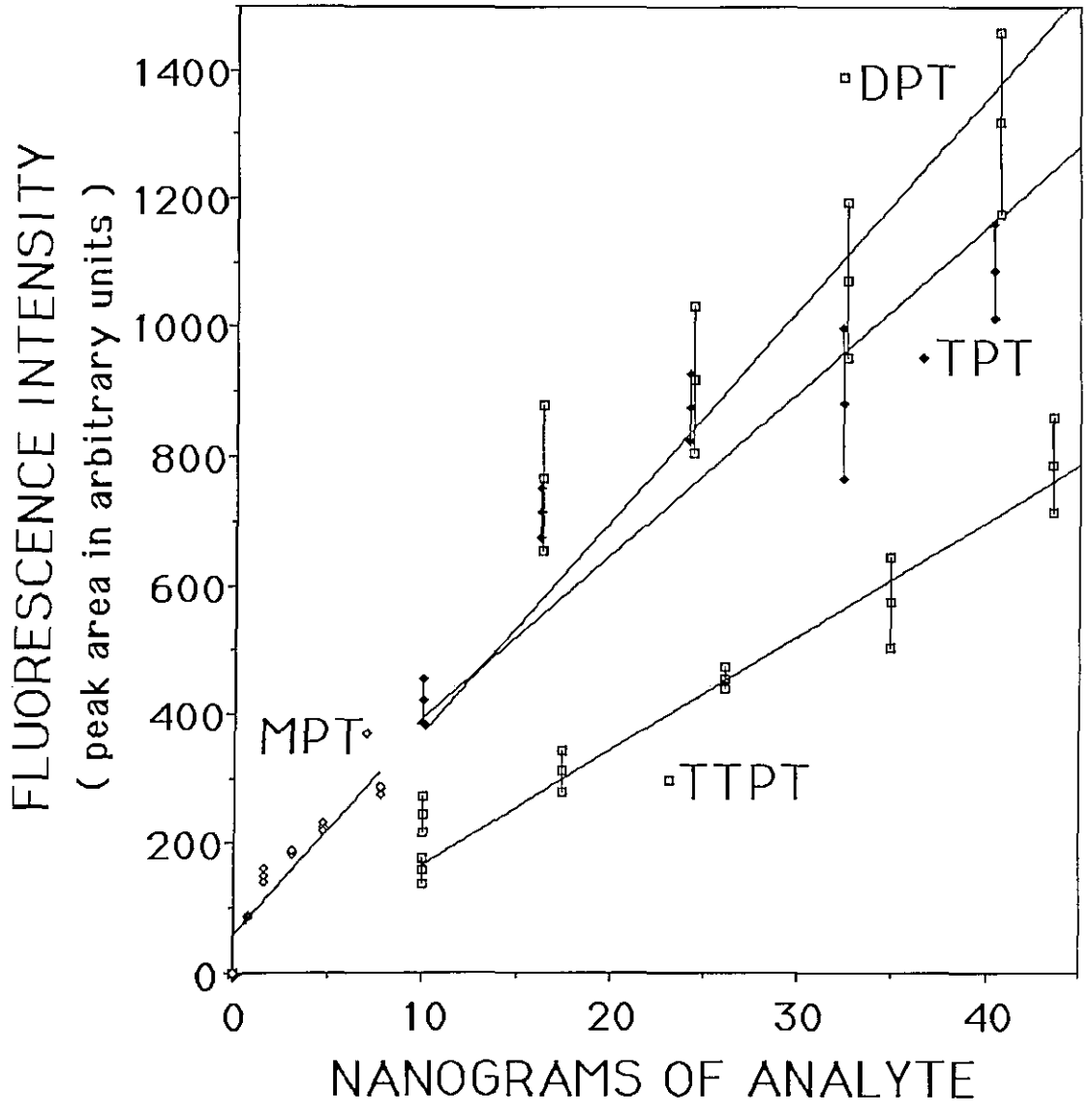

Figure 2. Fluorescence calibration curves for $MPTCl_3$, $DPTCl_2$, TPTCl, and TTPT excited at 313 nm. Error bars show ±SD.

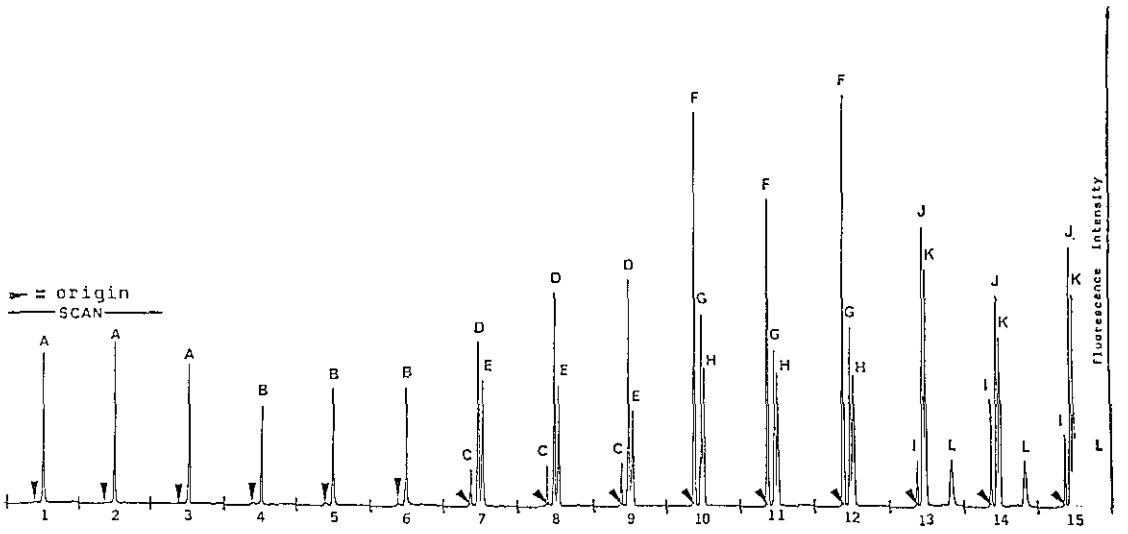

Figure 3. Fifteen chromatograms produced from 4 cm longitudinal densitometer scans across a 10 cm×10 cm HPTLC plate with 15 organotin samples. Components: A, 6 ng fenbutatin oxide; B, 7 ng TPTO; C, $MCyTBr_3$; D, 11 ng $DCyTBr_2$; E, 11 ng TCyTBr; F, 11 ng $MBTCl_3$; G, 11 ng $DBTCl_2$; H, 13 ng TBTCl; I, $MPTCl_3$; J, 12 ng $DPTCl_2$; K, 12 ng TPTCl; L, 13 ng TTPT.

References

[1] Poole, C. F., and Schuette, S. A., Contemporary Practice of Chromatography, Elsevier, Amsterdam (1984).
[2] Poole, C. F., Coddens, M. E., Butler, H. T., Schuette, S. A., Ho, S. S. J., Khatib, S., Piet, L., and Brown, K. K., J. Liq. Chrom. **8**, 2875 (1985).
[3] Laughlin, R. B., Guard, H. E., and Coleman, W. M., Env. Sci. Tech. **20**, 201 (1986).
[4] Woggon, H., and Jehle, D., Die Nahr. **17**, 739 (1973).
[5] Kimmel, E. C., Fish, R. H., and Casida, J. E., J. Agr. Food Chem. **25**, 1 (1977).
[6] Vasundhara, T. S., and Danhar, D. B., Fres. Z. Anal. Chem. **294**, 408 (1979).
[7] Ohlsson, S. V., and Hintze, W. W., J. High Resol. Chrom. & Chrom. Comm. **6**, 69 (1983).
[8] Arakawa, Y., Wada, O., and Manabe, M., Anal. Chem. **55**, 1901 (1983).
[9] Sherman, J., TLC Technical Series Vol. 2, Whatman Chemical Separation Inc., New Jersey, 1981.
[10] Brown, K. K., and Poole, C. F., J. High Resol. Chrom. & Chrom. Comm. **7**, 520 (1984).
[11] Brown, K. K., and Poole, C. F., L. C. Mag. **2**, 526 (1984).

Determination of Chromium(III) and Chromium(VI) by Ammonium Pyrrolidine Dithiocarbamate-Methyl Isobutyl Ketone-Furnace Atomic Absorption Spectrometry

K. S. Subramanian

Environmental Health Directorate
Health and Welfare Canada
Tunney's Pasture
Ottawa, Ontario
K1A 0L2, Canada

The determination of Cr(III) and Cr(VI) in environmental and biological systems is of interest because the toxicity of this metal depends on its oxidation state. Cr(III) is essential to mammals, while Cr(VI) is toxic. In addition to its existence in the two main oxidation states of +3 and +6, Cr occurs in the aquatic environment at $\leqslant$ ng/mL levels. Therefore, some form of preliminary separation and preconcentration is required to determine the low levels of individual Cr species by sensitive analytical techniques, such as graphite furnace atomic absorption spectrometry (GFAAS) [1,2].

This paper explores the feasibility of directly complexing both Cr(III) and Cr(VI) by ammonium pyrrolidine dithiocarbamate (APDC) at room temperature, extracting these subsequently into methyl isobutyl ketone (MIBK) and determining the individual Cr species in the MIBK phase by GFAAS.

A Perkin-Elmer Model 603 atomic absorption spectrometer equipped with a Perkin-Elmer HGA500 graphite furnace, an AS-1 autosampler incorporating a 10-μL pump, a PRS-10 printer and a Perkin-Elmer hollow cathode lamp operated at 25 mA at the Cr resonance line of 357.9 nm (spectral bandpass, 0.7 nm) were used for the determination of Cr. Argon served as the purge gas and its flow was interrupted during atomization.

The solution parameters studied include: pH of the aqueous phase, concentration of APDC, concentration of potassium hydrogen phthalate (PHP buffer, and length of time needed for complete extraction.

Complete transfer from aqueous to MIBK phase occurred in a single extraction at pH 2.5–4.0 for Cr(III) and pH 2.5–5.0 for Cr(VI) at final PHP and APDC levels of 0.1% and 1.2%, respectively. Thus simultaneous and quantitative extraction of Cr(III) and Cr(VI) were possible at pH 2.5–4.0. Also, Cr(VI) could be selectively and quantitatively extracted at pH 2.5–4.0, but at final APDC and PHP concentrations of 0.2% and 1%, respectively. In the case of Cr(III), the optimum APDC-to-metal and PHP-to-metal concentration ratios were $\geqslant 2.4\times10^4$ and 0.8×10^4 to 4.0×10^4, respectively (final concentrations: Cr(III), 50 ng/mL; APDC, 1.2%; PHP, 0.04–0.2%). Above 0.8% PHP, Cr(III) was not extracted whereas Cr(VI) was extracted. Thus selective extraction of Cr(VI) occurred when the APDC-to-metal and PHP-to-metal ratios were $\geqslant 4\times10^4$ and $\geqslant 2\times10^5$, respectively (final concentrations: Cr(VI), 50 ng/mL; APDC, 0.2%; PHP, 1%). Extractions of Cr(III) and Cr(VI) were complete on shaking for 20 min. and 10 min. respectively, at pH 3.5 and 22 °C. Both the Cr(III) and Cr(VI) chelates were stable for at least 30 days when the MIBK phases were transferred to dry centrifuge tubes soon after extraction. In summary, these studies showed that, by careful optimization of the concentrations of APDC, PHP, pH and extraction time, the APDC-MIBK system could be used to: (i) selectively separate Cr(VI) from Cr(III); and (ii) simultaneously extract Cr(III) and Cr(VI) at room temperature without the need to oxidize Cr(III) to Cr(VI).

The sensitivity (concentration at 0.0044 absorbance), detection limit (3 SD of blank) and linear range for both Cr(III) and Cr(VI) were identical and found to be (ng/mL): 0.2, 0.3 and 0–50, respectively, in the MIBK phase. The values in the aqueous phase depend on the phase volume ratio. A concentration factor of up to 20 was possible with MIBK. At 20-fold concentration the above values will be (ng/mL): 0.01, 0.02 and 0–2.5, respectively. Thus the method is sufficiently sensitive to permit determination of background levels of Cr(III) and Cr(VI) in unpolluted natural and drinking water samples. The precision, expressed as the coefficient of variation (CV), at 5, 10 and 20 times the detection limit of Cr was 33.3, 12.6 and 8.1, respectively. The reliability of the proposed procedure was assessed by analyzing the NBS multielement water standards SRM 1643a and SRM 1643b, and the National Research Council of Canada (NRCC) river water standard, SLRS-1. Both the NBS and the NRCC specify certified values only for total Cr. The observed values for total Cr of 18.1 ± 0.6 (SD), 17.8 ± 0.3, and 0.22 ± 0.05 ng/mL for SRM 1643a, SRM 1643b, and SLRS-1, respectively, compare favorably with the corresponding certified values of 17.3 ± 2.0, 18.9 ± 0.4 and 0.36 ± 0.04 ng/mL. Furthermore, our analysis revealed Cr(III) to be the dominant species in the NBS standards as confirmed by the good agreement for Cr(III) by the APDC-MIBK extraction procedure and an ion exchange procedure based on the use of a Bio-Rad SM-7 polyacrylic ester resin [1]. Thus the solvent extraction values for Cr(III) in SRM 1643a and SRM 1643b were (ng/mL): 16.0 and 16.4, respectively, while the corresponding ion exchange values were 14.6 ± 0.5 and 17.9 ± 0.5 ng/mL. The reliability of the APDC-MIBK-GFAAS procedure was also ascertained by doing recovery studies. The average percent recovery obtained for the addition of Cr(III), Cr(VI) and Cr(III)+Cr(VI) spikes to tap, well, treated and river water samples were quantitative.

No interferences were found from Ca, Mg, Na, K and a number of trace elements at levels exceeding those usually found in most fresh and drinking water systems. The humic acid concentration in the solution to be extracted for Cr(III) should be $\leqslant 2$ mg/mL. In the case of Cr(VI), up to 40 mg/L humic acid can be tolerated.

The method was applied to the determination of Cr(III) and Cr(VI) in a number of water samples according to the procedures outlined below.

• Determination of Cr(III)+Cr(VI). To 25 mL of sample, add 0.3 mL of 8% PHP, adjust pH to 3.5, and add 3 mL of 10% APDC and 5 mL of PHP-saturated MIBK. Extract for 20 min. Determine Cr(III)+Cr(VI) in the MIBK layer.

• Determination of Cr(VI). Proceed as above except for the addition of 3 mL of 8% PHP and 3 mL of 2% APDC and for the extraction time of 10 min.

• Determination of Cr(III). The value of Cr(III) is obtained as the difference between Cr(III)+Cr(VI) and Cr(VI). The concentration of Cr(III) is also determined by the SM-7 ion exchange procedure [1].

In all the above cases, the Cr atomic absorption signal was measured by using the dry/atomize program of 900 °C–30 s (ramp)–30 s (hold)/2500 °C–0 s (ramp)–6 s (hold).

References

[1] Subramanian, K. S., Méranger, J. C., Wan, C. C., and Corsini, A., Internat. J. Environ. Anal. Chem. **19**, 261 (1985).
[2] Subramanian, K. S., Anal. Chem. (in press).

Precision and Bias of Graphite Furnace Analysis of Environmental Samples

Gerald L. McKinney

U.S. EPA Region VII Laboratory
25 Funston Road
Kansas City, KS 66115

1. Introduction

This study was undertaken to examine the effects of several operational modes of graphite furnace analysis on the precision and bias of environmental trace element analysis. The modes compared were:

1. Method of Standard Additions (MSA) vs Direct Calibration
2. Single vs Double injections
3. Peak Height vs Peak Area Quantitation

The six solid and two water matrices studied are listed in table 1. These were chosen so that results obtained could be compared to a reference value. The elements studied were arsenic, selenium, cadmium, and lead.

Table 1. Sample types

1.	NBS Spinach
2.	NBS Orchard Leaves
3.	NBS Oyster Tissue
4.	NBS River Sediment
5.	EPA Sludge
6.	Urban Particulate
7.	Drinking Water
8.	Wastewater

2. Sample Preparation

The solid matrix samples were prepared using the nitric acid-hydrogen peroxide digestion originally proposed by the EPA EMSL/Cincinnati which is currently included in the EPA contract lab program protocol for low to medium concentration environmental samples.

The aqueous samples were not digested but were spiked to provide 50 μg/L of the elements of interest. Since the purpose of this study was to investigate instrumental precision and accuracy, samples were prepared only once and the four replicate determinations were performed on the same digestate. The precision estimates do not include any variability, due to that of digestion.

3. Instrumentation

Analysis was performed using a Perkin-Elmer Zeeman 5000 atomic absorption spectrophotometer equipped with an AS-40 auto-sampler and 3600 data station[1].

4. Analysis Protocol

The study was designed so that all three desired comparisons could be done from a single run by storing each atomization peak on a computer disk.

[1] Disclaimer: Mention of trade names does not constitute endorsement by U.S. EPA.

Each sample matrix was injected in duplicate in the following manner:

Cup 1—Straight sample.
Cup 2—Sample diluted 50% with 0.5% HNO_3.
Cup 3—Sample diluted 50% with 20 μg/L standard.
Cup 4—Sample diluted 50% with 50 μg/L standard.

A computer program calculates peak height and peak area for each atomization peak so that the first injection for cup 1 was used for the direct calibration single injection for both peak height and peak area. The average value obtained from the first and second injections was used for the duplicate injection calculation. A separate least squares linear fit program provided the MSA values from cups 2, 3, and 4. This protocol was repeated on three additional runs, usually on different days.

5. Results

All results were normalized to the appropriate percentage of the reference or theoretical value. The concentration in solution in μg/L is also shown. Thirteen of the 32 required dilutions varying from 1–2 to 1–200 to bring them on scale for HGA analysis. Table 2 shows the mean and standard deviation for each comparison.

Table 2. *Mean and standard deviation for comparison.*

	Element: Arsenic Sample type								Element: Selenium Sample type							
Comparison	1	2	3	4	5	6	7	8	1	2	3	4	5	6	7	8
Method of additions	121	97	102	88	26	116	111	105		15	86			110	107	109
Standard deviation	23	16	17	13	12	7	9	13		8	12			11	14	15
Direct calibration	92	82	81	67	26	97	100	97		23	41			88	97	95
Standard deviation	23	15	12	5	10	14	6	9		14	15			14	11	10
Single injection	92	82	81	67	25	97	100	97		23	41			88	97	95
Standard deviation	23	15	12	5	10	14	6	9		14	15			14	11	10
Double injection	111	78	79	67	27	97	99	94		27	37			105	92	96
Standard deviation	18	5	10	5	10	13	5	13		22	14			9	11	14
Peak height	72	71	64	64	16	88	89	77		19	33			70	98	108
Standard deviation	21	17	11	11	8	14	9	6		10	17			2	10	3
Peak area	92	82	81	67	25	97	100	97		23	41			88	97	95
Standard deviation	23	15	12	5	10	15	6	9		14	15			14	11	10

	Element: Cadmium Sample type								Element: Lead Sample type							
Comparison	1	2	3	4	5	6	7	8	1	2	3	4	5	6	7	8
Method of addition	97	78	110	101	103	109	101	118	111	110	95	110	108	111	110	109
Standard deviation	22	10	4	8	15	7	20	8	22	8	14	6	16	10	3	4
Direct calibration	105	99	98	84	99	103	107	101	100	87	104	95	102	92	99	91
Standard deviation	10	17	6	9	5	7	9	5	16	4	8	12	6	3	6	7
Single injection	105	99	98	84	99	103	107	101	100	87	104	95	101	92	99	91
Standard deviation	10	17	6	9	5	7	9	5	16	4	8	12	5	3	5	7
Double injection	106	132	99	84	100	110	112	112	110	86	98	97	100	92	99	94
Standard deviation	13	8	6	5	4	11	10	14	12	4	11	10	6	4	5	5
Peak height	93	102	82	65	66	101	88	91	82	93	113	94	99	91	108	73
Standard deviation	17	20	23	12	11	5	13	17	8	17	9	10	9	3	9	7
Peak area	105	99	98	84	99	103	107	101	100	87	104	95	101	92	99	91
Standard deviation	10	17	6	9	5	7	9	5	16	4	8	12	5	3	5	7

6. Statistical Evaluation

6.1 Bias

Comparison of methods for bias (differences between the modes compared) was accomplished by pooling the mean recoveries of each method and using Student's t test in the form:

$$t=\frac{\bar{d}\sqrt{n}}{s_d},$$

where $\bar{d}$ = average difference between each "method mean"
s_d = standard deviation of these differences
n = number of differences

If $t>t_{.975}$, i.e., 3.18 in the case of four replicates, then the means of the two methods are considered to be statistically significantly different.

6.2 Precision

Equality of pooled within-sample variance for the modes compared was tested using the F test in the form:

$$F=\frac{s_{m_1}^2}{s_{m_2}^2}, \quad \text{where } s_{m_1}^2>s_{m_2}^2$$

If $F>F_{.975}$, i.e., 15.4 in the case of four replicates, then there is a statistically significant difference between variances.

7. Discussion

7.1 Precision

There were no significant differences in variance for any of the comparisons as summarized in table 3. Precision is not improved with peak area as compared to peak height or method of additions vs direct calibration.

Although not significant in this study possibly due to the small number of replications, we believe generally that precision is degraded in MSA analysis due to the multiple injections required. One of the primary objectives of this work was to investigate the value of duplicate injections. This practice is common in many, if not most, analytical laboratories. Duplicate injections essentially double the analysis time. If precision is not improved, then single injections would improve a laboratory's efficiency. This study indicated no significant improvement in precision. It has been our experience that poor precision is usually due to what we call "correctable problems." These include poor injection practices; improper furnace conditions; tube, platform, or contract ring conditions; inadequate background correction; or improper matrix modification. These and other such conditions should be corrected before continuing analysis. Duplicate injections do not correct these conditions. As a result of this work and discussions with other analysts, we have discontinued the practice of duplicate injections.

Table 3. Statistical evaluation

Precision—F Test				
Comparison	As	Se	Cd	Pb
MSA vs DC	1.3	1.1	2.0	1.9
Pk Ht vs Pk A	1.0	1.7	2.9	1.3
Single vs Double	1.4	1.3	1.1	1.2

No statistically significant differences.

Agreement—Student's t				
Comparison	As	Se	Cd	Pb
MSA vs DC	4.7[a]	1.9	0.5	3.2[a]
Pk Ht vs Pk A	4.8[a]	2.4	3.4[a]	0.5
Single vs Double	0.5	0.6	1.8	0.6

[a] Indicates statistically significant difference.

7.2 Bias

In the context of this study, bias is concerned with the agreement of the two modes compared. As was anticipated, direct calibration produced results that were generally lower than those by the method of additions. We have observed that interferences do sometimes tend to bias direct calibration results low. We have also noticed a high bias in the MSA results which we have not been able to explain.

For Se and Cd, the differences between direct calibration and MSA were not statistically significant. The 15% difference found for arsenic was significant. Both direct calibration and MSA gave only 26% recovery for sample type 5—the EPA Municipal Digested Sludge sample. We believe, as do other workers, that the true value may be less than that found by analysis [1]. Looking at the other seven sample types, the MSA mean recovery

is 106% and the direct calibration is 88%, indicating that even though the MSA value is biased high, it is somewhat better than that resulting from direct calibration. The statistically significant difference found for lead is interesting in that the direct calibration results were somewhat better than the MSA results. The direct calibration averaged 96% recovery, and the MSA averaged 108%. Lead is a good example of the strides that have been made in eliminating interferences in graphite furnace. Only a few years ago, lead recoveries were often low. This was usually attributed to chloride interferences. Now accurate results may be obtained for lead even in hydrochloric acid.

Selenium analysis is a good example of how statistical evaluation may sometimes be misleading. The differences in precision and bias found between MSA and direct calibration were not statistically significant. However, the difference for the NBS oyster tissue was the largest of any observed, the recoveries being 86% for MSA and only 41% by direct calibration. Since selenium is often present in tissue at significant levels, accurate analysis is important. These results indicate that one would not want to attempt selenium analysis for tissue using these conditions by direct calibration. This example demonstrates that, for complex and difficult matrices, more work needs to be done to remove interferences. But just as this is evident, we also believe that it is possible to overcome these interferences. For selenium and arsenic, perhaps palladium or a mixed palladium matrix modification may be the answer (see [2]). Although there are cases such as the above where the method of additions is required, we feel that there are disadvantages other than the time required that are often overlooked and hence we avoid MSAs whenever possible. These include errors when the sample to spike ratio is inappropriate, or small errors in calibration and blank (baseline) that can be magnified in MSAs. The sum of the sample and spike can put analysis out of the linear range. Small variations in the individual readings in an MSA determination can produce larger errors in the final result. One example which is quite typical from this study demonstrates this last problem. In the MSA value for arsenic in orchard leaves, the fourth replicate was biased positive 49%. Since the correlation coefficient of calibration was low, this replicate was repeated. The individual readings of the second run were very close to the first run with the largest difference for the highest spike level. The difference between the first and second run for this was 7.7% (33.8 to 36.5 μg/L). In addition, the correlation coefficient improved and the bias was positive (only 15%). That is, a difference of 7.7% in one of the individual readings made a difference of 34% in the final result. This type of error is so common that we prefer to use direct calibration for the most accurate results for routine work such as verifying maximum contamination levels in drinking water or analyzing performance evaluation samples.

Errors introduced due to inappropriate spiking level and calibration error is discussed by Gaind and Odell [3]. They address the EPA contract lab "continuing calibration" criteria of ±10% and its effect on the probability of successful spike recovery. This probability is low and they believe the 10% limit is too wide.

8. Conclusion

We believe that the data from this study demonstrate that reliable analytical data can be achieved, whether these data are obtained from peak height or peak area, single or double injections, or direct calibration or the method of additions. Certainly, there are exceptions to every rule, but we believe that advances have made the interferences the exception. These advances include such things as improved background correction, delayed atomization, automatic injection, and matrix modification. We are approaching the "standardless graphite furnace analysis" proposed by Walter Slavin and co-workers [4]. In the absence of interferences, absolute calibration by a "characteristic mass" could be a powerful concept in accurate trace analysis.

References

[1] Adelman, H., Jeniss, S. W., and Katz, S. A., Amer. Lab. p. 31–35, Dec. 1981.
[2] Xiao-quan, Shan, Zhe-ming, Ni, and Li, Zhang, Atomic Spectrosc. 5, 1 (1984).
[3] Gaind, A., and Odell, G., "Consequence of Analytical Spiking Protocol and Continuing Calibration Specifications". Unpublished report to EPA Inorganic CLP, 1987.
[4] Carnick, Glen, Manning, David, and Slavin, Walter, "The Possibility of Standardless Graphite Furnace Analysis". Paper 580. Pittsburgh Conference on Analytical Chemistry and Applied Spectroscopy, 1984.

Volume 93, Number 3, May–June 1988
Journal of Research of the National Bureau of Standards

Accuracy in Trace Analysis

An Instrument for Determination of Energy Oxygen and BOD_5

Leonard L. Ciaccio

Ramapo College
Mahwah, NJ

and

Klaus Hameyer

Chemical Abstracts Service
Columbus, OH

"The biochemical oxygen demand (BOD) determination is an empirical test in which standardized laboratory procedures are used to determine the relative oxygen requirement of waste waters, effluents and polluted waters [1]." This method has several well-known drawbacks, i.e., 5-day duration of the test, lack of correspondence of the BOD bottle to the biological system of the receiving water body, and the nonquantitative nature of the BOD test [2]. Each of these factors seriously compromises the present testing procedure. The length of the analysis time, which is generally 5 days, makes the test practically useless [2,3] in real-time control of pollution, and the prescribed condition of carrying out the test at a constant temperature of 20 °C is an inconvenience.

The objective of this investigation was to develop an instrument which would measure biological oxygen demand by some parameter which was meaningfully related to the oxygen depleting activity of waste waters, precise, and of short measurement duration (1 hour or less). The variable chosen was energy oxygen, a thermodynamic value related to the substrate free energy of oxidation in cell synthesis [2–8].

Two factors, energy oxygen and endogenous oxygen, comprise ultimate biochemical oxygen demand [2,3,4]. Five-day BOD (BOD_5), may not necessarily exert the ultimate biochemical oxygen demand because 5 days may be too short a time for complete stabilization by the bacteria. Thus we can summarize

$$\text{BOD ultimate} = \text{Energy Oxygen} + \text{Endogenous Oxygen}$$

BOD_5 may be some percentage of BOD ultimate

Energy Oxygen, EO, is that amount of oxygen needed in energy reactions to provide synthesis of new biological cells and/or biologically stable organic substances from organic matter (bacterial food or organic pollutant) until none of the organic matter remains. This process is relatively rapid compared to endogenous respiration (consumption of endogenous oxygen) [3,4].

Endogenous Oxygen is that amount of oxygen used in reducing cellular materials to stable end products by a cyclic degradation process consisting of cell lysis—cell synthesis—cell lysis. Thus, a mass of bacterial cells is reduced ultimately to a relatively stable mass where life is maintained. This is a relatively slow process whose rate and extent of bacterial colony size is dependent on temperature. Thus the standard BOD_5 is determined at a given temperature, 20 °C, to obtain reproducible results.

The ABODA instrument, an acronym for automated biochemical oxygen demand analyzer, consists of an analyzing system and subsidiary systems which supply a measured volume of sample, standardize the dissolved oxygen probe and recorder scale, etc. The analyzer system is a loop containing an aeration cell in which the sample diluted with water is saturated with air, a pump, a Biological Reactor, a dissolved oxygen (DO) probe and finally, the aeration cell. The diluted sample is pumped around this loop, and the saturated DO level achieved in the aeration cell is decreased due to the interaction of the microorganisms in the Biological Reactor, the DO and the pollutant sample (food). The decreased DO level is measured by the DO probe. The signal from the DO probe is traced out on a recorder. An electronic integrator gives the area under the curve which represents the amount of oxygen consumed by the microorganisms in response to the sample [5,8]. This value is proportional to the energy oxygen. The energy oxygen is calculated using several factors such as a calibration factor for the electrode, scaling factor for the integrator, flow rate in the analysis system and sample size.

The EO diagram is obtained from the ABODA instrument, and the EO is obtained by integrating the area under the curve and calculating as follows:

$$\text{EO} = (\text{Area, mg of } O_2/\text{L}) \times (\text{time, } t_f - t_i \text{, min}) \times (\text{flow rate, mL/min})/(\text{volume of sample, mL})$$

The correlation of EO and BOD_5 values for five different concentrations of glucose—glutamate standards is given in table 1. A regression analysis resulted in a correlation coefficient, r^2, of 0.99.

Table 1. Correlation of EO and BOD_5 for glucose-glutamate

BOD_5 mg/L	EO mg/L
217	63.5, 57.9, 63.9
160	41.6
108	31.6
58.6	12.3, 15
27	7.8, 6.3

A series of raw sewage and primary (1°) effluent samples obtained from two different waste treatment plants were analyzed for their EO and BOD_5 values (see table 2). Plant R is a small domestic treatment plant with flow rates from 3 to 5 MGD, while plant BC treats a mixture of domestic and industrial wastes with a flow rate of about 100 MGD. A correlation coefficient, r^2, of 0.92 was obtained in a regression analysis of these data.

Table 2. Correlation studies of waste samples

Plant	Sample	EO	BOD_5
R	Raw	4.49	50.5
BC	Raw	5.91	61.0
BC	Raw	4.52	49.8
R	Raw	6.11	75.3
R	1°	3.21	34.1
BC	1°	5.90	39.8

A number of secondary effluent samples from three different plants were analyzed for their EO and BOD_5 values. Some of these values fall on a "best fit" line. However more extensive testing is needed to allow regression analysis for secondary effluent samples.

In all the EO determinations carried out in this investigation, the analysis time was an hour or less. The overall precision of EO analyses by the ABODA instrument and BOD_5 is given as weighted average % relative standard deviation value in table 3.

Table 3. Weighted average of 1% rel. std. dev. data

Sample	EO		BOD_5	
	%Rel. s.d.	No. analyses	%Rel. s.d.	No. analyses
Glucose-glutamate	±4.3	67	±4.4	29
Waste samples	±6.1	106	±9.6	111
Weighted avg.	±5.4	173	±8.5	140

In summary, the ABODA instrument measures EO which is correlated with BOD_5, precise (±5.4% SD), and it accomplishes an analysis in 1 hour.

References

[1] Standard Methods for the Examination of Water and Wastewater, 14th ed., Am. Public Health Assoc., New York (1976), p. 543.
[2] Stack, V. T., Jr., in Water and Water Pollution Handbook, L. L. Ciaccio, ed., Marcel Dekker, Inc., New York (1972), Vol. 3, Chap. 15.
[3] McCarty, P. L., Thermodynamics of Biological Synthesis and Growth, Proc. 2nd Int. Water Pollution, Res. Conf., Tokyo (1964), Pergamon (1965), p. 169.
[4] Servizi, J. A., and Bogan, R. H., J. Sanit. Eng. Div. Am. Soc. Civil Engrs. **89**, 17 (1963).
[5] Bhatla, M. N., Stack, V. T., Jr., and Weston, R. F., J. Water Pollut. Control Fed., **38**, 601 (1966).
[6] Lee, E. W., and Oswald, W. J., Sewage Industrial Wastes **26**, 1097 (1954).
[7] Vernimmen, A. P., Henken, E. R., and Lamb, J. C., J. Water Pollut. Control Fed. **39**, 1006 (1967).
[8] Stack, V. T., Determination of Rate of Consumption of Gases Dissolved in Liquids, British Patent 1,132,456 (1968).
[9] Ciaccio, L. L., and Hameyer, Klaus, Method and Apparatus for Automated Measurement of Energy Oxyen, U.S. Patent 4,063,792 (1978).

In-Situ Filtration Sampler for the Measurement of Trace Metals in Precipitation

Barbara J. Keller

Analytical Chemistry Unit
Illinois State Water Survey
Champaign, IL

An in-situ filtration sampler has been developed for use in measuring trace metals in precipitation. This sampler is a modification of the Aerochem Metrics Model 301 wet/dry precipitation sampler now in use in the National Atmospheric Deposition Program/National Trends Network (NADP/NTN). The sample is captured in a funnel and filtered directly into a precleaned and preweighed collection bottle. Upon collection, the bottle can be weighed to determine sample volume and immediately preserved with the appropriate amount of acid. Samples collected in this manner were

compared to those collected in high density polyethylene (HDPE) buckets according the standard NADP/NTN protocols for major ion sampling. These bucket-collected samples were filtered in the laboratory at different times throughout a week to approximate time lapses normally present in a large scale monitoring study. The metals investigated were aluminum, cadmium, copper, iron, lead, manganese, and zinc. Graphite furnace atomic absorption spectrophotometry was the method of analysis.

Filtration of aqueous samples followed by acidification has been shown to be necessary to preserve the natural distribution of metals since the particles present in the sample may adsorb or desorb metal ions rapidly [1]. Immediate filtration is particularly important in low volume deposition events where rapid pH changes can take place due to neutralization by natural dusts [2]. Since there are varying time lapses between collection in the field and filtration in the laboratory, the soluble/insoluble distribution of metals may be significantly changed in the final analysis. The in-situ filtration system partitions the sample as it falls, so that a more natural metal distribution is preserved. Also, sample handling is decreased, thereby decreasing opportunity for contamination.

The in-situ filtration system consists of a funnel and bottle assembly with an in-line filter. The top opening of the funnel is the same diameter as the standard buckets (30 cm), so that the catch area is the same. The HDPE funnel is connected to the fluorinated ethylene propylene (FEP) tubing via a polypropylene cone. The 0.4 μm polycarbonate membrane filter is housed in a tetrafluoroethylene (TFE) filter holder. The samples are collected directly into a 2-liter polyethylene bottle. After collection, the bottle is weighed and the sample is preserved with the appropriate amount of ultrapure nitric acid.

The Aerochem Metrics Model 301 wet/dry precipitation sampler was modified as follows:

1. The counterweight bar was cut and the middle portion removed, so that tubing could be connected from the collection funnel to the receiving bottle.
2. The bucket was shortened by 2.5 cm (off the top) to allow the funnel to nest at the top of the bucket. This was necessary to allow full closure of the sampler lid during dry periods.
3. A hole was cut in the bottom of the bucket for passage of the polypropylene cone and FEP tubing.

Direct comparisons between this system and the bucket collection system involved blank leachates and natural wet deposition samples. Blank leachate results for the two systems are shown in table 1. Blanks were poured into the bucket or funnel, left for 24 hours, and transferred to sample bottles and preserved. Acid cleaning the buckets lowered the iron values, but the zinc values increased to as high as 115 μg/L. The maximum concentrations found in the in-situ filtration system blank leachates were much lower for iron and zinc.

Table 1. Blank leachate analyses for HDPE sampling buckets and the in-situ filtration sampling system (percent frequency of method detection limit (MDL) concentrations)

Metal	MDL (μg/L)	HDPE buckets [a]	In-situ filtration system[b]
Al	3.5	100	82 (4.3)[c]
Cd	0.05	100	91 (0.08)
Cu	0.9	100	100
Fe	1.1	90 (16.1)	91 (1.2)
Pb	1.1	95 (2.8)	100
Mn	0.8	100	100
Zn	0.5	18 (14.7)	73 (2.9)

[a] pH 5.7 and pH 1.8, $n=40$
[b] pH 5.7, pH 4.3, and pH 3.4, $n=11$
[c] Numbers in parentheses are maximum values (μg/L).

Figure 1 shows results for the 24-hour sampling period during which a rainfall of 0.35 inches was collected. The bucket sample was filtered and acidified at 0, 1, and 3 days, while the in-situ filtration sample was acidified at the same intervals. The differences are obvious with much higher aluminum, iron, and zinc concentrations in the bucket samples.

To check for adsorption of metals onto the collector and/or filter surfaces, spike recoveries were determined for the in-situ filtration system. Results are presented in table 2.

Table 2. Single-operator precision and bias for trace metals determined from analyte spikes of samples (6 blanks, 2 synthetic, 5 wet deposition)[a]

Metal	Amount added, μg/L	*n*	Mean percent recovery, %	Mean bias, μg/L	Standard deviation, μg/L	Statistically significant bias?[b]
Al	18.5	12	95.7	−0.8	2.1	no
Cd	6.11	13	109.2	0.56	0.73	yes
Cu	11.0	13	100.0	0.0	0.6	no
Fe	11.1	12	89.2	−1.2	0.9	yes
Pb	20.8	13	101.9	0.4	1.5	no
Mn	10.1	13	107.9	0.8	0.5	yes
Zn	21.9	13	107.8	1.7	4.7	no

[a] Samples were spiked prior to filtration in the in-situ filtration collector.
[b] 95% confidence level [3]

The gravity filtration system evaluated in this study has some limitations. Precipitation with a high particulate load may require a pumping system, and below freezing temperatures necessitate the use of a heating system and/or insulation. Further research into these areas is planned.

The advantages of in-situ filtration are: preservation of the natural distribution of metals, decreased sample handling, and the inexpensive modification of available equipment.

References

[1] Rattonetti, A., Stability of Metal Ions in Aqueous Environmental Samples, National Bureau of Standards Special Publication 422, *Accuracy in Trace Analysis: Sampling, Sample Handling, and Analysis*, Proceedings of the 7th IMR Symposium (1974), (1976), 633–647.
[2] Peden, M. E. and Skowron, L. M., Atmospheric Environment **12**, 2343 (1978).
[3] Annual Book of ASTM Standards, Section 11, Vol. 11.01 (1) "Standard Practice for Determination of Precision and Bias of Methods of Committee D-19 on Water", Standard D 2777-77 (1983), 26–38.

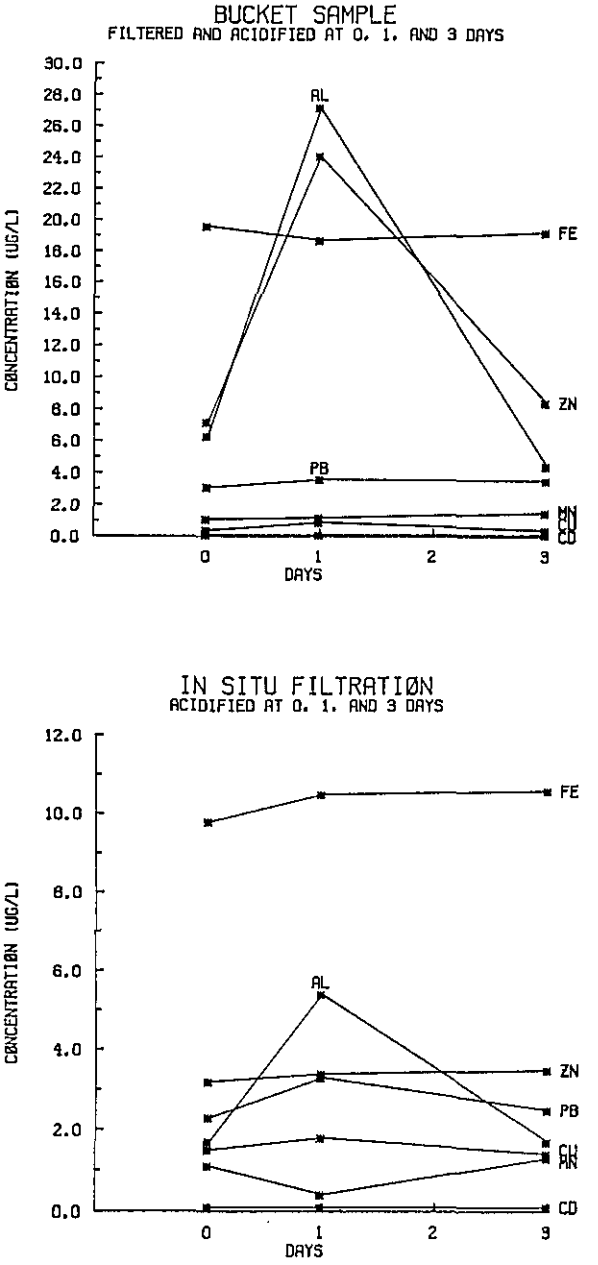

Figure 1. Trace metal concentrations of a rainfall of 0.35 inches, Champaign, IL, February 5, 1986.

Volume 93, Number 3, May–June 1988
Journal of Research of the National Bureau of Standards

Clinical/Biomedical Analysis

Quantitation of Arsenic Species in Urine for Exposure Assessment Studies

David A. Kalman

Department of Environmental Health
University of Washington
Seattle, WA 98195

1. Overview

Accuracy in trace level clinical or biomedical analyses is of increasing importance as population-based surveillance is more widely used to address issues of nutritional requirements, environmental exposures, and epidemiological outcomes. Among the uses of such surveillance, evaluation of community exposures from a local arsenic pollution source is one example. Urinary biological monitoring is a desirable tool used in conjunction with measurement of environmental levels of arsenic in order to permit assessment of total exposures and to provide a basis for consideration of the relative importance of different routes of exposure and of age-related behaviors in influencing exposure. Urinary arsenic concentrations are indicative of recent (previous 1–2 days) exposures to arsenic. When total urinary arsenic is measured, total arsenic intake is assessed. When exposures to inorganic arsenic (in the forms of oxides or salts of trivalent or pentavalent arsenic) are of interest, determination of urinary arsenic species comprising the major metabolites of inorganic arsenic exposures is most appropriate [1]. A recent two-year study of community exposures to environmental inorganic arsenic pollution utilized urinary arsenic speciation analysis to assess exposures. In these analyses, part-per-billion sensitivity was achieved with a mean precision of less than 12% coefficient of variation, and with excellent interlaboratory comparability.

2. Assay Method

The method utilizes a chemical reactor with addition of sodium borohydride to convert reducible arsenic compounds to the corresponding arsines and helium sparging to remove and concentrate arsines on a separation column maintained at cryogenic temperatures during trapping [2]. Following collection of all volatile arsenic, a temperature program is applied to the column and the eluted arsine species are detected by atomic absorption spectrometry using a microburner combustion cell [3]. Figure 1 shows a schematic of the analytical system. In order to increase sample throughput, two separate sample inlet trains were connected to the microburner cell using a 4-port glass valve. Arsine generation and cryogenic concentration could then occur on one inlet side while desorption and analysis was occurring on the other. Overall analysis time was thereby reduced to less than 15 minutes per sample, with up to 80 analyses being accomplished in a two-shift day. Analog signal output from the AA was integrated and concentrations computed using an electronic integrator. Direct serial interfacing to a MacIntosh-Plus microcomputer permitted us to download assay parameters and to transfer integrated results for processing in an electronic spreadsheet.

The analytical sensitivity of the method is very high, due principally to the efficiency of the detection system. The method mass detection limit was 1 ng per compound, or 1 ppb for a 1 mL urine sample. Sample volumes of up to 100 mL were permitted by the capacity of the reactor used. A typical output chart is shown in figure 2.

3. Achieving Accuracy

3.1 Quality Control Procedures for the Assay

Initial method validation was accomplished using pooled urine obtained from arsenic-exposed smelter workers. Three pools (high, ca. 25 ppb; medium, ca. 15 ppb; and low, ca. 5 ppb arsenic) were provided to four laboratories routinely determining arsenic in urine samples. Each lab assayed the samples using its own standards and procedures, which ranged from calorimetric assay of total arsenic to speciation assay by methods essentially identical to ours. Of the five labs

providing data, four showed good agreement (standard deviation of 3.6 ppb in high pool and 2.2 ppb in low pool), with the total arsenic assay slightly higher than the speciation assays. To maintain constant performance throughout the study, a benchmark sample was prepared using the mid-level urine pool frozen in 1500 aliquots. This sample was assayed daily for each inlet side at the beginning and end of each set of 7 samples. Control charts with 2-sigma limits were maintained daily. The daily analysis routine consisted of blanks, calibrants, benchmark samples, and replicate sample assays. Control samples in all accounted for approximately 26% of the analysis load.

3.2 Quality Assurance Procedures for the Project

Elements of the quality assurance effort were: the development of a QA manual for the assay and project; external audits by a technical team provided by EPA, Region X, EPA Las Vegas and its contractors, EPA RTP, and the Centers for Disease Control; and extralaboratory performance samples. The QA manual documented the SOP and subsequent modifications, set control limits and corrective actions required for out-of-control situations, and defined data validation criteria. Extralaboratory performance samples were provided quarterly by the EPA CLP QA office. In addition, blind resubmission of randomly-selected field samples and blind interlaboratory comparison samples shared with CDC were used to evaluate laboratory bias.

3.3 Assay Performance

Out-of-control events occurred approximately 6 times over the 14 months of intensive laboratory analysis. These events were typically related to failing source lamps, column degradation, or gas leaks. Blind sample resubmissions showed the same variation as within-lab reanalyses. All EPA performance audit samples were within control limits and were within 5 ppb of the reference value. Table 1 presents the summarized intra-laboratory QC results for the study.

Table 1. Quality control summary, AA/arsine speciation assay

Samples assayed	
Number of study samples	3728
Number of batches	375
Type of samples	water, urine, handwash
QC summary	
Blank analyses	
# required	424
# reported	424
# elevated blanks	none > LQL
Control samples	
# required	852
# reported	1186
mean "recovery" (% ref. value)	92.6±12.1
# outliers	128
definition of outliers	1 species not within $2-\sigma$ control limit
Replicate samples	
# required	249
# reported	251
mean precision	6.5% CV
# outliers	15 (6%)
definition of outliers	>25% CV and >2 ppb diff.

4. Biomonitoring Results and Discussion

The completed data set for this study consisted of slightly more than 9000 urine sample assay results plus several thousand environmental measurements including arsenic in soil, ambient air particulate, personal air particulate, water and locally-raised foods, house dust, road dust, surface dust from playgrounds and schoolrooms, hand loadings, and hair. Statistical path analysis of this data set using several models showed that:

— For this population, environmental arsenic variation explained only about 25% of urinary arsenic variation, with age, sex, diet, and urinary creatinine covariation explaining another 25%. Unexplained variation could be divided as follows: within individuals (26%), between individuals within households (15%), and between households (8%).

— The most significant environmental compartments influencing urinary arsenic were: indoor and outdoor air concentration (for entire population), and soil arsenic (for ages 0–6 and 7–13 only); $p < 0.01$ for each of these measures.

— Estimation of inhaled dose (based on personal air arsenic concentration and literature values for ventilation rate and retention of particulate) and comparison to mean arsenic daily intake (estimated by applying a steady-state pharmacokinetic model to those individuals whose urine values varied less than 25% between successive sampling days) showed that less than 15% of the arsenic intake could be contributed by inhalation, under reasonable worst-case assumptions.

— Dietary influences related to seafood consumption were not excluded by the use of speciation analysis. This was demonstrated both statistically and from feeding experiments, where some types of seafood (notably shellfish) produced significant short-term increases in urinary inorganic and methylated arsenic, as illustrated in figure 3.

5. Conclusions

We have demonstrated the feasibility of making large numbers of speciation measurements for urinary arsenic over a 14-month period, with good control of analytical performance and accuracy. Such measurements can permit the application of statistical tools to discern patterns of exposures leading to new insights regarding environmental pathways, target populations, and behavioral aspects of exposures. Needed developments to further this aim are reference materials with bioincorporated analytes, better procedures for normalizing urinary concentrations, and more complete pharmacokinetic characterization of arsenic for diverse age, sex, and exposure variables.

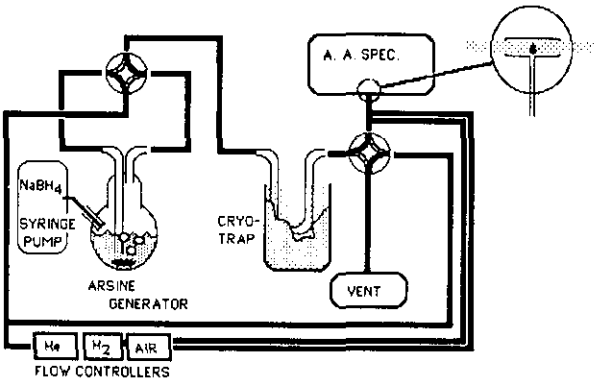

Figure 1. Analytical system schematic: Arsenic speciation assay.

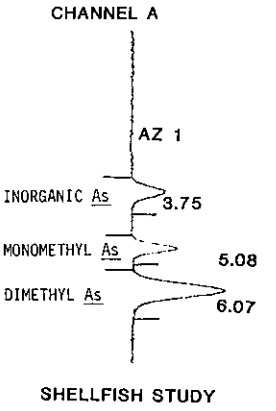

Figure 2. Typical analysis output.

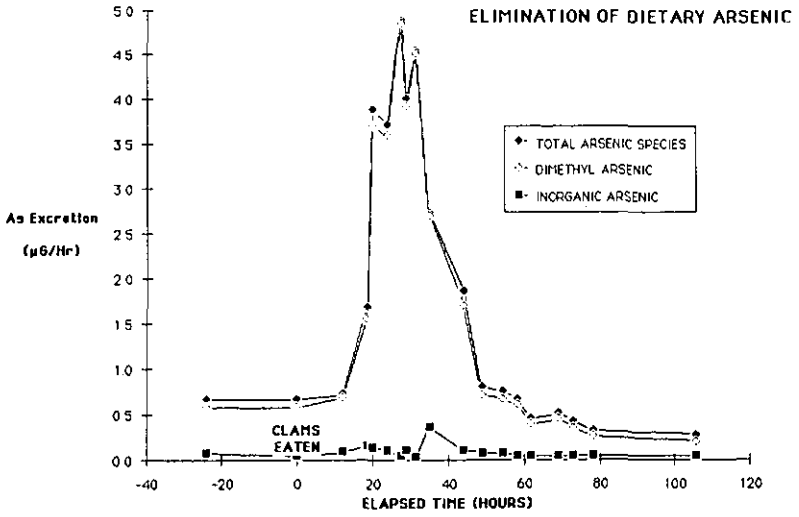

Figure 3. Time profile of excretion of urinary arsenic species following consumption of claws.

References

[1] Lauwerys, R., Industrial Chemical Exposure: Guidelines for Biological Monitoring, Biomedical Publications, Davis, CA (1983) pp. 12-14.
[2] Crecelius, E. A., Anal. Chem. 50, 826 (1978).
[3] Andreae, M. O., Anal. Chem. 49, 820 (1977).

Biological Reference Materials for Trace Element Analysis: What is New?

J. Versieck, L. Vanballenberghe, A. De Kesel, J. Hoste, B. Wallaeys, and J. Vandenhaute

Department of Internal Medicine
Division of Gastroenterology
University Hospital
De Pintelaan 185, B-9000 Ghent,
and Laboratory for Analytical Chemistry
Institute for Nuclear Sciences
Proeftuinstraat 86, B-9000 Ghent, Belgium

Introduction

In biomedical trace element research, reference materials are a relatively recent development: indeed, Bowen's Kale Powder became available only in the middle of the 1960s, NBS Orchard Leaves (SRM 1571) and NBS Bovine Liver (SRM 1577) in the beginning of the 1970s. In general, when compared to a number of real samples submitted to laboratories for elemental analyses, these reference materials have high or relatively high trace element concentrations. This is probably best illustrated when the levels expected in human blood plasma or serum (matrices which are frequently analyzed both because of their established biomedical importance and their ready availability) are considered. For example, for chromium and manganese, figures are as follows—370 and 14,950 ng/g (in Bowen's Kale Powder), 88 and 10,300 ng/g (in NBS Bovine Liver), and 1.5 and 5.5 ng/g dry weight (in human blood plasma or serum). So, although the above-mentioned, first generation biological reference materials rendered excellent services as a means to check the accuracy and precision of analytical techniques, large numbers of investigators were still largely left to their own devices.

Some reference materials are specifically aimed at researchers working on human blood plasma or serum, e.g., NBS Human Serum (SRM 909), Nycomed's Human Serum (STE 105), and National Institute for Environmental Studies' (NIES) (Japan) Freeze-Dried Human Serum. In all three cases, however, it is obvious that the original levels of several elements must have been drastically distorted during the collection and preparation of the

materials. For example, in reconstituted NBS Human Serum the nominal concentration of chromium is 91.3 ng/mL whereas the true level of the element in fresh plasma or serum is now widely believed to be approximately 0.15 ng/mL (or approximately 1.5 ng/g dry weight as mentioned above); in reconstituted Nycomed's Human Serum, the concentration of manganese was measured to be 23.5 ng/mL whereas the true level of the element in plasma or serum is now definitively established to be approximately 0.55 ng/mL (or approximately 5.5 ng/g dry weight as mentioned above). In fact, these materials give false feelings of confidence to inexperienced workers in search of reference materials to back their figures in real plasma or serum samples; obviously, they are only useful in a few instances, namely for the determination of iron, copper, and zinc, and, in the case of Nycomed's Human Serum, for the determination of selenium.

New Developments

Among researchers working on matrices with low trace element concentrations (or with "ultra-trace" element concentrations), the need for second generation biological reference materials with trace element levels close to those in real samples was very strongly felt. Efforts to meet their needs were undertaken in some centers.

NBS Non-Fat Milk Powder, SRM 1549

This material, issued in 1984, represents a matrix with some of the lowest trace element levels so far available. To the authors of this paper, not much is known about its collection and preparation. Recent publications [1,2] give very few details. Trace element levels (either certified or information values) are listed in table 1. Several years before (in the late 1970s), the International Atomic Energy Agency (IAEA) also issued a milk powder reference material (A-11). However, in the original intercomparisons it gave very unsatisfactory results for most elements so that a coordinated program was set up to improve the certification: the results were published only some months ago [3]. The most striking differences are a markedly higher chromium (17.7 ng/g) and mercury level (3.2 ng/g), a moderately higher arsenic (4.85 ng/g) and cadmium level (1.7 ng/g), but a definitely lower molybdenum level (92 ng/g) in the IAEA material.

Table 1. Trace element concentrations in recently developed biological reference materials

Element, unit	NBS Non-Fat Milk Powder, SRM 1549	NBS Bovine Serum, RM 8419 [a]	Freeze-Dried Human Serum, this paper
Al, ng/g dry weight	(2000)	132	20.2
Cr, ng/g	2.6	3.04	0.76
Mn, ng/g	260	26.4	7.7
Fe, μg/g	(2.1)	20.3	25.9
Co, ng/g	(4.1)	12.2	3.6
Ni, ng/g		18.3 [b]	(2.5)
Cu, μg/g	0.7	7.6	11.1
Zn, μg/g	46.1	11.2	9.6
As, ng/g	(1.9)	(3.5)	19.6
Se, μg/g	0.11	0.16	1.05
Br, μg/g	(12)		48.8
Rb, μg/g	(11)	(1.20)	1.85
Mo, ng/g	(340)	162	7.5
Cd, ng/g	0.5		2.0
Cs, ng/g		(2.2)	10.0
Hg, ng/g	0.3		(7.0)

[a] Values converted into ng/g or μg/g dry weight: recommended values, published in μg/L or mg/L [5], were multiplied by 10.15 (i.e., 100/(1.026×9.6)—1.026 being the specific gravity of the fresh serum (estimated) and 9.6 the percent residue after freeze-drying).

[b] Recently, lower values were reported by other researchers [6].

Figures in parentheses are information values only; the others are certified (NBS Non-Fat Milk Powder, SRM 1549, and Freeze-Dried Human Serum, this paper) or recommended values (NBS Bovine Serum, RM 8419).

NBS Bovine Serum, RM 8419

This is a very important material that became available in 1985 (pool of approximately 8 liters). Its collection and preparation (by C. Veillon and coworkers in Beltsville, MD) as well as its characterization (by C. Veillon and collaborating investigators both from Europe and the United States) were described [4,5]. It is interesting to note that the material was distributed in liquid form and that its recommended values were in μg/L or mg/L (ng/ml or μg/ml); for the sake of uniformity, however, values listed in table 1 were converted into ng/g or μg/g dry weight. Its main characteristics are obvious from the table. This material has now been analyzed by several researchers throughout the world. As indicated, in a footnote to the table, for nickel, values lower than that assigned were obtained by Andersen et al. [6]. As far as the authors of this paper are aware, the first batch of this material is now exhausted but a second is in preparation; preliminary results for a number of elements are similar to those measured in the first batch.

Freeze-Dried Human Serum

This second generation reference material was developed at the University of Ghent in Belgium by the authors. In 1981, a pilot study was set up to test the feasibility of the project; collections for the final pool were started in the second half of 1982. As donors, patients were selected for idiopathic hemochromatosis under treatment with phlebotomy. All were tested for hepatitis B surface antigen (HBsAg) as well as for antibodies against human immunodeficiency virus (HIV) and found to be negative. In December 1984, approximately 22 liters were accumulated. The collection and preparation of the material were discussed at the 7th International Conference on Modern Trends in Activation Analysis (Copenhagen, 1986); the written version of the text is in press [7]. The most important point that should be emphasized is that all imaginable precautions were observed to avoid contamination with exogeneous material! In 1985 and 1986, the material was homogenized and certified. A description of the whole process has been submitted for publication [8]. The values attached to the material are also catalogued in table 1. A comparison of the levels with those expected in lyophilized plasma or serum samples of apparrently healthy adults illustrates that the purpose of the project—preparing a reference material with low trace element levels, comparable to those in one of the most challenging matrices: real plasma or serum—was attained. Particular attention is drawn to the values for chromium, manganese, nickel, molybdenum, cadmium, and other difficult elements to measure reliably.

Conclusion

During the last 5 years, second generation biological reference materials have became available. Investigators engaged in low level trace element research finally have the means to check the accuracy and precision of their analytical procedures in the best possible conditions; in addition, for the first time they have at their disposal a possibility to evaluate the adequacy of some of their sample manipulation and preparation methods. With judicious use of the newly developed reference materials, it should be possible within a relatively short period of time to harmonize low-level trace element measurements by different researchers in human health and disease.

Acknowledgments

The authors acknowledge with thanks the contributions of numerous researchers to the certification of the second generation biological reference material described in this paper. Financial support was provided by the National Fund for Scientific Research in Belgium.

Note

The material described in this paper may be purchased ($150 per "unit," i.e., 12 samples of approximately 100 mg, or 8 samples of approximately 200 mg, or three samples of approximately 1 g, or one sample of approximately 2 g, or one sample of approximately 4 g of lyophilized material) from the University of Ghent via Dr. J. Versieck who should be contacted for further details.

References

[1] Alvarez, R., and Uriano, G. A., New Developments in NBS Biological and Clinical Standard Reference Materials, in: Biological Reference Materials, Wolf, W. R., Ed., John Wiley and Sons, Inc., New York (1985) p. 19.

[2] Alvarez, R., The Use of NBS Standard Reference Materials in Validating Trace Element Determinations in Biological Materials, in: Trace Elements in Man and Animals—TEMA 5, Mills, C. F., Bremner, I., and Chesters, J. K., Eds., Commonwealth Agricultural Bureaux, Farnham Royal (1985) p. 655.
[3] Byrne, A. R., Camara-Rica, C., Cornelis, R., de Goeij, J. J. M., Iyengar, G. V., Kirkbright, G., Knapp, G., Parr, R. M., and Stoeppler, M., Fresenius Z. Anal. Chem. **326**, 723 (1987).
[4] Veillon, C., Patterson, K. Y., and Reamer, D. C., Preparation of a Bovine Serum Pool to be Used for Trace Element Analysis, in: Biological Reference Materials, Wolf, W. R., Ed., John Wiley and Sons, Inc., New York (1985) p. 167.
[5] Veillon, C., Lewis, S. A., Patterson, K. Y., Wolf, W. R., Harnly, J. M., Versieck, J., Vanballenberghe, L., Cornelis, R., and O'Haver, T. C., Anal. Chem. **57**, 2106 (1985).
[6] Andersen, J. R., Gammelgaard, B., and Reimert, S., Analyst **111**, 721 (1986).
[7] Versieck, J., Hoste, J., Vanballenberghe, L., De Kesel, A., and Van Renterghem, D., J. Radioanal. Nucl. Chem., in press.
[8] Versieck, J., Vanballenberghe, L., de Kesel, A., Hoste, J., Wallaeys, B., Vandenhaute, J., Baeck, N., Steyaert, H., Byrne, A. R., and Sunderman, F. W., Certification of a Second Generation Biological Reference Material (Freeze-Dried Human Serum) for Trace Element Analysis, submitted for publication.

Detecting Contamination or Trends in the Concentrations of Trace Metals in Marine Environments

Eric A. Crecelius

Battelle/Marine Research Laboratory
439 West Sequim Bay Road
Sequim, WA 98382

1. Introduction

Three marine monitoring programs now in progress were designed to detect contaminated marine ecosystems and to quantify temporal trends in contaminant concentrations. These programs are the National Status and Trends "Mussel Watch" Program, which is funded by NOAA's Ocean Assessment Division, and the Beaufort Sea Monitoring Program and California Outer Continental Shelf Phase II Monitoring Program, which are both funded by the U.S. Department of Interior Minerals Management Service. As part of these monitoring programs, replicate samples of sediments and organisms from numerous stations are collected annually and analyzed for contaminants.

2. Field Sampling Methods

2.1 Sampling Rationale

Critical to the success of monitoring programs is the minimization of sampling variability. The sampling strategy was developed to effectively achieve the following:

- ensure uniformity of sampling techniques through establishment of and adherence to specific detailed field protocols;
- collect organisms from indigenous populations in areas considered integrative of contaminant inputs;
- collect undisturbed, depositional surface sediments from areas considered integrative of contaminant inputs;
- employ collection methods that minimize contamination;
- employ sample position-fixing techniques accurate to ± 100 m or better;
- sample for auxiliary parameters (shell length, sediment grain size, organic carbon) that may be used to normalize the variability of analytical data;
- plan subsequent collections during the same season and from precisely the same site coordinates.

2.2 Sediment Sampling Methods

Sediment was collected at three or more replicate stations within a site using a Kynar-coated grab sampler or box corer designed to collect undisturbed surficial sediment. Prior to subsampling the surface sediment, the quality and integrity of the sample was determined according to specified criteria. A grab sample was acceptable if it contained overlying water (siphoned prior to subsampling), and was not acceptable if the sampler over-penetrated the sediment. A Kynar-coated stainless steel sediment scoop was specifically designed to collect uncontaminated, undisturbed sediment from the grab sampler.

2.3 Organism Sampling Methods

In sampling for bivalves, the primary objective was to obtain three discrete samples from three sta-

tions within each site, representing site replicates. However, at sites where this was not possible, a pool of bivalves representative of the site also constituted an acceptable sample. Pooled site samples or composites were generated when bivalves were collected subtidally or when the distribution of intertidal populations did not permit discrete samples to be collected. Due to the low abundances of bivalves in some areas, alternate species, such as amphipods, crabs, and gastropods, were collected in baited epoxy-coated commercial steel minnow traps.

3. Analytical Methods

3.1 Analytical Rationale

The success of monitoring programs depends equally on both the design and execution of the analytical effort. The goal of the analytical program is to provide data of the highest quality via state-of-the-art techniques, provide documentation of the quality attainable (accuracy and precision), and improve the sensitivity of trend assessment by minimizing analytical variability. Based on these goals, the analytical strategy included the following objectives:

- ensure interlaboratory comparability of analytical techniques and provide method validation through participation in intercalibration exercises;
- ensure interlaboratory analytical uniformity through specific establishment of and adherence to detailed analytical protocols;
- document the quality of the data generated (based on observed limits of detection, precision, and accuracy) through adherence to detailed quality assurance protocols;
- measure auxiliary parameters such as shell length in bivalves, grain size, and total organic carbon in sediments in an effort to normalize contaminant data, correcting for variability resulting from biological, physicochemical, and geochemical processes.

3.2 Sediment Analysis

Sediment samples were freeze-dried and blended in a Spex mixer-mill, then 4 g were ground in a Spex ceramic ball mill. A 0.5-g aliquot of ground sediment was pressed into a 2-cm-diameter pellet and analyzed by energy dispersive x-ray fluorescence (XRF) [1] for Al, As, Ba, Cr, Cu, Fe, Mn, Ni, Pb, Si, V, and Zn. For the metals analyzed by atomic absorption, 0.2-g aliquots of the dry homogenate were digested with 4:1 nitric acid/perchloric acid in Teflon digestion bombs in an oven for 4 hours. After these samples were allowed to cool, hydrofluoric acid was added and the digestion bombs were returned to the 130 °C oven for 8 to 12 hours. The next day, boric acid was added to the solutions and the bombs were returned to the 130 °C oven for 8 hours. After cooling, solution volumes were calculated and the solutions stored in polyethylene vials until analyzed. Mercury was analyzed by cold vapor atomic absorption similar to the method of Bloom and Crecelius [2]. The other metals (Ag, Cd, Sb, Se, Sn and Tl) were analyzed by Zeeman graphite furnace.

3.3 *Tissue Analysis*

All samples were sized and shucked prior to tissue processing. Tissue samples were freeze-dried to a constant weight and ground to a powder in a plastic mixer-mill. Half-gram aliquots of dry tissue homogenate from each station sample were reserved for XRF analysis for As, Cu, Fe, Mn, Se, Si, and Zn. For all other analyses, half-gram aliquots of dry tissue homogenate from each station sample were weighed in an acid-cleaned, preweighed Teflon digestion bomb. These samples were predigested at 50 °C for 4 hours without the bomb sealed, using 4:1 nitric acid/perchloric acid, then sealed and digested at 130 °C for 4 hours. After cooling, samples were diluted with deionized-distilled water. Solution volumes were calculated and the sample solutions transferred to polyethylene vials for analysis. The analytical methods used to determine specific metals included cold vapor atomic absorption for Hg, hydride for Sn, and Zeeman graphite furnace for Ag, Al, Ba, Cd, Cr, Ni, Pb, Sb, and Tl.

4. Results and Discussion

Determining the intrasite variability for specific chemical parameters is a key step in the process of evaluating the incremental change that one can expect to detect at a given site. The determined variability includes both the intrasite or sampling variability and the analytical variability.

The intrasite variability for trace metals in sediment usually has a coefficient of variation (CV)

from 5% to 20%. However, the variability occasionally exceeds 50%. The variability appears to be primarily related to the intrasite variability in grain size, and secondarily related to analytical detection limits for some elements.

Measurements of mud content (silt plus clay) at several sites had a CV of greater than 100%. Usually, trace metal CVs at these sites were also very high, in the range of 40% to 80%. This relationship between the high CVs for mud and trace metals is not surprising because of the positive correlation of these metals with fine grain sediments.

The concentrations of the crustal elements (Al, Fe, Mn, and Si) are less influenced by grain-size variations than are the trace elements and, therefore, had the lowest intrasite CVs, usually less than the 10%.

The intrasite CV has a direct effect on the ability to detect either temporal trends or between-site differences. Statistical calculations (table 1) indicate that with a site replicate sample number of 3 and an intrasite CV of 0.1, a 1.4-fold difference in concentration would be detectable with 80% confidence using a two-sided t-test at the 0.05 significance level.

Intrasite variability for metals in bivalves is similar to that for sediments. Commonly, CV values for metals range from 10% to 20%, indicating that relatively small incremental changes in metal concentrations can be detected. For example, a 1.4-fold or 40% change can be detected if four site replicate samples have a CV of 0.1 (table 1).

Table 1. Minimum number of replicates necessary to detect a K-fold difference in geometric means with 80% confidence, using a two-sided t-test at significance level 0.05. Coefficient of variation of measurement (equals analytical plus sampling variability)

K[a]	0.1	0.2	0.3	0.4	0.5
1.1	19	71	157	278	433
1.2	6	20	44	77	120
1.3	4	11	22	38	58
1.4	3	7	14	24	36
1.5	3	5	10	17	25
1.6	3	5	8	13	19
1.7	3	4	7	10	15
1.8	2	4	6	9	13
1.9	2	3	5	8	11
2.0	2	3	5	7	10

[a] 1.4=40% change in value; 2.0=100% change (i.e., twofold change in value, etc.).

The temporal trends in Ba concentrations in California shelf sediments have been examined. Barium was analyzed at 13 stations both in October 1986 and January 1987. A paired t-test was used to test if the 13 station Ba means were different in October than in January. The means (724 and 738 μg/g Ba) were not significantly different at an $\alpha=0.05$. Assuming the variance in these data is a good estimate for future differences between the 13 stations, then an absolute difference of about 25 μg/g Ba, or a 4% change in Ba, could be detected with an $\alpha=0.01$. The power of the test used was $p=0.95$, or the probability that we reject the null hypothesis when we should.

References

[1] Nielson, K. K., and R. W. Sanders, Advances X-ray Anal. **26**, 385 (1983).
[2] Bloom, N. S., and E. A. Crecelius, Marine Chem. **14**, 49 (1983).

Determination of Manganese in Serum with Zeeman Effect Graphite Furnace Atomic Absorption

Daniel C. Paschal and George G. Bailey

Centers for Disease Control
U.S. Public Health Service
U.S. Department of Health and Human Services
Atlanta, GA 30333

1. Introduction

Manganese is widely distributed in the environment, comprising about 0.1% by weight average crustal abundance [1]. Among the more important commercial uses of manganese are iron alloys, nonferrous alloys, dry cells (as MnO_2), oxidizers (mostly as $KMnO_4$), and a large number of organomanganese compounds, notably methylcyclopentadienylmanganese tricarbonyl (MMT), used as a gasoline additive [2,3].

Under "normal" or non-occupational exposure conditions, low levels of manganese are found in serum, usually about 1 μg/L or less [4]. During occupational exposure, the levels of manganese in

serum or plasma are observed to rise, the manganese mainly bound to β-globulin or transferrin [4,5]. Manganese in blood is found mainly in the red cells, approximately 25 times higher in concentration than in serum [4]. The regulation of serum manganese levels seems to be homeostatic under "normal" conditions. Exposure to either inorganic or organic manganese has been shown to cause an increase in serum manganese [5].

Generally speaking, there are two conditions in which biological monitoring of manganese is important: 1) occupational exposure, in which serum manganese is elevated; and 2) some nutritional states in which a manganese deficiency is observed, reflected by near zero serum manganese [6].

The adverse health effects of increased manganese absorption include CNS effects, especially with organomanganese compounds. Symptoms which have been observed include dyspnea, fever, tachycardia, and Parkinsonian muscle weakness and rigidity [7]. Deficiency of manganese, on the other hand, has been suggested to be related to osteoporosis-like decalcification of bone [6].

The normal range of serum manganese values are from about 0.4 to 1.0 μg/L [8–10]. Any proposed method for manganese in serum must have a detection limit commensurate with these values. Of equal importance is the avoidance of contamination by manganese, which is ubiquitous.

The method to be described is suitable for measurement of serum manganese in either nutritional or occupational exposure settings. The detection limit is about 0.2 μg/L, with linearity observed up to 12 μg/L. Within run precision, as calculated by analysis of variance (ANOVA), is about 10% for analysis of reference material from the U.S. National Bureau of Standards.

2. Experimental

2.1 Instrumentation

A Perkin-Elmer Zeeman/5000 atomic absorption spectrophotometer[1] was used, equipped with an AS-40 autosampler and DS-10 Data Station (Perkin Elmer, Norwalk, CT USA). A Perkin-Elmer "Intensitron" hollow cathode lamp was used, with instrumental and spectroscopic parameters as in table 1. Pyrolytic graphite platforms and furnaces were used throughout.

[1] The use of trade names is for identification only and does not constitute endorsement by the U.S. Department of Health and Human Services.

Table 1. Furnace conditions for the determination of serum *manganese*

Step	1 (Dry)	2 (Char)	3 (Atomize)	4 (Cool)
Temp °C	180	1400	2400	20
Ramp (s)	5	5	1	1
Hold (s)	25	15	4	4
Flow (mL/min)	300	300	0	300
Recorder, (s)			−5	
Baseline, (s)			−1	

Lamp current 30 ma, wavelength 279.5 nm, slit 0.7 (ALT). Pyrolytic platform and furnace; 20 μL injected volume.

2.2 Reagents

Serum diluent was prepared with Triton X-100 (Fisher Scientific Catalog # CS-282-4M), using 500 μL diluted to 100 mL with ultrapure water. The water used was polished with a Milli-Q system (Millipore Corp.) to a resistance of 18 MΩ/cm.

2.3 Sample Collection

The collection of uncontaminated serum specimens is critical to the success of this determination.

Subramanian and Meranger [10] have described a procedure for serum collection which includes the use of plastic cannula to avoid manganese contamination. Veillon [11] has suggested the use of "siliconized" metal needles in which the surface has been rendered hydrophobic, thus minimizing metal contact with the specimen.

To apply this method to an osteoporosis study, a protocol was used for serum collection which is based upon our previous experience in collection of serum for determination of zinc and iron [12] and is similar to one described by Jarvisalo et al. for collection of uncontaminated whole blood for manganese determination [13]. In our protocol, two 15 mL portions of blood are collected sequentially in "standard" serum tubes using a 20 gauge multiple sampling needle (Becton-Dickinson Catalog # 5749), followed by collection of 7 mL of blood in a serum tube specially prepared to minimize trace metal contamination (Becton-Dickinson Catalog # 6526). After allowing the "trace metal" specimen to clot at room temperature, the blood was refrigerated at 4 °C and centrifuged to harvest the serum. Serum was transferred to 1.8 mL "Nunc" brand cryotubes (Catalog # 3-68632), and stored at −20 °C until analysis.

To evaluate the potential contamination from the collection and storage equipment used, a "lot test-

ing" procedure based on statistical methods of A. Wald [14] was performed. None of the collection or storage tubes or needles (N=10) tested had detectable manganese.

2.4 Contamination Control

In addition to the procedures referred to above, manganese contamination must be rigorously avoided in the specimen processing procedure itself. Glassware and plasticware were cleaned with aqueous detergent followed by rinsing with copious quantities of ultrapure water; then they were soaked overnight in 25% v/v reagent grade nitric acid. After additional rinses with ultrapure water, the plastic or glassware was then dried in a Class 100 facility, and stored in a dust-free area. Pipet tips were rinsed with ultrapure water, then with specimen or diluent before use. Linear polyethylene or polystyrene autosampler cups were cleaned as above [8,10,11].

2.5 Procedure

Prepare matrix modifier (0.5% v/v Triton X-100) on a weekly basis, to minimize contamination due to handling. Dilute the well-mixed serum with an equal volume of 0.5% Triton X-100, and inject 20 μL aliquots via the autosampler, making duplicate area measurements. Calibration is accomplished with a curve prepared with (1+1) Triton X-100/water, using the instrumental conditions given in table 1. Peak area was used for calibration throughout.

3. Results and Discussion

Determination of a series of "control" sera by the proposed method gave the results in table 2. The three pools determined had nominal manganese concentrations above those expected for "normal" sera; probably as a reflection of contamination during the collection or dispensing process. Accuracy of the procedure is evidenced by both analysis of RM 8419, with a nominal value of 2.6 μg/L, and by recovery estimates on "spikes" sera. Recovery of manganese to serum R576 gave an average of 102.9% for four replicate additions of 80, 160, and 240 pg manganese.

Table 2. Precision and accuracy study

Pool	Target value (μg/L)	Found	SD (within run)	SD (among run)	SD (total)
RM 8419	2.6	2.46	0.28	0.25	0.38
R576		4.86	0.23	0.49	0.54
"Low"		2.76	0.43	0.52	0.68

Twenty-two serum specimens were analyzed for manganese from participants in the initial phase of an osteoporosis pilot study. Results of these determinations gave a mean value of 1.3 μg/L, with a range of 0.56 to 2.7 μg/L. These data are quite similar to those reported by Subramanian [10], who reported data for 30 subjects. We feel that these results are indicative of a collection system that does not introduce appreciable manganese into the collected serum specimen.

Optimization of the char temperature, as described by Welz [15] is shown in figure 1. The char temperature chosen was sufficient to reduce the background absorbance to approximately 0.04–0.10 A without analyte loss. The characteristic mass, pg manganese required for an average absorbance area of 0.0044 A·s, is 3.2 pg, in good agreement with published values [16,17]. Linearity was evaluated by extending the calibration curve to about 0.30 A·s, which corresponds to serum with a manganese value of 12 μg/L. The calculated linear regression line gives an estimated slope of 8.57×10^{-3} A·s per μg/L for both diluted serum and water (both 1+1 with matrix modifier).

The proposed method is rapid, convenient, and accurate. It has been shown to be suitable for evaluation of "normal" subjects for a nutritional study. Contamination, often a limiting factor with serum transition metal studies, is successfully avoided with the simplicity of the procedure and use of a single aqueous diluent.

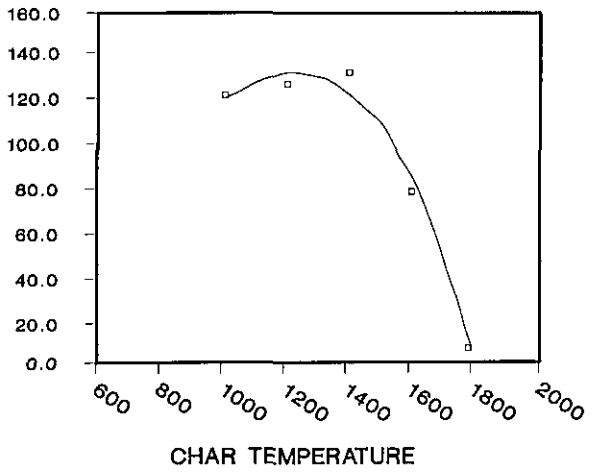

Figure 1. Char temperature optimization. R576 serum pool, 20 μL injection.

4. References

[1] Carson, B. L., Ellis, H. V., and McCann, J. L., Toxicology and Biological Monitoring of Metals in Humans, Lewis Publishers, Inc., Chelsea, MI (1986).
[2] Joselow, M. M., Tobias, E., Koehler, R., Coleman, S., Bogden, J., and Gause, D., Amer. J. Publ. Health **68**, 557 (1978).
[3] TerHaar, G. L., Griffing, M. E., Brandt, M., Oberding, D. G., and Kapron, M., J. Air Poll. Control Assoc. **25**, 858 (1975).
[4] Tsalev, D. L., and Zaprianov, Z. K., eds., AAS in Occupational and Environmental Health Practice, Volume I, CRC Press, Boca Raton, FL (1983).
[5] Gianutsos, G., Seltzer, M., Saymeh, R., Wu, M., and Michel, R., Arch. Tox. **57**, 272 (1985).
[6] Paul Saltman, University of California at San Diego, personal communication.
[7] NIOSH/OSHA "Health Guide for Manganese," in "Occupational Health Guidelines for Chemical Hazards," DHHS (NIOSH) Publication 81-123 January, 1981.
[8] Versieck, J., and Cornelius, R., Anal. Chim. Acta **116**, 217 (1980).
[9] Buchet, J. P., Roels, H., Lauwerys, R., Bruaux, P., Clays-Thoreau F., Lafontaine, A., and Verduyn, G., Env. Research **22**, 95 (1980).
[10] Subramanian, K., and Meranger, J., Anal. Chem. **57**, 2478 (1985).
[11] Veillon, C., Anal. Chem. **58**, 851A (1986).
[12] Laboratory Procedures Used by the Clinical Chemistry Division, Centers for Disease Control, for the Second Health and Nutrition Examination Survey (HANES II) 1976-1980, Elaine W. Gunter, Centers for Disease Control Laboratory Manual, Atlanta, GA 30333.
[13] Jarvisalo, J., Olkinuora, M., Tossavainen, A., Virtamo, M., Ristola, P., and Aitio, A., in Chemical Toxicology and Clinical Chemistry of Metals, Brown, S., and Savory, J., eds., Academic Press, London (1983).
[14] Wald, A., Sequential Analysis, Wiley, New York (1947).
[15] Welz, B., Atomic Absorption Spectroscopy, Verlag Chemie, Weinheim/New York (1976).
[16] Slavin, W., Carnrick, G., Manning, D., and Pruszkowska, E., At. Spectrosc. **4**, 69 (1983).
[17] Slavin, W., and Carnrick, G., At. Spectrosc. **6**, 157 (1985).

Appropriate Reference Parameters for the Evaluation of Elemental Analysis Data from Biomedical Specimens

Venkatesh Iyengar

NBS/USDA
Gaithersburg, MD

and Dietrich Behne

HMI, Berlin
F.R. Germany

Studies on the elemental composition of biological systems can be divided into four stages: experimental design, collection of valid samples, chemical analysis and data evaluation (and interpretation). Each of these steps is important for the overall success of an investigation. In our opinion, one aspect of data evaluation and interpretation of trace element studies, namely relating the elemental analysis data to a meaningful base, has not received adequate attention. In many cases this has resulted in wrong conclusions being reached, even if the elemental analysis has been carried out correctly. This frequently happens when the biological material consists of several components with different elemental content, and the ratio of these components differs from sample to sample [1].

Elemental analysis in bone samples is an example of this phenomenon, as several elements are unevenly distributed between the different bone compartments. The fluorine content of the trabecular bone, for instance, is greater than that in the compact substance by a factor of 3 [1]. As the ratio of spongy to compact substance varies along the bone, different fluorine contents are estimated for the whole sample, according to where the sampling has been carried out, although no changes in the fluorine levels in the different bone tissues have occurred. Forbes et al. [2] have reported a similar phenomenon for lead within a rib; expressed on the

basis of ash, Pb content decreases as the distance from the costochondral junction increases. This has been attributed to the increased ash content of the samples as the fraction of marrow changes. Therefore, it is necessary to specify the location of the bone section analyzed and its marrow content.

Similarly, the results of elemental analysis of whole blood may depend on the percentage of red blood cells in the sample [1]. This should always be considered when the elemental content is much higher in erythrocytes than in the blood plasma, as for instance, in the case of iron and lead. If not, changes in the hematocrit, which can occur as a function of several factors (such as pregnancy, age or disease) may lead to false conclusions being drawn about the quantities of these elements in the body.

Other examples of this source of error are the changes in the age distribution of erythrocytes after blood loss [3], which results in a higher zinc content of the red blood cells, changes in the water content of serum samples according to the body position during sampling (recumbent or upright) [4], or changes in the amount of fat or residual blood in a tissue, all of which can lead to alterations in the content of several elements.

Errors can also occur by redistribution of elements or water in certain organs due to the interruption of metabolic processes. For instance, significant changes in the weight of the whole organ can occur under post-mortem conditions [5]. This can lead to great differences in elemental concentrations, depending on whether they are related to the wet or the dry weight of the material. In such cases, it is necessary to know the total weight of the organ, as well as its water content, to be able to account for changes in elemental concentrations. It is obvious that meaningful data interpretation is not possible without this knowledge.

Many of the errors alluded to above can be avoided if one does not express the analytical value only in the usual way of amount per volume or weight of the sample, but also relates the data to other parameters such as the number of certain cells or the content of a protein. This enables changes in the tissue composition to be taken into account. For instance, in whole blood analysis errors due to changes in the hematocrit can be excluded, if the amount of hemoglobin, which reflects the number of red blood cells, is used as a base for expressing elemental concentrations.

Some examples of relevant parameters needed to evaluate elemental analysis data are shown in table 1. In table 2 additional features are listed, which should also be checked when elemental data are measured in biological materials.

The authors recognize that it is difficult to recommend a most suitable base, since this generally depends on the type of study and on the problems to be investigated. However, one can improve the present situation by paying adequate attention to documentation of supplemental information on relevant parameters and by including them in scientific publications. This would facilitate a meaningful intercomparison of results from different investigations.

In conclusion, it is important to present results from biological trace element investigations in an unambiguous way. A multidisciplinary approach is essential throughout the whole investigation. Only then will it be possible to eliminate the influence of presampling factors [6], to obtain biologically and analytically valid specimens for analysis [7,8] and to choose the most appropriate parameters for data evaluation and interpretation.

Table 1. Parameters for evaluation of elemental analysis data in biological specimens[a]

Specimens	Parameters
Body fluids	
Serum, plasma	Protein, water
Whole blood	Hematocrit
Urine	24 h volume, creatinine
Sweat	Volume
Amniotic fluid	Meconium, cells
Milk	Average daily output, fat content
Semen	Sperm count
Bile	Volume
Cells	
RBC, WBC, Platelets, Spermatozoa	Cell number and Haemoglobin (for RBC)
Soft tissues	
Organ samples	Whole weight of the organ
Placenta	Age of the placenta, total weight.
Hard tissues	
Bone	Percentage marrow, ratio spongy/compact, Ca/P ratio.
Teeth	Ratio pulp/enamel
Hair	Distance from surface
Diets[b]	24 h collection weights, average body weights of subjects
Feces[c]	24 h collection weights, average body weights of subjects

[a] Specific Gravity, dry/wet weight ratios, common for all fluids, moisture content common for both hard and soft tissues, diets and feces.
[b] Expressed as intake/day.
[c] Expressed as excretions/day.

Table 2. Checklist of essential features related to elemental analysis of biological systems

Specimen	Required information
Plasma	Amount and type of anticoagulant and its chemical purity
Serum	Body position during sampling, hemolysis status
Milk	Days past partum, specific fraction (hindmilk, foremilk) if entire volume not collected
Cells	Viability, (cell age), amount. Type and purity of stabilizer used, trapped plasma
Soft tissues	Residual blood, decidual tissue while *handling placenta, biopsy or autopsy*
Hard tissues	
bone	Biopsy or autopsy, renal function status sampling location
hair and nail	Origin and washing procedures for hair and nail
Diets	Proximate composition, caloric energy
Feces	Occult blood

References

[1] Behne, D., J. Clin. Chem. Clin. Biochem. **19**, 115 (1981).
[2] Forbes, W. F., Finch, A., Esterby, S. R., and Cherry, W. H., Studies of trace metal Pb levels in human tissues—III. The investigation of Pb levels in rib and vertebra samples from Canadian residents, in Trace Substances in Environmental Health-X, Hemphill, D. D., (ed.), University of Missouri, Columbia, MO, 41 (1976).
[3] Gawlik, D., Behne, D., and Gessner, H., Trace Ele. Med. **2**, 64 (1985).
[4] Juergensen, H., and Behne, D., J. Radioanal. Chem. **37**, 375 (1977).
[5] Iyengar, G. V., J. Path. **134**, 173 (1981).
[6] Iyengar, G. V., Anal. Chem. **54**, 554A (1982).
[7] Iyengar, G. V., and Kollmer, W. E., Trace Ele. Med. **3**, 25 (1986).
[8] Iyengar, G. V., J. Radioanal. Nucl. Chem. **112**, 151 (1987).

Ultra-Trace Elemental and Isotopic Quantification for Neonatal Nutrition Studies

L. J. Moore, J. E. Parks, M. T. Spaar D. W. Beekman and E. H. Taylor

Atom Sciences, Inc.
114 Ridgeway Center
Oak Ridge, TN 37830

and

V. Lorch

Intensive Care Nursery
Department of Pediatrics
University of Tennessee
Knoxville, TN 37920

Trace element accumulation in the human fetus occurs primarily in the third trimester of pregnancy, and premature birth interrupts this process. A study of zinc in low birth weight infants indicates that the fetus accrues 310 μg of Zn daily at the 30th week, increasing to 590 μg daily by the 36th week of gestation [1]. Similarly, the human fetus accumulates 80–90 μg of Cu/kg/day between 28 and 36 weeks, and by 40 weeks the fetus has accumulated almost 20 mg of Cu, one half of which is in the liver [2]. These and other essential trace elements play vital roles in the adult. Zinc is required for the synthesis of DNA, RNA, and protein, and as the zinc metallo-enzyme, regulates growth through DNA polymerase, RNA polymerase and thymidine kinase. References to these effects have been summarized [3]. Significant progress has been achieved recently using stable isotope tracers to assess the metabolic and nutritional roles of Ca [4], Zn [5], Se [6], and Mg [7] in adults and healthy infants. Techniques used for these studies include mass spectrometry, using electron impact ionization of metal chelates or thermal ionization of inorganic species. Trace elements at higher concentrations or in large samples have been determined with techniques such as atomic absorption (AA) or emission spectroscopy that do not address measurement needs for trace element and isotope tracer determinations in premature infants, healthy newborns, children, pregnant women, and other adults.

Little is known about the presence and function of trace and ultra-trace elements in pre-term infants whose birth weight is 500–2000 g. Only microliters of blood are available, and trace elements can occur in the blood at levels of parts per billion (ng/g) or lower. For a trace element level of 1 ppb, the total amount of the element available is 100 pg, or assuming vanadium, only 10^{12} atoms. Clearly a new and comprehensive method is required to access elemental and isotopic information at these levels. Resonance ionization spectroscopy (RIS) is being used to solve these problems.

RIS utilizes a source of tunable laser radiation that is resonant with a specific atomic energy level. In the simplest two photon RIS scheme (fig. 1, scheme 1), a second photon of the same energy promotes the excited electron to the ionization continuum, forming an atomic ion. This simple two photon process can be used to ionize approximately fifty elements, but a series of RIS schemes has been proposed by Hurst et al., to ionize all elements except He and Ne (fig. 1) [8].

Resonance ionization advantages are threefold: 1) sensitivity, 2) selectivity, and 3) generality. Ionization *sensitivity* is achieved by saturating the photon absorption cross section of the energy level such that every atom crossing the active ionizing laser volume is ionized with unit probability. Elemental ionization *selectivity* is achieved through wavelength tunability. By selecting appropriate non-overlapping wavelengths, elements can be measured quantitatively in the presence of $10^6 - 10^{12}$ of other elements. Resonance ionization is a *general* ionization process as described above.

Experimental

The experimental design was structured toward the longer term research goal: to provide for the neonatologist a total multi-elemental and isotopic diagnostic analysis using only a few microliters of blood. Thus, the chemical separations must be minimal, simple, and capable of providing a group separation in a form amenable to RIS analysis. We selected electrodeposition as an initial separation process and were successful in depositing nanogram or picogram quantities of Cu, Mo, Se, and V singly or simultaneously onto a high purity gold substrate directly from aqueous solution. Cu and Mo were deposited individually onto gold from processed serum samples and their concentrations determined by isotope dilution. To separate copper, the serum samples were wet-ashed with a nitric-perchloric acid mixture, evaporated to dryness, adjusted to the appropriate acidity, and the copper electrodeposited. To separate molybdenum, the sample was wet-ashed as above but the molybdenum was deposited from alkaline solution.

Following the multicomponent analysis theme, the laser and optical systems in Atom Sciences' Sputter-Initiated Resonance Ionization Spectrometer (SIRIS) (fig. 2) were modified to permit access to Cu, Zn, Mo, Se, and V within a single tunable laser dye range. Samples on gold foil were atomized by ion sputtering and the diluted isotope ratios were determined using a double-focusing mass spectrometer. The mass spectrometer was calibrated using gravimetrically prepared mixtures of isotopically natural copper and enriched ^{65}Cu.

Results and Discussion

The results of the SIRIS calibration are illustrated in figure 3a. The data points cover an isotope ratio range of nearly 600, from natural copper ($^{63}Cu/^{65}Cu = 2.244$) to the separated ^{65}Cu isotope ($^{63}Cu/^{65}Cu = 0.0038$). This range encompassed the anticipated $^{63}Cu/^{65}Cu$ range for the isotope dilution samples, nominally 0.05 to 0.4. The deviation of each observed ratio from its gravimetric value was summed over all the ratios, yielding a relative standard deviation (RSD) of 4.7%. Isotope ratio precisions internal to an analysis were typically 1–2%, with attendant standard errors of the mean of 0.2%.

The concentration of copper was determined in separately processed duplicate samples of human serum and plotted in figure 3b versus analyses of the same (but larger) samples by flame AA. The RIS sample sizes were 80–200 μL, and an overall accuracy of ±10% was estimated, which included contributions from inhomogeneities, RIS methodology and the flame AA results using larger (2–3 mL) aliquots. Using isotope dilution with ^{100}Mo, Mo was determined in high purity reagents and serum. Concentrations of Mo in reagents, pg/g, were: H_2O, 13; HNO_3, 44; $HClO_4$, 30; and an Mo concentration of 19 ng/g was determined for a 250 μL aliquot of Bovine Serum (RM 8419), compared to the suggested value of 16 ng/g [9].

Using SIRIS, sensitivities have been observed for Mo isotopes at the few pg level. Overall ionization and instrumental transmission efficiencies indicate potential absolute sensitivites of a few thousand atoms ($\leqslant 10^{-9}$ monolayer). The RIS elemental and isotopic analysis technology is expected

to be generally applicable in medicine and nutrition for metabolic and diagnostic studies.

Acknowledgments

C. Veillon provided the comparison flame AA results. Partial support for this work was provided by two grants: 1) An NIH Small Business Innovation Research grant, #1 R43 HD 21831-01 and 2) a grant from the Professional Medical Education and Research Foundation in Knoxville, TN.

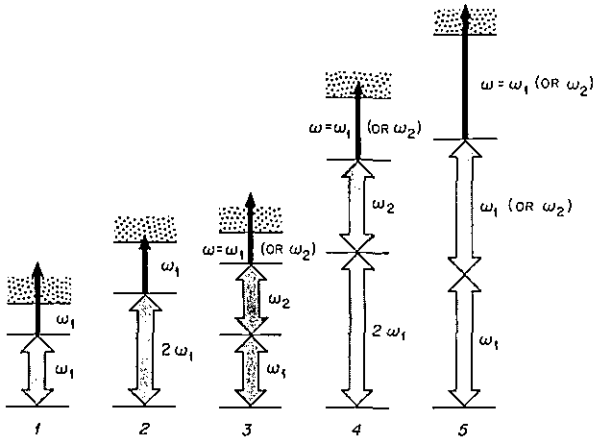

Figure 1. *A schematic illustration of five resonance ionization* processes that are possible using commercially available lasers (taken from Ref. [8]). RIS of Mo is by a generalization of scheme 1, where ω_1 refers to a frequency doubled laser beam. Analogously, RIS of Cu is by a generalization of scheme 3, where $\omega_1=\omega_2$=frequency doubled beams, although ionization is by ω_3=IR.

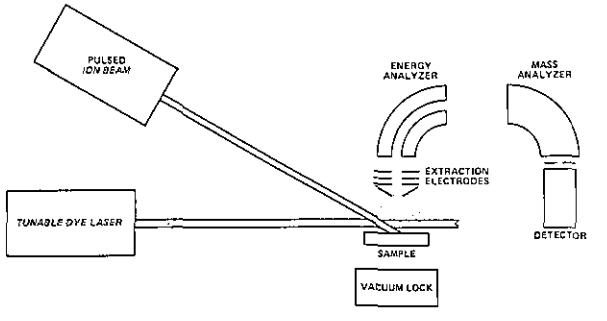

Figure 2. The sputter-initiated resonance ionization spectrometer (SIRIS) system used for the analytical determinations reported here. Condensed phase samples are atomized with an energetic argon primary ion beam ionized with a multi-color tunable dye laser system, and the ions are energy and mass analyzed with a double focusing mass spectrometer.

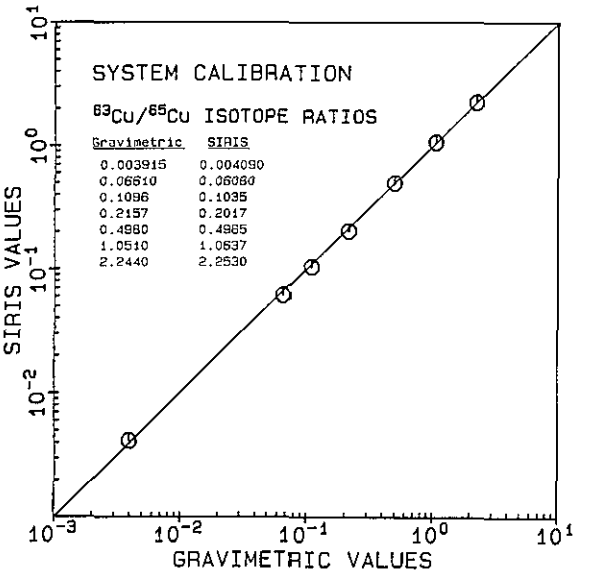

a

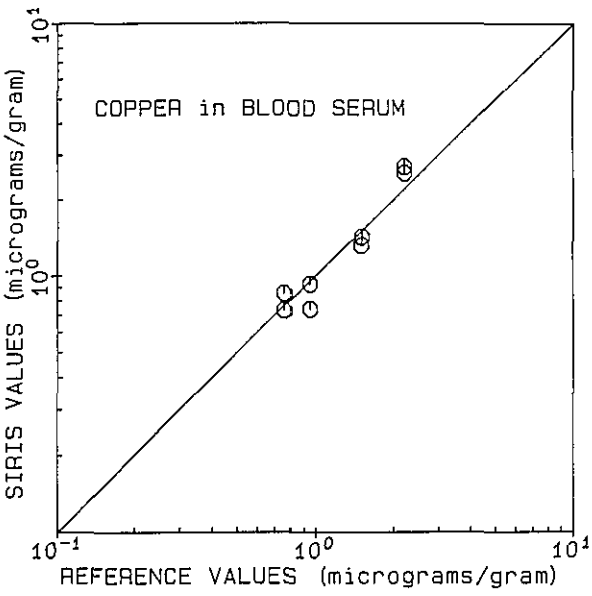

b

Figure 3. *a. A calibration of the SIRIS system using* $^{63}Cu/^{65}Cu$ isotope ratio standards, prepared by mixing natural copper ($^{63}Cu/^{65}Cu$=2.244) and the ^{65}Cu enriched isotope ($^{63}Cu/^{65}Cu$=0.0038). The relative standard deviation observed for the calibration was 4.7%; b. a plot of copper concentrations in bovine (RM 8419) and human serum determined with SIRIS, versus concentrations determined by flame AA using 2–3 mL samples. Serum sample sizes used for SIRIS were nominally 100 μL and were separate duplicate determinations. The lowest concentration reported here was for bovine serum (RM 8419), and was 0.76 μg/g compared to the suggested value of 0.73 μg/g (Ref. [9]).

References

[1] Dauncey, J., Shaw, J. C. L., and Urman, J., Ped. Res. **11**, 1033 (1977).
[2] Morris, F., Jr., Trace Materials, Seminar in Perinatology **3**, 369–379 (Oct. 1979).
[3] Johnson, H. L., and Sauberlich, H. E., Trace Elements Analysis in Biological Samples, in Clinical, Biochemical and Nutritional Aspects of Trace Elements, Ananda, S., Prasad, Ed., Alan R. Liss, Inc., New York, 405–426 (1982).
[4] Moore, L. J., Machlan, L. A., Lim, M. O., Yergey, A. L., and Hansen J. W., Ped. Res. **19**, 329 (1985).
[5] Janghorbani, M., Young, V. R., Gramlich, J. W., and Machlan, L. A., Clin. Chem. Acta **114**, 163 (1981).
[6] Turnlund, J. R., Michel, N. C., Keys, W. R., King, J. C., and Margen, S., Am. J. Clin. Nutr. **35**, 1033 (1982).
[7] Hachey, D. L., Blais, J. C., and Klein, P. D., Anal. Chem. **52**, 1131 (1980).
[8] Hurst, G. S., Payne, M. G., Kramer, S. D., and Young, J. P., Rev. Mod. Phys. **51**, 767 (1979).
[9] Veillon, C., Lewis, S. A., Patterson, K. Y., Wolf, W. R., Harnly, J. M., Versieck, J., Vanballenberghe, L., Cornelis, R., and O'Haver, T. C., Anal. Chem. **57**, 2106 (1985).

Use of High Resolution GC/MS for Obtaining Accuracy in Lipid Measurements

John Savory, Michael Kinter, David A. Herold, Judy C. Hundley, and Michael R. Wills

Departments of Pathology,
Biochemistry and Internal Medicine
University of Virginia
Charlottesville, VA 22901

Introduction

Inaccuracy in clinical chemistry measurements is a serious problem in both service and research laboratories. It is only by having procedures of proven accuracy available that the clinical chemist can gain assurance that a working method is providing meaningful data. Analytical uncertainties occur in all areas of clinical chemistry and two examples of such problems in the area of lipid analysis are discussed here.

Prostanoid Measurements

One excellent example in which difficulties with inaccuracy can be seen is in the measurement of prostanoids. Although these analyses are not yet routine clinical chemistry measurements, these metabolites of arachidonic acid are of great importance in a vast number of research studies. Disturbances of prostanoid production are seen in a wide variety of pathological conditions including diabetes mellitus, hypersensitivity and inflammation, cancer, reproductive problems, hypertension and cardiovascular disease. To emphasize the analytical problems associated with measuring prostanoids, a survey of the literature reveals an incredible spread of reported reference (normal) ranges for various prostanoids in human plasma. For example, reported reference ranges for 6-keto-$PGF_{1\alpha}$ are 0.4–5.0 pg/mL [1], 19–25 pg/mL [2], 160–228 pg/mL [3] and 1500–1700 pg/mL [4].

We have applied gas chromatography/mass spectrometry (GC/MS) to the measurement of prostanoids in plasma and in urine. Our procedure initially used an initial extraction, clean-up by high performance thin layer chromatography [1], derivatization, and detection by GC/MS at low or unit mass resolution using negative ion chemical ionization. Using this technique, assays of marginal performance were developed for the measurement of PGE_2, 6-keto-$PGF_{1\alpha}$, $PGF_{2\alpha}$, and TxB_2 in plasma. However, when urine was analyzed, there were many interferences due to the complex matrix and reliable analytical data could not be produced.

The purpose of the present investigation was to reduce these potential interferences from biological specimens, particularly urine, by applying stable isotope dilution with quantitation by capillary column gas chromatography and high resolution mass spectrometry. The use of high resolution mass spectrometry is notable because it provides the selectivity of detection previously obtained by extensive chemical clean-up. This selectivity of detection can result in lower limits of detection despite a reduction in absolute sensitivity since one source of noise, chemical noise, is reduced more rapidly.

Materials and Methods

Deuterium-labeled internal standards (d_4-PGE_2 and d_4-6-keto-$PGF_{1\alpha}$) were added to 10 mL of acidified urine (pH=2.5). Initial extraction of the prostanoids was by a C_{18} SEP-PAK extraction, elution and subsequent ethyl acetate extraction from

the eluate. Derivatization involved methoximation followed by a novel scheme in which the pentafluorobenzyl esters were formed prior to a silylation step in which the t-butyldimethylsilyl esters were formed in an apparent exchange reaction. Treatment with N-methyl-N-(t-butyldimethylsilyl)trifluoroacetamide (MTBSTFA) to produce the t-butyldimethylsilyl esters also, of course, formed the t-butyldimethylsilyl ethers.

Gas Chromatography/Mass Spectrometry. The mass spectrometer used was a double focusing, reverse geometry instrument (Model 8230, Finnigan MAT) with a SpectroSystem 300 data system. The instrument was operated in the electron ionization mode using 70 eV electrons. Data were acquired in a selected ion monitoring experiment, monitoring m/z 666.441 and 670.466 for PGE_2, and 798.537 and 802.503 for 6-keto-$PGF_{1\alpha}$ at a rate of 1 Hz. A DB-1 bonded phase fused silica capillary column, 20 m×0.32 mm, was used. Samples were injected on column at a temperature of 200 °C followed by a 15 °C/min ramp to 300 °C.

Results and Discussion

Recoveries through the entire extraction and derivatization procedure were 70.6% for PGE_2 and 64.4% for 6-keto-$PGF_{1\alpha}$. Quantitation at mass resolution of 10,000 eliminated all interferences in the PGE_2 chromatograms while a resolution of 1,000 was sufficient for the 6-keto-$PGF_{1\alpha}$ analysis with limits-of-detection of 50 pg/mL for each. For PGE_2 a lower limit-of-detection was obtained at a mass resolution of 10,000 (50 pg/mL), than was obtained at a mass resolution of 1,000 (80 pg/mL), illustrating the selectivity of detection. The method was linear to 10 ng/mL. Spot urine specimens in normal volunteers ranged from 80–570 pg/mL PGE_2 (n=12) and 77–185 pg/mL 6-keto-$PGF_{1\alpha}$ (n=6). This method, although difficult and expensive, provides excellent analysis of PGE_2 and 6-keto-$PGF_{1\alpha}$ in urine.

Cholesterol

Recent studies on the use of serum cholesterol as a risk factor in atherosclerosis indicate a need for improved analytical performance in routine assays. The Laboratory Standardization Panel of the NIH National Cholesterol Education Program has set goals of $<\pm 3\%$ for both bias and precision. Towards this end, the Panel has also established a definitive method, which uses isotope dilution mass spectrometry, and a reference method, which uses a colorimetric assay. There is, however, a continued need for the widespread availability of reference and pseudo-definitive methods with physical methods being preferred.

We have developed a GC/MS procedure for the measurement of serum cholesterol using a structural isomer, 7,(5α)-cholesten-3β-ol, as the internal standard which we used because the cost of a stable isotope labeled internal standard based assay was prohibitive due to the high concentration of endogenous cholesterol. In addition, the GC/MS measurement was made at a moderately high mass resolution (R=5000) to enhance the selectivity and ensure an interference-free assay. As was the case with the prostanoid measurements, high resolution mass spectrometry provided a highly selective measurement step. This selectivity, in this example, was used to eliminate interferences that were fundamental limitations to accuracy.

Materials and Methods

Reagent and Standards. The cholesterol Standard Reference Material (SRM 911a) and Certified Human Serum (SRM 909) were obtained from the National Bureau of Standards (Gaithersburg, MD 20899). The latter had a certified cholesterol concentration of 143.1 mg/dL.

A 0.5 mL aliquot of serum and a 0.5 mL aliquot of the internal standard solution (7,(5α)-cholesten-3β-ol) were pipetted into a centrifuge tube using an automatic pipettor and the sample hydrolyzed in alcoholic KOH at 37 °C for 3 hours. The sample was then extracted and derivatized with BSTFA (bistrimethylsilytrifluoroacetamide) for 0.5 h at 60 °C. The samples were then evaporated to dryness and reconstituted in 500 μL of tetradecane for analysis. A 211.4 mg/dL standard was also prepared by pipetting 0.5 mL of a standard cholesterol solution and 0.5 mL of the internal standard solution in a centrifuge tube, evaporating to dryness, and reconstituting the standard in 5 mL of methanol from which a 100 μL portion was transferred for derivatization.

Gas chromatography/mass spectrometry analysis was performed in a similar manner to the prostanoid assay. Selected ion monitoring of m/z 458.394 at a rate of 4 Hz was carried out with GC conditions the same except that a 20 °C/min ramp was used.

Results and Discussion

The 100 eV EI mass spectra of cholesterol and 7,(5α)-cholesten-3β-ol both showed molecular ions of large relative abundances, 70% and 100%, respectively. The molecular ion was therefore chosen as the ion to be monitored, maximizing our molecular specificity. These compounds were also quite easily separated using capillary column gas chromatography. Under our chromatographic conditions, the 7,(5α)-cholesten-3β-ol derivative eluted at 7:56 minutes and the cholesterol derivative eluted at 8:21 minutes. In addition, the signals obtained were quite large, allowing good counting statistics. No other chromatographic peaks were observed in the time window for which data were acquired, indicating good selectivity. A linear response, area cholesterol divided by area 7,(5α)-cholesten-3β-ol, was observed over a range of 0 to 1000 mg/dL. This linearity allowed the calculation of sample concentration using a response factor calculated from a single standard.

Concentration values for the Certified Human Serum determined by this method in a series of 7 analyses sets are shown in table 1. From these data the accuracy was excellent with an average concentration of 142.3 mg/dL indicating a bias of −0.6%. The between-run precision, SD=2.2 mg/dL, CV=1.6%, is approaching the target precision of 2.5% for a serum cholesterol reference method. The in-run precision, estimated from the average of the ranges for the duplicate determinations, is also acceptable, SD=2.3 mg/dL, CV=1.6%.

Table 1. Cholesterol concentrations for NBS Certified Human Serum

Analysis set	Cholesterol concentration, mg/dL			
	#1	#2	ave	range
1	144.2	144.1	144.2	0.1
2	140.4	146.7	143.6	6.3
3	142.0	138.4	140.2	3.6
4	138.0	141.9	140.0	3.9
5	146.0	145.2	145.6	0.8
6	142.9	141.8	142.4	1.1
7	142.1	138.6	140.4	3.5

The performance characteristics of this assay are within the goals established for a serum cholesterol reference method. Good accuracy was to be expected because of the high molecular specificity of gas chromatography/high resolution mass spectrometry. This specificity ensures an interference-free assay eliminating interferences as a fundamental limitation to accuracy.

A GC/MS reference method for the measurement of serum cholesterol using a structural isomer as an internal standard has been developed. The advantages of this method are the cost-effectiveness of using an unlabeled internal standard and the specificity of using gas chromatography/high resolution mass spectrometry. This assay will allow the establishment of reference serum cholesterol assays in laboratories with high resolution mass spectrometry capabilities and, therefore, lead to the wider availability of serum cholesterol reference methods in the future.

Conclusion

The selectivity of detection provided by high resolution mass spectrometry is a powerful tool in developing accurate analytical methods in clinical chemistry. In the case of prostanoid measurements, it is likely that GC/MS methods may be the only methods which provide good analytical data. In the case of serum cholesterol measurements, GC/MS reference methods may lead to an improvement in routine assay by allowing more careful quality control and assurance, and more accurate calibration materials.

Acknowledgments

Funding for the purchase of the high-resolution mass spectrometer was obtained from the National Institutes of Health, Division of Research Resources Shared Instrumentation Grant Program, grant number 1-S1-RR0-2418-01. Additional funding supporting this research by the John Lee Pratt Fund of the University of Virginia is also gratefully acknowledged.

References

[1] Smith, B. J., Ross, R. M., Ayers, C. R., Wills, M. R., and Savory, J., J. Liq. Chrom. **6**, 1265 (1983).
[2] Mitchell, M. D., Prostaglandins Med. **1**, 13 (1978).
[3] Hensby, C. N., FitzGerald, G. A., Friedman, L. A., Lewis, P. J., and Dollery, C. T., Prostaglandins **18**, 731 (1979).
[4] Chiabrando, C., Castognoli, M. W., Noseda, A., et al., Prostaglandins Leukotrienes Med. **16**, 79 (1984).

Volume 93, Number 3, May-June 1988
Journal of Research of the National Bureau of Standards

Some Atomic Absorption Spectrometric Applications to Clinical-Biomedical Trace Metal Analyses

Eleanor Berman

Division of Biochemistry
Cook County Hospital
Chicago, IL 60612

Following the introduction of atomic absorption spectrometric (AAS) instrumentation about 30 years ago, many specific and sensitive methods for determining trace metal concentrations in biological materials were developed. Yesterday's rare and esoteric investigations are today's routine clinical analyses. Levels of essential and toxic metals can be determined with relative ease for diagnostic purposes and following response to treatment. There is greater understanding of the chemistry and biochemistry of trace metals in health and disease as a consequence.

The Challenges

Atomic absorption spectrometric analyses of the trace metal content of biological materials are challenging. These materials are complex, containing components that can generate nonspecific molecular absorption signals which may bias absorption measurements of the trace metals of interest. Sodium, and to a lesser extent potassium and protein, represent the major interferences.

Biological materials usually require pretreatment before instrumental analyses: the extent necessary depends upon the material itself as well as the concentration of the analyte. Tissues must be solubilized while blood and urine may require the removal of the proteins.

The sensitivity or detection limit capability of the instrument is an important factor. Oftentimes trace analytes in biological tissues and fluids are below the detection limits of the analytical instrumentation and a preconcentration is required.

Unknowns and standards should be similar to obtain valid instrumental comparisons. A blank or zero concentration standard is included with each group of assays. Control materials should be determined concurrently to assure the quality of the assay. There are standard reference materials available for most trace metals.

Contamination

Many of the trace metals of clinical interest are common contaminants in the laboratory environment and in areas where samples are collected for analysis. Maintenance of a clean environment from the point of sample collection to the release of analytical findings is a continuous challenge for the trace metal analyst in a clinical laboratory. Rigorous, but practical, measures must be instituted and maintained to ensure that sample collection vessels, measuring devices, labware in general, water, and reagents are essentially free from trace metal contaminants. For example, determining trace metal residues on freshly cleaned labware and setting limits of acceptance can prove quite effective in maintaining the quality of labware and reagents, and ultimately, the quality of the analytical measurements.

Since the skin and clothing of subjects being investigated for exposure to toxic metals such as lead, cadmium, and mercury are often liberally dusted with the metals of interest, it is prudent for the laboratory to request, periodically, that sponges used in cleaning the venipuncture sites be submitted along with the blood specimens sent for analysis. If venipuncture sites are not cleaned adequately, sufficient contamination can be introduced into the blood samples to yield erroneously elevated levels.

To illustrate: the amount of lead removed by alcohol sponges from the venipuncture sites of 20 battery workers was found to range from 0.5 to 14.9 mg. Four to five separate sponges were required to free the skin area from lead contaminants. Initial lead content of the brand of alcohol sponges used in the study was 30 to 60 μg.

Lead, Cadmium, and Thallium

The many procedures described for determining the toxic metals lead, cadmium, and thallium vary in complexity from simple dilution with a surfactant to precipitation of proteins by nitric or tri-chloroacetic acids to chelation-solvent extraction techniques at different pH ranges [1]. In the latter case, we found a pH of 5.5 to 6.5 to be optimal.

Capability of the instrumentation available, as well as the population being investigated govern the choice of method adopted. Both flame and electrothermal atomization techniques can be employed. For flame methods larger sample size is needed while electrothermal atomization is usually more than an order of magnitude more sensitive. All techniques have their pitfalls. For example, versenate (EDTA) blocks the solvent extraction of lead as a dithiocarbamate [2]. EDTA is a stronger chelator of lead than is dithiocarbamate. Furthermore, the lead-EDTA complex is water soluble and is not extracted by an organic solvent. The addition of calcium can eliminate the versenate interference with the chelation-extraction of lead [3]. However, recoveries tend to be variable. The acid precipitation methods [4] for lead analysis are not influenced by versenate; however, versenate does not interfere with the chelation-extraction of cadmium, thallium, or mercury as dithiocarbamates.

Both techniques, chelation-extraction and acid precipitation, yield comparable results when blood samples from asymptomatic children and adults or NBS porcine blood lead controls are analyzed. However, higher values are obtained on blood samples drawn from symptomatic subjects [5]. Table 1 lists a comparison between the two methods.

Table 1. Comparison of blood lead values obtained by chelation-extraction and nitric acid precipitation methods

Subject	Status	Lead level μg% Chelation-extraction	Nitric acid
child	asymptomatic	36	34
child	asymptomatic	29	29
child	asymptomatic	58	58
child	symptomatic	56	34
child	symptomatic	56	29
child	symptomatic	143	93
adult	asymptomatic	24	23
adult	asymptomatic	45	44
adult	asymptomatic	57	58
adult	symptomatic	69	49
adult	symptomatic	57	44
adult	symptomatic	67	48

This pattern follows the subjects throughout treatment and subsequently. Since agreement between the two procedures was good when applied to control materials and blood samples from asymptomatic subjects, incidental error can be ruled out. It is possible, perhaps, that the low molecular weight protein described by Raghavan and Gonick [6] may be a factor in producing the discrepancies observed between the two methods when applied to blood lead analyses of symptomatic individuals. This protein, occurring in the red cells of lead exposed subjects, was found to bind considerable lead. Quite possibly, this bound-lead is precipitated along with the blood proteins.

Mercury

Determination of mercury in a clinical laboratory presents special challenges. Because of the volatility of elemental mercury and some of its compounds even at ambient temperatures, precautions must be taken to prevent losses of the element during the analytical process.

For obvious reasons mercury analyses should not be performed in a room containing a Van Slyke or comparable type apparatus. Furthermore, wearing of certain cosmetics, for example, eye shadows, by technical personnel doing these analyses should be prohibited. Many such preparations contain mercury salts.

Some current analytical methods utilize an adaptation of the cold-vapor technique wherein mercury is reduced to the elemental state and swept from solution by a stream of inert gas and into an absorption tube in an atomic absorption spectrometer. Mercury vapor, so measured, is essentially free from interferences due to matrix constituents [7,8].

This technique proves to be a bit awkward in the usual high volume clinical laboratory; however, we find chelation-extraction less cumbersome. Mercury in solution is chelated at pH 3–4 by ammonium pyrollidine dithiocarbamate and extracted into methyl isobutyl ketone. Standards and unknowns are compared in a graphite furnace programmed to dry and char at 75 °C. Background correction is necessary.

Therapeutic and Essential Elements

Determination of serum levels of the therapeutic metal lithium and the essential elements magnesium, copper, zinc, and iron can prove to be life saving guides to the immediate therapy indicated. Sample preparation involves only dilution or protein precipitation since levels of the metals are in the μg/mL range compared to mg/mL quantities for the toxic elements.

Lithium and copper are distributed equally between cells and serum. However, red cells contain more magnesium, zinc, and iron than does serum. To assure analytical accuracy, hemolysis should be avoided. Also, cells and sera must be separated shortly after sample collection.

Since aqueous solutions leach magnesium from glass containers, materials and reagents meant for magnesium analysis should be stored in plastic containers washed to reduce trace metal content.

Specimens for zinc analysis are best collected and stored in washed plastic containers to avoid contamination by the zinc present in rubber stoppers of the usual evacuated tubes.

Both flame and electrothermal atomization techniques can be applied to the analyses of these metals. Flame atomization is more practical for routine clinical determinations of lithium, magnesium, and zinc. Electrothermal atomization is preferred for copper and iron analyses. Background correction is essential for electrothermal atomization AAS.

References

[1] Berman, E., Toxic Metals and Their Analysis, Heyden and Son, Ltd., London (1980) 130.
[2] Stary, J., The Solvent Extraction of Metal Chelates, Pergamon Press, Ltd. (1964) 161.
[3] Zinterhofer, L. J. M., Jatlow, P. I., and Fappiano, A., J. Lab. Clin. Med. **78**, 664 (1971).
[4] Stoeppler, M., Brandt, K., and Rains, T. C., Analyst **103**, 714 (1978).
[5] Berman, E., Toxic Metals and Their Analysis, Heyden and Son, Ltd., London (1980) 132.
[6] Raghavan, S. R. V., and Gonick, H. C., Proc. Soc. Exptl. Biol. Med. **155**, 164 (1977).
[7] Magos, L., and Clarkson, T. W., J. Assoc. Offic. Anal. Chemists **55**, 966 (1972).
[8] Taylor, A., and Marks, A., But. J. Ind. Med. **30**, 293 (1973).

Inaccuracies in Clinical Chemical Analysis

Merle A. Evenson

University of Wisconsin
Hospital Clinical Laboratory
Departments of Medicine and
Pathology-Laboratory Medicine
Madison, WI 53706

Accuracy in clinical chemistry analyses remains vague and difficult to quantitate in individual samples. The analytical chemistry principles of standard addition, interference studies, reagent blank studies, the use of National Bureau of Standards' Standard Reference Materials (NBS-SRMs) and the development of definitive analytical methodology have contributed significantly to the improvement of the accuracy of clinical chemistry methods in the last 25 years. However, absolute accuracy for all biological samples remains an unattainable goal for the field of clinical chemistry analysis.

Clinical chemistry as a distinct field started to evolve principally from biochemistry shortly after the turn of this century. Analytical chemistry method development at that time was hindered by the unavailability of highly pure and stable chemical standards. Frequently, clinical correlation of laboratory numbers to the patient's medical condition was one of the major pieces of information that was used to assess the accuracy of the laboratory measurement. As commercial sources of chemical standards became available, products from different companies were compared and exchange of samples between laboratories ("round robins") revealed many accuracy and calibration problems with the analytical measurements. In the late 1950's when the AutoAnalyzer became commercially available from the Technicon Corporation, common calibration materials and reagents from Technicon greatly reduced the bias in laboratory results between different hospital laboratories. In addition, the precision of the analytical methods dramatically improved as a result of the Technicon mechanization of the measurement process. However, this increase in precision did not bring with it the expected improvement in accuracy.

The focused emphasis on increased accuracy in clinical chemistry analysis in the 1960's was initiated and led by the National Bureau of Standards

(NBS). In 1966, Dr. W. Wayne Meinke presented a talk at the national meeting of the American Association for Clinical Chemistry (AACC) on "Standards." In June of 1969, the National Institutes of Health (NIH) announced they would award 3 million dollars to NBS for the development of SRMs for the clinical chemistry laboratory. A progress report of the research at NBS was written by Dr. Meinke and appeared in *Analytical Chemistry* [1].

With the availability of the NBS-SRMs, clinical chemists quickly found they were unable to obtain the correct answers for the highly purified reference materials using their usual daily clinical laboratory instruments and methods. Further, if they used the NBS-SRM materials to calibrate the methods in daily use, the "normal ranges" would have to be significantly changed from the long established textbook values. This was not acceptable in most laboratories.

The Clinical Laboratory Improvement Acts of 1969 and 1973 and the Medical Device Law of 1976 forced accuracy issues and changes upon the field of clinical chemistry. This demand occurred at a time when the capabilities for improved accuracy were limited and when this goal was difficult to achieve.

The original intention of the improvement acts was to make sure that Medicare and Medicaid payments were being made for quality health care delivery. It appears that one of the achievements of the laws was the limitation of interstate commerce of samples and laboratory results. These laws also caused the proliferation of proficiency testing as a measure of the quality of a laboratory. We have since learned that proficiency testing is not a dependable way to detect inaccurate laboratory results.

The Medical Device law of 1976 produced a flurry of activity at the Food and Drug Administration (FDA) causing them to work on "reference methods" of analysis, while at the NBS, efforts were directed at development of "definitive methods." The definitive methods have been, and continue to be, successfully used and continue to be developed. These definitive methods have improved the quality of data and information that proficiency testing programs can obtain. The development of reference methods has not produced similar successes.

In the 1980's the FDA has had as one of its missions the classification and pre-market evaluation of many commercial products used in clinical laboratories. Initially, for analytical and instrumental methods of analysis, a requirement of FDA was that a new proposed method must produce results that have a high positive correlation with the previously accepted physical-chemical method of analysis. In the area of drug analysis, the accepted method was often gas or high pressure liquid chromatography, occasionally with mass spectrometry. After many months of testing, most of the original immunochemical methods presented to FDA did not meet the expected performance standards. The FDA developed a large backlog of 510(k)'s and the commercial companies discovered that by presenting their new methodology as "substantially equivalent" the approval rate increased and delay at FDA was shortened. This procedural change by the manufacturers and at FDA rapidly improved the efficiencies of handling the 510(k)'s at FDA.

Today, decentralization of clinical chemistry testing is occurring rapidly and estimates for the size of the business of home testing and doctor's office testing is at $400 million per year. Establishment and maintenance of high accuracy in these decentralized facilities are increasingly difficult to achieve.

Nerve tissue aluminum, urine cadmium, whole blood cyclosporine, serum theophylline, and serum cholesterol are five examples of analytes where methodologic difficulties and/or lack of accuracy can produce analytical results of poor quality. In the graphite furnace atomic absorption spectrometric (GFAAS) method of measuring aluminum in neuronal tissue [2] variations in the matrix, even after digestion, apparently cause inaccuracy problems [3]. In the GFAAS method of measuring cadmium in urine, the spectral interference of sodium in the sample is the most difficult matrix problem that can contribute to inaccurate results [4]. In the HPLC method of measuring whole blood cyclosporine [5], many metabolites, interferences due to hemoglobin and bilirubin, and nonreproducibility of the sample preparation steps all contribute to inaccurate results. Using immunochemical methods to measure serum theophylline creates inaccurate laboratory data when the samples are from patients that have renal failure. In the case of serum cholesterol analysis, the lower-than-desired accuracy is principally due to matrix interferences in the routine methodology used in clinical laboratories.

The above examples of inaccuracies would be much more serious but for the ways that physicians use laboratory results. If the quality of the analytical results are high then much more effort is invested in attempting to make logical decisions with that

data. If the quality of the laboratory is poor then the decision may be made to ignore the laboratory result and proceed to "care for the clinical condition of the patient." Alternately, the physician may decide to reorder the test a second time to see if a statistically different result is obtained.

Most interferences in analytical methodologies can be eliminated by a chromatographic sample preparation step prior to analysis. However, chromatographic separations are not usually automated, are poorly mechanized, and add time and expense to the analysis. In a high volume service clinical chemistry laboratory, the extra step required by a chromatographic separation is very undesirable. Therefore, today many inaccuracies remain with the routine methods used rather than adapt a cure for the accuracy problem by adding a manual chromatographic sample preparation step.

In conclusion, the development of highly accurate instrumental methods of chemical analysis for the clinical laboratory remains a very difficult task. When one includes the nonanalytical priorities in method development, then decreasing emphasis on accuracy is often accepted by members of this field. Decentralization of the service laboratory causes some additional reassessment of the criteria for test methods. A list of desired characteristics for test methodology can be created. That list of performance criteria in decreasing order of importance is: 24-hour availability of results, minimum sample pretreatment, wide selection of different types of tests, low operator skill, high precision, low total cost per analysis, short throughput time, and high accuracy.

Analytical chemistry has much to contribute to the field of clinical chemistry analysis but ways must be found to produce highly accurate test results while lowering the cost and decreasing the difficulty of the analysis. We as analytical chemists have addressed the cost issue but have not contributed much to the improvement of accuracy while simplifying the technical difficulty of the clinical laboratory tests. This last task then remains as a challenge for the near future.

References

[1] Meinke, W. W., Anal. Chem. 43, 28A (1971).
[2] Pierson, K. B., and Evenson, M. A., Anal. Chem. 58, 1744 (1986).
[3] Adan, L., Hainline, B. W., and Zackson, D. A., N. Eng. J. Med. 313, 1609 (1985).
[4] Carmack, G. D., and Evenson, M. A., Anal. Chem. 56, 907 (1979).
[5] Lensmeyer, G. L., and Fields, B. L., Clin. Chem. 31, 196 (1985).

Technical Difficulties Associated with the Formation of Carbon-11 Labelled Carboxylic Acids

Patricia Landais and Ronald Finn

National Institutes of Health
Clinical Center
Department of Nuclear Medicine
Bethesda, MD 20892

Positron Emission Tomography (PET) is an established method for probing biochemical processes in vivo and holds promise for being an established clinical tool [1–4]. PET produces cross-sectional tomographic images which monitor fundamental physiologic, biochemical and pharmacological processes such as glucose metabolism, oxygen utilization, blood flow, amino acid and fatty acid transport and metabolism, tissue receptor and drug binding characteristics. PET is similar to x-ray Computed Tomography (CT) and Magnetic Resonance Imaging (MRI) in that it is a computed tomographic technique. Unlike these clinical techniques, PET requires the injection of a positron emitting compound of particular physiologic interest. At present, the positron emitting radionuclides commonly being investigated include carbon-11 ($t_{1/2}$=20.4 m), nitrogen-13 ($t_{1/2}$=9.98 m), oxygen-15 ($t_{1/2}$=123 s) and fluorine-18 ($t_{1/2}$=109.8 m). The restrictions imposed upon the pharmaceutical chemist due to the physical half lives of these radionuclides mandate not only a sensitive, but also a rapid quality assurance program for the finished formulations. The preparation of a class of fatty acids is an excellent illustrative example of the technical difficulties and chemical subtleties associated with the research effort on short-lived radiopharmaceutical diagnostic compounds.

Biologically, long chain fatty acids are important substrates utilized to meet the myocardial energy requirements. It is theorized that PET might provide insight into changes in the utilization of these compounds as a result of therapies or organ

dysfunction caused by disease. Moreover, an added benefit of the successful synthesis of particular fatty acids is that it allows the radiopharmaceutical chemist the option of preparing other synthons, such as acid chlorides, aldehydes and alcohols.

Fatty acids labelled with radio-carbon are prepared from the corresponding organomagnesium halide. Although numerous fatty acids have been prepared utilizing this synthetic approach, few detailed reports exist. For this reason we now report our results on the preparation of (^{11}C)-cyclopropanecarboxylic acid and (^{11}C)-3,4-dimethoxybenzoic acid. These compounds are required as starting reagents for the preparation of (^{11}C)-cyclofoxy [1,2] and (^{11}C)-dopa [3,4] respectively.

Experimental

"No carrier added" (^{11}C)-carbon dioxide is produced in high radionuclidic and radiochemical purity by the ^{14}N(p, α)^{11}C nuclear reaction on a nitrogen gas target using the Japan Steel Works Limited Baby Cyclotron (BC-1710). The $^{11}CO_2$ is condensed from the nitrogen gas target stream on a vacuum line using a glass radiator trap cooled to −193 °C. Following complete removal of the nitrogen gas, the $^{11}CO_2$ is allowed to react with freshly prepared organomagnesium halide. After 2–3 minutes, the reaction is quenched by acid hydrolysis. In the experiments involving the addition of carrier, known quantities of carbon dioxide were added to the cyclotron produced product.

A catalytic concentration of 1,2 dibromoethane was used to initiate the reactions [6]. The concentration of the alkyl magnesium halide formed, with suitable correction made for non-Grignard basicity [5], was determined by acidimetric titration using CCl_4. Moreover, radio thin layer chromatography was used to establish the radiochemical purity of the synthesized fatty acid.

The chemical scheme and specific reactions leading to the products are shown in figure 1 and our analytical results are summarized in table 1.

Discussion

The reaction of Grignard reagents with radiolabelled carbon dioxide has proven to be an effective means of preparing labelled carbonyl compounds. The state of the magnesium surface has a significant impact upon the yield of the reaction and subsequent "side" reactions. It is important to use high chemical purity magnesium with a large surface area for the preparation of the organomagnesium reagent. The principal competing reactions that lead to a reduced yield of Grignard reagent are a) a coupling (Wurtz) reaction and b) a disproportionation reaction. These reactions are favored by elevated temperatures and excess halide concentration. Our experience indicates that the formation of the Grignard reagent proceeded smoothly when the alkyl bromide concentration was greater than 0.15 mol/L. The freshly prepared Grignard reagent exhibits a high chemical reactivity. Efforts to exclude oxygen, moisture and stable carbon dioxide are important to maintain the high specific activity and to minimize "side" reactions. Only freshly distilled solvents, flame-dried magnesium turnings and glassware, and an inert atmosphere are appropriate.

The radio thin layer chromatography shows that several radioactive products are formed which lead to lower chemical yield of the labelled fatty acid. These products could be the result of competing reactions resulting in ketone formation or alcohol formation from impure or excess Grignard reagent. In the preparation of "no carrier added" radiopharmaceuticals side product formation is generally limited by restricting reaction times.

In conclusion, the preparation of "no carrier added" carbon-11 labelled fatty acids is readily achievable utilizing organomagnesium compounds and carbon dioxide labelled with carbon-11; however, impure reagents and experimental conditions may reduce the concentration of the desired Grignard reagent. To find application in PET, the preparation of both radionuclidic and radiochemically pure compounds is of paramount concern. In the case of radiolabelled carboxylic acids, care must be exercised in determining the yield of Grignard reagent formation based solely upon assay of nonisolated intermediates.

Volume 93, Number 3, May-June 1988
Journal of Research of the National Bureau of Standards

Table 1. Formation yields of magnesium compounds and the corresponding carboxylic acids.

	Grignard reagent			Carboxylic acid	
	R'X	Ar-MgBr/Ar-Br	cycloPr-MgBr/cycloPr-Br	Ar-COOH	cycloPr-COOH
Experimental Yield	-	59 (32-100)*	71 (52-100)	42 (25-60)	52 (10-66)
	$BrCH_2-CH_2Br$	40 (7-76)	41 (8-71)		
	CCl_4	-	55 (42-66)		
Published Yield		-	80	95<	60-80

* The numbers in parentheses represent the extremes in our experimental results.

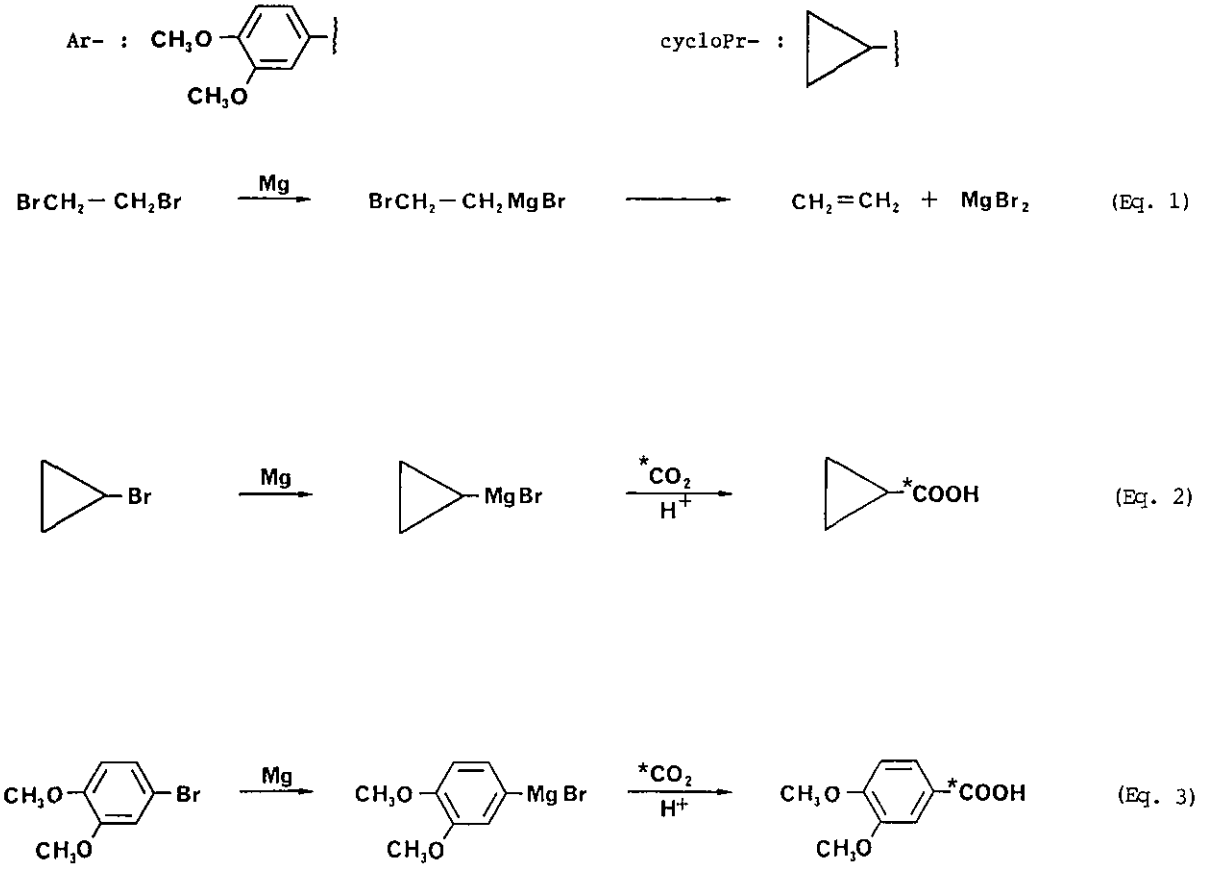

Figure 1. Activation of magnesium by entrainment eq (1) and reactions leading to the formation of radiolabelled cyclopropanecarboxylic acid eq (2) and 3,4-dimethoxybenzoic acid eq (3).

References

[1] Luthra, S. K., Pike, V. W., and Brady, F., J. Chem. Soc. Chem. Comm., 1423 (1985).
[2] McPherson, D. W. et al., J. Label Compds. Radiopharm. **23**, 505 (1986).
[3] Halldin, C., and Langstrom, B., Int. J. Appl. Radiat. Isotopes **35**, 779 (1984).
[4] Halldin, C., and Langstrom, B., Acta Chem. Scand. **B38**, 1 (1984).
[5] Vlismas, T., and Parker, R. D., J. Organometal. Chem. **10**, 193 (1967).
[6] Lai, Y. H., Synthesis **8**, 585 (1981).

The Development of Definitive Methods for Organic Serum Constituents

M. J. Welch, A. Cohen, P. Ellerbe, R. Schaffer, L. T. Sniegoski, and E. White V

Center for Analytical Chemistry
National Bureau of Standards
Gaithersburg, MD 20899

Methods in clinical chemistry must be fast, cost-effective, and relatively easy to perform. But, of more importance, they must be sufficiently accurate and precise for proper interpretation of the results by physicians. For the most common serum analytes, a variety of methods and instrumentation are used for each. These methods vary in performance and generally exhibit a bias versus each other. An accuracy base is needed to provide a means of evaluating reference and field methods and the performance of the laboratories using them. The concept of definitive methods was developed to provide such an accuracy base. The mechanism for this accuracy transfer is through serum pools with concentrations certified by definitive methods.

For a method to be considered definitive, it must be based upon sound theoretical principles, its accuracy must be tied to an absolute physical quantity, it must be thoroughly tested for sources of bias and imprecision, and it must produce results which approximate the "true value" within narrow limits.

In cooperation with the College of American Pathologists (CAP), the National Bureau of Standards (NBS) has a long-running program on development of definitive methods. Isotope dilution mass spectrometry (IDMS) is the technique of choice for definitive methods and has been used for many serum analytes, both organic and inorganic. The organic analytes for which candidate DM's have been developed at NBS include cholesterol [1], glucose [2], urea [3], uric acid [4], and creatinine [5]. These methods have been used to certify analyte concentrations in a freeze-dried human serum Standard Reference Material as well as a number of frozen and freeze-dried serum pools supplied by the Centers for Disease Control, the College of American Pathologists, and others.

Although the individual methods vary, they have several common features. All involve addition of a weighed amount of a stable isotope labeled analogue of the compound of interest to a weighed amount of serum, followed by an equilibration period. The labeled and unlabeled forms are isolated from most of the matrix, derivatized, and subjected to GC/MS measurement of the intensity ratio of an ion from the unlabeled analyte and the corresponding ion from the labeled compound. This intensity ratio is compared with intensity ratios of standard mixtures measured immediately before and after the sample measurement. With this approach relative standard deviations for independent preparations have ranged from 0.2–0.4%. Measurements made using other pairs of ions and different gas chromatography conditions are employed to assure the absence of bias in the measurements. The labeled analogue, the derivative, and the ions monitored for each analyte are listed in table 1.

Table 1. Labeled analogues, derivatives, and principal ions monitored for each analyte

Analyte	Labeled analogue	Derivative	Ions measured
Cholesterol	cholesterol-d_7	TMS ether	458,465
	cholesterol-$^{13}C_3$	"	458,461
Glucose	glucose-$^{13}C_6$	diacetonate	245,250
(2 methods)	"	butylboronate-acetate	297,302
Urea	urea-^{18}O	6-methyluracil-TMS	255,257
Uric Acid	uric acid-$^{15}N_2$	tetraethyl	280,282
(2 methods)	"	t-butyldimethylsilyl	567,569
Creatinine	creatinine-$^{13}C_2$	ethyl ester of N-(4,6-dimethyl-2-pyrimidinyl)-N-methylglycine	150,152

The technique has evolved with the field of analytical chemistry. The early methods developed for cholesterol and uric acid utilized packed column GC for sample introduction and magnetic switching between the two ions used for measurement.The peaks were broad enough to permit a sufficient number of measurement cycles across the peak for good precision. Support-coated open tubular columns (SCOT) were used for glucose, urea, and creatinine. Retention times were long to permit sufficient cycles. New methods for cholesterol and uric acid utilize fused-silica open tubular columns of high efficiency. To get sufficient measurement cycles across the narrow peaks required a different means of switching between ions. Switching by varying the accelerating voltage has never produced the necessary precision on the instrument used for this work. Instead, switching was accomplished by adding a DC voltage to the beam deflection plates located in front of the detector slit. This technique has proven to work very well over a small mass range (about 1%) with no loss of precision.

SRM 909, a freeze-dried human serum pool, has been analyzed by each of the definitive methods. These results are shown in table 2. Repeated measurements of glucose over several years have shown that glucose is unstable in this matrix. The decline in glucose concentration has averaged 0.7% per year. The other analytes are much more stable; cholesterol has shown a very small decrease over 6 years, uric acid is being measured this year, but does not appear to be significantly different. Urea and creatinine have not been remeasured, but the original certification measurements were done when the material was several years old and the material was found to be completely homogeneous from vial to vial with respect to these two analytes. We found for glucose and would expect to find for the other analytes that if they are degrading with time the vial to vial variations increase with time.

Table 2. Certified concentrations of organic analytes in SRM 909 lyophilized human serum with 99% confidence intervals

Analyte	Certified concentration mmol/L-g
Cholesterol	4.359 ± 0.017
Glucose	7.74 $^{+0.04}_{-0.15}$
Uric acid	0.570 ± 0.003
Urea	11.387 ± 0.049
Creatinine	0.1796 ± 0.0007

The new capillary column method for cholesterol has been compared to the old packed column method using SRM 909 and sera from the CAP proficiency testing program. The analyses were run about 1 year apart. The differences observed were small (<0.2%) and in both directions. The results from the new method are more precise and less likely to be biased by hidden interferences.

Future plans for the definitive method program include extending the technology to other analytes and to other matrices. The techniques developed here have been used to measure ascorbic acid in milk and cholesterol in a spiked coconut oil. For any new analytes, there must be available a high-purity well-characterized certified reference compound to tie the accuracy of the method to an absolute quantity. Planning is underway to explore the quantitative potential of isotope dilution liquid chromatography-mass spectrometry. If acceptable precision can be obtained by this technique, the range of compounds for which definitive methods are possible would be increased.

References

[1] Cohen, A., Hertz, H. S., Mandel, J., Paule, R. C., Schaffer, R., Sniegoski, L. T., Sun, T., Welch, M. J., and White, E., V, Clin. Chem. **26**, 854 (1980).
[2] White, E., V, Welch, M. J., Sun, T., Sniegoski, L. T., Schaffer, R., Hertz, H. S., and Cohen, A., Biomed. Mass Spectrom. **9**, 395 (1982).
[3] Welch, M. J., Cohen, A., Hertz, H. S., Ruegg, F. C., Schaffer, R., Sniegoski, L. T., and White, E., V, Anal. Chem. **56**, 713 (1984).
[4] Cohen, A., Hertz, H. S., Schaffer, R., Sniegoski, L. T., Welch, M. J., and White, E., V, Presented at the 27th Annual Conference on Mass Spectrometry and Allied Topics, Seattle, WA, June 3–8, 1979.
[5] Welch, M. J., Cohen, A., Hertz, H. S., Ng, K. J., Schaffer, R., Van Der Lijn, P., and White, E., V, Anal. Chem. **58**, 1681 (1986).

Volume 93, Number 3, May–June 1988
Journal of Research of the National Bureau of Standards

Recent Advances in the Analysis of PCBs and Pesticides in Human Adipose Tissue

James C. Peterson and Peter Robinson

Pacific Toxicology Laboratories
1545 Pontius Avenue
Los Angeles, CA 90025

Introduction

Due to their bioaccumulative and persistent nature, determination of PCB and organochlorine pesticide levels in human adipose tissue can be a useful biological indicator of exposure. The analytical methods previously used are relatively tedious, labor intensive and not readily amenable to automation. We have combined the use of sweep co-distillation cleanup [1] and high resolution gas chromatography with automated on-column injection to efficiently process and quantitate levels of these compounds in fat samples.

Methods

Tissue samples (200 to 500 mg) are dried with sodium sulfate and extracted three times with petroleum ether. The solvent is totally removed and the 100 to 500 mg of the remaining extracted fat is ready for cleanup by sweep co-distillation (SGE, Australia). The principle of sweep co-distillation is based on the differential volatility of fat and the organochlorine compounds of interest and utilizes a process which is similar to a preparative gas chromatograph. The rendered or extracted fat is injected directly into a heated tube filled with uncoated glass beads. The pesticides and PCBs are carried through the column by nitrogen, leaving behind the fat. The analytes are retained on a silica gel trap at the end of the glass head column and are eluted from the trap in two solvent fractions.

The first fraction is eluted with 7 mL of hexane and contains PCBs, hexachlorobenzene, mirex and a portion of the heptachlor (50%) and p,p'-DDE (30%). Fraction II is eluted with 8 mL of 20% ethyl ether in hexane and contains p,p'-DDT, p,p'-DDD, p,p'-DDE (70%), trans-nonachlor, oxychlordane, γ-chlordane, α-chlordane, heptachlor (50%), heptachlor epoxide, lindane, α-BHC, β-BHC and Dieldrin. The two fractions are reduced to 2 mL each before GC analysis. This cleanup technique allows processing of 10 samples simultaneously, requires relatively little solvent and provides very clean extracts with less than 1% residual fat. The virtually fat free extracts reduce the problem of capillary column fouling when on-column injections are made.

The use of high resolution capillary columns for the separation of PCBs and organochlorine pesticides reduces possible interferences and allows quantitation of individual PCB congeners. This is vital for the analysis of human tissue where metabolism significantly changes the pattern of PCB congeners.

Automated on-column injection (Varian Model 3500, Walnut Creek, CA) allows unattended GC operation while providing the benefits of on-column injection including superior injection reproducibility which eliminates the need for an internal standard.

PCB congeners give different electron capture responses, generally increasing with the number of chlorines. Even isomers with the same number of chlorines often have widely varying response factors. Therefore, quantitation based on the assumption of equal response for all congeners in a particular Aroclor mixture will produce inaccurate results, especially in adipose tissue, where metabolism significantly changes the pattern of PCB congeners in a mixture.

In order to determine individual congener response factors, mean weight percents for all the major PCB peaks in each Aroclor mixture were determined by first analyzing the Aroclors by GC/MS (EI). Assuming that each congener responds equally in the GC/MS, the area percents of the PCB peaks will be approximately equal to the mean weight percent for those peaks. These mean weight percents are used to calculate the amounts of individual congeners in Aroclor standards of known concentration, which, in turn, are used to calculate corresponding ECD response factors. A few of these response factors have been satisfactorily validated analyzing available pure PCB congener standards (Ultra Chemicals, Hope, RI).

A control lipid sample was prepared by spiking rendered pork lard with 1 mg/kg of Aroclor 1260 and 0.10 to 0.30 mg/kg of each of the organochlorine pesticides.

Results and Discussion

Quality assurance data collected over a 3-month period and representing 14 separate runs using the spiked lipid control (approximately once a week), indicates that this procedure produces excellent recoveries and precision (table 1). Each analyte, except for β-BHC (64%), has greater than a 78% recovery. PCBs, hexachlorobenzene and p,p'-DDE are recovered at slightly higher than 100%, most likely due to endogenous contamination in the lard used for spiking. Precision ranged from 8.3 to 13.5% relative standard deviation confirming the robust qualities of the method. Even p,p'-DDT which is the poorest performed in the sweep co-distillation process has satisfactory recoveries (78%) and precision (11.8%) indicating that p,p'-DDT breakdown is under control. Detection limits are 0.010 to 0.020 mg/kg for organochlorine pesticides and 0.050 mg/kg for PCBs.

Table 1. Recoveries and precision of PCBs and organochlorine pesticides in a spiked pork lard control (14 separate runs over a 3-month period).

Analyte	% Recovery	CV(%)
PCB (Aroclor 1260)	112	8.3
Hexachlorobenzene	105	9.1
α-BHC	93	13.5
Lindane	95	10.8
β-BHC	64	12.5
trans-Nonachlor	86	12.5
Oxychlordane	87	11.1
Heptachlor epoxide	95	10.8
γ-Chlordane	93	11.5
α-Chlordane	94	11.5
p,p'-DDE	114	12.5
p,p'-DDT	78	11.8
Dieldrin	86	12.6

Adipose tissue results from 136 analyzed human samples are presented in table 2. As evidenced by these results there are several ubiquitous analytes found in human adipose tissue. PCB levels were found in all samples analyzed and most closely resembled Aroclor 1260, with over 80% of the total congeners containing six or more chlorines. The relatively narrow concentration range of PCB, hexachlorobenzene, heptachlor epoxide, trans-nonachlor and oxychlordane residues indicates a similar exposure history to these compounds in the population.

On the other hand, Dieldrin, p,p'-DDT and its metabolite p,p'-DDE display a greater concentration variation suggesting individual differences in either exposure or metabolism. α-Chlordane, γ-chlordane and heptachlor were present in less than 1% of the individuals tested. However, their metabolites, oxychlordane and heptachlor epoxide, were always present. Similarly, lindane and α-BHC were rarely detected, but a biorefractory contaminant of technical lindane, β-BHC, was always present.

Table 2. Chlorinated hydrocarbon residues in 136 adipose tissue extracts analyzed

Analyte	Mean, mg/kg	Standard deviation	% of samples containing residues[a]
PCB	1.03	0.57	100
Hexachlorobenzene	0.048	0.027	100
β-BHC	0.087	0.061	100
Heptachlor epoxide	0.056	0.035	100
trans-Nonachlor	0.122	0.070	96
Oxychlordane	0.090	0.039	100
p,p'-DDE	1.82	1.35	100
p,p'-DDT	0.093	0.220	75
Dieldrin	0.055	0.066	98

[a] Present in less than 1%: α-chlordane, γ-chlordane, lindane, α-BHC.

References

[1] Luke, B. G., Richards, J. C., and Dawes, E. F., J. Assoc. Off. Anal. Chem. 67, 295 (1984).

Trace/Ultratrace Analyses of Unstable Compounds: Investigations on Hydrazobenzene and Azobenzene

S. Ahuja, G. Thompson, and J. Smith

Development Department
Pharmaceuticals Division
CIBA-GEIGY Corporation
Suffern, NY 10901

Trace analysis generally entails determination at parts per million (ppm) or μg/g level. Analyses performed at trace or lower levels (ultratrace) are difficult to carry out for several reasons. The difficulties relate to obtaining a representative sample, avoiding loss or contamination during sample preparation, finding a suitable method for resolving the component of interest without significant loss,

Volume 93, Number 3, May–June 1988
Journal of Research of the National Bureau of Standards

and, finally, having sufficient detectability in the range of interest to assure reliable quantitation. These problems are further compounded when one is dealing with compounds such as hydrazobenzene and azobenzene. Discussed below is a method developed to analyze these compounds which circumvents some of the problems encountered with them.

Experimental

A sample weight anticipated to contain ~10 ppm of hydrazobenzene or azobenzene is weighed accurately and shaken with 30 mL of pH 9.2 THAM buffer. This is followed by extraction with 10 mL of n-hexane. After centrifugation, 5 mL of the n-hexane layer is evaporated to dryness, at room temperature, with nitrogen and the residue is solubilized in 1.0 mL of acetonitrile. Twenty-five microliters are immediately injected into HPLC equipped with Partisil 10 μ C_8 column (25 cm×4.6 mm) and a dual channel detector (254 and 313 nm). Elution is carried out with a mobile phase composed of acetonitrile:acetate buffer, pH 4.1 (11:14). Both hydrazobenzene and azobenzene standards are treated similarly.

Results and Discussion

A review of the literature revealed that a normal phase HPLC method has been reported for the analysis of hydrazobenzene and azobenzene [1]. The method entails extraction of these compounds into n-hexane from 1*N* NaOH followed by analysis on Partisil-10 PAC column with a mobile phase containing 2.5% absolute ethanol. The published method suffers from the following shortcomings:

a. Hydrazobenzene and azobenzene show significant instability in 1*N* NaOH (table 1).
b. Azobenzene can isomerize into cis- and trans-isomers. Their separation is not demonstrated or accounted for in the method.
c. Parent compound (I) can degrade directly or indirectly into hydrazobenzene and azobenzene (fig. 1).
d. Selectivity of transformation products given in figure 1 is not demonstrated.

The properties of hydrazobenzene and azobenzene are given in figure 2. Hydrazobenzene is known to be an unstable compound, it oxidizes easily to azobenzene and other compounds and has $t_{1/2}$ of 15 minutes in wastewater [2]. Azobenzene, on the other hand, can isomerize or sublime even at 30 °C [3].

Table 1. Stability of hydrazobenzene and azobenzene

Medium	Time	%Loss Hydrazobenzene	%Loss Azobenzene
0.1*N* NaOH	30 minutes	82.9%[a]	4.6%[b]
pH 9.2 buffer	30 minutes	0.9%[c]	None found[d]

Original concentration in 10% acetonitrile:
[a] 11.8 μg hydrazobenzene/mL.
[b] 15.7 μg azobenzene/mL.
[c] 3.55 μg hydrazobenzene/mL.
[d] 2.59 μg azobenzene/mL.

To assure that the methodology would be reliable at ~10 ppm, suitable methods were developed for detecting these compounds at levels ⩽1 ppm, i.e., ultratrace levels. To further assure reliability of analyses, an effort was made to meet the following requirements for ultratrace analysis [4]:

a. Sample used for analysis was representative of the whole lot.
b. Methodology incorporated optimum separation and detection techniques.
c. Component of interest was allowed to suffer a minimum loss during various analytical operations.
d. Adequate steps were incorporated in the analytical method to account for losses that might occur due to sample preparation or degradation.

Furthermore, to assist other researchers in evaluating whether these methods could be useful for their investigations, the following analytical parameters were included:

Amount Present in Original Sample (APIOS)
Minimum Amount Detected in g (MAD)
Minimum Amount Quantitated in g (MAQ)

Investigations revealed that the optimum pH for extraction for both hydrazobenzene and azobenzene is 9.2. At this pH, these compounds can be easily extracted from the parent compound and are quite stable (table 1). The cis- and trans-isomers of azobenzene and hydrazobenzene can be resolved well with the reversed-phase HPLC method (fig. 3). Previous investigations had confirmed the selectivity of this method as it resolves compound I (t_R≃11 minutes) from other transformation products [5]. Data on spiked samples are given in table 2. An average recovery of 91% and 114% was obtained for hydrazobenzene and azobenzene respectively with relative standard deviation (R.S.D.) of

3–11%. The methods were found useful for quantitating ⩽ 1 μg of these compounds with respect to the parent compound (MAD=6–7 ng). The high recovery obtained for azobenzene is partly due to conversion of hydrazobenzene to azobenzene (~9%). Further improvements are being investigated.

Table 2. Recovery data of spiked samples. APIOS: ⩽10 μg/g of parent compound

Sample	Hydrazobenzene found	Azobenzene found
Parent compound	89.0±8.6% (n=7)	123±2.6% (n=6)
Capsules	89.6±10.8% (n=5)	98.7±10.2% (n=3)
Tablets	95.8±5.4% (n=3)	121±4.2% (n=3)
Average	91%	114%
R.S.D.	±5–11%	±3–10%
MAD (μg)	0.006 (6 ng)	0.007 (7 ng)
MAQ (μg/g)	<1	<1

Conclusions

1. Selective methods have been developed for analysis of hydrazobenzene and azobenzene.

2. The instability of hydrazobenzene in aqueous and organic solvents is well known. This problem has been effectively dealt with in that an average recovery of 91% was obtained for the active ingredient, capsules and tablets.

3. It was found that azobenzene is susceptible to isomerization and sublimation. The developed procedure provides an average recovery of 114% for the active ingredient, capsules and tablets. The high values are partly due to conversion of hydrazobenzene to azobenzene (~9%).

4. The developed methods provide reliable values (3–11% R.S.D.) for hydrazobenzene and azobenzene at a concentration of ⩽10 μg/g (⩽10 ppm) in terms of the parent compound.

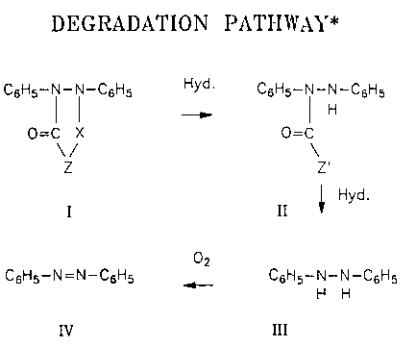

*S. Ahuja, 'Discovery of New Compounds by Thin-Layer Chromatography', *Techniques and Applications Of TLC*, J. Touchstone, Ed., Wiley, 1985

Figure 1. Degradation pathway of parent compound.

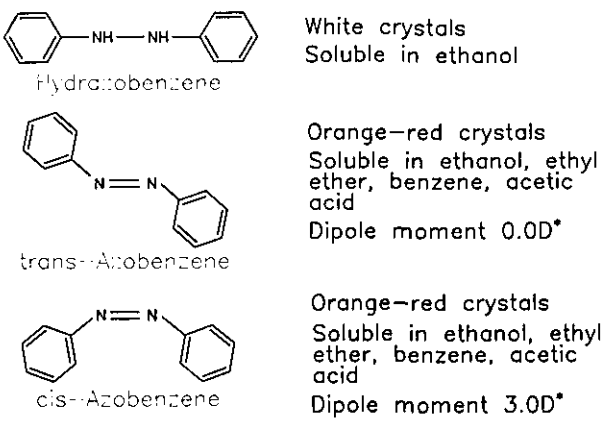

Properties: Weast, R. C., *Handbook of Chemistry and Physics*, C.R.C. Press, Inc., New York, p. C-91, -314, 1985.
* Jannsen, J., *J. Chem. Ed.* 46, 117, 1969.

Figure 2. Physical properties of hydrazobenzene and azobenzene.

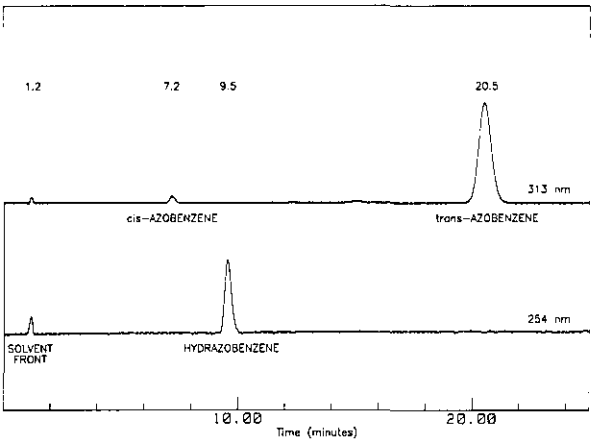

Figure 3. Chromatograms of azobenzene (cis- and trans-) and hydrazobenzene (0.05 μg of each compound injected and monitored at 313 nm and 254 nm).

References

[1] Matsui, F., Lovering, E. G., Curran, N. M., and Watson, J. R., J. Pharm. Sci. 72, 1223 (1983).
[2] Riggin, R. M., and Howard, C. C., Anal. Chem. 51, 210 (1979).
[3] Weast, R. C., Handbook of Chemistry and Physics, C. R. C. Press, Inc., Boca Raton, p. C664 (1985).
[4] Ahuja, S., Ultratrace Analysis of Pharmaceuticals and Other Compounds of Interest, John Wiley and Sons, Inc., New York, p. 1 (1986).
[5] Ahuja, S., Shiromani, S., Thompson, G., and Smith, J., Personal Communication, March 2, 1984.

Volume 93, Number 3, May–June 1988
Journal of Research of the National Bureau of Standards

Nutrient Analysis

Trace Element Speciation in Food: A Combined Enzymolysis—SEC-ICP-MS Approach

H. M. Crews, R. Massey, and D. J. McWeeny

Ministry of Agriculture
Fisheries and Food
Norwich, U.K.

and

J. R. Dean

The Polytechnic
Plymouth, U.K.

Trace elements in food can be either desirable, tolerable or undesirable. They occur in the diet as natural constituents of agricultural produce, as deliberate additives and as contaminants from environmental and processing sources. Historically, their significance to man has been assessed on the basis of total concentration of the element in the food item—or the total amount in the diet as a whole (with the exception of the measurement of mercury and to a lesser extent arsenic where specific forms are sometimes measured). In recent years the inadequacy of simply measuring the total concentration has been increasingly appreciated and efforts to provide information which is targeted more accurately to the needs of the nutritionist and the toxicologist are now being made.

Over the last few years, the MAFF Food Science Laboratory has had a small programme investigating ways of obtaining more meaningful information about the chemical forms of trace elements in food. As a first stage of a general approach to the problem, attention has been restricted to species which are soluble at around neutral pH after treatment with normal monogastric mammalian digestive enzymes. A procedure has been developed in which food is treated sequentially with pepsin at around pH 2 and with pancreatic enzymes at around pH 7 at 37 °C. A limitation of this procedure is that it is a "static" system, whereas absorption is dynamic; if there is equilibrium between soluble and insoluble species, the system will underestimate the amount which is potentially available biologically.

In some very simple experiments, food composites representing the cereal, meat, fish and green vegetable components of the UK diet were examined with and without the addition of small amounts of copper, zinc, cadmium and lead as inorganic salts. The properties of the endogenous element which was soluble after enzyme treatment has been compared with that of the added element. For all the foods studied, endogenous and added copper behaved similarly, but there were marked differences for some of the other elements. For instance, zinc from fish is largely insoluble, and added zinc also becomes insoluble; other foods release much zinc in soluble form. On the other hand, iron from meat is largely soluble but added iron becomes insoluble [1].

This investigation has been developed further in studies of the effect of one food upon the release of trace elements from another. The amount of acid-soluble cadmium available from crab meat is reduced by 75% by digesting it along with wholemeal bread; white bread has very little effect. Similar experiments show that addition of 10% soya to ground beef gives a much lower release of zinc from the beef—presumably a soya phytate effect. Processing of beef can affect the solubility of iron; inorganic iron as taken in dietary supplements is much more soluble if digested along with cereals and vegetables than with meat and fish [2].

The broad conclusions of these experiments were that: a) acidity enhances solubility, b) enzyme action changes solubility, c) processing can affect solubility, and d) presence of other foods can affect solubility. Even where an element was soluble, there were indications of changes in chemical form as a result of enzyme action, processing or the presence of other foods.

In devising an investigation of these changes, the criteria were that it should be, i) with foods containing levels of toxic elements typical of those in the normal food supply; ii) with systems which,

so far as possible, did not alter the chemical form of the element naturally present. The first point created problems, i.e., natural levels are close to the limits of reliable determination by atomic absorption spectrometry; dilution occurring on enzymolysis and separation of species produced nonmeasurable levels. One solution to this problem lies in the high sensitivity of ICP-MS [3] and the ability to use ICP-MS as a detector with LC columns.

Particular attention has been paid to steric exclusion chromatography as one of the most gentle forms of separation achievable. It is also a relevant separation of soluble macro molecules (which are unlikely to be absorbed) from lower molecular weight species which are more likely candidates for absorption. Additionally, some work with reversed-phase HPLC linked to ICP-MS has also been carried out.

With HPLC systems a guard column is used to protect the analytical column; post-column injections of standards are used for calibration checks. To minimize peak-broadening, aerosol transfer distance should be reduced by mounting the nebulizer system close to the torch. Flow rates above 0.5 to 0.7 mL/min can lead to signal instability unless precautions against condensation are taken. In an early piece of work, the cadmium content of crab meat with separation by HPLC and monitoring by UV and ICP-MS showed that the major protein peak has almost completely eluted before the cadmium peak corresponding to a somewhat lower molecular weight cadmium-containing protein.

More recent studies of the HPLC separation of the proteins from pig kidney before and after cooking show that in the raw state there are three peaks—the higher molecular weight materials disappear during cooking, i.e., are rendered insoluble by heat denaturation, whereas the heat-resistant metallothionein remains intact.

Another recent study concerns an organo-arsenical drug used in poultry production. In this, reversed-phase HPLC has been linked to the ICP-MS in much the same way for HPLC. This system allows good separation of "Roxarsone" from other low molecular weight substances and from interference from molecular ions formed from argon in the plasma in the presence of chloride ion.

Arsenic in extracts from muscle of chickens fed on a base diet and one supplemented with "Roxarsone" have been compared. The "Roxarsone" peaks correspond to arsenic concentrations of 7 and 10 ng/g in the muscles from treated birds and demonstrates that in the untreated birds the concentration is less than 2 ng/g.

The sensitivity foreseen with these systems is now a matter of reality rather than potential—and the ability to use it in speciation studies at tissue concentrations at the ng/g level is a matter of fact rather than of speculation.

References

[1] Crews, H. M., Burrell, J. A., and McWeeny, D. J., J. Sci. Food Agric. **34**, 997 (1983).
[2] Crews, H. M., Burrell, J. A., and McWeeny, D. J., Z. Lebensm. Unters Forsch. **180**, 405 (1985).
[3] Dean, J. R., Ebdon, L., and Massey, R., J. Anal. Atomic Spectrosc. **2**, 369 (1987).

Trace Element Determinations in Biologicals Using Atomic Absorption Spectrometry

Nancy J. Miller-Ihli

U.S. Department of Agriculture
Nutrient Composition Laboratory
Beltsville, MD 20705

Atomic absorption spectrometry (AAS) has been used for many years for trace element determinations in foods and other biological materials. The Nutrient Composition Laboratory of the U.S. Department of Agriculture has both conventional commercial single element AAS Spectrometers (Perkin-Elmer Models 603 (flame) and 3030 (Zeeman, furnace)) and a multielement AAS research spectrometer (SIMAAC) [1] which can provide multielement data using either flame or graphite furnace atomization [2–3]. The SIMAAC system consists of a 300 watt xenon arc lamp, an atomizer, an echelle polychromator modified for wavelength modulation, and a PDP 11/34 minicomputer responsible for high-speed data acquisition, data processing and report generation. The SIMAAC system can simultaneously determine up to 16 elements including: Al, Ca, Co, Cr, Cu, Fe, K, Mg, Mn, Mo, Na, Ni, Pb, Sn, V, and Zn. The extended range [4] provided by the system permits simultaneous measurement of elements whose concentrations may vary by as much as 4 orders of magni-

tude of concentration. The SIMAAC system has been used for a wide range of applications but the maximum potential of multielement AAS can be seen using graphite furnace atomization (GFAAS) [7–9] where sub-ng/mL detection limits can be achieved using μL-sized samples.

Successful single element or multielement AAS determinations cannot be achieved without suitable sample preparation procedures. As a result, research has been conducted to evaluate the following sample preparation procedures: 1) wet ashing; 2) dry ashing; 3) microwave dissolution; and 4) direct analysis of solids.

Wet Ashing

Wet ash sample preparation procedures are versatile and offer several advantages. First, wet ash procedures are applicable to a wide range of materials and suitable for all foodstuffs. Second, wet ash procedures are low temperature preparations and therefore provide reduced risk of loss of volatile elements. Third, high purity reagents are available for wet ash preparations and finally wet ash preparations are not labor intensive. Typically large batches of samples can be easily handled using a heating block or hot plates. A typical wet ash procedure appears in table 1. Basically, this is a HNO_3/H_2O_2 digestion done using ultrapure reagents (sub-boiling distilled HNO_3, National Bureau of Standards, Gaithersburg, MD; Perone Peroxide, DuPont, Wilmington, DE) and silanized quartz test tubes to prevent contamination. Typical wet ashing results for NBS SRM 1577a Bovine Liver and NBS SRM 1572 Citrus Leaves appear in tables 2 and 3. The average accuracy for the simultaneous multielement determination of these four elements was 100±9% and the average precision was 10% RSD.

Table 1. Wet ash digestion procedure

1. Weigh homogenized sample (0.5–1.0 g) into a silanized quartz test tube and add 2 mL 18 megohm water
2. Add 0.5–1.0 mL sub-boiling distilled nitric acid and heat samples (80 °C) overnight
3. Add 1 mL ultrapure hydrogen peroxide, repeating until samples are clear
4. Allow samples to go to dryness
5. Dilute to a final volume of 5–15 mL

Table 2. SIMAAC GFAAS results for wet ashed bovine liver[a] (μg/g, dry weight)

Element	Soln. conc. (ng/mL)	Certified value	SIMAAC value
Pb	30	0.34±0.08[b]	0.30±0.02[c]
Cr	10	0.088±0.012	0.099±0.009
Co	20	(0.18)	0.17±0.03
Mo	380	(3.4)	3.6±0.3

[a] Sample 1 g/10 mL.
[b] Values=95% confidence level.
[c] Values=1σ, n=6.

Table 3. SIMAAC GFAAS results for wet ashed citrus leaves (μg/g, dry weight)

Element	Soln. conc. (ng/mL)	Certified value	SIMAAC value
Mn	28[a]	23±2[c]	20±2[d]
Zn	38[a]	29±2	32±2
Cu	19[a]	16.5±1.0	15.5±0.7
Pb	18[b]	13.3±2.4	14.8±2.9
Cr	120[b]	0.8±0.2	1.0±0.1
Mo	23[b]	0.17±0.09	0.19±0.05

[a] Sample 0.6 g/500 mL.
[b] Sample 0.6 g/5 mL.
[c] Values=95% confidence levels.
[d] Values=1σ, n=6.

Dry Ashing

Dry ashing also offers several advantages as a sample preparation procedure. Dry ashing requires very few reagents, utilizes simple apparatus, requires little sample manipulation and is excellent for biological fluids. Dry ashing also shares the benefit of requiring minimal operator attention so it lends itself well to large "batch" preparations of samples. Table 4 contains a typical dry ash procedure using serum as an example. This procedure provides an optional 4-fold concentration step. Data for NBS SRM urine prepared using this procedure without the 4-fold concentration step appear in table 5. The average accuracy for the five elements determined simultaneously was 100±6% and the average precision was 9% RSD.

Table 4. Dry ash digestion procedure

1. Pipet 2 mL of urine into a silanized quartz test tube
2. Add 20 μL of 2% magnesium nitrate and vortex
3. Dry samples (or freeze and freeze-dry)
4. Place samples in muffle furnace and heat: 100 °C 1 h; 150 °C 1 h; 200 °C 1 h; 250 °C 1 h; 480 °C overnight
5. Dissolve ashed urine in 2 mL 5% sub-boiling distilled nitric acid

Microwave Dissolution

Microwave dissolution was evaluated because of its significant time savings and potential to provide lower blanks. The closed vessel procedure evaluated provides elevated temperatures and pressures leading to more complete digestions than can be attained using conventional preparation procedures. Microwave procedures also provide the ability to use reproducible conditions making sample dissolution less of an art and more of a science. The microwave digestion procedure utilized was based on the method of Kingston and Jassie [7] (see table 6). Equipment used consisted of an MDS 81 600 watt microwave oven (CEM Corp., Indian Trail, NC) equipped with a turntable and 60 mL teflon PFA vessels with relief valves (Savillex Corp., Minnetonka, MN). Analytical data for NBS SRM 1567 Wheat Flour appear in table 7 and data for an in-house tuna quality control material are summarized in table 8. Reference values for the tuna are based on analytical results obtained using conventional wet and dry ashing preparations and atomic absorption and emission methods. Both sets of data indicate that the microwave method provides suitable results (Wheat Flour: Average accuracy 100±7%, average precision 9% RSD).

Table 5. SIMAAC GFAAS results for dry ashed SRM urine (ng/mL)

Element[a]	Certified value	SIMAAC value
Cu	370±30[b]	331±33[c]
Pb	109±4	98±12
Cr	85±6	86±7
Ni	(300)	294±23
Cd	88±3	84±6

[a] 2 mL urine dry ashed and diluted to 2 mL (5% HNO_3).
[b] Values=95% confidence levels.
[c] Values= 1σ, n=5.

Table 6. Microwave preparation procedure[a]

1. Weigh 0.15–0.20 g material into teflon PFA vessel
2. Add 5 mL of sub-boiling distilled HNO_3 and seal vessels
3. Place samples on turntable and digest individually (25% power; 8 minutes)
4. Cool vessels and remove cap
5. Rinse cap with deionized distilled water
6. Place uncapped vessel on hot plate (130 °C) and heat (approx. 30 minutes)
7. Dilute to final volume (10 mL)

[a] Adapted from: Kingston, H. M. and Jassie, L. B., Anal. Chem. **58**, 2534 (1986).

Table 7. Results for microwave preparation of NBS wheat flour (μg/g, dry weight)

Element	Certified value	Flame AAS value
Mn	8.5±0.5[a]	7.7±0.5[b]
Zn	10.6±1.0	11.2±0.2
Fe	18.3±1.0	18.4±3.3
Cu	2.0±0.3	1.7±0.3
K	1360.±40.	1260.±29.

[a] Values=95% confidence level.
[b] Values= 1σ, n=6.

Table 8. Results for microwave preparation of tuna (μg/g, dry weight)

Element	Reference value	Flame AAS value
Mn	0.43±0.08[a]	0.64±0.08[b]
Zn	13.5±0.6	13.9±0.8
Fe	30.9±1.7	32.8±1.3
Cu	1.27±0.25	1.18±0.03
Mg	1076.±59	964.±8
Na	15,976.±793	16,367.±844
K	9,113.±425	8,238.±110

[a] Values=95% confidence level.
[b] Values= 1σ, n=6.

Direct Solids Analysis

The direct analysis of solids in the graphite furnace appears to be the ultimate solution to sample preparation problems related to contamination control and preparation time. Research has been conducted using slurry preparations of a wide range of materials [8]. Slurry preparations offer several advantages over conventional wet ashing and dry ashing procedures: 1) reduced sample

preparation time, 2) decreased possibility of analyte loss through premature volatilization, 3) reduced loss of analyte related to retention by insoluble residue, and 4) reduced opportunity for sample contamination. Slurry preparations also offer advantages over direct analysis of solids. First, slurries can be easily prepared and no special tools are required. In addition, any amount of the original powdered sample can be used and samples can be diluted if necessary. Finally, samples can be prepared in advance and handled easily. Slurries are typically prepared by weighing ~10 mg of finely powdered homogeneous material into a clean polypropylene tube and then diluting with 5–10 mL of 5% HNO_3 containing 0.04% Triton X-100. Slurries are mixed well on a vortex mixer and while mixing, a 1 mL aliquot is removed and placed into an acid soaked teflon autosampler cup. Slurries are then mixed using an ultrasonic probe (RAI, Hauppauge, NY) until the autosampler withdraws an aliquot for injection into the graphite furnace. Table 9 contains analytical data from the analysis of NBS SRM Citrus Leaves and SRM 1572. Table 10 contains results for NBS SRM 1632a Coal. Average accuracies were: 100±10% (Citrus Leaves); 100±14% (Coal) and average precisions were: 11% RSD (Citrus Leaves); 6% RSD (Coal). These and similar data for more than 12 materials suggest that the slurry technique is well suited to the analysis of homogeneous powdered biological and botanical materials.

Table 9. SIMAAC GFAAS results for slurry preparations of NBS citrus leaves SRM 1572 (μg/g, dry weight)

Element	Certified value	SIMAAC value
Mn	23±2[a]	19±1[b]
Zn	29±2	33±4
Fe	90±10	90±15
Cu	16.5±1.0	16.1±1.0
Pb	13.3±2.4	15.3±2.5
Al	92±15	80±18

[a] Values=95% confidence level.
[b] Values=1σ, n=5.

Table 10. SIMAAC GFAAS results for slurry preparations of NBS coal SRM 1632a (μg/g, dry weight)

Element	Certified value	SIMAAC value
Mn	28±2[a]	23±2[b]
Fe	11,100±200	12,100±1500
Cu	16.5±1.0	14.0±4.3
Cr	34.4±1.5	26.4±2.5
V	44±3	46±7

[a] Values=95% confidence level.
[b] Values=1σ, n=5

Comparison of Methods

NBS SRM 1577a Bovine Liver was prepared in duplicate using each of the four methods discussed. Analytical results appear in table 11 with the amount of time each preparation procedure required under routine operating conditions in our laboratory. It is clear that all sample preparation methods provided accurate analytical data for the four elements determined. The microwave and slurry preparation procedures offered significant time savings over the wet ashing and dry ashing methods which were performed in the typical batch mode of operation routinely employed in the lab. Presumably, the times for wet ashing and dry ashing could be reduced somewhat but, it is clear that the microwave and slurry methods offer significant advantages with regard to sample contamination as well as speed. Additional work is needed to ascertain whether these two faster methods are well suited for as wide a range of sample matrices as conventional wet ashing and dry ashing preparation procedures are.

Table 11. Comparison of methods (bovine liver, SRM 1577a)

Method	Mean concentration (μg/g)				Total time
	Mn	Zn	Fe	Cu	
Wet Ashing	10.9	125	184	159	36 h
Dry Ashing	9.7	120	190	153	24 h
Microwave	9.7	120	198	154	45 min
Slurry	10.9	131	210	153	5 min
Cert. Values:	9.9±0.8	123±8	194±20	158±7.	

Acknowledgments

I would like to thank F. E. Greene for her assistance with this project and H. M. Kingston for his technical input on the microwave dissolution work.

References

[1] Harnly, J. M., O'Haver, T. C., Golden, B., and Wolf, W. R., Anal. Chem. **51**, 2007 (1979).
[2] Miller-Ihli, N. J., Anal. Chem. **57**, 2892 (1985).
[3] Harnly, J. M., Miller-Ihli, N. J., and O'Haver, T. C., Spectrochim. Acta **39B**, 305 (1984).
[4] Harnly, J. M., and O'Haver, T. C., Anal. Chem. **53**, 1291 (1981).
[5] Kingston, H. M., and Jassie, L. B., Anal. Chem. **58**, 2534 (1986).
[6] Miller-Ihli, N. J., J. Anal. At. Spectrom., in press.

Reliable Measurement of Major, Minor, and Trace Elemental Nutrients

Milan Ihnat

Land Resource Research Centre
Agriculture Canada
Ottawa, Ontario K1A OC6, Canada

1. Introduction

A number of major, minor, and trace elements function as important nutrients in foodstuffs of crop and animal origin. These elements occur in a broad range of concentrations in an exceedingly vast array of foods available commercially and home-prepared. In disciplines such as regulatory compliance, product development, quality and safety, and research, reasonably reliable analytical information is mandatory for conclusions and decisions of impact. Although analytical scientists recognize the need for valid data, solid analytical information is at times elusive not only in the area of determination of chemical elements at low (trace) levels [1–5] but also when present as major constituents [6,7].

Of the many analytical techniques available for determination of inorganic nutrient constituents in biological matrices, those based on atomic spectrometry (AAS) are convenient and widely applied. The thrust of current research is to define impacts of a number of parameters on the performance of flame AAS (FAAS)-based methods of analysis of soil and biological materials to lead to reference methods for the measurement of major, minor and trace levels of elements of nutritional and toxicological pertinence. Some of these parameters as well as the excellent performance possible with well-applied versions of FAAS procedures are discussed.

2. High Reliability Flame Atomic Absorption Spectrometry

In spite of wide acceptance of the technique and the proliferation of published articles on its application, very few AAS-based methods have reached official method or reference method status [8]. Requirements for analytical data of the highest reliability (high precision and accuracy) in the author's research dealing with levels of elemental nutrients and toxicants in soils and biological tissues and with official and reference versions of procedures based on AAS have led to detailed investigations of a number of parameters bearing on method performance. Of the parameters listed in table 1, those

Table 1. Some factors bearing on the reliable application of acid decomposition-flame atomic absorption spectrometry to the determination of major, minor and trace elements in biological materials

Sample decomposition and solution preparation
Volumetric ware verification, calibration, operational technique
Sample drying and/or moisture determination
Volatilization or retention losses in dry ashing or wet decomposition
Incomplete destruction of matrix; recovery and analysis of insoluble residue
Contamination from ashing acids, acids and vessels
Procedural and standard reagent blanks, non-identical performance of method with pure reagents and samples
Standard solutions, materials and preparative techniques
Sample and standard solution dilution schemes
Spectrometric measurement
Instrument optimization, performance characteristics and operational techniques
Physical and chemical interferences
Non-atomic absorption
Calibration solutions (single analyte, composite or matrix-matched)
Calibration technique (calibration curve, bracketting)
Data handling and interpretation
Recording, data entry and calculation
Calibration curve fitting and calculation techniques
Interpretation and evaluation (controls, statistical treatment, data presentation basis)
Overall
Analyst, specialist training and experience
Data quality control (accuracy verification by recovery testing and performance with appropriate reference materials)

studied thus far include sample decomposition, solution preparation, standard solution preparation, calibration approaches, instrumental parameters and measurement protocols.

Experiments were conducted with four plant Standard Reference Materials as test materials, SRM 1570 Spinach, SRM 1571 Orchard Leaves, SRM 1573 Tomato Leaves, and SRM 1572 Citrus Leaves, from the National Bureau of Standards with the last product uncertified at the time of the study. Samples were dissolved with $HNO_3/HClO_4$ with further separate treatment of insoluble siliceous residues with HF for measurement of total concentrations of Na, K, Mg, Ca, Mn, Fe, Cu and Zn. Flame atomic absorption measurements were performed under optimized standard operating conditions. Measurement techniques were based on either bracketting of sample with appropriate standard solutions or second order calibration curves incorporating appropriate standard and procedural reagent blanks. Two types of working standard solutions were prepared with one set (regular standard) containing the eight analytes at concentrations required for analysis. The second set (matrix-matched) contained the analytes at approximate concentrations occurring in the plant materials being analyzed and, in addition, contained three other major constituents, Al, S and P present in the samples to match the analytes and matrices of the analytical samples. The scheme of analysis is depicted in figure 1.

Development and application of a high reliability version of an analytical procedure requires familiarity with all factors having a possible bearing on the precision and systematic errors of the overall procedure. The effect of calibration expressed as differences in elemental concentrations measured using regular and matrix-matched standard solutions is a function of element and sample type. Differences in concentrations ranged from 0.2% to 10.2% depending on element and matrix, indicating that for measurements of the highest reliability, systematic error arising from calibration can be reduced by using reasonable close matrix-matched standard solutions [9]. Effects of the two sample decomposition procedures leading to acid-soluble and total concentrations showed that error in analytical data, without considering any contribution from the residue, ranged from 0.04% for Mg in spinach to 42% for Na in orchard leaves for the three materials certified at the time of the study [9,10]. For high reliability analysis, decomposition technique must be assessed and contributions of residues must be incorporated either by separate decompositions or one step procedures [10,11].

That meticulous attention to detail can lead to a high precision and high accuracy procedure is demonstrated by information in tables 2 and 3, and figure 2. Figure 2, depicting concentrations of eight elements in spinach determined by FAAS as a function of subsample, shows generally a tight scatter about the means. The means are compared in table 2 with certified values issued by NBS with excellent agreement evident among the two sets of data. A more striking demonstration of FAAS method performance in this work is provided by comparison (table 3) of results by this method with those from several other diverse methods of analysis applied during the certification work of NBS Citrus Leaves. Outstanding agreement can be observed between FAAS-generated data and those for other methods including INAA which importantly does not involve sample decomposition. Analytical results from this FAAS work were obtained before knowledge of the composition of the Citrus Leaves and in fact the data were used by NBS in the certification exercise. It is thus evident that consideration of appropriate details and careful work can lead to a truly high fidelity analytical procedure based on flame atomic spectrometry.

Table 2. Concentrations of elements in NBS Spinach SRM 1570 determined by application of acid decomposition-flame atomic absorption spectrometry

Element	Total concentration, μg/g	
	This work ±SE[a]	Certified value
Na	1.504±0.005%	–
K	3.601±0.014%	3.56±0.03%[b,c]
Mg	8620±21	–
Ca	1.329±0.007%	1.35±0.03%[b,c]
Mn	173.3±0.5	165±6[c]
Fe	549±3	550±20[c]
Cu	12.1±0.1	12±2[c]
Zn	50.7±0.4	50±2[c]

[a] Typically 9 analyses; SE=standard error; SD=standard deviation.

[b] Values in weight percent.

[c] Uncertainty includes method imprecision, material inhomogeneity of entire SRM lot, and estimates of possible bias.

Table 3. Performance of high-precision, high-accuracy acid-decomposition flame atomic absorption spectrometry. Comparison with other methodologies/analysts for measurement of major and trace elements in Standard Reference Material 1572, Citrus Leaves

Method[a]	Concentration μg/g (mean±standard deviation)			
	K	Ca	Mn	Fe
FAAS	18140±160	31730±170	22.62±0.16	90.7±3.4
INAA	–	31710±60	22.6±0.14	89.3±4.3
				91.7±0.8
IDMS	18180±70	–	–	–
FES	18230±100	30400±840	–	–
		31000±3000		
ICPAES	–	31600±400	22.1±1.1	90.1±3.7
POLAR	–	–	–	95.2±1.2
NBS	18200±600[b]	31500±1000[b]	23±2[b]	90±10[b]

[a] FAAS : Flame atomic absorption spectrometry (this work)
INAA : Instrumental neutron activation analysis
IDMS : Isotope dilution mass spectrometry
FES : Flame or plasma emission spectrometry
ICPAES: ICP atomic emission spectrometry
POLAR : Polarography
NBS : Certified values established by NBS after analyses completed.
[b] Uncertainties of NBS data are 95%/95% statistical tolerance intervals or based on judgment.

Acknowledgments

The assistance of R. J. Westerby with flame spectrometric measurements is appreciated. R. Alvarez (NBS) kindly made available analytical information for citrus leaves.

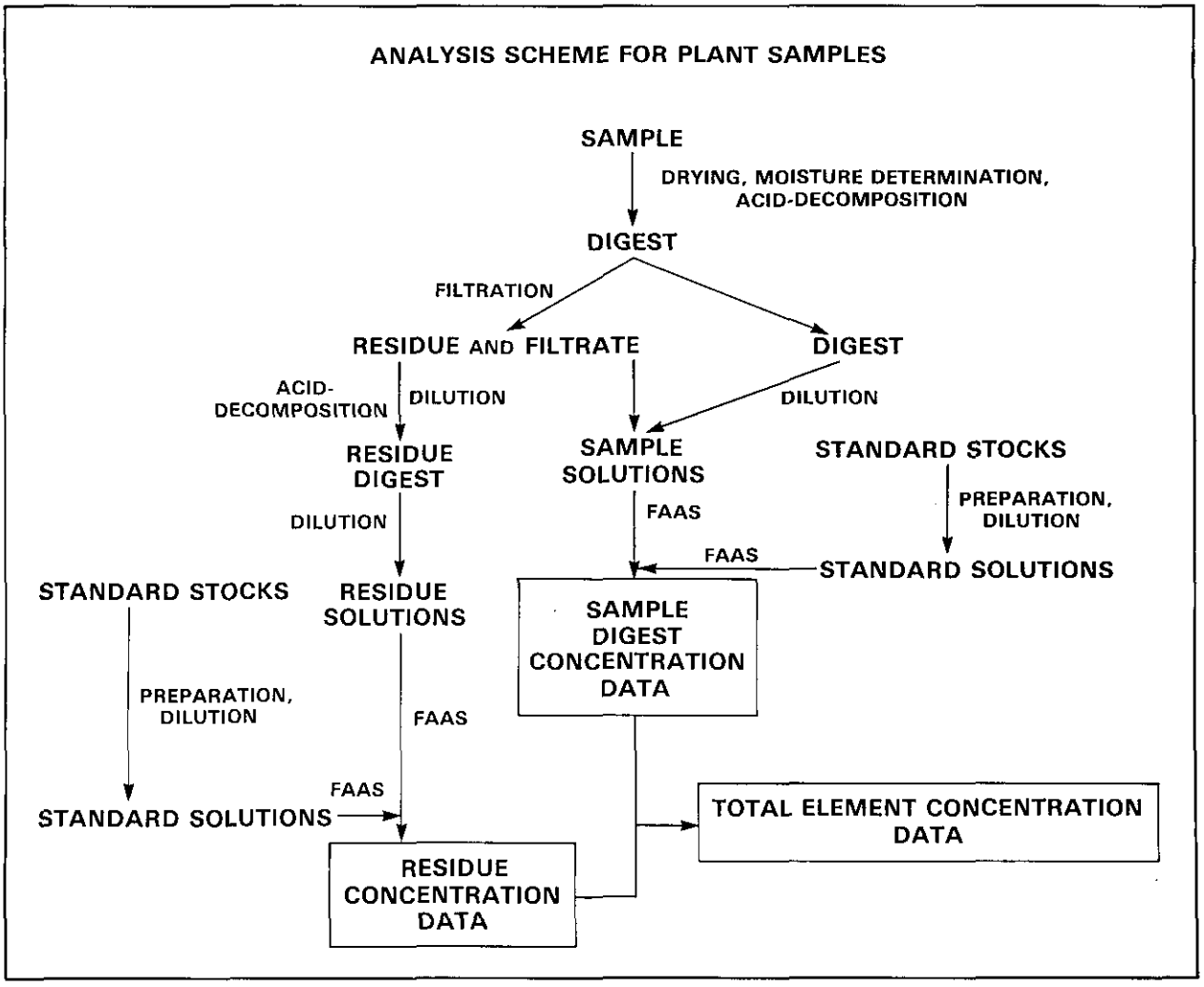

Figure 1. Scheme of analysis of plant samples by acid decomposition. Flame atomic absorption spectrometry for the determination of total elemental concentrations.

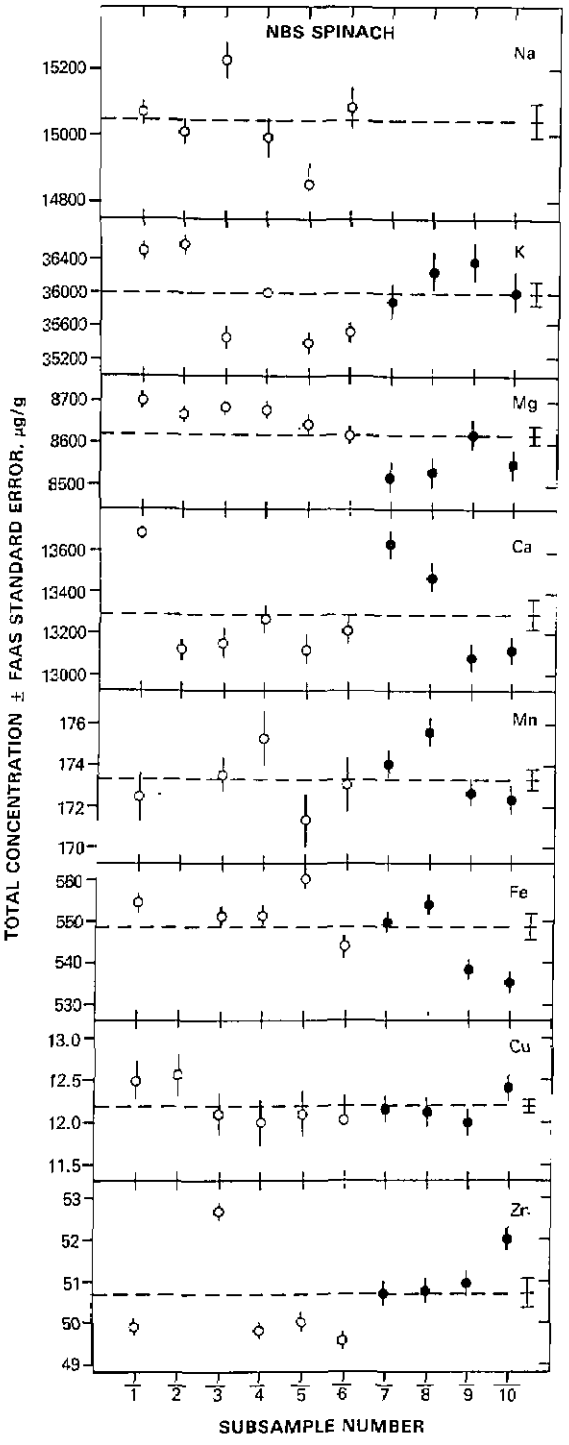

Figure 2. Total concentrations, with associated standard errors from the flame atomic absorption spectrometric step, of several major and minor elements in NBS SRM 1570 Spinach, as a function of subsample. Open and closed data points depict unfiltered and filtered solutions, respectively, used to measure acid-soluble concentrations; the data at extreme right are overall means ± standard error.

References

[1] Keppler, J. F., Maxfield, M. E., Moss, W. D., Tietjen, G., and Linch, A. L., Amer. Ind. Hyg. Assoc. J. **31**, 412 (1970).
[2] Hume, D. N., Fundamental Problems in Oceanographic Analysis, T. R. P. Gibb, Jr., (ed.), in Analytical Methods in Oceanography. Adv. Chem. Series 147, pp. 1–8, American Chemical Society, Washington, DC (1975).
[3] Parr, R. M., J. Radioanal. Chem. **39**, 421 (1977).
[4] Fukai, R., Oregioni, B., and Vas, D., Oceanologica Acta **1**, 391 (1978).
[5] Versieck, J., Trace Elements Medicine **1**, 2 (1984).
[6] Ihnat, M., Data Validity in Analytical Chemistry, in Proceedings Tenth National Shellfish Sanitation Workshop, Wilt, D. S., ed., pp. 95–105, Washington, DC, U.S. Department of Health, Education and Welfare Publication (FDA) 78-2098 (1979).
[7] Brown, S. S., Healy, M. J. R., and Kearns, M., J. Clin. Chem. Clin. Biochem. **19**, 395 (1981).
[8] Ihnat, M., Applications of Atomic Absorption Spectrometry to the Analysis of Foodstuffs, in Atomic Absorption Spectrometry, Cantle, J. F., ed., pp. 139–210, Elsevier, Amsterdam (1982).
[9] Ihnat, M., Fres. Z. Anal. Chem. **326**, 739 (1987).
[10] Ihnat, M., Commun. Soil Sci. Plant Anal. **13**, 969 (1982).
[11] Rains, T. C., NBS Spec. Publ. 492, Mavrodineanu, R., ed., Sec. 4., Washington, DC (1977).

ICP-AES: A Realistic Assessment of Its Capabilities for Food Analysis

J. W. Jones

Center for Food Safety and Applied Nutrition
U.S. Food and Drug Administration
Washington, DC 20204

Accurate determination of trace elements in foods is a formidable challenge for even the most capable analyst. The complex and disparate matrices of foods, coupled with the often very low concentrations of nutritive or toxic elements, combine to push the capabilities of existing trace element analytical methods to their limits.

Inductively coupled plasma atomic emission spectrometry (ICP-AES) is now a widely used technique for food analysis. Na, P, Ca, Mg, Fe, Zn, Cu, Mn and Sr can be readily determined in most foods by ICP-AES. However, several other important elements such as Al, Mo, Ni, Cr, Pb, Se, As, Cd, Co, V and Hg cannot be easily determined in most foods by ICP-AES unless extensive chemical procedures are used to concentrate these elements

to quantifiable levels in the analytical test solution, and to remove potentially interfering elements. Further, even with preliminary chemical separations of analytes from any given matrix, significant spectral interferences may remain, necessitating extreme care during the ICP-AES determination.

The U.S. Food and Drug Administration conducts a continuous nationwide monitoring program to estimate the dietary intake of selected food contaminants (including toxic elements) and nutritive elements. In this Total Diet Study representing the typical U.S. diets, 234 food types are prepared (e.g., peeled, cooked) as for consumption. The foods range in matrix complexity from drinking water to beef stew or chocolate cake. These 234 foods encompass the full range of "difficult" food types usually encountered in a food analysis laboratory. We have analyzed all of these foods for many of the elements above using ICP-AES to: a) estimate the approximate concentration ranges of the elements; and b) assess the capability of ICP-AES for accurate determination of some of the more difficult to determine elements such as V and Co.

During this project, we noted many problems with acid digestion procedures, separation chemistry, and the ICP-AES determinative step, all of which could adversely affect the accuracy of our determinations. Appropriate test portion sizes which are sufficient to provide enough analyte mass to quantify, but which also can be accommodated safely by the digestion procedure (nitric, perchloric, sulfuric acids) must be selected. Compatibility of the test portion size and the digestion procedure with the post-digestion chemistry (Chelex 100 ion exchange) is essential. Finally, the recognition of less common, but significant, spectral interferences for elements such as Ti is critical to obtain an accurate ICP-AES determination of V or Co.

For many of the 234 foods, it was not possible to obtain accurate ICP-AES estimates of some elements, most notably, Co and V. The concentrations of these elements were generally well below 10 ng/g (in about 75% of the foods), and in a few cases the presence of relatively high concentrations of Ti rendered useless the more sensitive ICP-AES emission lines for V and Co.

Nevertheless it was possible to estimate upper limit daily dietary intake values of these two elements. We were able to quantify Mo, Ni and Cd in most of the samples. Based on these analyses, we have estimated the U.S. daily dietary intakes. These estimates are expressed in ranges to include the various age/sex groups in the U.S. population. They are, in micrograms per day: Mo, 50–126; Ni, 69–162; Co, 3–12; V, 6–18; and Cd, 8–15.

These preliminary estimates clearly illustrate the very low intakes of elements such as Co, V, Cd, Mo, and Ni and the corresponding need for extreme care by the analyst in reporting low-level findings in foods. The potential exists for serious errors in ICP-AES determinations of these elements. This is illustrated in figures 1–3 for Co and V.

Figures 1 and 2 show two of the more commonly used ICP-AES Co emission lines. In figure 1, the Co line at 238.9 nm is seriously overlapped by an Fe line. Depending on the quality of the spectrometer and the experience of the analyst, the interference could quite conceivably go unnoticed, resulting in a gross overestimation of the Co levels in foods. The analyst who is able to recognize this serious Fe interference might elect to avoid it by selecting another Co emission line at 228.6 nm, a line with approximately equal sensitivity. For most foods, this line is adequate for obtaining at least upper-level limits for Co. However, in the presence of high Ti levels such as those found in some processed foods containing Ti additives, the line is rendered useless by a direct Ti overlap interference (fig. 2). Titanium is also a potentially major interference for V at 292.4 nm (fig. 3). Such interferences may easily go undetected even by an experienced ICP-AES analyst, since Ti is rarely determined in foods and the analyst has no obvious reason to suspect that the emission intensity observed at the Co or V lines is not, in fact, Co or V.

These examples serve to illustrate the care needed when ICP-AES is used to determine trace elements in foods. Highly experienced analysts in trace element chemistry and ICP-AES spectrometry are essential when ICP-AES is used to estimate these types of dietary intakes.

ICP-AES can be used successfully to estimate the levels of selected nutritive and toxic elements in foods. However, despite the low determination limits possible with ICP-AES, a great deal of effort is required to obtain consistently reliable results. These efforts include the use of relatively large test portions to obtain enough analyte element for quantitation, separation chemistry to concentrate the elements to quantifiable levels, contamination control, ICP-AES instrumentation capable of characterizing interferences, and highly experienced ICP-AES analysts who recognize interferences and other inherent limitations of the technique.

Volume 93, Number 3, May–June 1988
Journal of Research of the National Bureau of Standards

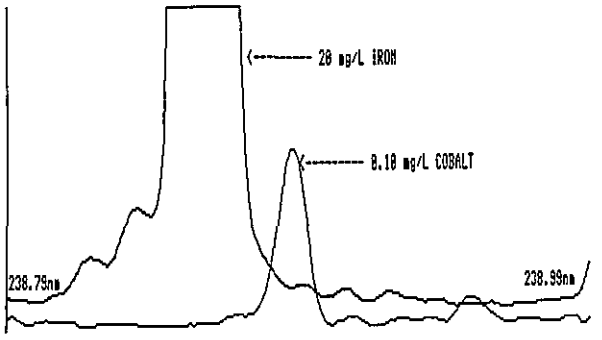

Figure 1. Spectral line overlap interference of iron on the 238.9-nm line of cobalt.

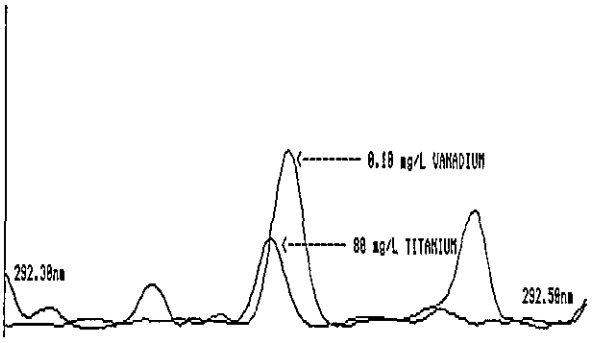

Figure 3. Spectral line overlap interference of titanium on the 292.4-nm line of vanadium.

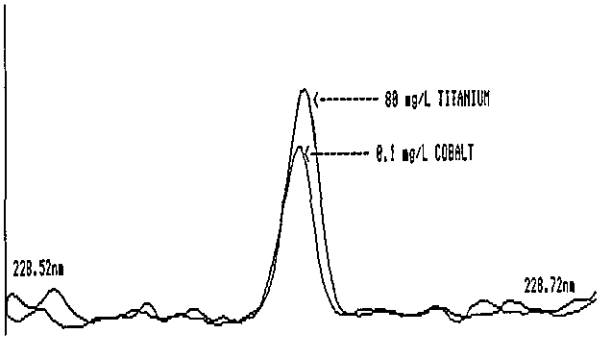

Figure 2. Spectral line overlap interference of titanium on the 228.6-nm line of cobalt.

Development of Multi-Purpose Biological Reference Materials

Venkatesh Iyengar

National Bureau of Standards
Gaithersburg, MD 20899
and
USDA
Beltsville, MD

James Tanner

FDA
Washington, DC

Wayne Wolf

USDA
Beltsville, MD

and

Rolf Zeisler

National Bureau of Standards
Gaithersburg, MD 20899

Biological trace element research is a multidisciplinary science in which both inorganic analysis and relevant biochemical parameters are important to carry out meaningful investigations. Therefore, ensuring adequate quality assurance encompassing all aspects of an investigation can be complex and multifaceted. In seeking solutions to these prob-

lems, it should be recognized that currently available reference materials (RM) are not fully adequate. The choice of the available RMs is limited even to meet the needs for inorganic constituents, while there are hardly any natural matrices available for organic components. Therefore, in attempting to generate new biological RMs, it is desirable to adopt a multipurpose view. The advantage of having a natural matrix certified for several groups of analytes needs no emphasis.

We have prepared a human mixed total diet to evaluate this concept. The diet material was prepared by pooling 201 foods in appropriate proportions [1]. One part of this material was stored as wet substance at −150 °C, and analyzed periodically for several organic nutrients, inorganic elements, and selected organic toxicants. AOAC methods for organic nutrients, flame atomic absorption spectrophotometry and inductively coupled plasma atomic emission spectrometry for elemental analysis and an ion-exchange separation method for phytic acid determination were used. Organic toxicants were assayed by gas chromatography [2].

The results for several organic nutrients are shown in table 1. These preliminary findings indicate that the diet material stored at −150 °C is stable for at least 1 year for organic nutrients. Unfortunately, extended observations were interrupted due to lack of sample material, since the organic nutrient analysis required large quantities of diet material. Some organic nutrients are very sensitive to handling operations. This may be one reason for the differences observed in vitamin C contents between diets I and II. Because of the experience gained from diet I, diet II was handled with additional care which may have resulted in a higher retention of vitamin C (table 1).

Table 1. Stability of organic nutrients in mixed total diets stored under liquid nitrogen cooling

Nutrient	Unit	Diet-I t=0	Diet-I t=1 yr	Diet-II t=0
Thiamine (B1)	mg	2.2	2.1	2.1
Riboflavin (B2)	mg	2.4	2.2	2.3
Vitamin B6	mg	1.5	1.8	1.8
Vitamin C	mg	20	26	42
Pantothenic acid	mg	6.4	8.7	8.5
Niacin	mg	24	28	26
Vitamin A	μg	564	590	745
Vitamin B12	μg	9	12	13
Biotin	μg	36	36	38
Total folates	μg	210	180	210

Proximate analysis of fresh material revealed 84% total volatiles, 3% fat, 9.2% carbohydrate, 3.4% protein, and an ash content of 0.7%.

A few organic pesticides/toxicants have also been identified in this material. These include lindane, heptachlor-epoxide and 4-4′ DDE. Follow-up studies to investigate stability of these components on storage are in progress.

The fresh diet material frozen at −150 °C was also investigated for its stability with respect to inorganic constituents. These results have been converted to freeze-dried basis, and are shown in table 2. As expected, no systematic trends in concentration changes were observed for most elements over the 6-month period of storage. Slight inconsistencies seen in the concentrations of Fe and Mg being somewhat lower at t=0, are mostly reflections of practical analytical problems encountered with this kind of study.

Table 2. Stability of mixed diet material for selected inorganic elements. Wet material stored for 6 months at −150 °C. Results are expressed on dry weight basis (concentration=μg/g±1 S.D.)

Element	t=0	t=6 months
Ca	1698±34	1667±56
Mg	543±26	617±14
K	6480±154	6080±180
Na	7040±230	6590±280
P	3235±37	3333±56
Cu	3.11±0.70	2.7±0.11
Fe	26.2±2.0	31.0±1.5
Mn	5.61±0.25	5.52±0.30
Zn	35.0±0.1	33.1±0.1

A second part of the diet composite was freeze-dried, homogenized and periodically investigated for inorganic elemental content. During this period, the material was stored in teflon jars at ambient temperature (20–25 °C). As seen from the results shown in table 3, no significant changes were observed over a period of 30 months of storage. There is also good agreement between the results shown in table 2 (stored as fresh material) and table 3 (stored as dry material).

Table 3. Stability of mixed total diet material for selected inorganic elements (dry material stored at 20 °C up to 30 months, μg/g, mean±1 S.D.)

Element	Initial[a] 1 month	After[b] 6 months	After[b] 18 months	After[b] 30 months
Ca	1643±45	1712±24	1618±46	1612[c]
Mg	608±10	618±4	594±16	611
K	6150±170	5510±120	5960±80	
Na	6320±40	5860±130	6120±95	
P	3337±33	3217±15	3198±50	3277
Cu	3.05±0.20	2.83±0.06	2.60±0.08	
Fe	30.0 ±1.0	31.0 ±1.5	29.5 ±0.9	31.2
Mn	5.63±0.03	5.30±0.06	5.21±0.05	5.23
Sr	---	2.83±0.04	2.7 ±0.07	
Zn	29.6 ±0.5	30.5 ±1.1	29.5 ±0.7	32.7

[a] AAS flame.
[b] AES-ICP.
[c] Results under this column are averages of two determinations.

Besides the inorganic constituents, phytate was also determined in the dry material, and was found to contain an initial level of 1.4±0.2 mg/g [3]. The storage stability of this constituent is being investigated.

This preliminary investigation has demonstrated the feasibility of exploring a total mixed diet matrix for certification as a multicomponent Standard Reference Material (SRM). A bigger batch of a second mixed total diet is under investigation as part of a systematic study to evaluate the stability of several components over a period of at least 3–5 years. The experience gained from this investigation has helped in understanding some of the practical difficulties faced in the preparation of a natural biological reference matrix for multiple components, especially organic constituents.

The authors are thankful to John Jones and Kathleen Cook (FDA) and Robert Watters (NBS) for elemental analysis, Michele Schantz (NBS) for organic analysis, and Eugene Morris (USDA) for phytate analysis.

References

[1] Iyengar, G. V., Tanner, J. T., Wolf, W. R., and Zeisler, R., Sci. Total Environ. **61**, 235 (1987).
[2] Schantz, M. M., and Chesler, S. N., Personal communication.
[3] Ellis, R., Kelsay, J. L., Reynolds, R. D., Morris, E. R., Moser, P. B., and Frazier, C. W., J. Am. Diet. Assoc. (1987), in press.

Accurate Measurement of Vitamins in Foods and Tissues

J. N. Thompson

Nutrition Research Division
Health Protection Branch
Tunney's Pasture
Ottawa, Ontario, Canada K1A OL2

Dramatic advances in the development of techniques and instruments in recent decades have improved the quality of all analytical work including that directed at determining vitamins. The pursuit of accuracy, however, still involves detailed examination of every step in a procedure, including studies on seemingly trivial manipulations. New methods must also be checked against established procedures and finally, tested in collaborative studies. The development and evaluation of methods for measuring vitamin A in Canada is described as an example. These procedures were designed to replace the antimony trichloride color reaction in the analysis of various materials ranging from serum collected in nutrition surveys to milk being checked for fortification.

Several publications have recommended simple fluorometric methods for the measurement of vitamin A in blood. Comparison of the results of fluorometric and colorimetric methods, however, revealed large differences. Investigations confirmed that blood contains at least one fluorescent carotenoid, phytofluene, which interferes in analysis for vitamin A [1]. Chromatographic purification or correction formulas were needed to eliminate the errors [2,3].

Milk, in contrast, contains little phytofluene. Fatty acids from milk include fluorescent lipids, but these can be removed by saponification. A simple method was developed for milk in which 1 mL was saponified and then extracted with hexane in a stoppered centrifuge tube [4]. The method could be used to examine large numbers of samples and it was adopted by several laboratories involved in milk analysis. Uniformity in milk analysis was maintained in Canada by a quality assurance program. Between 1979 and 1982, ten laboratories in Canada participated in a project in which 4 samples of milk were circulated for analysis on 20 occasions. The standard deviations of 6 laboratories using the fluorometric method were usually

less than 10%.

Liquid chromatography (LC) methods are now often recommended for the analysis of vitamins and there are many reports of the separation and detection of retinol, retinol esters and carotenoids. Methods have been developed for normal and reversed phase separations of retinol after saponification of retinol esters extracted directly from foods and tissues [5]. Retinol and carotenoids are often measured in extracts of serum by reversed-phase LC [6]. Unfortunately, collaborative tests of LC methods for measuring retinol in foods have yielded disappointingly high standard deviations, and few of the many LC methods proposed for the measurement of vitamin A in blood have been examined critically or collaboratively.

To assist the evaluation and development of methods for vitamin A, a reference LC method was designed for the analysis of foods and tissues. The method involved saponification of substantial amounts of sample in ethanolic pyrogallol. A small portion of the digest was extracted in centrifuge tubes, and the extract was evaporated under nitrogen in the presence of a trace of nonvolatile hexadecane. The residue was subjected to LC on a silica column. All-trans retinol was eluted after 5 minutes and small amounts of 13-cis isomer were eluted a minute earlier. Each step in the method was studied in detail and modifications were introduced to eliminate possible sources of error. The tests included comparisons of various methods of saponification, and investigations of distribution ratios for retinol between solvents and saponification digests. The stability of retinol was investigated during evaporation of solutions in common solvents. Two important points emerged. First, the vitamin was rapidly decomposed in chlorinated solvents; this decomposition was due to the presence of HCl and it was eliminated when the solvent was washed with alkali or water. Second, the vitamin was unstable after pure solutions in any volatile solvent were evaporated because it was then deposited alone on the inside surface of a dry container where it was difficult to protect, even with nitrogen. The survival of vitamin in many methods of analysis thus depends on poorly understood roles of protective materials in extracts which are derived accidentally from reagents or samples.

The tendency of retinol to decompose in air affects the accuracy of standards. Retinol purchased from suppliers typically contains more than 20% impurities and once a vial is opened, the contents deteriorate rapidly. Solutions of pure retinol could be prepared by collecting and pooling eluate from several LC runs, and the concentrations could be determined accurately from the absorbance. Although fresh preparations yielded excellent standards for LC, there appeared to be no reliable method of storing them for longer than a few days. Solutions in organic solvents decomposed when sealed under nitrogen, and exposure to traces of air accelerated the process. In contrast, solutions of retinol in cottonseed oil, which can be quantitatively diluted in solvent for use in LC, were relatively stable and their vitamin content fell less than 1% per month. Oil solutions were therefore prepared for use as standards in routine analysis, and they were calibrated at intervals by LC analysis using freshly purified retinol as a primary standard.

A Waters 990 photodiode array detector, which scans a range of wavelengths during LC and plots complete spectra of the eluate, was used to test for the presence of interfering substances. The detector confirmed that the main peak in the LC analysis for vitamin A in all samples was all-trans retinol. Moreover, the spectrum of the smaller, earlier peak was similar to that of the 13-cis isomer when extracts were prepared from infant formula or milk. The occurrence of the cis isomers was not confirmed in blood, however, and the small peak detected by the fixed wavelength detector at the retention time of the 13-cis isomer was concluded to be a polar carotenoid.

Adjustments of the saponification step permitted the reference method to be applied to oils, foods and feeds. Comparisons of the reference method with the fluorometric method indicated that the latter overestimated the true retinol content of unflavored milk by less than 10%.

Acknowledgments

The author is indebted to the staff of the Health Protection Branch laboratories, Longueuil, Quebec for data concerning food analysis and assistance in testing methods, and to Suzanne Duval for technical help in all studies. Investigations on blood are presently done in collaboration with Dr. T. O. Siu, Alberta Cancer Institute, and are supported by a grant from the Department of National Health and Welfare, Canada.

References

[1] Thompson, J. N., Erdody, P., Brien, R., and Murray, T. K., Biochem. Med. 5, 67 (1971).
[2] Thompson, J. N., Erdody, P., and Maxwell, W. B., Biochem. Med. 8, 403 (1973).
[3] Garry, P. J., Pollack, J. D., and Owen, G. M., Clin. Chem. 16, 766 (1970).
[4] Thompson, J. N., Erdody, P., Maxwell, W. B., and Murray, T. K., J. Dairy Sci. 55, 1070 (1972).
[5] Thompson, J. N., J. Assoc. Off. Anal. Chem. 69, 727 (1986).
[6] Thompson, J. N., Duval, S., and Verdier, P., J. Micronutr. Anal. 1, 81 (1985).

Effects of Ionizing Radiation on Nutrients in Foods

Donald W. Thayer, Jay B. Fox, Jr., Ronald K. Jenkins, Stanley A. Ackerman, and John G. Phillips

Eastern Regional Research Center
USDA, ARS
600 East Mermaid Lane
Philadelphia, PA 19118

Within the dose ranges and conditions envisioned for food irradiation processing, there is little, if any, measurable effect on nutritional value of proteins, amino acids, carbohydrates, and lipids. The protein efficiency ratios of a number of foods radiated at doses adequate to achieve commercial sterility were not significantly altered by the treatments. Though ionizing radiation does produce changes in carbohydrates, lipids, amino acids, and proteins, these reactions are minimized in foods irradiated under proper conditions [1]. It is important to stress that nutrients are protected by their molecular environment from ionizing radiation. These same nutrients in aqueous solution may undergo severe degradation when exposed to doses of ionizing radiation equivalent to those used for the treatment of foods. Irradiation at subfreezing temperatures in the absence of oxygen results in better products and greater retention of vitamins than does irradiation at ambient temperatures in the presence of air. The effects of high dose irradiation of meats *in vacuo* at temperatures of −30 °C or lower on their vitamin content have been reported in many studies.

The reactions of vitamins to ionizing radiation in fresh meats and poultry products irradiated at normal processing temperatures and in the presence of air for increased shelf life and/or elimination of food-borne pathogens are much less well known. This prompted the Food Safety Inspection Service to request the Agricultural Research Service to conduct a study of the effects of ionizing radiation on five vitamins in fresh poultry and pork meats. An experimental design was developed to determine the effects of gamma irradiation in the presence of air at processing temperatures between −20 °C and +20 °C and at doses between 0 and 7.0 kGy on the vitamins cyanocobolamin (B_{12}), pyridoxine (B_6), niacin, riboflavin, and thiamin (B_1) using response surface methodology [2] to predict the effects with reasonable accuracy in fresh poultry and pork chops. A response surface statistical design was chosen to provide a series of equations allowing the prediction of the effects of radiation treatments on vitamins over the entire area covered by the experimental design. Implicit in the design described below is the assumption that the vitamin content of the samples would not be altered by either freezing nor warming to temperatures of −20 °C or +20 °C, respectively. A radiation dose of 0.5 kGy was included in the study with pork chops because that would be representative for pork irradiated for the inactivation of trichina. The range of radiation doses and the irradiation temperatures were selected to include those which would have the greatest probability of being selected for elimination of food-borne pathogens other than *Clostridium botulinum* as well as for shelf-life extension for the product. Seven fresh center cut loin pork chops (1/2 inch thick) were used for each replicate sample with three replicates for each treatment (radiation dose and uncooked versus pork chops cooked after irradiation). Five replicate samples were used at the zero radiation dose (control) and at 3.5 kGy and 0 °C. Samples were irradiated at temperatures of −20°, −10°, 0°, +10°, and +20 °C and at doses of 0, 0.5, 1.75, 3.50, 5.26, and 7.0 kGy. The irradiation protocol is illustrated in table 1. The number of replicates indicated is twice that shown above because one-half were analyzed raw and the other after cooking. The protocol followed for poultry was similar except that four breasts per replicate were used and the 0.50 kGy radiation dose was eliminated. The discussion which follows will be limited to a partial presentation of the effects of thiamin as they relate to validity of the experimental design.

Table 1. Pork irradiation experimental design

Temperature °C	Radiation dose (kGy) 0	0.5	1.75	3.5	5.25	7.0
−20 °C		6		6		
−10 °C			6		6	
0 °C	10	6		10		6
+10 °C			6		6	
+20 °C		6		6		

Each replicate contained seven pork chops; one-half of the replicates were fried after irradiation.

The data obtained from the analyses of the samples described above were used to develop response surface equations which would predict the effect of the irradiation dose and temperature on each vitamin over the entire area covered by the design. From the equation for the response surface for thiamin loss the predicted losses in pork chops irradiated at 0 °C and then cooked were as follows: 0 kGy, −1.5% (−0.04%); 0.50 kGy, −10.1% (14.3%); 3.5 kGy, −48.7% (54.3%); and 7.0 kGy, −65.9% (69.7%). The values given in parentheses represent the average of the actual observed values. There was no loss of thiamin in the control on a sample weight basis upon cooking, but there was an overall weight loss of about 30%. The effect of temperature on the degradation of thiamin can be illustrated by comparison of the predicted results obtained at a dose of 3.5 kGy, losses of 32.7 (34.9%) and 63.3% (60.2%) at −20° and +20 °C respectively. The fit of the predicted values to the measured values is indicated by a R^2 value of 0.90 for the equation for the response surface.

The effect of radiation on thiamin was different in poultry from that observed in pork. The response surface equation for thiamin loss in chicken breasts cooked after irradiation predicted the following losses of thiamin at 0 °C: 0 kGy, +3.2%; 1.0 kGy, −0.38%; 2.0 kGy, −2.2%; 3.0 kGy, −5.9%; 3.5 kGy, −7.4%; and 7.0 kGy, −34.9%. Thus, in the range of greatest interest for the control of salmonella contamination (3.0 kGy) the loss of thiamin was very low especially when compared to losses in pork chops irradiated and cooked in the same manner.

References

[1] Kraybill, H. F., Handbook of Nutritive Value of Processed Food **1**, 81 (1982).
[2] Goodnight, J. H., and Sall, J. P., SAS User's Guide, SAS Institute, Inc., Raleigh, NC (1979).

Stable Isotope Dilution GC/MS for the Quantification of Food Contaminants

John Gilbert and James R. Startin

Ministry of Agriculture,
Fisheries and Food
Food Science Laboratory
Haldin House, Queen Street
Norwich NR2 4SX, UK

1. Introduction

As organic contaminants are present in foods at only low levels, and as the food derived extracts for analysis are invariably complex, determinative methods need to be of both a high sensitivity and specificity. Further requirements for an assay are a quantitative ability with a high precision, and the capability of handling large numbers of samples for food surveys. The approach of stable isotope dilution GC/MS fulfills all these requirements; the selected ion monitoring detection method provides high sensitivity and specificity, and the use of stable isotope internal standards enables quantification with relative standard deviations (RSD) of the order of only a few percent. With the use of highly specific mass spectrometric detection, sample clean-up can be minimized, and automated approaches to sample handling and preparation are thus possible, enabling large numbers of samples to be readily analyzed.

Isotope dilution depends on an initial equilibration of the analyte with the stable isotope analogue (usually deuterated or ^{13}C-labelled)—this is normally carried out at an early stage by the addition of the internal standard to a solvent slurry of the foodstuff and allowing it to stand for several hours. After equilibration the internal standard will, during extraction, clean-up and sample derivatization, effectively behave in an identical fashion to the analyte, and thus compensate throughout for recovery losses. The main disadvantage of this approach can be the cost of purchasing labelled internal standards, or where they are unavailable the need to carry out possibly lengthy syntheses.

2. Contamination of Foods by Migration from Plastic Packaging Materials

Plasticizers such as di-(2-ethylhexyl)adipate (DEHA), and various phthalates are present in both flexible films and in coatings which come into contact with foods during retail packaging or the use of plasticized "cling-film" in the home. Epoxidized soybean oil (ESBO) is used as a plasticizer and secondary heat stabilizer in food packaging and recently so-called polymeric plasticizers have been introduced. These components can migrate from the packaging materials into the foods for which monitoring is therefore necessary. Stable isotope dilution GC/MS methods have proved to be successful for quantification of the levels of migration.

The stable isotope internal standards d_4-DEHA, d_4-dibutylphthalate, d_4-dicyclohexylphthalate and d_4-diethylphthalate can be readily synthesized from their respective commercially available isotopically-labelled acids, and thereby obtained with high label incorporation and in high chemical purity. Food sample preparation for the determination of these plasticizers involves extraction with acetone/hexane, size-exclusion chromatographic clean-up (automated) in dichloromethane/hexane solvent and a final capillary GC/MS selected ion monitoring quantitative step. For DEHA determinations [1], ions at m/z 129 and 133 are monitored for d_0- and d_4-DEHA respectively, whilst for the phthalates m/z 149 and 153 provide common ions for monitoring a number of unlabelled phthalates and their respective internal standards [2]. The approach has been employed for monitoring migration in a large number of food samples of different types such as cheese, fresh and cooked meat, vegetables, confectionary products and even complete microwave cooked meals [3,4]. In no instance was there any evidence of interference from food components, and the limit of detection of the procedure was 0.1 mg/kg with a RSD of between 1 and 3% [1,2].

So-called polymeric plasticizers are in fact oligomeric mixtures of components, and for example the adipate-based plasticizer "Reoplex R346" has a number average molecular weight some five times greater than the monomeric counterpart. The isotope dilution GC/MS procedure [5] for determining polymeric plasticizer levels in foods involves transmethylation of the polymeric plasticizer to dimethyladipate (DMA), utilizing d_4-DEHA as an internal standard which is in turn transmethylated to d_4-DMA. Using a similar clean-up to that for the other plasticizers outlined above, the GC/MS determination is based on monitoring of m/z 143 and 147 for d_0- and d_4-DMA respectively. The method has been demonstrated as applicable to a diverse range of food types, and to have a limit of detection of 0.1 mg/kg and a RSD of about 4%.

ESBO is a multi-functional additive used at levels of between 3 and 7% in a range of plastics. This material is determined in foods by transmethylation of the triglycerides and then derivatization of the epoxide groups in the fatty acid esters to form compounds with characteristics particularly suitable for GC/MS selected ion monitoring. The initial transmethylation is carried out under basic conditions (sodium methoxide/methanol) to ensure protection of the epoxide group, and derivatization involves formation of the 1,3-dioxolane by treatment with cyclopentanone (followed by BF_3/diethyl ether). The method has been used down to a limit of 0.1 mg/kg without necessitating prior separation of the epoxides from the other naturally occurring fatty acid esters derived from the food lipids. The choice of ions for selected ion monitoring depends on whether the mono-, di- or tri-epoxidized fatty acid esters are to be monitored, but for example for the monoepoxidized species m/z 367 and 396 are detected. The isotopically-labelled internal standard is easily synthesized from commercially available ^{13}C-triolein, to give a method with an overall RSD of about 5%.

3. Pesticide Residues in Foods

The determination of pesticide residues in foods by stable isotope dilution presents some difficulties, firstly because of the large number of compounds that have to be simultaneously monitored, and secondly the high proportion of samples containing not detectable levels of pesticides which makes quantification the exception rather than the rule. For these reasons it is probably preferable to initially screen by another method and then re-analyze positive samples by GC/MS adding only the appropriate labelled internal standards for which quantification is required. For organochlorine pesticides at least 15 deuterated and/or ^{13}C-labelled standards are commercially available, but these surprisingly have not been utilized for residue analysis and to date our own experience has been limited to the quantification of hexachlorobenzene

(HCB) using the $^{13}C_6$-labelled standard [6]. For the analysis of eggs, sample preparation involves initial treatment with phospholipase, extraction with acetone/hexane and then clean-up of the lipid extract on a water deactivated alumina column. Selected ion monitoring is for m/z 284 and 286 for HCB and 292 and 294 for [$^{13}C_6$]HCB. The GC/MS program involves switching between a number of different ions, grouped for different retention time windows to enable monitoring of altogether 10 organochlorine pesticides plus respective isomers. For the future it is intended to increase the number of isotopically labelled standards utilized which will further increase the complexity of the multiple ion monitoring program.

4. Veterinary Drug Residues in Animal Tissue

Veterinary drug residues in foods, although obvious candidates for isotope dilution approaches to analysis, do present the same logistical problems as pesticides with the same requirement for multi-residue monitoring. For the determination of the sulphonamide drug, sulphamethazine in kidney samples by isotope dilution GC/MS [7], after addition of d_4-sulphamethazine to an acetonitrile slurry of the kidneys and allowing for equilibration, the clean-up involves solvent partition, diazomethane treatment to form the methyl derivative and then HPLC fractionation as a further clean-up stage. In the trapped HPLC fraction GC/MS selected ion monitoring for m/z 227 and 228 for sulphamethazine and 231 and 232 for the deuterated internal standard is carried out for quantification. The limit of detection of the method is around 0.05 mg/kg and the CV is between 3.7 and 5.7% for sulphamethazine spiking levels in the tissue from 0.2 to 1.2 mg/kg. Deuterated sulphamethazine had to be custom synthesized and other stable isotope-labelled drugs are not widely available commercially which hinders development of this approach, as does the fact that many drugs of interest are not amenable to GC. One possible way to overcome this latter difficulty is to maintain the use of isotope dilution but to use MS/MS which also confers advantages of reduced sample preparation and clean-up [8].

References

[1] Startin, J. R., Parker, I., Sharman, M., and Gilbert, J., J. Chromatogr. **387**, 509 (1987).
[2] Castle, L., Mercer, A. J., Startin, J. R., and Gilbert, J., Migration from plasticized films into foods. 3. Migration of phthalate, sebacate, citrate, and phosphate esters from films used for retail food packaging, Food Addit. Contamin., in press (1988).
[3] Startin, J. R., Sharman, M., Rose, M. D., Parker, I., Mercer, A. J., Castle, L., and Gilbert, J., Food Addit. Contamin. **4**, 385 (1987).
[4] Castle, L., Mercer, A. J., Startin, J. R., and Gilbert, J., Food Addit. Contamin. **4**, 399 (1987).
[5] Castle, L., Mercer, A. J., and Gilbert, J., Gas chromatographic-mass spectrometric determination of adipate-based polymeric plasticizers in foods, J. Assoc. Offic. Anal. Chem., in press (1988).
[6] Gilbert, J., Startin, J. R., and Crews, C., Pestic. Sci. **18**, 273 (1987).
[7] Gilbert, J., Startin, J. R., and Crews, C., J. Assoc. Publ. Analysts **23**, 119 (1985).
[8] Finlay, E. M. H., Games, D. E., Startin, J. R., and Gilbert, J., Biomed. Environ. Mass Spectrom. **13**, 633 (1986).

An Isotope Dilution Mass Spectrometric (IDMS) Method for the Determination of Vitamin C in Milk

P. Ellerbe, L. T. Sniegoski, J. M. Miller, and E. White V

Center for Analytical Chemistry
National Bureau of Standards
Gaithersburg, MD 20899

The accurate determination of constituents in food is necessary to establish dietary requirements. A non-fat milk powder (NFMP) has been developed as a Standard Reference Material (SRM) for use in validating methods for the analysis of milk and other biological materials. When this SRM was issued, L-ascorbic acid (vitamin C or AA) was measured by HPLC methods developed at NBS and by the AOAC microfluorimetric method.

An IDMS method has been developed as an independent method to measure AA in NFMP, using AA-13 C-1 as an internal standard. After the labeled AA is added to the NFMP and has equilibrated with the unlabeled AA present, samples are treated to remove protein, put over an anion exchange column, and freeze-dried. AA is converted

to the t-butyldimethylsilyl derivative and analyzed by capillary column GC/MS under a strict measurement protocol [1]. The two masses of interest are the $[M\text{-}C_4H_9]^+$ ions at 575 and 576. The ions are monitored using a mass switching system designed to provide accurate measurement of isotope ratios for the narrow GC peaks (12–15 seconds) typical of capillary columns.

Two independent sets of standards were prepared by weight from labeled and unlabeled ascorbic acid. Each set was used as standards to measure, according to the protocol, the weight ratios of the other set as if it were samples. The difference between the measured and weighed weight ratios within each set is calculated as a percent difference, which is a measure of the consistency of each independently prepared set with the other. As an example, the average percent difference for set 1 as standards and set 2 as "samples" was +0.06%. This set is consistent with the other set because the mean of the percent differences is acceptably low.

Analyses of the NFMP Standard Reference Material run in 1984 gave values of 53 (SD=5) μg/g by an HPLC method [2] and 49.6 (SD=4.2) by the AOAC method [2,3]. Analyses run in 1987 by two other HPLC methods [4] gave values of 35 (SD=1) and 41.4 μg/g. Table 1 gives the results of the IDMS analyses; the IDMS overall mean is 40.23 μg/g (SD=0.71).

There are two points to consider. Firstly, the value for AA appears to have fallen over 3 years, suggesting that AA is not stable in this matrix. It must be noted, however, that the measurement methods used in 1984 and 1987 were not the same. Secondly, there is a difference between the HPLC measurements made in the same year, and that one result does not agree with the IDMS result, thus indicating a problem with at least one of the methods.

In summary, L-ascorbic acid can be determined precisely in NFMP by an ID/MS method using a C-13 labeled ascorbic acid as the isotopic diluent. The discrepancy between the HPLC and IDMS methods is being investigated, but since the L-ascorbic acid content of this Standard Reference Material may change rapidly with time, a certified value for AA will not be assigned.

Table 1. Results of ID/MS analyses

Bottle	Sample	μg AA/g NFMP	SD	CV(%)
1	1	40.31		
	2	39.85		
	mean	40.08	0.33	0.82
2	1	41.11		
	2	40.55		
	3	41.16		
	4	41.21		
	5	41.01		
	6	39.68		
	mean	40.79	0.59	1.45
3	1	39.88		
	2	39.37		
	3	39.15		
	4	39.76		
	5	39.91		
	mean	39.61	0.34	0.85
overall mean		40.23	0.71	1.77

References

[1] Cohen, A., Hertz, H. S., and Mandel, J., et. al. Clin. Chem. **26**, 854 (1980).
[2] Certificate of Analysis 1549: Non-Fat Milk Powder.
[3] Tanner, J. T., Smith, J. S., and Angyal, G., et. al. J. Assoc. Off. Anal. Chem. **68**, 110 (1985).
[4] S. Margolis, NBS, private communication.

Volume 93, Number 3, May-June 1988
Journal of Research of the National Bureau of Standards

Accuracy in Trace Analysis

Materials Analysis on a Microscale

Prospects for Trace Analysis in the Analytical Electron Microscope

D. B. Williams

Department of Materials Science and Engineering
Lehigh University
Bethlehem, PA 18015

Background

The analytical electron microscope (AEM) uses a high energy ($\geqslant$100 kV) beam of electrons to generate a range of signals from a thin foil sample as shown in figure 1a [1,2]. Various detectors are configured in the AEM to pick up most of the generated signals (fig. 1b). Microanalysis is usually performed using the characteristic x-ray signal, detected by an energy dispersive spectrometer (EDS) although occasionally the electron energy loss spectrum is also used. This paper will emphasize x-ray microanalysis only. The specific advantages that the AEM has for microanalysis are two-fold. First the instrument can be operated as a high resolution transmission electron microscope, thus permitting the analytical information to be related directly to the microstructure of the sample. Second, in the AEM most microanalysis is performed with a probe size $<\approx 10$ nm and a specimen thickness $<\approx 100$ nm. This results in an analyzed volume $\approx 10^{-5}$ of that commonly encountered in bulk microanalysis, for example, in the electron probe microanalyzer (EPMA). This small volume means that the spatial resolution of microanalysis is relatively good (routinely <50 nm) but generally trace analysis in the AEM is relatively difficult, because generated signal intensities are low.

X-Ray Microanalysis in the AEM

The definition of "trace analysis" in this paper is assumed to be that commonly used in the EPMA, namely elemental concentrations $<\approx 0.5$ wt% [3]. Under these conditions the average counts in the x-ray characteristic peak, $\bar{N}$, approach the average counts in the background, $\bar{N}^b$.

One reasonable measure of analytical sensitivity used in the AEM field is the minimum mass fraction of one element that is detectable in the matrix of another. Using the criterion of Liebhafsky et al. [4], the peak is detectable if:

$$\bar{N} > 3(2\bar{N}^b)^{1/2} \tag{1}$$

This simple criterion can be combined with the Cliff-Lorimer equation [5] to give a minimum mass fraction of element B (C_B):

$$C_B = \frac{3(2I_B^b)^{1/2}}{I_A - I_A^b} \cdot C_A \cdot k_{AB}^{-1} \tag{2}$$

where I_A^b and I_B^b are background intensities for elements A and B; I_A is the integrated characteristic intensity from A; C_A is the concentration of A (in wt%) and k_{AB}^{-1} is the reciprocal of the Cliff-Lorimer sensitivity k-factor k_{AB} [5]. The equation can be rewritten [6] as:

$$C_B = \frac{3(2I_B^b)^{1/2}}{I_B - I_B^b} \cdot C_B \tag{3}$$

Results using eqs (2) and (3) have been given by Romig and Goldstein [7] ($\approx$0.5% Ni in Fe), Michael [6] ($\approx$0.07% Mn in Cu) and Lyman [8] ($\approx$0.1% Ni in Fe). The results of Michael [6] are shown in table 1. What is not apparent in these reported values is that since all the data were obtained from homogeneous samples, spatial resolution was of little consequence and was usually >50 nm which is the current limit for most thermionic source AEMs. The data in table 2 [9] are the first to compare the effect of spatial resolution on minimum detectability. These results show that a sensitivity <0.1 wt% Cr with moderate spatial resolution ($<\approx 50$ nm) can only be achieved with an AEM employing a field emission gun, such as the Vacuum Generators HB501. Thermionic source instruments such as the Philips EM430 can only demonstrate <0.1 wt% detectability with substantially poorer spatial resolution.

Table 1. Calculation of the minimum mass fraction of Mn detectable in Cu using eq (3)

I_{Mn}	I^b_{Mn}	$(I_{Mn}-I^b_{Mn})$	$3(2I^b)$	$C_{Mn}(MMF)=C_{Mn}\times\frac{3(2I^b)}{(I_{Mn}-I^b_{Mn})}$ wt%
11904	1995±189	9909±422	189±9	0.064±0.008
13769	2299±203	11470±454	203±9	0.059±0.007
10737	1860±183	8877±400	183±9	0.069±0.008
10547	1916±186	8631±394	186±9	0.072±0.009
				av. = 0.067±0.008 wt%

Specimen Cu 3.36 wt% Mn.
Data obtained at 120 kV, 20 nm probe size, 40 μA emission current, 70 μm C_2 aperture, W hairpin filament.
From refs [1,7]. Reproduced courtesy of Philips Electronic Instruments Publishing Group.

Table 2. Calculated MMF values for Cr after 200 s livetime and spatial resolution of microanalysis for a range of AEMs

Microscope	Probe current (nA)	Accelerating voltage (kV)	Sample Thickness (nm)	Cr MMF wt%	Calculated spatial resolution (nm)
HB-501	0.5	100	164	0.125	45
HB-501	1.7	100	164	0.069	45
HB-501	0.5	100	434	0.056	200
HB-501	1.7	100	434	0.035	200
EM430	0.5	100	164	0.181	70
EM430	0.8	300	164	0.135	25
EM430	0.5	100	434	0.054	200
EM430	0.8	300	434	0.053	70

Data from ref. [8]. Reproduced by permission of C. E. Lyman and San Francisco Press.

Future Prospects for X-Ray Analysis in the AEM

However, recent instrumental developments promise substantial improvement in trace analysis capability in the AEM. A combination of higher voltage beams (up to 400 kV), brighter (field emission) electron sources, improved microscope stage design [10] and x-ray spectrometry advances offer the prospect of extending the minimum mass fraction detectable by x-ray analysis down to ≈0.01 wt% [8]. If this can be achieved while maintaining spatial resolution at the 10 nm level or below, then the AEM will be close to detecting the presence of only a few atoms, as well as localizing them to within a few tens of unit cells.

From an experimental standpoint, Ziebold [11] has shown that C_B depends on several factors, namely:

$$C_B \propto (I_B \cdot I_B/I^b_B \cdot \tau)^{-1/2} \qquad (4)$$

where τ is the counting time to acquire the peak. Going to an intermediate voltage such as 300 kV, will increase the value of I_B (the peak intensity) and I_B/I^b_B (the peak to background ratio (P/B)) [8]. Unfortunately, there is no generally accepted definition of P/B. A recent attempt has been made to generate a "standard" sample from which to measure a "standard" P/B [12,13].

The standard sample is a 100 nm of evaporated Cr on a carbon film, supported on a Cu grid, and manufactured at the National Bureau of Standards.[1] The value of the P/B used is that originally suggested by Fiori et al. [14] and ratios the intensity in the full peak to the average background in a 10 eV channel. Thus the ratio is defined as P/B (10 eV).

Preliminary results (table 3) [13] indicate that modern AEMs show an enormous range in P/B (10 eV) at 100 kV and not all intermediate voltage instruments show the expected improvement at higher kVs. Nevertheless, an improved M_{DL} of ≈0.05 wt% in a 10 nm probe is estimated at

[1] Standard films may be obtained from Dr. E. B. Steel, Analytical Chemistry Division, Bldg. 222, Room A121, National Bureau of Standards, Gaithersburg, MD 20899.

300 kV. However, if an FEG were added to a 300 kV AEM, a probe current of 5×10^{-8} to 10^{-7} A should be available in a 10 nm probe. This increase in probe current would result in an increase in P of 100 times and would improve the M_{DL} by $\approx$10 times to 0.01 wt% in a nominal 100 to 200 nm thick film at 300 kV [8]. Such an improvement of over an order of magnitude in analytical sensitivity brings x-ray analysis in the AEM into the 100 ppm range similar to that obtained in the electron probe microanalyzer. None of these calculations takes into account the possibility of increasing the value of τ in eq (4). Typically τ is limited by contamination, specimen drift and operator fatigue. Contamination can be virtually eliminated by careful specimen preparation and good ($<10^{-8}$ Torr) vacuums. Specimen drift can now be compensated electronically [15], effectively eliminating operator fatigue and permitting such experiments as overnight counting, long-term digital mapping and other techniques, hitherto the realm of classical bulk analysis using the EPMA at the micron level.

Table 3. Peak to background (P/B (10 eV)) data for the CrK_α peak obtained from a standard thin film sample in a range of AEMs

AEM	kV	α°	Ω(sr)	P/B
1	120	20	0.13	1621
2	100	20	0.13	3346
2	200	20	0.13	3181
2	300	20	0.13	2991
3	300	25	0.13	2983
4	100	20	0.13	3177
5	200	72	0.03	2489
6	200	72	0.01	2873
7	100	10	0.02	3007
7	100	13	0.077	2690
8	100	13	0.077	3120
9	120	20	0.13	2879
10	100	30	0.13	2255
11	100	25	0.04	3040
12	200	34	0.005	2300
12	200	37	—	3300
13	120	20	0.13	3093

Reproduced courtesy of San Francisco Press.
α° = detector take-off angle above horizontal.
Ω = detector solid angle.

Acknowledgments

The author wishes to acknowledge the financial support of the National Aeronautics and Space Administration (NASA Grant NAG9-45) and many stimulating discussions with C. E. Lyman and J. R. Michael.

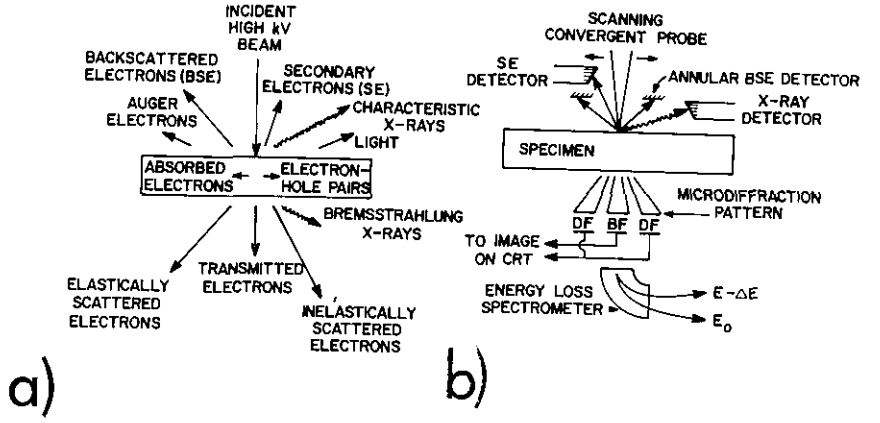

Figure 1. a. Schematic diagram showing the range of signals generated when a high kV electron beam strikes a thin foil sample.
b. Typical array of detectors in a modern analytical electron microscope.

References

[1] Williams, D. B., Practical Analytical Electron Microscopy in Materials Science, Philips Electron Optics Publishing Group, Mahwah, NJ (1984).
[2] Joy, D. C., Romig, A. D., and Goldstein, J. I., Principles of Analytical Electron Microscopy, Plenum Press, New York (1986).
[3] Goldstein, J. I., Newbury, D. E., Echlin, P., Joy, D. C., Fiori, C. E., and Lifshin, E., Scanning Electron Microscopy and X-ray Microanalysis, Plenum Press, New York (1981) p. 435.
[4] Liebhafshy, H. A., Pfeiffer, H. G., and Zemany, P. D., X-ray Microscopy and X-ray Microanalysis, Elsevier/North Holland, Amsterdam (1960) p. 321.
[5] Cliff, G., and Lorimer, G. W., J. Microsc. (U.K.) **103**, 203 (1975).
[6] Michael, J. R., M.S. Thesis, Lehigh University (1981) p. 41.
[7] Romig, A. D., and Goldstein, J. I., Detectability Limits and Spatial Resolution in STEM X-ray Analysis: Application to Fe-Ni Alloys, Microbeam Analysis—1979, San Francisco Press (1979) p. 124.
[8] Lyman, C. E., Microanalysis Limits on the Use of Energy Dispersive X-ray Spectroscopy in the Analytical Electron Microscope, Microbeam Analysis—1986, San Francisco Press (1986) p. 434.
[9] Lyman, C. E., and Michael, J. R., A Sensitivity Test for Energy Dispersive X-ray Spectrometry in the Analytical Electron Microscope, Analytical Electron Microscopy—1987, San Francisco Press (1987) in press.
[10] Williams, D. B., Towards the Limits of Microanalysis in the Analytical Electron Microscope, Electron Microscopy and Analysis—1987, The Institute of Physics (1987) in press.
[11] Ziebold, T. O., Anal. Chem. **36**, 322 (1967).
[12] Williams, D. B., Standardized Definitions of X-ray Analysis Performance Criteria in the AEM, Microbeam Analysis—1986, San Francisco Press (1986) p. 443.
[13] Williams, D. B., and Steel, E. B., A Standard Cr Thin Film Specimen to Measure the X-ray Peak to Background Ratio (Using the Fiori Definition) in Analytical Electron Microscopes, Analytical Electron Microscopy—1987, San Francisco Press (1987) in press.
[14] Fiori, C. E., Swyt, C. R., and Ellis, J. R., The Theoretical Characteristic to Continuum Ratio in Energy Dispersive Analysis in the Analytical Electron Microscope, Microbeam Analysis—1982, San Francisco Press (1982) p. 57.
[15] Vale, S. H., and Statham, P. J., STEM Image Stabilization for High Resolution Microanalysis, Proc. XIth Int. Cong. on Electron Microscopy, Kyoto 1986, Japanese Society of Electron Microscopy, Tokyo (1986) p. 573.

Accuracy in Microanalysis by Electron Energy-Loss Spectroscopy

Ray F. Egerton

Department of Materials Science and Engineering
State University of New York
Stony Brook, NY 11794-2275

The transmission electron microscope can focus electrons onto a small region of a specimen, typically 1 nm to 1 μm in diameter. If the specimen is suitably thin (preferably <100 nm) and the transmitted electrons enter a high-resolution electron spectrometer, an electron energy-loss spectrum is produced. This spectrum (fig. 1) contains a zero-loss peak, representing elastic scattering, one or more peaks in the 4–40 eV range (due to inelastic scattering from outer-shell electrons) and, at higher energy loss and lower intensity, characteristic edges due to ionization of inner atomic shells. These latter features are used in elemental microanalysis, usually by fitting a background in front of each edge and measuring the area I_c over an energy range Δ beyond each edge; see figure 1. The number of atoms (N per unit specimen area) of a particular element can be obtained from [1]:

$$N \simeq I_c/GI_l\sigma_c) \qquad (1)$$

The factor G makes allowance for any increase in detector gain between recording the low-loss region (area I_l) and the ionization edges; σ_c is a cross section for inner-shell scattering over the appropriate range of energy loss, which can be calculated from atomic theory or obtained experimentally. Energy-loss spectroscopy is therefore capable of providing absolute, standardless elemental analysis, although in practice it is usually the ratio of two elements which is of interest, in which case the quantities G and I_l cancel and need not be measured.

Energy-loss spectroscopy has been used to identify quantities of less than 10^{-20} g and concentrations of less than 100 ppm of elements such as phosphorus and calcium in an organic matrix [2,3]. However, the accuracy of quantitative analysis, using eq (1), is often no better than 20%. The main sources of error, and possibilities for their removal, are discussed below.

Background Subtraction

The pre-edge background is usually taken to be a power law: AE^{-r} where E represents energy loss, A and r being found by least-squares fitting over a pre-edge region. Particularly for lower-energy edges where the background is relatively high, alternative fitting functions or procedures have been used to reduce systematic errors [2,4–6]. Also because the background must be extrapolated rather than interpolated, statistical errors tend to be high [6]. Both types of error could be reduced by fitting over both the pre-edge and a post threshold region [7,8]. Where the elemental concentration is low, the use of digital filters [9] and differential-mode spectrum recording [2] is being developed.

Effect of Elastic Scattering

Equation (1) would be exact if inner-shell excitation were the only mode of scattering or if all scattered electrons contributed to the energy-loss spectrum. In practice, the spectrometer collects scattering only up to some angle β, and this fact is taken into account to first order by using a cross section $\sigma_c(\beta,\Delta)$ evaluated over the appropriate angular range. However, to reduce the background contribution from plural scattering, β is usually chosen to be in the range 3–15 mrad, and as a result most of the *elastically* scattered electrons are excluded from the spectrometer. With a crystalline specimen, diffracted beams contribute additional intensity to I_c, in the form of plural (elastic+inner-shell) scattering [1,10], causing N to be overestimated. The systematic error involved depends on the edge energy (which determines the angular width θ_E of the inner-shell scattering) and the specimen thickness and orientation (which determine the intensity of the diffracted beams); see figure 2. It is therefore not surprising to find that elemental ratios measured from test samples become inaccurate for thicker specimens or under strongly diffracting conditions [1,6,11]. Efforts are continuing to find a simple method of correcting for the diffracted electrons. In an amorphous material, the equivalent errors should be much reduced [1].

Accuracy of Inner-Shell Cross Sections

The accuracy of absolute quantification is clearly dependent on the accuracy with which σ_c is known; likewise, the accuracy of elemental ratios will depend on the *relative* accuracy of the inner-shell cross sections. K-shell cross sections can be calculated rapidly (on-line) by use of a hydrogenic approximation, probably to an accuracy of around 10% [12]. Hydrogenic L-shell cross sections require some empirical correction, originally based on photoabsorption data [13].

Hartree-Slater or Dirac-Slater calculations can be carried out for all atomic shells [14] and should be more accurate, though more time-consuming. Within the last year or two, systematic experimental determinations of K-, L-, and M-shell cross-section ratios have been made for the ionization edges of most interest [15,16]. As a result, correction parameters used in the hydrogenic L-shell program have been modified [6] and further refinement may be desirable. A parameterization scheme for all edges of practical importance is also being investigated since the measured cross-section ratios ("k-factors") apply only for given values of β, Δ and incident-electron energy.

Lens-Aberration Errors

Spherical and chromatic aberrations of any electron lenses between the specimen and spectrometer can cause a loss of energy resolution, spatial resolution and collection efficiency, all of which could lead to analysis errors, dependent on the values of β, edge energy, spatial resolution (e.g., incident-beam diameter) and the type of electron-optic coupling [6]. Severe effects have been reported in cases where one of the post-spectrometer lenses is operating with an object distance close to its focal length [17]. More work needs to be done to assess the performance of conventional microscope lenses at high energy loss.

Radiation Damage

The electron beam used for microanalysis can cause both structural damage and chemical change (mass loss) within the analyzed region, leading to errors in elemental ratios. With a high-brightness electron source, this problem is observable even with inorganic specimens [18]. Use of a liquid-nitrogen stage may reduce the radiation sensitivity, particularly of organic specimens. Parallel-recording spectrometers, now commercially available, will greatly increase the signal-collection efficiency and reduce the electron exposure required to obtain an acceptably noise-free spectrum. In fact, the radiation-damage problem is not so severe as in x-ray emission spectroscopy, where the collection

efficiency and fluorescence yield (for light elements) are both much lower.

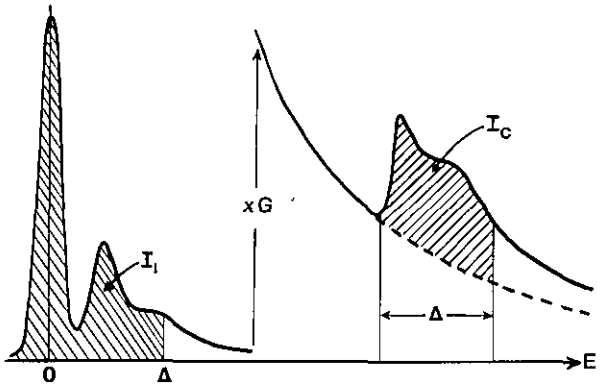

Figure 1. Schematic energy-loss spectrum with a gain increment G between the low-loss and high-loss regions.

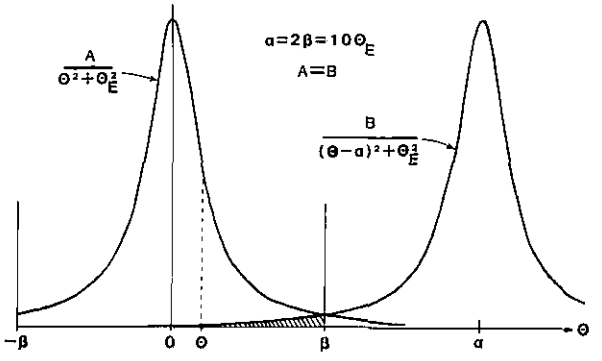

Figure 2. Angular distributions of inelastic scattering around the undiffracted beam and around a beam diffracted through an angle α. The shaded area represents the contribution from the diffracted beam to the intensity collected by an on-axis aperture of semi-angle β.

References

[1] Egerton, R. F., Ultramicroscopy **3**, 243 (1978).
[2] Ottensmeyer, F. P., Elemental Mapping by Electron Energy Filtration in Biology: Limits and Limitations, Electron Microscopy, (1986) (Proc. 11th Int. Cong., Kyoto) p. 53.
[3] Shuman, H., and Somlyo, A. P., Ultramicroscopy **21**, 23 (1987).
[4] Liu, D. R., and Williams, D. B., A New Background Extrapolation Procedure, Proc. 45th Ann. Meeting Elec. Micros. Soc. Am. (1987) p. 118.
[5] Kundmann, M. K., Analysis of semiconductor EELS in the low-loss regime, Microbeam Analysis (1986) p. 417.
[6] Egerton, R. F., Electron Energy Loss Spectroscopy in the Electron Microscope, Plenum Press, New York (1986).
[7] Steele, J. D., Titchmarsh, J. M., Chapman, J. N., and Paterson, J. H., Ultramicroscopy **17**, 273 (1985).
[8] Leapman, R. D., and Swyt, C. R., Removal of Plural Scattering in Electron Energy Loss Spectra from Organic Samples: A New Approach, Microbeam Analysis (1987) p. 273.
[9] Zaluzec, N. J., Spectral Processing and Quantitative Analysis in Electron Energy Loss Spectroscopy Using a Digital Filter Technique, Analytical Electron Microscopy (1987).
[10] Bourdillon, A. J., and Stobbs, W. M., Ultramicroscopy **17**, 147 (1985).
[11] Zaluzec, N. J., The Influence of Specimen Thickness in Quantitative Energy-Loss Spectroscopy, 41st Ann. Proc. Electron Microsc. Soc. Am., p. 388.
[12] Egerton, R. F., Quantitative Microanalysis by Electron Energy Loss Spectroscopy: The Current Status, Scanning Electron Microscopy (1984) part 1, p. 505.
[13] Egerton, R. F., SIGMAL: A Program for Calculating L-Shell Ionization Cross Sections, 39th Ann. Proc. Electron Microsc. Soc. Am. (1979) p. 198.
[14] Rez, P., and Ahn, C., Comparison of Theoretical EELS Edges with Experimental Data, Analytical Electron Microscopy (1984) p. 294.
[15] Malis, T., and Titchmarsh, J. M., A k-Factor Approach to EELS Analysis, EMAG 1985, Institute of Physics, Bristol, U.K.
[16] Hofer, F., Ultramicroscopy **21**, 63 (1987).
[17] Craven, A. J., and Buggy, T. W., Ultramicroscopy **7**, 27 (1981).
[18] Thomas, L. E., Ultramicroscopy **18**, 173 (1985).

Analysis at the Atomic Level: The Atom Probe Field-Ion Microscope

M. K. Miller

Metals and Ceramics Division
Oak Ridge National Laboratory
Oak Ridge, TN 37831

Introduction

The atom probe field-ion microscope (APFIM) is a unique analytical instrument that can analyze metals and semiconducting materials on the atomic scale. In recent years, the atom probe has developed into one of the most powerful instruments available for routine microstructural and microchemical analysis of materials. The types of investigations that have been performed have encompassed many diverse metallurgical subjects

including phase transformations, segregation, diffusion, catalysis, and radiation damage [1].

The Atom Probe Field-Ion Microscope

The atom probe combines an ultrahigh resolution field-ion microscope (FIM) with a mass spectrometer as shown in figure 1. The FIM is capable of producing images of the surface of a specimen in which each distinct point on the image is an individual atom. The mass spectrometer is used to chemically analyze the specimen with single atom sensitivity for all elements.

After cooling to cryogenic temperatures, the field-ion image of the specimen surface is obtained by first introducing a small amount of image gas (e.g., neon) into the ultrahigh vacuum chamber and then applying a positive voltage to the specimen. At a certain voltage, dependent on the sharpness of the needle-shaped specimen and the image gas used, the field-ion image will appear on the channel plate and phosphor screen assembly. In order to make a chemical analysis of a specific region, such as a precipitate, the specimen is rotated until the image of that feature falls over the aperture in the channel plate and screen assembly. This aperture serves as the entrance to the mass spectrometer. The surface atoms of the specimen may then be removed from the specimen by increasing the voltage on the specimen by the process of field evaporation. This is generally done in practice by the superposition of a short high-voltage pulse onto the standing voltage already on the specimen. In the pulsed laser atom probe (PLAP) that is used for semiconducting materials, a short laser pulse is used instead. Whereas ionized atoms are removed from the entire specimen, only those whose trajectories pass through the aperture are analyzed in the mass spectrometer. The rate of field evaporation can be precisely controlled so that only a few atoms or many layers are removed from the specimen surface with each field evaporation pulse. The composition of the analyzed volume is determined by simply counting the number of atoms of each element in comparison to the total number. No calibrations or conversions are required, although some care must be taken in selecting experimental conditions to ensure that no preferential evaporation or retention occurs. The three-dimensional morphology of the phases or microstructures present in a specimen may also be reconstructed from a sequence of field-ion micrographs taken after successive field evaporation using video recording of the images. This persistence size technique also permits an accurate determination to be made of the size of small precipitates and their number density. Analysis of precipitates can be applied when the number density of the second phase is relatively large, i.e., $>10^{20}$ m^{-3}. This type of analysis for less frequently occurring features is more difficult and time consuming because of the limited volume of material that is accessible for analysis in a field-ion specimen. The mass range of the atom probe is not restricted and the concentration of light elements may be readily determined. The negligible background noise level in the presence of the image gas enables chemical analysis to be made while viewing the field-ion image. The minimum detection level for trace elements is currently limited to approximately 10 appm because of the length of time required to collect sufficient ions.

In addition to the instrument outlined above, another variant known as the imaging atom probe (IAP) may be used to obtain elemental maps similar in form to those obtainable in an electron microprobe except with atomic spatial resolution [1].

Examples

The true uniqueness of the atom probe is clearly evident by its capability to chemically analyze a single atom. This type of analysis may be used to identify a segregant to a boundary as shown in figure 2. In this field-ion micrograph, a grain boundary in a boron-doped nickel aluminide specimen is decorated with bright spots. [2] The bright spots were identified as individual boron atoms by correlating the atom that produces the bright spot in the field-ion image with the atom that is collected in the mass spectrometer when it is field evaporated. This type of analysis is a specific example of selected area analysis and is used to determine the composition of small precipitates or compositional variations as a function of distance from features such as precipitates or boundaries. Precipitates smaller than 1 nm in diameter may be analyzed although the limited number of atoms that are available will control the statistical significance of the analysis.

An alternative procedure for examining a specimen is to use random area analysis. This approach is used to analyze specimens where the selected area analysis is not possible or other information is

desired. Situations where this method would be applied include clustering and cosegregation studies, high volume fraction microstructures such as found in systems that undergo spinodal decomposition, or systems where there is little or no contrast between the phases. In this method, a cylinder of atoms is collected from the specimen without regard to any feature in the image. In this way, the composition variations as a function of distance are measured. As material is removed, precipitates or clusters present in the specimen will eventually intersect the surface and those that emerge in the sampling volume will be analyzed. An example where this method was used [3] to detect small brightly-imaging boron clusters in other higher aluminum boron-doped nickel aluminide materials is shown in figure 3. The cluster size in this material was found to range from 2 to 7 boron atoms.

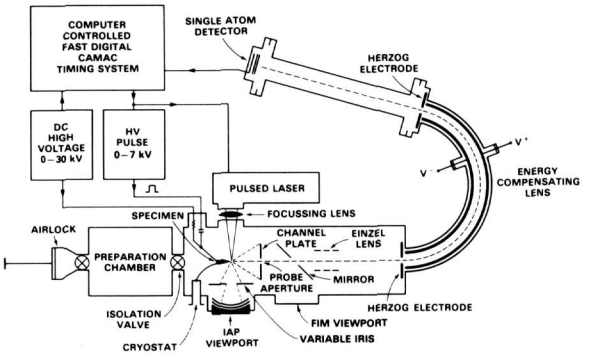

Figure 1. A schematic diagram of an atom probe field-ion microscope.

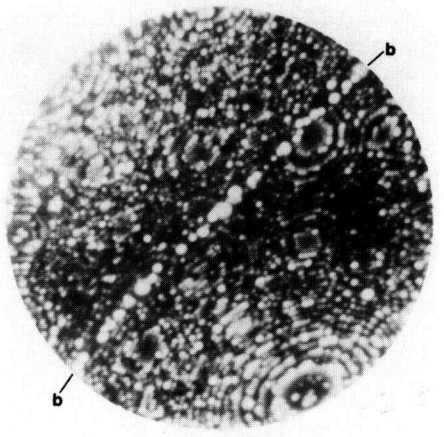

Figure 2. FIM micrograph of a boron-decorated boundary in rapidly solidified Ni–24.0 at. % Al–0.24 at. % B. Each bright spot is an individual boron atom.

Acknowledgment

Research sponsored by the Division of Materials Sciences, U.S. Department of Energy, under contract DE-AC05-84OR21400 with Martin Marietta Energy Systems, Inc.

References

[1] Miller, M. K., Inter. Mat. Rev. **32**, No. 5, (1987) in press.
[2] Horton, J. A., and Miller, M. K., Acta Metall. **35**, 133 (1987).
[3] Miller, M. K., and Horton, J. A., J. Phys. (1987) in press.

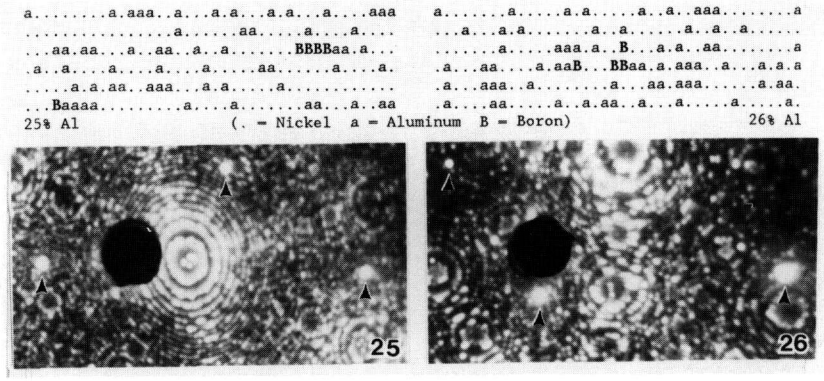

Figure 3. FIM micrographs and character plots of clusters in a Ni–25 at. % Al–0.48 at. % B and a Ni–26 at. % Al–0.48 at. % B. Each symbol in the character plots represents a single atom.

Volume 93, Number 3, May-June 1988
Journal of Research of the National Bureau of Standards

Accuracy in Trace Analysis

Imaging Microanalysis of Materials with a Finely Focused Heavy Ion Probe

R. Levi-Setti, J. Chabala, and Y. L. Wang

The Enrico Fermi Institute and
Department of Physics
The University of Chicago
Chicago, IL 60637

Scanning Analytical Heavy Ion Microscopy at High Lateral Resolution

Liquid metal ion sources (LMIS) in view of the quasi-point-like geometry of their emitting region and confined emission cone possess brightness ($\sim 10^6$ A cm^{-2} sr^{-1}) which is adequate for the realization of high current density (~ 1 A cm^{-2}), finely focused ($\geqslant 20$ nm) probes. A 40 keV scanning ion microprobe, which makes use of a Ga LMIS (UC-HRL SIM) is currently employed in our laboratory to obtain chemical maps of materials in a variety of interdisciplinary applications [1]. The instrument is composed of a two-lens focusing column, a high-transmission secondary ion energy analyzer and transport system, and an RF quadrupole mass filter for secondary ion mass spectrometry (SIMS). In addition, two-channel electron multiplier detectors, overlooking the target region, collect secondary electrons or ions for imaging of the surface topography and material contrast of a sample.

Although a lateral resolution of 20 nm has been attained, sensitivity considerations favor operation at somewhat larger (50–70 nm) probe size. The analytical image resolution is in fact critically dependent on the statistics of the mass analyzed signal [2], which in turn is determined by the rate of material removal by sputtering from the sample surface. Such a rate is proportional to the probe current, which decreases with the square of the probe diameter for chromatic-aberration-limited probes such as those extracted from LMIS. Thus at, e.g., 20 nm probe diameter, only 1–2 pA of probe current are available, the erosion rate is of the order $\sim 10^{-3}$ monolayers/s and probe-size resolution can only be attained for elements of high ionization probability which will provide the highest signal statistics over an acceptable recording time (>1 count/pixel in a 1024×1024 pixel scan for a 512 s acquisition time for the UC-HRL SIM).

In view of the well known range of ionization probabilities (ion fractions) among sputtered atomic species, as well as of sputtering yields, the attainable analytical lateral resolution of finely focused probes becomes target-species dependent due to the above considerations. It also follows that for species difficult to ionize, high resolution SIMS imaging microanalysis is altogether precluded, unless by recourse to postionization techniques [3].

Two examples of applications of the UC-HRL SIM to the study of materials will be illustrated in the present context.

Imaging Micro-SIMS of Aluminum-Lithium Alloys

SIMS techniques are uniquely suited to the study of Li because of the intense $^7Li^+$ signal emerging from fast ion bombardment of Li-containing materials. The high resolution imaging capability of the UC-HRL SIM can be fully exploited in this case, as demonstrated in preliminary studies of Al-Li alloys containing up to 12.7 at. % Li [4,5]. In these important alloys, the $^7Li^+$ signal is detected with a signal-to-noise ratio $\approx 10^5$, and it is feasible to image and identify grain boundary phases and precipitates in the <100 nm range of dimensions.

Samples of binary Al-Li alloys were solution treated for ~ 10 mins at 570 °C and water quenched. Some of the samples were then aged to give coarse distributions of either the equilibrium δ ($AlLi$) phase or a combination of δ and metastable $\delta'(Al_3Li)$. The samples were first mechanically polished and then electropolished to produce a flat surface for SIMS imaging.

A number of SIMS artifacts originating in the sample preparation process could be identified and subsequently avoided. These involve Li surface enrichment, surface oxidation and chlorine and carbon contamination. Sputter-cleaning of the samples *in situ* with a 2 kV Ar ion gun was generally necessary to obtain clean and artifact-free surfaces. An example of the detection of δ plates in Al-12.7 at. % Li aged 100 hours at 250 °C is shown in the $^7Li^-$ map of figure 1(a). The plates form in regular crystallographic orientations. A $^{34}AlLi^+$ image is shown in figure 1(b) where δ' particles (dark inclusions) are detected, showing distinctive morphologies that include dendritic growth and nucleation on dislocations. In the latter case, the Al-10.1 at. % Li sample was aged 4 hours at 290 °C.

Volume 93, Number 3, May-June 1988
Journal of Research of the National Bureau of Standards

Toward quantification, a calibration curve has been constructed from $^{7}Li^{+}/^{27}Al^{+}$ measurements performed on binary Al-Li alloys of known Li concentration. A linear relation between the $^{7}Li^{+}/^{27}Al^{+}$ ratio and the composition of the standard was observed, as shown in figure 2.

Imaging Micro-SIMS of Silicon Nitride Ceramics

Sintered silicon nitride is an advanced ceramic often used for high-temperature applications. The sintering process requires the addition of small amounts of oxides in a nitrogen overpressure to prevent dissociation above 1700 °C. Sintering agents such as MgO, Y_2O_3 and others, present in 1–10% weight concentrations, react with the silicon nitride phases and the secondary phases, which form along grain boundaries determine the mechanical properties of the ceramic.

Using the UC-HRL SIM, it has been feasible to obtain detailed mapping of the components of the interboundary phases in both yttria- and magnesia-doped silicon nitride [6]. Both fractured and polished surfaces of these ceramics can be readily analyzed in our microprobe, after coating with a thin (~5 nm) Au layer, which is rapidly sputtered away from the field of view under investigation.

In the case of Y_2O_3-sintered silicon nitride, the dominant interboundary phase is $YSiO_2N$, known to oxidize to $Y_2Si_2O_7$. SIMS mapping of these phases can be obtained for several break-up fragments such as Y^{+}, O^{-}, SiO_2^{-} and SiN^{-}. In addition differential resputtering of the implanted Ga^{+} probe ions provides detailed descriptions of the structure of the ceramic comparable to that which can be obtained with backscattered electrons. An example of the level of detail and resolution that can be attained in the imaging microanalysis of this ceramic is shown in figure 3. Figure 3(a) is a $^{69}Ga^{+}$ map, figure 3(b) a $^{89}Y^{+}$ map of the same fracture surface. The silicon nitride crystallites representing the ceramic matrix are clearly outlined in the Ga^{+} map, while the complementary Y^{+} map describes the distribution of the interboundary phase.

Quantification of the composition of the interboundary phase by SIMS is complicated by the presence of matrix effects and local ion yield enhancements in the presence of bound oxygen. Methods are being developed, based on image processing techniques, to perform vector scan microanalysis of either the matrix or the interboundary phases separately. Aided by suitable standards, it is expected that quantification on a microscale may become feasible by this approach.

Acknowledgments

This research was supported by the NSF Materials Research Laboratory at the University of Chicago, the Allied Signal Engineered Materials Research Center, and the National Science Foundation under Grant No. DMR-861 2254.

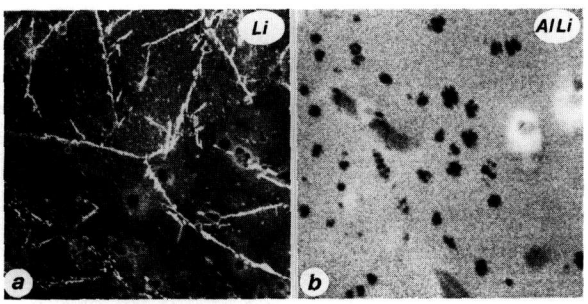

Figure 1. (a) $^{7}Li^{+}$ SIMS image of δ plates in Al-12.7 at. % Li alloy. 80 μm full scale. (b) $^{34}AlLi^{+}$ SIMS image of dendritic δ' particles in Al-10.1 at. % Li. 10 μm full scale.

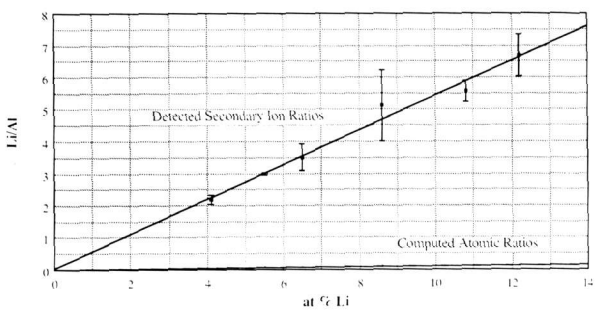

Figure 2. $^{7}Li^{+}/^{27}Al^{+}$ calibration obtained for the UC-HRL SIM from homogeneous as-quenched samples of binary Al-Li alloys.

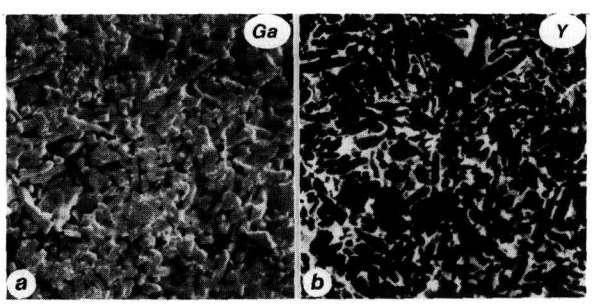

Figure 3. (a) Resputtered $^{69}Ga^{+}$ SIMS image of fracture surface of Y_2O_3-sintered silicon nitride ceramic, 20 μm full scale. (b) $^{89}Y^{+}$ image showing distribution of interboundary phase in same area as (a).

References

[1] Levi-Setti, R., Wang, Y. L., and Crow, G., Appl. Surf. Sci. 26, 249 (1986).
[2] Levi-Setti, R., Chabala, J., and Wang, Y. L., Scanning Micros. Suppl. 1, 13 (1987).
[3] Wang, Y. L., Levi-Setti, R., and Chabala, J., Scanning Microsc. 1 (1987).
[4] Williams, D. B., Levi-Setti, R., Chabala, J. M., and Newbury, D. E., J. Microsc. (1987) in press.
[5] Williams, D. B., Levi-Setti, R., Chabala, J. M., and Newbury, D. E., to be submitted to J. Microsc.
[6] Chabala, J. M., Levi-Setti, R., Bradley, S. A., and Karasek, K. R., Imaging Microanalysis of Silicon Nitride Ceramics with a High Resolution Scanning Ion Microprobe. Appl. Surf. Sci. (1987) in press.

Synchrotron Radiation Excited Fluorescence Micro-Analysis Using a New Imaging Technique

A. Knöchel, M. Bavdaz[1], N. Gurker[1], P. Ketelsen, W. Petersen, M. H. Salehi, and T. Dietrich

Universität Hamburg
Institut für Anorganische und Angewandte Chemie
Martin-Luther-King-Platz 6
D–2000 Hamburg, FRG

Introduction

The great importance and large field of applications the x-ray fluorescence analysis (XFA) found in the last decade are due to its extraordinary qualities. It is a very flexible method, it is nondestructive, fast and requires only a very simple sample preparation. It is not necessary to perform the analysis in vacuum, so samples containing volatile components pose no problem (e.g., biological and medical samples).

The penetration depth of x-rays ranges from a few μm up to several 100 μm and is thus much greater than that of electrons (used to excite the sample with scanning electron microscopy). The analyzed volume of the sample thus increases and results in a high sensitivity of the method. Additionally, x-rays cause much less radiation damage than corpuscular beams [1].

Using synchrotron radiation as a very powerful primary x-ray source, the sensitivity of the method is very high and is comparably good for all elements having $Z \geqslant 18$ [2,3]. Figure 1 shows the detection limits for synchrotron radiation excited x-ray fluorescence analysis (SYXFA). A 1 mg/cm^2 multielement sample was measured for 300 s using a beam diameter of 0.5 mm. The solid line indicates the detection limits measured using a white beam, the dotted line those using a graphite monochromator adjusted to eliminate the As-Kα/Pb-Lα interference.

The main advantages of applying synchrotron light as the primary radiation source in XFA could be summarized as follows:

- The high photon flux makes filtering, monochromatizing and masking of the primary beam feasible.
- A very broad continuous white spectrum allows simultaneous multi-elemental analysis featuring very good limits of detection (absolute $\geqslant 10^{-13}$ g, relative $\geqslant 0.1$ μg/g).
- Synchrotron radiation is linearly polarized in the storage-ring plane, thus improving the signal-to-noise ratio significantly.
- The source size is very small and the synchrotron beam is very well collimated, so a high spatial resolution is achievable (see later).
- Since the properties of synchrotron radiation are calculable, the evaluation of the measured data becomes easier and more reliable.

We are applying SYXFA to help solving different analytic problems that hardly could be approached with other methods. For example, we analyzed cosmic dust particles smaller than 10 μm in diameter to find out their composition. A second example is the analysis of the printing ink on very precious documents, including the 42-line bible by Gutenberg.

X-Ray Imaging

SYXFA becomes even more interesting if one succeeds in combining spatial resolving analysis with the high sensitivity of the method.

[1] Technische Universität Wien, Institut für Angewandte und Technische Physik, Karlsplatz 13, A-1040 Vienna, Austria.

X-ray imaging has experienced a renaissance in the last few years; microscopic details of specimens can now be imaged [4], but unfortunately only with soft x-rays. Zone plates show a low effective transmission (typically 10%) even in the soft x-ray region; for energies above 1 keV they are no longer applicable.

Reflecting optics also suffer from various difficulties; for use in microscopy, such optics are extremely complicated to make, since very high accuracies are required. The otherwise most promising multilayer reflection optics act as a relatively narrow band-pass filter and work only for a single defined x-ray energy.

We are therefore going another way to reach the goal of achieving high resolution imaging and still maintaining a good signal-to-noise ratio; using coded imaging techniques we are increasing the interaction area of the incident beam with the sample (fig. 2) [5–7]. Line-scanning increases the interaction area by the linear dimension of the measured image, and area-scanning enables us to irradiate up to 50% of the sample.

Line-scanning requires a linear and a rotational motion; the set of data-points measured at a given rotation angle is called a "profile." Figure 3 shows schematically the process of back-projecting the measured data [8]; the profiles have to be filtered prior to their backprojection in order to avoid reconstruction errors [9]. Since each data-point contains information about several sample-pixels, the loss of some data-points has very little influence on the resulting image.

An estimation of the relative errors in the reconstructed image is given in figure 4 (the signal area is defined as the percentage of the sample area contributing to the signal; 0/1-contrast was assumed).

The experimental set-up is outlined in figure 5. Several stops reduce the scattered radiation; the total-reflecting mirror is used to cut off x-rays that are too hard. The slit-aperture (No. 4 in fig. 5) is made very accurately and has a width down to 2 μm. The alignment of the rotation axis of the sample has to be adjusted very carefully with respect to the synchrotron-beam axis. Both axes have to be parallel better than a few tenths of an arc minute.

Figure 6 compares an image measured by line-scanning to another measured by conventional point-scanning. In both cases the sample was measured under the same conditions (geometry, measuring time, filtering, parameters of electronics and accelerator).

Discussion

By applying the line-scanning technique to scan the sample, it was possible to reach spatial resolutions down to 3 μm with SYXFA, still being able to measure trace elements. Nevertheless, this is a very demanding technique. A synchrotron radiation laboratory is necessary, a computer is needed to decode (backproject) the measured data, and a very tricky alignment of the experiment has to be performed.

Considering the fascinating properties of this SYXFA-microprobe, many interesting fields of applications promise interesting results, e.g., aerosols, pigments of printing-ink on historic documents or oil paints on canvas, blood particles, diffusion processes and structured multilayers (e.g., electronic circuits).

The experiments were generously supported by the "Bundesministerium für Forschung und Technologie." Thanks are due to the HASYLAB-team for their professional assistance.

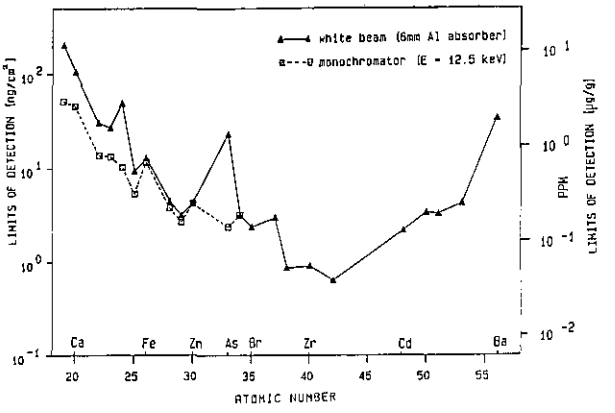

Figure 1. Detection limits for SYXFA [2].

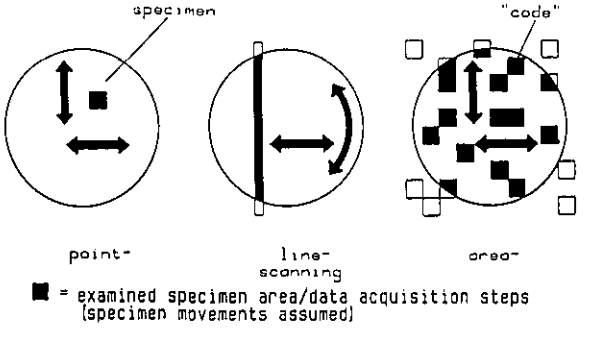

Figure 2. Different methods of x-ray scanning [7].

Volume 93, Number 3, May–June 1988
Journal of Research of the National Bureau of Standards

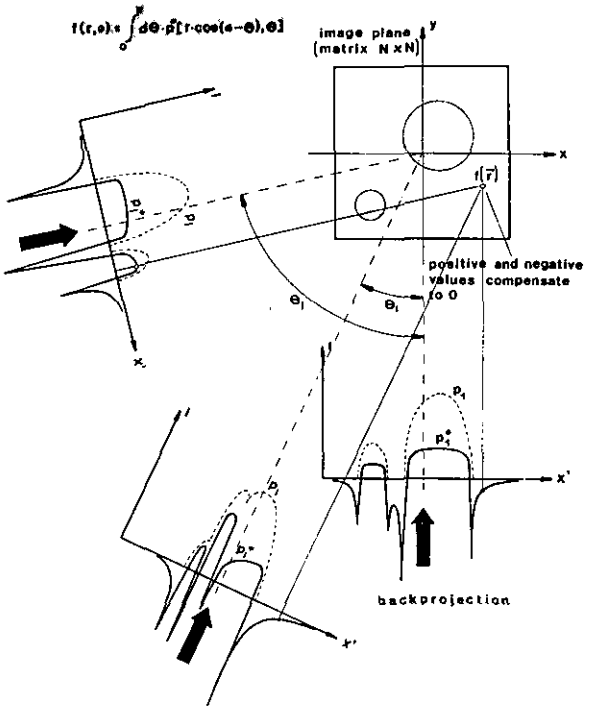

Figure 3. Filtered backprojection [8].

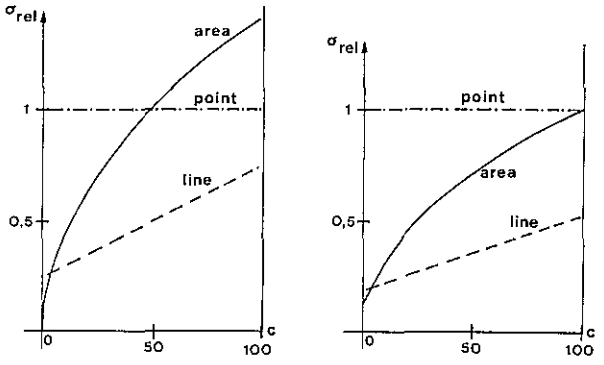

Figure 4. Estimated errors (σ_{rel}) in reconstructed images versus signal area (c,%) for different scanning methods (for the right plot the presence of a constant background was assumed).

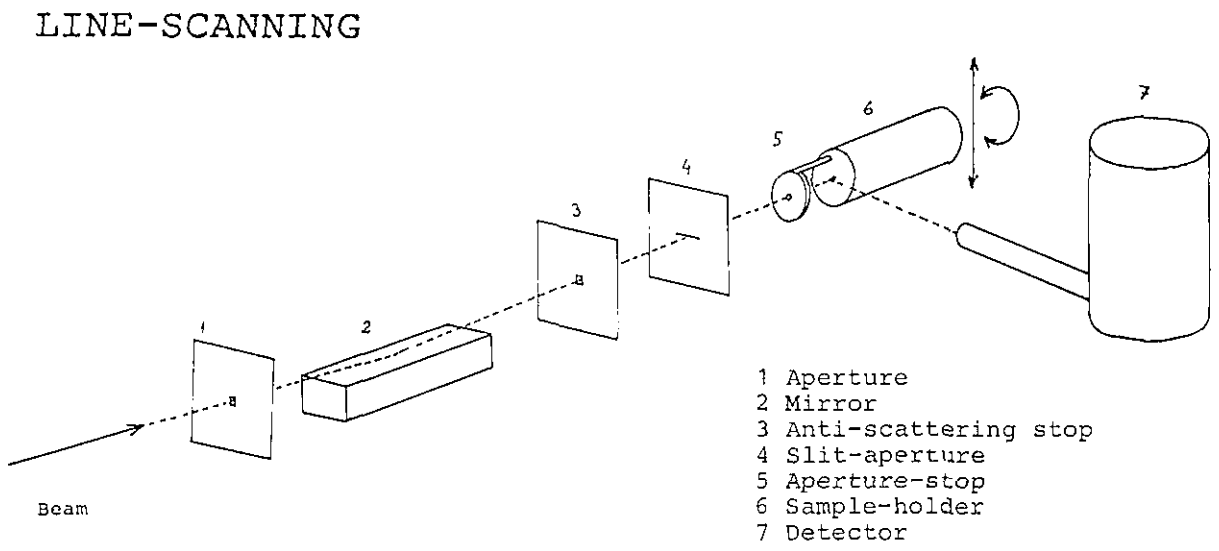

Figure 5. Experimental setup.

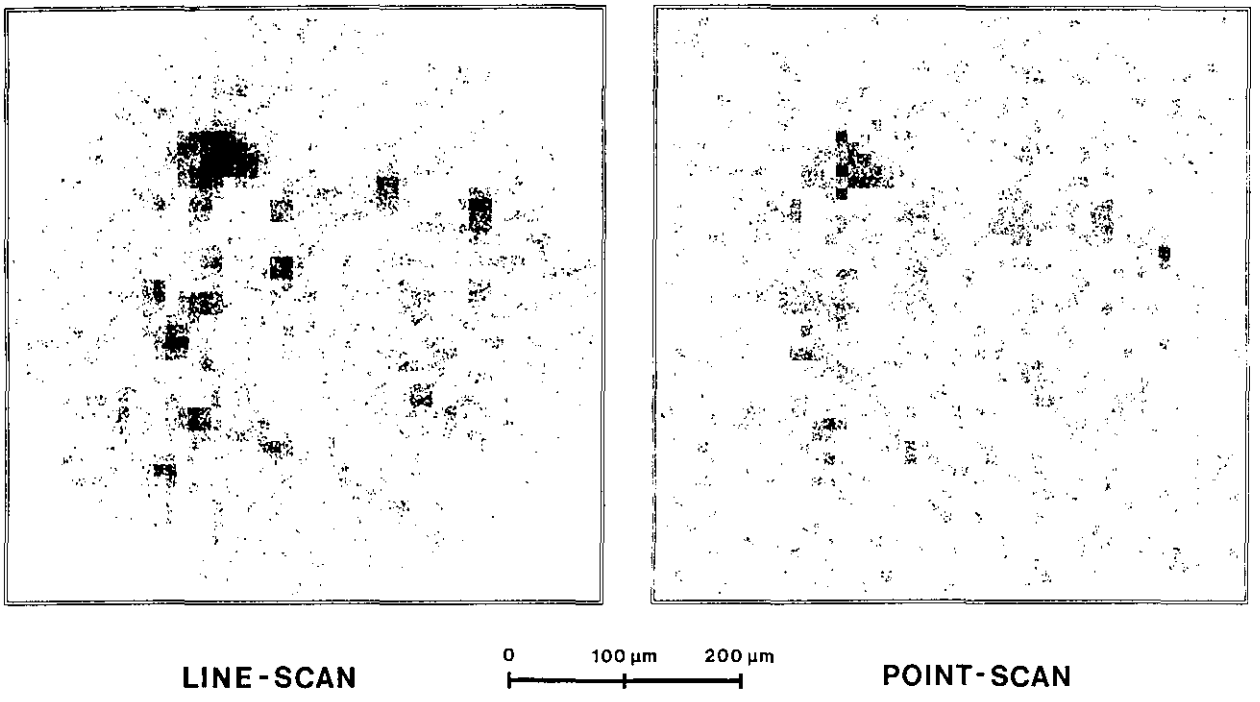

Figure 6. Comparison: line- and point-scanning (experimental; Sn grains in organic polymer matrix).

References

[1] Slatkin, D. N., Hanson, A. L., Kraner, K. W., Warren, J. B., and Finkel, G. C., Nucl. Instr. Methods **227**, 378 (1984).
[2] Petersen, W., Ketelsen, P., Knöchel, A., and Pausch, R., Nucl. Instr. Methods **A246**, 731 (1986).
[3] Knöchel, A., Petersen, W., and Tolkiehn, G., Anal. Chim. Acta **173**, 105 (1985).
[4] Niemann, B., Rudolph, D., and Schmahl, G., Nucl. Instr. Methods **208**, 367 (1983).
[5] Gurker, N., X-Ray Spectrometry **8**, 149 (1979).
[6] Gurker, N., Advances X-Ray Anal. **30**, in press.
[7] Gurker, N., X-Ray Spectrometry **14**, 74 (1985).
[8] Gurker, N., Advances X-Ray Anal. **23**, 263 (1980).
[9] Herman, G. T., Image Reconstruction from Projections: The Fundamentals of Computerized Tomography, Computer Science and Applied Mathematics, Academic Press, New York (1980).

Direct Solids Analysis Using Sputter Initiated Resonance Ionization Spectroscopy (SIRIS)

J. E. Parks, M. T. Spaar, and L. J. Moore

Atom Sciences, Inc.
114 Ridgeway Center
Oak Ridge, TN 37830

W. M. Fairbank, Jr.

Department of Physics
Colorado State University
Fort Collins, CO 80523

and

J. M. R. Hutchinson

Center for Radiation Research
National Bureau of Standards
Gaithersburg, MD 20899

Direct, determination of trace chemical species in solids is a fundamental analytical problem. The need to measure trace and ultra-trace concentrations of species in solids requires a method that is free of matrix effects and can be carried out with minimal contamination. Sputter Initiated Resonance Ionization Spectroscopy (SIRIS) is such a method, allowing a minimum of chemical pretreatment, the chief source of contamination, and providing a highly selective and sensitive measurement of essentially any element. SIRIS is an ultrasensitive analysis technique which uses an energetic ion beam to sputter a solid sample and Resonance Ionization Spectroscopy (RIS) to selectively and efficiently ionize neutral atoms of the element of interest in the atomized cloud. RIS and SIRIS have been adequately described elsewhere [1]. A primary advantage of SIRIS technology is the potential to reduce or eliminate the matrix effect in direct solids analysis by utilizing the predominant neutral population produced by primary ion bombardment. Since the origination of the patented SIRIS technology in 1981, numerous matrix types have been analyzed for a variety of elements. We have found that for metals, semiconductors, and alloys, trace elements can be quantitated interference-free over a broad range of concentrations by using a single point calibration. Complex matrices, such as biological or geological specimens, generally require internal standardization with separated isotopes.

We have reported [1] sensitivities for SIRIS as low as 2×10^{-9} (atom fraction) and demonstrated linearity down to the ppm level with aluminum, vanadium, boron, copper, silicon, and selenium in standard steel samples from the National Bureau of Standards. The SIRIS measurements showed good linearity with certified values, and the relative signals from the different elements were in good agreement with the standard values.

The principal results to be reported here come from using SIRIS to investigate the spatial distribution of trace elements in specially fabricated crystals or devices. Since the ion beam is pulsed (at 30 Hz and with 1 microsecond duration) during a measurement, only about an equivalent monolayer of material is sputtered away, and the analysis pertains strictly to the surface. However, use of the unpulsed beam can remove material rapidly (ion milling), and thus provide a profile of the element being measured with depth into the sample.

Figure 1 shows a SIRIS depth profile measurement of silicon-29 implanted into gallium arsenide. The SIRIS measurements were normalized to the known peak concentration of 5×10^{18} atoms/cm^3 and the depth scale was calibrated by measuring the sputtered crater with a Dektak profilometer. The profile is compared to LSS theory [2] and shows good agreement at depths near the peak concentration. At larger depths the agreement is poorer, the measurement showing higher concentrations than predicted by theory. This has been explained by Shepherd [3] to be the result of

Table 1. *Results of isotope dilution experiments with samples of Rocky Flats soil, phosphate ore, and graphite.* Samples were spiked with isotopes of U-235 and U-238 in the forms of both nitrates and oxides

Composition	Molecular form of U-235 spike	Molecular form of U-238 spike	Normalized SIRIS response	Normalized isotope ratio response
100% graphite	nitrate	nitrate	9.31	0.99
Soil with 15.2% graphite	nitrate	nitrate	3.43	1.03
100% graphite	nitrate	oxide	1.92	1.15
Soil with 19.2% graphite	nitrate	oxide	0.64	1.04
100% graphite	oxide	oxide	1.44	1.11
Soil with 23.1% graphite	oxide	oxide	0.67	1.16
Ore with 39.7% graphite	nitrate	ore	0.16	0.95
Ore with 74.8% graphite	nitrate	ore	1.52	0.72

channeling of the Si during implantation. He was able to avoid this effect by amorphising the gallium arsenide crystalline material before implanting. Our samples were not pre-amorphised and channeling was possible. Backgrounds near 1×10^{15} atoms/cm^3 were demonstrated.

The matrix independence feature makes SIRIS highly desirable for the analysis of layered materials where measurements are made as a function of depth and the analysis proceeds from one material through an interface into an adjoining material. A layered sample of gallium arsenide and aluminum gallium arsenide, (GaAs/AlGaAs/GaAs), grown by MBE and doped with silicon, was depth profiled with SIRIS. Figure 2 shows the makeup of the sample and a measurement of the aluminum concentration versus depth. This indicates a 150 Å depth resolution, consistent with the 10 keV argon ion beam used for sputtering. The depth scale was determined with the profilometer and the aluminum measurement shows that the position of the aluminum layer is in agreement with the stated composition. Figure 3 shows the depth profile of the silicon dopant in this sample. The silicon concentration in the top layer of GaAs was determined electrically, based on the sum of the N and P type carriers, to be 2×10^{18} atoms/cm^3. The electrical concentration is known to be different from the physical concentration, but the ratio of the physical concentration in the GaAs and AlGaAs layers was known from the MBE parameters to be 0.77. The ratio of the silicon concentrations in the AlGaAs layer to that in the GaAs layer was found to be 0.77 which was fortuitous since the SIRIS measurements have a precision of about 10%. The profile indicates that the silicon concentration changes at a depth consistent with the position of the interface indicated in the stated composition, and no discontinuities in the signal were observed at the interface.

The data of table 1 illustrate a different kind of analytical problem in a solid sample, the determination of a trace constituent, not in a simple, macroscopically homogeneous sample, but in a complex, heterogeneous mess, an unseparated soil or ore sample. Since admixture with graphite was used to reduce sample charging in the soil/ore samples, one set of measurements was made on graphite itself. It is clear that the absolute signal from (one isotope of) the uranium cannot be used to quantify the composition; the signal varies by about a hundred-fold over the three types of samples. However, an internal standard can be used satisfactorily, as evidenced by the nearly constant relation between the as-prepared and measured isotope ratios.

Acknowledgments

This work was supported in part by Air Force Wright Aeronautical Laboratories, Aeronautical Systems Division (AFSC), United States Air Force, Wright-Patterson AFB, OH 45433 and Electronic Systems Division, Air Force Systems Command USAF, Hanscom AFB, MA 01731. This work was also supported in part by the National Bureau of Standards.

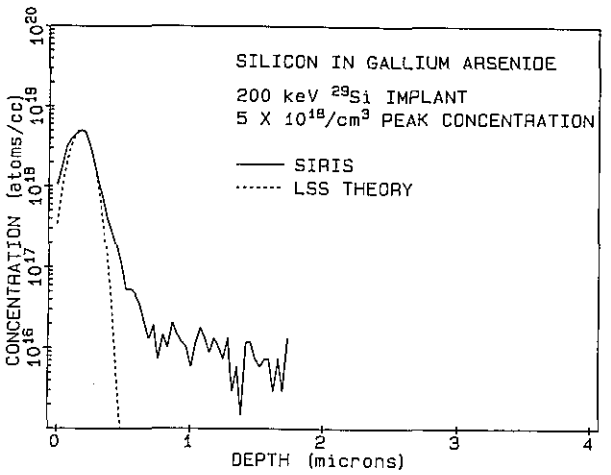

Figure 1. SIRIS depth profile of 200 keV silicon-29 ions implanted into gallium arsenide and compared with LSS theory.

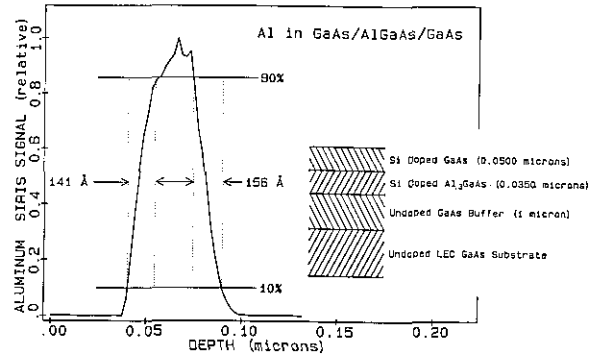

Figure 2. Composition of silicon doped, layered sample of GaAs/AlGaAs/GaAs and the aluminum concentration profile measured with SIRIS.

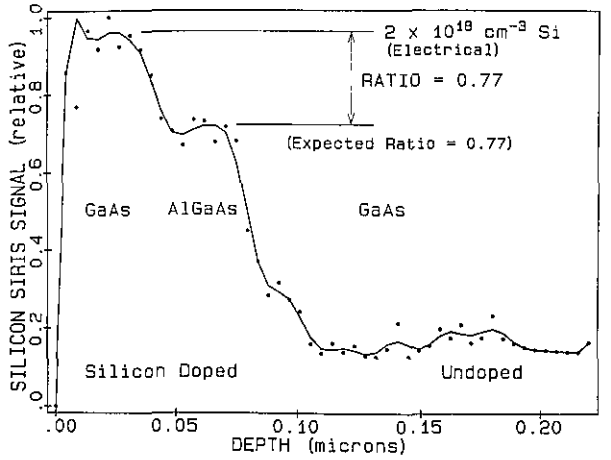

Figure 3. SIRIS silicon concentration profile in layered sample of GaAs/AlGaAs/GaAs.

References

[1] Parks, J. E., Optics News **12**, 22 (1986) and refs. therein.
[2] Lindhard, J., Scharaff, M., and Schiott, H. E., Mat. Fys. Medd. Dan. Vid. Selsk. **33**, No. 14 (1963).
[3] Shepherd, F. R., Vandervorst, W., Lau, W. M., Robinson, W. H., and SpringThorpe, A. J., in Secondary Ion Mass Spectrometry SIMS V, ed., by A. Benninghoven, R. J. Colton, D. S. Simons, and H. W. Werner (Springer, New York 1986).

Volume 93, Number 3, May–June 1988
Journal of Research of the National Bureau of Standards

Materials Analysis

The Accuracy of Surface Analyses

C. J. Powell

Surface Science Division
National Bureau of Standards
Gaithersburg, MD 20899

1. Introduction

Surface analysis is being increasingly used for a great variety of scientific and technological applications [1,2]. The composition of the outermost or several outermost atomic layers of a selected region on a specimen surface is frequently measured. It is also possible to measure the compositional variations with position on the surface and, in conjunction with removal of surface layers by ion bombardment, to obtain composition-versus-depth information. Such analytical information is often critical for the solution of a wide range of problems.

While many of the applications of surface analysis have been successful in fulfilling their intended purposes, there have been many difficulties in achieving high accuracy, as will be described below. The precision (repeatability) of many surface analyses is generally satisfactory for most purposes (often 1% and sometimes better). The precision depends largely on the extent of uniformity of different regions of a specimen surface (if replicate measurements are made), instrumental stability, the statistical quality (signal-to-noise ratio) of the acquired data, and the extent of specimen change during data acquisition. Specimen surfaces may change in composition during measurements due to decomposition or diffusion induced by the incident radiation; the composition may also change due to adsorption of molecules from the ambient vacuum, to segregation from the bulk (particularly if the surface is heated), or to differential sputtering effects on ion-bombarded surfaces. Thus, gains in precision obtained by increasing the measurement time may be offset by a loss of analysis accuracy if the surface composition changes. A similar problem arises with attempts to measure the composition of small regions with highly focused incident beams; as the beam diameter is decreased, the beam current is reduced and it can be counterproductive to increase the signal (sensitivity) by increasing the measurement time on account of beam-induced damage to the specimen.

A brief summary is given here of the many factors that can limit the accuracy of surface analyses made with the techniques in common use (Auger-electron spectroscopy (AES), x-ray photoelectron spectroscopy (XPS), and secondary-ion mass spectroscopy (SIMS)). Additional details are given elsewhere [2,3].

2. Factors Affecting the Accuracy of Surface Analyses

It is unfortunately not often possible for the average analyst to make credible claims for the accuracies of surface analyses made on practical materials. There are many factors which both complicate any analysis and make statements of systematic error (bias) either impossible or extremely difficult. Such factors can be classified as follows.

2.1 Specimen Complexity

It is often implicitly assumed that a specimen is compositionally homogeneous over the volume probed in the measurement. Many specimens, however, are inhomogeneous, as illustrated schematically in figure 1. Since surface-analysis techniques are sensitive to the outermost few atomic layers, it is necessary to characterize the variation of composition with depth on an atomic scale in order to ensure that observed spectral intensities can be meaningfully converted to elemental concentrations.

The surfaces of practical specimens are unlikely to be smooth, either on a microscopic or a macroscopic scale. Details of the surface topography (as well as local defects) can affect particle transport and the relative intensities of different spectral features. Similarly, complex specimen geometries (e.g., impurity particles, the presence of islands in deposited films, or thin lines on microelectronic

devices) may require an appropriate model calculation in order to drive a composition from observed signals.

If the specimen material is a single-crystal (or an epitaxial film on a single-crystal substrate), the angular distributions of emitted electrons (in AES or XPS) or ions (in SIMS) can be anisotropic. Changes of observed intensities of ~30% in AES have been found when the incident beam was deflected from one grain to another in a polycrystalline specimen or when the angle of incidence was varied [4,5]. Analyses of such transport anisotropies are complex.

2.2 Instrument Performance

It is clearly important that the intensity scale of an instrument be linear and change in known ways if instrumental parameters are varied. An early XPS laboratory intercomparison showed variations in intensity ratios for the major peaks in each of two pure metals of up to a factor of 10, a result attributed in part to erratic instrument performance [6]. A later XPS intercomparison showed an order of magnitude improvement [7] that was presumably due to instrumental advances. An instrument should also "view" a well-defined region of the specimen, particularly if there are compositional inhomogeneities in the plane of the specimen. Figure 2 nevertheless indicates how an XPS analyzer can view different specimen areas depending on the selected operating parameters [8]; such variations in observed specimen area need to be known when comparing intensities at different electron energies.

Modern instruments are typically supplied with computer systems and proprietary software developed by the manufacturer. Instrument automation has many advantages, but the software may have limitations that can cause unsuspected inaccuracies in an analysis [2]. An example of such a limitation is the use of oversimplified (yet convenient) methods for background determination and thus for intensity measurement in AES and XPS. It is usually difficult for an analyst to make desired changes to software.

2.3 Lack of Needed Reference Data and Reference Materials

Spectral lineshapes (in AES and XPS) and intensities (in AES, XPS, and SIMS) for a particular element often depend on the matrix in which the element is found. Individual parameters important in observed matrix effects are electron attenuation lengths and inelastic mean-free paths (AES, XPS), back-scattering factors (AES), ion neutralization cross sections (SIMS), and sputtering rates (SIMS). The magnitudes of the matrix effects on these individual parameters and on spectral intensities (sensitivity factors) need to be either documented or calculated from theory. A review of data compilations needed in AES and XPS has been published by Seah [9].

One of the most important matrix corrections in AES and XPS involves the electron inelastic mean-free path (IMFP). Accurate IMFP measurements are difficult to make and there has been considerable uncertainty over the IMFP dependence on electron energy and material. Figure 3 shows results of new IMFP calculations for 27 elements and 4 compounds and indicates the IMFP range that can be encountered [10].

Reference materials are needed for calibration of instrumental energy (AES, XPS) and intensity scales, demonstration of detection sensitivity, calibration of depth scales in sputter-depth profiling (SDP), and optimization of profiling parameters in SDP. A recent article gives details of the limited number of reference materials now available for these purposes [11].

3. Summary

The accuracy of surface analyses generally depends on the particular sample, the analysis technique, the analytical procedure, and the particular measuring instrument. Much useful progress has been made in recent years in developing improved methodologies and in providing needed reference data, reference materials, and reference procedures [12]. Surface analysts still need additional assistance in these areas to ensure that analyses of known accuracy can be made routinely.

Volume 93, Number 3, May–June 1988
Journal of Research of the National Bureau of Standards

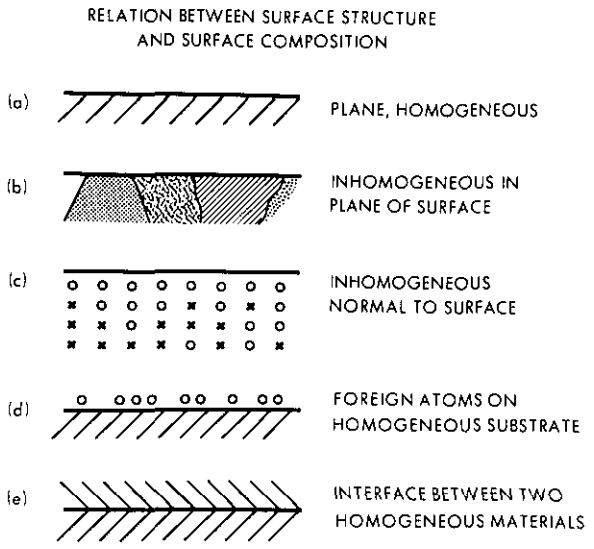

Figure 1. Idealized surface morphologies: (a) plane homogeneous surface; (b) a surface with lateral inhomogeneities consisting of several different surface phases; (c) a surface with depth inhomogeneities (the circles and the crosses represent different types of atoms); (d) a surface phase consisting of a submonolayer of foreign atoms on an otherwise homogeneous surface; and (e) an interface between two homogeneous bulk phases [3].

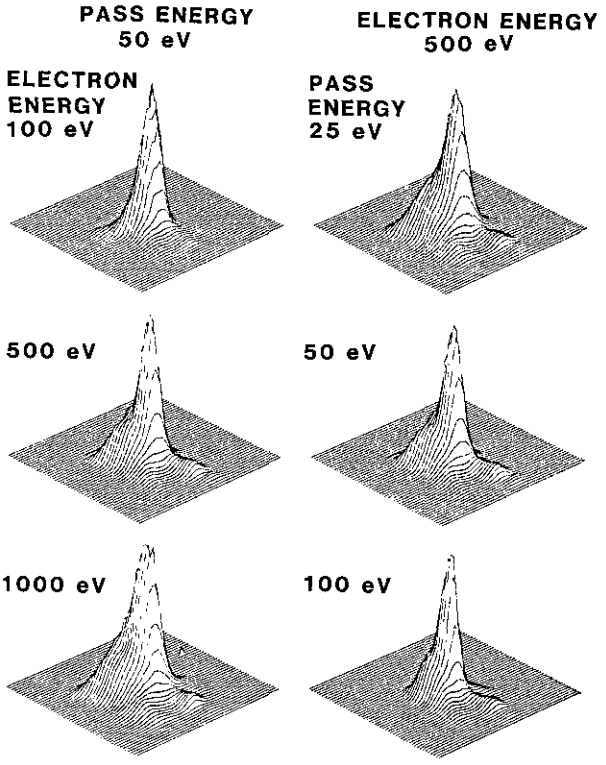

Figure 2. Images recorded with a double-pass cylindrical-mirror analyzer to show the specimen areas contributing to the detected signal for the indicated conditions of analyzer pass energy and electron kinetic energy. The horizontal (bottom left to right) distance is 13 mm and the vertical distance is 15 mm.[8].

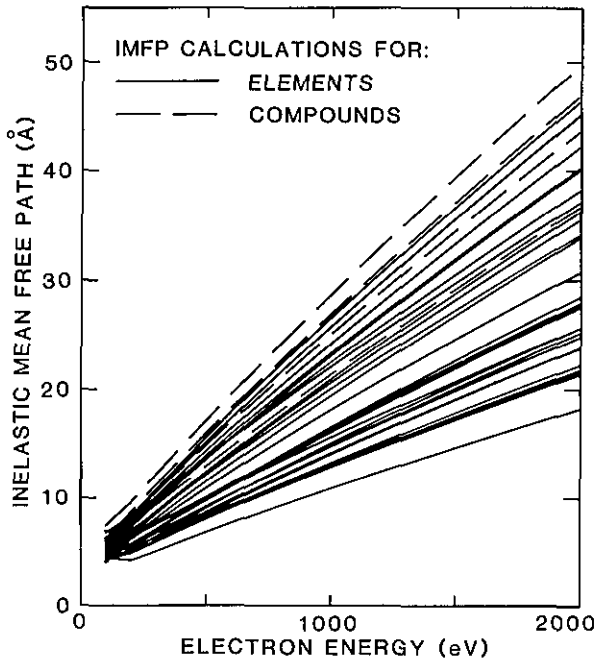

Figure 3. Plots of calculated electron inelastic mean-free paths versus electron energy for 27 elements (solid lines) and 4 compounds (dashed lines) [10].

References

[1] Powell, C. J., Aust. J. Phys. **35**, 769 (1982).
[2] Powell, C. J., Appl. Surf. Sci. **4**, 492 (1980).
[3] Powell, C. J., J. Vac. Sci. Tech. A **4**, 1532 (1986).
[4] Bishop, H. E., Chornik, B., Le Gressus, C., and Le Moel, A., Surf. Interface Anal. **6**, 116 (1984).
[5] Doern, F. E., Kover, L., and McIntyre, N. S., Surf. Interface Anal. **6**, 282 (1984).
[6] Powell, C. J., Erickson, N. E., and Madey, T. E., J. Electron. Spectrosc. **17**, 361 (1979).
[7] Seah, M. P., Jones, M. E., and Anthony, M. T., Surf. Interface Anal. **6**, 242 (1984).
[8] Erickson, N. E., and Powell, C. J., Surf. Interface Anal. **9**, 111 (1986).
[9] Seah, M. P., Surf. Interface Anal. **9**, 85 (1986).
[10] Tanuma, S., Powell, C. J., and Penn, D. R., Surf. Sci. (in press).
[11] Powell, C. J., Electronic Materials and Processes, edited by N. H. Kordsmeier, C. A. Harper, and S. M. Lee, Society for the Advancement of Material and Process Engineering, Covina, CA (1987), p. 252.
[12] Powell, C. J., Surf. Interface Anal. (in press).

Depth Profiling of Trace Constituents Using Secondary Ion Mass Spectrometry

Charles W. Magee

EVANS EAST, Inc.
The Office Center, Suite 1236
666 Plainsboro Road
Plainsboro, NJ 08536

Secondary ion mass spectrometry (SIMS) offers unique capabilities for in-depth elemental characterization of thin solid films. SIMS utilizes a beam of keV-energy ions to sputter off the outermost atomic layers of a sample. By performing mass/charge analysis of the ion population of these sputtered particles, one can determine the elemental composition of the sample surface. Since the instantaneous surface recedes into the bulk as sputtering continues, monitoring of the sputtered ions as a function of time yields in-depth concentration profiles of the detected elements. The technique is capable of detecting all elements—hydrogen through uranium—with sub part-per-million sensitivity for most elements. The technique is capable of depth resolution in the 50–100 Å range even at depths greater than 10,000 Å. SIMS, since it is a mass spectrometric technique, can also yield isotopic information, and can be made quantitative through careful instrument operation and use of standards.

Unfortunately, the raw data from a SIMS depth profile are of little use in solving problems. The depth scale of a depth profile obviously depends on the sputtering rate of the material being analyzed. However, the rates at which samples are sputtered by the primary ion beam vary widely with material and sputtering conditions (e.g., ion energy, ion species, angle of incidence) and must be measured for each set of samples being analyzed. This is easily accomplished after the analysis by measuring the depth of the sputtered crater by profilometry and equating sputtering time to sputtered depth.

Transforming a secondary ion intensity into an elemental concentration is somewhat more difficult. Because elemental sensitivities in a given matrix can vary by six orders of magnitude, and given the fact that a given element's sensitivity can vary over several orders of magnitude depending upon

the matrix in which it is found, standards are needed for virtually all elements in the matrix to be analyzed. Fortunately since SIMS is an inherently linear technique with small backgrounds, only one standard per element is required. Standards made by ion implantation are particularly good for SIMS because the number of impurity atoms added to the matrix is very accurately known (usually to within 1–2%), and virtually any element can be implanted into virtually any matrix. Using these methods, elemental concentrations in a SIMS depth profile can be measured to within 10–20% on a routine basis, and accuracies of better than 5% are possible. Depth scales on SIMS depth profiles can be measured to better than 5% given a standard of sufficient accuracy with which to calibrate the profilometer. Accuracies of this order in both concentration and depth are necessary in many semiconductor applications. Junction depths (depths into the semiconductor at which both p- and n-type dopants are of equal concentration) can be obtained from SIMS depth profiles, as well as areal densities of dopants (measured in atoms/cm^2 calculated by integrating the area of the profile of atoms/cm^3 vs depth in cm). Accuracies of a factor of two are not sufficient for these exacting applications.

Applications

Determination of total areal densities of dopants in semiconductors is often needed. Whether determining dopant areal densities of diffused species for use with electrical measurements (e.g., spreading resistance), or determining total retained dose of an ion-implanted sample which has undergone subsequent thermal processing, the high sensitivity of SIMS combined with its excellent depth resolution make it the clear technique of choice for these kinds of analyses.

SIMS is also the technique of choice in certain applications requiring highly accurate, high sensitivity analyses but without the need for depth resolution (e.g., a bulk analysis). One such example is the determination of oxygen grown into highly doped silicon boules. In normal Si material, which is grown doped p- or n-type at approximately 0.1 ppma, the oxygen concentration is usually measured by FTIR using ASTM procedure F121-80. Oxygen levels are of the order of 15 ppma. However, in highly doped material used for latch-up resistant CMOS circuits, the FTIR method cannot be used, yet the oxygen content of this material must be very rigidly controlled. SIMS has been shown to be able to determine the oxygen content in highly doped wafers of this type with accuracies of 10% relative at the 15 ppma level with counting statistics of better than 1%.

Semiconductor samples serve well to illustrate the extreme sensitivity of the SIMS technique. A depth profile was taken on a sample of GaAs which had been ion implanted with Si at an energy of 70 keV to a dose of 4.5E12/cm^2. Such a sample is quite commonly used in microwave technology. The profile of the implanted Si had a maximum concentration of only 10 ppma and was detected down in concentration to approximately 20 ppba. The truly remarkable fact about this analysis was that the data were taken from an area on the sample 200 micrometers square, and data were taken in depth increments of 20 Å. This resulted in an analyzed volume per data point of only 1E-10 cc or 1E-7 microliters in terms more familiar to organic chemists. In this extremely small volume, however, the sought-for-constituent was present at only 20 ppba, resulting in a detected amount of Si per data point of only 1E5 atoms, or 2E-19 moles, again in terms more familiar to organic chemists. There are very few other analytical techniques commonly practiced today which exhibit this kind of elemental sensitivity.

The excellent depth resolution of SIMS in combination with its sensitivity have made it indispensable in understanding the subtleties of ion implantation into semiconductors. Long ago SIMS showed that the depths of penetration of ions into silicon were not as predicted by early theoretical models. Subsequent models (e.g., SUPREM-III from Stanford University) have actually used SIMS depth profiles to refine their predictions of what the in-depth distribution of the implanted species should be. It was also shown by SIMS how an appreciable fraction of the implanted ions are guided into the channels between the rows of atoms in the single crystal samples used in the semiconductor industry. This caused the actual depth distribution of the implanted ions to be quite different from that calculated by even the newest models used to predict ion-implant profiles. SIMS also showed how this unwanted "ion channeling" effect could be eliminated by rendering amorphous by ion bombardment the near-surface region of the crystal in which the ion implant was to reside. This has recently proven very important as device engineers try to keep the implanted dopants very

close to the crystal surface which is important as dimensions of transistors shrink.

Conclusion

It is hoped that the reader has acquired some appreciation of the problems, yet power of quantitative depth profiling using secondary ion mass spectrometry. The technique needs standards to obtain the accuracy needed for most of the applications at which it has excelled, and no doubt, this is a serious problem. Yet, in the field of analytical chemistry there exist very few techniques which exhibit quantitative accuracies in the 10–20% range without the use of standards, (techniques such as atomic absorbtion certainly require standards). These problems with quantitation are more than made up for by the technique's sub-ppm sensitivity, and universal applicability in terms of both sample type and elemental coverage, especially when one considers that this degree of sensitivity and accuracy is obtainable with depth resolution in the 50–100 Å range.

Relative Sensitivity and Quantitation in Glow Discharge Mass Spectrometry: A Progress Report

J. C. Huneke

Charles Evans & Associates
301 Chesapeake Drive
Redwood City, CA 94063

Recent availability of commercial glow discharge mass spectrometer (GDMS) instrumentation, and the increasing industrial use of GDMS for bulk trace element characterization have necessitated rapid progress in understanding the systematics and requirements of GDMS analysis. GDMS approaches the ideal instrument for broad spectrum trace element analysis to ppbw levels. In the GDMS source the sample is the cathode for a dc discharge supported by 1 Torr of Ar or other gas. The composition of the atoms sputtered from the sample surface is the same as the bulk solid, providing a representative pool of atomized material for further analysis. Atoms are ionized in the plasma mainly by collision with metastable Ar atoms with energy levels near 11.5 eV, which is sufficient to ionize all but a few elements. Sputtered atoms diffuse through the plasma to the walls of the chambers, and ions formed near the exit orifice and leaving the chamber are mass analyzed and the mass separated ion currents measured. Ion currents out of the source are stable and high, and a few ion counts of an element can correspond to concentrations of less than a ppbw. For example, it has been determined that Fe present in Cu at a level of 5 ppbw can easily be measured to a precision of 10%.

With a few exceptions, GDMS ion yields vary by only an order of magnitude over the whole periodic table. Simple elemental survey analyses of solids can be provided by GDMS which are accurate to within the order of magnitude variation of relative GDMS yields. However, if material must be qualified within specified impurity limits or more accurate elemental contents are required, better measurement becomes essential and accurate relative sensitivity factors must be determined. There are no adequate theoretical or semi-empirical models of ion production out of the GDMS source yet available. Nor is there a good understanding of the effects of variations of physical factors on ion yield (i.e., pressure, discharge voltage and current, sample cell geometry, plasma gas composition). Relative elemental sensitivities must be determined by analysis under similar conditions of a standard material.

There are several constraints on appropriate standard material for the relative sensitivity determinations: (1) The full element survey capability of GDMS requires the widest possible element coverage for a specific matrix type, preferably within a single sample. (2) The ability to measure precisely elements present to the 10 ppbw level, coupled with the fact of analytical back contamination of 1E-3 to 1E-6 of the previous sample, requires accurate standard concentrations of 1–10 ppmw or less. (3) To ensure representative sampling suitable dopants are those dissolved in the matrix and not exsolved to grain boundaries or incorporated in separate phases since elements present in different phases may be sampled at different rates. (4) The physical shape of the standard and analytical samples must be similar to assure similar discharge conditions. (5) Standards must be characterized for sampling on the scale of 10–50 mm^2 surface area at a rate of 1 μm/min.

Since commercial GDMS is recent, standards generated for other methods must be used. Typically, available standards useful for GDMS characterization are designed (1) for analysis of larger areas, (2) for techniques less susceptible to heterogeneous distributions in multiphase assemblages, (3) are not particularly well characterized for elements below 10–100 ppmw concentration, and (4) are limited in the variety of dopant/matrix combinations.

The pattern of relative GDMS yields from an Ar plasma has been established using available standards, which are generally accurate to better than 10% for elements present at 10 ppmw or greater concentration. (Relative sensitivity factors as normally defined for quantitation purposes are the inverse of the relative GDMS yield illustrated in fig. 1.) There is a pronounced trend in yields across the group b transition elements, decreasing by an order of magnitude from high yields in groups 3b–5b to low yields in groups 1b–2b. The trend is general and not monotonic. A similar but separate trend is also observed for group a elements.

Relative GDMS yields determined using different standards of the same metal agree well within stated concentration errors, demonstrating an accuracy of GDMS analysis of 10–20%. Relative GDMS yields determined on the same metals but in a different laboratory (same manufacture of instrument) are generally quite comparable, but there are systematic differences by factors of two or three in the more electronegative elements, differences which are not well understood. Relative yields appear to be moderately sensitive to power levels and especially sensitive to plasma pressure. Until interlaboratory differences are resolved, relative GDMS yields determined on one instrument are accurate to no better than a factor of two for use on a comparable instrument.

The relative GDMS yields determined from a variety of standard metals (Al, Cu, Zn, Steel) typically agree within 30%, with Ni and Zn in Cu as notable exceptions indicating possible certification problems. The GDMS measurement is indeed matrix independent, as well as presently can be determined, and relative GDMS yields for application to one type of matrix can be reliably determined from a different standard type. The differences in the relative yield determinations from different metals may be due in no small part to the segregation of many of the elements into separate phases (clearly observed by SIMS imaging) with the consequence that sampling is not entirely uniform. Variations in GDMS measurements due to such segregation can be clearly exhibited and can be significantly reduced by sampling larger areas and by multiple sampling in a single measurement.

Regardless, not all elements are represented in standard metals, and theory or a suitable semi-empirical model must be invoked to obtain the relative GDMS yields necessary for quantitation. In a promising approach it has been demonstrated that a Saha-Eggert formalism exhibits the general features of the GDMS yield pattern (W. Vieth, pers. comm.). Relative GDMS yields calculated this way are improved compared to uniform yields, particularly for group b elements, but again accuracy is no better than a factor of three for the more electronegative elements.

In summary, while the precision of GDMS measurements is excellent for the measurement of almost all elements at concentrations as low as a few ppbw, the accuracy of trace constitutent analysis is quite variable (10–300%) depending on the source of the relative GDMS yields needed for quantitation. The instrument itself appears inherently more capable than can be demonstrated using presently available standards. Improved assessment of GDMS performance and precise relative GDMS yield determinations will require more careful selection and characterization of standard materials.

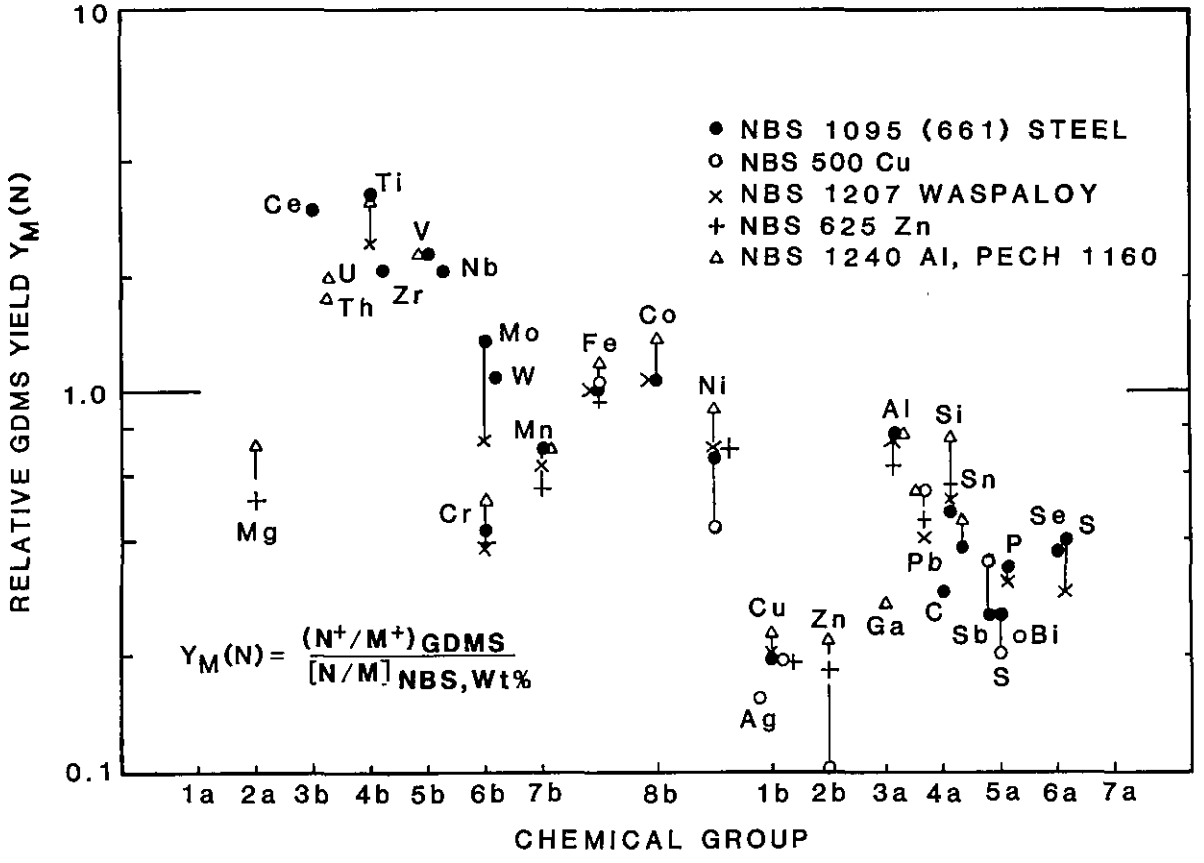

Figure 1. Relative GDMS yield from the glow discharge mass spectrometer analysis of several standard materials. Measurements were done at the same glow discharge power and pressure for each sample. Measured element ion currents are normalized to the *weight* fraction of the element in the standard to determine relative yield.

Applications of Mass Spectrometry in Polymer Analysis: Use of GC-GC-High Resolution MS to Identify Photo- and Oxidative Degradation Products of BPA-Polycarbonate

Woodfin V. Ligon, Jr., Arnold Factor, and Ralph J. May

General Electric Company
Corporate Research and Development
Schenectady, NY 12301

Introduction

A full understanding of any chemical process usually requires the complete elucidation of all of the reactants involved and all of the products produced. Even products produced in very minor quantities can be important because they may provide mechanistic clues.

The photooxidative degradation of polymers is an economically important process. If we are designing windows of a clear plastic then stability to light is all important in order to extend useful life. If we are designing certain kinds of single-use containers then we may wish them to degrade rapidly in order to minimize the potential for environmental contamination.

Identifying the products of the photooxidation process is, however, an unusual challenge for the analytical chemist. Especially in the early stages of the process, the products are likely to remain bound to the polymer backbone whose molecular weight may typically lie in the tens of thousands.

This means that we are really talking about a very small change in a very large molecule. Accordingly these products are often not amenable to the usual battery of organic analytical methods such as nmr and mass spectrometry. Mass spectrometry is limited by the high molecular weight and nmr (and often ir) are limited by the low effective "concentration" of the altered functional groups. Moreover, these processes are typically exceedingly complex—commonly producing 30 or 40 products. Relatively global surface techniques such as electron spectroscopy for chemical analysis (ESCA) while providing some insight into mechanism cannot possibly provide the detailed speciation needed to fully understand mixtures of this complexity.

A final impediment involves the fact that photooxidation is a surface phenomenon and, for this reason, altered products may have to be isolated from layers only few micrometers thick. As a result the total mass of "sample" available to the analyst may be quite small.

In this paper we discuss our approaches to understanding the photooxidation of Bisphenol-A (BPA) polycarbonate. A detailed experimental procedure will not be presented here and is in press elsewhere [1]. In keeping with the theme of this conference, this paper will concern itself with the relatively philosophical and strategic questions of the design of the analytical method for these trace components.

Discussion

The carbonate linkage of BPA-polycarbonate provides an attractive strategy for recovery of the photooxidatively altered portions of individual macromolecules. Simple base hydrolysis of the carbonate produces largely BPA and carbonate salts together with trace quantities of the various photooxidative products [2]. However, there is some concern that not all of the degradation products survive treatment with strong base. As an alternative, it was felt that degradation with lithium aluminum hydride (LAH) would both destroy the carbonate linkage (producing methanol) and reduce materials in a highly oxidized state (quinones, acids, etc.) to less polar, more easily characterized and more stable forms. However, it was recognized that use of a reduction step introduces some ambiguity in terms of speciation of the original photooxidation products. In order to facilitate speciation, it was decided to reduce aliquots of the altered polymer with both LAH and lithium aluminum deuteride (LAD). It was reasoned that if mass spectra of the LAH and LAD product mixtures were compared, then one could conclude that materials differing by one amu were derived from ketones or aldehydes whereas materials differing by two amu were derived from acids or esters. Reduction products of quinones would not retain the hydride and therefore would not retain the label.

Having decided on a degradation strategy, about 30 mg samples consisting of 10 μm thick slices of altered polymer were obtained from the surface of a photo-aged outdoor exposed specimen. In addition samples were taken from below the surface to act as controls on the analytical procedure. These samples were all subjected to LAH and LAD reduction.

Hydride reduction provided the photooxidation products in a form which was amenable to traditional techniques such as GC-MS. However we were then faced with the presence of a relatively large quantity of BPA that acted as a diluent for the products of interest which were present in trace quantities. High resolution gas chromatography could not be used directly because the amount of the major component (BPA) which could be injected without degrading chromatographic performance was limited to several micrograms. When this quantity of BPA was injected, the minor components were present in such small amounts that high resolution mass spectrometry was not practical. Although liquid chromatography could have been utilized to separate the BPA, it was reasoned that a two-stage gas chromatographic (GC) separation would provide many more theoretical plates and therefore minimize the probability that photo-products which very closely resembled BPA would be lost by co-elution. Furthermore a two-stage GC separation is much faster and highly efficient.

Using two-dimensional GC-MS methods, which have been described elsewhere [3], we obtained a primary separation by injecting milligram size aliquots of the product mixture onto a packed primary GC column. The entire effluent of this column was collected in a cold trap with the exception of the solvent and the PBA peak which were both vented. The components collected in the cold trap were then rechromatographed on a high resolution fused silica capillary and in separate analyses both low resolution and high resolution mass spectrometry data were obtained. Using this technique about 40 photooxidation products were resolved and characterized.

These data allowed the identification of products arising from ring oxidation, ring attack, side chain oxidation, and photo-Fries reactions.

References

[1] Factor, A., Ligon, W. V., and May, R. J., Macromolecules (1987) in press.
[2] Factor, A., and Chu, M. L., Polym. Degrad. Stab. **2**, 203 (1980).
[3] Ligon, W. V., and May, R. J., J. Chromatogr. Sci. **24**, 2 (1986).

Analytical Chemistry and Material Purity in the Semiconductor Industry

Purneshwar Seegopaul

Materials Research Corporation
Orangeburg, NY 10962

Analytical chemistry has evolved from a "hodge-podge" of empirical ideas into a highly visible, diverse and ubiquitous science. Perhaps the two most important industries that place significant demands on analytical chemistry are the biomedical and semiconductor fields. One can envisage a symbiotic relationship between analytical chemistry and the semiconductor industry. While improved analytical methods and instrumentation are constantly needed to support technological progress, it is technology development that provides the impetus and tools for enhanced instruments and thereby, analytical methodology.

The electronic revolution has resulted in significant miniaturization of devices on integrated circuits with complex multi-level structures. A typical VLSI circuit may contain up to a million devices! Obviously, this degree of complexity raises concern of yield, quality, and reliability. Materials play a critical role in these issues with the type and purity of the material directly influencing the profitability and very survival of semiconductor industries. For example, capacitance-voltage shifts caused by mobile ion impurities and ionization effects resulting from alpha-particles destroy the integrity of the devices. Table 1 shows the diversity of materials and their applications.

Table 1. Materials and their applications

Thermal print heads	
Ta_2O_5	Au
SiC	Al
SiO_2	Cr
TaN	

Optical disks	
Te	CaF_2
Bi	
Al	
Rh	
And alloys of above	

Thin film heads	
Ni-Fe	Al_2O_3
Fe-Si-Al	Au
SiO_2	
Al	

Hard disks—Winchester type	
Ni-Fe	SiO_2
Co-Ni	Cr
Co-Cr	Ni-V
C	
Co-Ni-Cr	

Integrated circuits	
Al(Al-Si, Al-Cu, Al-Si-Cu)	
Si	Mo & $MoSi_2$
W-Ti	Ta & $TaSi_2$
SiO_2	W & WSi_2
Au	Ti & $TiSi_2$
Pt	Doped Si

Optical magnetic disks
Gd-Co
Tb-Fe
Al
SiO_2
Th-Co-Fe
And other alloys

Liquid crystal displays	
ITO	SiO_2
ATO	Al_2O_3
Doped ZnS	Al
In-Sn Metal	

Thin film hybrids	
Cr	Au
Ni-V	TaN
W-Ti	Ta

Resistors	
Hybrids	Monolithic
Ni-Cr	Al-Ta
Cr-Si	
Cr/Cr_2O_3	Ni-Cr-Si
Cr-SiO_2	Ni-Cr-Al

Image sensors	
ITO	Cr
In-Sn	Al
SiO_2	

The enormous significance of material purity, however, is unfortunately clouded with the current practice of defining purity. At best, the purity phenomenon exists in a very arbitrary manner with its use subject to a myriad of interpretations. Purity of material in the semiconductor industry generally refers to the extent of the absence of impurities in the material. This then introduces the concept of total purity.

The ambiguity in purity data stems from the arbitrary and injudicious use of nine's without reference to acceptable and defined specifications. This method yields total purity by simply cumulative total impurity level from 100% to give the data in nine's. This is shown in table 2. It all seems too easy and simple! What does it mean? Was a six nine's (99.9999) pure material exhaustively analyzed and found only to contain 1 ppm total impurity out of all possible contaminants?

Table 2. Classification of purity by use of nine's

Three nine's	3N	99.9%	1000 ppm impurities
Four nine's	4N	99.99%	100 ppm impurities
Five nine's	5N	99.999%	10 ppm impurities
Six nine's	6N	99.9999%	1 ppm impurities

The system of defining, describing, and interpretating purity data needs to be modified. Such changes should be brought about by joint efforts of National Organizations, such as, NBS and ASTM in conjunction with material suppliers and users. Material purity, however, cannot be considered as an isolated issue. It is intricately linked to all the processes and techniques utilized to generate and guarantee the purity data. Table 3 lists some of the areas that are related to the whole concept of purity.

Table 3. Considerations in the purity debate

• Semantics	—	Meaning Comprehension/interpretation
• Specifications	—	Reference to purity Needs and material application
• Measurement process	—	Techniques Related functions
• Data reduction	—	"Numbers" game
• Data communication	—	Analytical terminology Certification of purity actual vs typical Correlation of purity data
• Reliability	—	Laboratory QC SPC Process stability and purity

Specifications that define purity are generally built with the manufacturing capability in conjunction with the material application. These specifications must be realistic and clearly defined with a critical list of parameters for evaluation; for example, a critical elemental list. The use of nine's may then become more practical.

Perhaps the most important area in this purity debate is the analytical process. Poor analytical practice and techniques generate useless data that distort the information. The analytical chemist is fortunate to have an impressive repertoire of modern techniques to discharge these responsibilities. Such techniques range from the simple potentiometric ion selective electrodes to the sophisticated glow discharge mass spectrometer. It is interesting to note that the choice of technique can have a direct influence on the purity in terms of the sensitivity and detection limits of the methods.

The interpretation and communication of the analytical data introduce the "numbers game." Data manipulation cannot be done without clearly defined conditions. Significant figures, use of absolute or rounded-off numbers, allowable deviations from the specified limits, etc., influence the final result and therefore, the purity. Confusion also arises from use of analytical parameters that are not in accordance with regulations, if any. For example, detection limits are being used with two and three standard deviations. Certification of the analytical data must indicate the use of actual results as opposed to typical values. The use of actual analysis data is more practical in terms of the risks involved and users of high purity materials must be aware of the significant difference in these numbers in their material and supplier evaluation.

The other critical consideration in the purity debate is the subject of reliability. Basically, this involves the need for comprehensive analytical quality control. Table 4 describes some of these parameters which include both internal laboratory and external control. Constant monitoring of accuracy and precision of procedures and data in conjunction with other aspects of the analytical process should be established as standard operating procedures. The use of reference samples and duplicates in analysis are absolutely critical for reliability which in turn produces real and useful information on material purity. A recent trend in the industry is the growing need for statistical process control (SPC). Obviously, SPC cannot be effectively utilized without accurate and precise data. Control charts are now necessary for certification of material purity! Material purity data is now being integrated with the actual process stability to monitor consistency.

The criticality of material purity, therefore, demands that the concept be clearly defined and specified for effective use and correlation of purity

data. This discussion highlights the issues that need to be resolved and focused on the role of the analytical chemistry in the process.

Table 4. Reliability of the analytical process

Analytical quality control
• Sampling
* Valid methods statistics
• Sample/data management
* Accountability
* Traceability
* Automation—LIMS
* Terminology and interpretation of data
• Internal quality control
* Procedures
* Accuracy
* Precision
* Facilities/personnel
• External quality control
* Round Robin Studies
* Accreditation
Statistical process control
• Process stability
• Purity vs consistency

Determination of Traces of Uranium and Thorium in Microelectronics Constituent Materials

Hideo Saisho, Masataka Tanaka, and Koichi Nakamura

Toray Research Center, Inc.
2-1, Sonoyama 3-Chome
Otsu, Shiga 520, Japan

Eiji Mori

Sunric Co., Ltd.
2-8-9 Keihinzima, Ota-ku
Tokyo 143, Japan

1. *Introduction*

Because of the problem of soft errors due to α-particle emission by uranium and thorium [1], determination of trace amounts of these metals in microelectronics constituent materials has recently gained considerable attention. In the present paper, four different techniques: chemical analysis (CA), instrumental neutron activation analysis (INAA), glow discharge mass spectrometry (GD/MS), and inductively coupled plasma mass spectrometry (ICP/MS) were studied using high-purity aluminum samples A, B, and C.

2. Experimental

2.1 Chemical Analysis

Samples (1–5 g) were decomposed with nitric and hydrochloric acids, evaporated to dryness, dissolved in nitric acid and subjected to chemical analysis.

2.1.1 Uranium Analysis [2,3] With sodium nitrate and aluminum nitrate added into nitric acid solutions of samples, uranium was extracted twice with a carbon tetrachloride solution of tributyl phosphate (TBP). The organic phase was back-extracted thrice with dilute hydrochloric acid after being washed with a sodium nitrate solution and hydrochloric acid. The aqueous phase was evaporated to dryness. The residue was fused with the addition of a fusing mixture consisting of potassium carbonate, sodium carbonate and sodium fluoride. The fused product was set in a fluorophotometer to determine the uranium by measuring the fluorescence intensity at 556 nm.

2.1.2 Thorium Analysis [4,5] Aluminum nitrate and EDTA were added to nitric acid solutions of samples and the resulting solutions were extracted twice with mesityl oxide. The organic phase was back-extracted thrice with water. The aqueous phase, with acids added, was decomposed by heating. The residue was dissolved in hydrochloric acid and with Arsenazo III added to this solution, thorium was determined by measuring the absorbance at 660 nm.

2.2 INAA

About 5 g of each sample was irradiated for 24 h at a thermal neutron flux of 5.5×10^{11} neutrons cm^{-2} s^{-1}. After cooling, the irradiated sample was counted for 10,000 s using a Ge (Li) detector. The cooling time was 6 to 8 days for uranium and 15 to 19 days for thorium. Uranium was determined by measuring γ-rays from 228 keV of ^{239}Np and thorium from 312 keV of ^{233}Pa.

2.3 GD/MS

The instrument used was a commercial GD/MS system (VG 9000, VG Isotopes). A pin-shaped

sample was prepared for measurement. Discharge was conducted, using argon as the discharge gas, with a voltage of 1.0 kV and current of 2.0 mA. Quantitative analysis was performed at a mass resolution of 5400 with a data acquisition time of 75 to 150 s per isotope.

2.4 ICP/MS

Using a PlasmaQuad (VG Isotopes), measurements were taken with two kinds of sample solutions: one was for acid-decomposition, and the other for chemical separation of uranium and thorium from an acid-decomposed solution as in the case of chemical analysis.

In mass spectrometry, the isotopes of uranium and thorium measured were ^{238}U and ^{232}Th, respectively.

3. Results and Discussion

3.1 Accuracy and Precision

The accuracy and precision of the chemical analysis were confirmed using NBS reference materials. As can be seen from tables 1 and 2, our chemical analysis methods were found to have acceptable accuracy and precision.

Table 1. Accuracy data for NBS reference materials

	This work (ppm)			
	Run 1	Run 2	Mean	Certified value (ppm)
1. Uranium SRM 616 (glass wafer)	0.068	0.069	0.068	0.0721±0.0013
2. Thorium SRM 614 (glass wafer)	0.75	0.74	0.74	0.748±0.006

Table 2. Precision data for the NBS 688 sample[a]

	Uranium (ppm)	Thorium (ppm)
Run 1	0.31	0.31
Run 2	0.33	0.31
Run 3	0.28	0.32
Run 4	0.30	0.30
Run 5	0.32	0.30
Mean	0.31	0.31
CV[b]	6%	3%

[a] SRM 688 (basalt rock): U, 0.37 ppm (non-certified). Th, 0.33±0.02 ppm (certified).
[b] Coefficient of variation [(standard deviation/mean)(100)]

3.2 Comparison of Results Obtained by Four Analytical Methods

Table 3 summarizes results obtained by chemical analysis, INAA, GD/MS and ICP/MS. So far as ICP/MS is concerned, results obtained by direct measurements of acid-decomposition solutions are omitted, because of unreliable nature of these results when the concentrations are lower than 100 ppb.

Table 3. Analytical results for high-purity aluminum samples obtained by four different methods

		Sample A		Sample B		Sample C	
		U	Th	U	Th	U	Th
CA	(ppm)	0.001	<0.01	0.010	0.02	0.080	0.07
INAA	(ppb)	<1	1.6±0.8	10±2	14±2	82±4	79±4
GD/MS	(ppb)[a]	<5	<5	15±3	18±2	121±17	119±8
ICP/MS[b]	(ppb)	$2._2$	$5._3$	12	12	79	84

[a] Ion beam ratio. Data not corrected using RSF. Mean ± standard deviation (5 determinations).
[b] Data obtained using the same solvent extraction procedure for CA.

Three samples subjected to chemical analysis and INAA provide close agreement. Results of measurements by ICP/MS with Samples B and C are in close agreement with those by chemical analysis and INAA. However, with Sample A with the lowest concentrations of both uranium and thorium, somewhat higher analytical values have been obtained in ICP/MS than in INAA. The spectral signals observed in ICP/MS from Sample A's uranium and thorium were apparently different from those of the blanks. On these grounds, the analytical values seem to have high accuracy.

The measured values by GD/MS are given in terms of ion beam ratios relative to that of an aluminum matrix. They are higher than the values obtained by the other three analytical methods with both Samples B and C. However, the ratio of the mean value of GD/MS to that of INAA falls in a range of 1.3–1.5 with both elements. Thus, by correction using this ratio or a relative sensitivity factor (RSF), satisfactory agreement can be obtained between the results from GD/MS analysis and the other three different analyses. If a more accurate RSF is obtained, it will become possible to make determinations of uranium and thorium very rapidly at concentration levels of 10 ppb or higher, as compared with the other three analytical methods.

Acknowledgment

The authors are grateful to Marubun Corporation (Tokyo, Japan) for the ICP/MS measurements.

References

[1] May, T. C., and Woods, M. H., 16th Proceedings of 1978 International Reliability Physics Symposium, p. 33, San Diego, CA, April 1978.
[2] Science and Technology Agency, Methods for Determination of Uranium, Japan Chemical Analysis Center, Chiba (1982) p. 9.
[3] Sandell, E. B., Colorimetric Determination of Traces of Metals, Interscience Publishers, Inc., New York (1959) p. 908.
[4] Grimaldi, F. S., Treatise on Analytical Chemistry, Part II, 5, Interscience Publishers, Inc., New York (1961) p. 139.
[5] Trofimova, L. A., and Syromyatnikov, N. G., Determination of Uranium, Thorium, and Zirconium with Arsenazo III without Chemical Separation, Zavodsk. Lab. (U.S.S.R.) 31, 1325 (1965); C.A. (U.S.) 64, 4254 (1966).

Multitechnique Approach to Trace Characterization of High Purity Materials: Gallium

S. Gangadharan, S. Natarajan, J. Arunachalam, S. Jaikumar, and S. V. Burangey

Ultratrace and Nuclear Methods Section
Analytical Chemistry Division
Bhabha Atomic Research Centre
Trombay, Bombay 400 085 India

1. Introduction

Compositional characteristics complement the structural aspects and in combination with certain correlated property measurements, provide complete characterization of materials. While characteristics completely govern the properties, the properties do not give a unique or complete account of the characteristics. The ultimate constraint in the characterization of ultrapure materials is the ability to maintain the integrity of the sample throughout the analytical measurement process. Developments in clean-room technology, coupled with the advances in plastics industry, have helped to push down the (environment and reagent) blank levels which has led to increased reliability in the quantitative measurement of impurities at ppb and sub-ppb levels of concentration. The stringent requirement of purity of materials for high technology demand compositional characterization for several (metallic) impurities which necessitates the use of diverse techniques like GFAAS, ICP/AES, activation analysis and electrochemical techniques, the choice of a given technique being guided by the sensitivity and selectivity it offers towards the characterization. To ensure good precision for measurements at ultratrace levels, the analytical methodologies should ensure minimum process blanks and afford (simultaneous) analysis of several critical elements related to (i) the manufacturing process, (ii) chemical similarity with reference to the matrix, and (iii) in the case of semiconductor materials, the donor, acceptor and neutral impurities.

1.1 The Facility

A (prototype) ultratrace analytical facility has been set up using indigenously available technology, to establish the attainable levels of cleanliness. The laboratory, designed to be at different levels of cleanliness, is better than class 100 at the work surface. The cleanliness with respect to (metallic) impurities has been monitored through the analysis of the air samples at several locations in addition to particulate counting. Distilled water, passed through a mixed bed ion exchange resin, is being routinely used. The levels of some of the impurities in that water, which reflect the cleanliness of the laboratory environment is as follows:

Element	Cd	Cu	Fe	Pb	Zn
Level ng/L	3	10	60	10	100

These levels have been maintained over several months of operation.

2. Approaches: Experimental

The multitechnique approach to trace characterization of gallium metal has been adopted. The philosophy behind the approach has been (i) to ensure cross-validation, i.e., generation of analytical results by at least two independent analytical methodologies wherever possible and obtain complementary information, (ii) to develop optimum instrumental

parameters during the final measurement, (iii) to analyze different aliquots of samples to check homogeneity and sample requirement, and (iv) analyze subsamples obtained from a large volume solution to generate an intra-lab comparison on the basis of inter-technique capabilities.

Direct analysis of Ga metal using NAA, though virtually free from process blanks, is limited to elements providing good sensitivity through long lived isotopes and requires proper configuration of the sample during irradiation to minimize flux perturbation. Analysis by ICP/AES, DPASV and GFAAS requires the sample to be brought into solution. Signal suppression of about 20% for ultra-trace constituents at ~100 ng/mL is noted in ICP/AES when Ga is present in ~1 ng/mL. Suppression of anodic waves as well as non-linear behavior with respect to standard addition has also been observed in DPASV. Direct analysis of Fe, Cu, Ni etc. in Ga at >1 ppm levels is possible by GFAAS but severe signal suppression for many elements is noted for trace constituents when even tens of micrograms of Ga is present.

2.1 APDC/MIBK Extraction

Solvent extraction of elements as their thiocarbamates has been investigated using APDC as the complexing agent and MIBK as the extractant. The optimum pH levels for complete extraction of trace constituents from citrate as well as tartrate media (which inhibit the extraction of Ga) have been investigated using GFAAS and radioactive tracers. Optimization of parameters like the quantity of Ga taken, the amount of buffer required as well as the concentration of APDC used for complexing the metals, was carried out to ensure that virtually no Ga extracts into the organic layer. The MIBK layer was directly analyzed by GFAAS. The tartrate medium provided a more consistent and effective separation in addition to reduced blanks than citrate medium. Current levels of the process 'blanks' for some trace elements (1-g sample basis) are given below:

Element	Cd	Co	Cu	Ni	Pb
blank levels (ppb)	1	8	45	40	70

2.2 Preconcentration of Trace Impurities on Ga Itself through Controlled Dissolution

A 1-g Ga sample was dissolved slowly in a 3:0.15 M mixture of $HCl:HNO_3$ at 95 °C for several hours until a residue of ~10 mg remained. This residue was carefully washed and weighed, dissolved in an $HCl:HNO_3$ mixture and aliquots of this solution were directly analyzed by GFAAS, ICP and DPASV. Theoretically this procedure should provide the least process blank, limited by the purity of the acids used. The process 'blanks' (1-g equivalent) as analyzed by ICP/AES and GFAAS are given below:

Technique/Element	Ag	Bi	Cu	Fe	Ni	Pb	
GFAAS	4	–	40	10	14	10	(ng/g)
ICP	–	90	40	–	–	–	

2.3 Preconcentration of Impurities in Aqueous Medium through Solvent Extraction of Ga in MIBK

Methyl isobutyl ketone is an excellent extractant of Ga from concentrated HCl medium. Our choice of MIBK as the extractant has been mainly due to much lower molarity of HCl required under similar operating conditions.

(i) 99.99% extraction of Ga (5 M) HCl, compared to di-isopropyl ether (7.6 M) and chlorex (12 M) and hence lower blanks.

(ii) Good phase separation compared to ether.

(iii) Presence of small amount of nitrate does not hamper Ga extraction; close to 80% recovery of Cd, Co, Cr, Cu, Mg, Mn, Zn at ~100 ng/mL level in presence of 250 mg Ga is obtained. The process 'blanks' (1-g sample equivalent) estimated by GFAAS and ICP are given below:

Element (ppb)	Al	Ca	Cd	Co	Cu	Mg	Mn	Ni	Pb	V	Zn
Technique ICP	60	20	20	30	40	15	15	60	–	30	40
GFAAS				11			10	20	50		

2.4 Other Approaches

Solvent extraction of Ga with ethyl-hexyl-phosphoric acid (DEHPA) affords preconcentration of more elements than MIBK and the extraction can be done at very low acidities. Currently, the purification of the reagent for suitability to work at nanogram levels is being attempted. Coprecipitation of several impurities by reductive precipitation with Pd under alkaline conditions appears very promising, but even pure $PdCl_2$ contains several trace impurities that need to be removed. An ion exchange procedure has been developed to purify $PdCl_2$ for nearly complete removal of several trace impurities, and efforts to minimize process blanks have been undertaken.

3. Results

Results on two of the samples characterized are summarized in tables 1 and 2. Current levels of process blanks (1-g basis) by various procedures described here indicate that the lab environment and analytical methodologies are capable of handling Ga samples of 99.9999+% purity, with respect to some specific impurities. While the purity required is related to end-use, we wish to point out the levels of Hg and Zn impurities in two samples. Ga samples obtained from a single source at different times showed varying levels of Hg, which appears to be related to sampling errors. Another sample, though very pure with respect to several elements, contained about 115 ppm of Zn which may be a source-related impurity. Similarly, levels of Al, V and Pb also appear to be source-related.

Table 1. Trace impurities (ppb) in gallium (sample A) (analytical techniques INAA(a), GFAAS(b), ICP/AES(c), DPASV(d))

Element	Direct	Cont. dissolution	MIBK ext.	APDC/MIBK
Ag		30(b)		
Au	76(a)	35(a), <100(b)		
Bi		50(c)		
Cd			4.2	7(b)
Co	7(a)		17(b)	12(b)
Cr	11(a)			
Cu		190(b),180(c)	280(b)?	190(b)
In	2.8(a)ppm			
Mn			<24(b),25(c)?	
Ni		725(b),590(c)	740(b)	820(b)
Pb		25(b),60(c) 60(d)?	20(b)	40(b)
Pd		<60(b)		
Sb	<3(a)	15(a)?		
Zn	300(a)			

4. Comments

The restrictive nature of the presence of gallium in suppressing analytical signals in ICP/AES, DPASV and GFAAS, requires the development of optimum conditions for sample processing and final measurement. Optimization techniques based on simplex and method of steepest ascent are currently being examined to develop an experimental design which permits (1) preconcentration of several trace impurities with virtually no Ga accompanying them, (2) identifying analysis conditions in ICP/AES and GFAAS that afford signal enhancement with reduced matrix interference with and without modifiers. These results will be communicated shortly.

Table 2. Trace impurities (ppb) in gallium (sample B) (analytical techniques INAA(a), GFAAS(b), ICP/AES(c), DPASV(d))

Element	Direct	Cont. dissolution	MIBK ext.	APDC/MIBK
Au	0.4(a)			
Bi		<50(c)		
Cd			2.4	5.5(b)
Co	5(a)		<11(b)	<8(b)
Cr	7(a)			
Cu		85(b),50(c)		43(b)
In	84(a)			
Mn			16(b)	
Ni		<14(b),<100(c)		<40(b)
Pb		26(b),60(c)	<10(b)	<100(b)
Sb	15(a)	26(a)?		
Zn	106 ppm(a)		114 ppm(a), 100 ppm(c)	

Volume 93, Number 3, May–June 1988
Journal of Research of the National Bureau of Standards

IV. Advances in Analytical Techniques

Chromatography/Separation Science

Open Tubular Liquid Chromatography and the Analysis of Single Neurons

J. W. Jorgenson, R. T. Kennedy, R. L. St. Claire III, J. G. White, P. R. Dluzneski, and J. S. M. de Wit

Department of Chemistry
The University of North Carolina
Chapel Hill, NC 27514

Liquid chromatography in open tubular columns (OTLC) offers a means of achieving separations of high resolving power within analysis times of minutes to hours. A theory which predicts the optimal dimensions for an open tubular column for a given set of analytical conditions has been developed [1]. This theory predicts that for a wide range of possible inlet pressures and analysis times the most efficient columns will result when the column inner diameter is between 1.5 and 3 μm. A column of 2 μm diameter and 2 meter length should be capable of producing a million theoretical plates for an analyte with a capacity factor of 10 (strongly retained) and a retention time of 100 minutes.

Mobile Phase Delivery and Sample Injections

Mobile Phase Delivery For columns of a few micrometers internal diameter, the flow rate of mobile phase is on the order of picoliters per second. Such flow rates are far below the capabilities of any existing commercial pumps. A simple system which uses the constant head pressure of helium gas for pumping mobile phase in OTLC columns has been described [1]. This system makes use of the fact that the flow impedance of the open tubular column is constant under isocratic conditions, and thus a constant head pressure yields a constant flow rate. For gradient elution purposes, a commercial gradient pumping system used with a solvent splitting arrangement has been described by Yang [2]. This system permits gradient elution for micro-packed columns and is applicable to open tubular columns as well. A minor amount of solvent waste is the only disadvantage of such a solvent splitting system.

Sample Injections A number of schemes for introducing samples into microcolumns have been described. As the inner diameter of the column is reduced, the need for low dispersion in the introduction process becomes more critical. A simple "static splitting" system which directs a small portion of sample to the column has been described [1]. This system is assembled from standard commercial chromatographic plumbing and is capable of injecting sample plugs of essentially any desired length onto columns of any internal diameter (the chromatogram shown in figure 2 was obtained from a 7 picoliter injection onto a 1.7 μm diameter column using this system). The length of the injected plug is controlled by the flow rate of mobile phase through the column and the timing of injection valves. The main disadvantage of this system is that sample volumes of approximately half a milliliter are required to fill the injection "loop" even though only a few picoliters may actually be injected. Judicious engineering of the system could reduce the volume of sample required to perhaps 10 microliters. An alternative approach capable of injecting subnanoliter volumes of sample will be described in the section on single cell analysis.

Column Preparation

A major problem in OTLC systems is the preparation of columns with sufficient stationary phase. Capillary tubing in micrometer sized dimensions is readily available, but successfully "coating" large enough amounts of stationary phase into the capillary is a serious challenge. We have prepared columns of two basic types. The first is based on borosilicate glass capillaries in which a superficially porous layer is formed on the surface by chemical leaching. Silane stationary phases may be

subsequently bonded to this porous layer. As an alternative, columns may be prepared by depositing polymeric stationary phase on the inner wall of fused silica capillaries.

Porous Layer Glass Capillaries Capillaries are drawn from borosilicate glass tubing using a conventional glass drawing machine. They are then heat treated at 600 °C for 24 hours, inducing a phase separation in the glass. Following heat treatment, the column is leached with a hydrochloric acid solution. This renders the surface porous by selectively removing the non-silica components of the glass and leaving behind a porous silica layer. This process increases the internal surface area of the capillary roughly thirtyfold over a geometrically smooth capillary. This surface is then suitable for bonding of silane stationary phases [1,3,4].

Polymer Layer Fused Silica Capillaries Fused silica capillaries with internal diameters as small as 5 μm are now commercially available. Capillaries of fused silica offer the advantages of greater flexibility and resistance to breakage over conventional glass capillaries. They also exhibit better UV transparency and lower intrinsic luminescence than borosilicate glass, significant advantages when on-column fluorescence detection is to be done. Unfortunately, little is known about methods to increase the internal surface area of fused silica in order to bond sufficient amounts of silane stationary phase. As an alternate approach we have devised a method for coating siloxane polymer stationary phases onto the surface of these capillaries [5,6]. The method relies on the fact that the polymer solubility is temperature dependent. In this procedure OV-17v, a polysiloxane with 49% phenyl, 49% methyl, and 2% vinyl substitution, is dissolved along with a small amount of benzoyl peroxide (as a cross linking reagent) into a solvent composed of 70% heptane and 30% cyclohexane at a temperature of 80 °C. The polymer and peroxide are both quite soluble in this solvent system at this temperature. The capillary is then filled with this solution while maintaining the capillary at the elevated temperature. After filling, the capillary is simply allowed to cool to room temperature, whereupon the polymer and peroxide "coprecipitate" onto the capillary surface. The remaining solvent is flushed from the capillary with helium gas and the column is slowly heated to 140 °C at which point the benzoyl peroxide decomposes to generate free radicals which initiate cross linking of the polymer chains. This produces an immobile and inextractable polymer layer which is useful as a stationary phase.

Detection

The tiny dimensions and high efficiency of OTLC columns dictate that detectors be extremely sensitive and contribute a minimum of additional dispersion to the chromatographic peaks. We have developed detectors for on-column fluorescence detection as well as on-column electrochemical detection. Post column gas phase photoionization detection [7] and mass spectrometric detection [8] have been developed as well.

Fluorescence Detection On-column fluorescence detection with a conventional arc lamp source [9] offers acceptable sensitivity with columns of diameters larger than 10 μm, but smaller capillaries require the use of lasers as sources [10]. Figure 1 is a chromatogram obtained on a 1.7 μm diameter fused silica column with a 7 picoliter injection of a solution 1 micromolar in both riboflavin and perylene. This corresponds to only 7 attomoles or 4 million molecules injected onto the capillary. The detection limit in this case is only 100,000 molecules, attesting to the high sensitivity possible with laser induced fluorescence detection.

Electrochemical Detection An on-column electrochemical detector based on a single carbon fiber as the working electrode has been developed. The fiber electrode is inserted into the outlet of the OTLC column with the aid of a micropositioner and a microscope. Current may be measured at a fixed potential (amperometric) [11,12] or the voltage may be scanned and current measured as a function of applied potential (voltammetric) with the aid of a microcomputer [13,14]. The minimum detectable quantity of analyte is roughly 10 attomoles in the amperometric mode and 100 attomoles in the voltammetric mode. Figure 2 is a chromatovoltammogram of a sample of tea obtained on a 15 μm reversed phase borosilicate glass capillary [15]. The additional dimension of "separation" offered by voltammetry may be a significant advantage when working with such a complex sample.

Analysis of Single Neurons

The small sample requirements and high sensitivity of the OTLC systems just described make them ideal for analysis of samples of small volume, such as the contents of individual cells. We have developed a method which permits us to isolate individual giant (120 μm) neurons from various ganglia of the land snail, *Helix aspersa*. These neurons are used because of their large size and because they can be reproducibly located from specimen to specimen. A single neuron is transferred to a 500

nanoliter microvial. It is disrupted and homogenized with a glass fiber, its contents centrifuged, and the supernatant drawn up into a micropipette. The tip of the micropipette is then inserted into the inlet end of an OTLC column and the cellular fluid [16]. Figure 3 is a chromatovoltammogram obtained from the neuron designated F76 (anatomical map of Kerkut et al. [17]). Four compounds, tyrosine, dopamine, serotonin, and tryptophan, have been identified and quantified in several different giant neurons of the snail. Finding two classical neurotransmitters, dopamine and serotonin, in the same cell is an interesting result. This analysis is made feasible by the ability of OTLC to work with exceptionally small samples.

Acknowledgments

Support for this work was provided by the Donors of the Petroleum Research Fund, administered by the American Chemical Society, the Alfred P. Sloan Foundation, and the National Science Foundation under Grant CHE-8607899.

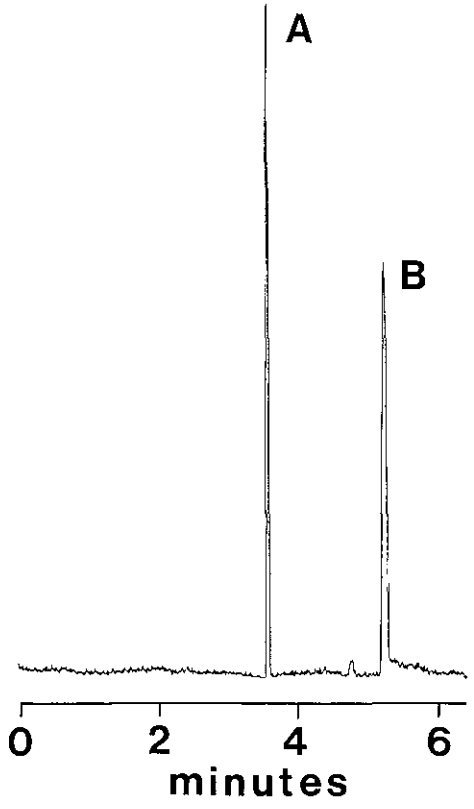

Figure 1. Chromatogram of riboflavin (A) and perylene (B) run on a 1.7 μm diameter fused silica column.

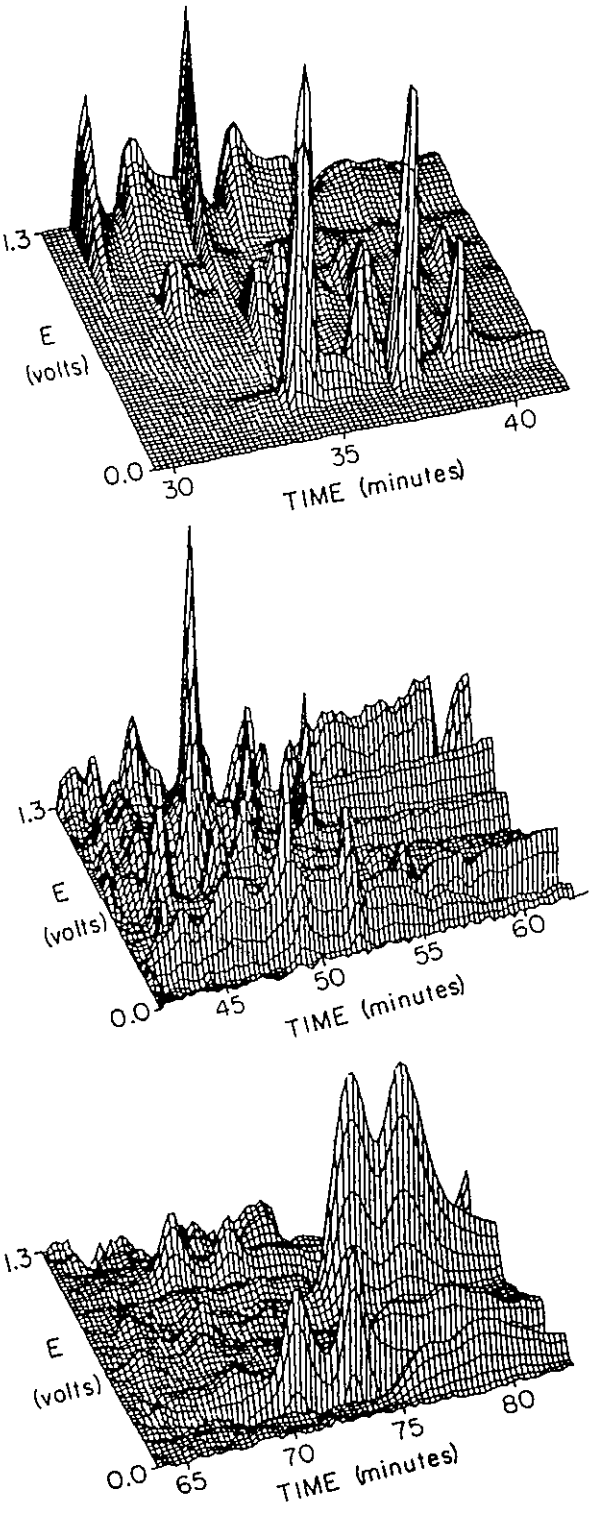

Figure 2. Chromatovoltammogram of a sample of tea, run on a 15 μm borosilicate reversed phase column.

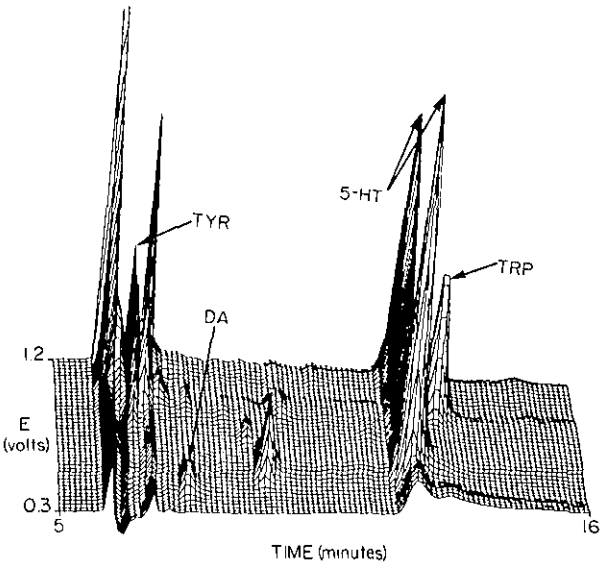

Figure 3. Chromatovoltammogram of the contents of a single neuron. Compounds identified are tyrosine (TYR), dopamine (DA), serotonin (5-HT), and tryptophan (TRP).

References

[1] Jorgenson, J. W., and Guthrie, E. J., J. Chromatogr. **255**, 335 (1983).
[2] Yang, F. J., Proceedings of the Sixth International Symposium on Capillary Chromatography, Huethig, Heidelberg, 861 (1985).
[3] St. Claire, R. L. III, Ph. D. Thesis, University of North Carolina (1986).
[4] St. Claire, R. L. III, and Jorgenson, J. W., J. Chromatogr., in press.
[5] Dluzneski, P. R., Ph. D. Thesis, University of North Carolina (1987).
[6] Dluzneski, P. R., and Jorgenson, J. W., Chromatogr. Commun., in press.
[7] de Wit, J. S. M., and Jorgenson, J. W., J. Chromatogr., in press.
[8] de Wit, J. S. M., and Parker, C. E., Jorgenson, J. W., and Tomer, K. B., Anal. Chem., in press.
[9] Guthrie, E. J., and Jorgenson, J. W., Anal. Chem. **56**, 483 (1984).
[10] Guthrie, E. J., Jorgenson, J. W., and Dluzneski, P. R., J. Chromatogr. Sci. **22**, 171 (1984).
[11] Knecht, L. A., Guthrie, E. J., and Jorgenson, J. W., Anal. Chem. **56**, 479 (1984).
[12] St. Claire, R. L. III, and Jorgenson, J. W., J. Chromatogr. Sci. **23**, 186 (1985).
[13] White, J. G., St. Claire, R. L. III, and Jorgenson, J. W., Anal. Chem. **58**, 293 (1986).
[14] White, J. G., and Jorgenson, J. W., Anal. Chem. **58**, 2992 (1986).
[15] White, J. G., Ph. D. Thesis, University of North Carolina (1986).
[16] Kennedy, R. T., St. Claire, R. L. III, White, J. G., and Jorgenson, J. W., Mikrochim. Acta, in press.
[17] Kerkut, G. A., Lambert, J. D. C., Gayton, R. J., Loker, J. E., and Walker, R. J., Comp. Biochem. Physiol. **50A**, 1 (1975).

High Performance Capillary Electrophoresis

B. L. Karger

Barnett Institute
Northeastern University
Boston, MA 02115

Electrophoresis is one of the most powerful tools currently available for the separation of charged species. Its impact in the biological sciences is very great with methods such as SDS polyacrylamide gel electrophoresis, DNA sequencing and two-dimensional gel electrophoresis as standard tools for biological analysis. Typically, electrophoretic methods today involve the use of slab gels or thin layer plates, with detection based on staining and/or blotting procedures. Such approaches are difficult to quantitate and automate and are generally slow. In addition, micropreparative operation involves extraction procedures following separation on the slab gel.

Currently, capillary electrophoresis is being developed as an instrumental approach to electrophoresis. Historically, columns or rods were initially introduced for electrophoretic separations; however, with development of slab gels, the rod technique became less used. However, the above cited limitations of slab gels have rekindled the interest in column operation. High performance capillary electrophoresis bears analogy to HPLC, in terms of injection, column, detection and sample collection. Today, fused silica capillaries of less than 100 μm diameter are typically employed for separation with efficiences in excess of 100,000 theoretical plates.

Equations (1)–(3) present the basic relationships of various parameters with respect to their influence on separation time (t), theoretical plates (N) and resolution (Rs).

$$t = \frac{lL}{\mu_{ep} V} \tag{1}$$

$$N=\frac{\mu_{ep}V}{2D} \tag{2}$$

$$Rs=\frac{1}{4}\frac{\Delta\mu_{ep}\sqrt{V}}{\sqrt{2D\bar{\mu}_{ep}}}, \tag{3}$$

where l=distance from injection to detector, L=total capillary length, V=applied voltage, μ_{ep}=electrophoretic mobility of the solute, and D=solute diffusion coefficient. In these equations, it is assumed that the major cause of band broadening is axial diffusion.

It can be noted that high voltages have a beneficial effect on all three parameters, yielding faster analyses, higher efficiencies and better resolution. The stumbling block toward ever-higher V is the Joule heating that accompanies the power generated from these systems ($W=I^2R$). We can control to some extent the current generated for a given field by a judicious selection of the buffer in terms of its conductivity and concentration; however, this choice is limited. On the other hand, the tube diameter influences Joule heating, both from the point of view of the number of current carriers and the ability to dissipate the heat generated. Smaller diameter tubes aid in the control of a constant temperature, hence, the use of narrow bore capillaries. A second specific advantage of fused silica is that the wall thickness can be maintained low for improved heat dissipation; indeed, wall thicknesses as small as 30 μm are possible. A polyimide coating on the fused silica permits practical use of narrow wall capillaries. Thus, for a given mobile phase, high fields (V/L) and fast separations are possible with fused silica capillaries. Of course, temperature control is important to achieve reproducible separation.

Our laboratory has focused on two approaches in capillary electrophoresis. First, in open capillary operation, we have incorporated chemical selectivity along with high performance separation for resolution of closely related species. Previously, Terabe introduced the use of micelles as a separation medium for the resolution of neutral species in capillary electrophoresis [1]. In this approach, a neutral species partitions within the interior of the micelle, the extent of partition being based on the hydrophobicity of the solute. The micelle moves at a fixed low rate through the capillary, acting as a "moving" stationary phase, in analogy to chromatography. Figure 1 shows a separation of neutral oligonucleotide bases, with solute elution of increasing hydrophobicity [2]. An alternative approach is the use of the surface of the micelle for separation. Figure 2 shows an electropherogram of a polythymidine mixture using SDS and 0.3 mM Cu(II) [2]. The copper is electrostatically attracted to the negatively charged surface of the micelle and differential ligand complexation results in separation. Many chemistries can be considered based on this surface adsorption approach. For example, surfactants with chiral chelates at the polar side can be used for chiral separations. We have separated D,L-dansylated amino acids using such a chelating surfactant and Cu(II). Thus, the selectivity of chromatography can be combined with the efficiency of capillary electrophoresis.

The second approach of our work involved the use of polyacrylamide gel capillary columns to provide a medium analogous to slab gel operation. We have successfully produced stable columns for the separation of important mixtures. Figure 3 shows a separation of myoglobin fragments using the approach of SDS-PAGE [3]. Retention was found to be linear with log MW. Indeed, further studies of proteins using a Ferguson plot, revealed a true size separation in these columns [3]. Thus, rapid molecular weight determination and assessment of protein purity is possible using this approach. Figure 3 illustrates another important advantage of this method relative to slab gel operation. Low molecular weight peptides can be separated and quantitated, whereas on slabs they often diffuse off the column.

We have continued work in this area with recombinant materials. Separation of recombinant human growth hormone from a proteolytic clipped variant (2 chain) has been achieved. In addition, the elution of methionine growth hormone (methionine at the N-terminal) has been successful. Other studies have involved oligonucleotides where size separation is again very important. These studies include micropreparative separation of impure mixtures.

Finally, the gel column can be used for entrapment of complexing species to create selective separation, as in affinity electrophoresis. As an illustration of this approach, we have entrapped β-cyclodextrin, a neutral cavity-complexation species. This agent has then been used to separate chiral species. The principles of separation have been established and the approaches to achieve optimum separation elucidated.

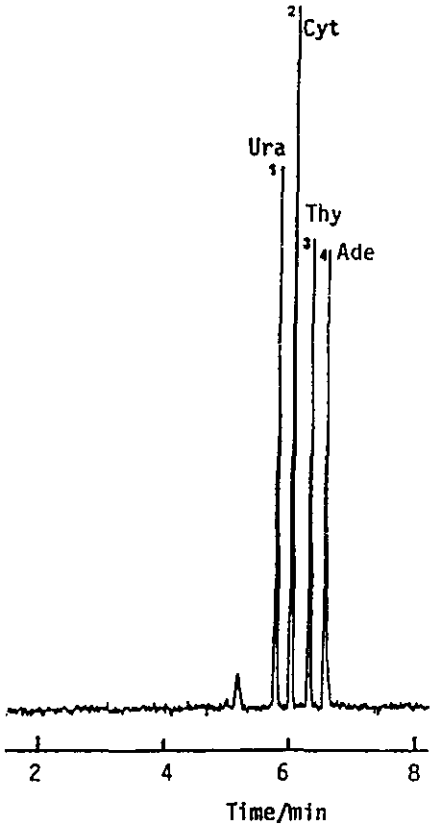

Figure 1. Separation of bases: (1) Ura, (2) Cyt, (3) Thy, (4) Ade. Buffer: 0.025 *M* sodium tetraborate, 0.05 *M* sodium dihydrogen phosphate, 0.1 *M* SDS, pH 7, capillary 650 mm×0.5 mm i.d. Column length 500 mm, applied voltage 14 kV, 50 μA, detection wavelength 210 nm.

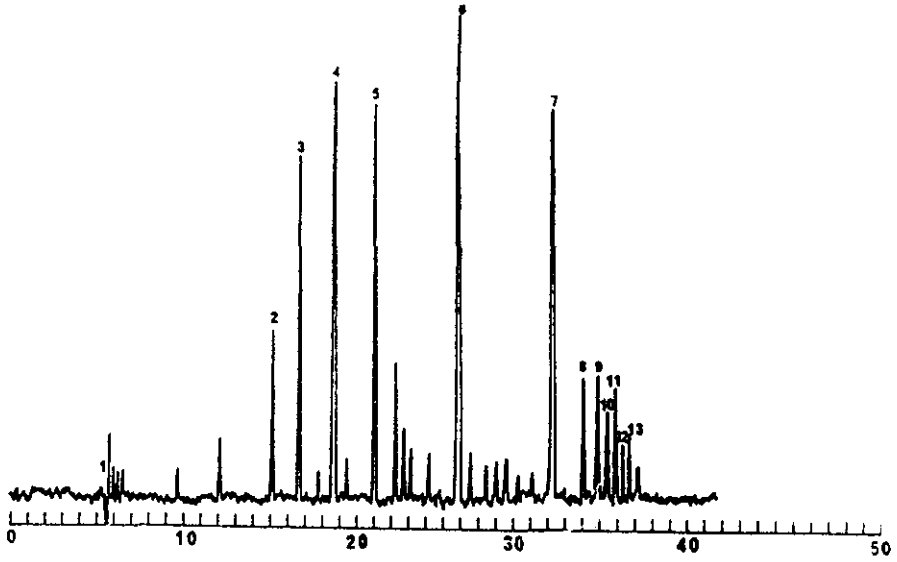

Figure 2. Separation of polythymidine mixture: (1) solvent, (2) $d(pT)_2$, (3) $d(pT)_3$, (4) $d(pT)_4$, (5) $d(pT)_6$, (6) $d(pT)_{10}$, (7) $d(pT)_{12}-d(pT)_{18}$, (8) $d(pT)_{12}$, (9) $d(pT)_{14}$, (10) $d(pT)_{15}$, (11) $d(pT)_{16}$, (12) $d(pT)_{17}$, (13) $d(pT)_{18}$. 0.3 m*M* Cu(II) added to the buffer. Buffer: 7 *M* urea, 5 m*M* Tris, 5 m*M* Na_2HPO_4, pH 7, capillary 650 mm×0.05 mm i.d. Column length 450 mm.

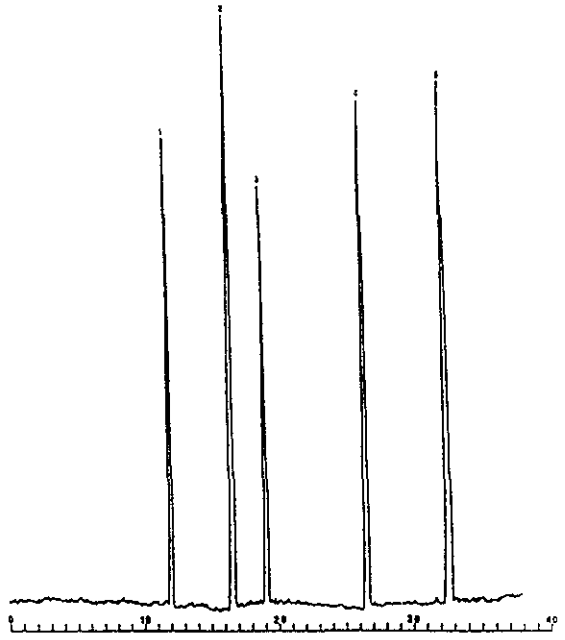

Figure 3. High performance capillary SDS-PAGE separation of myoglobin and several of its fragments. Conditions: 400 V/cm, 34 μA, 25 °C, migration distance 20 cm; fused-silica capillaries; 75 μm ID, T-12.5%, c=3.3%. Buffer: 0.1 *M* Tris-H_3PO_4 (pH=6.9), 0.1% SDS, 8 *M* urea.

References

[1] Terabe, S., Otsuka, K., and Ando, T., Anal. Chem. **57**, 834 (1985).
[2] Cohen, A. S., Terabe, S., Smith, J. A., and Karger, B. L., Anal. Chem. **59**, 1021 (1987).
[3] Cohen, A. S., and Karger, B. L., J. Chromatogr. **397**, 409 (1987).

Supercritical Fluid Chromatography: Application to Trace Analysis

Milton L. Lee, Nebojsa Djordjevic, and Karin E. Markides

Department of Chemistry
Brigham Young University
Provo, UT 84602

Supercritical fluid chromatography (SFC) is fast becoming the method of choice for many separations involving nonvolatile, reactive, and thermally labile compounds. In particular, supercritical car-

bon dioxide has found wide applicability as the mobile phase in SFC because of its low critical parameters, mild chemical properties, and excellent compatibility with a variety of detection systems. Supercritical fluids have lower densities and, hence, yield higher chromatographic efficiencies for equal analysis times when compared to liquids, and they possess solvating power to modify retention instead of relying on temperature for this purpose such as in gas chromatography.

Most SFC work in the past has been more qualitative in nature than quantitative. This is a result of the newness of the technique and efforts to explore the full range of its applicability. As the technique has become an established member of the analytical arsenal, more emphasis on quantitative aspects has arisen.

The most important contributing factors to the use of SFC in trace analysis are (a) sample introduction, (b) column inertness and resolving power, and (c) detector sensitivity. Packed columns have traditionally been preferred for trace analysis in chromatography because larger sample volumes could be injected onto such columns, thereby providing greater target analyte amounts for detection. However, these high surface area packings often exhibit some adsorption and/or catalytic decomposition of sensitive compounds, leading to lower sensitivities and reproducibilities. Furthermore, the carrier fluid flow rates are often too large to introduce directly into the desired detectors, and splitting of the column effluent is required. This again reduces the sensitivity. A compromise is achieved by using microbore columns packed with low surface area, highly deactivated microparticulate packings.

Capillary columns have the advantages that chromatographic peaks are narrower, the columns can be made more inert, and direct coupling, without splitting, to detectors is usually straightforward. Using the new dehydrocondensation deactivation reagents to mask surface silanol groups during column manufacture, polar compounds can be chromatographed using supercritical carbon dioxide with little or no reversible and irreversible adsorption at the subnanogram level. With such columns, underivatized carboxylic acids [2], steriods [3], polar pharmaceuticals [3], and drug metabolites have been successfully analyzed.

Polysiloxane stationary phases containing carefully designed organic pendant groups have broadened the scope of selectivity in capillary SFC. The incorporation of *n*-octyl, biphenyl, cyano, and liquid crystalline groups onto the polysiloxane backbone has increased the variety of selective stationary phases [4]. The biphenyl group has a very strong dipole induced-dipole character, while cyano groups are moderately polar as well as strongly polarizable. Geometric orientation is the interactive force that is characteristic of the liquid crystal groups. These useful interactive forces have demonstrated that the selection of stationary phases for use in SFC has a great influence on the separation of critical solutes.

The extremely low mobile phase flow rates (several microliters per minute) encountered in capillary SFC have encouraged the evaluation of a variety of detection systems for this technique. Particularly noteworthy is the relative ease experienced in adapting the flame ionization detector (FID), which is by far the most popular detector in gas chromatography, to capillary SFC. The main obstacle that had to be overcome was the decompression of the supercritical fluid at the column outlet through a carefully designed flow restrictor. The only apparent limitation is the required use of inorganic mobile phases that do not give responses in the detector.

Other flame-based detectors, thermionic [5] and flame photometric [6], which are also common to GC, can be used in capillary SFC. The only major limitation is the limited choice of mobile phases. Even CO_2 gives a weak response at the sulfur wavelength in the flame photometric detector and reduces the detector sensitivity by one order of magnitude. With nitrogen-selective thermionic detection, picogram detection limits can be obtained [5].

The optical detectors common to LC, i.e., uv-absorbance [7] and fluorescence [8], do not suffer from the problems of flow restriction (the restrictor is placed after the detector) common to the flame-based detectors. However, the small detector cell volumes necessary for the small diameter (<100 μm) capillary columns lead to reduced sensitivities. Novel detector cell designs incorporating focusing optics and optical fibers have greatly eliminated these problems, and very sensitive detectors are available. Again, picogram detection limits can be obtained for favorable compounds using a fiber-optic based fluorescence detector [7].

The greatest challenge in coupling SFC to detection systems is the successful interfacing to information-rich spectroscopic instruments such as mass spectrometers and infrared spectrophotometers. In the case of mass spectrometry, decompression into

a vacuum must occur before fragmentation. Recently, detection limits of low picograms in the full scan mode, and low femtograms in the selected-ion mode, were obtained using a coupled SFC-high resolution mass spectrometer system [9].

Sample introduction is the most difficult aspect of trace analysis in SFC. The sampling modes most widely used require splitting of a set volume delivered from a high pressure sample loop. This requires rather highly concentrated samples. Recently, solute focusing methods utilizing a retention gap, analogous to such methods used in capillary gas chromatography, have been applied in capillary SFC [10]. Proper manipulation of pressure and temperature is essential to achieving good chromatographic performance upon injection of large sample volumes. With 1-μL injection volumes, sub-ppm concentrations can be detected using an FID, and much greater detection limits can be achieved using more selective detectors.

References

[1] Woolley, C. L., Bartle, K. D., Markides, K. E., and Lee, M. L., J. High Resoln. Chromatogr./Chromatogr. Commun. **9**, 506 (1986).
[2] Markides, K. E., Fields, S. M., and Lee, M. L., J. Chromatogr. Sci. **24**, 254 (1986).
[3] Later, D. W., Richter, B. E., Knowles, D. E., and Andersen, M. R., J. Chromatogr. Sci. **24**, 249 (1986).
[4] Jones, B. A., Markides, K. E., Bradshaw, J. S., and Lee, M. L., Chromatogr. Forum **1**, 38 (1986).
[5] West, W. R., and Lee, M. L., J. High Resoln. Chromatogr./Chromatogr. Commun. **9**, 161 (1986).
[6] Markides, K. E., Lee, E. D., Bolick, R., and Lee, M. L., Anal. Chem. **58**, 740 (1986).
[7] Fields, S. M., Markides, K. E., and Lee, M. L., Ultraviolet-absorption Detection for Capillary Supercritical Fluid Chromatography with Mixed Mobile Phases, Anal. Chem., in press.
[8] Fjeldsted, J. C., Richter, B. E., Jackson, W. P., and Lee, M. L., J. Chromatogr. **269**, 423 (1983).
[9] Huang, E. C., Markides, K. E., and Lee, M. L., unpublished results.
[10] Djordjevic, N. M., Chang, H-C. K., Markides, K. E., and Lee, M. L., New Sampling Technique in Capillary Supercritical Fluid Chromatography, to be published

Ion Chromatography: From Anions to Metals

William F. Koch

Center for Analytical Chemistry
National Bureau of Standards
Gaithersburg, MD 20899

From its humble beginnings in 1975 [1], ion chromatography has grown and expanded its scope to the extent that the term ion chromatography may no longer adequately describe the technique. As initially conceived, ion chromatography was configured with an ion exchange separation, followed by an ion suppression system to permit electrolytic conductivity detection of the analyte without overwhelming background from the eluent. This patented configuration found its best application in the determination of anions at trace (1–100 μg/mL) levels, an area long in want of a fast, accurate and reliable method. Some cations, specifically the alkali and alkaline earth metals, were also determinable in the early days, but it was the capability to determine anions that drove the technique's popularity.

Soon, variations to the original concept were introduced, notably suppressorless or single column ion chromatography [2], and new types of detectors for ion chromatography. Amperometric and uv/visible spectrometric detectors have gained wide acceptance, especially in the determination of metals. Considerable effort was put into resin research to improve the sensitivity and resolution of the technique and to extend its capabilities to more ionic species. In some cases, ion exchange was no longer the dominant retention mechanism for the separation of various species. Hence, the term ion chromatography now is used to categorize any self-contained procedure based on chromatographic separation of ions followed by detection and quantification.

To typify the advances made in ion chromatography by noting recent work in the field at NBS, the detection limits for anion ion chromatography have dipped below 1 ng/mL for species such as sulfide and cyanide with amperometric detection, without preconcentration [3,4].

In other work, a method has recently been developed to determine alkali and alkaline earths in

the pg/mL range with in-line preconcentration [5]. During the development of this method at NBS, the factors investigated included: composition of the eluents, interference due to impurities in the delivery liquid and the possible means of eliminating them with a laboratory-packed trap column, and a comparison of suppression efficiencies between two types of suppressors. This method was used for the determination of Mg^{+2} and Ca^{+2} in SRM 2694, Simulated Rainwater, with precisions and accuracies better than 2% relative [5].

The frontier for ion chromatography is transition metal analysis with ongoing research along many fronts. New resins are being introduced and are being coupled to exotic detectors. The era of "hyphenated" techniques is burgeoning with ion chromatography showing up as the front-end separation method of choice. Recent work at NBS has coupled ion chromatography with direct current plasma emission spectrometry for the determination of phosphorus in copper-based alloys [6].

Future challenges for ion chromatography will be to enhance further its capabilities through improved speed, sensitivity, and resolution. Speciation of metals as a function of oxidation state and complexation will be an important goal. Innovative resins and a new generation of detectors will have to be developed. Fundamental research into the retention mechanisms leading to the separation will be essential.

In conclusion, ion chromatography has proven itself an invaluable tool to analytical chemistry. Its ultimate advantages will lie in its versatility and its capacity for ultra-trace analyses with minimal contamination and total automation.

References

[1] Small, H., Stevens, T. S., and Baumann, W. C., Anal. Chem. **47**, 1801 (1975).
[2] Gjerde, D. T., Fritz, J. S., and Schmuckler, G., J. Chrom. **186**, 509 (1979).
[3] Han, K., and Koch, W. F., Anal. Chem. **59**(7), 1016 (1987).
[4] Koch, W. F., J. Res. Natl. Bur. Stand. **88**, 157 (1983).
[5] Han, K., and Koch, W. F., LC-GC **6**, 56 (1988).
[6] Epstein, M. S., Koch, W. F., Epler, K. S., and O'Haver, T. C., Anal. Chem. **59**, 2872 (1987).

Quantification of Toxic Chemicals in Selected Human Populations

J. S. Holler, D. G. Patterson, and S. J. Smith

Center for Environmental Health
and Injury Control
Centers for Disease Control
Public Health Service
U.S. Department of Health and Human Services
Atlanta, GA 30333

The evaluation of risk posed by toxic chemicals to human populations requires a knowledge of the toxicity of compounds and the extent of human exposure to the compounds. The best estimate of exposure is obtained by measuring chemical residues or metabolites in biological samples and extrapolating the measurements to body burdens in study populations. Analytical methods developed at the Centers for Disease Control (CDC) typify the laboratory techniques needed to support epidemiologic studies. In these procedures, specific sample preparation techniques are used to isolate the target compounds, which are then measured by capillary gas chromatography combined with mass spectrometry. Many problems must be solved for these techniques to be applied successfully. Quality control materials must be generated that closely mimic actual specimens and that contain target analytes at appropriate concentrations. Sample contamination, both from internal and external sources, can be a major difficulty. The lack of analytical standards is usually a continuing problem for the analytical chemist, and a successful synthesis program can minimize this problem. Interpreting analytical results at or near the system's limit of detection poses more problems. Techniques must be developed to translate sample concentrations into valid estimates of total body-burden values.

A recent study in which chlorinated phenols and phenoxy acid herbicides in urine were measured exemplifies typical laboratory challenges in trace analysis. In this study, we compared children living near a chemical manufacturing site with a control group of unexposed children. An extensive sample preparation included acid hydrolysis, extraction with benzene, derivatization with diazoethane and column chromatography cleanup. The more volatile compounds are quantified by capillary column

gas chromatography/positive chemical ionization/mass spectrometry/mass spectrometry. Less volatile compounds are quantified by using electron capture negative chemical ionization in a single stage mass spectrometry mode. This study required a modified approach to quality control material in that target values were obtained during the analysis of actual specimens. In addition, we have used a multivariate quality control procedure to obtain a single quality control chart that is representative of the 12 study analytes. The synthesis of the pure derivatives provided an ideal material in estimating recovery and diagnosing chromatographic problems. With the method's improved detection limits and specificity, we had an increased frequency of detection for several of the study analytes compared with frequencies for previous studies.

Chemists have encountered significant analytical challenges in measuring 2,3,7,8-tetrachlorodibenzodioxin (TCDD) in tissue at the parts per trillion (ppt) level and measuring TCDD in serum at the parts per quadrillion (ppq) level. Such low levels of quantification can only be achieved by using high resolution mass spectrometry. The labor-intensive sample preparation activities have led to the application of automated procedures directed toward increasing sample throughput and optimizing use of the chemist's time. Such sample preparation requires a specialized approach to quality control, including the strategic placement of system blanks. Such low levels of quantitation require care in controlling artifacts and laboratory contamination. The reporting of quantitative results corrected for percent lipid in the samples permits the correlation of quantitative results between different sample matrices. The laboratory must be carefully organized to insure sample coordination, monitoring of quality control, and timely reporting of results. Finally, sample collection in the field has been challenging, particularly in the case of adipose tissue.

Interest in toxic chemical exposure will continue to challenge the analytical chemist to provide better laboratory measurements for assessing exposure. We are developing a method for quantifying a number of volatile organic compounds in human whole blood. Concerns about exposure to this class of compounds has led to controls and monitoring programs on drinking water systems, a major source of human exposure. Our method development has defined the analytical approach as a variation on the traditional purge and trap technique. Work includes adapting instrumental hardware specifically for this sample matrix. Major challenges include a short-lived quality control material, quality control for a significant number of "nondetects" and electronic data handling for the large number of samples involved. The overall objective of this work is to estimate the presence of a number of important volatile compounds in whole blood for a specific population of 1200 people. The results of this study should make it possible to estimate the types and magnitude of exposure encountered by the U.S. population.

Acknowledgment

This report was partially supported by funds from the Comprehensive Environmental Response, Compensation, and Liability Act trust fund.

An Evaluation of Jansson's Method to Deconvolve Overlapped Gas Chromatographic Peaks

Paul Benjamin Crilly

Hewlett-Packard Company
Box 900
Avondale, PA 19311

Introduction

It has been reported [1,2] that Jansson's Method [3] can be used to deconvolve severely overlapped gas chromatographic peaks. Initial testing [1,2] indicates the method will give improved performance over conventional graphical peak resolution techniques such as perpendicular drop and shoulder quantitation [4,5].

Jansson's Method is an iterative non-linear algorithm that uses the prior knowledge of peak non-negativity and maximum peak height for an improved estimate of the true chromatogram [3]. The method only requires a knowledge of the instrument's impulse response function and maximum peak height. Jansson's Method does not require any prior information on how many peaks are overlapped.

Volume 93, Number 3, May-June 1988
Journal of Research of the National Bureau of Standards

This paper will show the results of a comprehensive evaluation of Jansson's Method to resolve overlapped peaks that have been generated from two different sample mixtures. As a benchmark, these peaks were also resolved using shoulder quantitation and perpendicular drop techniques. As a second benchmark, these same sample mixtures were analyzed using an instrument with a relatively long column so that the peaks were fully resolved without using non-chemical peak resolving methods.

Theory

A gas chromatographic process can be modeled as follows [1]

$$g = h * x + n \tag{1}$$

where g is the observed peaks (raw data), h is the system impulse response function, x is the true peak shape, n is random noise and $*$ is the convolution operator. Variables g, h, x, and n are all functions of time. It is assumed the system is time invariant. The convolution of functions x and h can cause the perfectly resolved peaks in x to become severely overlapped.

Jansson's Method can be used to obtain an estimate of the true peak shape, x, (given functions g and h) as follows [3]

$$\hat{x}^{k+1} = \hat{x}^k + r\{\hat{x}^k\}[g - h * \hat{x}^k] \tag{2a}$$

with

$$r\{\hat{x}^k\} = b(1 - 2/c\,|\hat{x}^k - c/2|) \tag{2b}$$

where $\hat{x}^k$ is the k'th estimate of the true peak shape x, b is the relaxation constant, and c is the maximum peak amplitude. Relaxation function $r\{\hat{x}^k\}$ constrains the estimate to within its physical limits of 0 and c.

Experimental Procedure

The chromatographic analysis was done on a Hewlett-Packard 5890A Gas Chromatograph with a thermal conductivity detector. Two mixtures consisting of 50/50 and 10/90 concentrations of ethyl benzene and m-xylene samples were used to generate the chromatograms. Each sample was injected and analyzed 20 times so there would be a reasonable statistical basis for the goodness of any one method.

An instrument with a relatively short capillary column (10 meter) generated overlapped chromatograms whose resolution was 0.42 and are shown in the dotted line plots of figures 1 and 2. These overlapped peaks were resolved using Jansson's Method, shoulder quantitation and perpendicular drop techniques. The estimates obtained using Jansson's Method after 160 iterations are shown in the solid line plots of figures 1 and 2. Another set of chromatograms was generated using an instrument with a longer (50 meter) and narrower capillary column so that the peaks generated were fully resolved. For each method, the relative errors, peak quantity variances and relative retention time variances were calculated and are presented in tables 1 to 3.

Table 1. Relative error comparison for various peak resolving methods [2]

Sample concentration (%)	Relative Error: Long column[a] (%)	Jansson's Method[b,c] (%)	Shoulder quantitation[c,d] (%)	Perpendicular drop[c,d] (%)
ethyl benzene: 50	−0.04	+0.08	− 6.36	−35.35
m-xylene: 50	+0.04	−0.07	+ 6.07	+33.74
ethyl benzene: 10	+2.01	−4.68	−33.26	−78.67
m-xylene: 90	−0.20	+0.46	+ 3.27	+ 7.72

[a] Peaks were fully resolved without using non-chemical techniques.
[b] 160 iterations used.
[c] Original convolved peak had a resolution of 0.42.
[d] Since the peaks were so severely overlapped, implementing this method required prior knowledge that two peaks were present and their approximate retention times.

Table 2. Peak quantity variances for various peak resolving methods [2]

Sample concentration(%)	Peak Quantity Variance[a]: Long column	Jansson's Method[b]	Shoulder quantitation	Perpendicular drop
ethyl benzene: 50	0.26	0.31	0.23	10.09
m-xylene: 50	0.25	0.29	0.19	4.66
ethyl benzene: 10	8.63	3.39	11.60	19.05
m-xylene: 90	0.87	0.32	0.73	0.37

[a] Units are in percent standard deviation.
[b] 160 iterations used.

Table 3. Relative retention time variance for various peak resolving methods [2]

Sample concentration (%)	Relative Retention Time Variance[a] Long column	Jansson's Method[b]	Shoulder quantitation	Perpendicular drop
ethyl benzene: 50 m-xylene: 50	0.31	0.93	4.46	4.46
ethyl benzene: 10 m-xylene: 90	4.33	2.57	3.54	3.54

[a] Units are in percent standard deviation.
[b] 160 iterations used.

Results and Discussion

As table 1 indicates, the quantitation accuracy of peaks resolved using Jansson's Method is similar to what can be obtained using an instrument with a relatively long column and is about an order of magnitude better than the graphical methods. The peak quantitation accuracies for the graphical methods are similar to what Mikkelson et al. [4] and Altmayer [5] have reported. The peak quantity and relative retention time variances reported in tables 2 and 3 indicate Jansson's Method compares favorably to the long column method and is better than the graphical methods.

It should be noted that the overlapped peaks of figures 1 and 2 were overlapped to such a degree that it was almost impossible to implement the graphical methods since it was difficult to locate the peaks and valleys.

For a peak resolution of 0.42, a 10 Hz sample rate and pre/post smoothing using a nine point polynomial filter, Jansson's Method could deconvolve data whose signal-to-noise ratio was as low as 60:1. However, the signal-to-noise performance of Jansson's Method will depend on the noise power spectral density, degree of peak overlap, data system sampling rate and whether the data is pre and/or post smoothed. To a lesser extent, the signal-to-noise performance will depend on the number of iterations and the relaxation constant chosen.

In conclusion, Jansson's Method can be used to extend the capabilities of an instrument and provide faster analysis time. The initial results have been encouraging such that further research is justified.

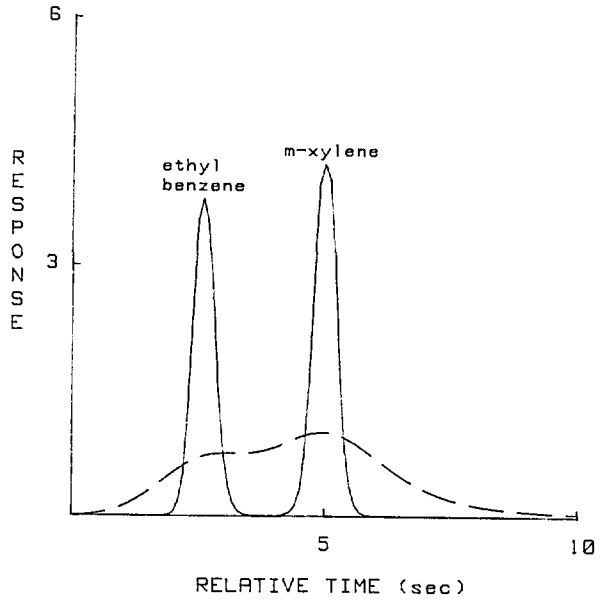

Figure 1. Solid line plot is the chromatogram of the 50/50 mixture of ethyl benzene and m-xylene deconvolved using Jansson's Method with 160 iterations. Dotted line plot is the original chromatogram [2].

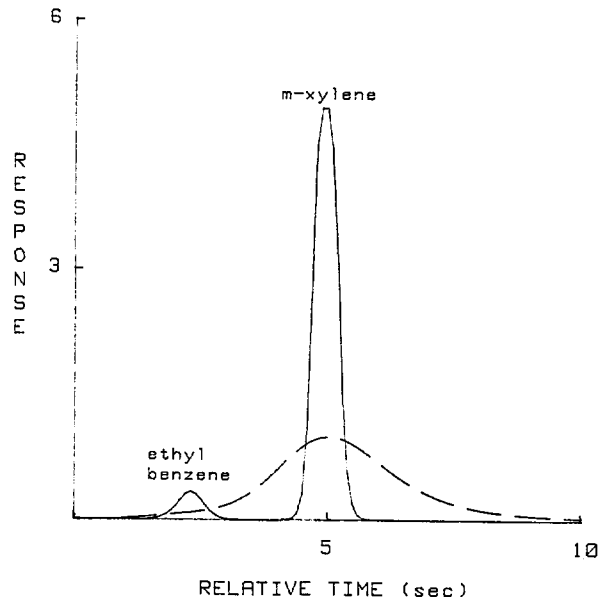

Figure 2. Solid line plot is the chromatogram of the 10/90 mixture of ethyl benzene and m-xylene deconvolved using Jansson's Method with 160 iterations. Dotted line plot is the original chromatogram [2].

References

[1] Crilly, P., J. Chemometrics (Sussex, England) **1**, 79–80 (1987).
[2] Crilly, P., Numerical Deconvolution of Overlapped Gas Chromatographic Peaks Using Jansson's Method, PhD Dissertation, New Mexico State University, Las Cruces, NM (May 1987).
[3] Jansson, P., Deconvolution With Applications in Spectroscopy, Academic Press, New York (1984).
[4] Mikkelson, L., and Davidson, I., Partially Resolved GC Peaks: Analytical Accuracy With an Electronic Integrator, Hewlett-Packard Technical Paper 45, Avondale, PA (1971).
[5] Altmayer, L., Information from Chromatography Real Time Quantitation, Hewlett-Packard Technical Paper 89, Avondale, PA (1979).

Volume 93, Number 3, May–June 1988
Journal of Research of the National Bureau of Standards

Accuracy in Trace Analysis

Mass Spectrometry

Inorganic Trace Analysis by Isotope Dilution Mass Spectrometry—New Frontiers

J. D. Fassett

Center for Analytical Chemistry
National Bureau of Standards
Gaithersburg, MD 20899

Isotope dilution mass spectrometry (IDMS) is used extensively at NBS in the certification of elemental concentrations in Standard Reference Materials. It is regarded at NBS as a "definitive method," that is, a method of proven high accuracy. Since the theme of this symposium is accuracy in trace element analysis, it is appropriate to review the role IDMS plays in accurate inorganic analysis. The thesis of this paper is that mass spectrometry is a dynamic technique, marked by continuous productive activity and change, and that new mass spectrometric methods and new ionization techniques promise to make IDMS more general, more available, and more cost effective. Furthermore, I argue that the adoption of this technique by analytical laboratories outside of reference laboratories would do much to broaden the accuracy base of the world's measurements.

In IDMS the quantity of an element present in a material is determined from the change produced in the isotopic composition of the element when a known amount of stable isotope (called a spike) is added. Thus, the technique is applicable to all elements with more than one stable isotope, or greater than 60 elements in the periodic table. In practice this number is reduced to those elements readily handled and ionized in the source of a mass spectrometer. In addition, some mononuclidic elements can be determined using radioactive isotopic spikes. For instance, procedures have been developed in our laboratory for iodine and thorium using ^{129}I and ^{230}Th.

An IDMS requires equilibrium of the spike isotope and the natural isotopes, and thus requires that the sample be dissolved. It is at this stage of the procedure that the potential sources of systematic error are most likely to occur. Clearly, if the sample does not completely dissolve, or, if the spike or sample isotopes are lost before equilibration, or, if contamination occurs in the dissolution process, the measured isotopic ratio will not reflect the accurate ratio of added spike atoms/sample atoms for that element. The analyst must be aware of these pitfalls.

The analyte concentration is determined knowing the isotopic composition of the spike and sample, the concentration of the spike, the weights of the mixed spike and sample, and the measured ratio. Thus, the spike must be calibrated. This calibration is accomplished doing a reverse IDMS procedure using gravimetrically prepared natural solutions from high purity materials. Also, both the natural and isotopic compositions must be verified.

The major source of separated isotopes is Oak Ridge National Laboratory [1], although there are alternative sources for some isotopes. The Electromagnetic Isotope Enrichment Facility (EMIEF) at Oak Ridge is currently used to produce 225 enriched stable isotopes of 50 elements. The isotopes in the sales inventory are for sale to anyone on a first-come, first-served basis. The cost of a separated isotope is roughly proportional to the extent of enrichment. However, the cost of the isotopic spike in IDMS is a minor part of the analysis and paradoxically becomes even less so in trace and ultratrace measurements. For instance, the ^{50}V spike costs \$131/mg. The cost of the μg of this spike used in spiking a sample with V at the ppm level is only 13 cents. More important, perhaps, is the future cost and availability of enriched stable isotopes. This issue has recently been discussed [2].

IDMS has traditionally been done using: thermal ionization mass spectrometry (TIMS) [3], an instrumental method used primarily in the nuclear and geochemical fields; spark source mass spectrometry (SSMS) [3], primarily at NBS; and, GC/MS electron impact ionization [4,5], using more widely available organic mass spectrometry instrumentation and techniques. There have been important advances in the traditional techniques and commercial instrumentation that are valuable in accurate, trace measurement using IDMS including: new procedures, higher sensitivity, and higher precision.

Examples of new thermal ionization procedures for IDMS are ones for sulfur [6] and vanadium [7]. The sulfur technique is novel in that the AsS^+ ion is generated and measured. The sulfur isotopes are shifted 75 mass units higher in the mass spectrum by the mononuclidic arsenic moiety. This technique has resulted in over 50 certification measurements since its development, illustrating the previous void in analytical techniques that could accurately measure sulfur at the parts-per-million level. The vanadium method uses pulse-counting TIMS and has been used to certify various materials from the ppb level to minor levels. This procedure illustrates one of the advantages of high-sensitivity IDMS procedures: large dynamic range capability. The sample is optimally spiked according to the concentration of the element of interest. Then, a subsample of the separated element is often adequate for determination of the altered isotopic ratio.

An illustration of the sensitivity achievable using TIMS is illustrated in the procedures developed for uranium [8]. The concentration of uranium in bovine liver (SRM 1577a) has been determined at the 700 pg/g level with a few percent precision from equivalent 0.25 g sample sizes. For these high sensitivity measurements, it is clear that accurate measurements require control and characterization of the analytical blank. Kelly has presented this topic at this symposium. The use of well-characterized, sub-boiling-distilled reagents helps keep reagent blanks to a minimum. The development of efficient and specific chemical separations, often involving microchemical procedures, has further helped to lower the limit of measurement for many elements.

Commercial instrumentation in TIMS now possess multicollectors and multisample turrets, as well as full automation. The multicollectors can demonstrate parts in 10^6 internal precision in favorable cases. Although this precision may be wasted in IDMS analysis, the traditional requirement for the production of long-lived, stable ion beams to reach high precision is considerably reduced. In many cases, this advance could reduce the need for very high purity elemental separations. Thus, the advances in commercial instrumentation promise to increase the throughput, reduce the labor costs, and, in general, reduce the overall cost of an IDMS measurement. In addition, one commercial vendor is selling a quadrupole-based thermal ionization instrument. Although not capable of the extremely high precision possible using a magnetic sector TIMS instrument, this relatively low cost instrument can make isotope ratio measurements with nominal 0.25% precision, certainly very adequate in many instances for accurate IDMS.

The general advances that have been made in sample pretreatment, automation, and separations that have been discussed at this symposium promise to reduce the front end labor costs of IDMS. More importantly, these advances could also do much to reduce the contamination that occurs in routine chemical operations. The very high sensitivity of many of the new and traditional mass spectrometric techniques will only be applicable when the limits imposed by the blank are overcome.

There have been a number of presentations at this symposium where the "new frontiers" of IDMS can be seen. Recently, two new techniques have been examined using isotope dilution: resonance ionization mass spectrometry (RIMS) and inductively coupled plasma mass spectrometry (ICP-MS). RIMS uses laser photoionization to produce ions from a gas phase reservoir of atoms [9]. Both the sensitivity and elemental selectivity of RIMS can be used to advantage in isotope ratio measurement. ICP-MS combines high sensitivity with breadth of elemental coverage, and, direct analysis of nebulized solutions [10]. The speed and convenience of the ICP-MS, and elemental coverage, in combination with its rapid commercialization give the analytical community an unprecedented opportunity to apply IDMS, and achieve accurate trace element analysis.

References

[1] ORNL Electromagnetic Separated Stable Price List, available from the Isotope Distribution Office, Oak Ridge National Laboratory, P.O. Box X, Oak Ridge, TN 37831.
[2] Hoff, R. W., Nucl. Instrum. Meth. Phys. Res. **B26**, 1 (1987).
[3] Moore, L. J., Kingston, H. M., Murphy, T. J., and Paulsen, P. J., Env. Int. **10**, 169 (1984).
[4] Veillon, C., Wolf, W. R., and Guthrie, B. E., Anal. Chem. **51**, 1022 (1979).
[5] Hachey, D. L., Blais, J.-C., and Klein, P. D., Anal. Chem. **52**, 1131 (1980).
[6] Paulsen, P. J., and Kelly, W. R., Anal. Chem. **56**, 708 (1984).
[7] Fassett, J. D., and Kingston, H. M., Anal. Chem. **57**, 2474 (1985).
[8] Kelly, W. R., and Fassett, J. D., Anal. Chem. **55**, 1040 (1983).
[9] Fassett, J. D., Moore, L. J., Travis, J. C., and DeVoe, J. R., Science **230**, 262 (1985).
[10] Houk, R. S., Anal. Chem. **58**, 97a (1986).

Volume 93, Number 3, May–June 1988
Journal of Research of the National Bureau of Standards

Applications of the Reaction Interface/Mass Spectrometer Technique to the Analysis of Selected Elements and Nuclides from Submicrogram Quantities of Biological Macromolecules and Xenobiotics

Donald H. Chace and Fred P. Abramson

Department of Pharmacology
George Washington University
School of Medicine
2300 Eye Street N.W.
Washington, DC 20037

Markey and Abramson [1] developed a microwave-powered chemical reaction interface, a device which converts a complex organic molecule in the presence of a reactant gas into small stable molecules which are detected by mass spectrometry. For a given reactant gas the molecules formed are a representation of the elemental composition of the original anlayte. The combination of the reaction interface and a mass spectrometer produces an isotope- or element-selective detector for samples either introduced directly into the reaction interface or flowing from a capillary gas chromatograph column.

Microgram and submicrogram samples of a variety of proteins were analyzed for their sulfur content relative to their carbon content by introducing the samples directly into the reaction interface. With CO_2 as the reactant gas, SO_2 at m/z 64 is produced. This quantifies the amount of sulfur which was introduced into the reaction interface. In the presence of N_2, HCN at m/z 27 is produced and is used to quantify the carbon content of the sample. The observed ratio of S/C for various proteins correlated well with the elemental formulas [2].

In the presence of SO_2, ^{14}NO at m/z 30 and ^{15}NO at m/z 31 are produced. Following administration of 50 mg of triple-labeled 5,5-diphenylhydantoin [1, 3(^{15}N); 2(^{13}C)] to a male beagle dog, a urine sample was selectively analyzed for its ^{15}N content by capillary gas chromatography—reaction interface/mass spectrometry. The corrected ratio of m/z 31 to m/z 30 produced a highly selective chromatogram showing only peaks of ^{15}N enrichment. Mass spectra of these peaks were obtained which permitted identification of phenytoin and several of its metabolites.

Supported by NIH Grant #GM36143.

References

[1] Markey, S. P., and Abramson, F. P., J. Chromatogr. **235**, 523 (1982).
[2] Abramson, F. P., and Markey, S. P., Biomed. Env. Mass Spectrom. **13**, 411 (1986).

Alkylation of DNA In Vivo: Development of Analytical Methodology for Trace Quantitative Analysis

R. G. Cooks, J. R. O'Lear, and C.-j. Chang

Departments of Chemistry
and Medicinal Chemistry
Purdue University
West Lafayette, IN 47907

1. Abstract

The application of tandem MS techniques to the determination of the site and extent of alkylation of DNA by chemical carcinogens is illustrated. It is shown that it is possible to i) separate many methyldeoxyribonucleosides and the common deoxyribonucleosides in a single LC run, ii) detect and quantify pure methyldeoxyribonucleosides at the 10^{-14} mole level by desorption chemical ionization tandem mass spectrometry, and iii) quantify the major methylated nucleosides resulting from treatment of calf thymus DNA or hamster V79 cells with methylnitrosourea (MeNU) or methylmethanesulfonate (MeMS). The ultimate aim is to use *in vivo* experiments to correlate mutagenicity and cytotoxicity of the alkylating agents with the type and distribution of the alkylated adducts and with their metabolic half-lives (metabolic persistence/repair) in cell cultures.

2. Significance

Alkylating agents [1] exhibit pronounced biological activity. Many are mutagenic in various genetic systems [1–3] and more than a dozen are being used clinically as anticancer drugs [4,5]. Reactions *in vitro* between alkylating agents and nucleic acids and their biological consequences in terms of transcription and translation activities have been reviewed [3,6]. Almost all nitrogen and oxygen atoms of DNA bases can be alkylated. In general, nitrosoureas (strong mutagens) yield a higher percentage of oxygen-alkylated products, suggesting that the cell transformation activity of alkylating agents may be related to the degree of oxygen-alkylation. In recent years, much interest has focused on O^6-alkylation of guanine because this modification can result in base mispairing [1,7–9]. Increasing attention has also been directed toward the formation and metabolic persistence of O^4-alkylthymine [10–12]. The formation of O^4-methylthymidine, 3-methylthymidine, 3-methyldeoxycytidine, and 1-methyldeoxyadenosine in V79 cells by MeMS or MeNU has been demonstrated in our study. Further studies on the extents of their formation and metabolic persistence of these modifications upon exposure to various alkylating agents at different dosages are essential for an understanding of their differential toxicity and mutagenicity at the molecular level.

3. Analytical Methodology

3.1 Overall Approach

Studies of DNA alkylation *in vivo* challenge analytical chemistry by requiring qualitative and quantitative analysis at high sensitivity for closely related compounds, some of which are involatile and thermally unstable and all of which occur in particularly complex matrices. Fortunately, recent progress in liquid chromatography and mass spectrometry offers capabilities to match these requirements. Figure 1 illustrates the protocol adopted.

Implicit in this methodology is the requirement for the synthesis of deuterium-labeled nucleosides. The methylated nucleosides examined in this investigation were 3-methyldeoxycytidine (m^3dc), 1-methyldeoxyadenosine (m^1dA), 7-methyldeoxyguanosine (m^7dG), 1-methyldeoxyguanosine (m^1dG), 3-methylthymidine (m^3T), O^4-methylthymidine (m^4T), O^2-methylthymidine (m^2T), 3-methyladenine (m^3Ade) and O^6-methyldeoxyguanosine (m^6dG). All compounds were synthesized as the trideuteromethyl nucleosides, and as the unlabeled methyl compounds.

The task of separation of isomeric alkylated nucleosides utilized high pressure liquid chromatography. Satisfactory separations of the various methylated compounds in reasonable times can be achieved by a procedure which uses ion-pair reverse-phase chromatography [13,14]. The technique of tandem mass spectrometry (MS/MS) [15,16] also provides separation capabilities as well as specific, sensitive detection and very rapid sample throughput. Desorption ionization, with tandem mass spectrometry, is the key to the application of mass spectrometry to this problem. The desorption ionization procedures [17,18] have had considerable influence on the application of mass spectrometry to the biological sciences [19], increasingly through the simultaneous use of MS/MS [20,21]. The particular form of desorption ionization used here, desorption chemical ionization (DCI), employs rapid heating of a sample held in a chemical ionization plasma [22,23].

Analysis of the pattern of alkylation of Chinese hamster V79 cells employs a triple quadrupole instrument for desorption chemical ionization followed by tandem mass spectrometry. Quantification is based on daughter spectra of the modified nucleosides for the major methylation products and on selected reaction monitoring spectra of the minor components. The rapidity and specificity of MS/MS analysis are important advantages which, coupled with its ultra-high sensitivity, permit the detection and quantification of 0.1–10 ng of individual modified nucleosides. It should be feasible for us to measure the alkylated nucleosides in the ranges of 0.1 to 10 picomoles resulting from *in vivo* alkylation of DNA with chemical carcinogens.

3.2 HPLC Separation

To allow the accurate determination by chemical ionization of the amounts of methylated nucleosides present relative to deuterium-labeled internal references, it was necessary to develop an HPLC system capable of separating these nucleosides. Although absolute resolution of each peak in the chromatographic system was not rigorously required, an initial objective was the complete resolution of all structural isomers being analyzed. The separation achieved with the high-pressure liquid chromatographic system (CH_3CN/H_2O; 50 mmol/L $HCOONH_4$; 3 mmol/L NEt_4Cl;

C-18 column) is excellent. The deoxyguanosine isomers, m^7dG, m^1dG and m^6dG; deoxyadenosine isomers, m^1dA and m^6dA; deoxycytidine isomers, m^3dC and m^5dC, as well as the thymidine isomers m^2T, m^3T, and m^4T are all completely separated.

3.3 Ionization Method

While DCI is not capable of ionizing the larger biomolecules which can be examined by ^{252}Cf-plasma desorption [24–26], secondary ion mass spectrometry (SIMS) [27,28] or fast atom bombardment (FAB) [29–32], it is a superior technique in this work since the absence of a matrix results in much lower detection limits than are achievable by the other methods. The suitability of this relatively simple ionization method for analysis of nucleosides has been recognized by others [33]. Experiments with solid (static) SIMS and laser desorption were successful, but failed to exhibit the low detection limits of DCI.

3.4 Tandem Mass Spectrometry: Daughter Ion Mode

The biologically significant minor alkylation product, m^6dG, could not be quantified by single-stage MS analysis [34] because of the poor signal-to-noise in the mass spectrum. MS/MS has therefore been used to increase specificity and sensitivity [13]. Figure 2a shows the daughter spectrum of m/z 166 for 10 ng (36 pmol) of m^5dG. The sensitivity is further improved by using ammonia instead of isobutane as ionization gas (fig. 2b). These data indicate a striking enhancement in specificity and sensitivity for tandem mass spectrometry over single-stage mass spectrometry.

3.5 Tandem Mass Spectrometry: Selected Reaction Monitoring Mode

The sensitivity of the MS/MS experiment can be enhanced even more by a selected reaction monitoring technique. Figure 2c shows the selected reaction monitoring spectrum of 0.01 nanogram (35 femtomole) of m^5dG. This technique has less specificity than scanning the entire tandem mass spectrum because only a few peaks are monitored; however, it has the important advantage of remarkably increased sensitivity due to the fact that all of the analysis time is spent monitoring reactions of interest. This advantage has also been demonstrated in determinations of m^7dG [34]. The procedure has the further advantage that the background noise level can be monitored by selecting for examination fragment ions which do not arise from the analyte.

3.6 Quantitative Analysis by Tandem Mass Spectrometry

Quantitation of pure methylnucleosides with tandem mass spectrometry by using internal standards labeled with deuterium yields excellent linearity in the low ng level [35].

4. Results of DCI MS/MS Analysis

4.1 Tandem Mass Spectrometric Analysis of Methylation of Calf Thymus DNA

Calf thymus DNA was methylated with methyl methanesulfonate [molar ratio (MeMS/DNA-P)=25] at pH 7 for 12 hours. Deuterium labeled 7-methyldeoxyguanosine and O^6-methyldeoxyguanosine were added to the methylated DNA as internal references, subjected to standard enzymatic degradation into nucleosides, and then separated by HPLC. The desorption chemical ionization daughter ion spectra of the corresponding HPLC fractions are shown in figure 3. The quantitative determination is readily made on the basis of the peak ratio of the CH_3-analyte and the CD_3-reference compound and the known amount of the reference compound. The results are shown in table 1, the last column of which is a comparison with the amounts of the methylated nucleosides estimated from other experiments.

4.2 Alternative Approach for Tandem Mass Spectrometric Analysis of Nucleosides

The DCI/MS/MS experiment using multiple reaction monitoring or daughter scans to characterize the protonated base is a considerable improvement over the earlier CI single-stage MS experiments. However, for *quantitation* of the *minor* products of methylation, the method suffers from unacceptably high background signals. An alternative approach for determining methyldeoxyribonucleosides is to measure the nucleoside molecular ion peak. The daughter ion MS/MS spectrum of the pseudomolecular ion ($M+H^+=282$) of O^6-methyldeoxyguanosine (1 ng) shows an intense peak at m/z 166, corresponding to the fragment of

Table 1. Quantitative MS/MS analysis of methyldeoxyguanosines in calf thymus DNA treated with methylmethanesulfonate (analysis at base level)

Nucleoside	[$^2H_3$] methyl nucleoside reference (nmol)	Relative ratio of [$^1H_3$] methyl [$^2H_3$] methyl nucleosides	[$^1H_3$] methyl nucleoside formed (nmol)	[$^1H_3$] methyl nucleoside estimated (nmol)
m^7dG	1.9	0.91	1.7	1.9[a]
m^6dG	3.9×10^{-3}	1.15	4.5×10^{-3}	3.9×10^{-3}[b]

[a] The amount of m^7dG formed is estimated from HPLC results using thymidine as an internal reference.
[b] The amount of m^6dG formed is roughly estimated from the earlier single-stage mass spectrometric analysis containing high experimental error due to the poor signal-to-noise ratio.

O^6-methylguanine. The corresponding spectrum of the solvent blank displays a very weak peak at *m/z* 166 despite the fact that the mass spectrum includes a strong 282 peak. The specificity of MS/MS therefore avoids contributions to the signal from the 282 background. We validated the quantification of O^6-methyldeoxyguanosine by mixing equal amounts of deuterated standard and analyte with enzymatically degraded nonmethylated DNA at the 4 ng level. After going through the analysis scheme the standard deviation was less than 0.2 ng. Therefore analysis at the nucleoside level appears to overcome the background interference problem. Application of this methodology gave results which are illustrated for m^6dG produced by MeNU action on calf thymus DNA (fig. 4). Note that the selected reaction monitoring experiment rather than the full daughter scan will be used to further lower detection limits.

In order to evaluate reproducibility, a sample resulting from methylation of calf thymus DNA with methylnitrosourea (pH 7, 3 hours, MeNU/DNA-P=5) was divided into three portions and separately analyzed (table 2). These results show reasonable precision although consideration of the data collection algorithm reveals a potential source of error. Since the reactions which characterize the labeled standard and the analyte are interrogated alternatively during the short period (2–3 s) that the sample is evaporated, discrimination against one or another signal may occur, depending on the relationship between the evaporation profile of the sample and the points at which data are acquired by the instrument. Consideration of this factor [35] should result in much better reproducibility.

Table 2. Quantitative DCI MS/MS analysis of O^6-methyldeoxyguansine in calf thymus DNA treated with methylnitrosourea (analysis at nucleoside level)

[$^2H_3$] nucleoside reference (mol)	[$^1H_3$] methyl nucleoside formed (mol) uncorrected
8.5×10^{-12}	2.8×10^{-11}
1.1×10^{-11}	3.8×10^{-11}
1.1×10^{-11}	5.4×10^{-11}

5. Conclusion

This project is helping in answering, at the molecular level, questions on the extent and types of reaction of alkylating agents with DNA, and how the *in vivo* persistence of these products correlates with relative cytotoxicity and mutagenicity. It is also providing powerful analytical techniques for the study of the differential toxicity of anticancer alkylating agents in terms of their interaction with cellular DNA. Screening for exposure to alkylating chemicals is a long-term objective for which, with further refinement of the methodology proposed here, the LC/MS/MS methods must be important candidates.

Acknowledgment

This work was supported by the National Cancer Institute (CA35904) and the Environmental Protection Agency (R811138).

Volume 93, Number 3, May–June 1988
Journal of Research of the National Bureau of Standards

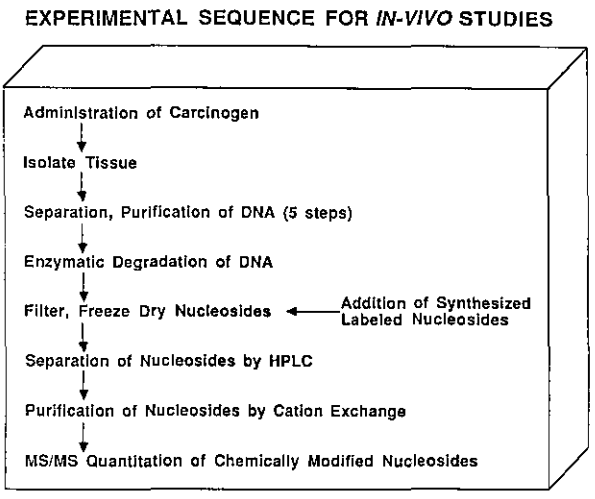

Figure 1. The analytical protocol.

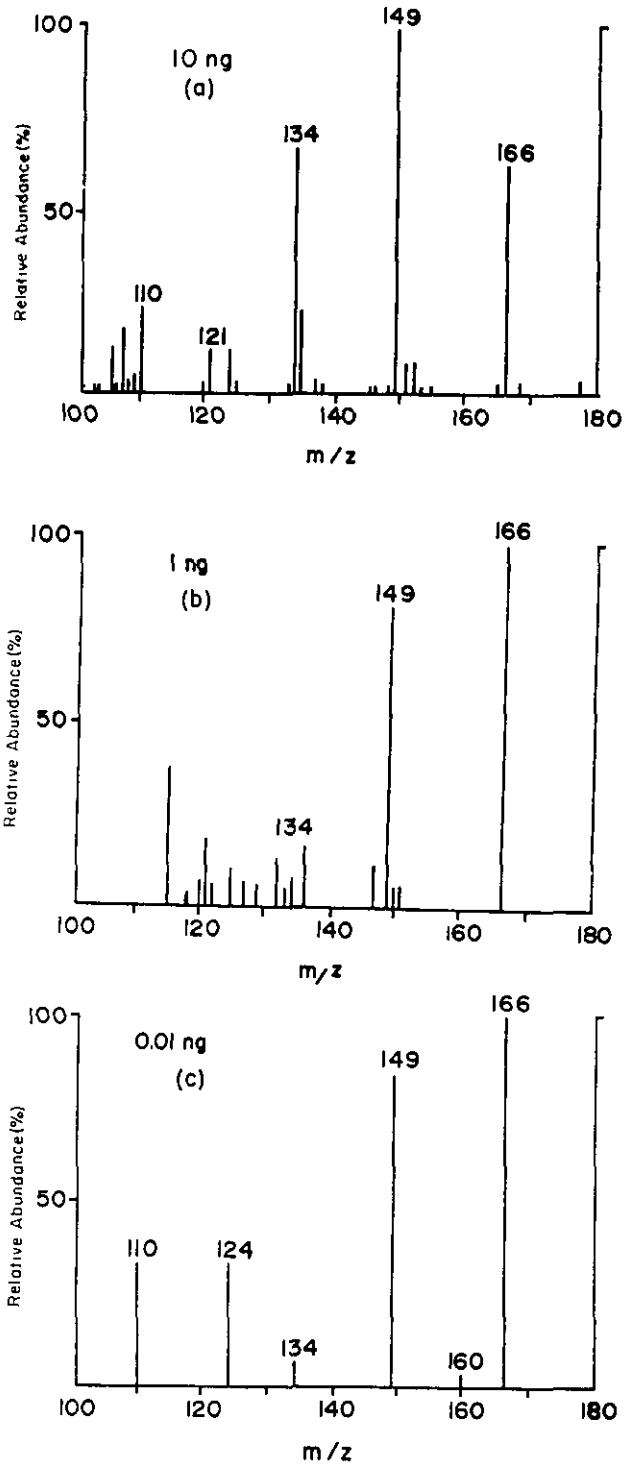

Figure 2. MS/MS data for O^6-methyldeoxyguanosine (a) daughter spectrum of $(M+H)^+$, m/z 166, isobutane CI, multiple Ar collisions, triple quadrupole 20 eV collision energy; (b) daughter spectrum, ammonia CI; (c) selected reaction monitoring, reactant ion 166.

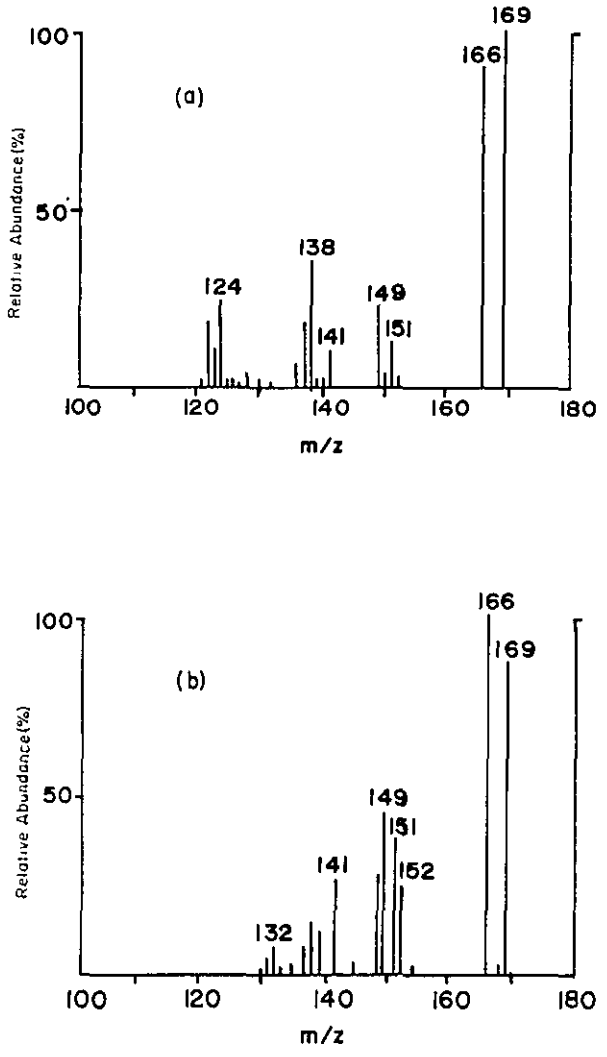

Figure 3. Daughter spectra (Ar, 20 eV, multiple collisions) for quantification of (a) m^7dG and (b) m^6dG using DCI selecting the protonated molecule (m/z 166) and internal standard (m/z 169) in each case.

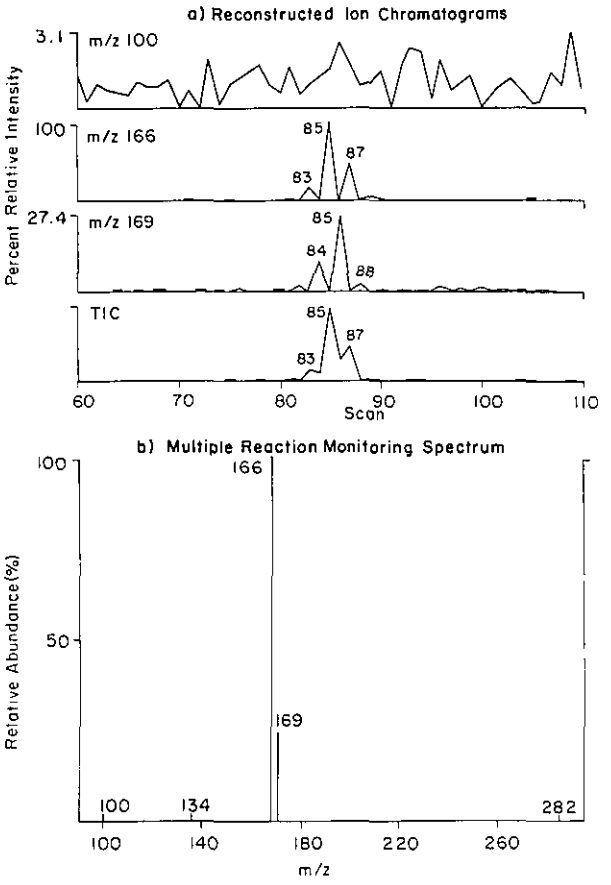

Figure 4. Multiple reaction monitoring experiment to quantitate m^6dG $(M+H)^+=166$ using the d_3 analog (10 ng) $(M+H)^+=169$ in a methylated calf thymus DNA sample. Ionization by DCI, 100 °C/s; fragmentation by 20 eV multiple collisions with argon (a) shows the individual ion chromatograms; (b) shows the multiple reaction monitoring data.

References

[1] Searle, C. E., Chemical Carcinogens, 2nd Ed., American Chemical Society, Washington, DC (1984).
[2] Bartsch, H., Malaveille, C., Camus, A.-M., Martel-Planche, G., Brun, G., Hautefeuille, A., Sabadie, N., Barbin, A., Kuroki, T., Drevon, C., Piccoli, D., and Montesano, R., *Mutat. Res. 76, 1 (1980).*
[3] Rao, T. K., Lijinsky, W., and Epler, J. L., Genotoxicity of N-Nitroso Compounds, Plenum Press, New York (1984).
[4] Rieche, K., Cancer Treat. Rev. **11**, 39 (1984).
[5] Wilman, D. E. V., and Connors, T., Molecular Aspects of Anticancer Drug Action, Neidle, S., and Waring, M. J. (eds.), Verlag Chemie, Weinheim (1983), p. 233.
[6] Singer, B., and Grunberger, D., Molecular Biology of Mutagens and Carcinogens, Plenum Press, New York (1983).
[7] Snow, E. T., Foote, R. S., and Mitra, S., Biochem. **23**, 4289 (1984).

Volume 93, Number 3, May–June 1988
Journal of Research of the National Bureau of Standards

[8] Newbold, R. F., Warren, W., Medcalf, A. S. C., and Amos, J., Nature **283**, 596 (1980).
[9] Eadie, J. S., Conrad, M., Toorchen, D., and Topal, M. D., Nature **308**, 201 (1984).
[10] Brennand, J., and Fox, M., Carcinogenesis **1**, 795 (1980).
[11] Dyroff, M. C., Richardson, F. C., Popp, J. A., Bedell, M. A., and Swenberg, J. A., Carcinogenesis **7**, 241 (1986).
[12] Safhill, R., and Fox, M., Carcinogenesis **1**, 487 (1980); Singer, B., Chavez, F., and Spengler, S. J., Biochem. **25**, 1201 (1986).
[13] Ashworth, D. J., Baird, W. M., Chang, C.-j., Ciupek, J. D., Busch, K. L., and Cooks, R. G., Biomed. Mass Spectrom. **12**, 309 (1985).
[14] DaSilva Gomes, J., and Chang, C.-j., Anal. Biochem. **129**, 387 (1983).
[15] Busch, K. L., and Cooks, R. G., Anal. Chem. **55**, 38A (1983).
[16] McLafferty, F. W., Tandem Mass Spectrometry, Wiley, New York (1983).
[17] Lyon, P. A., (ed.), Desorption Mass Spectrometry. Are SIMS and FAB the Same?, American Chemical Society, Washington, DC (1985).
[18] Magee, C. W., Int. J. Mass Spectrom. Ion Phys. **49**, 211 (1983).
[19] Burlingame, A. L., and Castagnoli, N., Jr., (eds.), Mass Spectrometry in the Health and Life Sciences, Elsevier, Amsterdam (1985).
[20] Maquestiau, A., and Flammang, R., Tandem Mass Spectrometry, McLafferty, F. W., (ed.), John Wiley & Sons, New York (1983), p. 401.
[21] Richter, W. J., Blum, W., Schlunegger, U. A., and Senn, M., Tandem Mass Spectrometry, McLafferty, F. W., (ed.), John Wiley & Sons, New York (1983), p. 417.
[22] Baldwin, M. A., and McLafferty, F. W., Org. Mass Spectrom. **7**, 1353 (1973).
[23] Esmans, E. L., Freyne, E. J., Vanbroeckhoven, J. H., and Alderweireldt, F. S., Biomed. Mass. Spec. **7**, 377 (1980).
[24] MacFarlane, R. D., Anal. Chem. **55**, 1247A (1983).
[25] Sundqvist, B., Hedin, A., Haakansson, P., Kamensky, I., Selahpour, M., and Saewa, G., Int. J. Mass Spectrom. Ion Proc. **65**, 69 (1985).
[26] MacFarlane, R. D., Springer Ser. Chem. Phys. **25**, 32 (1983).
[27] Benninghoven, A., J. Vac. Sci. Technol. **3**, 451 (1985).
[28] Wickramanayake, P. P., Arbogast, B. L., Buhler, D. R., Deinzer, M. L., and Burlingame, A. L., J. Am. Chem. Soc. **107**, 2485 (1985).
[29] Slowikowski, D. L., and Schram, K. H., Nucleosides Nucleotides **4**, 309 (1985).
[30] Slowikowski, D. L., and Schram, K. H., Nucleosides Nucleotides **4**, 347 (1985).
[31] Mitchum, R. K., Evans, F. E., Freeman, J. P., and Roach, D., Int. J. Mass Spectrom. Ion Phys. **46**, 383 (1983).
[32] Hogg, A. M., Kelland, J. G., Vederas, J. C., and Tamm, C., Helv. Chim. Acta **69**, 908 (1986).
[33] Virelizier, H., Hagemann, R., and Jankowski, K., Biomed. Mass Spectrom. **10**, 559 (1983).
[34] Chang, C.-j., Ashworth, D. J., Isern-Flecha, I., Jiang, X.-Y., and Cooks, R. G., Chem.-Biol. Interactions **57**, 295 (1986).
[35] O'Lear, J. R., Ph.D. Thesis, Purdue University (1987).

Ion Mobility Spectrometry after Chromatography—Accomplishments, Goals, Challenges

Herbert H. Hill, Jr. and Randy L. Eatherton

Department of Chemistry
Washington State University
Pullman, WA 99164-4630

The Promises

Ion mobility spectrometry was first introduced to the analytical community in 1970 as an ultra-trace organic technique under the name of plasma chromatography. Using highly sensitive ionization methods commonly employed in electron capture detectors coupled with an atmospheric pressure drift region to separate ions produced, it had the potential for widespread application in the separation and detection of trace quantities of organics.

The Problems

As researchers began to investigate the method, a number of serious problems rapidly became evident: Competitive ion-molecule reactions which occurred in the ionization region of the detector limited its use as a quantitative instrument when complex mixtures were introduced into the spectrometer. Long residence times (sometimes measured in hours) in the spectrometer prevented practical application to a large number of samples. Often spectra for a single component were found to contain multiple ion peaks, hopelessly complicating true multicomponent interpretation.

Recent Accomplishments

We designed and constructed an ion mobility spectrometer that was specifically suited for the detection of trace organics after separation by high resolution gas chromatography [1]. Using a unique unidirectional flow design, problems associated with long residence times in the spectrometer were eliminated. The high resolution gas chromatograph insured the purity of standards and enabled the in-

troduction of sufficiently small quantities of compounds such that only simple uncomplicated spectra were observed by the ion mobility spectrometer. Microprocessor-controlled operation of the ion gates in the drift tube permitted both selective and nonselective detection of chromatographic effluent [2] and the Fourier transform method of operation enabled spectra from rapidly eluting capillary chromatographic peaks to be captured "on the fly" [3]. It was also found that the linear range of the detector could be extended by the use of a photoionization source [4]. As a GC detector the IMD has been compared to the FID and the ECD for contamination effects [5] and has been applied to the detection of 2,4-D in soils [6] and for the determination of barbiturates [7].

Current Goals

More recently, our work has led to investigation of the mobility of ions produced from organic compounds with molecular weights higher than those that can be conveniently eluted from a gas chromatograph. One approach to achieve this goal has been to use supercritical fluid chromatography as the introduction method for IMS [8,9]. Besides the detection of medium range (500–5000 amu) molecular weight compounds, advantages of ion mobility detection after SFC include sensitive detection of compounds which do not contain chromophores, universal detection mode of operation, tunable selective detection, Fourier transform spectra of SFC separated compounds, and compatibility with a wide range of mobile phases.

Future Challenges

Now that interfaces and operational modes for the ion mobility detector have been developed for both gas and supercritical fluid chromatography, the methodology is being investigated for application to real samples. The real challenge for ion mobility spectrometry as a chromatographic detector, however, lies in the detection of compounds separated by liquid chromatography. A significant step toward achieving this goal is the recent development of an electrospray ion source for IMS. By introducing the effluent from a liquid stream into the spectrometer via an electrically charged capillary, we have been able to capture ion mobility spectra from nonvolatile compounds dissolved in the mobile phase. The practical utility of this method of ionization is currently under investigation.

References

[1] Baim, M. A., and Hill, H. H., Jr., Anal. Chem. **54**, 38 (1982).
[2] Baim, M. A., Schuetze, F. J., Frame, J. M., and Hill, H. H., Jr., Amer. Laboratory, Feb., 59 (1982).
[3] Knorr, F. J., Eatherton, R. L., Siems, W. F., and Hill, H. H., Jr., Anal. Chem. **57**, 402 (1985).
[4] Baim, M. A., Eatherton, R. L., and Hill, H. H., Jr., Anal. Chem. **55**, 1761 (1983).
[5] Baim, M. A., and Hill, H. H., Jr., J. Chromatogr. **299**, 309 (1984).
[6] Baim, M. A., and Hill, H. H., Jr., J. Chromatogr. **279**, 631 (1983).
[7] Eatherton, R. L., Siems, W. F., and Hill, H. H., Jr., J. High Resoln. Chromatogr. and Chromatogr. Comm. **9**, 44 (1986).
[8] Eatherton, R. L., Morrissey, M. A., Siems, W. F., and Hill, H. H., Jr., J. High Resoln. Chromatogr. and Chromatogr. Comm. **9**, 154 (1986).
[9] Rokushika, S., Hatano, H., and Hill, H. H., Jr., Anal. Chem. **59**, 8 (1987).

Quantitative Aspects of Glow Discharge Mass Spectrometry

N. E. Sanderson, P. Charalambous, D. J. Hall, and R. Brown

VG Elemental, Ion Path, Road Three, Winsford, Cheshire, England

The problems of quantitation that arise in the direct analysis of solid samples are well known. Amongst them are the preparation and certification of homogeneous standards, and the transfer of calibration factors from standards to similar or dissimilar matrices. These problems have been more aggravated as a result of the increased need for trace analysis at sub-ppm (microgram/gram) levels. Laboratory based instruments traditionally used in this area suffer from poor precision or large matrix effects.

The glow discharge mass spectrometer (GDMS) offers some attractive possibilities in this regard. The glow discharge source delivers a stable, high intensity, ion beam enabling good precision to be achieved from the electrical detection system. The method of ion formation in the source involves

sputtering neutral atoms from the sample and then ionizing them in the plasma. This two-step process is expected to considerably reduce dependence on matrix effects, giving relative ion yields that are not very sensitive to the material or chemical compositions of the sample. Finally, the application of high resolution mass spectrometry removes spectral interferences which in many cases would cause problems for elemental signals at ppm or lower. Results have been obtained by a number of laboratories operating GDMS (VG 9000—manufactured by VG Elemental), which show the above features. Table 1 is a compilation [1] of relative ion yields obtained from a range of standards of different materials. They have been normalized to the value for iron, and it can be seen that the relative yields vary by less than 30% for these dissimilar matrices.

The relative ion yields in table 1 can be used to construct a table of average relative sensitivity factors which can then be applied to matrices for which no convenient standard exists. The expectation is that, in general, this should provide quantitative analysis to within 30%, which is often sufficient at trace levels. Table 2 shows a test of this using a molybdenum sample [2]. After correction with average factors the results are well within 30% of the certified values. Other examples have been obtained. Quantitation can be further improved by using appropriate standards under controlled conditions. In these cases accuracies of 1–2% have been achieved.

Table 1. Relative ion yields for various matrices with the VG 9000 GDMS

Element	Ga	Al	Fe	Cu	Mean RIY	Max deviation %
B		1	1	1.2	1.1	9
Na	1	0.5	0.66		0.72	38
Mg	1	.77	.91		.89	13
Al	0.85	1	.63	1	.87	27
Si	.63	0.91	.5	1	.76	31
S	.5			0.34	.42	19
Cr	.5	.5	.5	.8	.6	33
F	1	1	1	1	1	
Cu	0.34	0.25	0.25	0.30	0.29	17
Ga	.5	.4			.45	11
Zn	.15	.2		.15	.16	25
Se	.3			.33	.34	3
Ge	.63		.5		.56	12
Cd	.18	.17		.17	.17	6
Sn	.34	.4	.42	.43	.42	2
Te	.34			.36	.35	3
Pb	.36	.34	.34	.38	.36	5

Table 2. Analysis of molybdenum sample following calibration with average sensitivity factors

Element	VG 9000 result using average sensitivity factors (ppm wt)	Quoted conc. (ppm wt)
Co	24	21
Cr	51	45
Cu	33	28
Fe	2125	1880
Mn	19	18
Ni	29	28
Si	151	133
V	1.4	1
W	5075	4700
Zr	99	120

Good internal and external precisions are inherent in achieving good quantitation. However, such measurements inextricably link sample homogeneity and instrumental reproducibility. Table 3 shows precisions [2] measured using a VG 9000 on 10 separate samples taken from a block of aluminum. Internal/external precisions of a few percent at the ppm level and 10–20% at the tens of ppb level show *both* good sample homogeneity and instrumental reproducibility. This exercise was in fact undertaken to assess the homogeneity of the material prior to a round-robin exercise.

Table 3. VG 9000 analysis of BCR high purity aluminum

Element	Conc. ppm (ion beam ratio)	RSD %
Mg	0.800 [a]	10
	.792 [b]	8.5
Si	.755	6.3
	.766	2.5
Ca	.126	19
	.149	15.4
Ti	.272	11.8
	.243	14.4
V	.048	6.3
	.047	6.4
Cr	.010	20
	.011	20
Mn	.036	8.3
	.038	7.8
Fe	.497	10
	.519	5.6
Ni	.042	26
	.054	14.8
Cu	.130	42
	.128	27.3
Zn	.017	23.5
	.019	10.5
Pb	.017	11.8
	.017	11.8
Th	.007	14.2
	.006	14.6
U	.005	20
	.005	20

[a] Upper level figures are internal measurements (same sample).
[b] Lower level figures are external measurements (different samples).

References

[1] Mykytiuk, A., and Berman, S., National Research Council, Ottawa; Private communication (1987).
[2] Hall, D. J., Robinson, P. K., and McKinnon, N., VG Applications Laboratory: Private communication (1987).

Studies of Limit of Detection on 2,4,6-Trinitrotoluene (TNT) by Mass Spectrometry

M. R. Lee, S. C. Chang, T. S. Kao, and C. P. Tang

Chung Shan Institute of Science and Technology
P.O. Box 1–4
Lung-Tan, Taiwan, R.O.C.

Various ionization methods including positive chemical ionization (PCI), negative chemical ionization (NCI) and electron impact (EI) were used to study the mass spectra of TNT. Methane, isobutane and ammonia were used as the CI reagent gases. The mass spectrometric quantitation in this study was performed by selected ion monitoring (SIM), with sample introduction via a short capillary column and a solids probe. The best TNT detection limit (ca. 0.020 ng) was obtained with the NCI-SIM technique with isobutane as a reagent gas.

Introduction

The trace analysis of explosives is of importance in forensic science and analytical problems encountered in this field involve the detection of nanogram quantities of explosives in extracts obtained from post-explosion residues [1]. The identification of an explosive residue usually involves extracting the debris with acetone or methanol, then separating the extract by chromatographic methods coupled with a detection technique. Single ion monitoring (SIM) by combined gas chromatography-mass spectrometry is the most promising technique to determine a trace amount of an explosive in an unknown mixture.

The mass spectra of a series of explosives have been reported [2–3]. This report describes the investigation of the limit of detection (LOD) of TNT by gas chromatography-mass spectrometry.

Experimental

All mass spectra were generated with a Finnigan Model 4023 combined gas chromatograph/mass spectrometer (GC/MS) equipped with a dual

CI/EI source. Ultra-high purity methane, isobutane and ammonia (Matheson, Morrow, GA) were used as CI reagent gases.

A 1000 ppm solution was prepared by dissolving purified TNT in acetone, then diluted to different desired concentrations as standard sample solutions. TNT was eluted on a two-meter-long fused silica capillary column (Supelcowax 10) using a helium carrier at 8 psig head pressure. The GC temperature was programmed from 80–250 °C at 30 °C/min. Triplicate 1.0 μL injections of each sample were made.

To operate the solid-probe, the temperature was kept at 40 °C for 2 minutes then heated to 60 °C directly. Triplicate 1.0 μL samples of a series of standard solutions were injected into separate 5 μL glass vials, allowed to air dry, and then introduced into the ion source via the solid-probe.

The selected ions monitored in different modes and the optimized quantitation conditions are listed in table 1. The quantification signal was obtained by the GC peak area, which was the integrated ion current during elution of TNT.

Table 1. Comparison of different methods with short capillary column GC/MS and solids probe for determination of TNT (Source temperature: EI at 250 °C, CI at 150 °C)

Technique	Reagent gas		Ion	LOD (ng)	
	Type	Pressure (torr)	monitored (m/z)	GS/MS	Solid-probe
EI			210	38	75
PCI	CH_4	1.0	228	8.3	21
NCI	CH_4	1.0	227	0.27	
PCI	i-C_4H_{10}	1.0	228	5.8	9.8
NCI	i-C_4H_{10}	1.0	227	0.02	
PCI	NH_3	1.2	168	12	35
NCI	NH_3	1.2	227	1.3	

Results

For the quantitative studies, the limit of detection (LOD) was calculated as the amount of sample necessary to give a signal-to-noise (S/N) ratio of 3. Based on the results of a series of standard TNT solutions, the calibration curves were constructed. From these calibration curves the limit of detection for EI, PCI and NCI with CH_4, i-C_4H_{10} and NH_3 as reagent gases were calculated and are tabulated in table 1. The relative standard deviations of integrated signals for the triplicate analyses having S/N ratio greater than 3 ranged from 5% to 25% for the PCI technique and 2% to 17% for NCI.

From table 1 and figure 1, it was found, as reported [4], that except for NH_3–NCI, the LOD by CI is at least one order lower than that by EI. Regardless of reagent gas used, the ion currents under electron capture conditions in the negative mode exceeds that in the positive ion mode by one or two orders of magnitude. The most sensitive result, an LOD of 0.020 ng was obtained in i-C_4H_{10}–NCI mode as shown in figure 1. Perhaps the energy transfer with isobutane is much less than with methane, and thus causes less fragmentation of the TNT molecular ion (M^-) which was selected as the monitored ion.

The results of quantification of TNT in standards with a solids probe are shown in table 1. The LOD of both PCI and EI modes are at the same levels. In the NCI technique we always obtained a false signal at the same retention time as TNT. Therefore, the LOD of this technique cannot be defined. All the calibration curves were nonlinear as shown in figure 2. The lower response (i.e., sensitivity) at low amounts injected may be due to adsorption in the entire system, including the glassware and syringe.

Conclusion

For the determination of TNT at trace levels, mass spectrometry has been shown to offer several advantages over other techniques. Comparing various MS monitoring modes with different reagent gases, the best monitoring mode for determination of TNT was shown to be isobutane negative chemical ionization with selected ion monitoring of the M^- of TNT at m/z 227. In a standard solution, the best TNT detection limit obtained with a short capillary column GC/NCI-SIM was 0.020 ng. Therefore, this NCI-SIM technique with its high sensitivity made it the preferred method for post-explosion residue analysis.

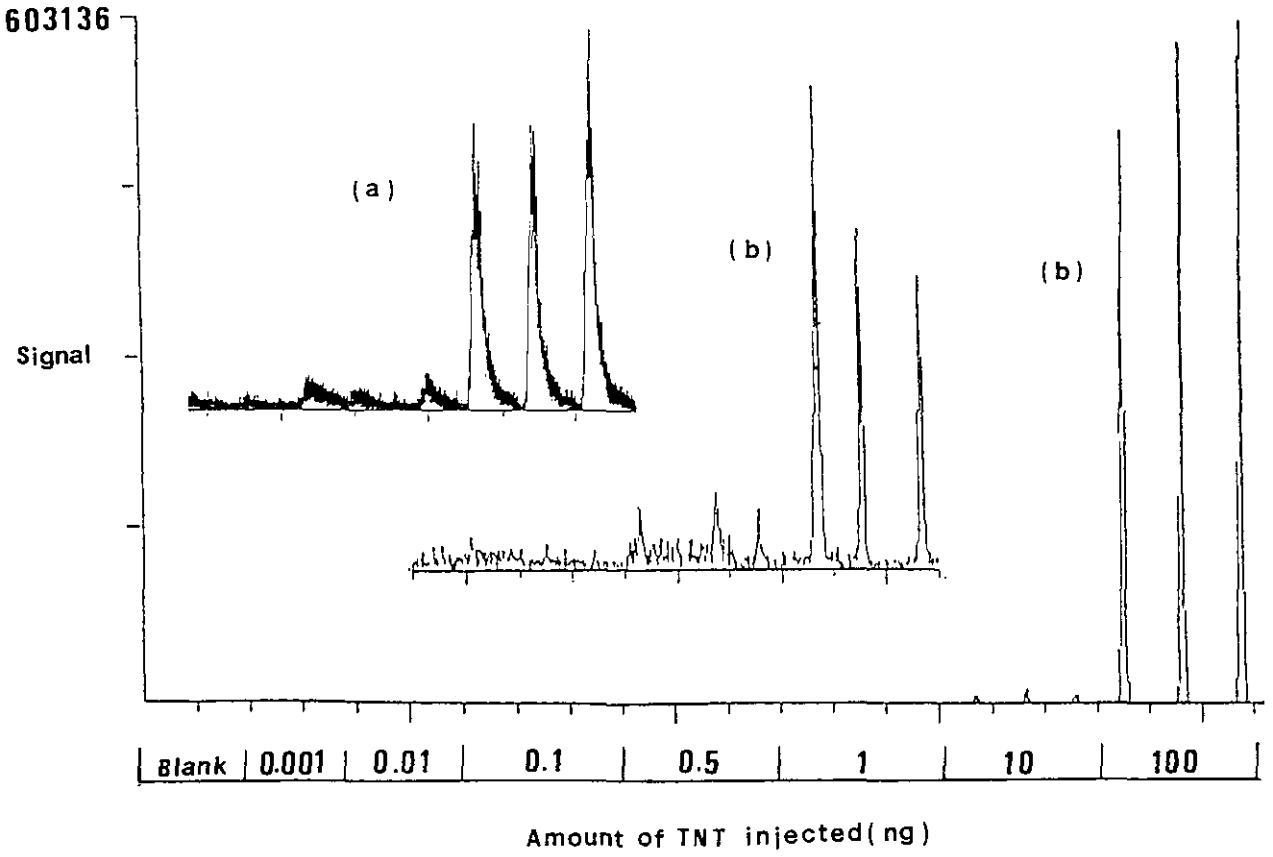

Figure 1. Quantitation of TNT by short capillary column a) NCI(i-C_4H_{10})—SIM(227), b) NCI(CH_4)—SIM(227).

Volume 93, Number 3, May–June 1988
Journal of Research of the National Bureau of Standards

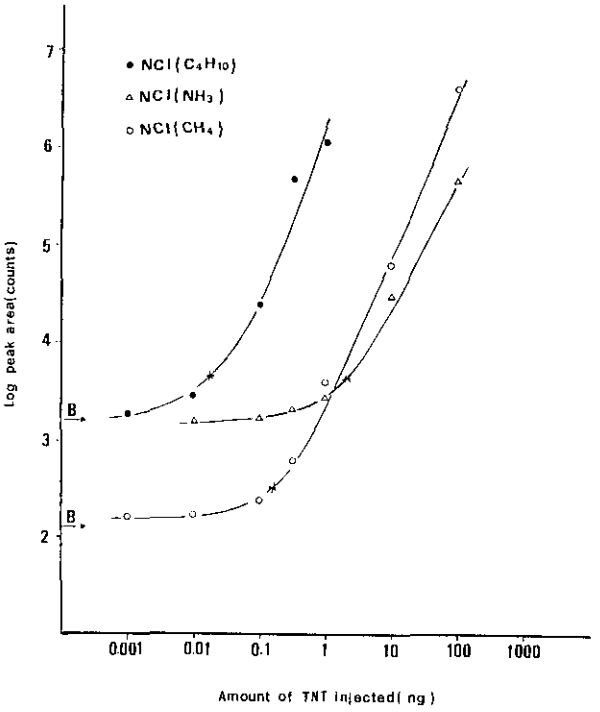

Figure 2. Calibration curves for the short capillary column NCI(i-C_4H_{10})–SIM(227), NCI(CH_4)–SIM(227) and NCI (NH_3)–SIM(227) quantitation of TNT.
B denotes the response of the acetone blank.
* indicates the LOD.

References

[1] Kraus, S., Proc. New Concepts Symp. Workshop Detect. Identif. Explos., Reston, VA, NTIS, Springfield, VA, p. 615 (1978).
[2] Yinon, J., Mass Spectrom. Rev. **1**, 257 (1982).
[3] Lee, M. R., Chang, S. C., Kao, T. S., and Tang, C. P., J. Explos. Propel., R.O.C. **2**, 60 (1986).
[4] Yinon, J., J. Forens. Sci. **25**, 401 (1980).

Absolute Cross-Section Measurements in XQQ Instruments: The NBS Round Robin

Richard I. Martinez

Center for Chemical Physics
National Bureau of Standards
Gaithersburg, MD 20899

Triple-quadrupole (QQQ) tandem mass spectrometry (MS/MS) is used for the analysis of multicomponent mixtures [1]. The analysis makes use of the collisionally activated dissociation (CAD) of "parent" ions. A "parent" ion may be a molecular radical cation, a protonated molecule, or a "progeny" fragment ion (daughter, granddaughter, etc., produced by the CAD of a larger precursor parent ion). A "parent" ion selected by the first quadrupole (Q1) interacts with a target gas within the second quadrupole (Q2). Q2 channels undissociated "parent" ions and "progeny" fragment ions into the third quadrupole (Q3) for mass analysis. The instrument thus produces a CAD spectrum of each initially selected "parent" ion.

But XQQ instruments (QQQ, BEQQ, etc.) are complex ion-optical devices [2–8]. So the choice of parameter settings and/or of instrument design can provide a distorted view of the molecular dynamics of the CAD process (e.g., if there are scattering losses due to poor ion containment within Q2, fringing fields between Q2/Q3, etc. [2–8]). So one observes instrument-*dependent* CAD spectra.

The key MS/MS parameters are:

1) the "target thickness"=(actual path length traversed by the ion in its complex oscillatory trajectory through the gas target)×(effective number density of the CAD target gas);

2) the type of target gas (influences the extent of energy transfer);

3) the center-of-mass interaction energy, E_{cm};

4) the energy level of the analyzing quadrupole Q3 relative to that of Q2;

5) the Mathieu parameter q_2 (rf voltage of Q2) and restrictive interquadrupole apertures of diameter $<1.4\ r_0$; and

6) differences in mass-dependent conversion gain of ion detectors.

For any *one* molecule, these key MS/MS parameters can cause the relative intensities among its var-

ious progeny ions to differ significantly when measured in different XQQ instruments.

This was clearly demonstrated in a recent international round robin [9] wherein very *different CAD spectra were observed for the same molecule*. That is, the relative intensities measured in different QQQ instruments for any given pair of progeny ions differed by factors ranging into the hundreds, even though the same *nominal* operating conditions were supposedly used in each of the QQQ instruments. So a CAD spectrum of a given species in one XQQ instrument presently cannot be used to identify and quantitate that same species in a different XQQ instrument. Moreover, real-time trace analysis often involves unknown transient species (e.g., reactive environmental pollutants and/or products of their photooxidation). Characterization of such species would be facilitated if one could do spectral matching against a generic, instrument-independent MS/MS CAD spectral database comprised of *known* ionic substructures (see [10,11]).

To obtain standardized instrument-*independent* CAD spectra, one must make appropriate corrections for ion-optical effects within each XQQ structure. To do so, one must provide a dynamically correct basis for selecting the key MS/MS parameter settings within each XQQ instrument.

The reactivity (kinetics) of a molecular system is an intrinsic and generic (transferable) property of that system. So the kinetics (reaction mechanisms and rate coefficients) of selected ion-molecule reactions can be used as molecular probes to determine which combination of key MS/MS parameters provide dynamically correct branching ratios for the CAD of polyatomic ions. To do so, all measurements must be made under pseudo-first order, single-collision conditions such that the following kinetic relations are applicable within a reaction zone of length L.

$$\begin{aligned} &\text{For } A^+ + B \rightarrow C^+ + S && [\alpha\sigma] \\ &\qquad \rightarrow D^+ + T && [\beta\sigma] \\ &\qquad \text{etc.} \end{aligned}$$

(σ = total cross-section; branching ratios $\alpha+\beta+\gamma+\ldots=1$),

$$\ln Y \equiv \ln\{[A^+]_0/[A^+]\} = \sigma[B]L \qquad (1)$$

and

$$\ln W_\alpha \equiv \ln\{\alpha[A^+]_0/(\alpha[A^+]_0-[C^+])\} = \sigma[B]L \qquad (2)$$

$$\ln W_\beta \equiv \ln\{\beta[A^+]_0/(\beta[A^+]_0-[D^+])\} = \sigma[B]L \qquad (3)$$

etc.

Equations (1)–(3), etc., place severe constraints [11] on the selection of the key MS/MS parameter settings. The key requirement, however, is that the XQQ instrument must have a *dynamically correct* design. That is, the design should make it possible to adequately control the key MS/MS parameters to provide an undistorted (unbiased) representation of the CAD dynamics (i.e., dynamically correct branching ratios, no back reactions, no impurity reactions, no scattering losses, minimal fringing fields, no mass discrimination, well-defined gas target, etc.). Instrument designs which are incompatible with these requirements cannot provide dynamically correct performance. A dynamically correct instrument is kinetically well behaved if the σ derived from eq (1) equals the σ from eq (2) for a charge transfer reaction with $\alpha=1$. Charge transfer reactions are dynamically equivalent to a "worst-case" CAD reaction system because they take place at large impact parameters with near-zero momentum transfer.

Work from this lab [10,12–14] has demonstrated that dynamically correct branching ratios α, β, ..., etc., can be measured in our kinetically well-behaved QQQ instrument [15] when the key MS/MS parameters are properly selected. For $N_2^+(SF_6,N_2)SF_x^+$ ($x=1-5$), $\alpha+\beta+\gamma+\delta+\epsilon\simeq 1.0$ when σ derived from eq (1) equals σ from eq (2), (3), etc. [14].

Our σ values for $Ar^+(Ar,Ar)Ar^+$ [10] and $Ne^+(Ne,Ne)Ne^+$ [12] agreed to within $\pm 10\%$ with experimental and theoretical results from the literature. So the largest *absolute* uncertainty in the effective target thickness $\{[B]L\}$, and therefore in our σ values is probably on the order of $\pm 10\%$. This $\pm 10\%$ error estimate is consistent with our observations that deviations from linearity in ln W vs P plots occurred only when single-collision conditions were exceeded. So single-collision conditions must be used if one is to develop and use a *generic, instrument-independent* MS/MS CAD spectral database [10,11].

The NBS Round Robin will provide a "zeroth-order" assessment about which XQQ instruments have dynamically correct designs, and therefore may be well suited for the generation of standardized reference CAD spectra. A test protocol is being formulated. It will involve: i) the in-situ target thickness calibration of each participant's XQQ instrument {by using eqs (1) and (2) with our σ for

$Ar^+(Ar,Ar)Ar^+$ [10] to determine the target thickness [B]L}, followed by ii) the experiment associated with figure 1(a) of [9].

References

[1] Yost, R. A., and Fetterolf, D. D., Mass Spectrom. Revs. **2**, 1 (1983).
[2] Dawson, P. H., Quadrupole Mass Spectrometry and its Applications, Elsevier, Amsterdam (1976).
[3] Dawson, P. H., Adv. Electronics Electron Phys. **53**, 153 (1980).
[4] Dawson, P. H., Int. J. Mass Spectrom. Ion Phys. **20**, 237 (1976).
[5] Dawson, P. H., and Fulford, J. E., Int. J. Mass Spectrom. Ion Phys. **42**, 195 (1982).
[6] Dawson, P. H., French, J. B., Buckley, J. A., Douglas, D. J., and Simmons, D., Org. Mass Spectrom. **17**, 205 (1982).
[7] Dawson, P. H., French, J. B., Buckley, J. A., Douglas, D. J., and Simmons, D., Org. Mass Spectrom. **17**, 212 (1982).
[8] Shushan, B., Douglas, D. J., Davidson, W. R., and Nacson, S., Int. J. Mass Spectrom. Ion Phys. **46**, 71 (1983).
[9] Dawson, P. H., and Sun, W.-F., Int. J. Mass Spectrom. Ion Processes **55**, 155 (1983/1984).
[10] Martinez, R. I., and Dheandhanoo, S., J. Res. Natl. Bur. Stand. (U.S.) **92**, 229 (1987).
[11] Martinez, R. I., Rapid Commun. Mass Spectrom. (1987), to be submitted.
[12] Martinez, R. I., and Dheandhanoo, S., Int. J. Mass Spectrom. Ion Processes **74**, 241 (1986).
[13] Martinez, R. I., and Dheandhanoo, S., Int. J. Mass Spectrom. Ion Processes, in press.
[14] Martinez, R. I., and Ganguli, B., Int. J. Mass Spectrom. Ion Processes, to be submitted.
[15] Martinez, R. I., Rev. Sci. Instrum., in press.

Assessment of the Analytical Capabilities of Inductively Coupled Plasma-Mass Spectrometry

H. E. Taylor and J. R. Garbarino

U.S. Geological Survey
Denver, CO

A thorough assessment of the analytical capabilities of inductively coupled plasma-mass spectrometry was conducted for selected analytes of importance in water quality applications and hydrologic research. A multielement calibration curve technique was designed to produce accurate and precise results in analysis times of approximately one minute. The suite of elements included Al, As, B, Ba, Be, Cd, Co, Cr, Cu, Hg, Li, Mn, Mo, Ni, Pb, Se, Sr, V, and Zn.

Experimental

Isotopes for analytical measurements were selected based on freedom from isobaric interferences, whenever possible. Experimental conditions were chosen to minimize both multiply charged and molecular ions.

Samples were run directly, after field filtration (0.45 μm) and preservation with ultrahigh purity nitric acid. To maximize measurement precision, samples were peristaltically pumped to a modified Babington-type nebulizer. Operating conditions of both the plasma and spectrometer are listed in table 1. Optimum ion lens settings varied from element to element as determined by simplex optimization techniques. Compromise settings were selected to facilitate multielement determinations.

Ion currents were measured in the "multielement" mode with a 0.25 second measurement time and 5 replicates. Low resolution conditions were selected with intensity measurements made at 3 points on each peak.

Table 1. Operating parameters

RF Power	1.2	kW
Plasma Ar flow	13	L/min
Aux. Ar flow	1.4	L/min
Aerosol Ar flow	0.5	L/min
Sample delivery	1.8	mL/min
Ion lenses		
Barrel	4.3	V.D.C.
Stop	−5.2	V.D.C
Einzels	−13	V.D.C.
Plate	−14	V.D.C.

Results and Discussion

Representative calibration curves are shown in figure 1 for selected representative elements Cd, Cr, Cu, Ni, and Tl. The curves are linear over at least four orders of magnitude. Similar curves were obtained for each of the other elements. Under these operating conditions, background currents were on the order of 10 counts per second.

Optimally, a coefficient of variation of 5% is obtained at a concentration of approximately 10 μg/L for each element. Below this concentration, the co-

efficient of variation increases rapidly, at 100 μg/L, it is increased to about 10%.

Drift is shown in figure 2 for representative elements, Cd, Pb, Li, and Sr, which were selected to cover the entire mass range. Drift is shown as a percentage change in ion current from its initial value. This illustration demonstrates that drift across the entire mass range is essentially random in nature and is sufficiently low in magnitude to obviate the need for internal standard compensation.

The effects of sample matrix composition on the accuracy of the determinations showed that matrix elements (such as Na, Ca, Mg, and K) that may be present in natural water samples at concentration levels greater than 50 mg/L resulted in as much as a 10% suppression in ion current for analyte elements. Figure 3 shows the effect of increasing potassium concentration on selected analyte elements, Li, Sr, Cd, and Pb.

Operational detection limits are listed in table 2 for each of the analyte elements. Detection limits were calculated at the 95% confidence level, and represent true detectability for each element.

Table 2. Detection limits (μg/L)

Element	Det. limit	Element	Det. limit
Ag	0.8	La	0.1
Al	1	Li	0.4
As	0.5	Mn	0.2
B	0.8	Mo	0.4
Ba	0.5	Ni	0.3
Be	0.4	Pb	0.4
Cd	0.6	Se	0.2
Co	0.1	Sr	0.2
Cr	0.6	Sn	2
Cu	0.3	Tl	0.2
Hg	7	V	0.5
		Zn	0.7

Conclusions

Several reference materials were analyzed to determine the degree of bias on the determinations. National Bureau of Standards Standard Reference Materials 1643a and 1643b and an assortment of U.S. Geological Survey Reference Materials were analyzed for each of the elements previously specified. A linear regression of the published values of concentration of these elements versus the experimentally determined concentrations show a linear relationship with a slope of 0.968 and a correlation coefficient of >0.99.

The data and examples presented show that the technique described is a suitable approach for analyzing natural environmental water for trace elements.

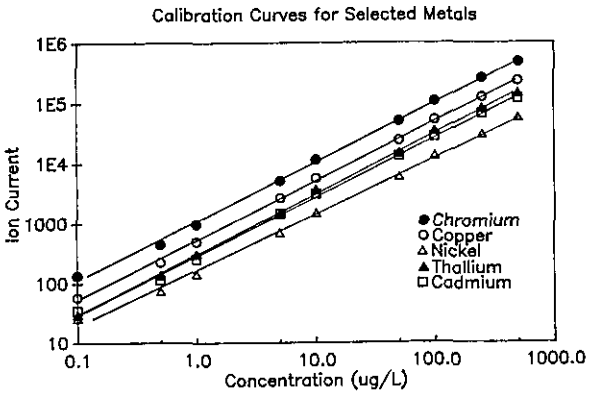

Figure 1. Calibration curves for selected metals.

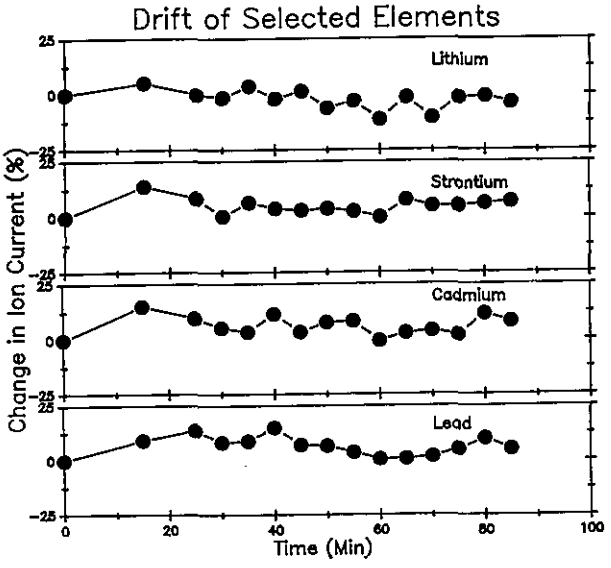

Figure 2. Drift of selected elements.

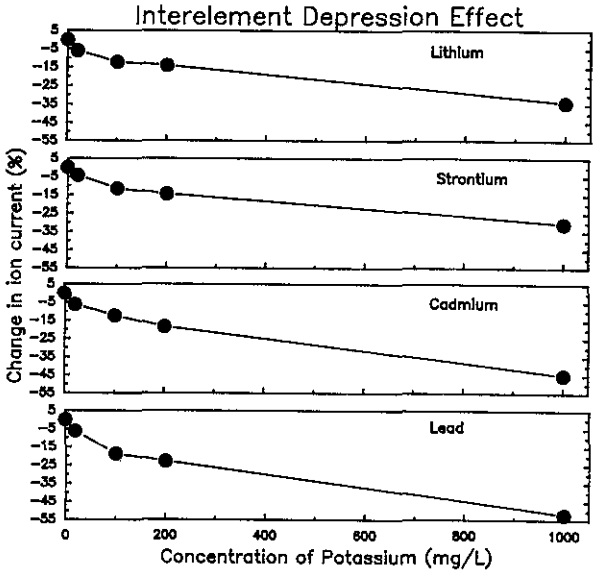

Figure 3. Interelement depression effect.

Volume 93, Number 3, May–June 1988
Journal of Research of the National Bureau of Standards

Accuracy in Trace Analysis

Molecular Spectroscopy

Fluorescence Spectrometric Determination of Nonfluorescent Compounds via Molecular Fragmentation

E. L. Wehry

Department of Chemistry
University of Tennessee
Knoxville, TN 37996

Molecular fluorescence spectrometry offers several important analytical advantages, including (a) achievement of very low limits of detection for intensely fluorescent analytes, (b) applicability to determine individual constituents of multicomponent samples without prior separation, (c) applicability to remote detection of analytes via fiber optic and/or laser probes, and (d) the high information content of luminescence measurements (excitation and emission spectra, decay times, polarization).

A principal shortcoming of fluorescence spectrometry is the fact that most organic and inorganic molecules exhibit low luminescence quantum yields and thus cannot be detected by fluorometry without first being converted to fluorescent derivatives. Accordingly, many procedures for derivatizing nonfluorescent analytes to form luminescent products have been devised.

Our work takes a somewhat different approach to fluorometric detection of nonfluorescent molecules. We exploit the fact that many small molecular fragments are intensely luminescent, including such common species as NH, OH, CN, CH, PO, and SH, as well as many atoms. Fluorescent fragments can be produced from virtually any nonfluorescent molecule. For analytical purposes, the key is to perform the fragmentation in a sufficiently reproducible manner that the fluorescence intensity of a fragment species can be related to the concentration of parent molecule present in the initial sample.

We presently perform molecular fragmentations in the gas phase, to avoid "cage effects" which often decrease the efficiencies of fragmentation processes in liquid or solid media to unacceptably low levels. From among the large number of possible techniques for molecular fragmentation, we have chosen laser photolysis (LP) and electron impact (EI) as the most promising methods.

In LP experiments, gaseous samples are fragmented by either the beam from an excimer laser (193 nm) or tunable radiation from an excimer-pumped dye laser. In EI methods, molecules are fragmented by 100-eV electrons from a conventional heated-filament electron gun. A certain fraction of fragment species are produced in electronically excited states and emit directly. If needed, a "probe" laser can be used to excite luminescence from fragments formed in their ground electronic states by LP or EI. Vacuum systems comparable in design and performance to those found in conventional mass spectrometers are usually used, though LP fragmentations can also in principle be applied directly to remote atmospheric sensing. Conventional fluorescence measurement and signal-processing techniques are used.

We will describe studies of the analytical characteristics (limits of detection, linear dynamic range, precision) for LP and EI fragmentation-fluorometric detection of a variety of nonfluorescent organic and organometallic compounds. The possibility of using low-temperature techniques (matrix isolation or supersonic expansion) to increase the selectivity of such measurements will be described. The complementarity of these measurements to mass spectrometry will be emphasized (most of the intensely emissive fragment species are neutrals, whereas ionic fragments are detected in mass spectrometry).

Volume 93, Number 3, May-June 1988
Journal of Research of the National Bureau of Standards

Accuracy in Trace Analysis

Enhanced Multidimensional Luminescence Measurements Through Cyclodextrin Complexation

I. M. Warner, G. Nelson, G. Patonay, L. Blyshak, and S. L. Neal

Department of Chemistry
Emory University
Atlanta, GA 30322

Cyclodextrins (CDxs) are cyclic oligosaccharides made up of 6, 7, or 8 glucopyranose units for α, β, and γ-CDx, respectively. These molecules are torus-shaped, with an interior cavity size ranging from 5 Å for the smaller α-CDx to 10 Å for the larger γ-CDx. While the CDx is water soluble, the cavity is characterized as hydrophobic. Consequently, an appropriately sized hydrophobic molecule can form an inclusion complex with the CDx. Often, the molecules involved in these complexes exhibit different properties than their uncomplexed forms, such as precipitation of the CDx complex, or a change in spectroscopic parameters of the included molecule. Cyclodextrin chemistry therefore offers a means for gaining selectivity and sensitivity in a variety of analytical measurements.

Many studies have demonstrated that the selectivity and accuracy of quantitative measurement of individual luminophors in a complex sample can be enhanced by simultaneous exploitation of multiple parameters. The combination of many multiple parameters could potentially provide specificity for the measurement. The most commonly used form of multidimensional luminescence measurement is the excitation-emission matrix (EEM), i.e., the measurement of the luminescence as a function of multiple excitation wavelengths (λ_{ex}) and multiple emission wavelengths (λ_{em}). In this talk, we discuss the use of CDxs to enhance selective detection via EEM measurements. Particular emphasis will be placed on the enhanced measurement of luminophors complexed with CDxs in the presence of select alcohols and quenchers. In addition, the use of solvent extraction and data analysis to reduce the dimensionality of the acquired EEM will be discussed.

Cyclodextrin complexation has been demonstrated to enhance the fluorescence of many types of included molecules. The lengthening of fluorescence lifetime [1], change in the fluorescence quantum yield [2], and shifts in the peak shape and position [3] have been observed as a consequence of complexation of fluorophors with CDxs. The addition of aliphatic alcohols to CDx systems has been shown to further enhance changes in these parameters [4]. These changes are often used to quantify the formation constants of a particular complex. Yet, in many instances, such changes are not of sufficient magnitude to quantify an analyte in a complex matrix.

One method of further enhancing the selectivity of CDx complexation is through the use of added quenchers. The accessability of some quenchers to a fluorophor is reduced by complexation of the fluorophor with CDxs. The presence of aliphatic alcohols further reduces the quenching of a CDx included fluorophor. A model system employing naphthalene and β-CDx will be discussed to demon-strate these principles. Appropriate Stern-Volmer type equations will be presented to explain the quenching phenomena observed in these studied.

Quenching may be successfully exploited for the analysis of a mixture of fluorescent molecules in the presence of CDx, where complexes of differing formation constants and protection from quenching interactions are present. In many cases, quenchers interact similarly with various classes of fluorescent molecules. Even the coupling of selective fluorescence measurements employing EEMs with quenching may not be sufficient to analyze a particular component. Quenching and CDx complexation offers a means of selectively analyzing a single component in a complex matrix. Figure 1 demonstrates the selective enhancement of pyrene in a five component mixture. These measurements will be discussed using fluorescence EEMs to demonstrate their utility in mixture analysis.

Cyclodextrin chemistry may also be successfully utilized in data reduction schemes for mixtures. Rank Annihilation schemes require the knowledge of one of the component spectra in order to elucidate other components present. Such a *priori* knowledge may not be available for some mixtures. The use of CDxs and quenchers can produce a single- or dual-component system from a more complex mixture, which can then be used as model component spectra. This type of data analysis scheme will be presented and discussed.

Research in the area of CDx extraction presently employs low solvent volumes and requires precipitation of the complex from aqueous solution.

Analyses are performed after removal of the included compound from the CDx cavity by shaking the solid complex with another organic solvent. We discuss the development of a solvent extraction scheme for polynuclear aromatic hydrocarbons (PAHs) which allows for isolation of individual components from mixtures. In conventional solvent extraction, a solute is partitioned between two immiscible solvents. In this study, CDxs are used as aqueous phase components to increase the solubility of PAHs in water and thus increase their aqueous extraction efficiencies. The stereoselectivity and hydrophobicity of the CDxs allows for some degree of selective extraction based on the formation constants between different PAHs and the particular CDx used. Thus, CDxs can discriminate between organic phase solutes in an extraction scheme. For example, aqueous γ-CDx extracts only perylene from an organic perylene-anthracene mixture.

Acknowledgments

We would like to acknowledge the National Science Foundation (CHE-8210886) and the Office of Naval Research for funding this research. I. M. Warner acknowledges support from a National Science Foundation Presidential Young Investigator Award (CHE-8351675). G. Nelson acknowledges support from an American Chemical Society, Division of Analytical Chemistry Fellowship sponsored by the Procter and Gamble Company. S. L. Neal acknowledges support from a National Organization of Black Chemists and Chemical Engineers Fellowship, sponsored by the Procter and Gamble Company.

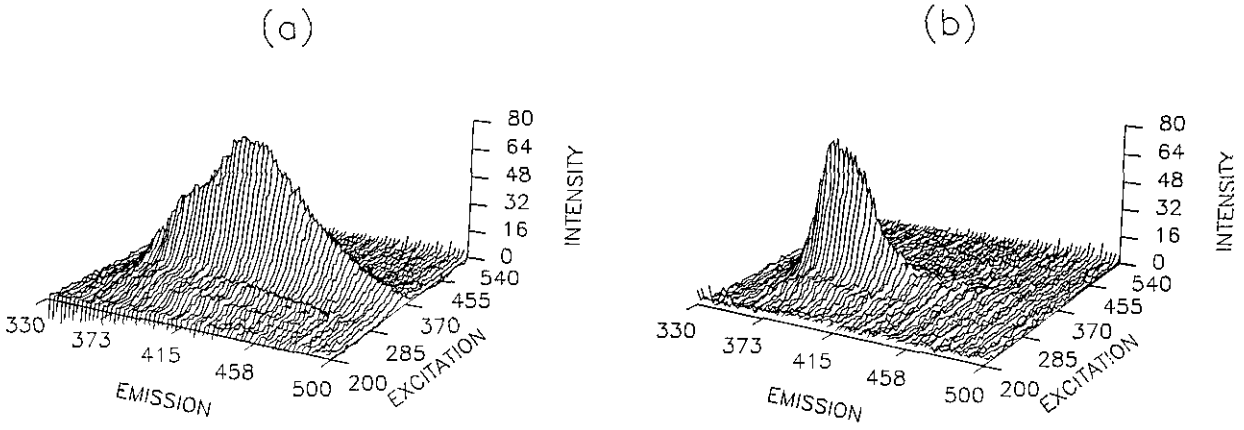

Figure 1. (a) EEM of five component mixture of acridine, 7,8-benzoquinoline, carbazole, fluoranthene, and pyrene. (b) Previous mixture in the presence of potassium iodide, 1% *tert*-butyl alcohol, and 1 millimolar β-CDx.

References

[1] Nelson, G., Patonay, G., and Warner, I. M., Fluorescence Lifetime Study of Cyclodextrin Complexes of Substituted Naphthalenes, Appl. Spectrosc., 1987, in press.
[2] Patonay, G., Shapira, A., Diamond, P., and Warner, I. M., J. Phys. Chem. **90**, 1963 (1986).
[3] Hoshino, M., Masashi, I., Ikehara, K., and Hama, Y., J. Phys. Chem. **85**, 1820 (1981).
[4] Patonay, G., Fowler, K., Shapira, A., Nelson, G., and Warner, I. M., J. Inclusion Phenom., 1987, in press.

Volume 93, Number 3, May-June 1988
Journal of Research of the National Bureau of Standards

Accuracy in Trace Analysis

High Resolution Nonlinear Laser Spectroscopy

John C. Wright

Department of Chemistry
University of Wisconsin
Madison, WI 53706

Ultra-trace analysis is often limited by the selectivity of an analysis procedure because at low concentration levels, there are a very large number of potential interferences. In spectrochemical analysis procedures, the selectivity is limited by two factors:

1. Spectral congestion where each individual component has a number of transitions and a multi-component sample will contain the contributions from all transitions of all components.
2. Line overlap where each transition has a linewidth that can be greater than the average separation between components in the mixture.

High resolution laser techniques were developed that address the problems listed above. The techniques are collectively called site selective laser spectroscopy. They relied upon the idea that a narrow band laser could be tuned to excite selectively an absorption line of a specific component or site within a sample so the resulting fluorescence spectrum came only from the site or component excited. One could simplify spectral congestion with this approach. One could also eliminate broadening that was caused by inhomogeneities in the samples because excitation within a broadened line would only excite components that had energy states resonant with the laser so the resulting fluorescence spectrum would not reflect the inhomogeneities. These methods were applied to matrix isolation, low temperature organic glasses, Shpol'skii systems, inorganic analysis using precipitates, and supersonic jet spectroscopy to measure a variety of inorganic and organic materials at ultra-trace levels. The methods all relied upon sample fluorescence and they failed if the samples were non-fluorescent.

We have recently shown that there is a new family of high resolution laser spectroscopies that have the same capabilities but do not require a fluorescent sample. These spectroscopies are based upon nonlinear mixing where several tunable lasers are focused into a material and new frequencies are formed at all of the sums and differences of the original laser frequencies. This nonlinear mixing is resonantly enhanced when some of the laser combinations match resonances of components in the sample. The nonlinear mixing can be used to perform atomic spectroscopy and molecular spectroscopy. We will concentrate on molecular spectroscopy in this discussion.

One can perform component selection by tuning the lasers to match resonances on one specific component in the sample. One would then expect to have that component contribute dominantly to the nonlinear mixing. One can also eliminate inhomogeneous broadening by tuning the lasers to match the resonances of specific sites within the inhomogeneously broadened line. Again, one would expect that those sites would contribute dominantly to the mixing and the nonresonant sites would be discriminated against.

We have tested these ideas in several model systems using four wave mixing spectroscopy. The two model systems are pentacene doped into p-terphenyl crystals and pentacene doped into benzoic acid crystals where p-terphenyl was added in small amounts to introduce controlled amounts of inhomogeneous broadening. The experiments were done at 2 K to eliminate thermal effects. There are four schemes that one can use to establish resonances with the pentacene molecules. In all of them, one establishes resonances with the vibrational levels, the excited electronic states, and the vibrational levels of the excited electronic state (which we will call vibronic states). The four schemes differ in which states are involved in the resonance associated with the emitted light. If the emitted light involves transitions between two levels that are not initially populated, the technique is classified as a nonparametric process. If one of the levels were initially populated, the technique is a parametric process. Theories for the ideas predict that each possibility will have a different ability to provide selectivity in the measurement.

The pentacene in p-terphenyl system was studied first. Pentacene has four different crystallographic sites in this crystal, some of which differ only slightly from each other. Conventional spectroscopy shows that the transitions from each

component appear together in the spectrum and lead to congestion. The nonlinear, four-wave mixing spectroscopy was applied to see if one could produce spectra from the individual sites without contributions from the other sites. We found that one could obtain single site spectra for the vibrational, electronic and vibronic states separately with high selectivity. There were, in fact, no contributions visible in the spectra from even the nearby sites.

The pentacene in benzoic acid doped with p-terphenyl system was studied as a model to see if one could eliminate inhomogeneous broadening. We used both parametric and nonparametric techniques to test the characteristic of each. We found that both methods could eliminate inhomogeneous broadening to the limit of our laser resolution.

This result was a surprise because the theory for the method predicts that only nonparametric methods could successfully eliminate inhomogeneous broadening. The explanation for the observation of parametric nonlinear mixing removing inhomogeneous broadening could only rest on the possibility that the character of the mixing changes as a function of the laser power because of the participation of excited state populations. A new theory was developed that treated saturation effects correctly and described excited state populations. The theory predicts intensity dependent changes in the relative intensity of the narrowed line to the non-narrowed line. It also predicts that the relative intensities are dependent upon the amount of inhomogeneous broadening. These predictions are consistent with the experimental observations.

At this point, we have succeeded in developing a new class of high resolution laser spectroscopy methods based on nonlinear mixing. The methods do not require that the sample emit light. We have applied the methods to molecular and atomic spectroscopy and are now ready to extend the methods to realistic samples and mixtures. The methods are capable of measuring both bulk concentrations and surface concentrations. Surface specific analysis is possible because nonlinear mixing processes that are based on three wave mixing are only allowed for noncentrosymmetric systems. Thus, three wave mixing will not be observed for the bulk of a material but it will be observed at the interfaces between materials. It is also important to realize that the selectivity is determined on the time scale of the lasers and is not limited by the lifetime of excited states. An environment can change while the excited state is occupied and the changes will act to broaden the spectral line. However, if a picosecond excitation is used in the line narrowing experiment, the motion will be frozen and one can eliminate the broadening. This idea has important implications for solution spectroscopy because the motion within a solvent acts to broaden all of the lines that one would normally observe. There is, in fact, a rich field of opportunity for the development of these spectroscopies that is only being hinted at in our present work and it will be exciting to see what capabilities lie in the future.

Acknowledgment

This work was supported by the Chemistry Division of the National Science Foundation under grant CHE-8515692.

Trace Analysis of Aromatic Compounds in Natural Samples by Shpol'skii Spectroscopy

P. Garrigues, E. Parlanti, and M. Ewald

Groupe d'Océanographie Physico-chimique
UA 348 CNRS Université de Bordeaux I
33405 Talence Cédex, France

Introduction

Polycyclic aromatic hydrocarbons (PAH) and their alkylated derivatives are generally mutagenic or carcinogenic compounds and are common trace components of environmental samples. Besides classical analytical methodologies such as capillary gas chromatography and liquid chromatography, high resolution spectrofluorometry (HRS) at low temperature in n-alkane matrices (Shpol'skii effect) is seeing an increasing interest [1–3].

Since the first observation in the early fifties [4], this method has been extensively applied to the analysis of common PAH (e.g., pyrene, benzo(a)pyrene...), of alkylated derivatives [5,6] or heteroatom containing PAH [7,8] in various crude samples or chromatographic extracts. Results presented in this abstract demonstrate the capability of the Shpol'skii spectroscopy to quantify the PAH priority pollutants.

Experimental Requirements

Fluorescence and phosphorescence spectra of aromatic compounds usually present broad bands at room temperature, having full widths at half-maximum (FWHM) of about 3 nanometers. A sharpening of the luminescence spectra is observed when PAH are incorporated into an appropriate n-alkane matrix frozen at low temperature ($T \ll 77$ K). The low temperature luminescence spectra exhibit a 0-0 transition with several sharp peaks ("quasi-lines") having FWHM about 0.1 nm called multiplet structure and related to different substitution sites of the aromatic molecules in the n-alkane lattice [9].

Experimental conditions for obtaining sharp emission spectra are specific. Particularly, a remarkable matching in length of long axis and short axis of the guest (aromatic) and the host (n-alkane) molecules seems to exist [10]. When this "key and hole" rule is not respected, broad band or complicated quasilinear emission spectra are observed.

A preliminary fast freezing of solution at 77 K in liquid nitrogen is also necessary to avoid aggregate formation [11]. Another feature is also the concentration dependence of the intensity of the quasi-lines. However at low concentration (about 10^{-6} M and less), the formation of aggregates is minimized and the reproducibility of fluorescence intensity is not altered [11,12].

Quantitative Analysis of Selected PAH

The American Environmental Protection Agency (EPA) has retained about 16 PAH as priority pollutants [13]. They have been partially identified by GC-MS or HPLC. Most of these molecules exhibit well resolved emission spectra (fig. 1) in n-octane at 15 K by using a low temperature spectrofluorometer previously described [14]. Perdeuterated PAH (deuterated pyrene and benzo(a)pyrene) have been used as internal standards and have been added to the total organic extract. These compounds exhibit a similar Shpol'skii emission spectra to that of the respective parent compound but with a spectral line shift of about 1 nm.

Most of the EPA PAH could easily be identified and quantified by this technique. Low molecular weight aromatic compounds (acenaphthene, acenaphthalene, fluorene, phenanthrene and anthracene) were difficult to detect due to their low fluorescence quantum yield. To evaluate the accuracy of this method, we have analyzed several organic extracts (diesel particulate, air particulate) used for intercalibration exercises organized by the National Bureau of Standards (Gaithersburg, MD USA). The results (imprecision less than 15%) obtained by Shpol'skii spectroscopy have been compared with values obtained by other analytical methodologies (HPLC coupled with fluorescence detection, GC coupled to mass spectrometry). As presented in figure 2, good agreement is observed among the three analytical techniques, demonstrating the reliability of Shpol'skii spectroscopy for quantitative analysis.

Conclusion

Partial results presented here show the analytical capability of high resolution spectrofluorometry in Shpol'skii matrices for the determination of different priority pollutant aromatic compounds in the total organic extract of natural samples.

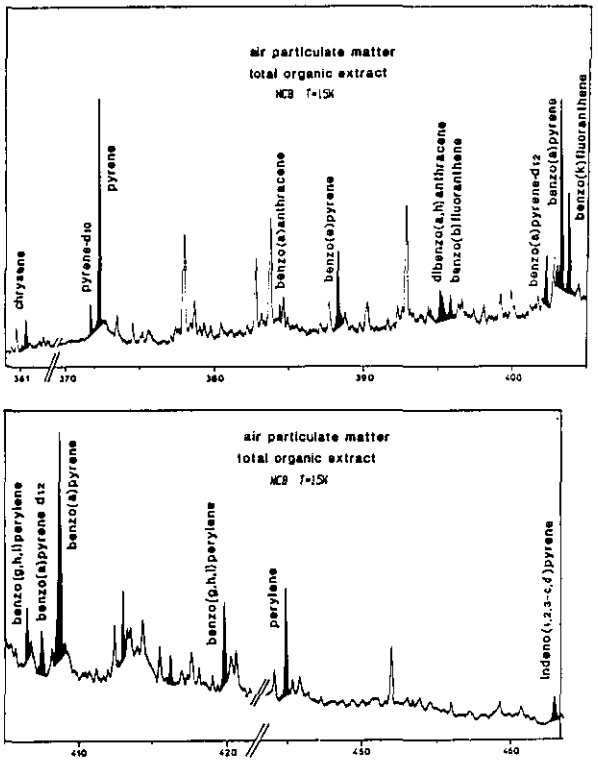

Figure 1. Fluorescence emission spectra of the organic air particulate extract in n-octane at 15 K. Deuterated pyrene and benzo(a)pyrene have been added as internal standards. Excitation wavelengths centered respectively at 275 nm (top) and at 290 nm (bottom).

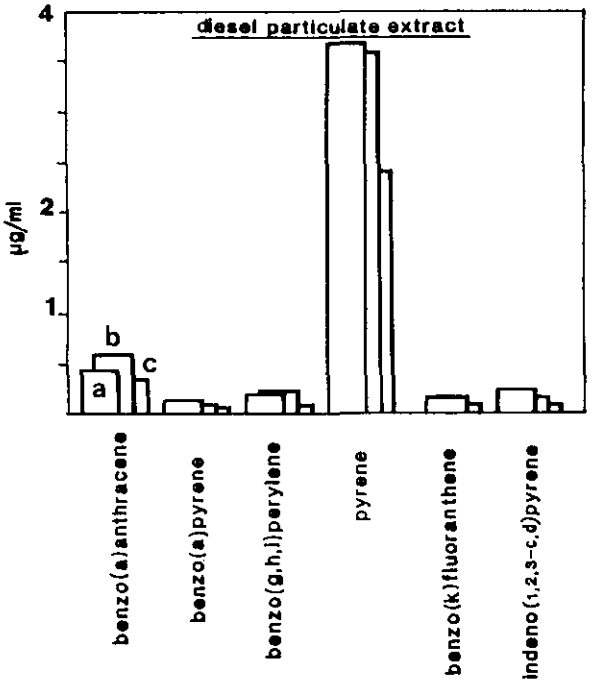

Figure 2. Comparison of the concentration values obtained on a diesel particulate extract for PAH determined by several analytical techniques (International Round Robin organized by the National Bureau of Standards, Gaithersburg, MD, USA): a) Capillary gas chromatography coupled to mass spectrometry (NBS values, ref. 15). b) Liquid chromatography coupled to spectrofluorometry (ref. 15). c) Shpol'skii spectroscopy values.

References

[1] Colmsjö, A., and Östman, C. E., Anal. Chem. **52**, 2093 (1980).
[2] D'Silva, A. P., and Fassel, V. A., Anal. Chem. **56**, 985A (1984).
[3] Garrigues, P., and Ewald, M., Anal. Chem. **55**, 2155 (1983).
[4] Shpol'skii, E. V., Sov. Phys. Usp. (Eng. Transl.) **5**, 522 (1962).
[5] Garrigues, P., and Ewald, M., Org. Geochem. **2**, 52 (1983).
[6] Garrigues, P., Parlanti, E., Radke, M., Willsch, H., and Ewald, M., J. Chromatog. **395**, 217 (1987).
[7] Garrigues, P., De Vazelhes, Ewald M., Joussot-Dubien, J., Schmitter, J. M., and Guiochon, G., Anal. Chem. **55**, 138 (1983).
[8] Dorbon, M., Schmitter, J. M., Garrigues, P., Arpino, P., Ewald, M., and Guiochon, G., Org. Geochem. **7**, 117 (1984).
[9] Lamotte, M., Merle, A. M., Joussot-Dubien, J., and Dupuy, F., Chem. Phys. Lett. **35**, 410 (1975).
[10] Garrigues, P., De Sury, R., Bellocq, J., and Ewald, M., Analysis **13**, 81 (1985).
[11] Garrigues, P., Lamotte, M., Ewald, M., and Joussot-Dubien, J., C. R. Acad. Sci. série II **293**, 567 (1981).
[12] Garrigues, P., Thèse de doctorat ès Sciences, Université de Bordeaux I (1985).
[13] US-EPA Effluents Guidelines Division, Washington (1977).
[14] Soclo, H. H., Garrigues, P., and Ewald, M., Analysis **14**, 344 (1986).
[15] May, W. E., Personal Communication (1987).

Sodium Taurocholate Micelles in Fluorometrix Analysis

Linda B. McGown and Kasem Nithipatikom

Department of Chemistry
Gross Chemical Laboratory
Duke University
Durham, NC 27706

Sodium taurocholate (3α,7α,12α-trihydroxy-5β-cholanoyl taurine, sodium salt), NaTC, is a micelle-forming bile salt. The three hydroxy groups on the cholic acid part of the molecule play an important role in the micellar characteristics of NaTC, and, along with the taurine group, serve to solubilize NaTC in aqueous solutions [1]. The most commonly observed micellar form has an aggregation number of four and can bind other molecules in the relatively hydrophobic interior, usually with a 1:1 stoichiometry [2]. The formation of secondary micelles has not been observed. Insoluble biological lipids can be solubilized by comicellization with NaTC [3] and NaTC can also form mixed micelles with detergent molecules [2]. The micellar properties of NaTC are relatively insensitive to experimental conditions. The aggregation number and critical micelle concentration (CMC) show very little dependence on pH in the range of 1.6–10 [1], on counterion concentration, and on temperature in the range of 10–60 °C [3]. A CMC of 3 mM was found from the shift in the absorption wavelength maximum of Rhodamine 6G [3].

We have used fluorescence probe molecules to study NaTC micelles alone and in NaTC-detergent mixed micellar solutions. Results were compared with those obtained for individual detergent micellar solutions, including SDS, Triton X-100 (reduced form) and CTAC. Pyrene was used as a probe of the micellar binding site polarity, and perylene was used in fluorescence lifetime and polarization studies. Nonradiative energy transfer

from pyrene to perylene was inhibited in NaTC micellar solutions, and promoted in SDS micelles and SDS-NaTC mixed micelles. Our studies indicate that the binding site characteristics of NaTC micelles, detergent micelles and mixed micelles are all distinctly different from each other.

We have also studied the effects of metal cations, including Eu^{3+}, Tb^{3+} and Al^{3+}, on the fluorescence intensities of polycyclic aromatic hydrocarbon (PAH) compounds in NaTC micelles. Enhancements as large as 18-fold were observed, and the extent of enhancement tends to increase with decreasing aqueous solubility of the PAH. The fluorescence of relatively soluble PAHs such as phenanthrene and carbazole was quenched by the metal ions in NaTC solutions, suggesting that the more soluble PAHs may not even be bound to the NaTC micelles. Calibration curves were found for several PAHs in NaTC solutions, and were used in the calculation of detection limits for the PAHs which were compared to detection limits obtained in SDS micellar solutions.

References

[1] Small, D. M., Molecular Association in Biological and Related Systems (R. F. Gould, ed.), Advances in Chemistry Series No. 84, pp. 31–52, American Chemical Society, Washington, DC (1968).
[2] Chen, M., Gratzel, M., and Thomas, J. K., J. Amer. Chem. Soc. 97, 2052 (1975).
[3] Carey, M. C., and Small, D. M., J. Colloid. Interface Sci. 31, 382 (1969).

Volume 93, Number 3, May–June 1988
Journal of Research of the National Bureau of Standards

Atomic Spectroscopy

Accuracy in Furnace Atomic Absorption Spectroscopy

W. Slavin

Perkin-Elmer Corporation
901 Ethan Allen Hwy.
Ridgefield, CT 06877

This paper holds that, when graphite furnace atomic absorption spectroscopy (GFAAS) is used correctly, it comes as close to being accurate as any analytical technique that has been proposed for trace metal determination. The signal for the analyte does not depend upon the particular matrix. Thus, if GFAAS is used correctly, it should be as close as is presently possible to providing a reference method for trace metals. The same simple standards should suffice for all samples whether they are biologicals, alloys or industrial products.

We admit that there still are situations for which this opportunity does not apply. Sometimes this is because we struggle to make do with outmoded instrumentation that was never designed for the modern graphite furnace or instrumentation that is not working properly. Sometimes it is because some of us don't want to solve our analytical problem in a simple way. If we try to take a simple and theoretically correct approach, failures of the system to work will help us understand why the theory does not apply.

By now there are more than a hundred papers in the literature confirming situations where the simple and general technique has been used [1], which has come to be called the stabilized temperature platform furnace (STPF). Of course, many more analysts are using these procedures without publishing because they have simply confirmed with reference materials or by comparison with earlier more laborious procedures that the simple methodology worked well.

Background Correction Error Sources in GFAAS

An important and frequent source of error is the failure of the background correction system to perform its role. Several methods for correcting matrix background errors have been proposed and almost every furnace measurement requires that some kind of background correction be made.

The earliest background correction relied on a measurement with continuum radiation that provided almost no signal for the analyte [2]. This worked very well if the background effects were not too large and if the beams from the two light sources were very carefully superimposed. There are many analytical situations which can be handled well with continuum source background correction but there are more situations which cannot.

In recent years the Zeeman effect has been adapted to background correction [3]. There are several advantages to Zeeman correction but the most important is that only one light source is necessary. This avoids the adjustment problem associated with continuum correction.

Smith and Hieftje [4] suggested that a single source could be used in two modes, the background correction mode being accomplished with an intense self-absorbed pulse from the lamp that is therefore insensitive to the analyte. The major limitation to their proposal, when it is applied to the graphite furnace, is that a considerable time is required after the large lamp pulse for the atomic cloud to dissipate. This delay forces a slow chopping frequency that is incompatible with the fast signals from the furnace.

Atomization Efficiency

The L'vov theory implies that it is possible to fully atomize the sample, or at least the analyte at the chosen furnace temperature. This was argued for many years but L'vov [5] and others have now shown that for the bulk of the elements determined in the furnace the efficiency of atomization is very close to 100%. Some elements are exceptions to this, and these elements cannot yet be determined

in the furnace with confidence that the matrix will not affect the efficiency. These troublesome elements are mainly among the rare earth and some of the alkali and alkaline earth elements. Furnaces that avoid graphite, e.g., by using tantalum [6], may make these elements accessible to interference-free AAS.

Another implication of the requirement for full atomization of the analyte is that the matrix components will not form strong vapor phase bonds that remove the analyte from the atomic state required for AAS. The halides form such vapor phase bonds with many metals and this continues to be troublesome [7]. Matrix modifiers are used to stabilize the analyte so that a char step can be used to remove much of the halide. However, present commercial furnaces have cold ends which condense some portion of the vaporized halide during the char step. This condensed halide is revaporized in the atomization step producing an interference in some situations. Indeed it is this problem that limits the amount of halide that can be present to a few percent for several analytes.

There are several ways to handle this. One is to make a furnace that is free of cold ends [8]. Another way is to avoid the char step entirely and depend upon the halide to have diffused out of the furnace before or after the analyte is vaporized. This usually requires Zeeman correction because the background signals become large when the char step is avoided. We have used this successfully for Tl in the presence of large amounts of chloride but we haven't studied this approach on a general basis yet.

Instrumental and Methodological Quality Assurance

Every instrument and every analytical method has the potential for error. Certainly, making available reference materials in a wide variety of matrices, accurately characterized for the many trace metals that must be determined, is an important step towards satisfying this need for quality assurance. We routinely use NBS Standard Reference Material (SRM) 1643 (Trace Metals in Water) as a test of our analytical conditions and of our standards.

This paper has emphasized that the analytical curve from simple standard solutions applies equally to a wide range of matrices. The slope of the linear portion of an analytical curve for each element is reported as characteristic mass, the mass of analyte in pg that produces a 1% absorption (which is 0.0044 absorbance) signal. These are integrated signals so the units are absorbance seconds (A·s). We have shown that instruments with similar furnace geometries provide very similar characteristic masses [9]. Thus, obtaining the expected characteristic mass for a particular analyte is a useful quality assurance indicator.

There are many experimental situations which can alter the apparent characteristic mass and three elements, Ag, Cu and Cr, have been chosen for a test procedure to be used for several purposes. The test confirms that our instrument is working well each day, that different instruments are working similarly and confirms that Zeeman instruments are working well when they leave our factory.

NBS SRM 1643b Trace Metals in Water is used without dilution to avoid pipetting and contamination errors. Instrumental conditions are used which introduce as few variables as possible. No matrix modifier or char step is used. Some of the test data and experience with this test have been reported [10] but much more work must still be done.

While most graphite furnaces are still purchased for routine determination of trace metals in widely varied materials, there is a gradual acceptance of the new furnace technology as the primary means for calibrating standards to be used for other faster but less accurate techniques. There are still instrumental improvements ahead and considerable work is required to simplify the analytical procedures by making fuller use of the new furnace technology.

References

[1] Slavin, W., *Graphite Furnace AAS—A Source Book*, Perkin-Elmer Corp. (1984) 993.
[2] Koirtyohann, S. R., and Picket, E. E., Anal. Chem. **37**, 601 (1965).
[3] de Loos-Vollebregt, M. T. C., and de Galan, L., Prog. Anal. At. Spectrosc. **8**, 47 (1985).
[4] Smith, S. B., Jr., and Hieftje, G. M., Appl. Spectrosc. **37**, 419 (1983).
[5] L'vov, B. V., Nikolaev, V. G., Norman, E. A., Polzik, L. K., and Mojica, M., Spectrochim. Acta **41B**, 1043 (1986).
[6] Sychra, V., Kolihova, D., Vyskockova, D., and Hlavac, R., Anal. Chim. **105**, 263 (1979).
[7] Slavin, W., Carnrick, G. R., and Manning, D. C., Anal. Chem. **56**, 163 (1984).
[8] Frech, W., Baxter, D. C., and Hütsch, B., Anal. Chem. **58**, 1973 (1986).
[9] Slavin, W., and Carnrick, G. R., Spectrochim. Acta **39B**, 271 (1984).
[10] Slavin, W., Manning, D. C., Carnrick, G. R., J. Anal. At. Spectrom., in press.

Volume 93, Number 3, May–June 1988
Journal of Research of the National Bureau of Standards

Microwave Induced Plasmas as Sources for Atomic Spectrometry

Joseph A. Caruso

Department of Chemistry
University of Cincinnati
Cincinnati, OH 45221

1. Introduction

Microwave induced plasmas (MIPs) have been studied for their potential applicability as analytical sources for over 20 years. In 1965 the MIP was described as an elemental emission detector for gas chromatography (GC) by McCormack and coworkers [1]. Because of its initial low power operation of less than 100 Watts, this plasma, with He primarily as the plasma gas, has been most successfully applied for introduction of gaseous samples. Hence, it is understandable that GC sample introduction [2], hydride generation [3], electrothermal vaporization [4] and other means of gaseous sample introduction have been successfully applied with the MIP. Until recently, solution aerosol introduction was not a particularly viable means of introducing sample to the MIP. However, with the use of the more robust MIPs of up to 500 Watts of generator power [5,6], good analytical figures of merit have been obtained with aerosol introduction of samples.

This presentation discusses the use of Ar and He microwave induced plasmas as spectrochemical sources for gaseous sample introduction and with solution nebulization methods of sample introduction. The first topic focuses on the application of the GC technique; the accuracy available through determination of elemental ratios; and the resulting empirical formulae for a series of control compounds for which empirical formulae have been established. Low level detection at the ng to sub-ng levels is available, however, the comparisons with standard materials to establish accuracy are not prevalent in the literature, although hydride generation has been utilized with NBS Orchard Leaves [3]. The discussion involving solution introduction through nebulized aerosols will consider both optical emission detection and mass spectrometric detection [7,8]. With both of these schemes, a variety of standard reference materials (SRMs) or alternate method comparisons can be made.

2. Gaseous Sample Introduction into MIPs

Element specific detection for GC has the advantages of low level detection, empirical formula determination and potential to overcome problems from lack of chromatographic resolution. The latter is because each element's optical emission or elemental mass may be monitored simultaneously or in rapid sequence. With MIP detection of organic compounds, C or H can serve as universal detectors whereas halogens, phosphorous, sulfur, oxygen and other elements can provide element specific chromatograms. This potential for overcoming problems associated with peak overlap is illustrated in figure 1 [9]. Multielement simultaneous detection is done through use of a polychromator [9]. In these instances, each chromatographic peak is monitored for the various elements contained in the eluting compound. If only single element detection is required, then the experiment can be simplified through the use of a modest monochromator.

One of the areas explored in recent years involves the use of a laminar flow plasma torch (LFT) to replace the open tube quartz torch which has been the most popular plasma containment device. Plasma stability is critical to performing the GC-MIP experiment. By producing a laminar gas flow, the plasma remains centered and therefore optical coupling is much more effective since plasma wander is minimized [9]. With this torch, optical emission detection levels at the sub-ng levels are possible. Low gas flows on the order of 60 mL/min are necessary. Plasma centering also minimizes torch degradation—an essential requirement for the laboratory analyst. Empirical formulae can be determined if the appropriate elemental ratio is determined. Partial empirical formulae for a series of chlorodioxins determined by GC-MIP with the LFT are given in table 1 [9]. A more comprehensive table is given in [2] which includes many contributions from a large number of workers. These rather extensive data suggest suitable accuracy is possible for empirical formula determination with GC-MIP even in a widely varying chemical (structural) environment.

Table 1. Partial dioxin empirical formulas obtained with the LFT

Compound	Partial empirical formulas		Error	
	Actual	GC-MIP	Atom[a]	amu[a]
2,7-CDD	C_6H_3Cl	C_6H_3Cl	0%	0%
1,2,4-CDD	$C_{12}H_5Cl_3$	$C_{12}H_5Cl_3$	0%	0%
1,2,3,4-CDD	C_3HCl	C_3HCl	0%	0%
1,2,4,6,7,9-CDD	C_6HCl_3	$C_6H_2Cl_3$	33%	1%
1,2,3,4,6,7,9-CDD	$C_{12}HCl_7$	$C_{11}HCl_7$	3%	3%
1,2,3,4,6,7,8,9-CDD	C_3Cl_2	C_3Cl_2	0%	0%

[a] See text for explanation, Appl. Spectrosc. 39, 948 (1985), ref. 9.

Certain elements form volatile hydrides when treated with sodium borohydride. Robbins and Caruso investigated the use of these for gaseous sample introduction of the As and Sb volatile hydrides as applied to NBS SRM 1571 Orchard Leaves. These data are presented in table 2 [3]. These data show that it is possible through the gaseous (hydride) sample introduction to the MIP to achieve accuracies within acceptable ranges for SRM 1571.

Table 2. Comparison of values obtained for NBS Orchard Leaves, Lot 1571[c]

	Value given μg/g	Value detmd. sequentially μg/g	Value detmd. simultaneous μg/g
As	10.0±2[a]	9.0±4[b]	8.9±1.2[b]
Sb	2.9±0.3[a]	2.3±0.3[b]	2.9±0.3[b]

[a] Two standard deviations "of entire range of observed results."
[b] Average deviation of four determinations.
[c] From reference [3].

3. Solution Nebulization for Sample Introduction to the MIP

Studies by Haas [5], and Brown et al. [6] have shown that sufficient plasma density is produced when operating at 500 Watts generator power to allow solution introduction of samples into the Ar MIP for optical emission. Other workers have illustrated that with desolvation even a 180 Watt plasma can yield useful analytical data with mass spectrometric detection [8]. With low power MIPs, solution nebulization gave detection levels one to two orders of magnitude poorer than those available from the ICP. In addition, the tolerance to matrix interferences was poor. At the low powers, the plasma was simply not robust enough to accommodate desolvation as well as excitation, particularly in the presence of solvent vapor which acts to detune the plasma. At the higher power levels, however, enough energy is efficiently coupled to the flowing gas stream to achieve much better analytical performance with the plasma.

With a direct solution nebulization, the moderate power MIP was studied to ascertain its suitability for metal ion determinations in solution. Discharge power, plasma viewing mode, cavity depth, nebulizer type and discharge containment mode were investigated [5]. Cu, Al, Pb, Cr, Mn, Fe, Hg, Cd, Zn, Mg, and Ni were investigated in 2% HNO_3 solution as well as a synthetic ocean water (SW) with nearly 3% dissolved solids. For the acid solutions, the detection levels paralleled those of the ICP at low ppb levels, while in the SW, the ion lines provided poorer detection and the atom lines still afforded excellent detection levels. Additional studies with NBS SRM 1577 Bovine Liver showed good agreement with the certified values. Further

Table 3. Analysis of NBS SRM 1577 Bovine Liver by MIP and ICP[d]

Element	Certified value, ppm	MIP, ppm	% RSD	% difference with certified	ICP,[a] ppm	% RSD	% difference with certified	ICP,[b] ppm	RSD	% difference with certified
Cu	1.27±10%	1.37	1.4	8.08	1.34	2.3	5.7	1.3	ND[c]	4.2
Fe	2.29±20%	2.21	1.9	3.67	2.36	4.0	2.9	2.6	ND	10.6

[a] Leeman Labs Plasma Spec ICP 2.5, university laboratories.
[b] Jarrell Ash Atom Comp 1140, US FDA.
[c] Not determined.
[d] From reference 6.

studies provided a comparison with two ICPs. Again, the comparison was very good in these experiments. One of the ICP studies was done at the local FDA laboratories and the other with the Department of Chemistry ICP. Table 3 illustrates these comparisons.

With solution introduction into the MIP possible, Douglas and co-workers [8] did the first MIP-MS studies with a 180 Watt Ar plasma. Their results were excellent, however, no further MIP-MS studies were completed until recently [7]. Douglas' work is particularly pertinent to this discussion since this study utilized comparisons with a number of SRMs. NBS SRM 362 Steel, AISI, was analyzed by both a simple calibration plot and by the method of standard additions. For the elements studied, the standard addition experiments provided the best comparisons with certified values. They also studied trace elements in NBS SRM 1643a Trace Elements in Water. Simple calibration in most cases was unsuitable while standard additions or matrix matching provided a much better comparison with certified values. Of the latter two, it would be difficult to say which of them is better. These authors also studied trace elements in SRM 1571 Orchard Leaves by MIP-MS and showed that good comparisons were possible if the standard additions technique was used.

In summary, microwave induced plasmas are capable optical emission and plasma mass spectrometric sources. If properly applied, they can yield excellent analytical data giving both accurate and precise results at the trace elemental level.

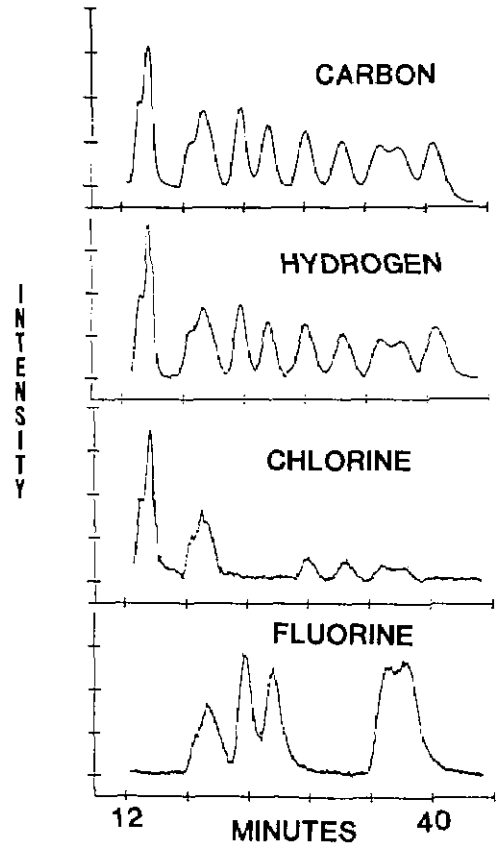

Figure 1. Background-corrected chromatograms of the pyrethroids taken with the LFT for carbon, hydrogen, chlorine, and fluorine channels Permethrin, Cyfluthrin, Flucythrinate (2 peaks), Fenvalerate (2 peaks), Fluvalinate (double peak), and Deltamethrin.

Acknowledgment

The author is grateful to those who have directly contributed to the experiments presented in this presentation, Drs. M. Eckhoff, M. L. Bruce, D. L. Haas, P. G. Brown, and R. D. Satzger. Thanks are also extended to Messrs. A. H. Mohamad and J. M. Workman. JAC is grateful to NIOSH and NIEHS who have supported this work through the years.

References

[1] McCormack, A. J., Tong, S. G., and Cooke, W. D., Anal. Chem. **37**, 1470 (1965).
[2] Mohamad, A. H., and Caruso, J. A., "Element-Selective Plasma Emission Detectors for Gas Chromatography," in Advances in Chromatography **26**, p. 191 (1987), J. C. Giddings, ed., Marcel Dekker Inc., New York.
[3] Robbins, W. B., and Caruso, J. A., J. Chrom. Sci. **17**, 360 (1979).
[4] Rose, O., Fricke, F. L., and Caruso, J. A., Talanta **23**, 317 (1976).
[5] Haas, D. L., and Caruso, J. A., Anal. Chem. **56**, 2018 (1984).
[6] Brown, P. G., Haas, D. L., Workman, J. M., and Caruso, J. A., Anal. Chem. **59**, 1435 (1987).
[7] Satzger, R. D., Fricke, F. L., Brown, P. G., and Caruso, J. A., Spectrochim. Acta **42B**, 705 (1987).
[8] Douglas, D. J., Quan, E. S. K., Smith, R. G., Spectrochim. Acta **38B**, 39 (1983).
[9] Bruce, M. L., and Caruso, J. A., Appl. Spectrosc. **39**, 942 (1985).

Volume 93, Number 3, May–June 1988
Journal of Research of the National Bureau of Standards

Graphite Furnace AAS: Application of Reduced Palladium as a Chemical Modifier

D. E. Shrader, L. M. Beach, and T. M. Rettberg

Varian Instrument Group-AA Resource Center
205 W. Touhy Ave.
Park Ridge, IL 60068

Chemical modification techniques are widely used in graphite furnace atomic absorption spectrometry (GFAAS). Palladium is a very effective chemical modifier and can be used to stabilize many elements to several hundred degrees higher than the temperatures possible with current methods [1–9]. Of the elements tested, the greatest temperature shifts are achieved for the semi-metallic elements such as As, Se, Te, Bi, Sb, Pb, Tl, Ga, Ge and P. Ash temperatures can be raised 400–800 °C higher than current methods allow. Temperature shifts are somewhat less for the transition elements and ash temperatures can be raised 200–500 °C. Palladium has no similar effect on elements in Groups I and II of the Periodic Table. The change in stability is believed to be due to the formation of an intermetallic species. This improvement in stability permits more efficient removal of matrix constituents during the ash step and vaporization into a hotter environment during the atomize step. Background and interference problems are thus reduced or eliminated.

Steps taken to guarantee that palladium is present as the reduced metal as early as possible greatly improve performance of the modifier. The palladium modifier solution can be pre-injected and the graphite tube heated to 1000 °C. Such a method has been used to stabilize mercury [10]. It is assumed that at this temperature palladium metal is present on the graphite surface. The sample can then be introduced. The addition of a reducing agent such as 5% hydrogen in 95% argon, ascorbic acid, or hydroxylamine hydrochloride also appears to guarantee that the palladium is present as the metal early in the temperature program. The use of hydrogen as a reducing agent appears to be the method of choice for a number of reasons. It is cleaner, leaves no residue, and is less subject to contamination. It is also easy to use. A pre-mixed gas of 5% hydrogen in 95% argon can simply be introduced into the furnace. More importantly, the problem encountered with high concentrations of nitric acid is eliminated with the use of hydrogen.

Reduced palladium metal allows the retention of the analyte element on the graphite surface until a higher gas phase temperature is achieved. This appears to give many of the analytical advantages normally associated with platform atomization while using the simpler wall atomization technique.

Investigations to elucidate the mechanism of palladium chemical modification have been conducted. Also, comparison of palladium modifier methods with current modifier methods in spike recovery studies from difficult matrices was accomplished.

Scanning electron micrographs of graphite surfaces with palladium deposits obtained by different reduction methods were obtained to investigate whether the physical form of palladium influenced the modifier behavior. It was found that reduced palladium metal was indeed present on the graphite surface after reduction and that the most effective reduction method was the use of 5% hydrogen in 95% argon with a palladium solution containing 1% glycerol. The scanning electron micrograph of the surface produced under these conditions is shown in figure 1. The palladium particles are considerably smaller and more highly dispersed than those produced by other methods. The average particle diameter is 0.05–0.15 μm. The smaller particles result in a great increase in palladium surface area. Spike recovery studies from difficult matrices showed that smaller, highly dispersed particles produced improved interference performance.

The interference performance of a palladium/hydrogen/glycerol method for tin was compared with the performance of a commonly used method. The commonly used method requires the use of the platform and chemical modifiers of ammonium dihydrogen phosphate and magnesium nitrate. Wall atomization was used for the palladium method. The results of this study are listed in table 1. While both methods performed well in concentrated HCl, in most instances the palladium gave slightly better interference performance. It was significantly better in overcoming interferences from NaCl and seawater matrices. Other elements have been tested in the same matrices and, in virtually every instance, palladium gave as good as or better interference performance (wall) as did the currently used methods (platform).

Table 1. Tin recoveries from interferent matrices

Interferent	Current method 200 μg $NH_4H_2PO_4$ 10 μg $Mg(NO_3)_2$ Platform	Palladium method 20 μg Pd 150 μg glycerol 5% hydrogen Wall
5 μL 2.5% NaCl (125 μg)	22%[a] 26%[b]	91%[a] 110%[b]
5 μL 5.0% NaCl (250 μg)	0 0	92% 107%
5 μL Seawater	0 0	87% 99%
5 μL concentrated HCl	97% 92%	96% 100%
5 μL concentrated HNO_3	79% 87%	92% 93%
5 μL 20% H_2SO_4	39% 58%	60% 79%
5 μL 0.5% Na_2SO_4 (25 μg)	87% 85%	101% 101%
5 μL 1.0% Na_2SO_4 (50 μg)	82% 85%	103% 100%

[a] Peak height.
[b] Peak area.

The palladium modifier method has been utilized with numerous real samples as well as synthetic interferent matrices to test its applicability. The direct determination of selenium in biological fluids has shown excellent accuracy using palladium modification. Thallium has been accurately determined in brackish waters, soil digests and digested fish tissue. Work with other real samples is continuing.

In many situations, quite low concentrations of palladium may be used and accurate results still obtained. Table 2 compares recommended chemical modifier concentration ranges. The use of lower modifier concentrations decreases the possibility of analyte contamination and associated analysis problems.

In summary, reduced palladium chemical modification for graphite furnace AAS has been shown to be very useful. It can be used to improve difficult graphite furnace analyses. It has been applied to over 20 analyte elements and in each case has produced beneficial effects. It does not require the added complexity of platforms as it produces the same effects chemically. Reduced palladium may be as close to a "universal" modifier as possible for graphite furnace AAS.

Table 2. Recommended modifier concentration ranges (μg/mL)

Modifier	Element	Current methods	Palladium method
Nickel	As	Up to 5000	50–1000
	Se	Up to 5000	50–1000
Mixed	Cd	Up to 20,000[1000]	50–1000
$PO_4+[Mg(NO_3)_2]$	Pb	Up to 20,000[1000]	50–1000
	Sn	Up to 20,000[1000]	50–1000
$Mg(NO_3)_2$	Fe	Up to 5000	50–1000
	Mn	Up to 5000	50–1000

Volume 93, Number 3, May–June 1988
Journal of Research of the National Bureau of Standards

Accuracy in Trace Analysis

Figure 1. Scanning electron micrograph of reduced palladium metal on graphite surface (20,000x magnification).

References

[1] Shan Xiao-quan, Ni Zhe-ming, and Zhang Li, At. Spectrosc. **5**, 1 (1984).
[2] Shan Xiao-quan, Ni Zhe-ming, and Zhang Li, Talanta **31**, 150 (1984).
[3] Shan Xiao-quan, and Hu Kaijin, Talanta **32**, 23 (1985).
[4] Shan Xiao-quan, and Wang Dian-Xun, Anal. Chim. Acta **173**, 315 (1985).
[5] Liu Ping, Keiichiro Fuwa, and Kazuko Matsumoto, Anal. Chim. Acta **171**, 279 (1985).
[6] Schlemmer, G., and Welz, B., Poster 077, presented at Colloquium Spectroscopicum Internationale XXIV, Garmisch-Partenkirchen, FRG, September (1985).
[7] Niskavaara, H., Virtasalo, J., and Lajunen, L., Spectrochim. Acta, **Part B 40**, 1219 (1985).
[8] Voth-Beach, L., and Shrader, D., Spectroscopy **1**(10), 49 (1986).
[9] Voth-Beach, L., and Shrader, D., Jour. of Anal. At. Spect. **2**, 45 (1987).
[10] Grobenski, Z., Erler, W., and Voellkopf, U., At. Spectrosc. **6**, 91 (1985).

The Determination of Trace Elements in Uranium Oxide (U_3O_8) by Inductively Coupled Plasma Emission Spectrometry and Graphite Furnace Atomic Absorption Spectrometry

Patricia M. Santoliquido

U.S. Department of Energy
New Brunswick Laboratory
9800 South Cass Avenue
Argonne, IL 60439

The observations and data presented here are drawn from a larger project which has as its objective the certification of a set of reference materials, known as CRM 123 (1–7), for the 18 trace elements contained in each of the seven levels which make up the set. Level 7 is high purity U_3O_8. Portions from the bulk of this same material were used as the base material for all the other concentration levels, which were made by adding known concentrations of impurity elements. CRM 123 (1–7) is a replacement for a previous reference material of the same type called CRM 98 (1–7). When that reference material was certified the workhorse methods were flame atomic absorption and spectrophotometric methods. Both graphite furnace atomic absorption (GFAA) and inductively coupled plasma emission spectrometry (ICP) had become established methods of analysis since then. The characterization of CRM 123 (1–7) provided an opportunity to take advantage of the greater sensitivity these newer methods could provide. In general the two techniques are complementary rather than competitive. A look at the characteristics of each method shows why we should have different expectations for each.

GFFA has a small linear dynamic range. The sensitivity for uranium is low; therefore, direct analysis without prior separation of uranium is possible. Volatile elements are the most sensitive analytes, so this should be a good method for cadmium, for example. A search of the literature [1–4] showed that the trail had already been blazed and that accurate results could be achieved in a 0.1 *N* nitric acid medium as long as the standards are matrix-matched for uranium as well. The amount of uranium present affects sensitivity. For cadmium there was no particular pattern for the sensitivity

changes. For manganese, chromium, and aluminum there was a gradual decrease in sensitivity with more than 100 micrograms of uranium present (fig. 1). The change for magnesium and copper was much more dramatic (fig. 2). Copper and magnesium were determined using pyrocoated tubes; the other elements were determined using regular graphite tubes.

In contrast to GFAA, ICP has a large linear dynamic range and is very sensitive for uranium and the more refractory elements that GFAA does poorly. The large linear dynamic range means that the same sample size may be used for many different concentration levels. The high sensitivity for uranium is a major problem and 1,458 ICP spectral lines have been identified for uranium [5]. Not only are direct spectral interferences a problem but with uranium as the matrix the wings from these lines are so high that they completely obscure any trace elements present. Separation of the uranium prior to measurement of the trace elements is essential. The literature [6–9] shows that a number of different approaches have been successful. A tributyl phosphate extraction from a 1.6 *N* nitric acid medium was chosen for this work. This proved to be successful for many elements. In separate analyses a cupferron separation was used for zirconium and an α-benzoin oxime extraction was used for molybdenum.

Both GFFA and ICP are relatively straightforward techniques. For GFAA the problem areas are environmental magnesium and chromium memory. For ICP it is spectral interference and structured background that we must watch out for. Background structure becomes increasingly important at lower concentrations—not only for wavelength selection but also for choosing background correction positions. By GFAA there are six elements that can be determined directly in uranyl nitrate solution: cadmium, chromium, aluminum, copper, magnesium, and manganese. By ICP after appropriate separations a larger group may be determined. These elements are aluminum, calcium, iron, nickel, copper, molybdenum, sodium, manganese, vanadium, zirconium, and magnesium. The method using GFFA is better for cadmium and chromium while the method using ICP is better for calcium, iron, nickel, molybdenum, sodium, vanadium, and zirconium. There are four elements, however, that are done equally well by each 5,2 method. These elements are aluminum, magnesium, copper, and manganese. Results for these elements are given in tables 1 to 4. Neither technique showed a systematic bias throughout all concentration levels, although for some levels of copper and manganese GFAA exhibited a small positive bias.

Table 1. Aluminum determinations, μg/g U, mean $\pm s_x$, n=10

Level	Added to base	ICP	GFAA
123-1	200	207.5±2.3	202.6±7.3
123-2	100	97.6±1.1	99.1±3.3
123-3	50	47.6±0.6	51.2±1.9
123-4	20	19.9±0.4	23.3±1.2
123-5	10	10.1±0.2	12.1±1.0
123-6	5	5.0±0.1	6.1±0.4
123-7	0	<0.9	<2.2

Table 2. Magnesium determinations, μg/g U, mean $\pm s_x$, n=10

Level	Added to base	ICP	GFAA
123-1	100	100.8±1.3	103.9±5.8
123-2	50	50.3±1.7	51.2±0.2
123-3	20	20.3±0.2	20.3±0.8
123-4	10	10.7±0.7	11.4±0.6
123-5	5	5.6±0.1	5.5±0.4
123-6	2	3.4±0.3	2.5±0.2
123-7	0	1.8±0.4	<1.0

Table 3. Copper determinations, μg/g U, mean ± s_x, n=10

Level	Added to base	ICP	GFAA
123-1	50	49.6±1.3	56.0±2.1
123-2	25	23.4±0.4	27.7±0.5
123-3	10	8.8±0.2	12.9±0.5
123-4	5	5.0±0.1	6.8±0.6
123-5	2.5	2.70±0.05	2.5±0.1
123-6	1	1.18±0.06	1.2±0.1
123-7	0	0.20±0.07	<0.6

Table 4. Manganese determinations, μg/g U, mean ± s_x, n=10

Level	Added to base	ICP	GFAA
123-1	50	51.1±1.5	52.7±1.3
123-2	25	25.4±0.4	29.4±0.6
123-3	10	10.9±0.2	12.7±0.3
123-4	5.0	5.45±0.07	5.7±0.2
123-5	2.5	2.90±0.04	3.25±0.08
123-6	1.0	1.14±0.03	1.33±0.08
123-7	0	0.30±0.02	0.24±0.03

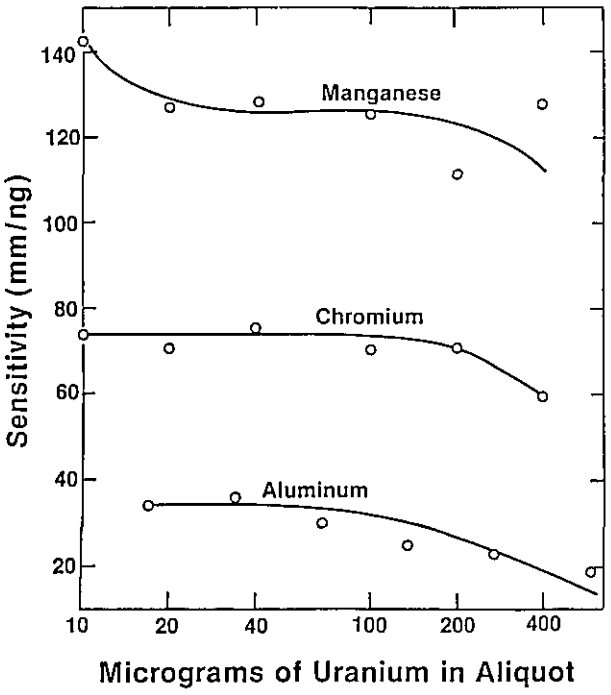

Figure 1. Influence of uranium concentration on sensitivity for aluminum, chromium and manganese by GFAA.

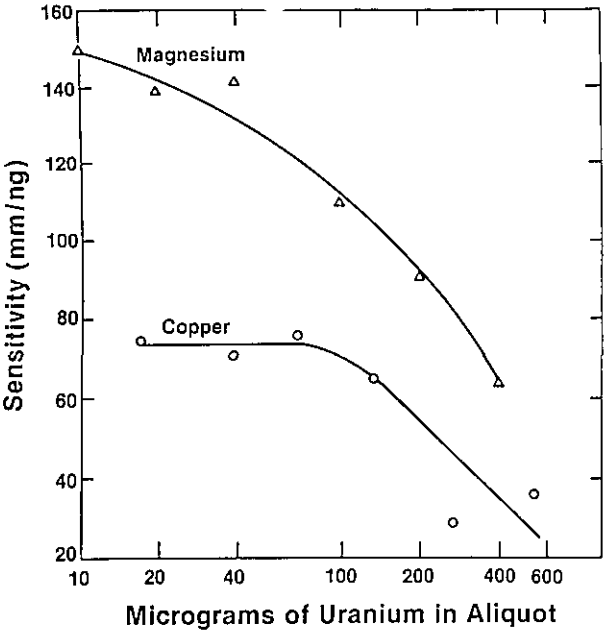

Figure 2. Influence of uranium concentration on sensitivity for copper and magnesium by GFAA.

References

[1] Bagliano, G., Benischek, F., and Huber, I., At. Abs. Newsl. **14**, 45 (1975).
[2] Patel, B. M., Bhatt, P. M., Gupta, N., Pawar, M. M., and Joshi, B. D., Anal. Chim. Acta **104**, 113 (1979).
[3] Patel, B. M., Gupta, N., Purohit, P., and Joshi, B. D., Anal. Chim. Acta **118**, 163 (1980).
[4] Patel, B. M., Goyal, N., Purohit, P., Dhobale, A. R., and Joshi, B. D., Fresenius Z. Anal. Chem. **315**, 42 (1983).
[5] Wohlers, C. C, ICP Inf. Newsl. **10**, 593 (1985).
[6] Maney, J. P., Luciano, V., and Ward, A. F., Jarrell—Ash Plasma Newsl. **2**, 11 (1979).
[7] Floyd, M. A., Morrow, R. W., and Farrar, R. B., Spectrochim. Acta **38B**, 303 (1983).
[8] Bear, B. R., Edelson, M. C., Gopalan, B., and Fassel, V. A., The Determination of Boron and Cadmium Impurities in Uranium Oxide and Uranium Metal by ICP-AMES, in Analytical Spectroscopy—Proceedings of the 26th Conference on Analytical Chemistry in Energy Technology, Knoxville, TN, October 11–13, 1983, W. S. Lyon, Ed., ACSS Volume 19, Elsevier Science Publishers B. V., Amsterdam (1984) p. 187.
[9] Seshagiri, T. K., Babu, Y., Jayanth Kumar, M. L., Dalvi, A. G. I., Sastry, M. D., and Joshi, B. D., Talanta **31**, 773 (1984).

ICP Trace Element Analyses from Fusion Dissolution

D. Brown, G. Legere, and P. Burgener

Technical Services Laboratories
1301 Fewster Drive
Mississauga, Ontario, Canada L4W 1A2

Lithium Carbonate-Boric Acid Fusion Digestion for ICP

The fusion digestion procedure of using a mixture of lithium carbonate and boric acid to prepare silicate rocks for analysis is not new. At Technical Service Laboratories (TSL) this fusion procedure has been used to perform "whole rock" analysis by ICP since 1979. Others, [1-4], have published values for the major rock constituents by ICP, X-ray, and other analytical techniques after a lithium carbonate-boric acid fusion. In the last 3 years at TSL however, minor elements were also determined on the same solution from which the majors were measured. With careful quality control procedures and a constantly updated interference correction matrix, minor elements can be also obtained with

detection limits as low as 1 ppm for some elements. The unique buffering effect of the fluxing material produces stable background levels which allows for easier correction of interelement concomitants.

As part of our ICP quality control program, major and minor element data have been compiled on international rock standards. The accuracy of the minor element data produced over the 3-year time period demonstrates the ability of the fusion to produce detection limits similar to that of other dissolution methods used prior to analysis by ICP.

Procedure

The digestion procedure used is similar to other digestion procedures using lithium metaborate published by Walsh [2], although several changes have been developed to make routine analysis simpler.

Approximately 200 mg of previously dried and sieved (−200 mesh) sample is weighed accurately to ±0.1 mg and is added to 1.50 g of dried fluxing material in a graphite crucible. The fluxing material is obtained by combining ground 99.9% pure boric acid and 99.99% pure lithium carbonate in a ratio of 2:1 by weight. The flux mixture is thoroughly blended, dried overnight and weighed into a prepared crucible. The flux-sample mixture is preheated to 400 °C for 1/2 hour and then heated to almost 1200 °C in a nitrogen atmosphere. The hot melt is gently swirled in the crucible and quickly poured into a 250 mL polypropylene bottle containing a mixture of 50.00 g of 16% v/v reagent grade HNO_3 and the Cd internal standard. The bottle is then placed on a rotary shaking tray for at least 2 hours. After shaking, the solutions are diluted with 70.00 g of double deionized water and decanted into test tubes ready to be run on the ICP. By this method, one person can completely prepare 120 samples in an 8-hour period.

For analysis, the samples are placed on a Gilson linear belt auto-sampler with a 30-second rinse cycle and a 30-second analysis time. A summary of the instrumentation and operating parameters used for the analyses are summarized in tables 1 and 2.

Table 1. Summary of instrumentation and operating parameters used for TSL analyses

Spectrometer #1	Jarell-Ash 975 Atomcomp, 0.75 m, 2400 grooves/mm Fixed 50 μm slits, with PDP-8 and IBM pc computers
Spectrometer #2	Jarrell-Ash 975 Atomcomp, 0.75 m, 2400 groves/mm Scanning spectrum shifter of 50 μm slits with IBM pc computers
Plasma torch	Mak torch to fit 8" Jarrell-Ash from Sherritt Gordon Research
Argon flows	Outer 10 L/min Support 1.5 L/min Nebulizer 0.8 L/min
Generator	Plasma Therm Model HFP-2000D, 27.1 MHz, with Autopower control
RF Power	Presently operating at 0.75 kW but in past have operated at 1 kW incident power
Nebulizer	Legere high salt nebulizer
Load coil	Presently using 1 1/2 turn copper oil but have previously used 3 1/2 turn copper coil

Table 2. Analytical wavelengths (Å) used for ICP analyses

Spectrometer #1								
Si	I	2881.6	Ti	II	3349.4	Cu	I	3247.5
Al	II	3961.5	Mn	II	2576.1	Ni	II 2x	2316.2
Fe	II	2599.4	P	I	2136.2	Sr	II	4077.7
Ca	I	4226.7	Ba	II	4554.0	V	II	2924.0
Mg	II	2795.5	Be	I	2348.1	Zn	II 2x	2062.0
Na	I	5889.9	Co	II	2286.0	Zr	II	3438.2
K	I	7664.9	Cr	II	2677.2			
Spectrometer #2								
Th		2837.3	Cu	I	3247.5	Co	II	2286.0
Y	II	3710.3	V	II	2924.0	Zn	I	2138.6

Calibration is achieved for the major oxides and Ba, Sr, Zr by running five international rock standards MRG-1, SY-2, NIM-G, NIM-L, and NBS Dolomite with a reagent blank and deriving an intensity vs concentration curve from these standards. For the minor elements, a synthetic solution is created by adding 1 or 2 mL of 1000 mg/L Spex or Inorganic Ventures plasma grade standards to a reagent blank and diluting as normal. This solution gives 5000 and 10000 ppm equivalence in the rock. With the advantage of the linear intensity vs con-

centration of the ICP source, and the buffering effect of the flux material, one point calibration has proven sufficient for the levels of trace elements one finds in silicate rocks. By having a fusion flux to buffer the solution, spectral baselines are more stable from sample to sample, making it easier to perform spectral overlap corrections from either a direct line or a wing.

Interelement interference correction is achieved by running blank reagent solutions doped with typical levels of the interfering elements found in whole rock solutions. Spex plasma grade standards were again used for the doping material where possible; otherwise, solid pure oxide forms of the element were obtained from Johnson Matthey and prepared under the same conditions as the samples.

The intensity obtained in an element channel is stored in the form of a matrix for each of the interfering elements. This matrix is updated monthly or when any of the operating parameters are changed. The matrix, after reagent blank subtraction, is used to correct for the interfering element in each analyte channel.

Results and Discussion

Analyses of selected international standards are given in table 3. Additional data are available for other standards including NIM-N; JR-1, JA-1, and JB-2 (Japan); NBS 1633a, and NBS 98a. As is usual, there are several precautions to note for this fusion using graphite crucibles. As indicated by Ingamells [1] some of the flux-sample mixture may stick to the walls of the crucible after the hot melt has been poured into the polypropylene bottle. To collect the remainder from the crucible, it is allowed to cool and the walls are gently scraped with a spatula and reheated to almost 1200 °C. The remainder is poured into the already swirling solution, and the stirring action is resumed. By doing this, the crucible will be completely free of sample and flux.

To minimize the sticking of the flux mixture to the walls of the crucible, the walls are gently scraped with a reaming tool to build up a carbon layer on the surface. Nevertheless, it has been found that no amount of pretreatment can eliminate entirely the sticking of the flux to walls of the crucibles for every sample.

The accuracy of this method of analysis for the major oxides is predominantly dependent upon two factors; the accuracy of the standards used to form the calibration curves and the stability of the plasma emission source. The latter of these problems covers the fluctuations of viewing height, power supplied by the radio frequency generator, and analyte transportation to the plasma. In this case, power to the plasma is monitored by an autocontroller. But no attempt has been made to monitor the effects of any power fluctuations at the plasma itself (i.e., monitoring an argon line). Any short term fluctuations in power are smoothed by the length of the 30-second integration time.

The analyte transport to the plasma is monitored via the Cd internal standard. The sole purpose of the internal standard is to account for variations in nebulizer efficiency from sample to sample. One internal standard cannot, alone, accurately monitor changes in power levels and sample dilution errors (even though it appears as if it does when plasma emission conditions remain stable). In our experience, however, no internal standardization of any form can account for changes in viewing height. The gas flows through the nebulizer orifice must remain very stable to keep the analytical zone constant for extended periods of time. If this condition is not met, gross changes in calibration and interelement spectral interferences will occur.

The major source of analytical error for the minor elements is predominantly determined by how accurately the emission line profiles can be corrected for interelement interferences. It is commonly the case where one finds that what one assumed to be a direct line overlap from a concomitant is simply contamination in the spectral correction solution. Yet the biggest sources of error when performing these spectral corrections routinely are the stability of the position of the observation zone in the plasma, and the temperature variations of the spectrometer itself. Unless the spectrometer has an independent temperature control, the room in which it is situated should have its temperature and humidity stabilized to within a few degrees. Otherwise, any matrix corrections performed must take into account drift of the position of the analytical lines with respect to the nearby interfering elements.

A change of observation height within the plasma can lead to incorrect matrix corrections since emission line strengths of different atomic and ionic populations vary with viewing height. Either the nebulizer's characteristics (e.g., gas flow) must remain constant, or, careful monitoring and adjustment must be done continuously with an apparatus such as a mass flow controller.

Table 3. TSL ICAP analyses on selected international rock standards

	GA (Fr)			MICA-Fe (Fr)			NIM-P			NBS 70a		
	TSL values Mar 84–Jul 85 ($N=17$)		Abbey [5]	TSL values Jul 84–Aug 86 ($N=16$)		Abbey [5]	TSL values Aug 84–Apr 86 ($N=19$)		Abbey [5]	TSL values Sep 84–Apr 86 ($N=16$)		NBS values
	Average	s[a]		Average	s		Average	s		Average	s	
SiO_2	69.62	0.35	69.96	34.34	0.24	34.55	51.21	0.62	51.10	67.27	0.38	67.10
Al_2O_3	14.68	0.10	14.51	19.51	0.23	19.58	4.17	0.05	4.18	17.97	0.14	17.90
Fe_2O_3	2.75	0.02	2.77	25.44	0.25	25.76	12.67	0.16	12.76	0.07	0.02	0.07
CaO	2.47	0.02	2.45	0.48	0.14	0.43	2.61	0.07	2.66	0.11	0.02	0.11
MgO	0.93	0.01	0.95	4.60	0.04	4.57	25.30	0.46	25.33	0.03	0.01	
NaO	3.47	0.06	3.55	0.20	0.02	0.30	0.26	0.04	0.37	2.42	0.07	2.50
K_2O	4.01	0.11	4.03	8.83	0.15	8.79	0.10	0.05	0.09	11.75	0.22	11.80
TiO_2	0.37	0.01	0.38	2.59	0.02	2.51	0.19	0.01	0.20	0.00	0.00	0.01
MnO	0.09	0.00	0.09	0.35	0.00	0.35	0.22	0.00	0.22	0.00	0.00	
P_2O_5	0.12	0.01	0.12	0.40	0.02	0.45	0.04	0.02	0.02	0.01	0.01	
BaO	0.09	0.00	0.09	0.02	0.00	0.02	0.00	0.00	0.01	0.01	0.00	0.02
SrO	0.04	0.00	0.04	0.00	0.00	0.00	0.00	0.00	0.00	0.01	0.00	
ZrO	0.02	0.00	0.02	0.11	0.00	0.11	0.00	0.00	0.00	0.00	0.00	
	Average	s		Average	s		Average	s		Average	s	
Be	3	1	4	7	1	8?	<1	1	<1	1	1	
Co	8	5	5	25	5	20	110	5	110	5	5	
Cr	10	5	12	90	5	90	2.1%	0.3%	2.4%	<5	5	
Cu	18	10	16	35	10	4?	10	5	18	5	5	
V	37	5	38	135	10	135	250	5	230	<5	5	
Zn	64	5	80	1210	30	1300	120	10	100	<5	5	

[a] s = standard deviation.

For our purpose, the use of the Legere Teflon nebulizer has eliminated gas flow variations in the nebulizer itself, thus ensuring a constant observation zone within the plasma for weeks at a time without need of adjustment.

A safe detection limit of 5 ppm is found for the trace elements (Ba, Co, Cr, Cu, Sc, Sr, Y, Zn, and Zr) in silicate rocks fused with lithium carbonate and boric acid, except for Be, which has an extremely sensitive line, and has a detection limit of 1.

However, in table 3, only values catalogued over the last 3 years are given. The additional elements included in the list above are those which have only recently been measured. It is hoped that in future months detection limits of 5 ppm or better can be achieved for Th, W, Sb and Sn.

References

[1] Ingamells, C. O., Anal. Chim. Acta **52**, 323 (1970).
[2] Walsh, J. N., and Howie, R. A., Mineralogical Mag. **43**, 967 (1980).
[3] Burmann, J., Ponter, C., and Bostrom, K., Anal. Chem. **50**, 679 (1978).
[4] Govindaraju, K., Mevelle, G., and Chouard, C., Anal. Chem. **48**, 1325 (1976).
[5] Abbey, S., Energy, Mines and Resources Canada Studies in "standard samples" for use in the general analysis of silicate rocks and minerals, Geological Survey Paper 80-14.

Volume 93, Number 3, May-June 1988
Journal of Research of the National Bureau of Standards

Accuracy in Trace Analysis

Automation and Application of a Direct-Current Plasma Emission Spectrometer

M. S. Epstein

Inorganic Analytical Research Division
National Bureau of Standards
Gaithersburg, MD 20899

R. E. Jenkins

Rice University
Houston, TX 77251

and

K. S. Epler and T. C. O'Haver

Department of Chemistry
University of Maryland
College Park, MD 20742

The direct-current plasma (DCP) coupled to an echelle spectrometer has been used for over 6 years in our laboratory as one of several independent methods for the certification of Standard Reference Materials (SRMs). The demanding certification process requires maximum performance from an analytical method as well as a good understanding of the method capabilities and limitations. We have made a number of modifications to the conventional DCP spectrometer to improve accuracy, precision, and analysis speed. Figure 1 is a schematic diagram of the entire DCP spectrometric system with all modifications and enhancements. This paper discusses these modifications and their application to a number of analytical problems.

Conversion from Unmodulated to Wavelength-Modulated Detection

The advantages of wavelength-modulated detection over unmodulated detection schemes have been well-documented in the literature [1–3]. Signal-to-noise ratio (SNR) enhancement in the presence of background emission flicker noise, reduction of baseline drift, nulling of line spectral interferences and rapid background correction are some of the advantages of wavelength-modulated detection. Unmodulated detection is superior when spectral resolution is critical or when the limiting system noise is detector shot-noise. The DCP spectrometer and detection system were modified so that either unmodulated or wavelength-modulated schemes could be employed.

Reduction of Spectrometer Wavelength Drift

Severe nonlinear drift of emission intensity was a recurrent problem with one of our two DCP/echelle emission spectrometers. The drift was a result of the extreme sensitivity of the spectrometer to thermal variations and vibration. Two approaches were taken to reduce the spectrometer drift. The first involved thermal regulation of the spectrometer baseplate at a temperature higher than attained during normal operation, and vibrational isolation of the spectrometer. These actions significantly reduced both long- and short-term intensity fluctuations.

Since the major heat source affecting the spectrometer was the plasma, another approach was removal of the plasma from contact with the spectrometer baseplate. The plasma was housed in a separate vented enclosure, and an optical rail with appropriate focusing optics was positioned between the spectrometer and the plasma. This configuration also effectively eliminated wavelength and order drift as major sources of intensity drift.

Automation of Sample Introduction, Data Collection, and Processing

An enhanced Apple II+ microcomputer (3.5 MHz 65C02 processor) coupled to an autosampler and controlled by a BASIC program was used to automate the DCP spectrometer operations. Figure 2 illustrates both the hardware and software design of the system. The autosampler was controlled through the three game control annunciator outputs of the Apple II+ and autosampler status was monitored through two game control pushbutton inputs. The three annunciator outputs were converted to five control states needed to program the autosampler by a binary-to-BCD converter. Voltage output from the spectrometer, either from a current-to-voltage converter (unmodulated system) or from a lock-in amplifier (wavelength-modulation system), was converted to digital data by a 12-bit ADC and processed by the BASIC program. Standard and sample weights and dilution factors are entered into the program at the start of an analysis and a report of sample concentrations is generated at the completion. Options to apply drift

correction or to use a standard addition correction are also included in the software.

Removal of Interfering Species Using Ion-Exchange Chromatography

The most straightforward approach to eliminate matrix-induced interferences, and the one that requires the least number of compromises, is the complete separation of analyte from interfering species. When chromatographic methods are directly coupled to spectrometric methods for on-line separations, sensitivity and accuracy may be further enhanced by preconcentration of the analyte on the chromatographic column.

We have applied an anion exchange method using an activated alumina (acid form) column for on-line preconcentration of phosphorus. Activated alumina has been found by several researchers [4,5] to be a useful column packing material for adsorption of oxyanions. The column is quite useful for the determination of phosphorus in acid digests of iron and copper-based alloys, since the direct DCP determination is complicated by iron and copper spectral interferences. Phosphorus is retained on the column while iron and copper are not retained and elute with a water wash of the column. With preconcentration times of 30 minutes, phosphorus detection limits are 20 times better than obtained using continuous aspiration. A detection limit of 10 ng/mL is obtained under these conditions, corresponding to a detection limit of 0.1 μg/g in the metal alloy. Results from the determination of phosphorus in several SRMs, as shown in table 1, were in good agreement with certified values or other independent techniques.

Table 1. Determination of phosphorus in standard reference materials using preconcentration on an activated alumina column

Sample	P, μg/g[a]	Other values	Method[b]
SRM 1252			
Phosphorized copper	84±8	85±2	Molybdivanadophosphoric acid method (ASTM E-62) [6]
SRM 875			
Cupro-nickel	21.4±1.8	20±5	Certified value
SRM 1767			
Low-alloy steel	37±1	39±2	Modified ASTM 350-84 heteropolymolybdate procedure [7]
SRM 365			
Electrolytic iron	15±1	12±2	Modified ASTM 350-84 heteropolymolybdate procedure [7]
		14±2	Molecular absorption spectrometry [8]
		12.5	Indirect ICP method [8]
		25±5	Certified value

[a] Uncertainty expressed as 95% confidence limits.
[b] Values obtained by other techniques or certified values.

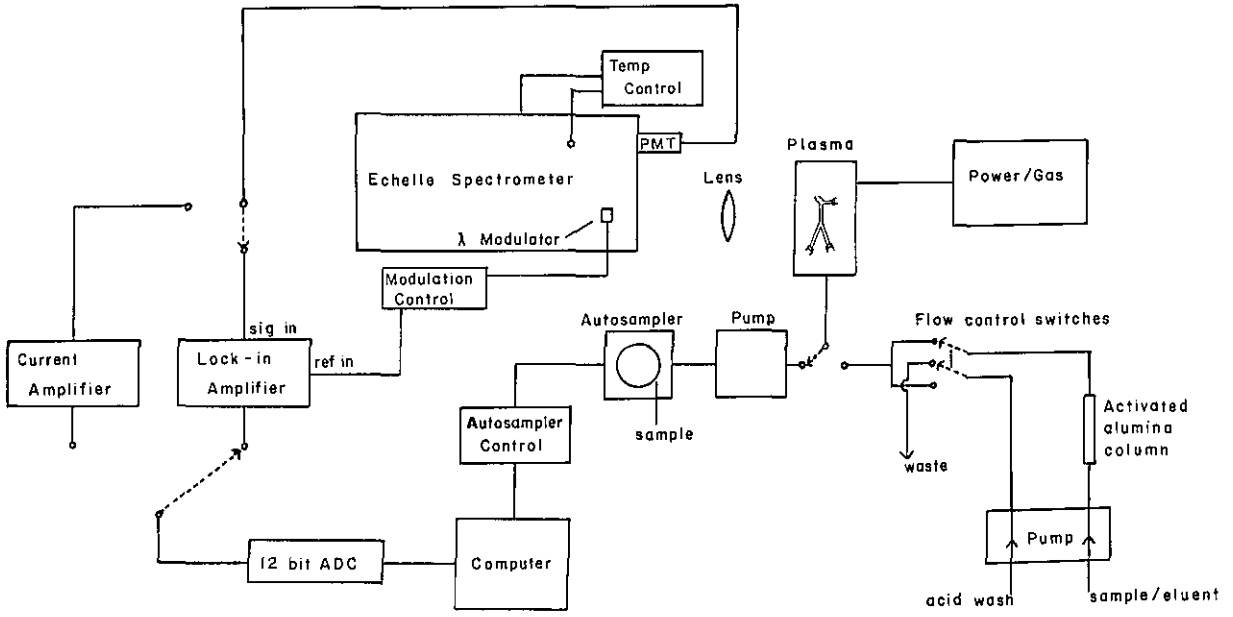

Figure 1. Schematic diagram showing all components of the DCP spectrometric system.

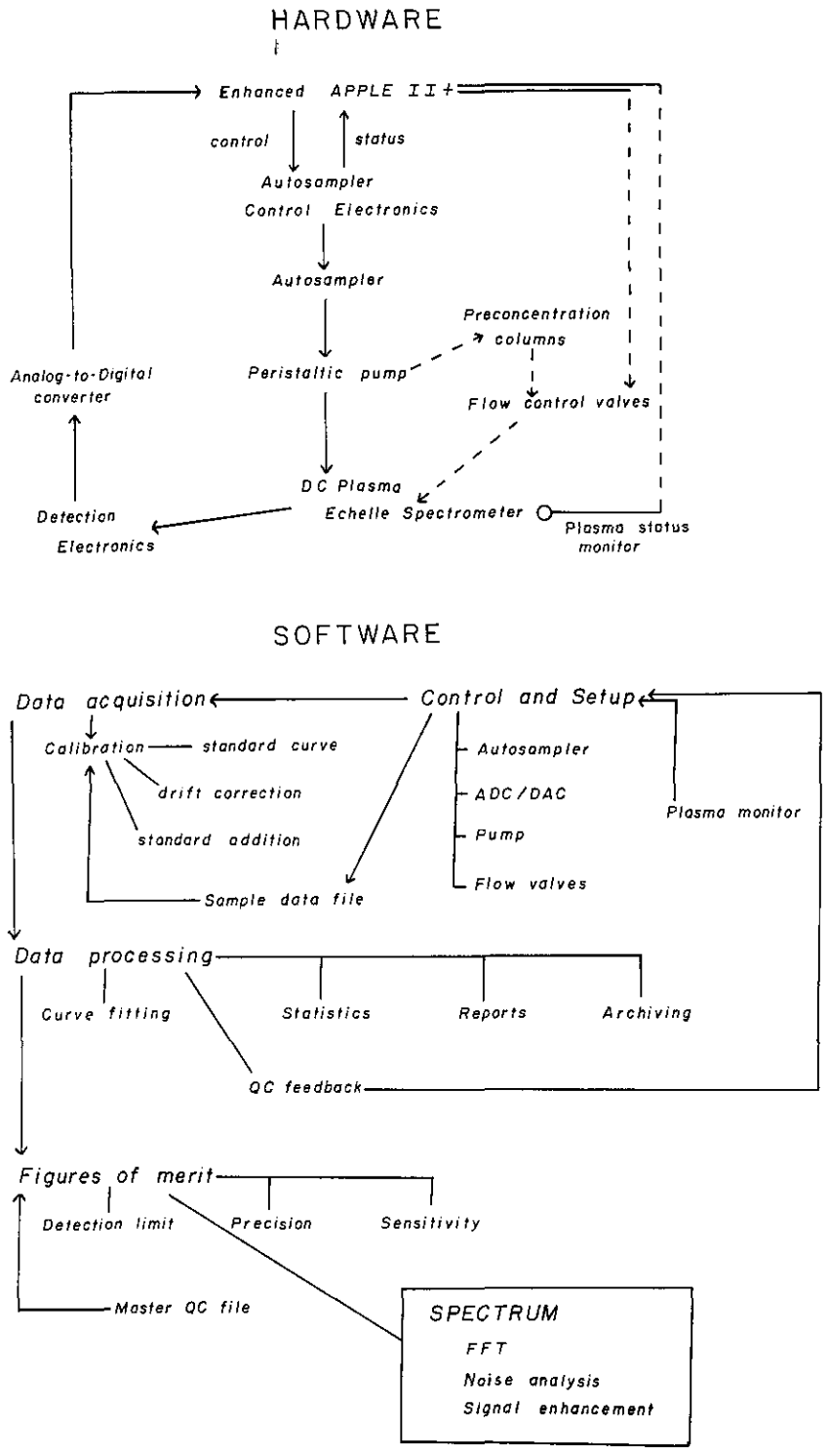

Figure 2. Software and hardware flow diagrams for the DCP spectrometric system. Dashed lines in the hardware diagram indicate components that are not yet automated.

References

[1] Snelleman, W., Rains, T. C., Yee, K. W., Cook, H. D., and Menis, O., Anal. Chem. **42**, 394 (1970).
[2] Epstein, M. S., and O'Haver, T. C., Spectrochim. Acta **30B**, 135 (1975).
[3] Epstein, M. S., and Winefordner, J. D., Prog. Analyt. Atom. Spectrosc. **7**, 67 (1984).
[4] McLeod, C. W., Cook, I. G., Worsfold, P. J., Davies, J. E., and Queay, J., Spectrochim. Acta **40B**, 57 (1985).
[5] Cook, I. G., McLeod, C. W., and Worsfold, P. J., Anal. Proc. *23*, 5 (*1986*).
[6] Deardorff, E. R., Private Communication, National Bureau of Standards, March 1981.
[7] Smith, M. V., and Burke, R. W., Private Communication, National Bureau of Standards, August 1987.
[8] Wittman, A., and Schuster, L., Spectrochim. Acta **42B**, 413 (1987).

Flow Injection-Inductively Coupled Plasma Spectrometry: A New Strategy for Ultratrace Analysis

C. W. McLeod, Y. Zhang, I. Cook, and A. Cox

Department of Chemistry
Sheffield City Polytechnic
Sheffield, S1 1WB, U.K.

and

A. R. Date and Y. Y. Cheung

British Geological Survey
64 Grays Inn Road
London, WC1X 8NG, U.K.

In the last decade few analytical techniques have made a greater impact in trace inorganic analysis than ICP emission spectrometry. Noteworthy features of the technique are well documented, but lack of sensitivity and susceptibility to spectral interferences have ensured that alternative techniques such as atomic absorption spectrometry remain competitive. The conventional approach to improving method sensitivity is to undertake relatively time-consuming sample pretreatment procedures such as ion exchange, solvent extraction, co-precipitation etc. With the advent of flow injection analysis [1] there has been a considerable interest in the development of on-line microcolumn concentration techniques for atomic spectrometry [2,3]. In the experiment relatively large volumes of sample are passed through a microcolumn in the flow injection (FI) manifold and retained analytes are subsequently eluted by injection of a small volume of eluent. Activated alumina offers a novel route for analyte preconcentration since it can function both as an anion and a cation exchanger depending upon solution pH. Under acidic and basic conditions alumina exhibits a high affinity for oxyanions and cations, respectively:

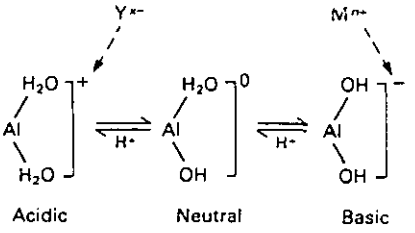

On-line Trace Enrichment: Acidic Alumina

The acidic form of alumina has a high affinity for a range of oxyanions and, as a result, FI-ICP methodology has been devised for the determination of phosphorus in steels, chromium VI in waters and sulphate in waters. The FI manifold consisted of a peristaltic pump, dual injection rotary valve, and a microcolumn (20 mm×1.5 mm i.d.) of acidic alumina. In operation, samples were injected into the carrier stream and oxyanions were retained on the column whereas cationic species were unretained. An injection of ammonium or potassium hydroxide was then used to elute analyte into the ICP. Typical emission-time responses corresponding to on-line enrichment of chromate are presented in figure 1. The approach provided the basis for development of a rapid speciation scheme for inorganic chromium by virtue of the fact that the microcolumn has a high affinity for anionic chromium VI in contrast to that for chromium III. Thus on injection of samples containing the two chromium species, chromium III was not retained by the column and hence time-resolved emission signals corresponding to the two oxidation states were monitored. Analytical data for the determination of chromium III and chromium VI in a reference water (SRM 1643a, National Bureau of Standards) certified for total chromium content are given in table 1.

Table 1. Analytical data (μg/L) for chromium III and chromium VI in water CRM (NBS 1643a)

Injection volume	Cr III	Cr VI
200 μL	15.0±1.2	not detected
2 mL	14.8±1.0	1.96±0.32

On-line Trace Enrichment: Basic Alumina

Recent studies have indicated that the FI manifold with basic alumina offers a relatively nonselective route for multielement preconcentration of divalent and trivalent cationic species over a wide pH range (pH 3–10). The emission-time responses for six elements given in figure 2 reveal rapid exchange kinetics for the elution process. Also the same integration window (integration time of 17 s) is appropriate for monitoring the transient signals and this complies with the signal processing requirements of multichannel spectrometers. Minimal retention of the alkali elements, sodium, potassium and lithium was noted (except at pH>10) and hence the technique offers a matrix isolation capability for those samples containing high concentrations of sodium and potassium. The same conclusion, however, does not apply to alkaline earth cations. Typical experimental conditions were: carrier stream, ammonium hydroxide (0.02 *M*); eluent, nitric acid (2 *M*); samples buffered to pH 6 and containing tartaric acid (0.5 *M*) as complexing agent. Use of tartaric acid was found to maintain a high deposition efficiency over a wide pH range relative to results for simple aqueous solutions without complexing agent. In addition the breakthrough capacity of the column was extended for the former case and this enabled the use of extended sampling times (e.g., 10 min at 8 mL/min) to achieve relatively high preconcentration factors. This aspect is illustrated in figure 3, in the case of manganese, where it can be seen that a 10 min sampling time corresponded to a preconcentration factor of about 500. Similar results were realized for barium, calcium, cadmium, cobalt, chromium, copper, iron, magnesium, nickel, lead, and zinc. At the 10 μg/L level and for 2 min sampling (sampling rate 8 mL/min) relative standard deviations for the specified elements were in the range 0.8–2.0% (exceptions Pb 3.9%; Ni 4.3%). For an assessment of accuracy the procedure was applied to the determination of trace elements in a certified reference water (SLRS-1, National Research Council of Canada). The data presented in table 2 reveal some inaccuracies (particularly Cd, Co, and Pb) and this was considered to be due to contamination in sample preparation/processing.

Table 2. Analytical data (μg/L) for water CRM (NRCC SLRS-1)

	FI-ICP-ES[a]	Certificate
Cd	0.028	0.015±0.002
Co	0.058	0.043±0.010
Cu	3.10	3.58±0.30
Fe	33.3	31.5±2.1
Mn	1.30	1.77±0.23
Ni	1.10	1.07±0.06
Pb	0.70	0.106±0.011
Zn	1.23	1.34±0.20

[a] 3 min sampling time; in duplicate.

Conclusion

A FI system incorporating a microcolumn of activated alumina has been devised for rapid on-line preconcentration in ICP emission spectrometry. Preconcentration factors of at least 100-fold are realized for a wide range of cationic and anionic species at sampling times of several minutes. The FI experiment may be coupled to alternative techniques including flame atomic absorption spectrometry and solution spectrophotometry and hence there is considerable scope for redeployment of such instrumentation for ultratrace analysis.

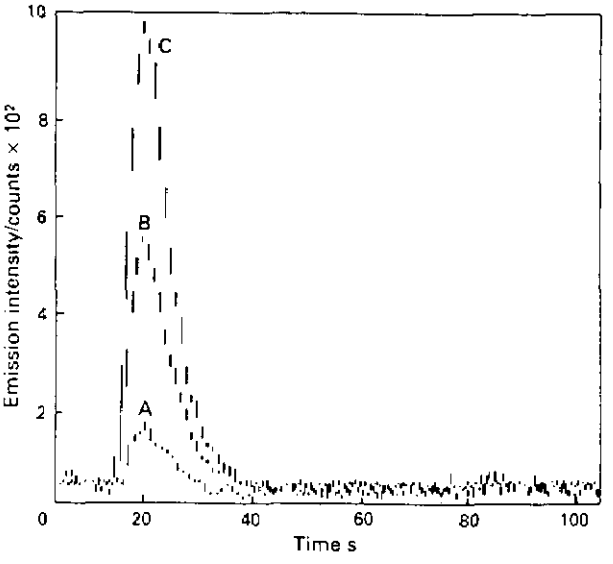

Figure 1. Effect of sampling volume on emission (267.7 nm)-time responses for Cr VI (20 μg/L): A, 200 μL; B, 1 mL; C, 2 mL. Elution, ammonium hydroxide (200 μL, 1 *M*).

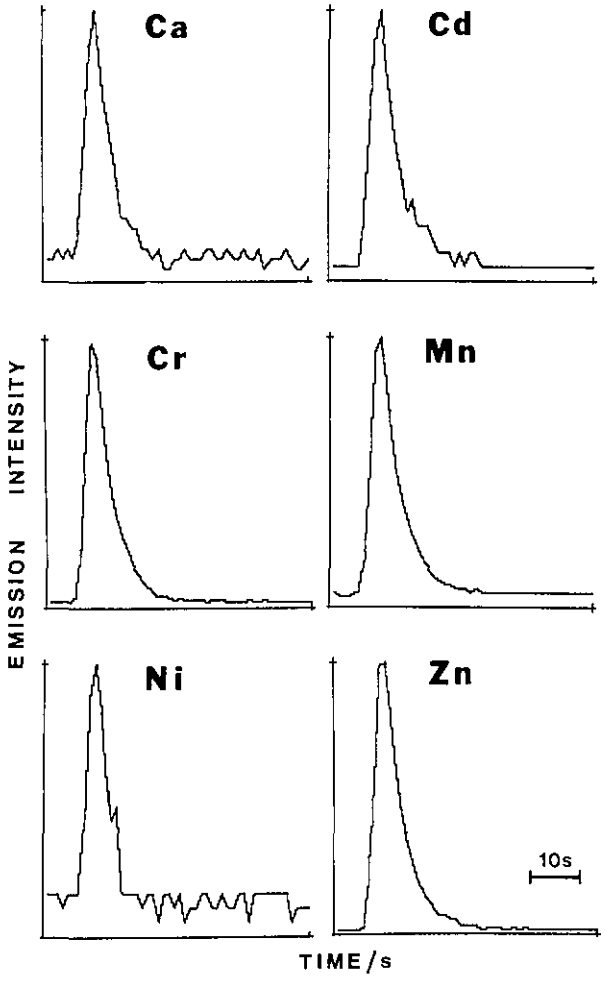

Figure 2. Multielement elution profiles: sample injection, multielement solution (250 μL, 0.1 μg/mL); elution, nitric acid (250 μL, 2 *M*).

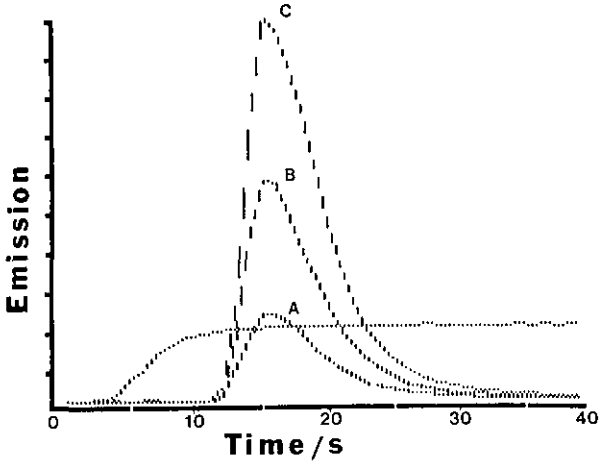

Figure 3. Effect of sampling time on emission (257.6 nm)-time responses for Mn (10 μg/L): A, 2 min; B, 5 min; C, 10 min. Sampling rate, 8 mL/min. Elution, nitric acid (250 μL, 2 *M*). Steady state response, conventional nebulisation (Mn 1 μg/L).

References

[1] Ruzicka, J., and Hansen, E., "Flow Injection Analysis," Wiley-Interscience, New York (1981).
[2] Christian, G. D., and Ruzicka, J., Spectrochim. Acta **42B**, 157 (1987).
[3] McLeod, C. W., J. Analyt. Atomic Spec. 2, 549 (1987).

Some Applications of Isotope Analysis of Lead in Food by ICP-MS

H. M. Crews, R. C. Massey, and D. J. McWeeny,

Food Science Laboratory
Ministry of Agriculture
Fisheries and Food
Norwich, U.K.

and

J. R. Dean and L. Ebdon

Department of Environmental Science
The Polytechnic
Plymouth, U.K.

Introduction

The lead concentration in food items is usually low, but accurate measurements of these concentrations are necessary if useful estimates of dietary intake are to be made. Measurements of lead at around 10 ng/g are usually beset by the two problems of sensitivity and, more importantly, matrix effects when atomic absorption techniques are employed. The advent of instruments in which samples are aspirated into an ICP torch (as an ion-source) interfaced with a mass spectrometer (as an ion-counter) open up new possibilities for the accurate measurement of lead in food at normal levels.

The present work explores the relative merits of two approaches, viz., standard additions and isotope dilution analysis (IDA). The latter relies upon the fact that in ICP-MS, measurements are made on a mass-by-mass basis and therefore each isotope of an element is measured separately. Where an isotope is normally present in food at low abundance, addition of a known amount of the element artifi-

cially fortified with this isotope and measurement of the ratio of the abundance of this isotope as compared to one of those which has not been fortified (IDA), will allow calculation of the amount of analyte present in the sample. The techniques have been assessed on samples of wines and aqueous slurries of a food powder (dried milk).

Satisfactory measurement of isotope ratios under these circumstances indicates the potential of IDA by ICP-MS for: a) accurate measurement of lead at low levels in food; b) metabolic and nutritional studies; and c) assessment of geographical origin of food.

Experimental

All measurements were made with a VG Plasmaquad. Solutions were pumped at 1 mL min^{-1} into a fixed cross-flow nebulizer (Jarrell-Ash) fitted into a water-cooled Scott-type double-pass spray chamber maintained at 10±3 °C.

For isotope dilution analyses, samples were enriched with ^{206}Pb at 5 ng·mL^{-1}; for standard additions, samples were spiked with 0, 1, 5 or 10 ng·mL^{-1} natural Pb. Milk powders were aspirated as a slurry in Triton X-100 [1].

Results and Discussion

Comparison of isotope concentration as measured by repeated scanning from 203 to 210 *m/z* and by "peak-hopping," i.e., repeated measurements at each mass unit in turn showed that the former usually gave a better precision. Although the peak-hopping routine allowed more time to be spent in measuring the low-abundance isotopes and hence might be expected to arrive at a more precise assessment, this advantage was offset by the inaccuracy due to noise at the peak crest (fig. 1). Since peak-hopping is essentially based on peak-height measurement it proved somewhat less precise than the peak-area based scanning mode. Typically the coefficients of variation for measurements of 208/206 at 10 ng·mL^{-1} were around 0.5% for scanning mode as compared to 2.5% by peak-hopping (table 1). However the latter was conducted in 13 seconds as compared to 130 seconds; if a slightly impaired precision is acceptable the speed of throughput by peak-hopping may be attractive. Recently improved software may make the precision more nearly comparable to that from scanning.

The accurate and precise measurement of lead isotope ratios (table 2) after correction for mass discrimination using NBS SRM 981 Lead enabled the technique of IDA to be used to measure the lead content of dried milk powders and of wine (table 3). The accuracy of IDA was confirmed by standard additions, small differences in concentration at the ng·g^{-1} level were observed and this is of importance for clinical and nutritional studies.

Table 1. Measurement of 10 ng mL^{-1} Pb (SRM 982), 208/206 ratio using scanning and peak hopping modes

	Scanning[a]	Peak hopping[b]
Certified	1.000	1.000
Measured mean ($n=10$)	1.082	1.098
RSD, %	0.5	2.6
95% Confidence limits of ratio	±0.003	±0.022

[a] 480 sweeps; 512 channels 500 μs/channel.
[b] Dwell time/mass ∝ % abundance; total run 13 s.

Table 2. Measurement of lead isotope ratios in milk powder slurries and wines using scanning mode

	208/206	(%RSD)	207/206	(%RSD)
Certified (SRM 981)	2.168		0.915	
Milk Powders				
European	2.063	(8.0)	0.890	(7.0)
Australian	2.167	(7.6)	0.959	(11.3)
Italian Wines				
Barola 1975	2.121	(2.6)	0.858	(2.0)
Barola 1978	2.243	(1.4)	0.873	(1.3)
Barola 1979	2.154	(2.2)	0.854	(2.1)
Borgogoni 1979	2.137	(0.9)	0.873	(0.7)
Australian Wines				
Gawler River Valley 1983	2.164	(2.5)	0.940	(2.7)
Hunter Valley 1985	2.090	(2.7)	0.849	(4.0)

Table 3. Lead concentration in milk powder (ng g^{-1}) and wine (ng mL^{-1})

Sample	Isotope Dilution Analysis	Standard Additions
Milk Powder		
European	21.±09[a]	30±16[a]
Australian	16.2±1.5	33±16
Italian Wines		
Barola 1975	92.7±2.7	106±9.5
Barola 1978	83.8±1.2	94±3.5
Barola 1979	101.4±3.7	99±8
Borgogoni 1979	143.4±2.5	150±10
Australian Wines		
Gawler River Valley	49.8±1.1	56±4
Hunter Valley	30.8±1.0	42±4.5

[a] ±1 standard deviation.

The 207/206 lead ratio of lead from the Broken Hill area of Australia is reported at 0.960. This value is consistent with the data reported for the Australian milk powder (table 2). There is some indication that the Gawler River Valley wine reflects this ratio but this needs to be confirmed. None of the Italian wines show evidence of contamination by lead originating from Broken Hill. Fuller details of this and related studies are published elsewhere [2].

Summary

1. *The accuracy and precision* achievable using scanning and peak modes for measurements of lead isotope ratios were studied. If sufficient time and sample materials were available scanning gave better accuracy and precision (table 1).

2. *Isotope ratios* in milk powders and wines of European and Australian origin have been compared. Australian milk powder has a 207/206 lead ratio consistent with that determined for lead in the Broken Hill area of Australia (table 2).

3. *Isotope dilution analysis (IDA)* gave more precise data than standard additions as a means of measuring total lead content in milk powder slurries and wine. Accurate and precise data for both matrices were obtained using IDA-ICP-MS (table 3).

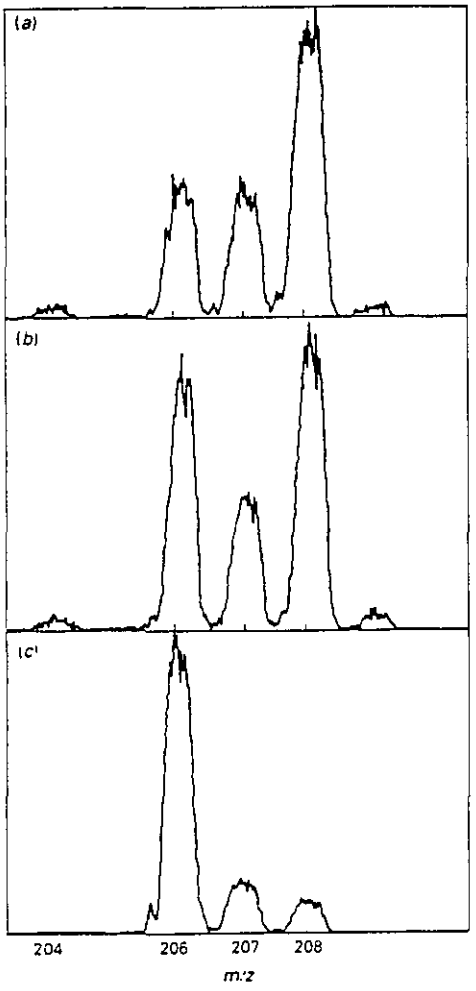

Figure 1. Mass spectra of 10 ng mL^{-1} Pb: (a) Natural Pb; (b) Lead and (c) enriched ^{206}Pb.

References

[1] Sparkes, S. T., and Ebdon, L., Anal. Proc. **23**, 410 (1986).
[2] Dean, J. R., Ebdon, L., and Massey, R., J. Anal. Atomic Spectr. **2**, 369 (1987).

Volume 93, Number 3, May-June 1988
Journal of Research of the National Bureau of Standards

Accuracy in Trace Analysis

Improving Accuracy in Graphite Furnace Atomic Absorption Spectrometry Through Peak Shape Monitoring

Markus Michaelis and Wolfhard Wegscheider

Institute for Analytical Chemistry, Mikro- and Radiochemistry, Technical University Graz
A-8010 Graz/Australia

and

Hugo M. Ortner

Metallwerk Plansee GmbH
A-6600 Graz/Australia

Due to the good detection limits of graphite furnace atomic absorption spectrometry (GFAAS), situations frequently arise when an analyte is determined in the presence of a large excess of concomitants. It is in these cases when the improvements made in furnace design, heating rate optimization, Zeeman background correction, platform atomization and application of matrix modifiers are still not sufficient to provide the analytical chemist with reliable data.

On the other hand, large gains in mechanistic insight have not yet yielded a model that can successfully cope with atomization characteristics in samples with a large matrix/analyte ratio. Typical accounts of the current state are found in [1] for explicit differential equations formulations and in [2] for the Monte Carlo approach, but there is no real difference in the predictive abilities of the two. Nevertheless, it is clear that a wide variation of peak shapes are observed and qualitatively monitored by everyone practicing GFAAS.

In this work we describe a characterization of peak shapes by various parameters, such as appearance time, mean, mode, peak width, area/height, skewness and kurtosis. This is done by attempting to alter the peak shape systematically through deliberate addition of concomitant elements in a fractional factorial experiment [3,4]. The observed shape parameters are then linked to the characteristic mass after discarding those that vary with analyte mass.

Experimental

A Perkin-Elmer 5000 with HGA 500 and AS 40 autosampler was used throughout. The computations were run on a Perkin-Elmer 7500 data station and on an IBM PC-XT. All data given are Zeeman background corrected and all samples are atomized from a platform. Two different platforms were used. One was the vendor-supplied pyrolytic graphite platform, and the other one was produced from the same type by physical vapor deposition of TaC [5]. A general account of the analytical properties of this TaC-coated platform for ETAAS can be found elsewhere [6]. All reagents were of analytical grade. Doubly distilled water and subboiled nitric acid were employed.

Sn, Se, and Rh served as model analytes to study the behavior of elements different in both chemistry and volatility. Ten micrograms of each palladium and magnesium as nitrates were used as matrix modifiers for Se, and 200 μg ammonium dihydrogen phosphate was used for Sn. First, temperature programs were optimized for standard solutions and not altered for any of the subsequently described experiments. Generally, atomization temperatures from the TaC-coated platform tended to be higher than for the ordinary total pyrolytic graphite platform [5].

Calibration curves were run to establish the linear range, but—more importantly—the dependence of peak shape parameters on analyte mass. From this the concentration levels were chosen for the interference experiments to be well within the linear range. Cr, Fe, Na, Zn, Mg and Al were chosen as potential interferents and added as nitrates in a 29000 (Sn) to 40000 (Se) fold molar excess over the analyte. A fractional factorial design in these interferents was set up which was replicated once, giving a total of 64 profiles [4]. These were recorded in random order with 2 atomizations of the standard solution and 2 atomizations of a blank solution before and after the run of 64.

Results and Discussion

Peak shape parameters can serve as a reduced description of the entire atomization curve and should be defined to carry information on the (largely) unknown fundamental mechanisms in GFAAS. In this work it was assumed that—if not the mechanisms—at least kinetic and thermody-

namic parameters governing the processes would be altered by the presence of interferents and result in changes of peak shape. Consequently, the observed atomization curve could be regarded as a faithful representation of the free atom population in the detection volume and should be accessible to a nonparametric description. The peak shape parameters used in this study are given in table 1. As these parameters were chosen to model sensitivity in unknown samples, it is required that they be fairly insensitive to analyte mass. This could be shown to be the case for all, but the parameter "length" [7] which was therefore not used in further studies.

Table 1. Peak shape parameters

Name	Description
area/height	(self explanatory)
appearance time	time when signal rises significantly above baseline noise
length	time interval from appearance time to drop of the signal below significance
standard deviation	width of the peak measured by assuming the signal to be the probability density curve of the free atom population in the analysis volume
mode	time of peak maximum
mean	arithmetic mean time of the peak
skewness	measure of asymmetry of peak [3]
kurtosis	measure of slimness of peak [3]
baseline noise	absorbance corresponding to the average spread of baseline noise

Figure 1 shows the change in kurtosis with the type of interferent and with the resulting characteristic mass. Of course, in a real analytical setting situations may arise where the interferent is not identifiable. It is therefore necessary that the characteristic mass is modelled independent of the nature and mass of an interferent. This can be attempted using only the peak shape parameters.

The technique employed for this modelling is known in the literature as partial least squares (PLS) regression [8]. The data from the interference study, supplemented by the four data on the standards were subjected to PLS. A subset of the data was randomly removed for the modelling step and used to assess the predictive ability afterwards. Table 2 gives an overview of the results. The optimal number of dimensions for the PLS model varied between 2 and 6 with 62 profiles fitted; six atomization curves were used for predictions. The relative importance of the different peak shape parameters is different for each data set. Detailed results on this subject will be published elsewhere [9].

Table 2. Results of modelling characteristic mass from peak shape parameters

Element	Platform	Rel. residuals %	Rel. prediction error %
Se	pyro	2.0	11
	TaC-coated	2.4	4.7
Rh	pyro	2.8	4.5
	TaC-coated	8.6	10.6
Sn	TaC-coated	0.6	8.6

The success of these initial experiments is obvious. In practice the applicability of the proposed scheme will depend (i) on whether the majority of changes in peak shape can be observed in the initial experimental design, and (ii) on the validity of the implicit assumption that most interferences manifest themselves by changes of peak shape. Both questions cannot be answered without full insight into the mechanisms of atomization. In the meanwhile, the approach can serve as a means to warn the analyst about the unexpected occurrence of interferences. The model for characteristic mass can serve to improve accuracy. This by itself should help to make data from ETAAS more reliable.

Acknowledgments

This work has been supported in part by the Fonds zur Förderung der gewerblichen Wirtschaft (Vienna). The help of Thai My Phe with partial least squares calculations is gratefully acknowledged.

Volume 93, Number 3, May–June 1988
Journal of Research of the National Bureau of Standards

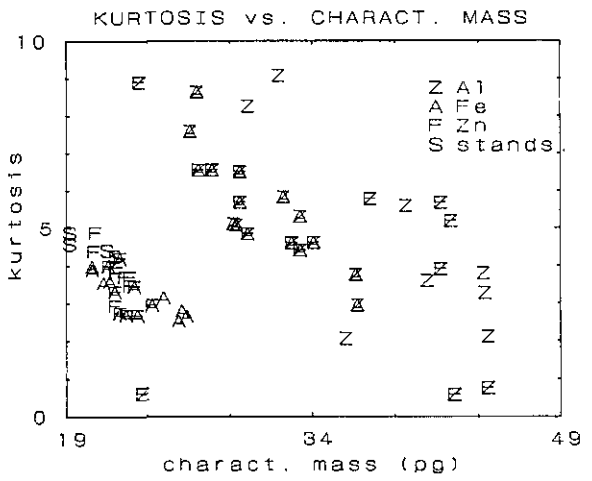

Figure 1. Variation of kurtosis with nature of analyte and change of characteristic mass.

References

[1] Chakrabarti, C. L., Chang, S. B., Thong, P. W., Huston, T. J., and Shaole Wu, Talanta **34**, 259 (1987).
[2] McNally, J., and Holcombe, J. A., Anal. Chem. **89**, 1105 (1987).
[3] Box, G. E. P., Hunter, W. G., and Hunter, J. S., Statistics for Experimenters, Wiley, New York (1978).
[4] Wegscheider, W., Knapp, G., and Spitzy, H., Fresenius' Z. Anal. Chem. **283**, 9 (1977).
[5] Schintlmeister, W., Pacher, O., Kailer, K., and Wallgram, W., Ion Plating Beschichtungen aus hochschmelzenden Metallen, Proc. 10th Plansee Sem. **2**, 635 (1981).
[6] Michaelis, M., Thesis, Technical University Graz (1986).
[7] Wegscheider, W., Michaelis, M., and Ortner, H. M., Peak Shape Parameters as Indicators for the Occurrence of Interferences in Graphite Furnace Atomic Absorption Spectrometry, in *Atomspektrometrische Spurenanalytik* (Welz, B., ed.), vol. 3, in press.
[8] Wold, S., Wold, H., Dunn III, W. J., and Ruhe, A., The collinearity problem in linear regression. The partial least squares approach to generalized inverses. Umea University, Report UMINF-83.80 (1982).
[9] Wegscheider, W., Michaelis, M., Thai My Phe, and Ortner, H. M., in preparation.

Analysis of Trace Elements in Methamphetamine Hydrochloride by Inductively Coupled Plasma-Mass Spectrometry

Tohru Kishi

National Research Institute of Police Science
6, Sanbancho, Chiyoda-ku
Tokyo 102, Japan

Introduction

Drug abuse is a serious problem in the world and these drugs are synthesized in clandestine laboratories. The determination of the manufacturing source provides important information regarding drug traffic [1,2]. One of the stimulants imported illegally, methamphetamine, is a serious social problem in Japan.

Methamphetamine is synthesized from ephedrine or methyl benzyl ketone as the raw material. In Asian areas, ephedrine is used as a starting material and methamphetamine is prepared by catalytic reduction of chloroephedrine by palladium-barium sulfate [3] or by reduction of ephedrine with hydrogen iodide and red phosphorus [4] as shown in figure 1.

The identification of catalyst and/or reagents based on final product analysis have been studied by radiochemical neutron activation analysis (RNAA) [2]. Palladium, barium, and iodine were determined as trace elements in methamphetamine hydrochloride.

In this paper, these trace elements were determined directly by inductively coupled plasma-mass spectrometry (ICP-MS) and the results are compared with those of neutron activation analysis (NAA).

Experimental

Reagents

Methamphetamine hydrochloride was prepared by Emde's method [3] or Nagai's method [4] as shown in figure 1.

Procedure

For the ICP-MS, samples were dissolved in water in a concentration of 0.1–1%, and then the ana-

lytes determined by the Seiko ICP-MS SPQ-6100. The plasma operating conditions were: rf power 1.35 kW; nebulizer gas flow rate, 0.5 L/min; plasma gas rate, 16 L/min; auxiliary gas rate, 1 L/min. The plasma was sampled at a depth of 8 mm from the load coil. The mass spectrometer was a quadrupole type, and the measurement time was 2 ms per point with a scan increment of 0.125 amu. For quantitative analysis, the intensity of Na-23, Br-79, Pd-106, I-127 and Ba-138 were integrated.

For NAA, samples were sealed in polyethylene bags. After 5 hours irradiation in a thermal neutron flux (1×10 n·cm^{-2}·s^{-1}), Na-24 and Br-82 were directly determined while Pd-109 and Ba-131 were precipitated as palladium-dimethylglyoxime complex and barium sulfate, respectively. After 5 min irradiation, I-128 was determined in the chloroform layer after radiochemical separation.

Results and Discussion

Mass Spectra of Methamphetamine Hydrochloride

ICP/MS spectra of methamphetamine hydrochloride solution are shown in figure 2 for the mass range m/z 1 to 200. Barium, palladium, bromine, and sodium, were detected in the methamphetamine hydrochloride prepared by Emde's method and iodine, bromine, and sodium were detected in the methamphetamine hydrochloride prepared by Nagai's method. Barium and palladium originated from palladium-barium sulfate catalyst and sodium and bromine from sodium hydroxide and hydrochloric acid as neutralization reagents. Iodine originated from hydrogen iodide.

For the mass range m/z 20 to 70, many ions were observed, because the sample solution contained large amounts of nitrogen and chlorine; thus, further investigation is required for the determination of trace elements in this region.

Analytical Calibration Curve

The analytical calibration curves shown in figure 3, obtained in the integration mode, show a useful working range of 3 orders of magnitude. These were linear for 0.1–10 μg/mL of sodium, for 0.01–1 μg/L of bromine and iodine and for 0.001–0.1 μg/mL of palladium and barium.

These data were obtained from reference solutions containing palladium, barium, iodine, bromine and sodium. The range of these calibration curves was established by considering the practical concentration of each element [2]. Therefore these elements were determined simultaneously, when one sample solution was measured.

Quantitative Analysis

Trace elemental concentrations determined by ICP-MS are listed in table 1. The result of INAA and RNAA are listed in parentheses. The results of ICP-MS and NAA are almost the same except for concentrations of bromine. Concentrations of bromine by ICP-MS were larger than those by NAA. Argon dimer ion peak (m/z 80) is very close to the bromine ion peak (m/z 79). Consequently, it might interfere in the peak area calculation of bromine peak (m/z 79).

Table 1. Trace elements in methamphetamine hydrochloride by ICP-MS (μg/g)

Synthetic method	Na	Br	Pd	I	Ba
Emde's	240(220)	130(80)	1.0(1.0)	-	1.0(1.0)
Nagai's	20(20)	90(80)	-	5(7)	-

( ): Determined by INAA and RNAA
- : Not detected

Conclusion

The trace elements in methamphetamine hydrochloride (stimulant) were determined by ICP-MS and NAA. Part per million levels of sodium, bromine, palladium, barium and iodine, which originated from the catalyst and/or reagents, were found in the methamphetamine hydrochloride crystal. From these results, trace amounts of reagent and catalyst remained in the final product and a specific synthetic method could be determined by analysis of the methamphetamine prepared in clandestine laboratories.

Acknowledgments

The author thanks Seiko Instruments & Electronics Ltd. for the ICP/MS measurements.

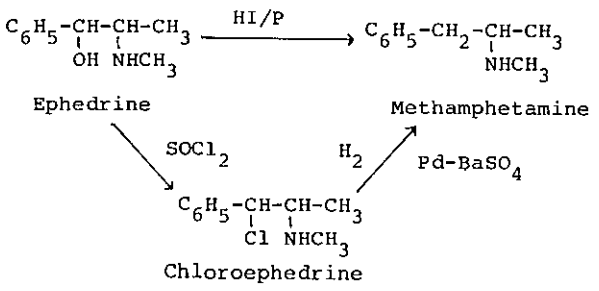

Figure 1. Synthesis of methamphetamine from ephedrine.

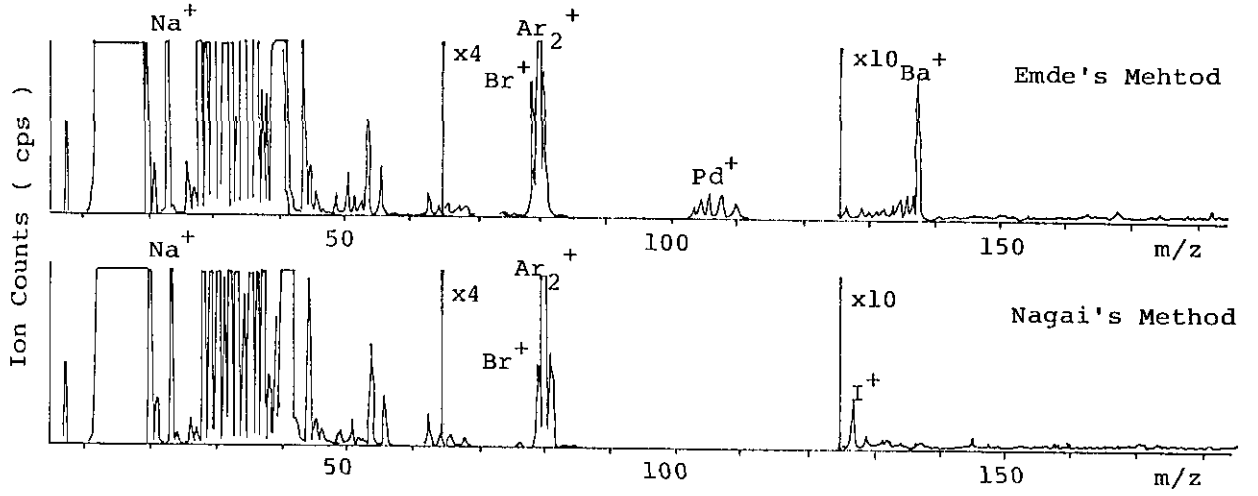

Figure 2. ICP-MS spectra of methamphetamine hydrochloride.

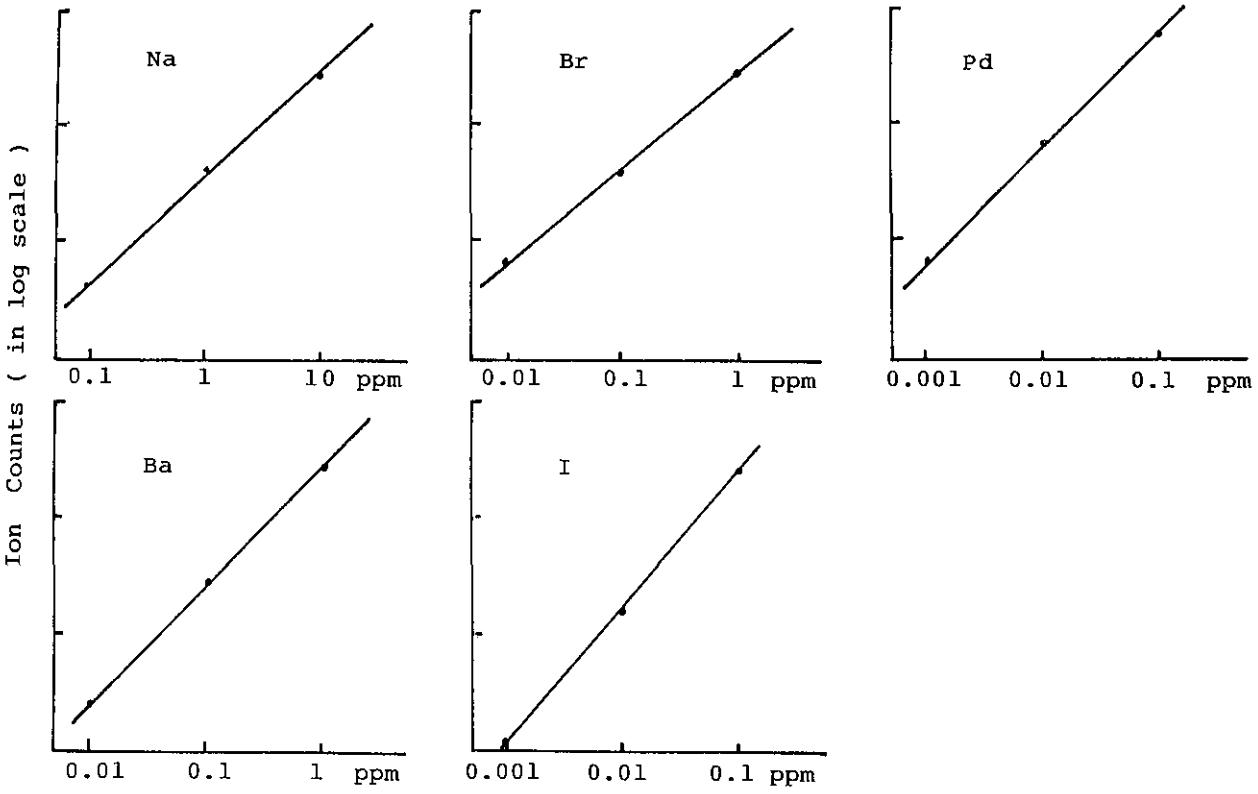

Figure 3. Analytical calibration curve of Na, Br, Pd, Ba, and I.

References

[1] Kishi, T., 7th International Conference, Modern Trends in Activation Analysis, Copenhagen (1986) 1141.
[2] Kishi, T., Inoue, T., Suzuki, S., Yasuda, T., Oikawa, T., and Niwaguchi, T., Eiseikagaku **29**, 400 (1983).
[3] Emde, H., Helv. Chim. Acta **12**, 384 (1929).
[4] Nagai, N., Yakugaku Zassi **139**, 901 (1893).

Volume 93, Number 3, May-June 1988
Journal of Research of the National Bureau of Standards

Nuclear Methods

MeV Ion Beam Analysis

J. A. Cookson and T. W. Conlon

Harwell Laboratory, UKAEA
Oxfordshire OX11 ORA, UK

1. Introduction

The main techniques traditionally used in MeV Ion Beam Analysis are Particle Induced X-ray Emission (PIXE), Rutherford Backscattering (RBS) and Nuclear Reaction Analysis (NRA), which, broadly speaking, utilize light ($m \leqslant 4$) ions. These techniques can also be applied in the channeling mode to study the structural properties of crystalline materials (such as foreign atom location, radiation damage, and interface studies). The techniques have the common feature that all are based on processes that occur spontaneously in the interaction of light ion beams with solids. Since these processes are well understood and are very well established in the literature [1–3], this review will treat them only with regard to improvements in their quantification (sec. 3).

Heavy ion beams in solids exhibit additional properties that can be utilized in materials. For example, they transfer large amounts of energy in collision with other nuclei; they slow down rapidly and in doing so generate regions of very high ionization density. Analytical methods based on the generation of fast recoils, on the nuclear physics process of coulomb excitation and on the heavy ion induced desorption of atoms and molecules are under development and are described in section 2.

Both the light and heavy ion techniques can be applied either in the broad beam or microbeam mode. New developments are taking place in the production and focusing of micrometer size beams for analysis where lateral resolution is important. These advances, which could revolutionize the prospects for microbeam systems, are described in section 4.

2. Advanced Analysis Techniques

The power of MeV ion beam analysis can be extended in several ways: by the use of heavy ions, by measuring more than one parameter of the interaction process, and by the application of coincidence techniques. Some examples are given below.

2.1 ERDA

The Elastic Recoil technique (ERDA) utilizes fast heavy ions to produce recoil substrate atoms that are ejected from the substrate and can be subsequently analyzed. In contrast to the light ion techniques that generally provide only one parameter (usually a particle or proton energy), both recoil mass and recoil energy can be measured.

ERDA is in routine use as a single parameter technique, where an energy spectrum of all the ions recoiling from the specimen can be interpreted to give depth profiles of the various elements (see fig. 1). There are several ways of developing a two-parameter version of ERDA so that a separate energy spectrum is produced for each type of recoiling ion. One technique carries out mass spectrometry of the ions with electric or magnetic fields. Another possibility is the application of the stopping power equation $E\mathrm{d}E/\mathrm{d}x = kMQ^2$ where $\mathrm{d}E$ is measured in a thin detector and the total energy E in a thick detector. M and Q are the ion mass and charge.

Also used is the time-of-flight (TOF) technique in which the velocity V of the ion is obtained from its transit time over a fixed distance, so that, if the ion energy ($\frac{1}{2}MV^2$) is also measured, the mass M can be uniquely determined.

All of these options, extensively used in nuclear physics experiments, are being investigated in various laboratories world-wide for material science uses [2,3]. However, no detailed comparison of the respective merits of the various options has yet been published.

2.2 Coulomb Excitation Studies

RBS has proved extremely useful in characterizing heavy element distributions in light element

substrates but, because it measures only a single parameter (i.e., E) and because of the small change in mass-energy product between neighboring elements, it is unable to resolve distributions of elements that are similar in mass (e.g., P in Si, Ga in As compounds). ERDA is very useful for determining multi-light element depth distributions, especially with two-parameter measurement of M and E (as indicated above). However, unless very heavy high energy ions are used, the recoil energies imparted to elements such as P, Si, Ga and As are insufficient to enable them to escape from the substrate.

Coulomb excitation in coincidence with RBS (e.g., called CBS) offers a solution to this class of problem. In this case the two-parameter measurement of RBS energy and gamma-ray energy from the recoiling nuclei is sufficient to distinguish the depth profiles of different nuclides even if their mass is the same. This is because each nuclide has a unique gamma-ray signature.

Figure 2 shows a preliminary test of the method, but insufficient data is yet available to determine the limits of depth resolution and sensitivity.

Bakir et al. [6] have reported an earlier attempt to combine RBS and PIXE (i.e., utilizing x-rays rather than the gamma-rays from Coulomb Excitation discussed above). They used 34 MeV ^{16}O ions and grazing angle RBS to demonstrate a depth resolution of 70 Å and a sensitivity of 10^{16} atoms/cm^2 from medium mass elements (Cu on Ge substrate).

2.3 Particle Desorption Mass Spectrometry (PDMS)

The high ionization density of both fission fragments and accelerated heavy ions has been utilized to investigate the ion induced desorption of atomic and molecular species from surfaces. Some species are often detected by TOF spectrometry as discussed above for ERDA. The phenomenon was first observed by MacFarlane and Torgerson [7] and used for the characterization of large, volatile biomolecules.

Most recently Schweikert et al. [8] have investigated the prospects of developing a technique based on this process for surface analysis. In contrast to the routinely used techniques, which require fluences of typically $10^{12}-10^{15}$ ions/cm^2 for analysis (and appreciably more for the coincidence techniques), useful information can be obtained from PDMS with much lower fluences (especially when fission fragments are used). The detection limit was 100 μg/g for lithium in glass, and microscopic analysis on areas as small as 11 μm diameter was demonstrated. To provide depth information, the technique must be combined with surface erosion.

3. Advances in IBA Microbeams

There are now upwards of 30 groups worldwide regularly using the various IBA techniques with finely focused or collimated beams to measure the lateral elemental distributions of a very wide variety of materials [9,10]. The present state-of-the-art beam quality is the 100 pA of beam in a spot with FWHM of 1 μm beam achieved at Oxford and Melbourne. These groups mainly use PIXE, which has the highest cross sections of the IBA techniques, to perform trace element analysis of biological and medical thin specimens with 1 μm resolution. All the other IBA techniques are used for a very wide range of applications, but usually at lower positional resolution.

At present the highest resolution microbeams use Van de Graaff accelerators with standard ion sources to illuminate an aperture which acts as the object for a single, demagnifying magnetic quadrupole lens. Although attempts [9] are being made to improve the focusing lens, it seems likely that significant reductions of the spot size below 1 μm, or major increases in the current density at the present spot size, will require improvement of the brightness (defined roughly as current per unit area and solid angle) of the accelerator beam.

A simplified view of the factors involved indicates that reduction of the spot diameter by a factor 10 without loss of current could be achieved fairly simply if there were an increase in beam brightness of 10^4. This implies that if the extra brightness of a field ionization source could be utilized, a microbeam size of 0.1 μm should be possible.

The type of field ionization source developed for low energy scanning transmission microscopy [11] has an intrinsic brightness about 10^6 greater than the sources used in Van de Graaff accelerators. Legge et al. have demonstrated [12] such a source giving 21 nA at 4×10^5 greater brightness than an RF source, and have discussed [13] how the brightness might be maintained through an MeV accelerator.

An adaptation of the field ion source by Böhringer et al. [14] uses a small pimple formed on a tungsten tip to give even brighter beams, but with only a few hours lifetime so far.

Liquid metal sources [15] can give ion brightnesses comparable with those achieved in hydrogen field ionization source, and have the advantage that longer source life can be anticipated as the emission is from a continuously renewed "Taylor Cone" of liquid metal. So far, a gallium source has been shown [16] to work satisfactorily in a Van de Graaff accelerator at Harwell for non-microbeam use. For microbeam purposes the chosen metal is lithium which is very suitable for RBS work and also has NRA and PIXE uses. Indications are that a very simple lithium ion source system of the type shown in figure 3 would provide an appreciably brighter beam than a normal Van de Graaff ion source, but considerable development is still needed to retain that brightness as far as the microbeam object aperture.

4. Improved Quantification

A feature that makes all four of the main IBA techniques very different from most other analytical techniques is that their concentration and depth information are very little influenced by the chemical form of the specimen. This lets them contribute only stoichiometric information for chemical characterization, but it has the very beneficial effect of making their results almost independent of matrix considerations.

The PIXE technique [1] has had its widest application as a very efficient means of analyzing pollution-covered thin filters. An intercomparison of PIXE measurements with a wide range of other techniques has been described by Bombelka et al. [18] who conclude that for most contaminants giving adequate counting statistics the PIXE accuracy is better than 10%, although for S, with the lowest energy x-rays considered, allowance was needed for the filter thickness.

The rapid measurement capability of the PIXE technique is now becoming routinely applied to thick targets. These measurements are more difficult than for thin targets because the x-rays are produced at different energies and depths as the beam penetrates the specimen material and there is attenuation of the x-rays as they escape from the specimen. These introduce extra uncertainties [19] in the measurement, of which the main ones arise from the x-ray attenuation coefficients and to a lesser extent the energy dependence of the x-ray production. The analysis needs to contain some iteration as the yield of each element depends on the presence of the others. An extra aspect of this interdependence is the fluorescent production of x-rays that can occur as PIXE x-rays are absorbed in the matrix.

For biological materials, where x-ray attenuation is not very severe, PIXE measurements of IAEA H-8 Horse Kidney and NBS 1572 Citrus Leaves have been made by Clayton [20], who shows that for elements with Z above 18 the concentration values assumed for H, C, N and O, which are of course not measured in PIXE, affect the analysis very little. The agreement of these PIXE results with the certified values is generally at the few percent level.

Geological materials usually present a more severe challenge because of the greater influence x-ray attenuation has on the measured intensities. Nevertheless Rogers et al. [21] have shown that with sophisticated data processing, very satisfactory results can be achieved for geological standard materials.

The RBS technique normally uses ^{4}He ions of about 2 MeV to measure depth profiles. For all except the very lightest target nuclei, the cross sections can be calculated to better than 1% accuracy provided that a screening correction [22] is applied to the Rutherford scattering law. The main extra information that is needed to interpret the RBS spectra is the way in which the incident and scattered particles lose energy as they travel through the specimen. There is now a comprehensive set of stopping power values available [23] that is believed to be accurate for ^{4}He ions in most pure solid elements to better than 5%. The stopping powers for compounds are usually calculated using the Bragg Rule, but deviations of a few percent from this are believed to occur for low energy beams due to atomic binding effects.

Although the accurate knowledge of the scattering cross section does, in principle, allow RBS to be independent of standards, most practitioners find it more convenient to normalize their results to well-characterized standards. The best known of these are a series of Bi implants in silicon known as Harwell Series I, II and III, and well-characterized Ta films produced at the École Normale Supérieure in Paris. Accuracy of about $\pm 1\%$ is suggested [24] for the Harwell series I implants, but larger uncertainties occur among the Series II

specimens [25]. RBS measurements of quantities of material can be better than ±5%, making use of such standards. The accuracy of RBS depth measurements can approach how well we know the stopping power of the ions used, i.e., perhaps 5%, and does not suffer from the uncertainties in sputtering rates that plague many depth profiling techniques.

ERDA, like RBS, relies on stopping power data and Rutherford cross sections. The stopping powers usually are the main source of uncertainty because, not only are the values for heavy ions less well known (typically ±10%) than those involved in RBS, but they have greater effects on the observed spectra. Each element measured in ERDA involves a different type of ion escaping from the target, and then passing through an absorber foil and a detector dead layer, before giving an energy signal. Nevertheless, accuracies of quantification and depth scale at the ±10% level can be regularly achieved. Better stopping power data would allow improvement of ERDA accuracy.

The cross sections for *NRA* do not have any simple variation with projectile or energy or from element to element, and most NRA measurements rely on comparisons with standards. Stopping powers are needed to relate results from the specimen to those from the standards, and are of course particularly important in NRA depth profiling.

An interesting indication of the accuracies that can be achieved in IBA is given by an intercomparison of three of the techniques carried out by six laboratories [26]. The two specimens consisted of nominal thickness of 30 and 100 nm of tantalum pentoxide grown anodically on Ta foil. Table 1 shows agreements among the measurements at better than the 5% level although the different groups have treated even the same techniques in different ways and relied upon different cross-section and stopping power information.

This work forms part of the Underlying Research programme of the UKAEA.

Table 1. A summary of the results of an intercomparison by Seah et al. [26], using NRA, RBS and ERDA, of the thickness and composition of 30 nm and 100 nm Ta_2O_5 films

Technique	Laboratory	Oxygen thickness, 10^{21} atoms/m^2		Ratio	Tantalum thickness, 10^{21} atoms/m^2	
		30 nm	100 nm		30 nm	100 nm
NRA	Liège	1.84±0.25	5.51±0.74	0.333±0.003		
NRA	Compiègne	1.73±0.05	5.12±0.15	0.337±0.001		
NRA	Paris	1.75±0.03	5.24±0.08	0.334±0.002		
NRA	Chalk River	1.80±0.06	5.37±0.17	0.336±0.003		
RBS	Compiègne					2.08±0.07
RBS	Surrey			0.326±0.003	0.71±0.02	2.18±0.05
RBS	Harwell			0.325±0.007	0.68±0.05	2.08±0.15
ERDA	Harwell	1.73±0.14	5.64±0.45	0.307±0.026		
Average		1.77±0.05	5.38±0.21	0.328±0.010	0.70±0.02	2.11±0.06

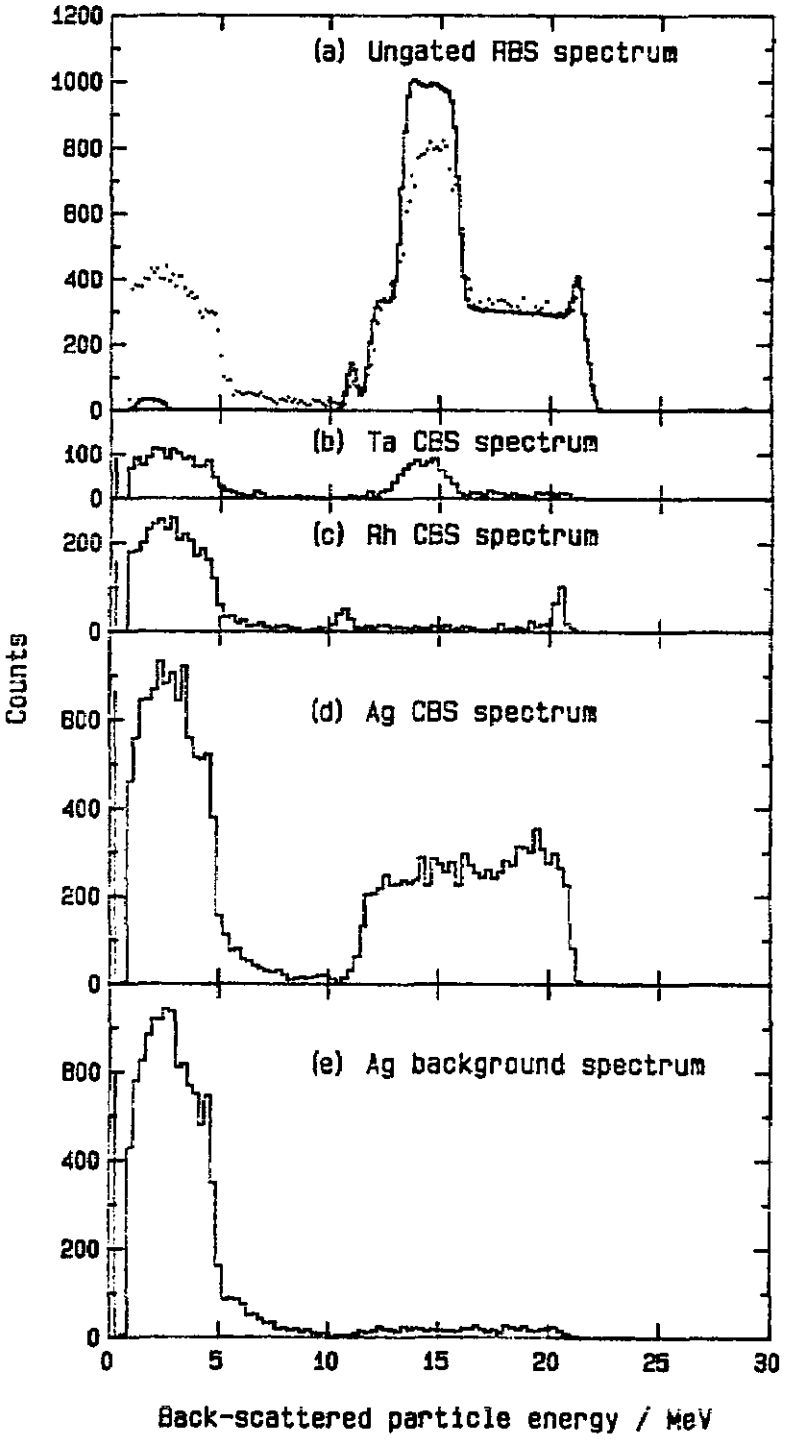

Figure 1. A one-parameter ERDA measurement with 30 MeV ^{35}Cl ions incident on an amorphous Si solar cell produced by plasma decomposition of silane and B_2H_4. The solid line is a simulation assuming uniformity of H and B concentration with depth. A surface C peak appears near channel 570 [4].

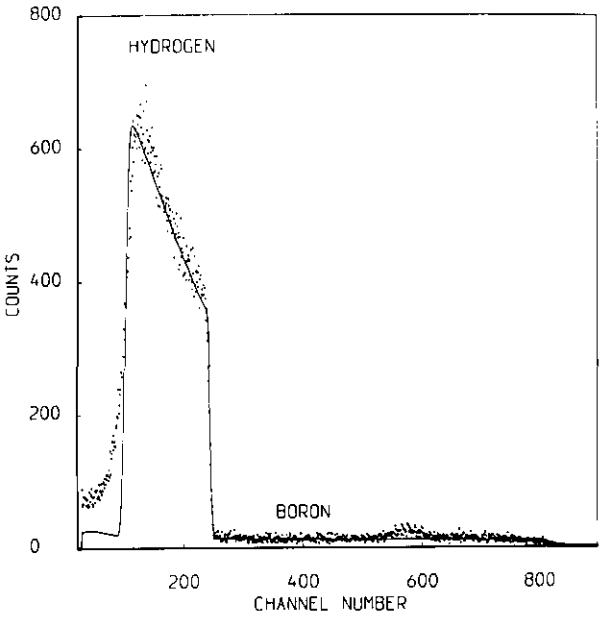

Figure 2. Spectra from the analysis of a composite target consisting of thin foils of Al, Ag, Rh, and Ta (with the Al at the front). The beam is 40 MeV ^{16}O and RBS is carried out at 170°. The CBS spectra are obtained by gating the RBS by characteristic gamma-rays from the various nuclides [5].

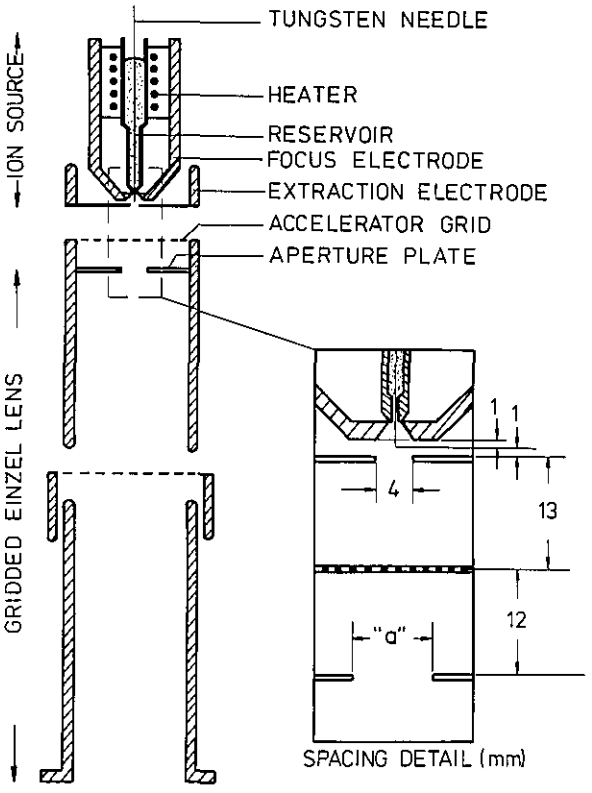

Figure 3. A schematic drawing of a liquid metal ion source and a gridded focusing lens [17]. A more sophisticated lens design would be needed for MeV microbeam applications.

References

[1] Proc. Fourth Int. Conf. on PIXE . . . , Nucl. Inst. Meth. **B22** (1987).
[2] Proc. Conf. Appl. Accel. in Res. and Ind., Nucl. Inst. Meth. **B24/25**.
[3] Proc. Seventh Int. Conf. on IBA, Nucl. Inst. Meth. **B15**.
[4] Read, P. M., Sofield, C. J., Franks, M. C., Scott, G. B., and Thwaites, M. J., Thin Solid Films **110**, 251 (1983).
[5] Asher, J., Parker, D. J., and Montague, S., 1987 (private communication).
[6] Bahir, G., Kalish, R., and Tserruya, I., Nucl. Inst. Meth. **168**, 227 (1982).
[7] MacFarlane, R. D., and Torgerson, D. F., Science **191**, 920 (1976).
[8] Schweikert, E. A., Summers, W. R., Beug-Deeb, M. U. D., Filpus-Luyckx, P. E., and Quiñones, L., Anal. Chim. Acta **195**, 163 (1987).
[9] Proc. First Int. Conf. on Nucl. Microprobe Tech. and Appl., Oxford, 1987, Nucl. Inst. Meth. (to be published).
[10] Principles and Applications of High-Energy Ion Microbeams (eds., Watt, F., and Grime, G. W.), Adam Hilger, Bristol, 1987.

[11] Levi-Setti, R., Nucl. Inst. Meth. **168**, 139 (1980).
[12] Allan, G. L., Zhu, J., and Legge, G. J. F., Fourth Aust. Conf. on Nucl. Techs. (1985) p. 49.
[13] Jamieson, D. N., Coleman, R. A., Allan, G. L., and Legge, G. J. F., ibid p. 111.
[14] Böhringer, K., Jousten, K., and Kalbitzer, S., see [9].
[15] Clampitt, R., and Jeffries, D. K., Low Energy Ion Beam Conf., Salford, 1978, no. 38.
[16] Read, P. M., Cookson, J. A., and Alton, G. D., Nucl. Inst. Meth. **B24/25**, 627 (1987).
[17] Read, P. M., Alton, G. D., and Maskrey, J. T., see [9].
[18] Bombelka, E., Richter, F.-W., Ries, H., and Wätjen, U., Nucl. Inst. Meth. **B3**, 296 (1984).
[19] Campbell, J. L., and Cookson, J. A., Nucl. Inst. Meth. **212**, 427 (1983).
[20] Clayton, E., Nucl. Inst. Meth. **B22**, 145 (1987).
[21] Rogers, P. S. Z., Duffy, C. J., and Benjamin, T. M., Nucl. Inst. Meth. **B22**, 133 (1987).
[22] L'Ecuyer, J., Davies, J. A., and Matsunami, N., Nucl. Inst. Meth. **161**, 337 (1979).
[23] Ziegler, J. F., Biersack, J. P., and Littmark, U., The Stopping Range of Ions in Solids, Vol. 1 (ed., Ziegler, J. F.), Pergamon Press, New York, 1985.
[24] Cohen, C., Davies, J. A., Drigo, A. V., and Jackman, T. E., Nucl. Inst. Meth. **218**, 147 (1983).
[25] Jackman, T. E., Davies, J. A., and Chivers, D. J., Nucl. Inst. Meth. **B19/20**, 345 (1987).
[26] Seah, M. P., David, D., Davies, J. A., Jackman, T. E., Jeynes, C., Ortega, C., Read, P. M., Sofield, C. J., and Weber, G., Nucl. Inst. Meth. (1987), to be published.

Classical Pitfalls in Contemporary Nuclear Data Analysis

K. Heydorn

Isotope Division
Risø National Laboratory
DK-4000 Roskilde, Denmark

Nuclear methods of analysis are important as an alternative to chemical methods, and often serve as reference methods, because they rely on entirely different principles, associated with the atomic nucleus rather than the electronic configuration of the elements. Although a variety of nuclear analytical methods are found, they almost invariably resort to the process of counting for the final measurement. Sophisticated electronic equipment for counting, as well as associated program systems for data processing, are now commercially available as integrated units, and most analytical chemists will have to use these systems as "black boxes."

Under proper conditions these systems are a great boon to practitioners of nuclear analytical methods, because they extract the maximum possible information from the data. However, it is important to be aware of their limitations, which may give rise to erroneous results without warning.

A recent example is the determination of Zn in a BCR candidate reference material RM 279 Sea Weed by a variety of methods, including instrumental neutron activation analysis. Only highly experienced laboratories from the European Community were invited to participate in the certification, and even then the results by INAA ranged from 48 to 57 mg/kg without any overlap between laboratories.

Such discrepancy is unacceptable for a well established analytical technique such as INAA with a reputation for being without significant systematic errors. Unfortunately this example is not unique, and an attempt is therefore made in what follows to point out possible pitfalls or sources of error that might be overlooked in contemporary nuclear analytical methods.

Calibration Errors

Direct comparison between a sample and the corresponding primary standard, subjected to exactly the same treatment, is necessary to achieve the highest accuracy in the determination of an element [1]. In radiochemical neutron activation analysis it is possible to transform the sample so that it becomes identical with the comparator with respect to physical form, shape, self-absorption and other factors affecting the calibration; in INAA this is obviously not possible.

Instead it becomes necessary to correct the calibration for differences between sample and standard, and to select counting conditions where these corrections are as small as possible. Failure to do this may lead to considerable systematic error.

The use of substances of ill-defined or unknown composition as comparator standards may lead to gross errors; only pure elements or compounds with known stoichiometry should be used. Reference materials, whether certified or not, do not serve as calibrants, but only for the purpose of checking calibrations.

Calibration based on elements other than those to be determined is in principle possible, when the nuclear parameters are taken into account by the k_0-factors [2]. This eliminates the need to have pri-

mary standards of all elements available in the laboratory, but failure to correct for differences between the actual conditions of measurement and those used in the determination of the k_0-factors may lead to systematic errors.

One such example is the use of k_0-factors for the determination of selenium using ^{75}Se as indicator isotope, where failure to make coincidence corrections in close counting geometry leads to significant errors; such correction is of course taken into account automatically when a ^{75}Se comparator standard is counted in the same counting position as the sample.

Even in an apparently simple case of chromium in zircalloy, where the ^{51}Cr has only a single photopeak, and where the matrix element is used as a comparator, systematic errors are still difficult to eliminate in the k_0-method.

Identification Errors

Neglecting to identify all photopeaks in a spectrum may lead to serious systematic errors, because without such information it is impossible to ascertain the lack of interference needed to determine an element using a single photopeak.

Such interferences are particularly dangerous when determining elements with indicator isotopes having only one strong γ-line, e.g., Cr, Zn, and Hg. While interferences of ^{75}Se on ^{203}Hg and ^{46}Sc on ^{65}Zn are well-known, interference from ^{152}Eu on ^{65}Zn is often not considered and has in the past caused significant errors in some types of sample.

The reverse situation may also apply, when an automatic resolution of double peaks seems to indicate the presence of a close-by γ-ray in a perfectly pure spectrum. The number of counts in the photopeak proper is thus reduced, resulting in reported results being too low.

Photopeak Area Evaluation Errors

A priori information on the presence or absence of interference in the processing of γ-spectra is a prerequisite for obtaining accurate results. However, even when an absolutely pure photopeak is at hand, peak areas are evaluated differently by different calculation methods particularly if the peak-to-base ratio is small.

The use of partial peak areas (PPA) to obtain optimum precision [3] also improves the accuracy when the same peak fraction is used for the comparator of the same element. In k_0-calibration only total peak areas (TPA) are applicable, and the ratio TPA/PPA varies from 1.00 to 1.26 [4] depending upon the magnitude of the peak.

The use of least-squares fitting methods appears to solve this problem, but the calculated peak area still depends on the functional representation of the peak used in the program. This assumes importance in the evaluation of the reference pulser peak used to correct for dead-time and pile-up losses during counting. This peak is not Gaussian-shaped, and the channel contents are not governed by the Poisson statistics; an attempt to evaluate this peak by least-squares fitting of a model peak therefore leads to strong bias.

Resolution of doublets leads to different results, depending on whether the program is based on consultation with a library or not [5]. The first category has a greater risk of leading to errors of the second kind, as mentioned in the preceding paragraphs, whereas the second category is more likely to fail to discover the presence of small or closely lying interfering peaks. For closely located peaks that are not resolved, some programs do not calculate the combined peak areas, but may yield completely false results.

The only way of detecting these or other systematic errors in the analysis of nuclear spectrometry data is to apply at least two independent methods and only release results when these methods concur.

References

[1] Heydorn, K., Neutron Activation Analysis, CRC Press, Boca Raton, p. 75 ff. (1984).
[2] de Corte, F. , Simonits, A., de Wispelaere, A., Hoste, J., Accuracy and applicability of the k_0-standardization method, Proc. 7th Int. Conf. Modern Trends In Activation Analysis, Vol. I, Copenhagen, p. 581 (1986).
[3] Heydorn, K., and Lada, W., Anal. Chem. 44, 2313 (1972).
[4] Ref. [1] p. 156.
[5] Christensen, L. H., and Heydorn, K., J. Radioanal. Nucl. Chem. 110 (1987).

Volume 93, Number 3, May–June 1988
Journal of Research of the National Bureau of Standards

A Uniform Concept for Error Estimation in Gamma-Ray Spectrometry

Péter Zagyvai, Lajos György Nagy, and József Solymosi

Technical University of Budapest
Department of Physical Chemistry
Hungary

Introduction

The estimated errors of peak areas are primarily important results for the complete analytical process (e.g., activation analysis or environmental radiocontamination assay). Many excellent program routines were offered in the literature for determining peak areas; however, no unambiguous solution has been given so far for assigning accurate error estimation methods.

As an introduction to our "uniform concept" some basic principles are to be stated:

- The error estimation would establish an accurate confidence limit around the calculated results: this region would include the "true value." Thus the error is a measure of accuracy rather than that of precision.
- The above condition is met only if the estimated error combines all statistical (random) and systematic (bias) errors.
- The methods for peak area determination and error estimation, respectively, would be closely interdependent.
- The actual formulation is strongly related to the given detection system.

Theory

Of course it is necessary that a uniform method be used for calculating peak areas of singlets and multiplets as well. The "apportioning" method proved satisfactory for resolving overlaps:

$$I_i = \frac{a_i \cdot s_i}{\sum_{j=1}^{K} a_j \cdot s_j} \cdot I_{ST} \qquad (1)$$

where

I_{ST} is the total count rate of the multiplet determined by summing and baseline subtraction,
K is the number of overlapping peaks
I_i is the count rate of the i'th peak,
a is the net peak height, and
s is the peak width.

Peak heights are computed from least squares fit with fixed and previously calibrated widths. The error of the i'th count rate is given by eq (2):

$$(\Delta I_i)^2 = \frac{(\Delta a_i)^2}{a_i^2} + \frac{\sum_{j=1}^{K} (\Delta a_j)^2}{\left(\sum_{j=1}^{K} a_j\right)^2} + \frac{(\Delta I_{ST})^2}{I_{ST}^2} \cdot I_i^2 \qquad (2)$$

The first two terms represent the "bias" error, the third one contains the "random" error. Peak height errors Δa are generated in the least squares fit.

The count rate I for singlets is the maximum of the summed and baseline-subtracted net counts (I_S) and the integral of the fitted peak shape function (I_F). If we consider this step as a "one component apportioning," the error of the count rate is given by eq (3):

$$(\Delta I)^2 = \frac{(\Delta a)^2}{a^2} + \frac{(\Delta a)^2}{a^2} + \frac{(\Delta I_S)^2}{I_S^2} \cdot I^2 \qquad (3)$$

The resemblance of eqs (2) and (3) is quite clear.

If the radioactivities attributed to the identified isotopes are calculated not individually but in a common least squares procedure (called interference correction), the estimated peak area errors must be applied as weight factors in the least squares solution.

Results

Numerous reference materials were analyzed to confirm the reliability of both the peak area computation and error estimation methods (such as Bowen's kale, NBS and IAEA reference materials). In testing the experimental standard deviations, it was revealed that some analytical results were biased. However, most results were still reliable because the known true values in most cases did fall into the calculated confidence intervals.

Volume 93, Number 3, May-June 1988
Journal of Research of the National Bureau of Standards

Summary

We elaborated a uniform formulation for calculating estimated count rate errors in gamma spectrometry. Experimental results confirmed that our method gave accurate confidence limits combining both random and bias errors.

Accuracy in CPAA for C, N and O and in ERDA and NRA for H

T. Nozaki

Department of Hygienic Sciences
Kitasato University
Kitasato, Sagamihara,
Kanagawa 228, Japan

1. Introduction

Trace amounts of H, C, N and O can be determined by only a few methods, often with rather poor accuracies. Charged particle activation analysis (CPAA) is highly reliable for C, N and O, and is used for calibration of other methods. Elastic recoil detection analysis (ERDA) and nuclear reaction analysis (NRA) have recently been utilized for H and D near the surface. Accuracies in these analyses are discussed on the basis of our experimental data.

2. Accuracy in CPAA

2.1 Advantage and Error in CPAA

The advantage of CPAA for C, N and O consists of inherent high sensitivity, freedom from various contaminations, and reliability in the use of comparators. The following reactions are used for activation: $^{12}C(^3He,\alpha)^{11}C$ or $^{12}C(d,n)^{13}N$; $^{14}N(p,\alpha)^{11}C$; and $^{16}O(^3He,p)^{18}F$. Uncertainty in the measurement of bombarding particle beam current frequently becomes a major cause of error in CPAA. Also, some bombardment damage of the sample often results in noticeable overestimation of C and O.

2.2 Precision for O and C

We analyzed O in a silicon wafer repeatedly nine times from 1982 to 1985 by the nondestructive measurement of the ^{18}F annihilation radiation with a Ge(Li) detector [1]. The results gave the mean value of 10.04 ppm wt with $\sigma=0.18$ ppm.

We examined chemical separation of ^{11}C in Si, using ^{11}C-containing Si prepared by proton bombardment of B-doped Si [1]. The following separation method was selected: alkali-dissolution of the pulverized sample; $KMnO_4$ oxidation of the ^{11}C under microwave heating to 700 °C; and generation of $^{11}CO_2$ and its conversion into $Li_2{}^{11}CO_3$. The measurement of ^{11}C activity before and after the separation and of carrier recovery indicated that $9.0\pm2.0\%$ of the ^{11}C apparently disappeared. Our results obtained by this separation has thus been corrected for this 9%.

For the separation of ^{13}N, dry fusion into $^{13}N_2$ and wet distillation as $^{13}NH_3$ are used [1]. Carbon in 27 plates of GaAs made from a single rod were analyzed by the dry method in different machine times of two cyclotrons. The mean results were 24.6 ppb wt with $\sigma=2.6$ ppb. For the last five plates taken from adjacent parts of the rod, the results were 23.25 ± 0.84 ppb. We separate ^{18}F by precipitation as $KB^{18}F_4$ [2]. This method has shown satisfactory precision.

2.3 Calibration of IR Spectrophotometry

Our calibration curve for IR spectrophotometry of C in Si is shown in figure 1 [1]. About 70 carefully prepared samples were submitted to round-robin IR measurement in 24 organizations. About 1/3 of them were then analyzed by CPAA; some of them were also analyzed by SIMS. The differences between the results of CPAA and SIMS are probably caused by the presence of background in SIMS. Satisfactory calibration curves were obtained also for O and N in Si [3,4]. Efforts are now being made to obtain a reliable calibration curve for C in GaAs.

3. Accuracy for ERDA and NRA for H

Figure 2 shows ERDA spectra of a H- and D-containing amorphous silicon film on a Si wafer [5]. The detection efficiency is seen to depend highly on the detection angle. No suitable substances are found as comparators for H and D, and their quantities are usually obtained in comparison with an internal standard element by the use of the theoretical relationships and experimental parameters. The H content of amorphous silicon films obtained by ERDA and vacuum fusions are given in

table 1 [5]. At present, the accuracy for H by ERDA is notably lower than for C, N and O by CPAA. The depth profiling of H and D is possible by ERDA, as is seen in figure 2; but further studies are necessary.

In the depth profiling of H by the $^{1}H+^{15}N\rightarrow^{12}C+\gamma(4.44\ MeV)$ reaction, it is easy to get the shape of the profile reproducibly but difficult to obtain an absolute value for H within a 20% uncertainty. We now use D as an activatable tracer, determining it by the reactions $D+^{3}He\rightarrow\alpha+p(14\ MeV)$ and $D+^{15}N\rightarrow^{16}O+n(or\ p+\beta^{-})+\gamma(6.13, 7.11\ MeV)$ [6]. Experimental data are required concerning the accuracy of these methods.

Table 1. Hydrogen content of amorphous silicon films measured by three methods (10^{17} atoms/cm^2): ERDA, vacuum extraction with the measurement of volume (VOL) and heat conductivity (HC)

Film thickness (nm)	ERDA	VOL[a]	HC[b]	VOL/ ERDA	HC/ ERDA
1065	7.36	7.92	7.38	1.08	1.00
830	5.77	6.54	5.90	1.17	1.06
672	4.25	5.60	5.11	1.32	1.20
650	3.78	5.26	4.40	1.39	1.16
526	4.53	4.40		0.97	
510	3.96	3.63		0.92	
310	2.40	3.07	2.67	1.28	1.11
270	1.85	2.19	1.89	1.18	1.02
Average				1.16 ±0.17	1.09 ±0.08

[a] By Prof. Ogawara, Science Univ. of Tokyo.
[b] By Dr. Nomura, Mitsubishi Metals Co.

4. Conclusion

At present, accuracy can be determined for the CPAA of C, N and O. For the ERDA and NRA determination of H and D, experimental data are still too scarce for consideration of accuracy.

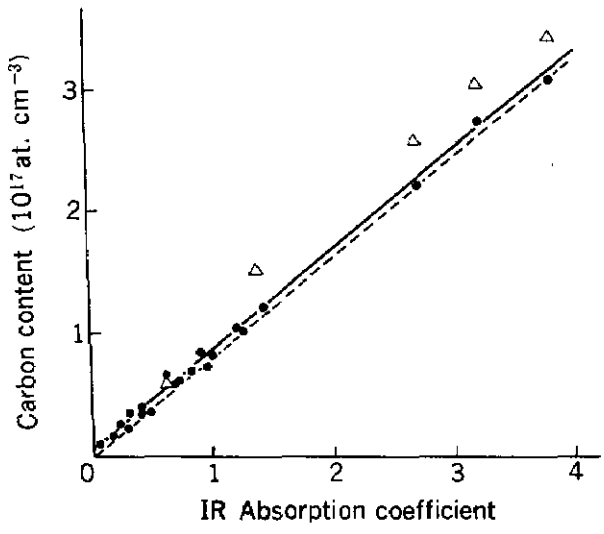

Figure 1. Calibration curve for IR spectrophotometry of C in Si (605 cm^{-1}, at room temperature). Solid line, before correction for C in IR reference Si; (C concentration, 4.3×10^{15} at. cm^{-3}); broken line, after the correction; Δ, results of SIMS.

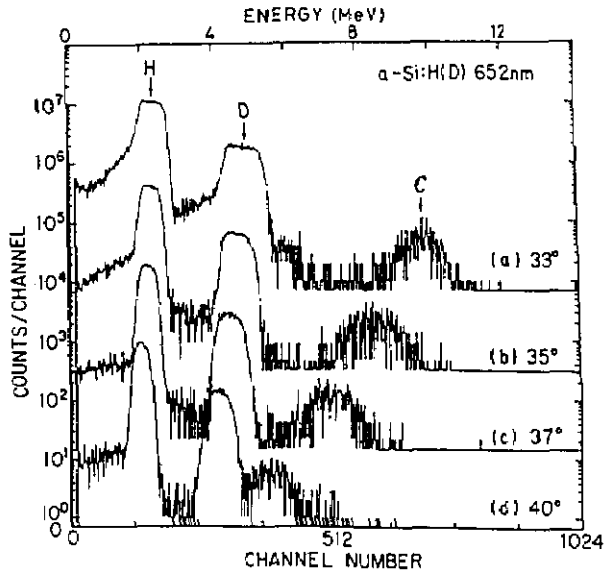

Figure 2. ERDA spectra for various detector angles. Sample: H- and D-containing amorphous silicon film 652 nm thick; incident particle: 42.3 MeV Ar; target angle: 30 °C; absorber: 10 μm Al foil.

References

[1] Fukushima, H., Kimura, T., Hamaguchi, H., Nozaki, T., Itoh, Y., and Ohkubo, Y., Proc. 7th Modern Trends in Activ. Anal., Copenhagen (June 1986) p. 335.

[2] Nozaki, T., J. Radioanal. Chem. **72**, 527 (1982).
[3] Itoh, Y., Nozaki, T., Masui, T., and Abe, T., Appl. Phys. Lett. **47**, 488 (1985).
[4] Iizuka, T., Takasu, S., Tajima, M., Arai, T., Nozaki, T., Inoue, N., and Watanabe, M., J. Electrochem. Soc. **132**, 1707 (1985).
[5] Nagai, H., Hayashi, S., Aratani, M., Nozaki, T., Yanokura, M., and Kohno, I., Nucl. Instr. Methods **B28**, 59 (1987).
[6] Nozaki, T., Itoh, Y., Hayashi, S., and Qui, Q., Proc. 7th Modern Trends in Activ. Anal., Copenhagen (June 1986) p. 47.

A Fast-Neutron Diagnostic Probe

C. M. Gordon, C. W. Peters, and T. K. Olson

Consolidated Controls Corporation
Lockport Place
Lorton, VA 22079

A novel, nuclear method for instrumental analysis of elements has been developed. The system, called a "neutron diagnostic probe (NDP)," has several unusual capabilities that are especially applicable to nondestructive, 3-dimensional analysis in solid materials or inaccessible spaces. The prototype instruments that have been assembled and tested demonstrate that the NDP system can penetrate several inches of solids, locate inaccessible inhomogeneities by time-of-flight ranging, and perform elemental analysis of the located volume of interest. This neutron diagnostic probe utilizes a combination of associated-particle, neutron time-of-flight spectroscopy; inelastic gamma-ray spectroscopy; and a recently developed sealed-tube neutron generator. The NDP interrogates a material or inaccessible space with an electronically collimated and timed beam of fast neutrons which have great penetrating power. Highly penetrating, inelastic gamma rays produced in the interrogated volume by the neutrons are detected and analyzed. The spatial production of these gamma rays is analyzed to "image" the distribution of materials within the volume of interest. The energies of the gamma rays from each substance within the space examined are analyzed to determine the concentrations of the elements in each volume element. An inelastic gamma-ray energy spectrum characteristic of every element except hydrogen can be obtained.

The name of this associated-particle technique [1] is derived from the alpha particle "associated" with a 14-MeV neutron produced by the $T(d,n)He^4$ reaction in the neutron generator. Because the associated particle is produced simultaneously with the fast neutron and is emitted in the opposite direction, its detection specifies the subsequent trajectory of the individual neutron. This capability makes it possible to define a timed and directed "beam" of 14-MeV neutrons traveling away from a continuous $T(d,n)He^4$ generator at about 5 cm per nanosecond. By using time-of-flight, range gating, only gamma rays generated by neutron reactions within a known sensitive volume at a predetermined distance from the generator are recorded.

The key element in the instrumentation is the sealed-tube neutron generator (STNG) shown schematically in figure 1. The basic design of the neutron generator is similar to that described by Reifenschweiler [2,3], using the $T(d,n)He^4$ reaction, a getter-controllable mixture of deuterium and tritium gases and a self-loading target. The innovations in the STNG used for this work are: 1) the inclusion of an internal alpha detector to supply time and direction information by the associated-particle technique and 2) provision for focusing the ion beam on the target to ensure a "point source" of 14-MeV neutrons.

In operation, the radiation detectors and nuclear electronics are arranged as shown in the block diagram of figure 2. Light signals from the ZnS alpha scintillator are amplified by a photomultiplier (PM) and preamplifier, shaped by a constant-fraction discriminator (CFD) and routed to the "start" input of a time-to-amplitude converter (TAC). The alpha signals are also counted and stored in the multichannel analyzer (MCA) data acquisition system for subsequent normalization of the spectral information. The gamma rays generated by inelastic neutron interactions in the interrogated sample are converted to energy spectra with a 15 cm diameter by 36 cm long NaI(Tl) scintillation spectrometer. These signals are shaped (CFD) and routed to the "stop" input of the TAC to provide a range-proportional, time-of-flight spectrum at the TAC output. The time-of-flight spectrum is proportional to range because the 14-MeV neutrons travel from the STNG to the interrogated sample at a constant 5 cm/ns and the gamma rays produced in the sample travel at 30 cm/ns to the NaI(Tl) detector. Signals from the portion of the time-of-flight spectrum that corresponds to the range position of the sample are selected to open a gate circuit (linear gate)

and pass only gamma-ray signals that occur within the appropriate delayed-coincidence, time gate.

The gamma-ray pulses are also linearly amplified and because of the time gate (range gate) only those analog signals of gamma rays originating in the selected sample volume are digitally converted (ADC) and recorded in the data acquisition system. This range-gating technique (time gate of about 3 ns) eliminates nearly all background. In general the background count rate (N_c) is expressed as

$$N_c = \tau N_\alpha N_\gamma,$$

where τ is the duration of the time gate while N_α and N_γ are the random count rates in the alpha detector and gamma detector respectively. In the system described here $N_\alpha \approx 3\times10^3$ s^{-1} and $\tau \approx 3\times10^{-9}$ s, therefore a random rate $N_\gamma \approx 1\times10^4$ s^{-1} in the gamma detector only generates $N_c \approx 10^{-1}$ s^{-1} background counts. As with all nuclear methods, the ultimate precision of the measurements will depend on signal-to-noise ratio and counting statistics, i.e., a standard deviation of approximately $\pm\sqrt{N}$ where N is the total count. In circumstances requiring background subtractions or other data manipulations the usual rules for propagation of precision indices apply.

In an application that might be called "remote trace analysis" the timed beam of 14-MeV neutrons was directed through about 1 inch of steel to monitor Na_2SO_4 corrosive agent on turbine blades. Measurements at less than 1/10,000 Na were made. Thus far the neutron diagnostic probe has been used mostly in areas of bulk analysis of oil shale, coal and sandstone and detection of concealed explosives or contraband, however it is expected to find additional applications for special-purpose instrumental trace analysis where requirements of nondestructive imaging and inaccessibility are paramount.

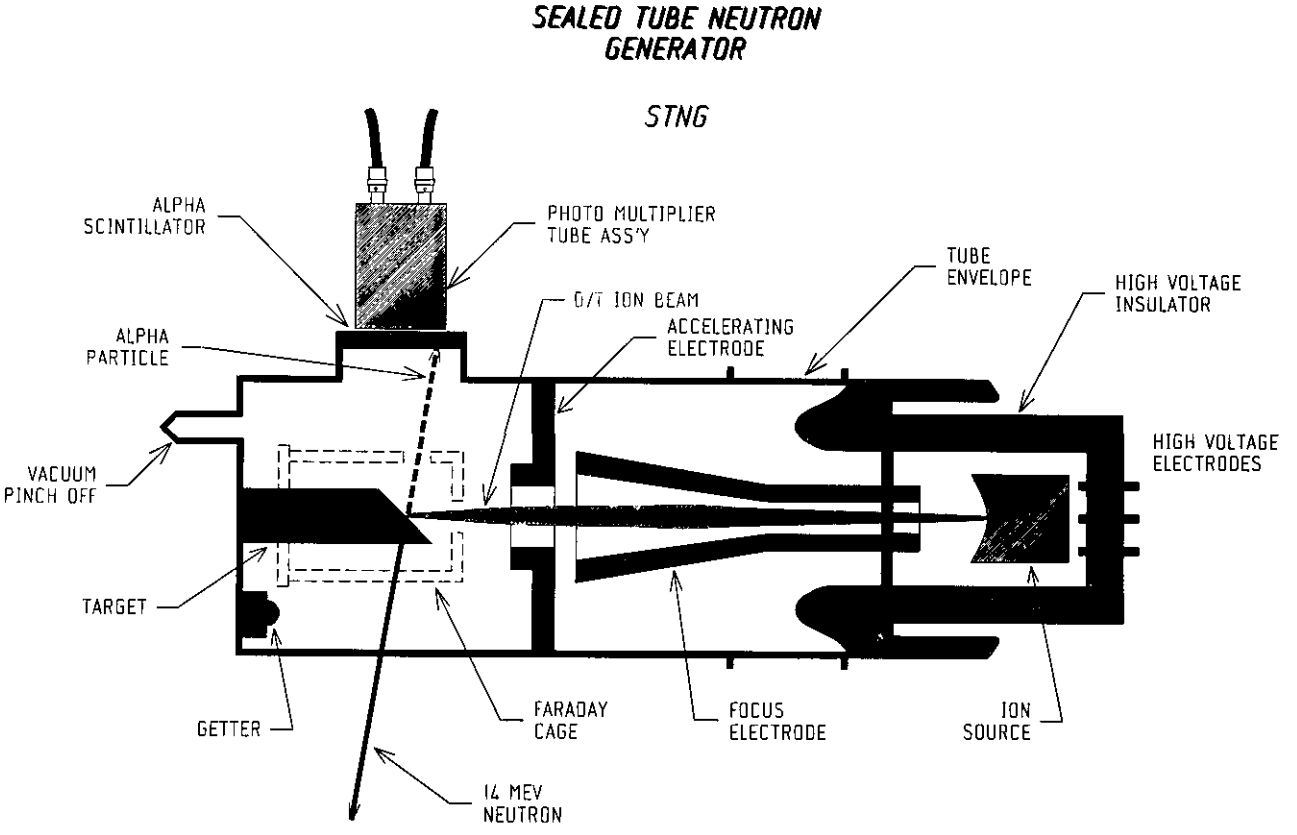

Figure 1. A schematic diagram of the neutron generator.

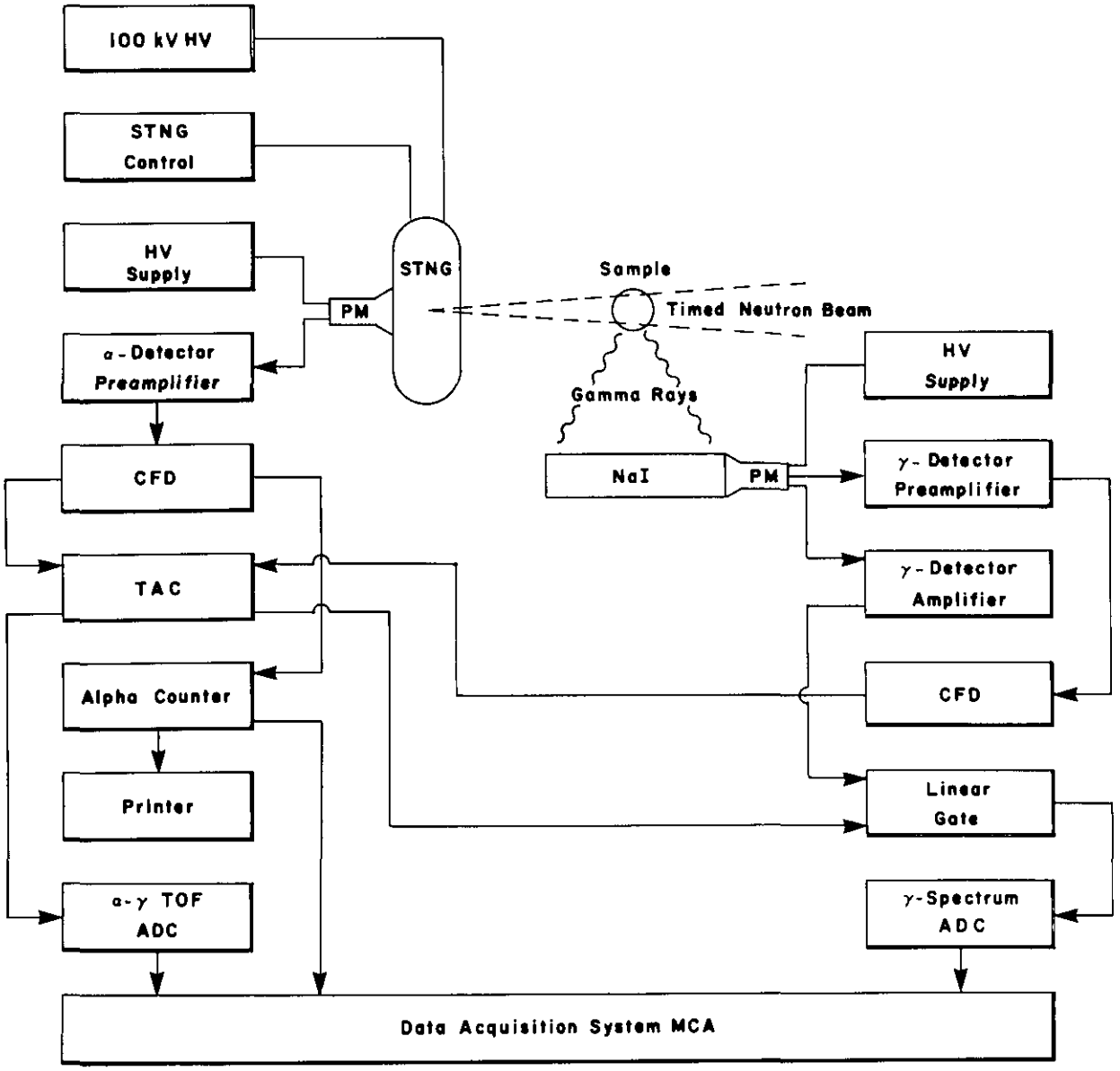

Figure 2. A block diagram of the experimental arrangement.

References

[1] Neiler, J. H., and Good, W. M., *Fast Neutron Physics*, J. B. Marion and J. L. Fowler, eds., Interscience Publishers Inc., New York (1960) p. 607.
[2] Reifenschweiler, O., Natl. Bur. Stand. Spec. Publ. 312, Vol. II, 905 (1969).
[3] Reifenschweiler, O., Philips Res. Rpts. **16**, 401 (1961).

Volume 93, Number 3, May–June 1988
Journal of Research of the National Bureau of Standards

Electrochemistry

Trace Analyses of Impurities in Povidone by Square Wave Voltammetry

Robert M. Ianniello

GAF Chemicals Corporation
Analytical Research & Development
1361 Alps Road
Wayne, NJ 07470

Povidone (polyvinylpyrrolidone) is a water soluble polymer used in a variety of pharmaceutical, beverage, cosmetic, and agricultural applications. The free radical-induced polymerization of vinylpyrrolidone using aqueous hydrogen peroxide/ammonia as an initiator allows for rapid, easily controlled reactions. However, the reactivity of the various components can give rise to trace levels of undesirable by-products. The analytical methods available for these impurities utilize dissimilar procedures with time consuming sample preparation steps; and the need for high product quality requires methods with low detection limits for which many of the established procedures are not suitable.

A general approach for the analysis of impurities in our laboratory has involved the use of square wave voltammetry (SWV) for the quantitation of electroactive species. This technique couples the ability to determine species at very low levels (sub ppm) with analysis speed, making it ideal for aiding in process optimization. The version of square wave voltammetry used in our laboratory was developed by Osteryoung [1] and first commercialized by Bioanalytical Systems. In the technique, a pulse train of square waves is superimposed on a staircase wave form. A single square wave cycle (forward and reverse pulse) is generated per staircase step. Current is sampled near the end of each forward and reverse pulse. The difference in currents generated from the forward/reverse signals yields the analytical current response. The very nature of the experiment results in the following advantages:

a) Scan rate, which is dependent primarily on square wave frequency, is fast. A typical experiment covering a potential range of 1 V may take only 5 seconds by SWV compared to 3 minutes by other pulse voltammetric techniques.
b) For reversible systems, enhanced peak currents are obtained as the net current is the difference between a positive forward current and a reverse current which is *opposite* in sign.
c) As a pulse technique, discrimination against charging current improves the detection limit.
d) Multiple scanning is used with signal averaging to improve the signal-to-noise ratio.
e) Diagnostic information can be obtained (as in cyclic voltammetry) by observing the individual forward and reverse currents.

Two impurities which have been analyzed successfully by the technique are acetaldehyde [2] and ammonium ion [3]. In the first case, acetaldehyde is irreversibly reduced at the mercury electrode in basic media. This allows for its direct detection via SWV. In the second case, ammonium ion is rendered electroactive by derivatization with formaldehyde to form hexamethylene tetramine. The derivative is then reduced in acid media at the mercury electrode. In both cases, superior sensitivity and detection limits are obtained, compared to conventional techniques.

References

[1] Osteryoung, J., and Osteryoung, R. A., Anal. Chem. **57**, 101A (1985), and references therein.
[2] Ianniello, R. M., Colonnese, R., and Machnicki, N., J. Assoc. Off. Anal. Chem. **70**, 566 (1987).
[3] Ianniello, R. M., Ibid., 1987, in press.

Volume 93, Number 3, May–June 1988
Journal of Research of the National Bureau of Standards

Accuracy in Trace Analysis

Voltammetric Sensors Using Chemically Active Electrode Materials

Calvin O. Huber

Department of Chemistry
University of Wisconsin-Milwaukee
Milwaukee, WI 54301

Voltammetric analytical techniques have ordinarily used relatively inert conducting materials in order to maximize the range of available applied potential and to enhance selectivity of the electrode reactions by control of applied potentials. A number of investigators have recently been examining modification of electrode surfaces in order to improve selectivity and sensitivity which are essential components to enhanced accuracy at trace levels. These modifications include bonded chemical functionalities, adsorption, polymers, use of electrode paste vehicle solubility, enzyme attachment and others. In the work reported here the use of several chemically active electrode materials is reported.

In flow-through voltammetric devices, such as for HPLC and FIA detectors, the chemical history of the electrode surface is relatively easily managed so that sometimes chemically active electrode materials can offer advantages. Further, these on-stream voltammetric configurations offer the advantages of controlled convection, electrode surface history, and ease of detector design. In this laboratory some recent studies exemplifying such an approach have involved nickel/nickel oxide [1–3], copper/copper oxide and silver iodide [4] as working electrode materials.

Nickel electrodes have allowed the smooth oxidation of hydroxyl and amine as well as more easily oxidized organic functional groups. The typical electrode conditions include 0.1 *M* sodium hydroxide as electrolyte. Often 0.1 m*M* nickel sulfate is added to the electrolyte to enhance long-term activity to slower reacting analytes. Typically a flow rate of 1 mL/min and a sample injection volume of 25 μL is used. The anodic current is controlled by redox reaction rate of the electrodes higher oxide lattice sites with the analyte molecule. This allows for low concentration level determinations of sugars, alcohols, glycols, amino acids, proteins, nucleic acids and nucleic acid constituents. Although the carrier stream is alkaline, acidic samples can be readily accommodated using the flow injection technique. The low-pH sample plug first produces a cathodic component to the signal as part of the electrode oxide layer is reduced, but as the pH increases with the passing of the low-pH segment a fresh, high-activity oxide layer is produced which oxidizes the end of the sample plug. Samples with pH as low as two can be accommodated. Layers of nickel oxide adsorbed on metals other than nickel yielded similar reactions to those using a nickel substrate.

Several proteins have been determined at concentrations as low as 1 mg/L [3]. Sensitivity is enhanced by increased temperature. Side- and end-hydroxyl and amino groups as well as sulfhydryl groups are oxidized, thus the technique is general for proteins, not limited to sulfide or bisulfide as for most electroanalytical methods, or to aromaticity as in UV-absorbance methods. Denaturation of human serum albumin in 0.1 *M* NaOH was followed by the technique. The results obtained correlate with a model based on random coil chain length control of denaturation rates interrupted by disulfide bond breakage delays.

A series of alcohols and glycols was studied. The anodic reaction rates, i.e., anodic amperometric sensitivities, could be correlated to the electron withdrawing nature of the moiety bonded to the primary reactant methylene-ol ($-CH_2OH$) of the analyte. Rate constants vary by more than an order of magnitude from isopropanol to 1,2-propanediol. The linear range was more than two orders of magnitude, extending to lower detection limits of less than one micromolar.

The nickel electrode work has been extended to HPLC detection for amino acids by post-column mixing of 0.2 *M* sodium hydroxide at a T connection with a 0.1 mm × 1.3 m mixing tube [2]. As predicted by hydrodynamic theory, no significant band broadening was observed.

Consideration of Pourbaix diagrams indicates that cathodic pretreatment of a nickel electrode can generate a temporary high pH near the electrode surface. On stepping to anodic potentials a temporary anodic current for analytes should then be observed. Applying this approach resulted in the determination of ethanol in a pH 7 carrier solution with a linear response, a sensitivity of 3.3 μA/m*M* and a lower detection limit of 0.8 m*M*. This relatively high limit was primarily due to high background current.

Analytes subject to anodic determination at

nickel can also be determined using a copper anode. Conditions are similar to those for nickel except that the applied potentials must be 200 mV more positive than for nickel. The anodic reaction rate constants with copper are typically somewhat greater than with nickel, however the applied potential results in increased background noise so that copper offers no signal-to-noise advantage over nickel.

When the background electrolyte contains nickel as suspended nickel hydroxide as described above, copper, nickel, cobalt, silver, platinum, and gold electrodes yield similar analytical currents. These results indicate that suspended nickel hydroxide adsorbs to the metal electrode surfaces and essentially converts them to nickel oxide electrodes.

Silver iodide in its room-temperature crystal form is sufficiently conducting so that it can carry the currents necessary for analytical amperometry. The electrode material is contacted using silver epoxy. The cathodic electrode mechanism involved generation of iodide at the silver:silver iodide interface yielding a current proportional to the rate of oxidation of iodide ions at the silver iodide:solution interface. Hypochlorous acid at sub-parts-per-million level thus yields cathodic currents for pH 6 solutions whereas pH 3 must be used for cathodic amperometry of monochloramine [4]. Accordingly a direct, linear response analytical technique for concentrations from more than 5 mg chlorine per liter down to about 10 μg chlorine per liter was developed for either monochloramine or the sum of hypochlorous acid plus monochloramine. The concentrations determined were sufficiently low to allow determination of the rate constant for monochloramine formation under realistic water treatment concentration, pH, and ionic strength conditions. The rate constant obtained was 3.2×10^6 L/mol/s, in agreement with earlier reported values extrapolated from higher concentrations and less moderate pH solutions.

References

[1] Hui, B. S., and Huber, C. O., Anal. Chim. Acta **134**, 211 (1982).
[2] Kafil, J. B., and Huber, C. O., Anal. Chim. Acta **175**, 275 (1985).
[3] Yuan, C. J., and Huber, C. O., Anal. Chem. **57**, 180 (1985).
[4] Morrison, T. N., and Huber, C. O., Amperometric Measurement of Chlorine at a Pulsed Silver Iodide Electrode, The Chemical Quality of Water and the Hydrologic Cycle, p. 337, D. McKnight, ed., Lewis Publishers, Ann Arbor, MI (1987).

Adsorptive Stripping Voltammetry—A New Electroanalytical Avenue for Trace Analysis

Joseph Wang

Department of Chemistry
New Mexico State University
Las Cruces, NM 88003

Stripping voltammetry is a powerful electroanalytical technique for trace metal measurements [1]. However, conventional stripping measurements are limited to about 25 metals that electrolytically deposit and/or form an amalgam with mercury. Hence, alternative preconcentration schemes, based on nonfaradaic processes, are desired for extending the scope of stripping voltammetry toward additional analytes.

An extremely useful, sensitive and versatile preconcentration scheme can be achieved via controlled interfacial accumulation of the analyte onto the surface of the working electrode [2]. The voltammetric response of the surface-confined species is directly related to its surface concentration, with the adsorption isotherm providing the relationship between the surface and bulk concentrations of the adsorbate. The most frequently used isotherm is that of Langmuir.

The surface-active characteristics of numerous organic analytes (that commonly complicate their conventional voltammetric measurements) can be exploited for obtaining effective adsorptive accumulation. Trace levels of reducible and oxidizable compounds, such as cardiac glycosides, tetracyclines, phenothiazines, riboflavin, streptomycin, bilirubin, diazepam, tricyclic antidepressants, or mitomycin C, can thus be determined at mercury and carbon electrodes. (Using carbon paste electrodes, both adsorption and extraction occur simultaneously.) Figure 1 illustrates the inherent sensitivity of differential pulse adsorptive stripping voltammetry, as applied to measurement of 5×10^{-9} mol/L digoxin. In addition to low molecular weight compounds, large biological macromolecules, e.g., cytochrome C, chlorophyll, fer-

ritin, or DNA can also be measured. In such cases, the adsorptive approach results not only in enhanced sensitivity, but also a more favorable interaction between the electrode and the redox center of the molecule (due to conformational changes), and hence with enhanced reversibility.

In addition to organic analytes, the formation and interfacial accumulation of appropriate surface-active metal complexes onto the hanging mercury drop electrode permit trace measurement of additional metals. Figure 2 illustrates the steps involved in such measurements of metal ions. In particular, the unique voltammetric and interfacial behaviors of metal chelates of dihydroxyazo dyes allow convenient trace measurement of titanium, thorium, aluminum, iron, uranium, manganese, yttrium, or gallium. Other chelators, e.g., dimethylglyoxime, catechol, oxine, tropolone, or cresolphthalexon, are useful for trace measurements of nickel, vanadium, molybdenum, tin or lanthanum, respectively. Overall, this activity resulted in procedures for measuring more than 25 trace metals; coupled with conventional stripping schemes, about 45 elements are now measurable by stripping analysis. Simultaneous measurement of 2–3 metals is possible, based on an appropriate separation of the metal-chelate peak potentials. Because of its fundamentally different detection principles, the metal chelate approach provides different speciation information compared to conventional stripping measurements, with the fraction of metal measured including the free ion and metals displaced from natural complexes during the formation of the strong adsorbable chelate. When the chelating ligand is present in large concentration excess compared to natural ligands, and a very strong chelate is formed, the *total* metal content is determined. The different nature of the response results in improved performance for metals, e.g., tin or gallium, measurable also by conventional stripping schemes, because interferences (e.g., overlapping peaks, intermetallic compounds) are minimized. Short preconcentration periods result in detection limits as low as $10^{-10}-10^{-11}$ mol/L. Lower levels, e.g., 10^{-12} mol/L platinum, can be achieved upon coupling with catalytic reactions (i.e., controlled adsorptive accumulation of the catalyst). Such dual amplification is expected to play an increasing role for ultratrace measurements of species exhibiting adsorption-dependent hydrogen catalytic processes. At low analyte levels ($10^{-7}-10^{-10}$ mol/L), for which the method is usually applied, a linear adsorption isotherm is obeyed and the response is linear. New strategies, such as the use of permselective electrode coatings or the medium-exchange approach, result in substantial improvements in the selectivity and reproducibility. For example, the medium-exchange approach allows convenient measurement of dopamine in the presence of large excess of ascorbic acid. Interferences due to coadsorbing surfactants can be minimized by covering the electrode with a cellulose acetate film.

Adsorptive stripping voltammetry is now a highly sensitive and rapid technique, applicable to analyses in various fields. Its utilization is expanding rapidly and will continue to do so in the near future.

Acknowledgments

The support of the National Institutes of Health (Grant No. GM 30913-04) and the NM Water Resources Research Institute is acknowledged.

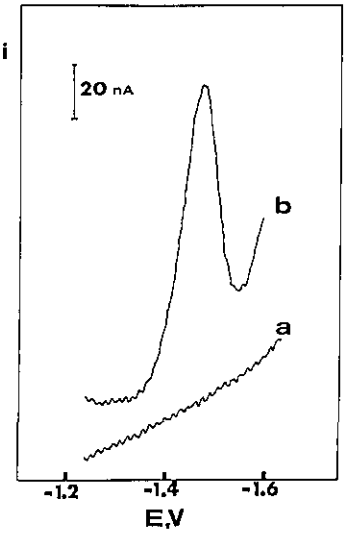

Figure 1. Voltammograms for 5 nmol/L digoxin using (a) no and (b) 15-minute accumulation.

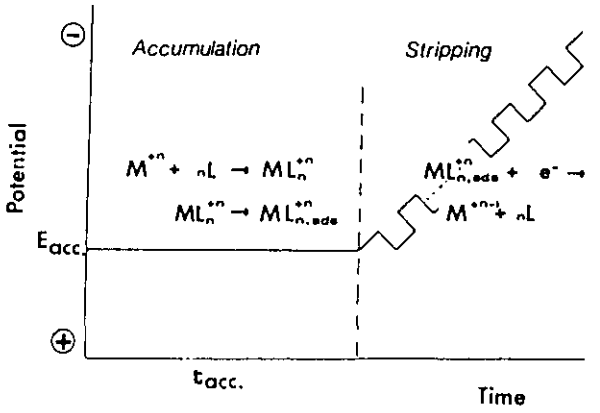

Figure 2. Steps in adsorptive stripping measurements of a metal ion based upon the formation, accumulation and reduction of its surface active complex.

References

[1] Wang, J., Stripping Analysis: Principles, Instrumentation and Applications, VCH Publishers, Weinheim (1985).
[2] Wang, J., Am. Lab. **17**, 41 (1985).

Electrochemical Enzyme Immunoassay

H. Brian Halsall, William R. Heineman, Sarah H. Jenkins, Kenneth R. Wehmeyer, Matthew J. Doyle, and D. Scott Wright

Analytical and Biochemistry Divisions, and
Biomedical Chemistry Research Center
Department of Chemistry
University of Cincinnati
Cincinnati, OH 45221-0172

"Immunoassay" defines the body of techniques which use the antibody (Ab) macromolecule, usually of the IgG class, for the detection and quantitation of an enormous range of simple and complex antigen (Ag) molecules. The success of the methods relies on both the specificity and formation constant of the Ab used, and the ability to detect the interaction between Ab and Ag. Sensitive assays in complex matrices require some kind of label to be present to provide this ability.

The development of immunoassay methods has in large part been driven by the available technology. Thus, although one of the first immunoassays using a label was electrochemically based [1], the state of that art in 1951 was relatively primitive, and could not meet the analytical demands of the Ag. Some years later, Yalow and Berson [2] developed immunoassays based on the radioisotopic label (RIA). For the first time, Ab selectivity was married to very low detection limit technology, and the result was an enormous growth rate in the use of RIA in both the clinical and research laboratory.

RIA has the significant advantage that the label used is not a normal constituent of physiological samples, and interferences of this type are therefore absent. RIA, however, has the disadvantages that accompany radioisotope handling, together with an inability to distinguish label which is bound from that which is not. There has therefore been an enormous effort to find suitable replacements for the radiolabel.

Where the low detection limit of RIA was not required for a successful assay, labels detectable by spectroscopic methods have become important. Where very low detection limits are demanded, then the concept of amplification of, or by, the label has been developed. The most successful of these have been enzyme linked using an immunosorbent phase for Ag extraction (ELISA), although assays based on the lysis of label-containing liposomes are also exhibiting very low detection limits.

In our hands, electrochemically based immunoassays at very low detection limits have also used enzyme amplification and ELISA, with either NAD/NADH and glucose-6-phosphate dehydrogenase [3], or phenyl phosphate/phenol and alkaline phosphatase [4]. The greatest sensitivity thus far has been obtained with ELISA coupled with liquid chromatography with electrochemical detection (LCED) [5].

The power of this approach can be readily illustrated by examining the evolution of its use in an assay for IgG, itself an important analyte. This evolution covers three principal stages of development and a reduction in detection limit of five orders of magnitude.

The basic methodology is shown in figure 1. The assay is essentially a "sandwich" ELISA, using an alkaline phosphatase labelled second Ab for amplification. Oxidative flow amperometry at +875 mV

on a carbon paste electrode is used for quantitation of the phenol produced. The phenyl phosphate substrate is electroinactive at this potential, and does not interfere. All analyses were conducted using a 20 μL injection loop for LCEC.

The first stage of development used a polystyrene cuvette of 750 μL as the solid phase to which the primary Ab was passively adsorbed, and Tween 20 as a blocking agent to minimize nonspecific adsorption of reagents to the plastic surface. Under optimal conditions, a detection limit of 500 attomoles of analyte IgG (or 300 million molecules) was obtained [6]. However, not counting the primary Ab adsorption step, this was a lengthy assay, requiring some 7 hours for completion.

The second stage of development was directed at reducing the level of the nonspecific background. This was achieved by incorporating bovine serum albumin in all solutions except that used for the adsorption of the primary Ab to the solid phase. This provides for more efficient blocking of the exposed surface, and prevents the adsorption of the second Ab-conjugate, which is the primary source of nonspecific signal [5]. Figure 2 shows the calibration curve for this stage, with a detection limit of 50 attomoles, or 30 million molecules [5] for exactly the same incubation conditions as for stage one. The length of the assay was not affected, therefore, remaining at 7 hours.

The third stage incorporated two major changes involving the nature of the solid surface and the attachment of the primary Ab to it. Since the concentration of phenol produced by unit activity of enzyme depends upon the volume of the container, whereas the amount produced does not, then increasing the surface area to volume ratio of the container should dramatically reduce the time needed for detectable quantities of phenol to be produced. This will be enhanced by a change in container geometry that reduces the diffusion pathlength for substrate. Reducing the diffusion pathlength will similarly shorten the time required for both the Ag and conjugate incubation steps.

Both of these characteristics were provided by using glass microcapillary hematocrit tubes of 70 μL volume. The primary Ab solid phase was prepared by covalently attaching the Ab to a polymer deposited on the glass surface. As in stage two, both bovine serum albumin and Tween 20 were used as blocking agents in all solutions except for the primary Ab attachment. A simple modification of the injection port permitted the direct displacement of the contents of the capillary into the injection loop. Figure 3 shows the calibration curve for this assay, for which the detection limit was 4×10^{-3} attomoles, or 2800±150 molecules. The total time of the assay, again after preparation of the primary Ab surface, was 28 minutes.

The design of the electrochemical flow cell in use permits a further reduction in its volume. By then reducing the volume of sample in the capillary, the limit of detectable amount should be readily lowered by an order of magnitude with no increase in assay time.

Acknowledgments

The financial support provided by the National Science Foundation, BioAnalytical Systems, and the University of Cincinnati University Research Council is gratefully appreciated.

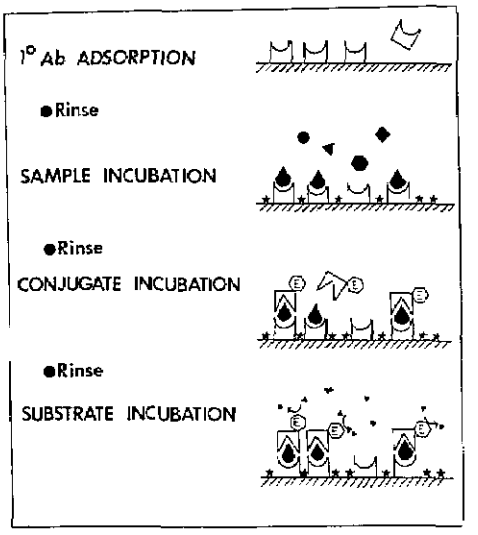

Figure 1. Heterogeneous assay protocol. Small stars represent *blocking reagents (Tween 20 and bovine serum albumin) to minimize* nonspecific adsorption of conjugate.

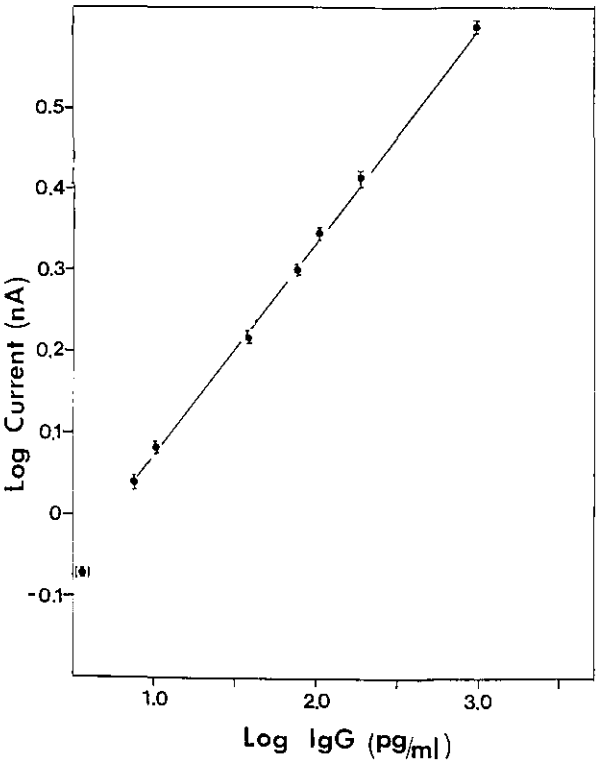

Figure 2. Calibration curve for Stage 2 assay in polystyrene cuvettes of 750 μL.

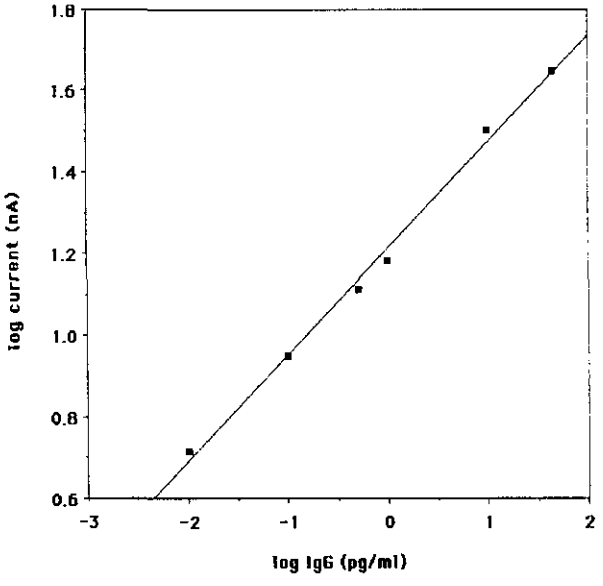

Figure 3. Calibration curve for Stage 3 assay in glass capillaries of 70 μL.

References

[1] Breyer, B., and Radcliff, F. J., J. Chromat. **117**, 35 (1951).
[2] Yalow, R. S., and Berson, S. A., Nature **184**, 1648 (1959).
[3] Eggers, H. M., Halsall, H. B., and Heineman, W. R., Clin. Chem. **28**, 1848 (1982).
[4] Wehmeyer, K. R., Doyle, M. J., Halsall, H. B., and Heineman, W. R., in Electrochemical Sensors in Immunological Analysis (ed., T. T. Ngo), Plenum, New York, 1987.
[5] Jenkins, S. H., Heineman, W. R., and Halsall, H. B., Anal. Biochem. (1987), in press.
[6] Wehmeyer, K. R., Halsall, H. B., and Heineman, W. R., Clin. Chem. **31**, 1546 (1985).

Stripping Voltammetric Assay of Trace Technetium with a TOPO Coated Glassy Carbon Electrode

J. M. Torres Llosa, H. Ruf, K. Schorb, and H. J. Ache

Kernforschungszentrum Karlsruhe
Institut für Radiochemie
D-7500 Karlsruhe, Federal Republic of Germany

It has been the goal pursued in the investigations described here to determine technetium trace concentrations using the sensitive method of stripping voltammetry with a chemically modified working electrode which responds in a highly selective manner. The attention was focused on the most stable +7 oxidation state of the radioelement, which is present in the majority of cases while searching also for the possibility of discriminating Tc-IV which sometimes occurs simultaneously in the samples to be analyzed.

One kind of electrode modification which was considered promising in this respect consisted of coating a glassy carbon electrode (GCE) with tri-n-octylphosphinoxide (TOPO) which already proved its worth in stripping voltammetric uranium assays of sea water samples without requiring an additional separation step [1,2]. For it is known that, similar to uranium, technetium also reacts with TOPO to give a stable complex [3] which can be extracted from hydrochloric acid solutions and the composition of which is reported to be $HTcO_4 \cdot 2$ (TOPO) [4].

According to this consideration it should be possible to preconcentrate technetium from chloride-containing acid solutions on the surface of a TOPO coated GCE (TOPO-GCE) via complexation. This approach in principle should be capable of exploitation for stripping voltammetric technetium assays as in the case of uranium.

Since the coefficient of Tc-VII distribution in the TOPO-HCl system attains its maximum of slightly over 100 at about 3 *M* HCl [3], which is equivalent to an extraction extent of at least 99%, it was obvious to attempt enrichment from about 3 *M* HCl acid solutions.

It became apparent that the expected accumulation of technetium from strongly HCl-acid solutions according to the outlined principle actually takes place [5]. (The technetium isotope used in this work was the long-lived Tc-99.) A glassy carbon electrode modified with TOPO results in a well defined reduction peak after contact of only some minutes duration with solutions of low pertechnetate concentrations down to the 10^{-8} *M* level. The potential of the signal which occurs as a peak during measurement in the DP mode is approximately −350 mV (vs Ag/AgCl). The signal is generated after enrichment if a voltage scan starting at 0 V is directed towards negative potentials. Stripping voltammograms recorded in this way for Tc-VII solutions of different concentrations are shown in figure 1. It is obvious from the correlation coefficient $R = 0.9987$ calculated from the measured signal heights and the amounts of technetium present that a linear relationship exists which is well suited for calibration purposes.

As a confirmation of the enrichment effect the analytical technetium signal rises first at a linear rate with longer enrichment time (see fig. 2). But if the reaction time is extended more this increase in signal amplitude becomes visibly smaller which is evidence of the limitation of the active electrode surface capacity.

It appears from figure 3 that it is actually the TOPO layer (prepared by pipetting and heat drying an appropriate volume of an ethanolic TOPO solution on the electrode) which is responsible for technetium fixation. In the absence of TOPO no enrichment at all takes place at the open-circuit GCE.

Best sensitivities are attained if high negative pulse amplitudes (−100 mV or more) as well as a voltage scan of approximately 60 $mV \cdot s^{-1}$ are employed.

Which electrochemical reaction of Tc-VII underlies the analytical signal recorded has not yet been investigated. Statements which have been made in the literature with respect to polarographic waves at similar half-wave potentials recorded so far by mercury electrodes in acid pertechnetate solutions are contradictory. This equally applies to measurements performed in 4 *M* HCl.

In accordance with the reported possibility of extracting Tc-IV with TOPO [6], Tc-IV can also be enriched at the TOPO-GCE and subsequently a voltammetric peak can likewise be observed. However, the potential of this peak unfortunately deviates only slightly from that of Tc-VII so that perfect assay of both species in this way is difficult. In order to elucidate the extent of interference, measurements were made with Tc-IV (prepared by electrolytic reduction of Tc-VII in 6 *M* HCl according to [7]) to which various amounts of Tc-VII had been added. The stripping voltammograms thereby obtained in favorable cases seem to enable a rough estimate to be made of the Tc-IV and Tc-VII fractions.

Uranium, as reported [1,2], gives rise to a stripping peak which is situated at −480 mV (vs. Ag/AgCl) under the experimental conditions chosen in this work. While the obstacles resulting from low uranium content should not be serious, samples containing a preponderance of uranium preclude the assay of technetium with the TOPO-GCE.

Except for some other metals which can be extracted from strongly acid solutions using TOPO (this applies to Fe, Mo, Zn, Nb and Sn-IV [3]) as well as for considerably interfering oxygen, the technetium assay studied here is hardly disturbed by other elements.

The analytical procedure described will be profitable not the least to the present relevant investigation of solutions which arise from the prophylactic studies on the leachability of technetium after the attack of chloride brines in vitrified nuclear waste proposed for deep disposal in salt mines.

Also stripping chronopotentiometric measurements performed at the technetium loaded TOPO-GCE will provide analytically interesting data. Pronounced potential-time plots are recorded during galvanostatic reduction both with Tc-VII and Tc-IV; the transition times observed are dependent on the technetium concentration.

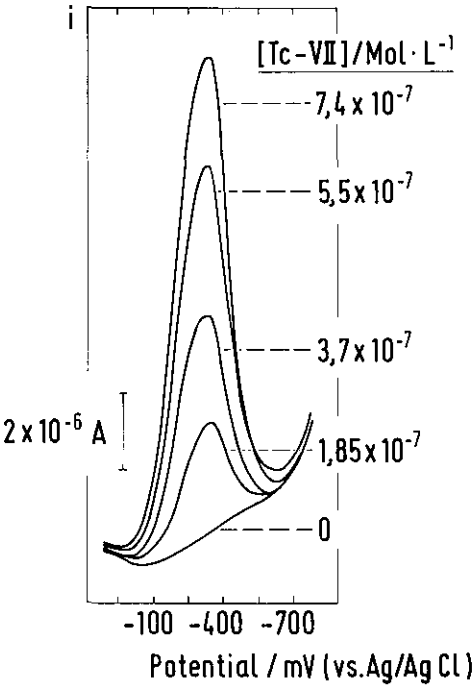

Figure 1. DP stripping voltammograms recorded in TcO_4^- solutions of different concentrations with the TOPO-GCE after enrichment in the absence of an applied electrolytic voltage. Supporting electrolyte: 3 *M* HCl; enrichment time: 200 s; pulse amplitude: −250 mV; scan rate: 10 mV·s^{-1}.

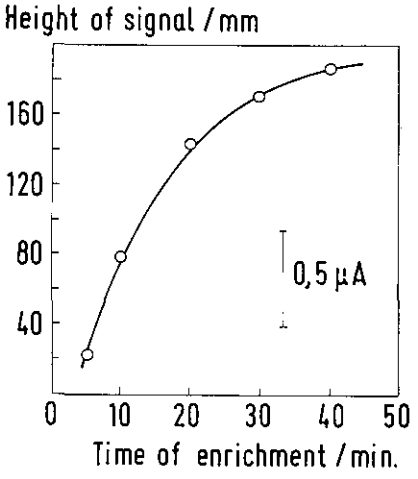

Figure 2. DP stripping voltammograms recorded with the TOPO-GCE in a 10^{-7} *M* TcO_4^- solution after different enrichment times. Pulse amplitude: −100 mV; scan rate: 15 mV·s^{-1}.

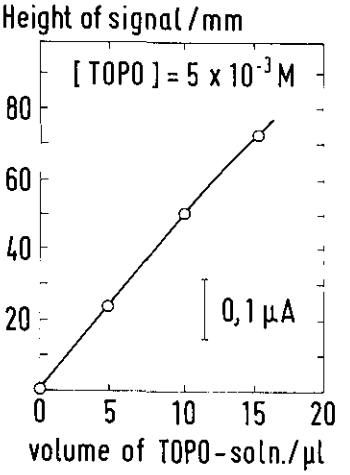

Figure 3. DP stripping voltammetric Tc signal heights at −350 mV (versus Ag/AgCl) recorded at the TOPO-GCE as a function of enrichment time. Tc-VII concentration: 10^{-7} *M*; pulse amplitude: −100 mV; scan rate: 15 mV·s^{-1}.

References

[1] Lubert, K. H., Schnurrbusch, M., and Thomas, A., Anal. Chim. Acta **144**, 123 (1982).
[2] Izutsu, K., Nakamura, T., and Ando T., Anal. Chim. Acta **152**, 285 (1983).
[3] Ishimori, T., and Nakamura, E., JAERI 1047 (1963).
[4] Boyd, G. E., and Larson, Q. V., J. Phys. Chem. **64**, 988 (1960).
[5] Torres Llosa, J. M., Diplomarbeit (Thesis), Universität Karlsruhe (1987).
[6] Colton, R. C., Dalziel, J., Griffith, W. P., and Wilkinson, G., Nature **183**, 1755 (1959).
[7] Mazzocchin, G. A., Magno, F., Mazzi, U., and Portanova, R., Inorg. Chim. Acta **3**, 263 (1974).

Volume 93, Number 3, May–June 1988
Journal of Research of the National Bureau of Standards

Accuracy in Trace Analysis

Electrochemical Studies of Dithiocarbamates and Related Compounds

S. Gomiscek, M. Veber, and V. Francetic

E. Kardelj University
Department of Chemistry and
Chemical Technology
YU-61001 Ljubljana, Yugoslavia

and

R. Durst

Center for Analytical Chemistry
National Bureau of Standards
Gaithersburg, MD 20899

Dithiocarbamates (DTC) and related compounds are widely used in chemistry, chemical technology, agriculture, and medicine. Therefore, the determination of DTC is of interest not only from a theoretical but also from a practical point of view. Many spectroscopic and electrochemical procedures for their determination have been reported in the literature. Among them, potentiometric monitoring of their concentration seems to be the most promising, in particular if measurements are to be performed in flow systems or with automatic analyzers. As a consequence, there is a demand for a reliable electrode sensor for the DTC^- ion.

Some reports have already appeared in the literature [1–3] on DTC ion-selective electrodes using either solid or liquid membranes which enable the DTC^- concentration to be determined down to 1×10^{-5} mol/L. Additionally, because of the chelating properties of DTC toward many metal ions, the electrodes are also sensitive to these ions. Therefore, it is not surprising that most of these reports have been concerned more with the potentiometry and potentiometric titration of metal ions than with the determination of DTC^- ions using the DTC ion-selective electrode.

The purpose of our work is the development of a sensitive, simple and long-lasting tetramethylenedithiocarbamate (TMDTC) based electrode sensor which would allow the determination of DTC^- as well as metal ions. The dithiocarbamate ion-selective electrode based on the heterogeneous solid membrane (AgTMDTC, Ag_2S, graphite) was prepared and its performance was evaluated.

Experimental

The potentiometric measurements were performed using an Iskra MA 5706 pH meter equipped with a saturated calomel reference electrode and the AgTMDTC/Ag_2S/graphite ISE as the indicator electrode. The polarographic and voltammetric measurements were made using PRG5 Solea-Tacussel and PAR 174 polarographs. All reagents were of A.R. quality. NH_4TMDTC was prepared in our laboratory, special care being taken to ensure its purity.

Results and Discussion

Because DTC form slightly soluble complex salts with metal ions in aqueous solutions (K_{sp}:1×10^{-13}–1×10^{-30}) they can be used in the preparation of membranes for ISE. For this purpose a precipitate of freshly prepared AgTMDTC and Ag_2S was thoroughly homogenized with a graphite powder (2:1:5), and paraffin oil added to obtain the paste. The electrode shows rectilinear dependence of the potential on the $TMDTC^-$ activity/concentration in the range 1×10^{-6}–5×10^{-3} mol/L. The selectivity of the ISE was estimated for some interfering cations, anions and ligands (table 1). The electrode is useful not only for the determination of $TMDTC^-$ and Ag^+ ion, and the titrimetric determination of metal ions which form slightly soluble complex salts with the $TMDTC^-$ ligand but also in the study of chemical equilibria of DTC systems (K_{sp},K_a). In addition to the metal ions and DTC^- ligand, soluble metal DTC complex salts should not be neglected in the solubility studies. The existence of these species (fig. 1) is clearly indicated by polarographic measurements [4]. The specificity of the AgTMDTC/Ag_2S/graphite ISE can be used to explain the discrepancies between the K_{sp} values reported [5,6] by the determination of the activity of DTC^- ions. It was also applied to the determination of the dissociation constants K_a of DTC acids (fig. 2) by measurements of the activity of $TMDTC^-$ ions at different pH values in a 1×10^{-4} mol/L NH_4TMDTC solution. The agreement between experimental and calculated values was found to be consistent for $pK_a=3.1\pm0.20$ (fig. 2).

Table 1. Selectivity coefficients $k_{i,j}$ for some interfering ions and ligands

Interfering ion	C_i(mol/L)	C_j(mol/L)	$k_{i,j}$
$DDTC^-$	10^{-4}	5.4×10^{-5}	1.84
PO_4^{3-}	10^{-5}	3.1×10^{-5}	0.32×10^{-3}
Cl^-, Br^-	10^{-5}	N.I.	N.I.
I^-	10^{-5}	4.6×10^{-5}	0.22
ETU	10^{-5}	7.4×10^{-3}	1.35×10^{-3}
Urea, ascorbic and tartaric acid	10^{-5}	N.I.	N.I.

N.I.–No interference

Selectivity coefficients $k_{i,j}$ for some cations

Cation	$k_{i,j}$	log $k_{i,j}$
Ag^+	1	0
Cu^{2+}	5×10^{-3}	−2.28
Cd^{2+}	3×10^{-5}	−4.47
Zn^{2+}	1×10^{-7}	−7.02

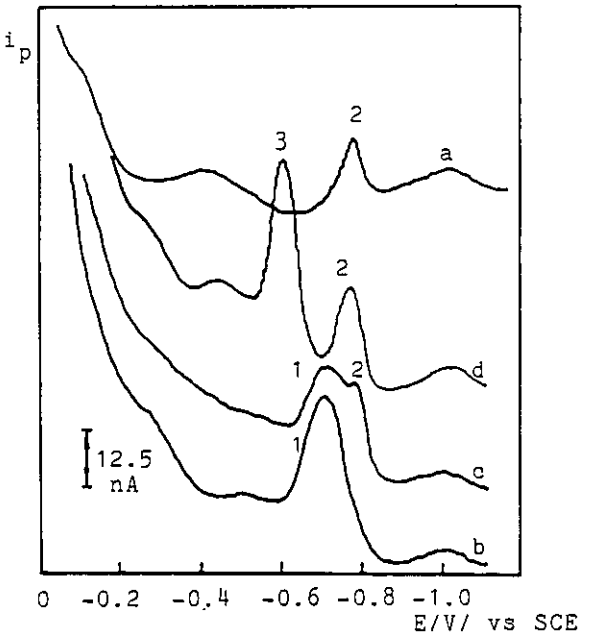

Figure 1. *i-E* curves obtained with differential pulse polarography; a=$Cd(TMDTC)_2$ under heterogeneous equilibrium; b=2.5×10^{-6} mol/L $TMDTC^-$; c=2.5×10^{-6} mol/L $TMDTC^-$+5.0×10^{-7} mol/L Cd^{2+}; d=2.5×10^{-6} mol/L $TMDTC^-$+5.0×10^{-6} mol/L Cd^{2+}. The peaks correspond to $TMDTC^-$ (1), $Cd(TMDTC)^+$ (2) and Cd^{2+} ions (3).

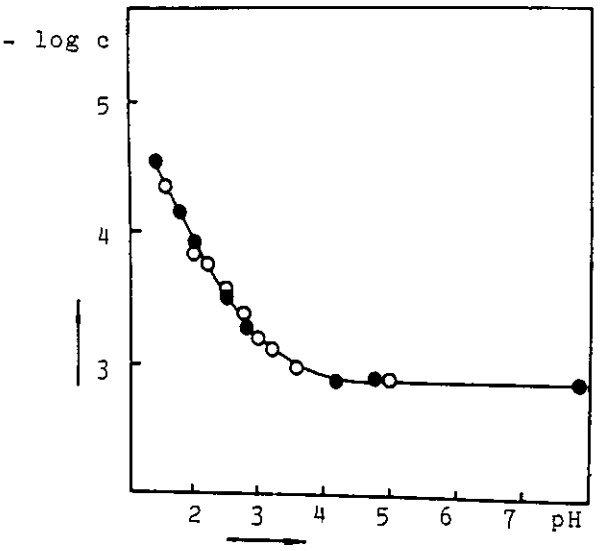

Figure 2. The determination of K_a with the AgTMDTC/Ag_2S/graphite ISE; $c_{NH_4TMDTC}=1\times10^{-3}$ mol/L, 0.1 mol/L KCl (pH was adjusted with H_2SO_4 and NH_3), O experimental values, ● calculated values for $pK_a=3.1$.

References

[1] Hassan, Saad S. M., and Habib, M. M., Anal. Chem. **53**, 508 (1981).
[2] Hassan, Saad S. M., and Habib, M. M., Analyst **106**, 1281 (1981).
[3] Itoh, Y., and Niiyama, K., Fres. Z. Anal. Chem. **320**, 573 (1985).
[4] Veber, M., Francetic, V., and Gomiscek, S., Vestn. Slov. Kem. Drus. **31**, 123 (1984).
[5] Hulanicki, A., Acta Chim. Acad. Sci. Hung. **27**, 41 (1961).
[6] Arnac, M., and Verboome, G., Anal. Chem. **46**, 2059 (1974).

Volume 93, Number 3, May–June 1988
Journal of Research of the National Bureau of Standards

Accuracy in Trace Analysis

Bioanalytical/Biosensors

Biochemical Applications of Chromatography/SIMS

K. L. Busch, M. S. Stanley, K. L. Duffin, and J. C. Dunphy

Department of Chemistry
Indiana University
Bloomington, IN 47405

The balanced capabilities of a high resolution separation method coupled with a flexible detection method such as mass spectrometry results in powerful analytical methods including gas chromatography/mass spectrometry and liquid chromatography/mass spectrometry. However, separations for diverse applications such as organic synthesis, pharmacological analysis, and biochemical separations are still based on static chromatography, defined as a method in which the separation of sample components is based on a spatial separation, rather than on a difference in retention times. Although capabilities for separation of very complex mixtures for static chromatography (thin layer or paper chromatography or electrophoresis) do not rival the very high resolution achievable with the gas and liquid chromatography, the resolution is adequate for a large number of applications, and the ease and low relative cost of the methods are advantageous. General detection methods for organic compounds separated by these forms of chromatography still seem relatively crude. Color development, charring, staining, or fluorescence measurements provide the location of sample spots, but little information about sample identity. In many cases, sample identity is suggested on the basis of an R_f identical with that of the standard. Such a match is a necessary but not a sufficient means of compound identification.

Over the past 2 years, we have constructed a secondary ion mass spectrometer (SIMS) that accommodates large chromatograms within the source, and sputters organic ions from the surfaces to produce the mass spectrum of samples directly from the chromatogram. Details of instrument construction have been reported [1]. In essence, the chromatogram is moved in the x and y axes into and out of the point of instrument focus, defined as the locus of the primary ion beam, and the secondary ion extraction optics of a quadrupole mass spectrometer. Data in four dimensions are generated: x, y, m/z ratio, and relative abundances of the ions in the mass spectrum [2–4].

Analytical advantages of the chromatography/SIMS instrument include an independent access order to sample spots, variable integration time for spectral measurement, variable spatial resolution adjusted in real time to maximize analysis efficiency, the ability to store sample as well as data generated in its analysis, preservation of all sample applied to the chromatogram, the ability to analyze chromatograms from outside sources, and the ability to calibrate the instrument with each chromatogram [5]. We have demonstrated application of chromatography/SIMS to a variety of biochemical samples and have used the mass spectral data to identify compounds contained in the chromatogram, and to increase the resolution of the chromatographic separation. The mass spectrometer is a "biosensor" that can either be operated as a general detector, or in concert with functional-group-specific-derivatization reactions that have been concurrently developed.

Figure 1 illustrates part of the data array measured in an analysis of a mixture of chenodeoxycholic acid (A) and cholic acid (B) separated by thin layer chromatography (metal-backed silica gel plate, 20 μm thickness). A dominant ion in the positive ion SIMS of chenodeoxycholic acid appears at m/z 357; similarly, the SIMS spectrum of cholic acid contains an abundant ion at m/z 355. The mass spectral data acquired over the range of x and y coordinates is reconstructed for ions of these masses. These data were acquired with a cesium ion gun with moderate spatial resolution. The maximum sample spot diameter is 1 mm, and 5 μg of each compound were present in the spot. Spectra could be recorded for several hours in each analysis (sample consumption rate is a few tens of picograms per second), and the same distribution is recorded if the chromatogram is removed from the mass spectrometer, stored, and reanalyzed later.

Figure 2 represents the analysis of pyridostigmine bromide separated by thin layer chromatography. The structure of this drug is shown; the SIMS spectrum contains an abundant ion for the intact cation at m/z 223. Variation of this particular ion with x and y is shown in the abundance plot. The same data are shown plotted as isoabundance contours. Each ion in the SIMS spectrum derived from the sample exhibits similar contours, and pattern recognition programs can be used to link such ions together to form a mass spectrum of the compound free of background.

The chromatography/SIMS method has been extended to the indirect analysis of electrophoretograms. Although aqueous gels can be dried for analysis, this often degrades the spatial resolution of the separation and makes the gel difficult to handle. The high vapor pressure of water (even at low temperatures) precludes direct analysis of electrophoretic gels by SIMS. Standard sample transfer techniques such as Southern and Western blots are used to transfer samples to nitrocellulose and diazotized media, then analyzed by SIMS. Bradykinin and a series of related peptides have been so separated and analyzed; the SIMS spectra obtained are identical to those obtained from a discrete sample.

Control of the physical and chemical nature of the chromatographic surface underlies the success of chromatography/SIMS. For maximum sensitivity, the sample should be in an ionic state, and should exhibit surfactant properties in the phase transition matrix used for the analysis [4]. Figure 3 is the positive ion SIMS spectrum of a mixture of five pyrylium salts (10 μg each) used for derivatization of primary amine groups in peptides. The recorded spectrum contains only ions from the pyrylium salt of the structure shown, which was synthesized specifically for its surface activity. No ions from the other pyrylium salts, or from the matrix, are observed. Several peptides have been derivatized with this surface-active agent. In addition to increased sensitivity, determination of the sequence of the peptide by MS/MS analysis of the parent ion of the derivative is greatly simplified.

Acknowledgments

Our research in chromatography/SIMS has been supported by the Whitaker Foundation, NIH, and NSF. The data on pyridostigmine bromide is derived from a collaborative study with Adam Vincze of the Israel Institute for Biological Research.

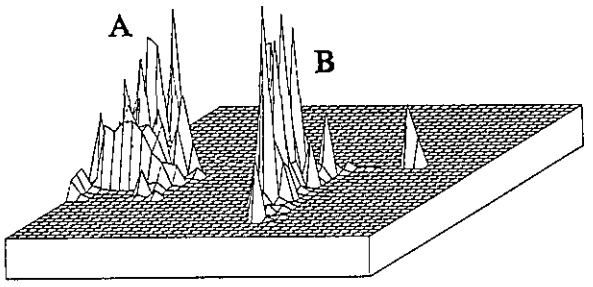

Figure 1. Reconstruction of the abundances of the ions at m/z 357 (chenodeoxycholic acid, A) and m/z 355 (cholic acid, B) as a function of x and y coordinates of the thin layer chromatogram on which they were separated.

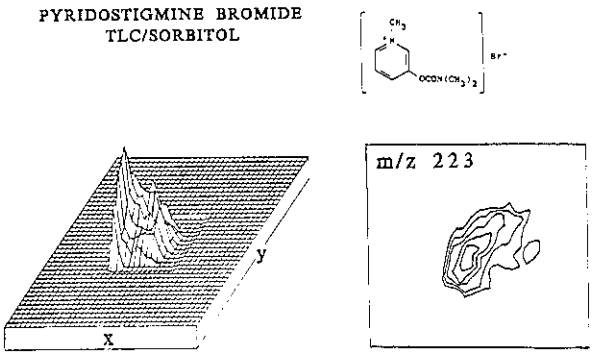

Figure 2. Abundance and isoabundance contour plots of the ion at m/z 223 corresponding to the intact cation of pyridostigmine bromide, separated from related drugs in a silica gel thin layer chromatogram.

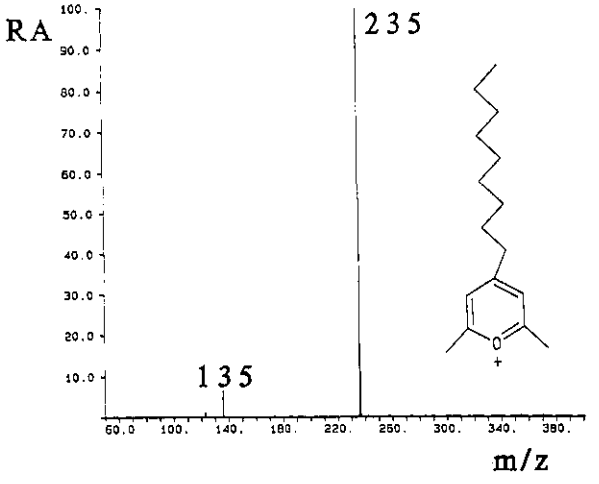

Figure 3. Positive ion secondary ion mass spectrum of a mixture of five pyrylium salts of equal concentration, showing only the ions corresponding to the pyrylium salt of the structure shown, illustrating the surfactant properties of this salt in the matrix used.

References

[1] Fiola, J. W., DiDonato, G. C., and Busch, K. L., Rev. Sci. Instrum. **57**, 2294 (1986).
[2] Busch, K. L., Fiola, J. W., DiDonato, G. C., Flurer, R. A., and Kroha, K. J., Adv. Mass Spectrom. **10**, 855 (1986).
[3] DiDonato, G. C., and Busch, K. L., Anal. Chem. **58**, 3231 (1986).
[4] Stanley, M. S., and Busch, K. L., Anal. Chim. Acta **194**, 199 (1987).
[5] Busch, K. L., TrAC **6**, 95 (1987).
[6] Stanley, M. S., Duffin, K. L., Doherty, S. J., and Busch, K. L., Anal. Chim. Acta, in press.
[7] Duffin, K. L., and Busch, K. L., manuscript in preparation.

Chemiluminescence Detection in Flowing Streams—Immobilized and Solid-State Reagents

Timothy A. Nieman

Department of Chemistry
University of Illinois
1209 W. California St.
Urbana, IL 61801

Chemiluminescence (CL) reactions yield light as one of their products. Luminol (5-amino-2,3-dihydro-1,4-phthalazinedione) is one of the CL reagents most commonly used in analysis. In aqueous alkaline solution, luminol is oxidized to yield 3-aminophthalate and light. Perhaps the most analytically useful oxidant is hydrogen peroxide, for which a reaction catalyst is required. Typical catalysts are peroxidase, hemin, transition metal ions, or ferricyanide. The luminol CL system most often used consists of luminol + H_2O_2 + catalyst + OH^-. Measurements of CL intensity can be used to quantitate any of these species. Thus, luminol CL has been used to determine catalysts or species labelled with catalysts, peroxide, or species which can be converted into peroxide, and luminol, or species labelled with luminol.

For quantitative determination of any one species involved in this reaction, one needs a way to deliver the other reaction components into the reaction zone or vessel. In flowing stream situations, either flow injection analysis or liquid chromatography, one would have a stream of analyte into which were flowed streams of the other necessary reagents as shown in figure 1. If the analyte were peroxide, then reagents 1 and 2 would be luminol and catalyst.

Such a system requires solutions of these reagents plus the necessary pumps, tubing, and mixers to deliver them and results in dilution and broadening of the sample plug. Our research effort has explored various ways to contain these reagent components in solid-state or immobilized format so that the usual reagents solutions, pumping, and tubing can be eliminated, and the reagents incorporated in-line as indicated in figure 2.

Immobilized luminol is of use for determinations of catalyst species or for determination of peroxide (and species such as glucose, cholesterol, etc., which can be enzymatically converted into an equivalent amount of peroxide). We have covalently bound luminol to silica, controlled-pore glass, and Ambersorb particles via various silane and linkage molecules. By using glutaraldehyde to bridge between the amine group on luminol and the amine group on an aminoalkylsilane, loadings of 15 mg luminol/g support are achieved for supports with about 400 square meters surface area/gram. This material is packed into a column placed into the flow stream. The immobilized luminol is stable in neutral solution, but injection of a portion of an alkaline solution will release a controlled amount of luminol (via hydrolysis of the bond between luminol and glutaraldehyde); the amount released is dictated by the pH and volume of the solution injected. We have also contained luminol simply by adsorption onto Ambersorb and released it in the same manner. Advantages to release of luminol prior to the CL reaction include improvement in the CL quantum efficiency and increased flexibility in engineering the contact with the other reagents. By use of this material in flow injection, a detection limit of 0.1 μM for peroxide is obtained.

An immobilized catalyst is of use for determination of peroxide (and analytes enzymatically converted to peroxide) or analytes that have been labeled with luminol or related compounds. An approach that we have investigated involves use of electrogeneration of luminol CL. Luminol can be oxidized at a positively-biased electrode, and CL results if oxygen or hydrogen peroxide are present. Electrogeneration of luminol CL offers the unique characteristics that the CL emission is confined to near the electrode surface and that the reaction can be turned "on" and "off" via control of electrode potential. The net electrogenerated CL (ECL) intensity due to peroxide injections appears as peaks on top of an appreciable and inescapable back-

ground due to oxygen. This background ECL however, does not prevent one from obtaining peroxide detection limits below 1 μM. The ECL intensity varies with both pH and potential. The net ECL to background ECL ratio is a maximum at pH 10. Gold and glassy carbon electrodes are preferable to platinum, but gold is somewhat better than glassy carbon. Potentials more negative than +0.3 V yield insignificant ECL; potentials of +0.4 to +0.6 V yield maximum ECL intensity. Long-term stability of the ECL signal is improved by use of a potential waveform which alternates between a positive potential where luminol is oxidized and a negative potential (about −0.2 V) where the electrode surface is reduced.

If luminol or luminol-labeled species are the analyte, then one needs both peroxide and catalyst as the reagents. Because the catalyst can be achieved electrochemically, it makes sense also to consider electrochemical generation of the peroxide from oxygen and water. In a stream flowing through an electrochemical flow cell, as long as the oxygen concentration, pH, flow rate, and electrode behavior remain constant, the amount of peroxide produced at the electrode per unit time will remain constant so that a constant concentration of peroxide will be achieved in the flowing stream. Use of a glassy carbon generating electrode, poised at about −1.0 V, yields sufficiently high peroxide concentrations over the pH 9.5 to 11 range to be useful with luminol CL; those solution pH values are also compatible with the luminol CL reaction. By using two electrodes in series (an upstream electrode to generate peroxide and a downstream electrode for luminol ECL) we have determined luminol from 0.1 nM to 10 μM.

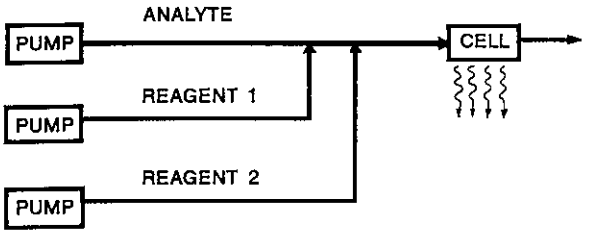

Figure 1. Typical chemiluminescence flow system using dissolved reagents.

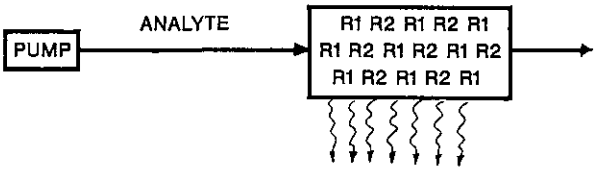

Figure 2. Possible chemiluminescence flow system with immobilized reagents (R1 and R2).

Applications of Lasers in Bioanalytical Chemistry

Edward S. Yeung

Department of Chemistry
Iowa State University
Ames, IA 50011

The combination of laser detectors and liquid chromatography (LC) has led to new types of analytical measurements in solution. LC has benefited from these selective detectors because, for complex biological matrices, complete separation of the analytes is rarely possible. Examples are polarimetry for distinguishing biologically important species from the bulk biological fluids and two-photon excited fluorescence. Laser spectroscopy has also benefited from the sample clean-up step provided by the LC, and the fact that the LC baseline allows a convenient reference measurement.

Absorption is a difficult spectroscopic measurement in remote monitoring situations. A well defined pathlength must be present to avoid nonlinear response. Unlike fluorescence, the measured radiation is at the same wavelength as the incident radiation, and scattered light is a problem. It is possible to use two optical fibers to direct light in and then out of the sample area, at the expense of a larger probe volume and potential cross-talk between fibers. When one fiber is used, reflections and scattering from the optics must be overcome. We use index-matching fluids to compensate for reflections at the end faces of the fiber. By modulating the laser source at a high frequency, the phase difference of the signals at the entrance of the fiber and at the remote optical region can be adjusted to 90°. Then, a lock-in amplifier can be used to distinguish

the two, leading to accurate absorbance values (figs. 1 and 2). We used this system for remote absorption detection of the effluent from a microbore LC column, and good detection capabilities were obtained.

In the last decade, the use of high performance liquid chromatography (HPLC) for protein separation and purification has increased dramatically. Reversed-phase (RP) separations are popular because of the high resolving power available and widespread use of RP-HPLC in many other areas. But the conditions which produce good separations are known to significantly change the protein structure. Broadened or multiple peaks resulting from subjecting a single protein to RP-HPLC have been observed by several researchers for a variety of proteins. The HPLC of soybean trypsin inhibitor was reexamined by using simultaneous optical activity and ultraviolet absorption detection (fig. 3). Ratio plots of the two detector responses allow easy identification of impurities that were not related to the protein (fig. 4). The specific rotations of each of the separated components can be derived. We find that one denatured form has a distinctly lower specific rotation while another form shows no change in specific rotation. The on-column denaturation rate here was found to be slower than that from previous w[illegible]. Column pretreatment may have resulted in milder column conditions through the elimination of irreversibly adsorbing sites.

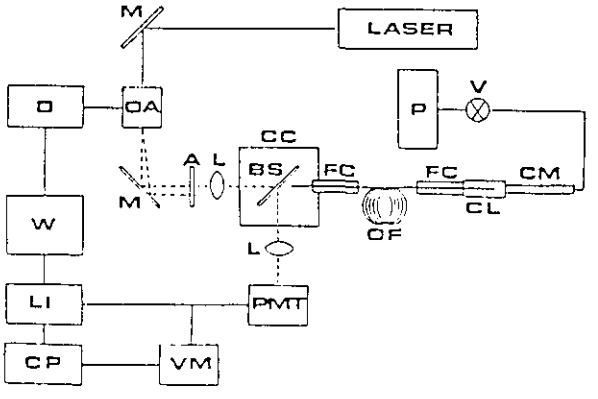

Figure 1. Fiber optic absorbance probe and chromatographic system: P, pump; V, injection valve; CM, microbore column; CL, absorbance cell; FC, fiber chuck; OF, optical fiber; CC, coupling cell; BS, beam splitter; L, lens; A, aperture; M, mirror; OA, Bragg cell; Laser, HeNe laser; D, driver; W, square-wave generator; LI, lock-in amplifier; CP, computer; VM voltmeter; PMT, photomultiplier tube.

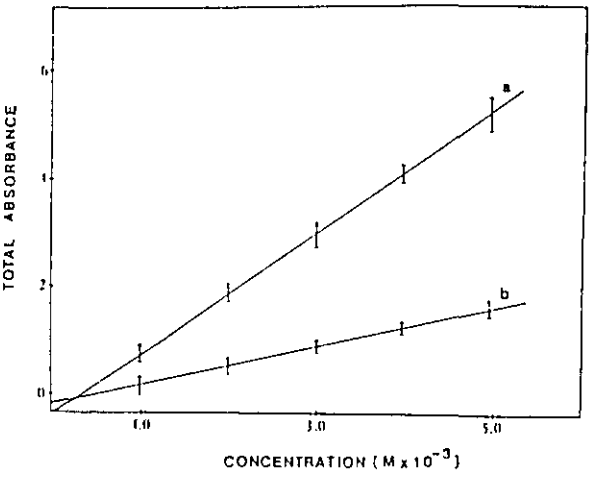

Figure 2. Beer's law plots of (a) modulated and (b) nonmodulated bromcresol green absorbance signals. Plots represent 95% confidence intervals for three replicate measurements.

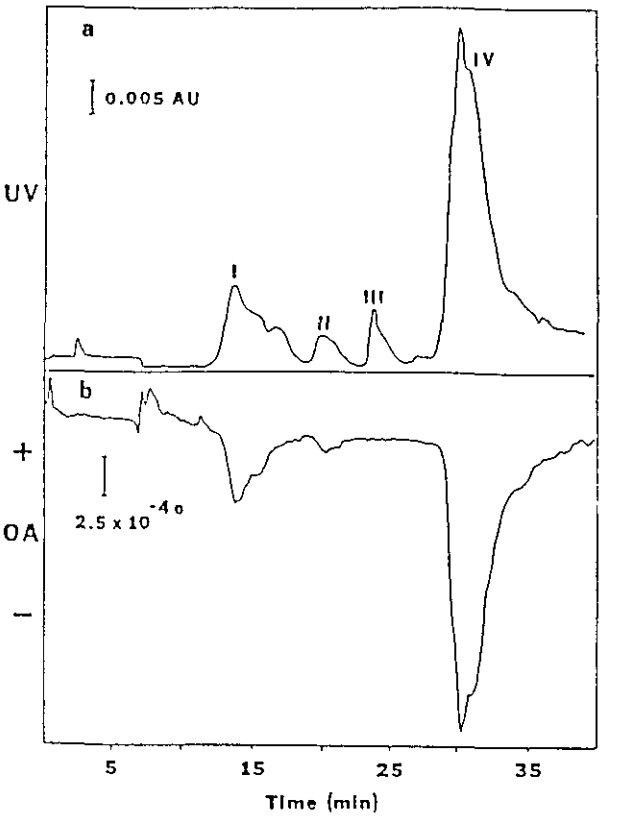

Figure 3. Ultraviolet absorbance (a) and optical activity (b) chromatograms of soybean trypsin inhibitor. 115 μg injected.

Volume 93, Number 3, May–June 1988
Journal of Research of the National Bureau of Standards

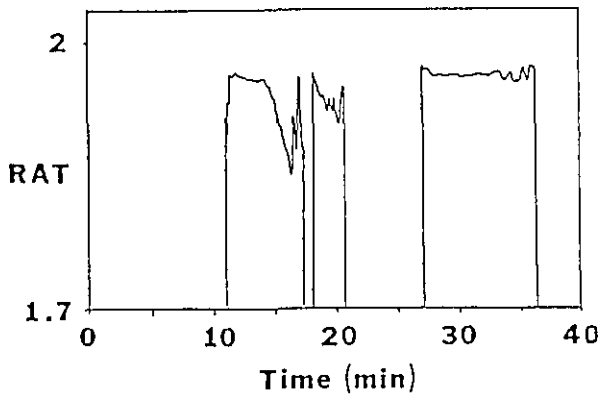

Figure 4. Plot of ratio (RAT) values versus time for the chromatograms shown in figure 3.

Trace Biogenic Amine Analysis with Pre-Column Derivatization and with Fluorescent and Chemiluminescent Detection in HPLC

T. Kawasaki, O. Wong, C. Wang, and T. Kuwana

Center for Bioanalytical Research
University of Kansas
Lawrence, KS 66046

Background

Research at the Center for Bioanalytical Research (CBAR) is aimed toward the development of highly sensitive and selective methods for the analysis of biological substances. The late Professor Takeru Higuchi, in creating the Center in 1983, initially focussed on target analytes such as amines, amino acids, peptides and polypeptides. Although methods such as RIA provide sensitive and selective analysis, a decision was made to develop fluorescence, chemiluminescence and electrochemistry for detection and liquid chromatography for separation; i.e. selectivity. Since most amino acids and peptides are optically and electrochemically "silent," it is necessary to derivatize these substances so that they can be detected. The objective of the present work was to develop a derivatization scheme with LC separation and with fluorescence (FL) and chemiluminescence (CL) detection of catecholamines and other biogenic amines in biological samples.

It is well known that electrochemical (EC) methods offer high sensitivity detection for LC analysis of catecholamines in biological samples [1–5]. Luminescence detection methods, such as FL and CL, are also capable of providing high sensitivity detection [6–9], particularly when the weakly fluorescing amines are fluorescent labelled [8–14] by derivatization. Fluorogenic reagents such as ortho-phthalaldehyde (OPA) and fluorescamine (FCA), which are specific for primary amines [15,16], have been used to enhance the sensitivity of catecholamines for LC analyses. The OPA method has been significantly improved by CBAR with the development of a new fluorogenic reagent, 2,3-naphthalenecarboxaldehyde (I, NDA), which in the presence of cyanide ion, reacts with primary amines to give the intensely fluorescent product, 1-cyano-2-substituted-benz[f]isoindoles (II, CBI) [18].

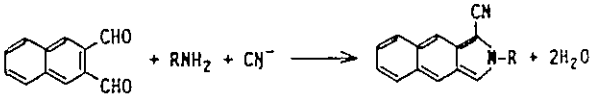

I, NDA II, CBI

The stability and FL quantum yields of the CBI-amine derivatives were superior to those from the OPA-thiol reaction [18]. The reaction of NDA with dopamine (DA), norepinephrine (NE), and the trace amines, octopamine (OA) and tyramine (TA), as a pre-column fluorogenic LC derivatization method, for the simultaneous determination of DA and NE in urine has been studied.

Experimental

Instrumentation: Optical absorbance, fluorescence and chemiluminescence measurements were made with a Shimadzu Model UV-260 spectrophotometer, a Farrand System 3 scanning spectrofluorometer, and an ATTO Model AC220 luminometer, respectively. The isocratic LC system consisted of a LKB Model 2150 dual-piston pump equipped with a Rheodyne 7125 sample injector with a 5 μL sample loop. For some of the LCCL studies, an ISCO Model 314 syringe pump was used.

Chromatography and Derivatization Procedures: CBI derivatives of catecholamine standards were separated using a TSK ODS-120T column (4.6×150 mm, 5 μm). The mobile phase was 50% acetonitrile in 10 mM potassium phosphate (pH 2.5, adjusted with phosphoric acid). The flow rate was 1 mL/min. For DA and NE analysis in urine samples, the mobile phase was isocratic elution with 38% acetonitrile and 6% THF in 10 mM phosphate buffer at pH 2.5. Derivatizations were conducted in borate buffer with dihydroxybenzylamine (DHBA) as an internal standard. Final concentrations were [NDA]=0.2 mM, [CN]=0.2 mM and [DHBA]=5 μM. For the urine samples, alumina was used for sample clean-up. Desorption of catecholamines from alumina was accomplished by washing (30 seconds) the alumina with two successive portions (200 μL) of 0.1 M phosphoric acid.

Results and Discussion

Figure 1 shows the absorbance-time profile for the reaction of NDA-CN with DA and NE in borate buffer (pH 9) at room temperature. Under these conditions, the reaction is completed in less than 5 minutes with the CBI-catecholamines exhibiting excellent chemical stability. The rapidity and completeness of the NDA-CN reaction under mild aqueous conditions are an important feature compared to that of the fluorescamine method [16], which requires the fluorescamine reagent to be solubilized in an anhydrous organic solvent to prevent deleterious hydrolysis from occurring. Also, compared to the usual OPA-thiol method [15], the CBI product has enhanced chemical stability. Figure 2 shows typical optical (A) absorbance and (B) fluorescence emission spectra of a CBI-amine derivative. The optical absorbance in the visible region of the spectrum allows the use of a low-powered He-Cd laser for excitation, which is currently under development [21].

Figure 3A shows the separation of a mixture of five CBI derivatives by reverse phase LC under isocratic conditions. The five derivatives were separated to baseline resolution within 15 minutes. Addition of 10 mM SDS in the mobile phase enhanced the FL intensities of the trace amines, CBI-OA and CBI-TA but had little effect on the other three (fig. 3B). Using DHBA as the internal standard, good linear response (linear regression correlation coefficient >0.995) was obtained in the range of 0.5 to 10 pmol of amine injected on-column. Detection limits for these amines are in the range of 20–60 femtomoles (S/N=2) with the commercial 10 μL FL detector.

Chromatograms for the determination of DA and NE in 1 μL urine samples containing DHBA as the internal standard with the NDA-CN procedure indicate that these substances can be quantified at less than 0.5 μM concentrations.

Chemiluminescence

Chemiluminescent detection of the CBI-catecholamines used bis(2,4-dinitrophenyl)oxalate (DNPO) as the oxalate. The hydrogen peroxide and DNPO in acetonitrile solvent are post-column mixed the LC eluant and the CL emission detected with the ATTO cell of 40 or 60 μL volume. The sensitivity of the CL system is demonstrated by the baseline separation of a mixture containing 1 femtomole each of DA, NE and DHBA. Calibration curves with DHBA as the standard exhibit excellent linearity over two orders of magnitude with a detection limit of 0.01 pg.

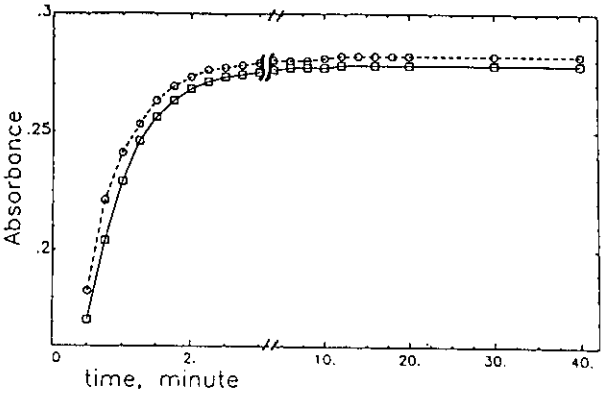

Figure 1. Absorbance-time profile for the reaction of NDA-CN with DA and NE.

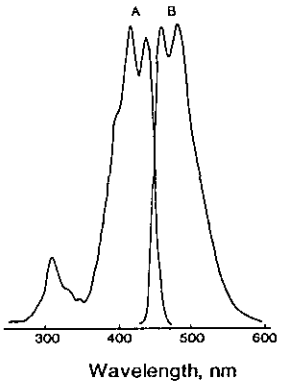

Figure 2. Typical optical absorbance (A) and fluorescence emission (B) spectra of a CBI-amine derivative.

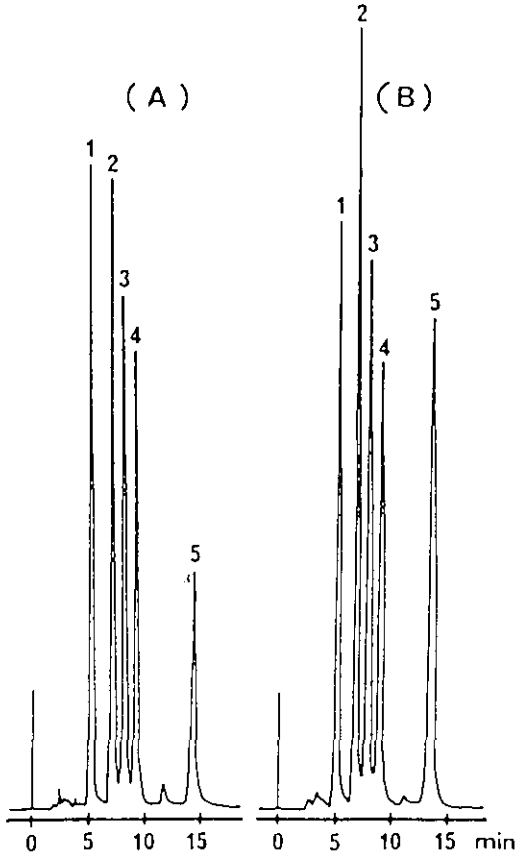

Figure 3. Isocratic reverse-phase LC separation of five CBI derivative (A). Same separation after addition of SDS (B).

References

[1] Rice, M. E., Oke, A. F., Bradberry, C. W., and Adams, R. N., Brain Res. **151** (1985).
[2] Elworthy, P. M., and Hitchcock, E. R., J. Chromatogr. **380**, 33 (1986).
[3] Moleman, P., and Borstrok, J. J. M., Biogenic Amines **3**, 33 (1985).
[4] Westerink, B. H. C., and Mulder, T. B. A., J. Neurochem. **6**, 1449 (1981).
[5] Causon, R. C., Carruthers, M. E., and Rodnight, R., Anal. Biochem. **116**, 223 (1981).
[6] Kobayashi, S., Sekino, J., Kazumasa, H., and Imai, K., Anal. Biochem. **112**, 99 (1981).
[7] Mellbin, G., J. Chromatogr. **6**, 1603 (1983).
[8] Imai, K., in Methods in Biogenic Amine Research, Eds., Parvez, S., Nagatsu, T., Nagatsu, I., and Parvez, H., Elsevier, New York (1983) Chapter 2.
[9] Imai, K., Toyo'oka, T., and Miyano, H., Analyst **109**, 1365 (1984).
[10] Mori, K., and Imai, K., Anal. Biochem. **146**, 283 (1985).
[11] Todoriki, H., Hayashi, T., Naruse, H., and Hirakawa, A., J. Chromatogr. **276**, 45 (1983).
[12] Imai, K., J. Chromatogr. **150**, 135 (1975).
[13] Yui, Y., and Kawai, C., J. Chromatogr. **206**, 586 (1981).
[14] Yui, Y., Kimura, M., Itokawa, Y., and Kawai, C., J. Chromatogr. **177**, 376 (1979).
[15] Roth, M., Anal. Chem. **43**, 880 (1971).
[16] Udenfriend, S., Stein, S., Bohlen, P., Dairman, W., Leihgruben, W., and Weigle, M., Science **178**, 871 (1972).
[17] Benson, J. R., and Hare, P. E., Proc. Natl. Acad. Sci. USA **72**, 619 (1975).
[18] Matuszewski, B., Givens, R. S., Srinivasachar, K., Carlson, R. G., and Higuchi, T., J. Org. Chem. **51**, 3978 (1986).

Homogeneous Electrochemical Immunoassay Using a Chemically Modified Electrode

Rosanne Kannuck and Jon M. Bellama

Department of Chemistry and Biochemistry
University of Maryland
College Park, MD 20742

and

Richard A. Durst

Center for Analytical Chemistry
National Bureau of Standards
Gaithersburg, MD 20899

An alternative to enzymatic detection and amplification of antigen/antibody interactions is the use of lipid bilayer structures known as liposomes. The concept in using this type of structure is that a specific "marker" is released from within the liposome when an antigen/antibody binding event has taken place on the liposome surface. Amphophilic

phospholipid molecules spontaneously aggregate in aqueous media to minimize the interaction free energy per lipid molecule. This aggregation results in the formation of closed bilayer structures consisting of an aqueous internal cavity separated from the external solution by a lipid membrane. If the aqueous solution used in the liposome preparation contains high concentrations of any of a variety of dyes, proteins, or ionic species, the result is that the marker is entrapped within a closed bilayer. The physico-chemical properties of the liposome are governed by the type of marker used, chemical composition of the liposome (the types of amphophiles used), molecular size and charge of the marker species, and membrane surface ligands.

The membrane surface ligands are either antigens or antibodies that have been covalently bound to the surface of certain phospholipid head group entities, such as an amine molecule, and impart the immunogenic properties to the liposome. After a binding event occurs, the liposomes will act as a receptor for complement attack, that is, a series of naturally occurring serum proteins which recognizes the event and lyses (disrupts) the membrane.

Recent work in this laboratory has demonstrated the feasibility of encapsulating high concentrations (50 mmol/L) of potassium ferrocyanide in liposomes and detecting the released marker by differential pulse voltammetry [1]. We have found, however, that modification of the electrode is necessary to overcome the interferences encountered in the immune lysis of liposomes and to enhance the oxidative peak current of the liposome-released ferrocyanide. This latter step is accomplished by electrostatically binding the released marker at the electrode surface via a technique described by Whiteley and Martin [2] as ion-exchange voltammetry (IEV). The ferrocyanide ion is electrostatically bound within a siloxane polymer film on the electrode surface by the exchange with iodide present in the film as a methylpyridinium iodide (fig. 1).

A film thickness of 1.2 μm was shown to be adequate coverage for electrode protection. Figure 2 illustrates the ion-exchange capabilities of these electrodes in serum matrices, where each data point is the average of three different electrodes in 1×10^{-5} mol/L ferrocyanide (final concentration). Peak currents measured at a bright Pt (0.635 cm^2) electrode for this concentration are typically on the order of 0.1 μamp. Therefore, it is seen that even with 60% serum in the matrix, the signal obtained is five times greater at the modified electrode.

Our research utilizes liposomes immunologically sensitized by the addition of 1 mole percent dinitrophenol-capped phosphatidylethanolamine (DNP-cap PE) to liposomes prepared from a mixture of dimyristoylphosphatidylcholine (DMPC), cholesterol, and dicetyl phosphate (DCP) in a 5:4:1 mole ratio. Using this technique, we have been able to demonstrate an analysis for anti-DNP IgM using the DNP-fixed liposomes and measuring the ferrocyanide signal as a secondary response for the presence of IgM.

The amount of complement greatly affects the permeability of the lipid bilayer. We have found that a 1:4 dilution of the serum results in a peak current (due to the nonspecific ferrocyanide leakage) of less than 0.5 nA over the background. A greater concentration of serum can result in as much as 86% of the entrapped marker leaking from within the membrane prior to a lysing event.

The linear response of ferrocyanide release as a function of IgM content in the sample is illustrated in figure 3. From these results the inefficiency of this particular complement lysis is evident. If the peak current resulting from a surfactant lysis of the membrane is defined as 100% release of the marker, the response of the IgM-saturated DNP-liposomes (between 100 and 200 μL of IgM supernate) implies that only 6–10% of the marker is released. Future research using this technique will include investigating alternate complement sources (such as guinea pig) which will hopefully prove to be more reactive and improve the sensitivity of the assay.

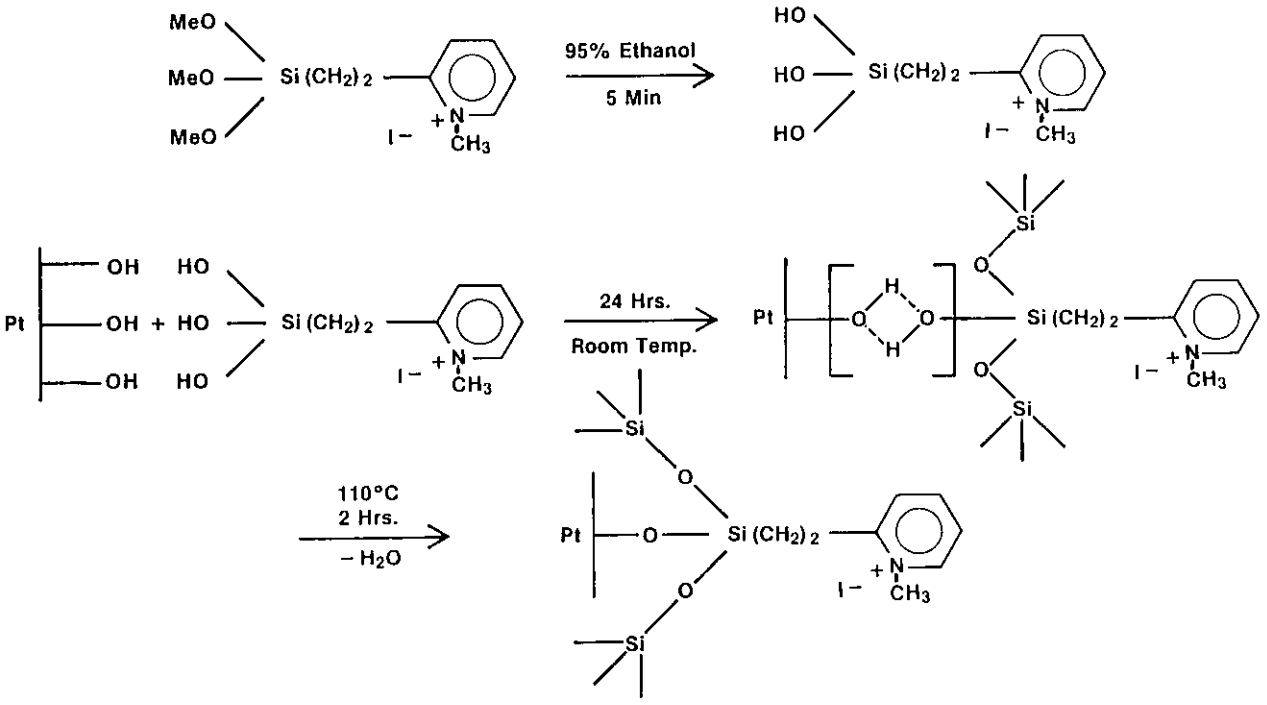

Figure 1. Reaction sequence for fabrication of silane-modified electrodes with approximately 100% of the sites methylated.

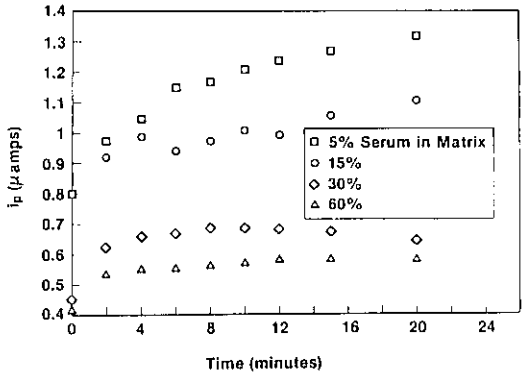

Figure 2. Ferrocyanide uptake for 1.2 μm thick polymer modified electrodes for increasing amounts serum in the sample matrix.

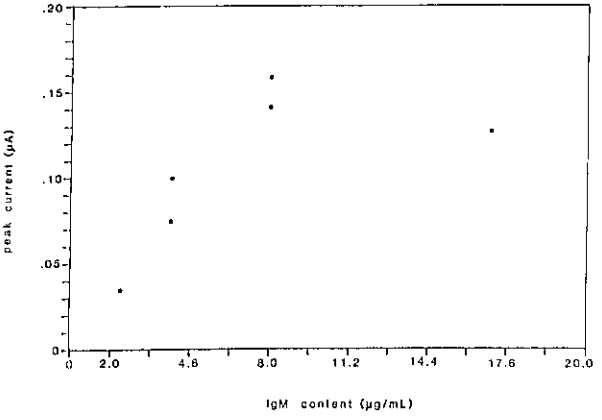

Figure 3. Analytical response (working) curve for DNP/Liposomes. Voltammograms were recorded at a modified electrode versus a Ag wire quasi reference electrode. Samples were incubated for 30 minutes at 37 °C and the released ferrocyanide preconcentrated for 30 minutes prior to scan.

References

[1] Kannuck, R. M., Bellama, J. M., and Durst, R. A., Anal. Chem. **60**, 142 (1988).
[2] Whiteley, L. D., and Martin, C. R., Anal. Chem. **59**, 1746 (1987).

Volume 93, Number 3, May–June 1988
Journal of Research of the National Bureau of Standards

Microprobe Techniques

Accuracy in Quantitative Electron Probe Microanalysis

K. F. J. Heinrich

National Bureau of Standards
Gaithersburg, MD 20899

Electron probe microanalysis (EPMA) is based on the interpretation of x-ray spectra emitted by specimens which were exposed to a focused, accelerated electron beam. One of the attractions of this technique is the simplicity of the x-ray emission line spectra which is particularly striking if we do not pay attention to the fine details of x-ray spectrometry such as line position and shape changes with chemical composition or the extended structure of absorption edges. In close analogy, the inventor of EPMA, R. Castaing, found in early investigations that quite simple approximations to quantitation with this technique could yield results of remarkable analytical accuracy, considering the state of art of instrumentation at that time, and the small volumes from which the compositional analysis was elicited [1]. While Castaing favored a simple approach based on physical principles, Ziebold and Ogilvie [2] chose an empirical technique based on the use of composite standard materials; again, a pleasing simplicity was observed, and the empirical method is still widely used, particularly in the analysis of minerals.

As experience and areas of applications widened, it became obvious that to increase the accuracy of the procedure, some of this apparent simplicity had to be abandoned. Fortunately, the availability of small computers permitted the on-line execution of more involved data reduction schemes; larger computers could be used in Monte Carlo simulations of the events in the target [3], and the quality of estimates of pertinent parameters, such as the x-ray absorption coefficients, was also improved [4].

The x-ray line spectra observed in EPMA are caused by electrons which penetrate the specimen surface with energies which typically range between 5 and 30 keV. In the typical flat, thick specimen, most of the electron paths are contained within a homogeneous specimen matrix. The penetrating electrons lose energy due to inelastic interactions which usually are treated as a continuous process and described by Bethe's law of electron deceleration or by expressions related to this law [4]. The direction of the penetrating electron is altered mainly due to inelastic collisions; the scattering of electrons causes a significant number of electrons to be re-emitted from the specimen (backscattering), and the fraction of electrons which are backscattered depends strongly on the mean atomic number of the target.

The backscattered electrons conserve most of the energy they had when entering the specimen; therefore, a significant fraction of the energy which would otherwise cause x-ray emission is lost through backscattering, and the loss varies strongly with specimen composition.

A small fraction of electron-target interactions, described by ionization cross-sections produces x-rays, and the x-ray emission directed toward the specimen surface suffers attenuation which is determined by the distribution in depth of the loci of excitation and by the x-ray absorption coefficients of the specimen.

Besides this primary x-ray generation, processes such as fluorescent x-ray generation by continuous as well as characteristic x-rays affect the relation between x-ray emission intensity and specimen composition. It is common, though not justifiable by present standards of computation, to group the data processing steps into three multiplicative factors (Z,A,F), which, respectively, represent the "atomic number correction" (i.e., consideration of electron deceleration and backscatter), the "absorption correction" (which only considers the attenuation of primary x-rays), and the "fluorescence correction" (which describes, usually in an oversimplified way, the generation and attenuation of x-rays excited by other characteristic x-ray lines). The fluorescence due to the continuum is ignored in most data reduction schemes.

In addition to the uncertainties in parameters involved in the aforementioned processes, the accuracy of the procedure is affected by lack of flatness and homogeneity of the standards whose emission is compared with that of the specimen, by errors in the determination of the composition of nonele-

mental standards, and by statistical and systematic errors in the measurement of x-ray lines and in the separation of line intensity from spectral background. The errors in estimating the characteristics of the detector system, with exception of deadtime effects, cancel when the emission from the specimen is divided by that from the standard. The estimate of achievable accuracy of EPMA and the comparison of diverse approaches must therefore involve consideration of theoretical aspects, of errors in the values of parameters used in the procedure, and of operational errors in specimen and standard preparation and in analysis. In the development of current "correction procedures," theoretical, mathematical and measurements aspects are interwoven. For instance, the distribution in depth of x-ray generation can either be calculated by Monte Carlo calculations, which are limited by the accuracy of available parameters, or by exeriments with sandwich tracer targets. To further complicate things, some Monte Carlo calculations use techniques empirically adjusted to fit the available experimental evidence. Since the precision of measurement of relative x-ray intensities is better than the accuracy of results on specimens of known composition, there is room for improvement; but, to achieve this, the diverse potential source of errors will have to be unraveled and tested separately.

References

[1] Castaing, R., and Descamps, J., J. Phys. Radium **16**, 304 (1955).
[2] Ziebold, T. O., and Ogilvie, R. E., Anal. Chem. **36**, 322 (1964).
[3] Heinrich, K. F. J., Newbury, D. E., and Yakowitz, H., eds., NBS Spec. Publ. **460**, U.S. Dept. of Commerce, 1976.
[4] Bethe, H. A., Ann. Phys. (Leipzig) **5**, 325 (1930).

Quantitative Secondary Ion Mass Spectrometry

M. Grasserbauer

Institute for Analytical Chemistry
Laboratory for Physical Analysis
Technical University Vienna
Getreidemarkt 9
A-1060 Wien, Austria

1. Introduction

Secondary Ion Mass Spectrometry [SIMS] provides a unique analytical potential due to the fact that all elements can be analyzed with high sensitivity and isotopic specificity, that elemental and molecular (bonding) information can be gained and that micro, surface and bulk analysis can be performed. The major limitations of SIMS are determined by the complexity of the mass spectra, the large variation of the secondary ion yields for different elements, and also for a particular element in different matrices (chemical matrix effect), and by the disorder induced into the analytical zone due to the high energy ($E_0 = 1-20$ keV) of the primary ions [1,2].

To overcome these limitations *in praxi*, the following approach for quantitative trace analysis is most useful:

- Use of reactive ion sputtering (oxygen or cesium) to increase the secondary ion yield and to achieve a chemical modification of the surface zone which reduces the chemical matrix effects.
- Use of high performance instrumentation which allows the identification (and separation) of interfering species by high mass resolution.
- Quantitation with relative sensitivity factors (RSFs) obtained from external or internal calibration.
- Systematic study of all sources of analytical errors, particularly of the measurement process, as described by Powell [3].
- Development of problem oriented measurement techniques and analytical strategies, combining SIMS with other analytical techniques yielding confirmatory and supplementary information (example ref. [4]).

Quantitation procedures and the general problems associated with quantitation of secondary ion mass spectra are discussed in several excellent pub-

lications [1,2,5–7]; thus this paper will concentrate on specific tasks of quantitative analysis with SIMS. These tasks are: multielement, ultratrace analysis of metals; high-accuracy, depth distribution analysis of dopants in silicon; and quantitative interface analysis.

2. Multielement Ultratrace Analysis of Metals

The need arises mainly from microelectronics, with its extreme purity requirements for metals used for the production of electrode lines and interconnects in VLSI devices: In refractory metals used for 1 Mbit and 4 Mbit storage devices, alkali elements and U, Th must not exceed 10 ng/g; the concentration of transition metals must be below 100 ng/g.

Due to the limited potential of NAA for ultratrace analysis of refractory metals, only mass spectrometric techniques can be considered for direct solid state analysis. A comparison of the useful yields [8] (SSMS : 10^{-8}–10^{-7}, GDMS 10^{-7}, SNMS 10^{-9}, SIMS 10^{-1}–10^{-5} [using reactive ion bombardment]) shows the large basic potential of SIMS.

The need to establish RSFs with reference materials characterized for trace elements—a disadvantage compared to SSMS, GDMS and SNMS—makes the analytical procedure more elaborate. Figure 1 contains the basic steps for the preparation and characterization of the reference material (doping with 40 elements, in the μg/g-range, round robin analysis, test of homogeneity with SIMS) and the analysis of the materials [9].

Thirty elements are analyzed with oxygen primary ions, 10 with cesium. Interferences are eliminated by energy filtering, peak stripping and high mass resolution. Several mass spectra or depth profiles are recorded to obtain a fairly representative value within a reasonable time (ca. 2 hours). Material consumption per analysis is ca. 1 μg (1–10 mg for SSMS, 1–10 mg for GDMS). With optimized measurement techniques, detection limits (calculated from the analysis of the reference materials) between 1 pg/g and 100 ng/g are obtained with SIMS (SSMS 10–100 ng/g, GDMS 1–10 ng/g) [9–11].

For the assessment of accuracy, chemical matrix effects were studied by comparing results obtained with oxygen bombardment (with and without saturation) and cesium bombardment and using different external standards (doped materials and ion implants). The values lie typically within a factor of 2 [10]. Furthermore, a comparison of SIMS with GDMS and SSMS (including NAA results on a few elements) for W and Mo showed that the agreement of SIMS with the other methods is on the same order (typically within a factor 2) as between GDMS, SSMS and NAA, respectively. This indicates the absence of large systematic errors in the SIMS results due to a chemical matrix effect. It was found that the major source for deviations between the different methods is the inhomogeneity of the materials analyzed. This again shows the need for reference materials that are homogeneous on the nm to cm scale.

For homogeneous materials, an analytical accuracy of SIMS for the ultratrace analysis of U and Th in aluminum of 10% has been reported [12]. This corresponds well with the experiences obtained in the analysis of semiconductors.

With these figures of merit, SIMS can be considered as another major technique for ultratrace analysis. It is—up to now—the only method for ultratrace analysis in thin films—a task which is of great interest to study the process related contamination of metallization layers. As an example for the application of SIMS, figure 2 shows the ultratrace analysis of the impurity content in molybdenum as a function of the number of electron beam refining steps. The increase of impurity levels after the 6th step is due to the inhomogeneity on the cm-scale of the cast molybdenum [11].

3. High-Accuracy, Depth Distribution Analysis of Dopant Elements in Silicon

SIMS is presently the most important technique for distribution analysis of dopant elements in semiconductors [4,13–17]. For silicon under optimized conditions (table 1), detection limits in the range between 10^{14} and 3×10^{15} cm^{-3} can be obtained. The accuracy of the concentration values in a profile is on the order of 5% (B) to 20% (P); that of the depth scale ~5% (using actual crater depth measurements) (see also [13]). The accuracy of SIMS profiles can be determined in two different ways:

a) Comparison of profiles quantified with the internal calibration ("fluence") method with those obtained using external (homogeneous) reference materials. Fluence measurements by an independent technique like NAA or RBS are valuable to check the accuracy of fluence

values obtained from measurement of the implantation current.

b) Comparison of profiles obtained with different techniques exhibiting independent systematic errors [16,19]. Such comparative analyses are of great significance to study the artefacts [18] which occur in SIMS depth profiling. For all dopant elements, only electrical measurements [e.g., spreading resistance (SR)] can be applied to annealed specimens. There is however a systematic deviation between elemental and electrical profiles at concentrations above the (electrical) solubility limit and at the deeper side of the profile, for which SR profiles seem to be steeper. Comparison of elemental profiles is even more difficult: only for ^{10}B a "reference technique"—NAA exists which exhibits the sufficient accuracy—at least for annealed specimens [19]. For non-annealed materials, differences between SIMS and NAA depth profiles for B in silicon have been observed [20]. For the dopant elements As, P, and Sb, chemical etching has to be applied for NAA depth profiling. Moderate depth resolution and rather large analytical errors are encountered. For Sb, RBS can be applied for depth profiling. Although the method is considered to be largely free from systematic errors, it exhibits only a rather poor depth resolution and a high detection limit. Thus the depth profiles obtained with RBS can only be compared with SIMS profiles in a very limited manner.

Summarizing this discussion of the assessment of the accuracy of SIMS depth profiles (which is presented in detail in ref. [16]), it must be stated that there is a significant lack of independent methods to study SIMS artefacts. The most successful approach still seems to be the systematic investigation of ion-solid interactions, thus creating a broader understanding for physical processes like sputtering and secondary ion formation [21].

Table 1. Optimized analytical conditions and practical detection limits for surface distribution analysis of dopant elements in silicon with SIMS [4]. $\left(\frac{M}{\Delta M}\right)_{pr.}$ = practical mass resolution used during measurement.

Isotope	Primary ion	Detected ion	Interfering ion	$\left(\frac{M}{\Delta M}\right)_{pr.}$	Detection limit (atoms cm^{-3})
^{10}B	O_2^+	$^{10}B^+$	$^{30}Si^{3+}$	500	10^{14}
^{11}B	O_2^+	^{10}B	$^{10}BH^+$	400	10^{14}
^{31}P	Cs^+	$^{31}P^-$	$^{30}SiH^-$	4500	$1{\cdot}10^{15}$
^{75}As	Cs^+	$^{75}As^-$	$^{29}Si^{30}Si^{16}O^-$	4500	$3{\cdot}10^{15}$
^{121}Sb	Cs^+	$^{121}Sb^{28}Si^-$	$C_xH_y^-$,	400	$3{\cdot}10^{15}$
^{123}Sb	Cs^+	$^{123}Sb^{28}Si^-$	$Si_xO_y^-$ (?)	400	$3{\cdot}10^{14}$

Up to this point the discussion has been concentrating on "pure" silicon matrices. In industrial practice the combined system SiO_2/Si is usually of great interest. This means depth profiling through an insulator/semiconductor system with a changing matrix. Compensation of charging and matrix effects is necessary to achieve quantitative results. This problem is especially serious if an element must be measured at high mass resolution, like P ($M/\Delta M \sim 4500$). New techniques are necessary to obtain stable and accurate profiles through the layer system SiO_2/Si [22]: They apply computerized peak centering routines in switching between references mass and analytical ion to eliminate magnetic drift and hysteresis effects. Secondly, a complete charge compensation is achieved by measurement of the intensity of the reference ion ($^{30}Si^+$) at the steep flank of the energy of distribution. This intensity value is extremely sensitive to charging: a surface charge of only 1 volt influences the reference intensity by 10%. Changes in this reference ion intensity are used to monitor the process of charge compensation by adjustment of the sample potential. The third step—compensation of the chemical matrix effect—is performed by oxygen saturation of the sample surface during analysis. To control the degree of surface saturation the secondary ion ratio SiO_2^+/Si_2^+, which is extremely sensitive towards oxygen coverage of the surface, is measured. With this procedure it is possible to control the compensation of the chemical matrix effect eight times more accurately than by monitoring only atomic ions (e.g., the reference mass).

These extensive computer based measurement techniques finally allow the measurement of the distribution of P across thick oxide films into the silicon matrix with high accuracy (estimated to be ~30% for a point on the profile) for determining the technically very important assessment of the segregation of this dopant element during oxidation of silicon in device manufacturing (fig. 3).

Distribution analysis of dopant elements in semiconductors by SIMS is by far not fully developed yet. Due to the increasing demands posed by semiconductor technology new challenges arise, e.g., for simultaneous multielement depth profiling, for which new computerized measurement approaches have to be established [23], or in high lateral resolution dopant analysis in devices with finely focused ion beams [24], or for high depth resolution profiles of very shallow or multilayer structures [25], or finally the problem of quantitation through layers of changing matrices [26].

4. Quantitative Interface Analysis

Quantitative analysis at interfaces is subject to pronounced artefacts and erroneous results due to cascade and recoil mixing, changes in sputter rates and ionization yields and ion beam induced diffusion (e.g., for alkali elements) [27]. Extensive investigations are usually necessary to achieve a quantitative result, as shown here in an exemplary manner for the study of the distribution of the dopant element Cr between GaAs and the covering Si_3N_4 layer [28]. Figure 4 shows the SIMS profiles of $^{52}Cr^+$, $^{28}Si^{2+}$ and $^{75}As^+$ obtained with oxygen primary ions in a GaAs material before and after annealing. Cr peaks are observed in GaAs adjacent to the interface (A) in both cases and in the Si_3N_4 layer (B) after annealing. Ion implantation of Cr into a Si_3N_4/GaAs structure also showed these two peaks, indicating that peak A was an artefact due to chemical yield enhancement by oxygen at the interface analysis of the annealed sample. Analysis with Ar^+ primary ions showed only peak B, thus raising the question about the origin of chemical signal enhancement. Modelling of the primary ion implantation and sputter process yielded the origin of peak B. Due to the higher stopping power of GaAs compared to Si_3N_4 for the primary oxygen ions, these are enriched in the near interface layer of GaAs when sputtering through the interface (enrichment factor ~2). Secondly the sputter rate of GaAs is a factor of 3.3 higher than that of Si_3N_4. Both effects combined lead to a signal increase for Cr in the near-interface zone of GaAs of about a factor of 10.

Once peak A was identified as an artefact, the real distribution of Cr could be established by fitting a Gaussian profile to peak B. The accuracy of this method was tested by comparison of the amount of outdiffused Cr from GaAs with that corresponding to peak B. An agreement for both Cr values of 30% was found.

5. Further Challenges

Quantitative SIMS has by far not reached its limits. Due to the increasing necessity for quantitative distribution analysis of trace elements particularly in high technology materials [29] a strong motivation for the development of instrumentation and analytical procedures is provided. Some of the most significant areas of current and future activities are compiled in the following (subjective) selection:

i) Analysis of laterally heterogeneous systems, e.g., metals with precipitates: reduction of selective sputter effects by chemical surface reactions to obtain depth profiles with a high dynamic range (fig. 5) [30], combination of ion microscopy and mass spectrometry to establish calibration curves [31].

ii) "Monolayer" analysis—quantitative analysis is limited by the low number of atoms available for a data point, e.g., the detection limit for Al in a thin SiO_2 layer on silicon is ca. 1 μg/g for a consumption of 0.1 atomic layer (d_A=250 μm)—corresponding to a removal of 10,000 Al atoms [32]. Laser resonance ionization SIMS employing high transmission TOFs promises to extend detection limits to the ng/g range or some tens of atoms, respectively [33].

iii) Three-dimensional quantitative distribution analysis, employing elaborate image processing techniques. The resistive anode encoder based systems [34] seem to be particularly promising. Availability of the full 3-D information will allow correlation of all information which can be gained with SIMS—a tremendous advantage for (usually complex) technical materials.

iv) Phase identification by quantitative evaluation of cluster ion intensities in the secondary ion mass spectrum. Pattern recognition techniques have been shown to have great value for selection of the appropriate features most typical for a particular compound or phase [35]. Identification of phases (precipitated in a matrix or at interfaces) is in principle possible even if their size is below the spatial resolution of SIMS.

v) Application of chemometric techniques to extract and verify information obtained from SIMS spectra and profiles, e.g., factor analysis [36] or fuzzy theory [37] to evaluate depth profiles.

vi) Compilation of sputter coefficients, ionization probabilities, useful yields [38], and relative sensitivity factors. These data would be of great value for choosing optimal measurement parameters and could enable assignment of at least semiquantitative values to secondary ion intensities for systems where a suitably matched reference material is not available. Recent investigations on semiconductor [39] and refractory metal [10] matrices indicate that RFSs can be transferred from one matrix to another by the use of scaling factors.

vii) Development of (further) models for sputtering and ionization which reflect the physical processes occurring under reactive ion beam bombardment.

Acknowledgments

Support of activities by the Austrian Scientific Research Council and the Industrial Research Fund is gratefully acknowledged. The author wants to thank his coworkers and partners in the scientific cooperations, whose names are contained in the list of references.

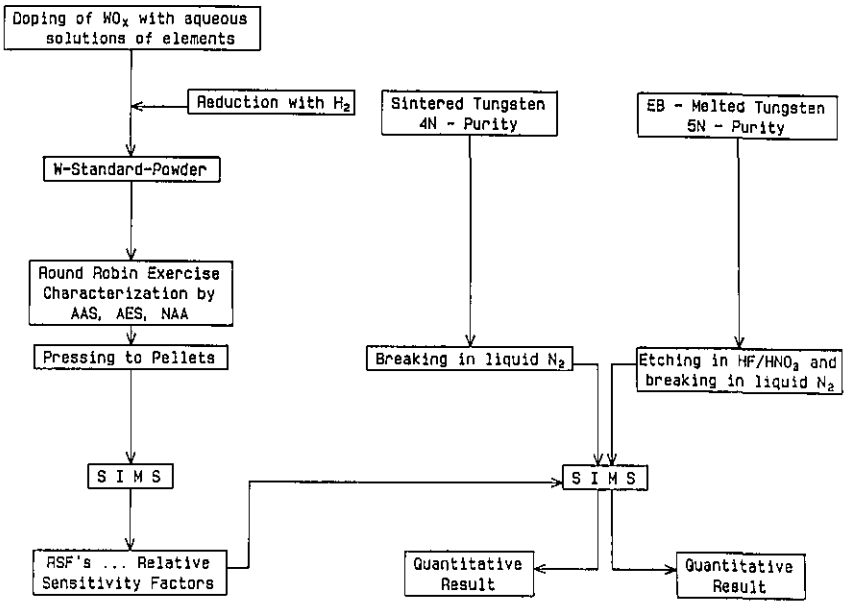

Figure 1. Scheme for quantitative multielement ultratrace analysis of refractory metals (example: tungsten) with SIMS [9].

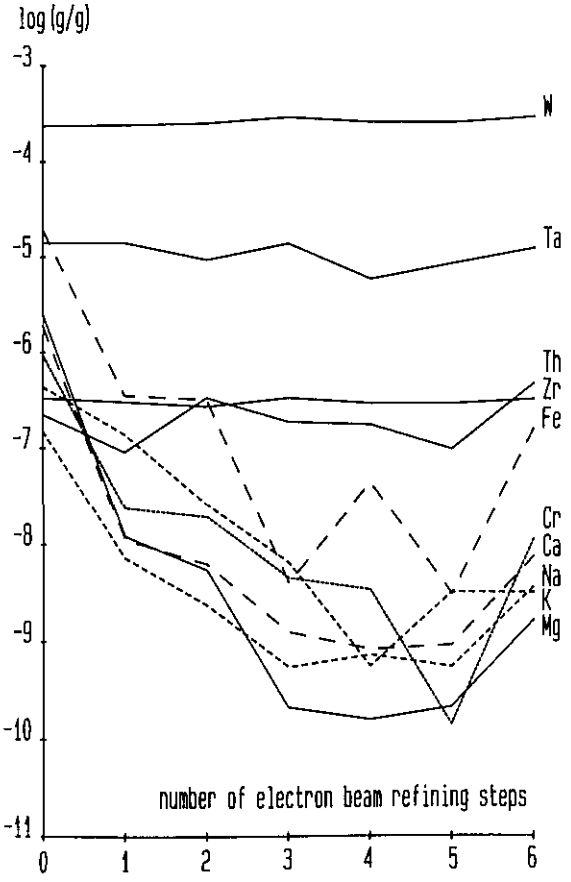

Figure 2. Quantitative ultratrace analysis of impurities in molybdenum with SIMS: Relation between impurity concentration and numbers of electron beam refining steps [11].

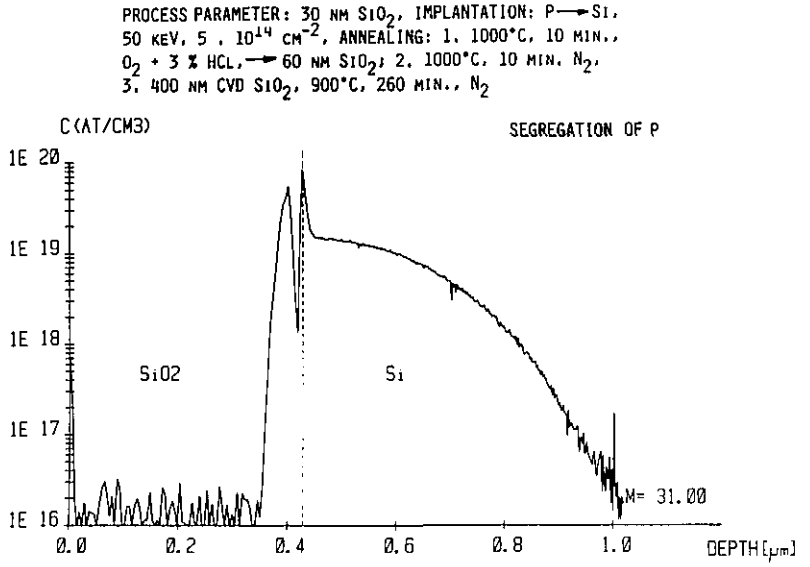

Figure 3. Quantitative phosphorus profile measured at high mass resolution ($M/\Delta M = 4500$) in the SiO_2/Si system for determination of the segregation coefficient.

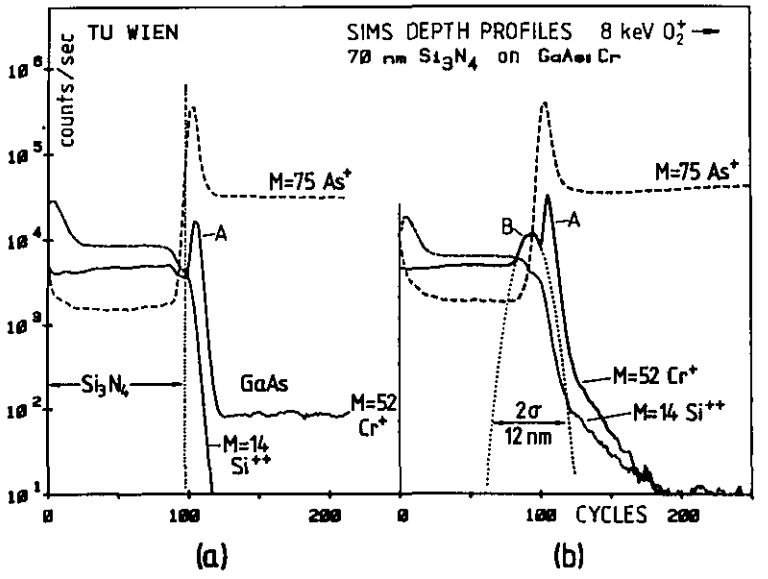

Figure 4. Depth profiles of 70 nm $Si_3N_4/GaAs$ doped with $3.5\times10^{16}cm^{-3}$ Cr. Left: before annealing. Right: after annealing. Primary ions: oxygen [28].

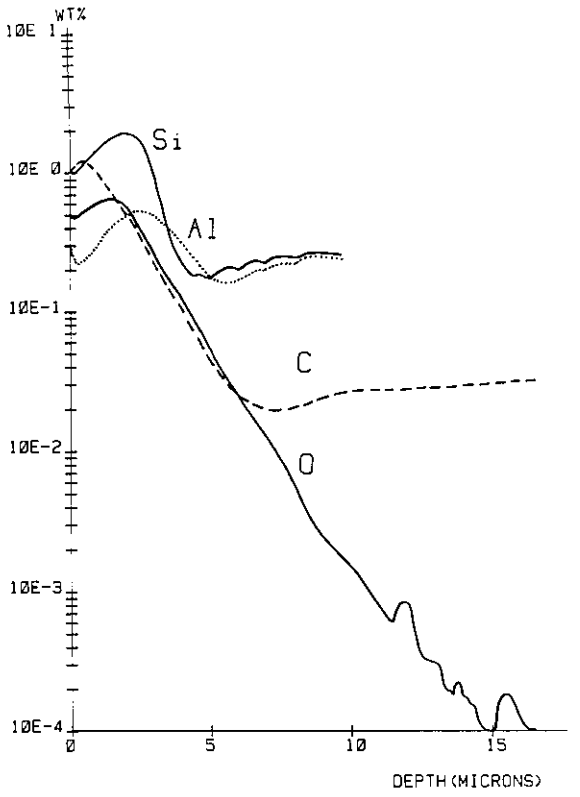

Figure 5. Quantitative depth profiles of C, O, Al and Si in FeAl (0.24), Si(0.25) alloy after annealing in CO-atmosphere [30].

References

[1] Benninghoven, A., Rüdenauer, F., and Werner, H. W., Secondary Ion Mass Spectrometry, John Wiley and Sons, Inc., New York (1987).
[2] Wittmaack, K., Surf. Sci. **89**, 668 (1979).
[3] Powell, C., J. Res. Natl. Bur. Stand. (U.S.) **93**, 387 (1988).
[4] Grasserbauer, M., Stingeder, G., Pötzl, H., and Guerrero, E., Fres. Z. Anal. Chem. **323**, 421 (1986).
[5] Heinrich, K. F. J., and Newbury, D. (eds.), Secondary Ion Mass Spectrometry, Natl. Bur. Stand. (U.S.) SP 427, Gaithersburg (1975).
[6] Morrison, G. H., Springer Ser. Chem. Phys. **19**, 244 (1982).
[7] Wittmaack, K., Nucl. Instr. Meth. **168**, 343 (1980).
[8] Reuter, W., Springer Ser. Chem. Phys. **44**, 94 (1986).
[9] Wilhartitz, P., Virag, A., Friedbacher, G., Grasserbauer, M., and Ortner, H. M., Fres. Z. Anal. Chem., in press.
[10] Grasserbauer, M., Charalambous, P., Jakubowski, N., Stuewer, D., Vieth, W., Beske, H. E., Virag, A., and Friedbacher, G., Mikrochim. Acta I, 1987, in press.
[11] Virag, A., Friedbacher, G., Grasserbauer, M., Ortner, H. M., and Wilhartitz, P., Metall., in press.
[12] Huneke, J., private communication.
[13] Magee, C. W., J. Res. Natl. Bur. Stand. (U.S.) **93**, 390 (1988).
[14] Werner, H. W., Diagnostic Techniques for Micro-Electronic Materials, Processes and Devices, Proc. NATO Adv. Study Institute, Microelectronic Materials and Processes, Levi, R. A., (ed.), M. Nijhoff, Amsterdam, 1987.
[15] Boudewijn, P. R., and Werner, H. W., Springer Ser. Chem. Phys. **44**, 270 (1986).
[16] Grasserbauer, M., Pure Appl. Chem., in press.
[17] Zinner, E., J. Electrochem. Soc. **130**, 199C (1983).
[18] Wittmaack, K., Rad. Eff. **63**, 205 (1982).
[19] Ehrstein, J. R., Downing, R. G., Stallard, B. R., Simons, D. S., and Fleming, R. F., Comparison of Depth Profiling ^{10}B in Silicon Using Spreading Resistance Profiling, SIMS, and Neutron Depth Profiling, ASTM, Special Technical Testing Publ. 850, 409, Philadelphia, 1984.
[20] Simons, D. S., Chi, P., Downing, R. G., Ehrstein, J. R., and Knudsen, J. F., Progress toward a Semiconductor Depth Profiling Standard, Proceedings of the SIMS VI Conference, Versailles, 1987, J. Wiley, Chichester, in press.
[21] Wittmaack, K., J. Vac. Sci. Technol. **A4**, 1662 (1986).
[22] Stingeder, G., Traxlmayr, U., Guerrero, E., Grasserbauer, M., and Pötzl, H., Quantitative Distribution Analysis of Phosphorus with SIMS in the Layer System SiO_2/Si, Mat. Res. Soc. Symp. Proc. 69, 329 (1986) Philadelphia.
[23] Stingeder, G., Piplits, K., Gara, S., Grasserbauer, M., Budil, M., and Pötzl, H., Silmultaneous Quantitative Distribution Analysis of Dopants in Silicon by High Mass Resolution SIMS, Proceedings of the SIMS VI Conference, Versailles, 1987, J. Wiley, Chichester, in press.
[24] Ruedenauer, F. G., and Steiger, W., Ultramicroscopy, in press.
[25] Boudewijn, P. R., Leys, M. R., and Roozeboom, F., Surf. Interface Anal. **9**, 303 (1986).
[26] Galuska, A. A., and Morrison, G. H., Pure Appl. Chem. **59**, 229 (1987).
[27] Kirschner, J., and Etzkorn, H.-W., Physical Limitations of Sputter Profiling at Interfaces—Model Experiments with Ge/Si Using KARMA, in Thin Film and Depth Profile Analysis (Oechsner, H., ed.), Springer Berlin 1984, p. 103.
[28] Traxlmayr, U., Stingeder, G., Fallmann,W., and Grasserbauer, M., Fres. Z. Anal. Chem. **319**, 855 (1984).
[29] Grasserbauer, M., Anal. Chim. Acta. **195**, 1 (1987).
[30] Stingeder, G., Wilhartitz, P., Schreiner, M., and Grasserbauer, M., Fres. Z. Anal. Chem. **319**, 787 (1984).
[31] Thorne, N., and Degreve, F., Trends in the Application of SIMS to Metallurgical Studies, Proceedings of the SIMS VI Conference, Versailles, 1987, J. Wiley, Chichester, in press.
[32] Stingeder, G., Grundner, M., and Grasserbauer, M., Surf. Interface Anal., in press.
[33] Gruen, D. M., Pellin, M. J., Young, C. E., and Calaway, W. F., The Impact of High Efficiency Laser Postionization Techniques on Surface and Bulk Mass Spectrometric Analysis, Proceedings of the SIMS VI Conference, Versailles, 1987, J. Wiley, Chichester, in press.
[34] Evans, C. A., A Review of Current Activities in the Acquisition, Manipulation and Processing of Digitized Secondary Ion Images, Proceedings of the SIMS VI Conference, Versailles 1987, J. Wiley, Chichester, in press.
[35] Wilhartitz, P., and Grasserbauer, M., Mikrochim. Acta II, 313 (1986).
[36] Gaarenstrom, S. W., Appl. Surf. Sci. **26**, 561 (1986).
[37] Otto, M., Chemometrics for Material Analysis, Mikrochim. Acta I, 1987, in press.

[38] Stevie, F. A., Kahora, P. M., Singh, S., and Kroko, L., Atomic and Molecular Relative Secondary Ion Yields of 46 Elements in Si for O_2^+ and Cs^+ Bombardment, Proceedings of SIMS VI Conference, Versailles, 1987, J. Wiley, Chichester, in press.
[39] Wilson, R. G., and Novak, S. W., Systematics of SIMS Relative Sensitivity Factors versus Electron Affinity and Ionization Potential for Si, Ge, GaAs, GaP, InP and HgCdTe Determined from Implant Calibration Standards for about 50 Elements, Proceedings of the SIMS VI Conference, Versailles, 1987, J. Wiley, Chichester, in press.

Quantitative Compositional Mapping on a Micrometer Scale

Dale E. Newbury

Microanalysis Research Group
Center for Analytical Chemistry
National Bureau of Standards
Gaithersburg, MD 20899

Introduction

Quantitative electron microprobe analysis has been restricted traditionally to application at single points or along scan vectors generated by beam or stage scans. However, from the very beginning of this field, the direct visualization of elemental spatial distributions by means of x-ray area scans or "dot maps" has been a powerful adjunct to quantitative analysis [1]. A dot map is created by marking the beam positions at which characteristic x-rays are detected by writing a white dot on a cathode ray tube scanned in synchronism with the beam position on the specimen. The spatial distribution of a selected elemental constituent can be depicted with a dot map at the micrometer level of resolution. Because of the great inherent value of information presented in a visual fashion, dot maps have become a major operating mode of the electron microprobe. However, dot maps are qualitative in nature and suffer from several key deficiencies. Quantitative information is lost because count rates are not recorded; the image information is recorded on film and is inflexible for subsequent processing; the ability to detect mass concentrations below 10 weight percent is severely limited by time constraints; and the method suffers from poor sensitivity to small concentrations changes measured against a high average concentration level.

Compositional Mapping

The development of true compositional mapping with the electron microprobe has recently been achieved in the microprobe laboratories at the National Bureau of Standards working in conjunction with the National Institutes of Health [2]. The basic methodology consists of recording under computer control scan matrix arrays of actual x-ray count rates, derived from both wavelength-dispersive and energy-dispersive x-ray spectrometers. These x-ray intensity matrices are then subjected, on a pixel-by-pixel basis, to complete conventional quantitative analysis procedures. These procedures include all of the usual steps, such as deadtime correction, background correction, standardization against intensities measured on pure elements or simple compounds, and matrix factor correction to account for effects due to electron scattering, x-ray absorption, and secondary fluorescence [3]. In addition to these conventional corrections, specific corrections must be applied to scanned images to compensate for the effect of defocussing of the wavelength-dispersive spectrometers which arises when the beam is scanned off the optic axis of the instrument. This defocus correction can be applied either mechanically by scanning the specimen stage or by rocking the diffraction crystal in synchronism with the scan. Alternatively, the correction can be generated mathematically by making use of the geometric equivalence between spatial scanning on the specimen with a fixed spectrometer diffraction condition and scanning the x-ray peak with the spectrometer while the beam is fixed on the specimen. This equivalence can be used to calculate the spatial dependence of the defocussing at any magnification from a spectrometer scan of the peak [4].

The resulting matrices of concentration values can be displayed as images in which the gray level or color encoding is based not merely upon the x-ray intensities but rather upon the actual concentrations of the elemental constituents. An example of a quantitative compositional map of a zinc diffusion zone at the grain boundaries of a polycrystalline copper sample is shown in figure 1 [5]. This image, which was collected in a matrix scan of 9 hours duration, depicts concentrations as low as 0.2

weight percent. The digital compositional images can be subjected to a wide variety of image processing algorithms to enhance the visibility of weak contrast and to highlight specific composition ranges, substantially improving the flow of information and overcoming many of the limitations of the classical dot mapping method. For example, as shown in figure 2a, by making use of digital processing to achieve contrast expansion, it becomes possible to view small concentration changes against a high average background, e.g., a 5 weight percent change in the silver constituent can be seen against a general background of 65 weight percent silver for grain boundary diffusion zones in a polycrystalline silver-gold alloy. The corresponding deficiency in the gold constituent in this specimen can also be visualized, as shown in figure 2b. In addition to various gray scale image processing algorithms, color scales can also be employed with digital image processing to improve the visibility of desired information. Through the use of carefully constructed "logical" color scales, such as the thermal color sequence (which involves assigning a concentration scale to the color sequence: black, red, orange, yellow, white), compositional ranges covering two decades can be directly visualized. Most importantly, the compositional images are supported by the availability of the quantitative compositional information, including statistics, at every pixel. This information is available for interrogation at any time. Thus, when a structure of interest is recognized in the compositional image, the actual concentrations determined at individual pixels, vectors or areas can be immediately examined.

The extension of quantitative compositional mapping to reach "trace" levels of detection in images depends on two requirements. First, the analytical system must be capable of performing with instrumental stability in electron dose and x-ray detection efficiency to less than 0.1 percent deviations over the long time periods, of the order of 10 hours, which are required to accumulate sufficient x-ray counts. Secondly, since the x-ray bremsstrahlung is strongly dependent upon atomic number, accurate modeling of the x-ray background is needed in order to subtract this contribution from the peak intensities [6]. With careful attention paid to the problem of background correction, compositional mapping has been demonstrated to permit imaging of concentration levels as low as 1000 ppm in materials of intermediate and high atomic number, and levels of 100 ppm can be detected in low atomic number systems such as biological specimens [7].

While this new methodology will not replace conventional single point analysis because of the time requirements of compositional imaging, the combination of compositional images and quantitative analysis is a powerful aid to the solution of many problems. The advent of increasingly powerful laboratory computer systems will allow implementation of imaging systems as a common feature in future analytical facilities.

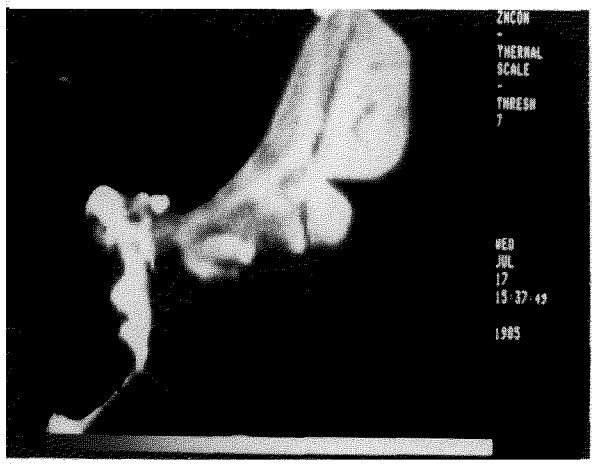

Figure 1. Quantitative compositional map of zinc at the grain boundaries of polycrystalline copper. Concentrations ranging from 0–10 weight precent are mapped. Image field width = 100 micrometers.

Volume 93, Number 3, May-June 1988
Journal of Research of the National Bureau of Standards

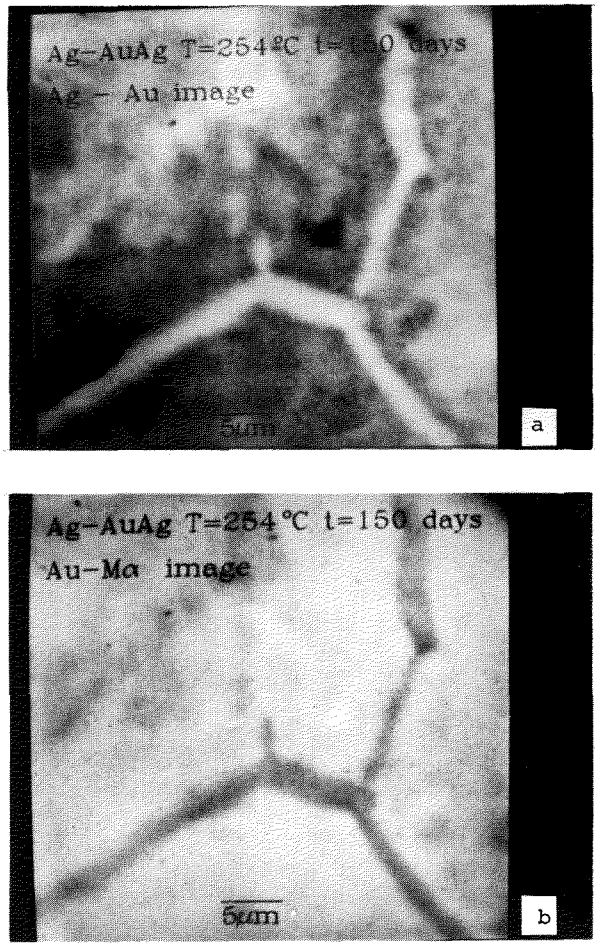

Figure 2. Quantitative compositional maps of grain boundary regions in polycrystalline silver-gold alloy: a) distribution of silver, with contrast enhancement to show an enrichment of 5 weight percent silver against a background of 65 weight percent silver; b) corresponding gold image, showing the deficiency of gold in the grain boundary region. Image field width = 50 micrometers.

References

[1] Duncumb, P., X-ray Microscopy and Microradiography, ed. by V. E. Cosslett, A. Engstrom, and H. H. Pattee, Academic Press (1957) 435.
[2] Marinenko, R. B., Myklebust, R. L., Bright, D. S., and Newbury, D. E., J. Microsc. **145**, 207 (1987).
[3] Goldstein, J. I., Newbury, D. E., Echlin, P., Joy, D. C., Fiori, C. E., and Lifshin, E., Scanning Electron Microscopy and X-ray Microanalysis, Plenum Press, New York (1981) 305.
[4] Myklebust, R. L., Newbury, D. E., Marinenko, R. B., and Bright, D. S., Defocus Modeling for Compositional Mapping with Wavelength-Dispersive X-ray Spectrometry, Microbeam Analysis, San Francisco Press (1986) 495.
[5] Piccone, T. J., Butrymowicz, D. B., Newbury, D. E., Mannig, J. R., and Cahn, J. W., Scripta Met., 839 (1982).
[6] Myklebust, R. L., Newbury, D. E., Marinenko, R. B., and Bright, D. S., Background Correction in Electron Microprobe Compositional Mapping with Wavelength-Dispersive X-ray Spectrometry, Microbeam Analysis, San Francisco Press (1987) 25.
[7] Garruto, R. M., Swyt, C., Fiori, C. E., Yanagihara, R., and Gajdusek, D. D., Lancet, 1353 (1985).

Transferring Accuracy to the Trace Level and Then to the Field

Paul De Biévre[1]

Central Bureau of Nuclear Measurements
Commission of the European Communities—JRC
B-2440 Geel, Belgium

The problem of arriving at an "accurate" determination in trace analysis—determining a "true" small amount in a large amount—requires the assessment of the performance of the measurement method used to an appropriate detail.

In the case of "direct" measurement techniques of trace concentrations, i.e., assaying directly a small amount relative to the large matrix sample, the evaluation should include the assessment of the reproducibility of the linear, or non-linear response of the measurement chain and of the high sensitivity detector over many orders of magnitude down to small concentrations. (See example in fig. 1.) To allow this assessment, a set of synthetic isotope mixtures can be prepared gravimetrically and used to examine the measurement chain and detector. An example of such a set is given in table 1. Its preparation is described elsewhere [1]. The built-in ratio $^{235}U/^{238}U \approx 1$ (certified to 0.02%) can be used to determine any systematic errors in the "excitation" or "ion" source and correct the observed $^{233}U/^{235}U$ or $^{233}U/^{238}U$ ratios. Comparison of the latter to the certified values (given to $\pm 0.03\%$) then provides a means to determine systematic errors of the (sensitive) detectors used in the trace analysis (e.g., electron multipliers) and to determine possible deviations from linearity of the (electronic) measurement equipment used. It is also possible to determine the reproducibility of these systematic

[1] Professor at the University of Antwerp.

Table 1. Set of (isotopic) reference materials to test the linearity of a detector/amplifier measurement system

Code number	Description	Atomic isotope ratios $^{233}U/^{235}U$ ±0.03% of value	Atomic isotope ratios $^{235}U/^{238}U$ ±0.000 30	Unit
CBNM-IRM-				
072/1	Uranyl-	1.000 33	0.991 03	1 mg U in 1 g
072/2	nitrate	0.699 67	0.991 68	solution
072/3	solution	0.499 85	0.992 12	
072/4		0.299 87	0.992 56	
072/5		0.100 01	0.992 99	
072/6		0.050 091	0.993 10	
072/7		0.019 994	0.993 17	
072/8		0.010 165	0.993 19	
072/9		0.005 000 0	0.993 20	
072/10		0.002 001 2	0.993 21	
072/11		0.000 968 92	0.993 21	
072/12		0.000 500 88	0.993 21	
072/13		0.000 101 82	0.993 21	
072/14		0.000 019 996	0.993 21	
072/15		0.000 001 999 5	0.993 21	

errors and/or deviations allowing to correct for them. It is important to point out that the uncertainties of such corrections must be carried on and correctly propagated until the final result in any measurement of unknowns.

We now have a means for specialized measurement laboratories to verify how their detector and measuring equipment is really performing at (very) low signals, i.e., at the trace element level and a first example obtained is given in figure 2.

In the case of measurement techniques which assay small amounts in weighed samples, the "jump" to the trace level is performed through weighing (by using small weights) and the problem becomes one of assaying a trace amount with a known, proven, or provable accuracy.

Every indication is there that this will have to come from isotope-specific—or should I say nuclide-specific?—methods on the basis of the fact that isotopes are very specific representatives of elements and specificity is an essential key to accuracy.

We have at present a few nuclide-specific assay methods in our array of analytical assay methods:

- Those which use the property of one nuclide as in a specific nuclear reaction ("activation analysis"); the degree of specificity will influence heavily the potential for accuracy; the degree of quantitative knowledge of every parameter concerned will determine the size of the total "inaccuracy."
- Those which modify an isotope (nuclide) abundance ratio R_x in the sample ("isotope dilution"), by the addition of a "spike" which is a known number of atoms of the same element as the unknown but with another R_y value for the abundance ratio of the same isotopes (an "enriched" stable isotope- or "nuclide"); this spike acts as an almost ideal "internal standard" and the measurement is reduced to the determination of the new isotope abundance ratio R_B in the blend resulting from the change induced by R_y in R_x. Of course, proper isotopic homogenization and complete destruction of the matrix (this makes the assay matrix—independent) in a closed system, is an absolute prerequisite for this type of assay.

Isotope- or nuclide-specific methods do have inherently more potential for accuracy since they measure isotopes and not elements. Isotopic atoms are measured on the basis of properties of the atom nucleus (e.g., difference in mass) which are shielded from chemical interferences before or during the measurement, by identical outer electron clouds. They can therefore potentially lead to greater accuracy (when the isotopic measurement methods are correctly applied of course). It is to be expected that isotope- or nuclide-specific methods will more and more deliver reference values and methods for elemental trace analysis in the future.

Thus the measurement of an element concentration ratio (= conventional analytical chemistry) is replaced by the measurement of isotope abundance

ratio. The essential step of isotopic homogenization can be guaranteed when properly carried out, because it takes advantage of the fact that the outer electron clouds (i.e., the chemical form) of both sample and spike isotopic atoms are identical. This ensures that both will behave in the same way and end up in the same chemical forms after chemical destruction of the sample. At the moment of full isotopic homogenization, the end result is in fact "frozen in." Any chemical effect in a later stage of the process, e.g., losses in normal purification or separation stages, will therefore affect equally the isotopes of sample and spike in the same way and leave their abundance ratio—the end result—unchanged.

The "accurate" values obtained as explained above for trace elements in unknown samples, can now be carried to the field by Interlaboratory Measurement Evaluation Programmes (IMEPs) where measurements on these samples are collected and graphically displayed around the "reference value." One could also call such a programme an "external" measurement evaluation.

Current work at the Central Bureau for Nuclear Measurements (CBNM) aims at following the route described above to establish reference values for IMEPs. An example of what this yields is given in figure 3, taken from the nuclear field: even after suitable calibration with available Reference Materials, a picture develops showing considerably larger spread than what laboratories believe to be their uncertainty. It is a surprisingly classical picture which can be produced for any assay measurement in any field at any concentration level. Only the ordinates and the title of the picture must be changed, the general nature of the picture remains the same (see an example in fig. 4). In other words, the concept is expected also to be applicable to the trace analysis field.

The question arises where such "reference value" or "baseline" takes its authority from and why. Since it is very difficult to unequivocally establish these baseline values, this should be done by specialized institutes or laboratories (the "standards" laboratories in the world) along the following lines:

(a) It must be absolutely transparent how the value intended to be the "closest approximation of the true value" (i.e., intended to be accurate), is arrived at, based on a detailed explanation of each step in the characterization process which leads from our bank SI units to the value pretending to be able to serve as "reference," and

(b) It must be absolutely transparent how the "uncertainty" or "inaccuracy" of the value is arrived at, based on the establishment of a list of uncertainty contributors which are identified qualitatively and individually quantified by various appropriate procedures so that their component contribution to the total "inaccuracy" is clearly visible; a work model for that is given in table 2.

Table 2. Proposed Work Model to Establish a "Composition of Uncertainty"

		%
a)	repeatability of measurement expressed as 2s	.....
	$(6 \leq n \leq 10)$	———
b)	repeatability of correction factors expressed as 2s	.....
	$(6 \leq n \leq 10)$	
	1st correction factor	.....
	2nd correction factor	.....
	|	.....
	|	.....
	|	.....
	nth correction factor	.....
	———	———
	subtotal = $\sqrt{(1st)^2 + (2nd)^2 + ...(nth)^2}$	.....
c)	Estimate of possible (as yet) unknown systematic errors	
	on a 2s basis	
	1st	.....
	2nd	.....
	|	.....
	|	.....
	|	.....
	nth	.....
	———	
	subtotal = $\sqrt{(1st)^2 + (2nd)^2 + ...(nth)^2}$	———
	TOTAL	.....

Note that such IMEP programmes are result-oriented and not method- or procedure-oriented. In the graphs presenting the results, distinction is clearly made between:

- The state of the practice (SOP) which is materialized in the spread of the results and in the (non-)deviation from the established reference values.

• Same form of the state of the art (SOA) which is materialized in the uncertainty level of the "reference values" which must be demonstrated to be reliable enough and usable for such "external" QA programmes.

Conclusions

1. It has been shown how the response of measuring equipment can be evaluated for (non-) linearity over many orders of magnitude, this possible error contributor being separated from the contributors located in the "source" or "excitation" part of the measurement method.

2. Isotope- or nuclide-specific methods have a great potential to serve "reference" purposes so badly needed in trace analysis.

3. IMEPs with carefully established baselines should carry references to the field.

4. "Standards-" or "Reference-" Institutes should consider it as part of their basic mission to deliver regularly "baseline-values" for real life samples which are circulated as "blind" samples amongst the laboratories wanting to assess their true measurement capability through an "external" evaluation programme.

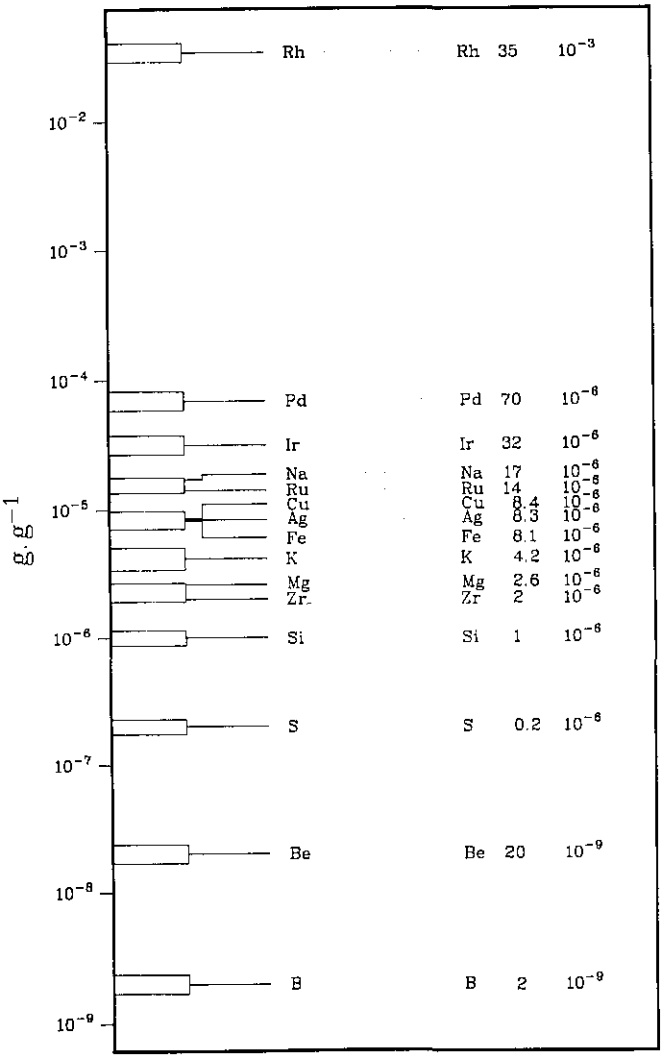

Figure 1. Example of dynamic range of trace concentrations: impurities in Pt metal (Spark Source Mass Spectrometry).

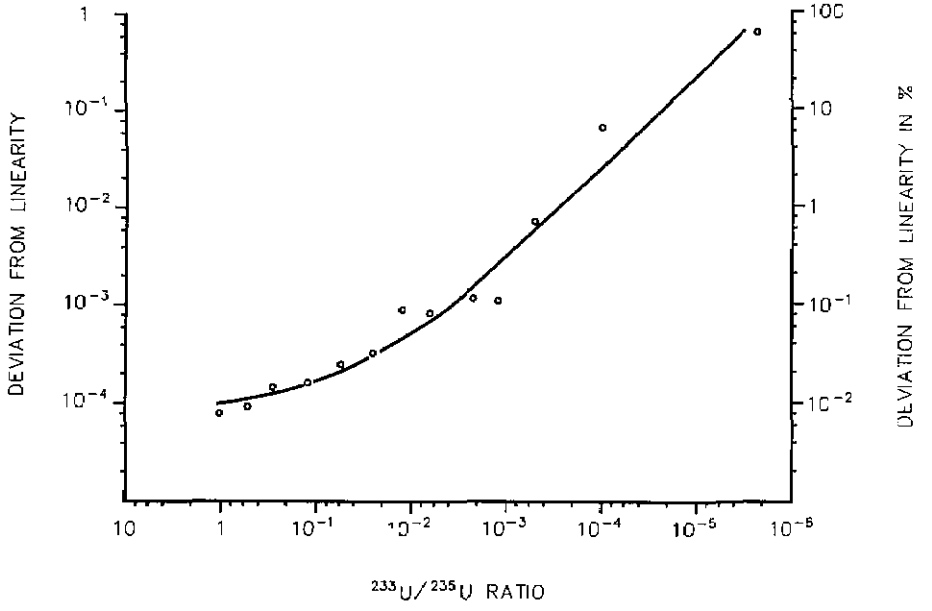

Figure 2. Test of the response of a mass spectrometer as function of the ratio to be measured.

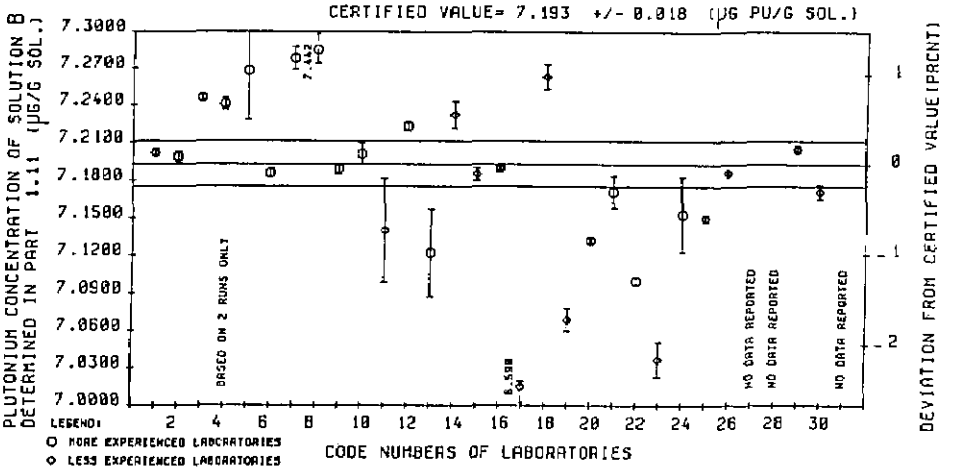

Figure 3. Interlaboratory measurement evaluation programme on Pu assay amongst 31 laboratories (Reference Value: CBNM by IDMS).

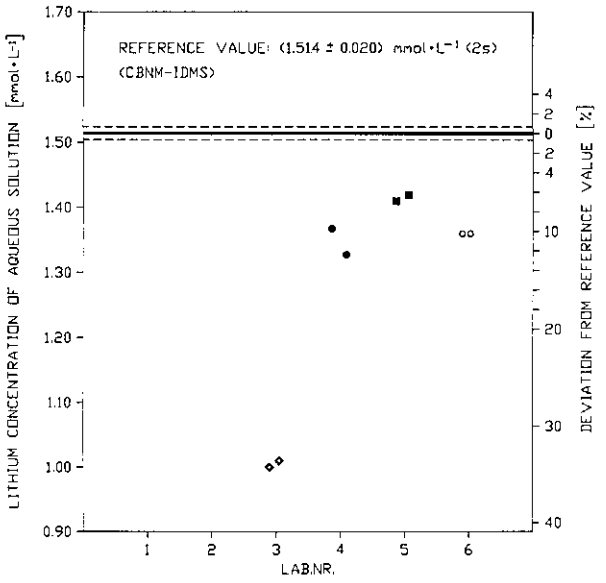

Figure 4. Interlaboratory measurement evaluation programme on Li assay amongst 61 laboratories (Reference Value: CBNM by IDMS).

References

[1] Lycke, W., De Bièvre, P., Verbruggen, A., Hendrickx, F., and Rosman, K. J. R., "Isotopic Reference Material Set for Testing the Linearity of Isotope Mass Spectrometers," CBNM IRM 072, 1987; Proc. EURO ANALYSIS VI, September 1987, Paris (to be published).